

Exposure of cardiac microvascular endothelial cells to harmful stimuli: A study of the cellular responses and mechanisms.

Amanda Genis



*Dissertation presented for the degree of Doctor of
Philosophy (Medical Physiology) in the
Faculty of Medicine and Health Sciences at
Stellenbosch University*

Supervisor: Prof Hans Strijdom

Co-supervisor: Prof Barbara Huisamen

° 2014

DECLARATION:

By submitting this dissertation electronically, I declare that the entirety of the work contained therein is my own, original work, that I am the sole author thereof (save to the extent explicitly otherwise stated), that the reproduction and publication thereof by Stellenbosch University will not infringe any third party rights and that I have not previously in its entirety or in part submitted it for obtaining any qualification.

Signature:

Date: 15 October 2013

.
. .
.

. y

ABSTRACT:

Exposure to harmful stimuli can render vascular endothelial cells dysfunctional, characterised by reduced nitric oxide (NO) bioavailability. Endothelial dysfunction (ED) is a reversible precursor of ischaemic heart disease (IHD), and understanding the mechanisms underlying the development of ED could lead to clinical strategies in preventing/treating IHD. Very little is known about the responses of cardiac microvascular endothelial cells (CMECs) to pro-ED stimuli, as most studies are conducted on macrovascular endothelial cells.

The current dissertation set out to comprehensively investigate the responses of cultured primary adult rat CMECs to known harmful stimuli, viz. hypoxia and tumor necrosis factor-alpha (TNF- α ; pro-inflammatory cytokine). We were interested to investigate whether this distinct endothelial cell type would develop classical features of ED, and if so, what the underlying mechanisms were. First we aimed to establish a baseline characterization of the CMECs under control conditions. Next, we developed a model of hypoxia-induced cell injury and measured apoptosis/necrosis, intracellular NO and reactive oxygen species (ROS), expression and activation of signalling proteins involved with NO-biosynthesis, hypoxia and apoptosis, and differential regulation of proteins. Finally, we characterised CMEC responses to treatment with TNF- α . We assessed apoptosis/necrosis, intracellular NO and ROS levels, NO-biosynthesis pathway proteins and large-scale differential protein regulation. The above measurements were performed by morphological assessment (light and fluorescence microscopy), FACS analysis, western blotting and large-scale proteomic analyses.

Data showed that CMECs shared many baseline features with other endothelial cell types, including morphological appearance, LDL-uptake, NO-production, and expression of eNOS protein. In a novel observation, proteomic analysis revealed the expression of 1387 proteins. Another novel finding was the high abundance of structural mitochondrial proteins, suggesting that CMECs require mitochondria for non-respiration purposes as well. High expression of vesicle, glycolytic and RAS signalling proteins were other features of the baseline CMECs. CMECs exposed to hypoxia responded by increased apoptosis/necrosis and expression of the hypoxia-marker, HIF-1 α . Interestingly, hypoxic CMECs showed increased eNOS-NO biosynthesis, associated with increased mitochondrial ROS and reduced anti-oxidant systems, suggestive of oxidative stress. In accordance with the literature, several glycolytic proteins were up-regulated. A novel finding was the up-regulation of proteins involved with protein synthesis, not usually described in hypoxic cell studies. The CMECs responded to TNF- α -treatment by exhibiting hallmarks of ED, namely attenuated biosynthesis of PKB/Akt-eNOS-derived NO and the development of outspoken response to oxidative stress as indicated by the up-

regulation of several anti-oxidant systems. The data showed that TNF- α treatment elicited classical TNF-Receptor 1-mediated signalling characterized by the dual activation of pro-apoptotic pathways (BID and caspase-3) as well as the protective, pro-inflammatory IKB-alpha-NF-KB pathway.

In conclusion, this is the first study of its kind to describe a comprehensive characterisation of CMECs under baseline and injury-inducing conditions. On the whole, although it appeared as if the CMECs shared many responses and mechanisms with more frequently researched endothelial cell types, the data also supplied several novel additions to the literature, particularly with the application of proteomics. We believe that this dissertation has provided more insights into endothelial heterogeneity in the vascular system and into the mechanisms adopted by CMECs when exposed to stimuli typically associated with cardiovascular risk.

OPSOMMING:

Blootstelling aan skadelike stimuli kan tot disfunksionaliteit van vaskulêre endoteelselle lei wat deur verlaagde biobeskikbaarheid van stikstofoksied (NO) gekenmerk word. Endoteeldisfunksie (ED) is 'n omkeerbare voorganger van isgemiese hartsiekte (IHD), en 'n beter begrip van die onderliggende meganismes van ED kan lei tot die ontwikkeling van kliniese strategieë vir die voorkoming/behandeling van IHD. Baie min is bekend oor die respons wat in kardiaal mikrovaskulêre endoteelselle (CMECs) uitgelok word na blootstelling aan pro-ED stimuli, omdat meeste studies op makrovaskulêre endoteelselle uitgevoer word.

Die huidige proefskrif het daarna gemik om die respons van primêre kulture van volwasse rot CMECs op bekende skadelike stimuli, nl. hipoksie en tumor nekrose faktor-alfa (TNF- α ; pro-inflammatoriese sitokien) in diepte te ondersoek. Ons was veral geïnteresseerd om vas te stel of hierdie spesifieke endoteelseltipe die klassieke kenmerke van ED sou ontwikkel, en indien wel, wat die onderliggende meganismes sou wees. Eerstens het ons beoog om 'n basislyn karakterisering van CMECs onder kontrole toestande daar te stel. Vervolgens het ons 'n model van hipoksie-geïnduseerde selskade gevestig en apoptose/nekrose, intrasellulêre NO en reaktiewe suurstofspesies (ROS), sowel as die uitdrukking en aktivering van proteïene betrokke by NO-biosintese, hipoksie en apoptose en differensiële regulering van proteïene gemeet. Laastens het ons die respons van CMECs op behandeling met TNF- α gekarakteriseer. Ons het apoptose/nekrose, intrasellulêre NO en ROS vlakke, NO-biosintese-seintransduksieproteïene en grootskaalse differensiele regulering van

proteïene gemeet. Bg. metings is uitgevoer deur gebruik te maak van morfologiese evaluasie (lig -en fluoressensiemikroskopie), vloeisitometriese analises, western blot analises en proteomiese analises.

Data het getoon dat die basislyn eienskappe van CMECs grootliks met dié van ander endoteelseltypes ooreenstem, insluitende morfologiese voorkoms, LDL-opname, NO-produksie en die uitdrukking van eNOS proteïene. In 'n nuwe waarneming, het die proteomiese data die uitdrukking van 1387 proteïene aangetoon. 'n Ander nuwe bevinding was die voorkoms van 'n groot aantal strukturele mitokondriale proteïene, wat daarop dui dat die CMECs mitokondria ook vir nie-respiratoriese doeleindes gebruik. 'n Hoë uitdrukking van vesikulêre, glikolitiese en RAS-seintransduksie proteïene was ook kenmerkend van die basislyn CMECs. CMECs wat aan hipoksie blootgestel is, het reageer met 'n verhoging in apoptose / nekrose en verhoogde uitdrukking van die hipoksie merker, HIF-1 α . 'n Interessante bevinding was dat eNOS-NO biosintese sterk toegeneem het in die hipoksiese CMECs wat met verhoogde mitokondriale ROS en verlaagde anti-oksidadant sisteme (aanduidend van oksidatiewe stres) gepaardgegaan het. In ooreenstemming met die literatuur, is verskeie glikolitiese proteïene opgereguleer. 'n Nuwe waarneming was die opregulering van proteïene wat betrokke is by proteïensintese, iets wat nie normaalweg in hipoksie-studies beskryf word nie. Die CMECs het op TNF- α behandeling gerespondeer deur tekens van ED te toon, naamlik 'n afname in die NO afkomstig van PKB/Akt-eNOS biosintese en die ontwikkeling van uitgesproke reaksie op oksidatiewe stres soos aangedui deur die opregulering van verskeie anti-oksidadant sisteme. Die data het ook aangedui dat TNF- α behandeling tot klassieke TNF-reseptor 1 bemiddelde seintransduksie gelei het, wat gekenmerk was deur die tweeledige aktivering van pro-apoptotiese seintransduksiepaaie (BID en kaspase-3) sowel as die beskermende, pro-inflammatoriese IKB- α -NF-KB seintransduksiepad.

Ten slotte: hierdie is die eerste studie van sy soort wat die kenmerke en response van CMECs onder basislyn en pro-besering omstandighede in diepte beskryf. Alhoewel dit oor die algemeen wil voorkom asof die CMECs baie in gemeen het met ander, beter nagevorste endoteelseltypes, het die data egter ook verskeie nuwe bevindinge tot die bestaande literatuur gevoeg, spesifiek die data afkomstig van die proteomiese analises. Ons glo dat hierdie proefskrif meer insig verleen t.o.v. die heterogeniteit van vaskulêre endoteelselle asook t.o.v. die megansimes wat deur CMECs aangewend word wanneer hulle aan skadelike stimuli (geassosieer met kardiovaskulêre risiko) blootgestel word .

ACKNOWLEDGEMENTS:**I would like to thank the following people:**

- My supervisor, Prof Hans Strijdom, for his support and guidance throughout this study and his complete commitment as a leader to our research group. I would also like to acknowledge him in all the personal growth and accolades that this study added to my career as a researcher.
- My family for their love, support and never-failing belief in me. With your steadfast belief in me and lots of patience, many “impossibilities” were turned into “realities”.
- My endothelium-research group also deserves a special thank you. Every single person contributed to the end results in some way or another.
- All the members from the department for support and assistance.
- My Heavenly Father for love and grace that knows no bounds and without Whom, this study and thesis, would not have been possible.

List of tables

Chapter 1:

- Table 1.1: Overview of the endothelium-derived vaso-active factors, responsible for regulating vascular tone (page 14).
- Table 1.2: The regulation of NOS protein expression and activity in the heart (page 16).
- Table 1.3: Selection of in vitro endothelial cell studies investigating the effects of TNF- α stimulation (page 51).
- Table 1.4: Summary of the detrimental effects of TNF- α in the heart (page 53).
- Table 1.5: ADMA in a nutshell (page 59).
- Table 1.6: The activity, regulation and expression of the main NOXs in the cardiovascular system (specifically the endothelium) (page 83).
- Table 1.7: Methods for Clinical Assessment of Endothelial Function (page 106).

Chapter 2:

No tables in chapter 2.

Chapter 3:

- Table 3.1: List of identified proteins in the baseline CMEC proteome known to be predominantly expressed in vascular endothelial cells (page 155).
- Table 3.2: Comparison of selected proteins identified in the baseline CMECs of the present study with those identified in other studies performed on similar or other endothelial cell types (page 156-157).

Chapter 4:

- Table 4.1: List of hypoxia-induced up regulated proteins in CMECs (≥ 1.5 -fold) (page 192).
- Table 4.2: List of hypoxia-induced down regulated proteins in CMECs (≥ 1.5 -fold) (page 193).

Chapter 5:

No tables in chapter 5.

Chapter 6:

Table 6.1: High confidence differentially expressed phosphorylated proteins in TNF- α treated (5 ng/ml; 24 h) CMECs as determined by 2-D DIGE (page 272).

Table 6.2: Selected list of strongly represented proteins (detected in TNF- α samples only) (page 276).

Table 6.3: Selected list of strongly represented proteins (up-regulated in TNF- α samples) (page 277).

Table 6.4: Selected list of underrepresented proteins (down-regulated in TNF- α samples) (page 278).

Table 6.5: Cellular components associated with TNF- α -induced up regulated proteins and proteins detected only in TNF- α stimulated cells (page 282).

Table 6.6: Biological processes associated with TNF- α -induced up regulated proteins and proteins detected only in TNF- α stimulated cells (page 283).

Table 6.7: Molecular functions associated with TNF- α -induced up regulated proteins and proteins detected only in TNF- α stimulated cells (page 284).

Table 6.8: Cellular components associated with TNF- α -induced down regulated proteins and proteins detected only in control (untreated) cells (page 285).

Table 6.9: Biological processes associated with TNF- α -induced down regulated proteins and proteins detected only in control (untreated) cells (page 286).

Table 6.10: Molecular functions associated with TNF- α -induced down regulated proteins and proteins detected only in control (untreated) cells (page 287).

Chapter 7:

No tables in chapter 7.

List of figures

Chapter 1:

- Figure 1.1: Global distribution of cardiovascular disease (CVD) (page 2).
- Figure 1.2: Top ten causes of mortality in the Western Cape in 2009 (page 3).
- Figure 1.3: Profile of the 2006 Heart of Soweto Cohort (page 4).
- Figure 1.4: Effects of LDL particles on the vessel wall (page 6).
- Figure 1.5: The anatomical structures of arteries, arterioles, and capillaries (page 6).
- Figure 1.6: A fluorescence digital image of Bovine Pulmonary Artery Endothelial Cells (BPAEC) (page 9).
- Figure 1.7: Illustration showing the structure of Nitric Oxide (page 13).
- Figure 1.8: Metabolite-controlled production of NO (page 18).
- Figure 1.9: Classical mode of action of NO in vascular smooth muscle by activation of sGC and generation of cGMP (page 21).
- Figure 1.10: The cyclooxygenase pathways (page 29).
- Figure 1.11: ECs (EC's) in arteries, veins, and capillaries (page 36).
- Figure 1.12: Classification of ECs in the heart (page 39).
- Figure 1.13: Cardiac endothelial cells (page 40).
- Figure 1.14: ECs in the heart (page 41).
- Figure 1.15: Role of TNF- α in ED (page 50).
- Figure 1.16: Schematic overview of biochemical pathways related to ADMA (page 55).
- Figure 1.17: Metabolic and biochemical responses of ECs to hypoxia (page 67).
- Figure 1.18: Pathophysiology of hyperglycaemia induced ED (page 71).
- Figure 1.19: Vascular ROS (page 76).
- Figure 1.20: Coupled vs. uncoupled eNOS (page 77).
- Figure 1.21: Potential sources of ROS in ECs (page 81).

- Figure 1.22: Schematic representation of NOX2 and NOX4 and oxidases (page 82).
- Figure 1.23: Pathophysiological effects and the interplay between increased plasma cholesterol and O₂ – levels, and EC responses (page 88).
- Figure 1.24: Exposure of ECs to cardiovascular risk factors and the resultant pathophysiological changes (page 93).
- Figure 1.25: Schematic overview of eNOS uncoupling (page 100).
- Figure 1.26: Oxidative and nitrosative stress (page 101).
- Figure 1.27: The central role of ED in the causation and progression of atherosclerosis (page 103).
- Figure 1.28: ED: the pathophysiological link between risk factors and CVD (page 105).

Chapter 2:

- Figure 2.1: Procedure for passaging and labelling of cells (page 113).
- Figure 2.2: Schematic diagram of a flow cytometer (page 116).
- Figure 2.3: A: A representative density dot plot of a CMEC representative sample (page 117).
B: A representative histogram plot of a CMEC representative sample (page 117).
- Figure 2.4: A: Density plot of a representative sample showing the sub-population of cell samples staining positively with PI (necrosis) (page 119).
B: Histogram plot, showing the corresponding PI fluorescence intensity (page 119).
- Figure 2.5: A: Density plot of a representative sample showing the sub-population of cell samples staining positively with Annexin V (apoptosis) (page 119).
B: Histogram plot, showing the corresponding Annexin V fluorescence intensity (page 119).
- Figure 2.6: A density plot showing the simultaneous measurement of necrosis and apoptosis in one sample (page 120).
- Figure 2.7: Positive control protocol with the NO donor, DEA/NO (100 µM), to validate the NO-specificity of DAF-2/DA (page 122).

- Figure 2.8: A: Measurement of DAF-2/DA fluorescence following treatment with increasing DEA/NO (100µM, 500µM & 1mM) concentrations for 30 minutes (page 123).
B: Histogram showing mean fluorescence intensity measured in absolute control, DAF-2/DA-control and positive control (page 123).
- Figure 2.9: Positive control protocol with the O₂- donor, DMNQ (100 µM), to validate the relative O₂-specificity of DHE (page 126).
- Figure 2.10: A: Measurement of DHE fluorescence following treatment with increasing DMNQ concentrations (10µM & 100µM) for 30 minutes (page 127).
B: Histogram showing mean fluorescence intensity measured in absolute control, DHE-control and positive control (page 127).
- Figure 2.11: Positive control protocol with authentic peroxynitrite (100 µM), to validate the relative peroxynitrite-specificity of DHR-123 (page 128).
- Figure 2.12: A: Measurement of DHR-123 fluorescence following treatment with increasing authentic peroxynitrite concentrations (100µM, 500µM & 1mM) for 30 minutes (page 129).
B: Histogram showing mean fluorescence intensity measured in absolute control, DHR-123-control and positive control (page 129).
- Figure 2.13: Positive control protocol with H₂O₂, (100 µM) to validate the relative H₂O₂-specificity of DCF (page 130).
- Figure 2.14: A: Measurement of DCF fluorescence following treatment with H₂O₂ (100 µM) for 30 minutes (page 131).
B: Histogram showing mean fluorescence intensity measured in absolute control, DCF-control and positive control (page 131).
- Figure 2.15: Protocol for sample preparation from cells to Bradford Assay (page 135).
- Figure 2.16: Example of a typical gel setup for a 14 sample western blot analyses (page 136).
- Figure 2.17: Workflow for identifying proteins in CMECs (page 139).
- Figure 2.18: A: The LTQ Orbitrap Velos mass spectrometer situated in the Proteomics Unit of the University of Stellenbosch (page 140).
B: Nano-electrospray source (page 140).
C: Nano-electrospray source magnified on screen (page 140).

Chapter 3:

- Figure 3.1: Validation of morphological appearance of confluent CMEC culture (page 147).
- Figure 3.2: Flow cytometric analysis of the percentage cells staining positively for the Dil-ac-LDL fluorescent probe in cells from different culture generations (page 148).
- Figure 3.3: Validation of endothelial cell purity. Representative fluorescence microphotograph (page 149).
- Figure 3.4: Total baseline expression of selected NOS-NO signalling proteins in our CMECs (page 151).
- Figure 3.5: Workflow for identifying proteins in CMECs under baseline conditions (page 154).
- Figure 3.6: Functional annotation analysis (DAVID Bioinformatics) of the proteins identified in baseline CMECs showing the top 10 most enriched annotation clusters with their respective enrichment scores and GO terms (page 158).
- Figure 3.7: Intracellular NO-levels measured by the mean fluorescence intensity of DAF-2/DA (page 160).
- Figure 3.8: Mitochondrial abundance in CMECs stained with MitoTracker™ Red (page 164).

Chapter 4:

- Figure 4.1: The hypoxia protocol (page 179).
- Figure 4.2: Workflow for proteomic analyses of CMECs under hypoxic conditions (page 180).
- Figure 4.3: Hypoxia time-response studies with necrosis expressed as % PI staining cells (page 182).
- Figure 4.4: Hypoxia time-response studies with apoptosis expressed as % Annexin V (page 182).
- Figure 4.5: Necrosis in hypoxic CMECs compared to hypoxic H9C2 myoblasts at 24 hours (page 183).
- Figure 4.6: Apoptosis in hypoxic CMECs compared to hypoxic H9C2 myoblasts at 24 hours (page 183).
- Figure 4.7: HIF-1 α expression in hypoxic CMECs (page 184).
- Figure 4.8: Total eNOS expression in hypoxic CMECs (page 186).
- Figure 4.9: Hypoxia-induced (24 hours hypoxia) increase in NO production measured as mean 4,5-diaminofluorescein-2/diacetate (DAF-2/DA) fluorescence intensity expressed as percentage of control (page 187).

- Figure 4.10: Hypoxia-induced cell injury (24 hours hypoxia) demonstrated by increased oxidative stress measured as % dihydrorhodamine-123 (DHR-123) mean fluorescence intensity of control (page 188).
- Figure 4.11: P22 phox expression in hypoxic CMECs (page 189).
- Figure 4.12: Nitrotyrosine expression in hypoxic CMECs (page 190).
- Figure 4.13: Functional annotation clusters of strongly represented proteins in hypoxic CMECs (page 194).
- Figure 4.14: Oxidative stress measured as % dihydroethidium (DHE) mean fluorescence intensity of control (page 199).
- Figure 4.15: A: Proteomic analysis of HSP 90 (page 204).
B: Total HSP 90 expression in hypoxic CMECs (page 204).
- Figure 4.16: A: Proteomics analysis of either tubulin beta-5 (Accession No: P69897) or tubulin beta-2C (Accession No: Q6P9T8) in hypoxic CMECs (page 207).
B: Total β -tubulin expression in hypoxic CMECs (page 207).
- Figure 4.17: A cartoon depicting the major findings in the hypoxic CMECs (page 211).

Chapter 5:

- Figure 5.1: Protocol for treatment of CMECs with 0.5 ng / ml, 5 ng / ml or 20 ng / ml (24 hours) for subsequent FACS and western blot analyses (page 217).
- Figure 5.2: Protocol for treatment of CMECs with 20 ng / ml TNF- α and Ox-LDL (40 μ g / ml) for 30 minutes for subsequent FACS analysis NO production, oxidative stress and nitrosative stress (page 219).
- Figure 5.3: Protocol for treatment of CMECs with 20 ng / ml TNF- α for 24 hours in medium supplemented with either 0, 5 or 10 % foetal bovine serum (FBS) for subsequent FACS analysis of superoxide production (DHE fluorescence) (page 221).
- Figure 5.4: TNF- α effects on necrosis at different concentrations (0.5, 5 and 20 ng / ml for 24 hours) (page 223).
- Figure 5.5: TNF- α effects on apoptosis at different concentrations (0.5, 5 and 20 ng / ml for 24 hours) (page 223).
- Figure 5.6: TNF- α effects on mean DAF-2/DA fluorescence at different concentrations (0.5, 5 and 20 ng / ml for 24 hours) (page 225).
- Figure 5.7: TNF- α effects on mean DHE fluorescence at different concentrations (0.5, 5 and 20 ng / ml for 24 hours) (page 228).

- Figure 5.8: TNF- α effects on mean DCF fluorescence at different concentrations (0.5, 5 and 20 ng / ml for 24 hours) (page 228).
- Figure 5.9: TNF- α effects on mean DHR-123 fluorescence at different concentrations (0.5, 5 and 20 ng / ml for 24 hours) (page 229).
- Figure 5.10: TNF- α effects on phosphorylated eNOS (phospho Ser 1177) at different concentrations (0.5, 5 and 20 ng / ml for 24 hours) (page 232).
- Figure 5.11: TNF- α effects on total eNOS expression at different concentrations (0.5, 5 and 20 ng / ml for 24 hours) (page 233).
- Figure 5.12: TNF- α effects on the phosphorylated eNOS / total eNOS expression at different concentrations (0.5, 5 and 20 ng / ml for 24 hours) (page 234).
- Figure 5.13: TNF- α effects on phosphorylated PKB/Akt (phospho Ser 473) at different concentrations (0.5, 5 and 20 ng / ml for 24 hours) (page 237).
- Figure 5.14: TNF- α effects on total PKB/Akt expression at different concentrations (0.5, 5 and 20 ng / ml for 24 hours) (page 238).
- Figure 5.15: TNF- α effects on the phosphorylated PKB/Akt / total PKB/Akt expression at different concentrations (0.5, 5 and 20 ng / ml for 24 hours) (page 239).
- Figure 5.16: TNF- α effects on total HSP 90 expression at different concentrations (0.5, 5 and 20 ng / ml for 24 hours) (page 241).
- Figure 5.17: TNF- α effects on total caveolin-1 expression at different concentrations (0.5, 5 and 20 ng / ml for 24 hours) (page 243).
- Figure 5.18: TNF- α effects on total p22-phox expression at different concentrations (0.5, 5 and 20 ng / ml for 24 hours) (page 245).
- Figure 5.19: TNF- α effects on nitrotyrosine expression at different concentrations (0.5, 5 and 20 ng / ml for 24 hours) (page 247).
- Figure 5.20: TNF- α effects on I κ B- α expression at different concentrations (0.5, 5 and 20 ng / ml for 24 hours) (page 249).
- Figure 5.21: Effects of TNF- α (20 ng / ml) and Ox-LDL (40 μ g / ml) on mean DAF-2/DA fluorescence intensity for 30 minutes (page 251).
- Figure 5.22: Effects of TNF- α (20 ng / ml) and Ox-LDL (40 μ g / ml) on mean DHE fluorescence intensity for 30 minutes (page 251).
- Figure 5.23: Effects of TNF- α (20 ng / ml) and Ox-LDL (40 μ g / ml) on mean DCF fluorescence intensity for 30 minutes (page 252).
- Figure 5.24: Effects of TNF- α (20 ng / ml) and Ox-LDL (40 μ g / ml) on mean DHR-123 fluorescence intensity for 30 minutes (page 252).

Figure 5.25: Effects of growth media with different serum contents (0%, 5% and 10% FBS) on mean DHE fluorescence intensity in CMECs treated with TNF- α (20 ng / ml) for 24 hours (page 254).

Figure 5.26: The effects of 40 μ g / ml OA pre-treatment on the mean DAF-2/DA fluorescence intensity in TNF- α -treated CMECs (20 ng / ml; 24 hours) (page 259).

Figure 5.27: The effects of 20 ng / ml TNF- α on iNOS expression (page 260).

Figure 5.28: TNF- α effects on mean DAF-2/DA fluorescence at different concentrations (0.5, 5 and 20 ng / ml for 24 hours) in CMECs and AECs (page 261).

Figure 5.29: Acetylcholine-induced aortic ring relaxation (page 262).

Chapter 6:

Figure 6.1: Workflow for the proteomic analyses of untreated, control and TNF- α -treated (TNF- α : 5 ng / ml for 24 hours) samples (page 270).

Figure 6.2: A two dimensional gel from Applied Biomics, containing the spots from which certain spots were eventually selected for further analysis (page 272).

Figure 6.3: The location of the HSP 90-alpha spot indicated on the 2D gel showing reduction in abundance between control (left) and TNF- α -treated (right) samples (page 273).

Figure 6.4: A western blot analysis of CMECs treated with 0.5, 5 and 20 ng / ml TNF- α for 24 hours, showing a decrease in HSP 90 expression when compared to control (page 279).

Figure 6.5: A: Classical signalling pathways of TNF- α receptor type 1 (TNFR1), showing activation of TRADD and NF- κ B (page 290).

B: Western blot analysis of CMECs treated with 5 ng / ml TNF- α for 24 hours, showing a decrease in IKB α expression when compared to control (page 290).

Figure 6.6: PEA-15 regulates TNF- α -induced apoptosis (page 292).

Figure 6.7: Western blot analysis of TNF- α treated (5 ng / ml for 24 hours) CMECs, showing a decrease in cleaved caspase-3 when compared to control (page 293).

Figure 6.8: The BID pro-apoptotic signalling pathway activated by TNF- α -TNF R1 activation (page 293).

Figure 6.9: The proposed mechanism of TNF- α -induced mitochondrial ROS production (page 296).

Figure 6.10: Fluorescence microscopy of: Panels A and B: control and TNF- α -treated cells respectively), followed by addition of mitochondrial ROS-sensitive MitoSox, detecting mitochondrial ROS production (red stain). (Panels C and D: control and TNF- α -treated cells respectively) (page 296).

Figure 6.11: A cartoon depicting the summary of the most significant intracellular events in TNF- α -treated CMECs based on the results in this chapter (page 299).

Chapter 7:

Figure 7.1: The downstream signalling pathways of TNF- α and TNFR1 and TNFR2 (page 304).

Figure 7.2: Protocol for treatment of CMECs with 20 ng / ml TNF- α with or without 1 μ g / ml of TRB1 for 30 minutes for subsequent western blot analysis (page 307).

Figure 7.3: Protocol for treatment of CMECs with 20 ng / ml TNF- α with or without 1 μ g / ml of TRB2 for 30 minutes for subsequent western blot analysis (page 308).

Figure 7.4: Protocol for treatment of CMECs with 20 ng / ml TNF- α with or without 1 μ g / ml of TRB2 and 1 μ g / ml of TRB2 for 30 minutes for subsequent western blot analysis (page 309).

Figure 7.5: The effects of TNF- α receptor blockade (1 μ g / ml) on phosphorylated eNOS in TNF- α (20 ng / ml)-treated CMECs (page 311).

Figure 7.6: The effects of TNF- α receptor blockade (1 μ g / ml) on total eNOS expression in TNF- α (20 ng / ml)-treated CMECs (page 312).

Figure 7.7: The effects of TNF- α receptor blockade (1 μ g / ml) on phosphorylated / total eNOS ratios in TNF- α (20 ng / ml)-treated CMECs (page 313).

Figure 7.8: The effects of TNF- α receptor blockade (1 μ g / ml) on phosphorylated PKB/Akt in TNF- α (20 ng / ml)-treated CMECs (page 315).

Figure 7.9: The effects of TNF- α receptor blockade (1 μ g / ml) on total PKB/Akt expression in TNF- α (20 ng / ml)-treated CMECs (page 316).

Figure 7.10: The effects of TNF- α receptor blockade (1 μ g / ml) on phosphorylated / total PKB/Akt ratios in TNF- α (20 ng / ml)-treated CMECs (page 317).

Figure 7.11: The effects of TNF- α receptor blockade (1 μ g / ml) on HSP 90 expression in TNF- α (20 ng / ml)-treated CMECs (page 319).

Figure 7.12: The effects of TNF- α receptor blockade (1 μ g / ml) on caveolin-1 expression in TNF- α (20 ng / ml)-treated CMECs (page 321).

Figure 7.13: The effects of TNF- α receptor blockade (1 μ g / ml) on iNOS expression in TNF- α (20 ng / ml)-treated CMECs (page 323).

- Figure 7.14: The effects of TNF- α receptor blockade (1 μ g / ml) on p22 phox expression in TNF- α (20 ng / ml)-treated CMECs (page 325).
- Figure 7.15: The effects of TNF- α receptor blockade (1 μ g / ml) on nitrotyrosine expression in TNF- α (20 ng / ml)-treated CMECs (page 327).
- Figure 7.16: The effects of TNF- α receptor blockade (1 μ g / ml) on IK β α expression in TNF- α (20 ng / ml)-treated CMECs (page 329).
- Figure 7.17: The effects of TNF- α receptor blockade (1 μ g / ml) on cleaved caspase-3 expression in TNF- α (20 ng / ml)-treated CMECs (page 331).
- Figure 7.18: The effects of TNF- α receptor blockade (1 μ g / ml) on cleaved PARP expression in TNF- α (20 ng / ml)-treated CMECs (page 333).
- Figure 7.19: Simplified schematic overview of: A: TNF- α NOS-signalling (page 336)
B: TNF- α + TRB1 NOS-signalling (page 337)
C: TNF- α + TRB2 NOS-signalling (page 338)
D: TNF- α + TRB1&2 NOS-signalling (page 339).
- Figure 7.20: Simplified schematic overview of: A: TNF- α oxidative/nitrosative stress-signalling (page 341)
B: TNF- α + TRB1 oxidative/nitrosative stress-signalling (page 342)
C: TNF- α + TRB2 oxidative/nitrosative stress-signalling (page 343)
D: TNF- α + TRB1&2 oxidative/nitrosative stress-signalling (page 344).
- Figure 7.21: Simplified schematic overview of: A: TNF- α IK β α -signalling (page 346)
B: TNF- α + TRB1 IK β α -signalling (page 347)
C: TNF- α + TRB2 IK β α -signalling (page 348)
D: TNF- α + TRB1&2 IK β α -signalling (page 349).
- Figure 7.22: Simplified schematic overview of: A: TNF- α apoptosis-signalling (page 351)
B: TNF- α + TRB1 apoptosis-signalling (page 352)
C: TNF- α + TRB2 apoptosis-signalling (page 353)
D: TNF- α + TRB1&2 apoptosis-signalling (page 354).

List of Abbreviations**Units of measurement**

%	-	percentage
°C	-	degrees celsius
µg	-	microgram
µl	-	microlitre
µM	-	micromolar
g	-	gram
kDa	-	kilodalton
l	-	litre
mg	-	milligram
min	-	minute
ml	-	millilitre
mm	-	millimeters
Mr	-	molecular weight
sec	-	second
ng	-	nanogram
pg	-	pictogram

Chemical compounds, enzymes and peptides.

AA	-	arachidonic acid
ACE	-	angiotensin converting enzyme
Ach	-	acetylcholine
Ac-LDL	-	acetylated-low density lipoprotein
ADMA	-	asymmetric dimethyl-arginine
AGE	-	advanced glycation end-product
ALK1	-	activin-receptor-like kinase 1
Ang II	-	angiotensin II
Ann V	-	annexin V
ASK	-	apoptosis signal-regulating kinase
ASS	-	argininosuccinate synthase
ATP	-	adenosine-5'-triphosphate
AT1R	-	angiotensin II type 1 receptors
AT2R	-	angiotensin II type 2 receptors
bFGF	-	basic fibroblast growth factor
BH ₂	-	dihydrobiopterin
BH ₄	-	tetrahydrobiopterin
BMP	-	bone morphogenetic protein
Ca ²⁺	-	calcium

[Ca ²⁺] _i	-	intracellular calcium
CaM	-	Ca ²⁺ /calmodulin
CaMKII	-	Ca ²⁺ /calmodulin-dependent protein kinase
cAMP	-	cyclic adenosine monophosphate
CBS	-	cystathionine β-synthase
CCO	-	cytochrome c oxidase
CETP	-	cholesterylester transport protein
cGMP	-	cyclic guanosine monophosphate
cGKI	-	Cyclic Guanosine Monophosphate Kinase I
cGKII	-	Cyclic Guanosine Monophosphate) Kinase II
COX	-	cyclooxygenase
CSD	-	caveolin scaffolding domain
CSE	-	cystathionine γ-lyase
CYP 450	-	cytochrome P450
DII4	-	delta-like 4
DAF-2/DA	-	4,5-diaminofluorescein-2/diacetate
DCF	-	2',7'-Dichlorofluorescein
DDAH	-	NG,NG-dimethylarginine dimethylaminohydrolase
Depp	-	decidual protein induced by progesterone
DEA/NO	-	diethylamine NONOate diethylammonium salt

DHE	-	dihydroethidium
DHFR	-	dihydrofolate reductase
DHR-123	-	dihydrorhodamine-1, 2, 3
Dil-ac-LDL	-	1,1'-dioctadecyl-3,3,3',3'-tetramethylindo-carbocyanine
DISC	-	death-inducing signalling complex
DMA	-	Dimethylarginine
DMNQ	-	2,3-dimethoxy-1,4-naphthoquinone
ECM	-	extracellular matrix
EDCFs	-	endothelial-derived contracting factors
EDHF	-	endothelium-derived hyperpolarizing factor
EDRF	-	endothelium-derived relaxing factor
EDTA	-	ethylenediaminetetraacetic acid
EETs	-	epoxyeicosatrienoic acids
EGM	-	endothelial growth medium
EGTA	-	ethylene glycol tetraacetic acid
eNOS	-	endothelial nitric oxide synthase
EPAS -1	-	endothelial PAS domain protein 1
ERK	-	extracellular signal-regulated kinase
ET-1	-	endothelin-1
FADD	-	Fas-associated death domain

FBS	-	foetal bovine serum
GPCRs	-	G protein coupled receptors
GSH-Px	-	glutathione peroxidase
GTP	-	guanosine triphosphate
H ₄ B	-	tetrahydrobiopterin
HDL	-	high density lipoproteins
13-HPODE	-	13-hydroperoxyoctadecadienoate
HETE	-	hydroxyeicosatetraenoic acid
HIF-1	-	hypoxia inducible factor-1
HMGB1	-	high mobility group box protein 1
HMG-CoA	-	-hydroxy-3-methylglutaryl-CoA
H ₂ O ₂	-	hydrogen peroxide
H ₂ S	-	hydrogen sulfide
HSP 90	-	heat shock protein 90
IBMX	-	isobutyl-methyl-xanthine
ICAM-1	-	intercellular adhesion molecule-1
IGF	-	insulin-like growth factor
IKK	-	kinase IκB kinase
Iκβ _α	-	I kappa beta alpha
IL	-	interleukin

IFN	-	Interferon
iNOS	-	inducible nitric oxide synthase
JNK	-	stress-related c-Jun N-terminal kinase
LDL	-	low density lipoproteins
L-NMMA	-	N ω -Methyl- L -arginine acetate salt
LOX-1	-	lectin-like receptor for oxidized low-density lipoproteins - 1
LPS	-	lipopolysaccharides
LTBR	-	lymphotoxin- β receptor
MAPK	-	mitogen-activated protein kinases
MCP-1	-	monocyte chemo-attractant protein-1
MLCP	-	myosin light chain phosphatase
MMPs	-	matrix metalloproteinases
MST	-	mercaptopyruvate sulfurtransferase
MYPT1	-	myosin targeting protein 1
NaCl	-	sodium chloride
NADPH	-	nicotinamide adenine dinucleotide phosphate
NaF	-	sodium fluoride
Na ₄ O ₇ P ₂	-	tetra-sodium diphosphate
NaVO ₃	-	sodium orthovanadate
NF-E2	-	nuclear factor, erythroid derived 2

NF- κ B	-	nuclear factor κ B
NIK	-	NF-kappa-B- inducing kinase
NO	-	nitric oxide
NOS	-	nitric oxide synthase
NO _x	-	nitrite and nitrate
nNOS	-	neuronal nitric oxide synthase
NRP1	-	neuropilin 1
N-SMase2	-	neutral sphingomyelinase 2
O ₂	-	oxygen
OA	-	oleanolic acid
OONO ⁻	-	peroxynitrite
Orn	-	l-ornithine
Ox-LDL	-	oxidised low density lipoprotein
PAF	-	platelet-activating factor
PAI-1	-	plasminogen activator inhibitor-1
PARP	-	cleaved poly(ADP-ribose) polymerase
PBS	-	phosphate buffered saline
PDE	-	phosphodiesterase
PDGF	-	platelet-derived growth factor
PGD ₂	-	prostaglandin E2

PG	-	prostaglandin
PGE ₂	-	prostaglandin D2
PGF _{2α}	-	prostaglandin F2alpha
PGI ₂	-	prostacyclin
PI	-	propidium iodide
PKA	-	protein kinase A
PKB/Akt	-	protein kinase B / Akt
PKC	-	protein kinase C
PLA	-	phospholipase A
PLC	-	phospholipase C
PLD	-	phospholipase D
PMSF	-	phenylmethylsulphonyl fluoride
PRMTs	-	protein arginine methyltransferases
PVDF	-	polyvinylidene fluoride
RAGE	-	receptor for advanced glycation end-product
RIP	-	receptor-interacting protein
RNA	-	ribonucleic acid
ROS	-	reactive oxygen species
Ser	-	serine
SDMA	-	symmetric dimethylarginine

SDS	-	sodium dodecylsulfate
sGC	-	soluble guanylate cyclase
SK1	-	sphingosine kinase 1
SNAP	-	S-nitroso-N-acetyl-penicillamine
SNP	-	sodium-nitroprusside
SOD	-	superoxide dismutase
Sph1P	-	sphingosine-1-phosphate
STAT3	-	signal transducer and activator of transcription-3
TACE	-	TNF- α converting enzyme
TBST	-	tris-Buffered Saline — 0.1% Tween 20
TCA	-	tricarboxylic acid
TE	-	transendothelial
TGF β	-	transforming growth factor- β
Thr	-	threonine
TNF- α	-	tumour necrosis factor- α
TNFR1	-	tumour necrosis factor receptor 1
TNFR2	-	tumour necrosis factor receptor 2
TRADD	-	TNF receptor-associated death domain
TRAF	-	TNF receptor-associated factor
Tris	-	tris(hydroxymethyl)-aminomethane

TXA ₂	-	thromboxane A ₂
TXB ₂	-	thromboxane B ₂
VCAM-1	-	vascular cell adhesion molecule-1
VEGF	-	vascular endothelial growth factor
VVOs	-	vesiculo-vacuolar organelles
vWF	-	von Willebrand factor
WPBs	-	Weibel-Palade bodies
XO	-	xanthine oxidase

Other

ADC	-	Analogue-to-Digital Conversion
AIDS	-	acquired immunodeficiency syndrome
ANOVA	-	analysis of variance
BAECs	-	bovine aortic endothelial cells
CVD	-	cardiovascular disease
CMECs	-	cardiac microvascular endothelial cells
CPAECs	-	calf pulmonary artery endothelial cells
DALYs	-	disability adjusted life years
DAVID	-	Database for Annotation, Visualization and Integrate Discovery
DC	-	dendritic cell

2-DE	-	two-dimensional gel electrophoresis
EC	-	endothelial cell
ECs	-	endothelial cells
ECL	-	enhanced chemiluminescence
EECs	-	endocardial endothelial cells
FACS	-	flow-assisted cell sorting
FASP	-	filter-aided sample preparation
FSC	-	forward scatter
FSS	-	fluid shear stress
GO	-	gene ontology
HAECs	-	human aortic endothelial cells
HIV	-	human immunodeficiency virus
HoS	-	Heart of Soweto
HUVECs	-	human umbilical vein endothelial cells
IHD	-	ischemic heart disease
IP	-	ischaemic preconditioning
I/R	-	ischaemia/reperfusion
LC-MS	-	liquid chromatography–mass spectrometry
LTQ	-	linear trap quadropole
LV dP/dt max	-	maximal rate of left ventricular pressure development

LV	-	left ventricle
MRC	-	Medical Research Council
PPAEs	-	porcine pulmonary artery endothelial cells
PPAR	-	peroxisome-proliferator activated receptor
SDS-PAGE	-	sodium dodecyl sulfate polyacrylamide gel electrophoresis
SEM	-	standard error of the mean
SHR	-	spontaneously hypertensive rats
SR	-	sarcoplasmic reticulum
SSC	-	side scatter
TEM	-	transmission electron microscopy
VSMC	-	vascular smooth muscle cells
WHHL	-	The Watanabe heritable hyperlipidaemic
WHO	-	World Health Organization
YLL	-	years life lost
ZOF	-	Zucker Obese Fatty rats

TABLE OF CONTENTS:

	PAGE NO.
Declaration	ii
Abstract	iii
Opsomming	iv
Acknowledgements	vi
List of Tables	vii
List of Figures	ix
List of Abbreviations	xviii
Chapter 1: Literature Review	
1.1 Ischaemic Heart disease (IHD)	1
1.1.1 Incidence.....	1
1.1.2 Vascular disease and the development of IHD	5
1.2 Introduction to vascular endothelium	8
1.2.1 Structure and function	8
1.2.2 Endothelium derived factors and their role in endothelial function	12
1.2.2.1 <i>Nitric Oxide (NO)</i>	12
1.2.2.1.1 <i>Nitric oxide synthase (NOS)</i>	15
<i>eNOS activation and phosphorylation</i>	17
1.2.2.1.2 <i>The physiological effects of NO in the heart</i>	20

	<i>NO-sGC- cyclic guanylyl monophosphate (cGMP) signalling</i>	20
	<i>Effects on myocardial contractility: inotropic and lusitropic actions</i>	22
1.2.2.1.3	<i>Metabolic effects of NO</i>	24
1.2.2.1.4	<i>NO in myocardial hypoxia</i>	24
	<i>NO production during hypoxia/ischaemia</i>	24
	<i>Myocardial reperfusion / reoxygenation and beneficial effects of NO</i>	25
	<i>Detrimental effects of NO during ischaemia-reperfusion</i>	25
1.2.2.1.5	<i>NO in the heart – summary</i>	27
1.2.2.2	<i>Prostacyclin & Thromboxane A2</i>	28
1.2.2.3	<i>Endothelium–derived hyperpolarizing factor (EDHF)</i>	30
1.2.2.4	<i>Endothelin-1 (ET-1)</i>	31
1.2.2.5	<i>Angiotensin II (Ang II)</i>	32
1.2.3	<i>Endothelial heterogeneity, macrovascular vs. microvascular ECs and cardiac EC subtypes</i>	33
1.2.3.1	<i>General endothelial heterogeneity</i>	33
1.2.3.1.1	<i>Structural Classification of Vascular Endothelium</i>	33
	<i>Continuous Nonfenestrated</i>	34
	<i>Continuous Fenestrated</i>	34
	<i>Discontinuous Fenestrated</i>	35
1.2.3.2	<i>Endothelial Heterogeneity in the Heart</i>	37
1.2.3.3	<i>Cardiac microvascular endothelial cells (CMECs)</i>	42

1.3	Endothelial responses to harmful stimuli	43
1.3.1	Vascular endothelium is a target of harmful stimuli.....	43
1.3.1.1	<i>Tumour Necrosis Factor alpha (TNF-α), Asymmetric dimethylarginine (ADMA), hypoxia, hyperglycaemia, oxidized-low density lipoprotein (ox-LDL) and oxidative stress.....</i>	43
1.3.1.1.1	<i>TNF-α</i>	43
	<i>Cardioprotective properties of TNF-α</i>	54
1.3.1.1.2	<i>Asymmetric dimethylarginine (ADMA).....</i>	54
	<i>Targets of ADMA.....</i>	56
	<i>Degradation of ADMA (The DDAHs).....</i>	56
	<i>Cellular ADMA.....</i>	56
	<i>Cardiovascular Effects of ADMA</i>	57
1.3.1.1.3	<i>Hypoxia</i>	60
	<i>Endothelial cell–neutrophil interactions.....</i>	60
	<i>Tissue remodelling.....</i>	63
	<i>Physiological relevance.....</i>	65
	<i>Metabolic effects of hypoxia on ECs.....</i>	65
	<i>Hypoxia as a cause of ED.....</i>	68
	<i>Hypoxia modulates NOS activity and NO bio-availability.....</i>	68
1.3.1.1.4	<i>Hyperglycaemia</i>	70
1.3.1.1.5	<i>Oxidized low density lipoprotein (Ox-LDL)</i>	72

	<i>Oxidized LDL and endothelial injury / ED</i>	72
	<i>Oxidized LDL and its receptor LOX-1 in endothelium</i>	72
	<i>Ox-LDL and atherosclerosis</i>	74
1.3.1.1.6	<i>Oxidative stress</i>	74
	<i>Risk factors / diseases associated with oxidative stress</i>	74
	<i>Cellular mechanisms of oxidative stress</i>	75
	<i>Cellular and Enzymatic Sources of ROS in the Vessel Wall</i>	78
	<i>Biochemical Consequences of ROS Production in the Vessel Wall</i>	84
1.3.1.2	<i>Cardiovascular risk factors associated with harmful stimuli</i>	85
1.3.1.2.1	<i>Diabetes mellitus (including insulin resistance and hyperglycaemia)</i>	85
1.3.1.2.2	<i>Dyslipidaemia (including hypercholesterolaemia)</i>	86
1.3.1.2.3	<i>Hypertension</i>	89
1.3.1.2.4	<i>Smoking</i>	89
1.3.1.2.5	<i>Aging</i>	90
1.3.1.2.6	<i>Other known factors that contributes to ED</i>	91
1.3.2	<i>Early endothelial responses to harmful stimuli</i>	91
1.3.2.1	<i>Endothelial Activation</i>	91
1.3.2.2	<i>Endothelial Dysfunction (ED)</i>	94
1.3.2.2.1	<i>Definition and features</i>	94
1.3.2.2.2	<i>Proposed mechanisms of ED</i>	95
1.3.3	<i>Progression to atherosclerosis</i>	102

1.3.4	Clinical relevance of endothelial function	104
B.	Motivation and Aims	107
(i)	Problem identification, rationale and motivation.....	107
(ii)	Aims of the study	108
Aim 1:	Baseline characterization of commercially purchased primary CMEC cultures	108
Aim 2:	Characterization and investigation of hypoxia-induced responses in CMECs.....	108
Aim 3:	Characterization and investigation of TNF- α -induced responses in CMECs.....	109
Chapter 2:	Materials & Methods	
2.1	Materials	110
2.1.1	General materials used.....	110
2.2	Cardiac microvascular endothelial cells (CMECs)	111
2.2.1	Passaging procedure	112
2.3	Methods	114
2.3.1	General methods used in this study.....	114
2.3.1.1	<i>Flow cytometric analyses.....</i>	114
2.3.1.1.1	<i>Cell viability Measurements.....</i>	118
2.3.1.1.2	<i>Nitric Oxide (NO) Measurements</i>	121
2.3.1.1.3	<i>ROS Measurements.....</i>	124
2.3.1.2	<i>Western blot analyses</i>	132
2.3.1.3	<i>Proteomics analyses.....</i>	137

2.3.1.3.1	<i>Protein isolation</i>	137
2.3.1.3.2	<i>One dimensional sodium dodecyl sulfate polyacrylamide gel electrophoresis (1-D SDS-PAGE) followed by in-gel trypsin digestion</i>	137
2.3.1.3.3	<i>Filter Aided Sample Separation</i>	138
2.3.1.3.4	<i>Mass spectrometry</i>	141
2.3.1.3.5	<i>Proteomic data analysis</i>	141
2.3.1.3.6	<i>Functional annotation analyses of proteins</i>	142
2.4	Statistical analyses	143
Chapter 3:	Characterization of primary CMEC cultures	
3.1	Introduction	144
3.2	Specific Aims	145
3.3	Morphology, functional characterization and baseline protein expression of CMECs	146
3.3.1	Morphology and functional characterization	146
3.3.2	Expression of proteins involved with NOS-NO biosynthesis in CMECs	150
3.4	Comprehensive characterisation of the baseline CMEC proteome	152
3.5	The effect of various harmful stimuli on the NO production of CMECs – FACS analysis	159
3.6	Discussion	161
3.6.1	Characterization of the morphology, culture specificity and expression of critical proteins involved with NOS-NO biosynthesis in CMECs	161
3.6.2	The CMEC proteome under baseline conditions	162

3.6.3	The effect of various harmful stimuli on the NO production of CMECs (FACS analysis)	166
3.6.3.1	<i>Angiotensin II (100 nM for 24 hours)</i>	167
3.6.3.2	<i>In vitro simulation with hyperglycaemia: Glucose (25 mM for 24 hours)</i>	168
3.6.3.3	<i>Hypoxia (O₂ < 0.6 %)</i>	169
3.6.3.4	<i>Oxidised-LDL (40 µg / ml for 24 hours)</i>	170
3.6.3.5	<i>ADMA (500 µM for 24 hours)</i>	172
3.6.3.6	<i>TNF-α (5 ng / ml and 20 ng / ml for 24 hours)</i>	172
3.7	Conclusion	173
Chapter 4:	Characterization and investigation of hypoxia-induced responses in CMECs.	
4.1	Introduction	175
4.2	Methods	177
4.3	Results	181
4.3.1	Validation of the hypoxia protocol.....	181
4.3.2	eNOS-NO biosynthesis; oxidative stress; nitrosative stress	185
4.3.3	Proteomic analyses	191
4.4	Discussion	195
4.4.1	Validation of hypoxia-inducing protocol	195
4.4.2	eNOS-NO biosynthesis, oxidative stress and nitrosative stress.....	196
4.4.3	Proteomics analysis.....	200

4.4.3.1	<i>The CMEC proteome under hypoxic conditions: Up regulated and strongly represented proteins</i>	200
4.4.3.2	<i>The CMEC proteome under hypoxic conditions: Down regulated proteins</i>	205
4.5	Conclusion	208
Chapter 5:	TNF-α-induced responses in CMECs: Baseline investigations.	
5.1	Introduction	212
5.1.1	TNF- α induces a down-regulation of NOS-NO biosynthesis	212
5.1.2	TNF- α induces an up-regulation of NOS-NO biosynthesis.....	214
5.2	Specific Aims	215
5.3	Methods	215
5.3.1	The effects of different TNF- α concentrations	215
5.3.2	Short term treatment of CMECs with TNF- α (20 ng / ml) for 30 minutes.....	218
5.3.3	Investigating the effects of modification of the serum content of growth medium on ROS production	220
5.4	Results	222
5.4.1	The effects of different TNF- α concentrations: 0.5, 5 and 20 ng / ml.....	222
5.4.1.1	<i>Cell viability measurements (FACS analysis)</i>	222
5.4.1.2	<i>NO production measurements (FACS analysis)</i>	224
5.4.1.3	<i>Reactive oxygen species measurements (FACS analysis)</i>	226
5.4.1.3.1	<i>TNF-α 0.5 ng /ml for 24 hours</i>	226
5.4.1.3.2	<i>TNF-α 5 ng /ml for 24 hours</i>	226

5.4.1.3.3	<i>TNF-α 20 ng /ml for 24 hours</i>	227
5.4.1.4	<i>Western blot analysis of eNOS signalling</i>	230
5.4.1.4.1	<i>eNOS</i>	230
5.4.1.4.1.1	<i>TNF-α 0.5 ng /ml for 24 hours</i>	230
5.4.1.4.1.2	<i>TNF-α 5 ng /ml for 24 hours</i>	230
5.4.1.4.1.3	<i>TNF-α 20 ng /ml for 24 hours</i>	231
5.4.1.4.2	<i>PKB/Akt</i>	235
5.4.1.4.2.1	<i>TNF-α 0.5 ng /ml for 24 hours</i>	235
5.4.1.4.2.2	<i>TNF-α 5 ng /ml for 24 hours</i>	235
5.4.1.4.2.3	<i>TNF-α 20 ng /ml for 24 hours</i>	235
5.4.1.4.3	<i>HSP 90</i>	240
5.4.1.4.3.1	<i>TNF-α 0.5 ng /ml for 24 hours</i>	240
5.4.1.4.3.2	<i>TNF-α 5 ng /ml for 24 hours</i>	240
5.4.1.4.3.3	<i>TNF-α 20 ng /ml for 24 hours</i>	240
5.4.1.4.4	<i>Caveolin-1</i>	242
5.4.1.4.4.1	<i>TNF-α 0.5 ng /ml for 24 hours</i>	242
5.4.1.4.4.2	<i>TNF-α 5 ng /ml for 24 hours</i>	242
5.4.1.4.4.3	<i>TNF-α 20 ng /ml for 24 hours</i>	242
5.4.1.5	<i>Western blot analysis of proteins associated with oxidative stress: p22-phox</i>	244
5.4.1.5.1	<i>TNF-α 0.5 ng /ml for 24 hours</i>	244
5.4.1.5.2	<i>TNF-α 5 ng /ml for 24 hours</i>	244

5.4.1.5.3	<i>TNF-α 20 ng /ml for 24 hours</i>	244
5.4.1.6	<i>Western blot analysis of proteins associated with nitrosative stress: nitrotyrosine</i>	246
5.4.1.6.1	<i>TNF-α 0.5 ng /ml for 24 hours</i>	246
5.4.1.6.2	<i>TNF-α 5 ng /ml for 24 hours</i>	246
5.4.1.6.3	<i>TNF-α 20 ng /ml for 24 hours</i>	246
5.4.1.7	<i>Western blot analysis of proteins associated with NF-KB signalling: IκB-α</i>	248
5.4.1.7.1	<i>TNF-α 0.5 ng /ml for 24 hours</i>	248
5.4.1.7.2	<i>TNF-α 5 ng /ml for 24 hours</i>	248
5.4.1.7.3	<i>TNF-α 20 ng /ml for 24 hours</i>	248
5.4.2	The effects of short term treatment with TNF- α (20 ng / ml): 30 minutes	250
5.4.2.1	<i>NO production measurements (FACS analysis)</i>	250
5.4.2.2	<i>ROS measurements (FACS analysis)</i>	250
5.4.3	The effects of reduced serum content in growth medium on superoxide production in CMECs treated with TNF- α (20 ng / ml): 24 hours	253
5.5	Discussion	255
5.5.1	The effects of different TNF- α concentrations: 0.5, 5 and 20 ng / ml (24 hours)	255
5.5.2	Short term treatment of CMECs with TNF- α (20 ng / ml) for 30 minutes.....	264
5.5.3	The effects of reduced serum content in growth medium on superoxide production in CMECs treated with TNF- α (20 ng / ml): 24 hours	264
5.6	Conclusion	265

Chapter 6:	A characterization and investigation of TNF-α-induced responses in CMECs: A proteomic analysis.	
6.1	Introduction.....	267
6.2	Methods	268
6.3	Results	271
6.3.1	Pilot studies: 2D-DIGE-phosphoproteomics (Applied Biomics)	271
6.3.2	Large-scale protein expression and regulation analyses: Main Study	274
6.4	Discussion	288
6.4.1	Pilot Studies: Applied Biomics.....	288
6.4.2	The main study: Proteomic analysis of TNF-alpha (5 ng / ml) treated CMECs (performed at the Proteomics Unit, Stellenbosch University)	288
6.5	Conclusions.....	298
Chapter 7:	Investigating the role of the TNF receptors and subsequent signalling events.	
7.1	Introduction.....	300
7.1.1	TNFR1	300
7.1.1.1	<i>Activation of NF-κB.....</i>	301
7.1.1.2	<i>Activation of the MAPK pathways.....</i>	301
7.1.1.3	<i>Induction of death signalling</i>	302
7.1.2.	TNFR2	302
7.2	Methods	305
7.3	Results	310

7.3.1	NOS signalling	310
7.3.2	Western blot analysis of oxidative stress: p22 phox	324
7.3.3	Western blot analysis of nitrosative stress: nitrotyrosine.....	326
7.3.4	Western blot analysis of NFK β signalling: IK β α	328
7.3.5	Western blot analysis of apoptosis signalling.....	330
7.4	Discussion	334
7.5	Conclusion	355
7.6	Limitations.....	355
 Chapter 8:		
	Final Conclusions	358
	Shortcomings of the present study.....	361
	Future directions	362
	Outputs that resulted directly or indirectly from this study	363
1.	Peer-reviewed journal publications.....	363
2.	Published Peer-reviewed Conference Abstracts	363
3.	Conference outputs	364
4.	Other outputs.....	365
	References	366

CHAPTER ONE

Literature Review

1.1 Ischaemic Heart disease (IHD)

1.1.1 Incidence:

Cardiovascular disease (CVD) is the number one cause of death in the world. In 2008, 7.3 million people died of IHD and 6.2 million from cerebrovascular disease (Mendis *et al.*, 2011). According to a report by the World Health Organization (WHO) in 2011 on the top 10 leading causes of death by broad income group (www.who.int/mediacentre/factsheets), IHD was the 4th most common cause of death in low-income countries (6.1% of deaths), the main cause of death in middle-income countries (13.7% of deaths) and high-income countries (13.6% of deaths) and remains the largest cause of deaths worldwide (12.8% of deaths) (Figure 1.1). This surpasses the threat of other major communicable diseases such as tuberculosis and HIV/AIDS worldwide.

According to the “Western Cape Mortality Profile – 2009 (<http://www.mrc.ac.za/bod/WesternCapeMortalityProfile2009>), CVD was the highest cause of death in the Western Cape, followed by Diabetes (an independent risk factor for CVD). Furthermore, CVD was the third highest cause of premature death (Years of Life Lost – YLL) in 2009 (Figure 1.2). The Heart of Soweto (HoS) study investigated the emerging problem of CVD in urban black African patients presenting for the first time at the cardiac unit of a tertiary-care centre in Soweto (Pretorius *et al.*, 2011). Data from the HoS indicated a high prevalence of traditional cardiovascular risk factors such as hypertension and obesity, with almost two-thirds of the patients in the study cohort presenting with multiple risk factors (Pretorius *et al.*, 2011). Furthermore, 12% of this study cohort was diagnosed with coronary artery disease. Overall, the findings of the HoS and other studies are pointing to significant increases in the prevalence of CVD amongst people of African heritage in South Africa as a result of epidemiological transition and

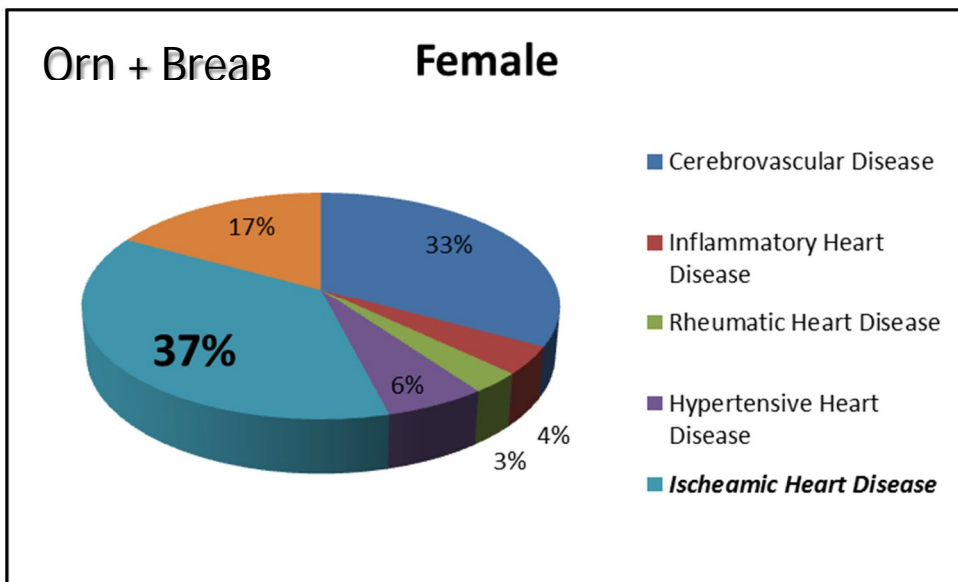
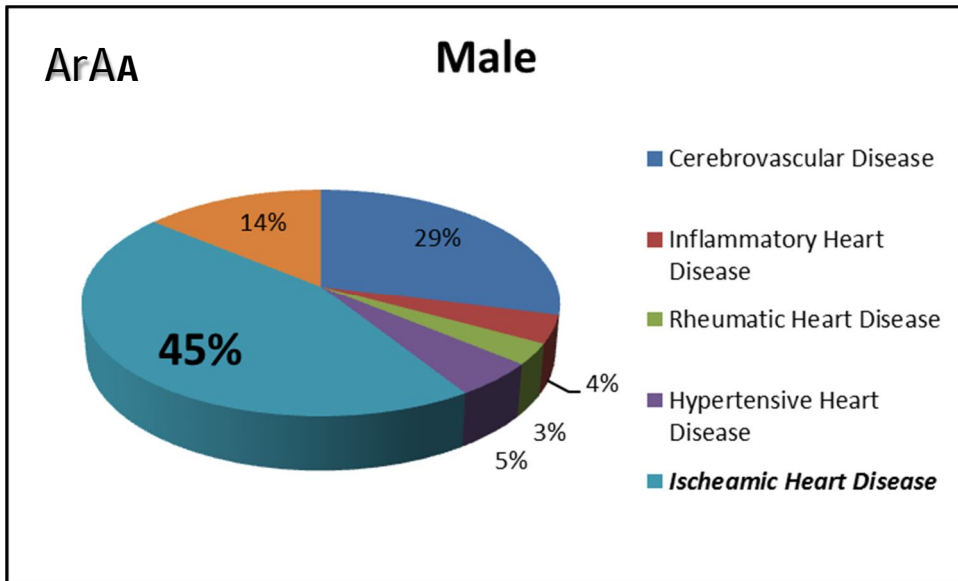
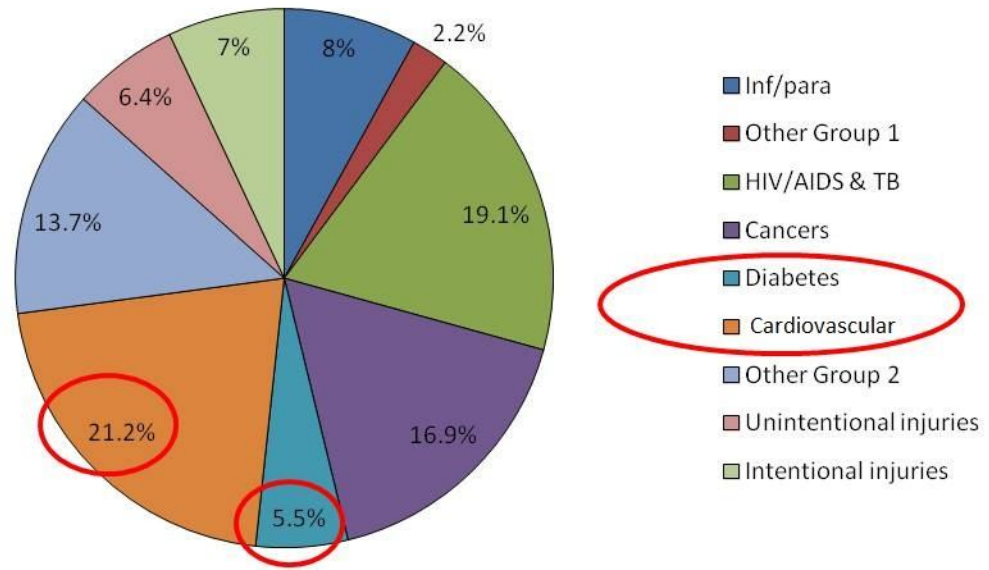


Figure 1.1: Global distribution of CVD burden (DALYs - Disability Adjusted Life Years) due to heart attacks, strokes and other types of CVD in males (A) and females (B) respectively (adapted from Mendis *et al.*, 2011).

A: Western Cape Deaths 2009, N = 46,254



B: Western Cape YLLs 2009, N = 823,518

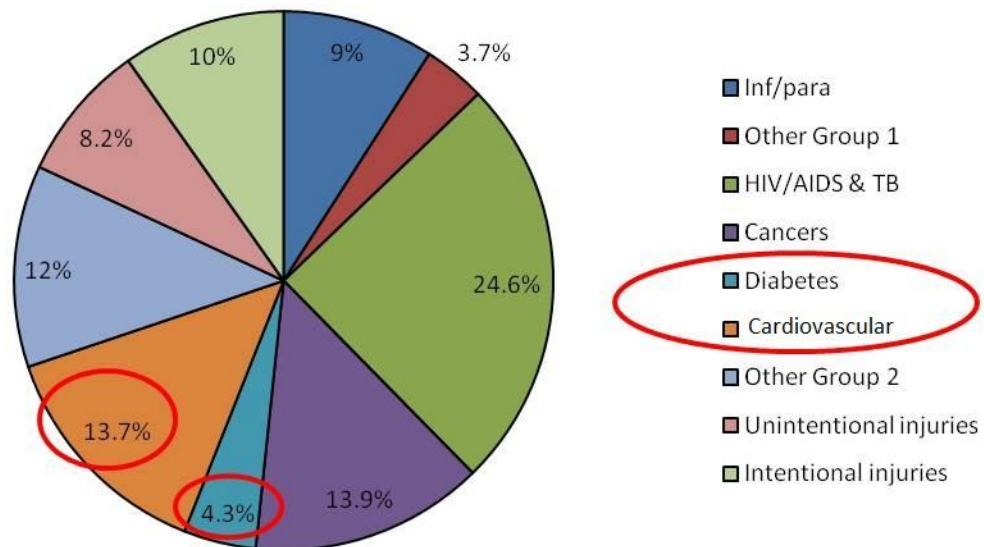


Figure 1.2: Top ten causes of mortality in the Western Cape in 2009: A – Deaths and B: premature deaths (years life lost - YLL) (<http://www.mrc.ac.za/bod/WesternCapeMortalityProfile2009>).

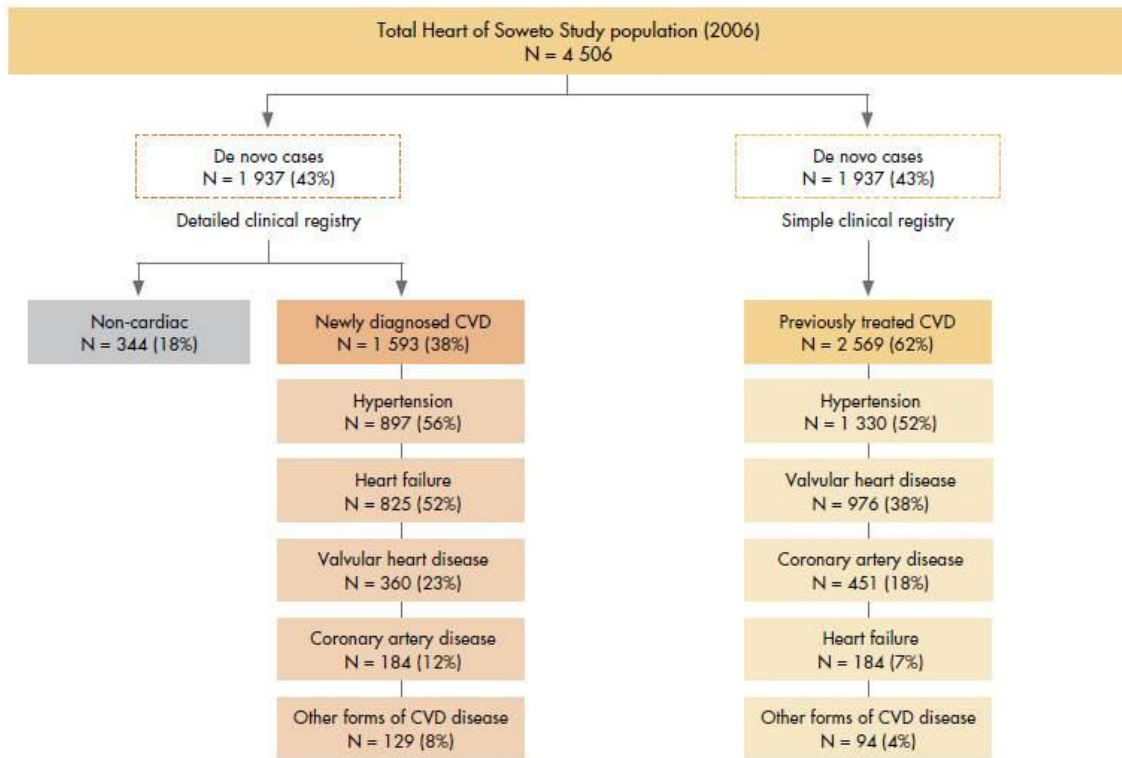


Figure 1.3: Profile of the 2006 HoS Cohort (Sliwa *et al.*, 2008).

chronic diseases of lifestyle. The profile of the HoS cohort discussed above is illustrated in figure 1.3.

It is clear from the above studies and reports, that IHD is a major cause of morbidity and mortality in both developed and developing countries worldwide. In addition, and of concern, is the fact that CVD and IHD are becoming increasingly prevalent among younger people and people of African heritage in South Africa. To further stress the importance and burden of CVDs, it is envisaged that cardiovascular deaths will escalate to 23.4 million by the year 2030 (WHO, 2009).

1.1.2 Vascular disease and the development of IHD:

A multitude of factors are responsible for the development of IHD. Hypertension, smoking, dyslipidaemia, diabetes mellitus, physical inactivity and obesity are all associated with the development of atherosclerosis and IHD and considered to be major risk factors for cardiovascular mortality worldwide (WHO, 2009).

Atherosclerosis, the underlying pathological phenomenon responsible for the development of IHD, is a chronic progressive vascular disease, characterized by plaque formation and subsequent fissure, erosion or rupture of the plaque with thrombosis of the plaque surface (Lahoz *et al.*, 2007) A complication of coronary atherosclerosis can be the development of myocardial ischaemia and ultimately myocardial infarction (Choi *et al.*, 2009).

Plaque formation is characterized by the invasion of the arterial wall by circulating low density lipoproteins (LDL) particles, where they accumulate in the intima and undergo chemical modifications, such as oxidation. Modified LDL can induce endothelial cell (EC) activation and expression of adhesion molecules on EC surfaces. Furthermore, intimal macrophages can internalize modified LDL particles through scavenger receptors and become foam cells—a key process in the development of the atherosclerotic plaque. Oxidized lipids probably modulate smooth muscle cell functions, for example by

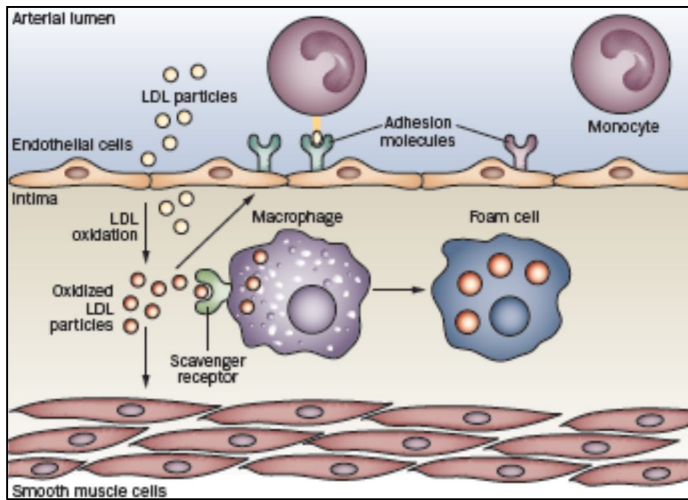


Figure 1.4: Effects of LDL particles on the vessel wall (Rocha & Libby, 2009).

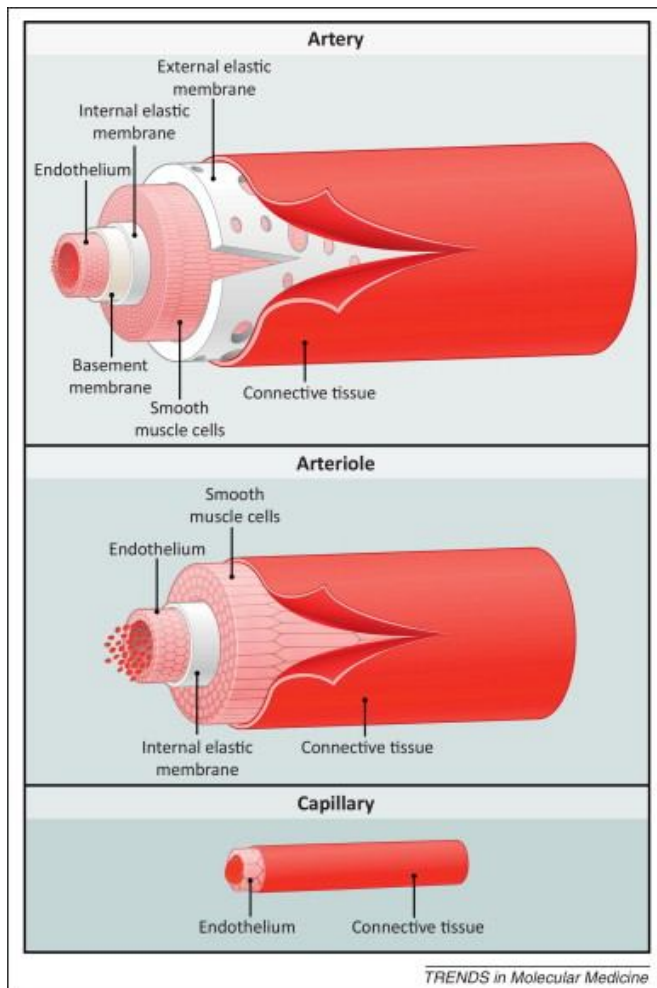


Figure 1.5: The anatomical structures of arteries, arterioles, and capillaries (showing the endothelium as the barrier between the vascular space and the underlying tissues) (La Sala *et al.*, 2012).

increasing their adhesion to macrophages and foam cells in the plaque (Rocha and Libby, 2009) (Figure 1.4).

Critical events in the early stages of atherosclerosis include endothelial activation and dysfunction (Schafer and Bauersachs, 2008; Vanhoutte PM, 2009; Södergren *et al.*, 2010). The vascular endothelium regulates vascular tone and structure, cellular proliferation and interacts with both cellular and hormonal mediators from the circulation and the vascular wall (Chan and Losclzo, 2011; Mas, 2009). EC activation is an important precursor and feature of atherosclerotic vessels (for detailed discussion, see Chapter 1, section 1.3.2.1). ECs are activated by cytokines (such as tumor necrosis factor alpha; TNF- α), Angiotensin II (AngII), oxidative stress, oxidized LDL, and infectious agents (Lee HS *et al.*, 2010; Divchev and Schieffer, 2008), upon which the activated ECs express adhesion molecules (e.g. vascular cell adhesion molecule-1; VCAM-1) and chemokines (e.g. monocyte chemo-attractant protein-1; MCP-1)(Mochizuki *et al.*, 2010; Kiechl *et al.*, 2012; Haas *et al.*, 2010). Therefore, inflammatory processes play a critical role in atherogenesis. There is substantial evidence indicating that impaired endothelial function is a feature of the early stages of atherosclerosis (Corrado *et al.*, 2008). Endothelial dysfunction (for detailed discussion, see Chapter 1, section 1.3.2.2), characterized by decreased activity or bio-availability of endothelium-derived nitric oxide (NO), is an important precursor of atherosclerosis and its complications (Grover-Páez *et al.*, 2008; Nacci *et al.*, 2009). A deficiency of NO in vascular endothelium has been shown to result in vasoconstriction, platelet aggregation, thrombus formation, increased vascular smooth muscle proliferation, and enhanced leukocyte adhesion/invasion to the endothelium (Binglan *et al.*, 2010; Isenberg *et al.*, 2008; Moore *et al.*, 2010; Furie *et al.*, 2008; Tsihliis *et al.*, 2011; Ortega *et al.*, 2010).

From the above, it is clear that the vascular endothelium is a primary target of harmful circulating stimuli associated with cardiovascular risk factor conditions. Therefore, the relative state of vascular endothelial health is a critical determinant and predictor of CVD in general, and atherosclerosis and IHD in particular; in fact, ED has been described as the *primum movens* of coronary artery disease (Sitia *et al.*, 2010).

1.2 Introduction to vascular endothelium.

1.2.1 Structure and function:

The endothelium is a thin, monolayer of cells (endothelial cells - ECs) lining the lumen of all blood vessels in the circulatory system, forming an interface between circulating blood and sub-endothelial tissues (Van der Oever *et al.*, 2010). The adult human endothelium is estimated to have a surface area of between 1 to 7000 m² (Limaye and Vadas, 2006; Mas, 2009), consisting of $1-6 \times 10^{13}$ ECs and accounting for about 1 kg of total body weight (Sumpio *et al* 2002; Limaye and Vadas, 2006). Traditionally regarded as a structural and selectively permeable barrier between the vascular space and the underlying tissues (see figure 1.5) (La Sala *et al.*, 2012; Simionescu, 2007), we now know that the vascular endothelium is also a dynamic organ, with several important “house-keeping” functions in health and disease (Limaye and Vadas, 2006).

ECs are flat with large central nuclei and a diameter of ~0.5 μm (Mas, 2009). ECs have a circular shape in capillaries and venules whereas in arteries and arterioles they are spindle shaped and arranged in the same direction as blood flow (Mas, 2009; Aird, 2007)(see figure 1.6 for a fluorescence digital image of Bovine Pulmonary Artery ECs). ECs show distinct phenotypic characteristics from site to site in the vascular tree (Van der Laan *et al.*, 2004). This phenomenon is also referred to as endothelial heterogeneity (Aird, 2007a).

The location of the endothelium at the interface between the blood and the vessel wall, bestows upon it an important role in several functions, such as vasoregulation, the provision of an anti-thrombotic surface facilitating laminar blood flow and selective permeability (McMurtry and Michelakis, 2012). These activities are most evident in the microcirculation where the EC surface area: blood volume ratio is maximal (Limaye and Vadas, 2008). Nutrients and macromolecules may diffuse out of the bloodstream through intercellular spaces (the result of cellular contraction) between ECs and may lead to tissue oedema/swelling (Oudega, 2012).

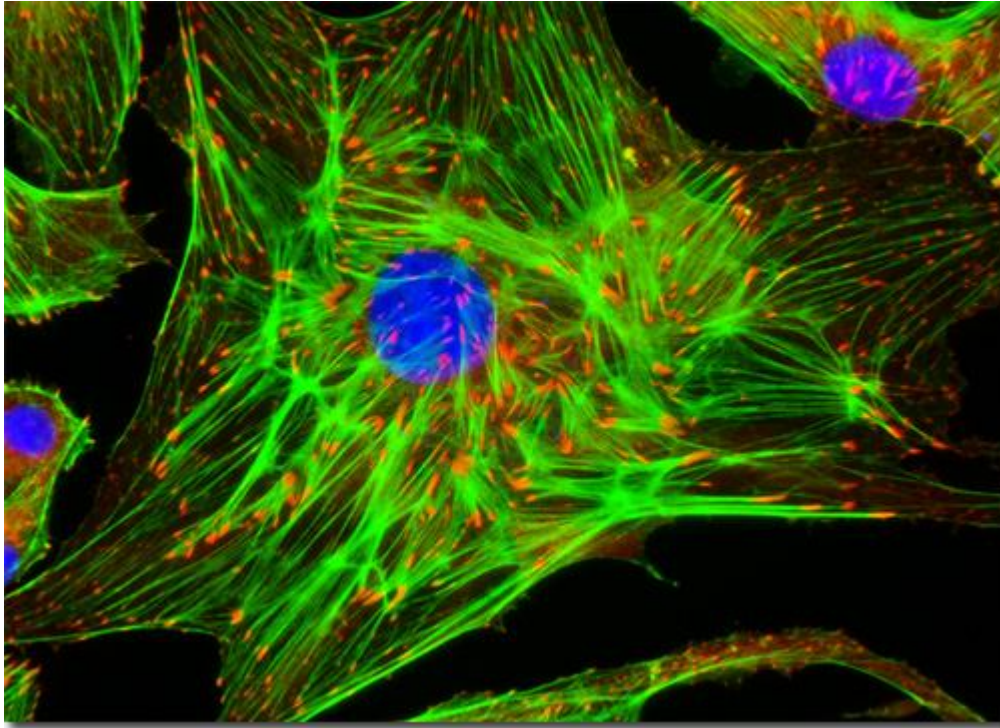


Figure 1.6: A fluorescence digital image of Bovine Pulmonary Artery ECs (BPAEC). (<http://micro.magnet.fsu.edu/primer/techniques/fluorescence/gallery>). Permission granted to re-use image.

Alternatively, nutrients and other molecules may be actively transported by transcytosis through the cells themselves. The endothelium is also responsible for regulating the growth of the surrounding connective tissue (Brábek *et al.*, 2010). In its basal inactive state, it prevents the proliferation of smooth muscle via the secretion of transforming growth factor- β (TGF β) and surface expression of heparan-like molecules (Patel *et al.*, 2010). When activated, however, cytokine/growth factor production by the dysregulated endothelium results in unchecked smooth muscle proliferation (Weakley *et al.*, 2010). Enhanced secretion of platelet-derived growth factor (PDGF) along with insulin-like growth factor (IGF) and basic fibroblast growth factor (bFGF) by the dysfunctional endothelium has mitogenic effects on smooth muscle cells, and can play a role in atherosclerotic plaque formation (Tajsic and Morrell, 2011; Perrault and Zahradtka, 2011). Endothelial activation may result from diverse insults such as disordered local cytokine production, viral infection, free radical formation or oxidation of lipids. Disruptions in endothelial function have been implicated in several diseases including atherosclerosis, cancer metastasis, inflammatory diseases and hypertension (Calcerrada, 2011), diabetes mellitus, Raynaud's disease, scleroderma, Kawasaki's disease, vasculitides and in transplant rejection (Limaye and Vadas, 2006).

Caveolae are particularly abundant in ECs (Van Nieuw Amerongen *et al.*, 2011). Resembling little caves (50–100 nm in diameter) in the plasma membrane, they were described for the first time more than 50 years ago (Yamada, 1955). Caveolae are believed to be involved in various cell functions, including a number of vesicular transport processes such as transcytosis, endocytosis and potocytosis (Conner and Schmid, 2003, Johannes and Lamaze, 2002; Nabi and Le, 2003), the cholesterol homeostasis (Ikonen and Parton RG, 2000), intracellular sorting of proteins and lipids (Sprong *et al.*, 2001) and the establishment of cell polarity (Manes *et al.*, 2003). It has also been proposed that caveolae, caveolins, and cavins play an important role in regulating EC signalling and function and thereby the cardiovascular and pulmonary function at cell and systemic levels (Sowa, 2011). Caveolae are required for the proper organization of signalling pathways that support numerous signalling events, through sequestration of receptors and downstream signalling regulators (Sowa, 2011). Caveolin-1 is the major coat protein responsible for caveolae assembly (Gratton *et al.*, 2004). Caveolin-1 itself may positively

or negatively regulate signalling via direct or indirect protein–protein interactions with resident caveolar proteins. Experiments suggest that caveolin proteins in ECs are themselves regulated by intracellular signalling events (Gratton *et al.*, 2004). Caveolin-1 can be phosphorylated on tyrosine 14 in response to oxidative (Sotgia *et al.*, 2012; Volonte *et al.*, 2001) and shear stress (Rizzo *et al.*, 2003), likely by src family kinases (Labrecque *et al.*, 2003). Caveolae play a critical role in the regulation of endothelial nitric oxide synthase (eNOS) and this has been studied intensively in recent years (Xu Y *et al.*, 2008). Direct interaction between endothelial nitric oxide synthase (eNOS) and caveolin-1, the structural protein of endothelial caveolae, inhibits activity of the enzyme (by competing with activating Ca^{2+} /calmodulin) and this has been confirmed by many studies (Bucci *et al.*, 2000; Cohen W *et al.*, 2004 and Gratton *et al.*, 2004).

Similar to most metabolically active cells, ECs contain substantial numbers of mitochondria (Dranka *et al.*, 2010; Mas, 2009). Interestingly though, adenosine-5'-triphosphate (ATP) production in ECs is relatively independent of mitochondrial oxidative pathways and therefore the mitochondria of ECs have been somewhat neglected. However, they are emerging as agents with diverse roles in modulating the dynamics of intracellular calcium and the generation of reactive oxygen species (ROS) and NO (Davidson and Duchon, 2007). This led to a proposal that the principal role of mitochondria in ECs may be to release NO and ROS as signalling molecules (Quintero *et al.*, 2006). Rod-shaped structures called Weibel-Palade bodies (WPBs) are uniquely expressed by ECs (Weibel and Palade, 1964) and are the major stores of the pro-coagulant von Willebrand factor (vWF) and some pro-inflammatory proteins including P-selectin (Mas, 2009).

The thin layer of ECs, covering the internal surface of blood vessels, cardiac valves, and numerous body cavities, play a critical role in vascular homeostasis. It does so by “sensing” changes in hemodynamic forces and blood-borne signals and “responding” by the release of vasoactive substances. A critical balance between endothelium-derived relaxing and contracting factors maintains vascular homeostasis (Verma and Anderson, 2002). These factors will be discussed in more detail in the next section.

1.2.2 Endothelium derived factors and their role in endothelial function.

The endothelium can release a host of factors in response to its environment and thereby regulate vascular homeostasis (see table 1.1).

1.2.2.1 Nitric Oxide (NO)

The binary molecule with chemical formula NO is also known as nitrogen monoxide (Figure 1.7). NO acts as a free radical, with key roles in both normal physiological processes and disease states (Gonenc *et al.*, 2011). Historically, NO was regarded as a by-product of combustion of substances in the air, as found in automobile exhaust fumes, fossil fuel power plants, and during the electrical discharges of lightning in thunderstorms (Neill *et al.*, 2008). The discovery that the endothelium-derived relaxing factor (EDRF) was in fact NO was rather astonishing, as NO had up till then been perceived as nothing more than a toxic environmental pollutant (Strijdom *et al.*, 2009a).

In fact, the discovery of that endogenously produced NO acted as an important cardiovascular signalling molecule resulted in the Nobel Prize for Medicine and Physiology being awarded to Furchgott, Ignarro and Murad in 1998 (http://www.nobelprize.org/nobel_prizes/medicine/laureates/1998/). It was proclaimed "Molecule of the Year" by *Science* journal 1992 (Culotta and Koshland, 1992). It is now known that NO is an important cellular signalling molecule involved in many physiological and pathological processes (Bryan *et al.*, 2009), and a powerful vasodilator with a short half-life of a few seconds in the blood (Saeed *et al.*, 2007).

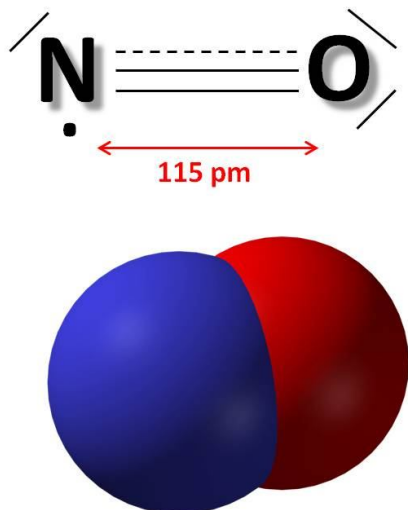


Figure 1.7: Illustration showing the chemical structure of NO (adapted from <http://en.wikipedia.org/wiki/File:Nitric-oxide-3D-vdW.png>).

Table 1.1: Overview of the endothelium-derived vaso-active factors, responsible for regulating vascular tone (Mudau M *et al.*, 2012).

OVERVIEW OF ENDOTHELIUM-DERIVED VASO-ACTIVE FACTORS		
Endothelium-derived factors	Physiological effects	Enzymatic source and mechanism of action
Nitric Oxide (NO)	<ul style="list-style-type: none"> • Potent vasodilator. • Inhibits inflammation, vascular smooth muscle cells (VSMCs) proliferation and migration, platelet aggregation and adhesion and leukocyte adhesion. • Regulates myocardial contractility. • Regulates cardiac metabolism. • Cardio-protective during ischaemia-reperfusion injury. 	<ul style="list-style-type: none"> • Synthesized by the enzymes, eNOS, nNOS and iNOS, with eNOS being the major source of NO during physiological conditions. • Diffuses from ECs to underlying VSMCs where it binds to soluble guanylyl cyclase (sGC), leading to a cascade of events that ultimately result in vascular relaxation.
Prostacyclin (PGI₂)	<ul style="list-style-type: none"> • Vasodilatory agent. • Inhibits platelet aggregation. 	<ul style="list-style-type: none"> • Derived from arachidonic acid by cyclooxygenase-2 (COX-2).
Endothelium-derived hyperpolarizing factor (EDHF)	<ul style="list-style-type: none"> • Exerts vasodilatory effects, particularly in small arteries of diameter $\leq 300\mu\text{m}$. 	<ul style="list-style-type: none"> • Its identity is still under suspicion with proposed candidates such as potassium ions and hydrogen peroxide.
Endothelin-1 (ET-1)	<ul style="list-style-type: none"> • A potent vasoconstrictor. 	<ul style="list-style-type: none"> • Synthesized by endothelin-converting enzyme. • Exerts its effects via two receptors: ET_A expressed on ECs and ET_B on WSMCs. ET_A receptors promote vasoconstriction, whereas ET_B receptors promote NO production and ultimately reduction in ET-1 production.
Thromboxane A (TXA₂)	<ul style="list-style-type: none"> • A potent vasoconstrictor. 	<ul style="list-style-type: none"> • Derived from arachidonic acid by COX-1.
Angiotensin II (Ang II)	<ul style="list-style-type: none"> • A potent vasoconstrictor. 	<ul style="list-style-type: none"> • Synthesized by angiotensin converting enzyme. • Elicits its effects via two receptors: AT₁ which promotes vasoconstriction and cell proliferation, and AT₂ which antagonizes the effects of AT₁.

To date, a vast number of studies have indeed proven that this molecule is endogenously synthesized in the body and plays a vital role in maintaining a healthy cardiovascular system (Strijdom *et al.*, 2009a). Owing to its gaseous and free radical nature, NO is able to diffuse easily between cells and tissues and react with a variety of molecules in the body (Strijdom *et al.*, 2009a). Following its identification as the EDRF, it was reported that NO is synthesized from the amino acid L-arginine by a family of enzymes known as NO synthase (NOS) (Bruckdorfer, 2005).

1.2.2.1.1 Nitric oxide synthases (NOS)

NOS is the main enzymatic source of NO in the body. The enzymatic synthesis of NO is accomplished by three NOS isoforms: neuronal NOS (nNOS), endothelial NOS (eNOS) and inducible NOS (iNOS) (see Table 1.2). The activation of the first two enzymes depends on calcium, whereas iNOS is regarded as calcium-independent (Reuter *et al.*, 2010). It has been reported that nNOS and eNOS are constitutively expressed, whereas iNOS is induced mainly by an immune response or inflammatory stimulation (Tsutsui M *et al.*, 2006; Tsutsui M *et al.*, 2009). However, it has been shown that iNOS is constitutively expressed in neurons (Buskila and Amitai, 2010), kidney (Heemskerk *et al.*, 2009), liver (Diesen and Kuo, 2010), lung (Rus *et al.*, 2010), colon (Baccari *et al.*, 2012) and keratinocytes (Schmitz *et al.*, 2012), whereas eNOS can be expressed at a level higher than its constitutive level under various conditions such as exercise (Gielen *et al.*, 2011), estrogen stimulation (Hien *et al.*, 2011), hyperthermia (Harris MB *et al.*, 2003) and shear stress (Lam CF *et al.*, 2006; Balligand JL *et al.*, 2009). Hence, in light of the most current research reports, the expression and activity of the NOS isoforms seem to be variable and cell-specific. In the case of vasodilation, NO produced by ECs diffuses to the smooth muscle cells to activate soluble guanylate cyclase (sGC), and by doing so it causes vascular relaxation (Reuter *et al.*, 2010), even when both cell types have the capability of expressing the same NOS isoform.

Table 1.2: The regulation of NOS protein expression and activity in the heart. Abbreviations: +, stimulation; -, inhibition (Modified from Massion *et al.*, 2003).

NOS protein expression		NOS activity	
nNOS			
+ / 0	Chronic angiotensin II	+	Hsp90
-	Chronic intermittent hypoxia	-	dystrophin deletion (mdx mice)
iNOS			
+	IL1 β , INF γ LPS, TNF α +IL6 Phenylephrine (α -AR) Norepinephrine(α and β) Isoproterenol (β 2) Hypoxia High glucose C-reactive protein Estrogen		
-	Corticoids , Cyclosporine A, FK506	-	Arginine deficiency
eNOS			
+	Shear stress Exercise Hypoxia (acute , chronic) Hormones and autacoids: Estrogens (ER β) , Insulin Angiotensin II (AT2 and calcineurin) Drugs and toxins: Angiotensin converting enzyme inhibitors Angiotensin II type 1 receptor antagonists Some Ca ⁺⁺ channel blockers β adrenoceptors antagonists Statins Nicotin Nicorandil Pertussis toxin	+	Myristoylation Palmitoylation Serine 1177 phosphorylation: Stretching , AMPK , Insulin , Corticoids Hsp90 , as in chronic hypoxia Dynamin Shear stress Acute pacing Hormones and autacoids: Bradykinin Estradiol VEGF Acetylcholine Substance P Histamine Angiotensin II Drugs: β 3-agonist Ca ⁺⁺ channel blockers ACE inhibitors Statins
-	Lipopolysaccharides LDL (native , glycosylated and oxidized) Hyperglycemia Cortisol Milrinone SNAP, 8-Br-cGMP and IBMX Erythropoietin	-	Caveolin-1 Caveolin-3 NOSTRIN Phosphorylation changes: hyperglycemia (Ser1177-) AMPK (Thr495+) BH4 deficiency ADMA ROS

NO synthesis and its resulting effects depend not only on the cell type in which it is produced, but also on the particular conditions experienced by the cells, the organ, and the whole organism at the time of its production. For example, NO production by vascular ECs is usually continuous and in relatively small amounts, contributing to the maintenance of normal blood pressure and blood homeostasis (Reuter *et al.*, 2010). During septic shock, however, iNOS expression is induced in vascular ECs, which in turn release high concentrations of NO, a process associated with vasoplegia, persistent hypotension, and decompensation (Reuter *et al.*, 2010; Lopez JA *et al.*, 2004; Ganda *et al.*, 2010). In another example, metabolically controlled production of NO can be affected by the distribution and expression of arginases (enzymes that catalyze the production of L-ornithine and urea from L-arginine) and dimethylargininases (Bratt JM *et al.*, 2009; Bratt JM *et al.*, 2010; Greene AL *et al.*, 2005), limited substrate concentration (L-arginine), or local concentrations of citrulline (a competitive inhibitor of NG,NG-dimethylarginine dimethylaminohydrolase (DDAH)(Zhang P *et al.*, 2011) and asymmetric dimethylarginine (ADMA)(a noncompetitive inhibitor of eNOS with a K_i of 0.4 μM (Wang CY *et al.*, 2009) (see figure 1.8). Interactions of NOS isoforms with other trafficking proteins at the cellular and subcellular levels may also determine the fate of NO (Schilling K *et al.*, 2006; Zimmermann K *et al.*, 2002; Konig P *et al.*, 2005; Konig P *et al.*, 2002).

In an article by Villanueva and Giulivi (2010), it is hypothesised that the compartmentalized production and effects of NO define its role in pathophysiology, and therefore modulating its localized production might be the key for effective pharmacological interventions and for understanding genetic differences in pathophysiology.

eNOS activation and phosphorylation

The activity of eNOS is largely determined by posttranslational modifications such as multisite phosphorylation, subcellular localization, and eNOS-protein interactions (Schulz *et al.*, 2009). The eNOS phosphorylation sites associated with enzyme activation includes Ser1177 and Ser633, whereas the phosphorylation site at Thr495 inhibits eNOS catalytic

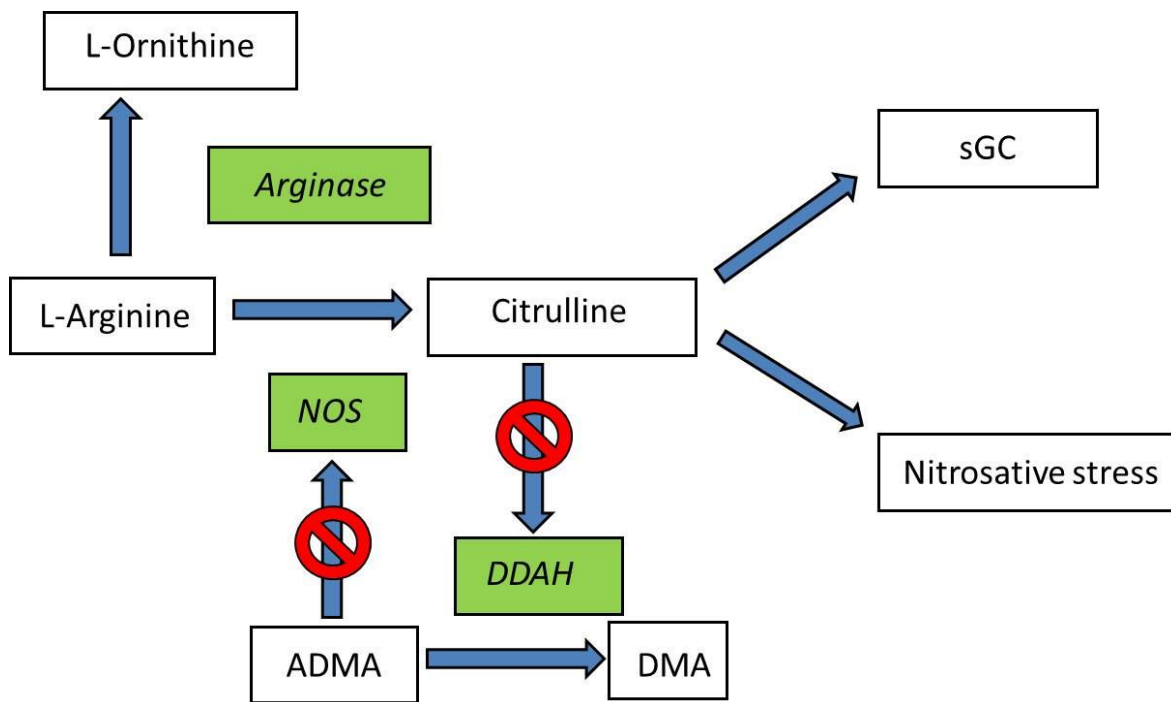


Figure 1.8: Metabolite-controlled production of NO. NO is produced by NOS from L-arginine. NO can interact with specific targets, such as soluble guanylyl cyclase (sGC) and cytochrome c oxidase (CCO), or with other molecules, such as superoxide anion, to trigger nitrosative stress. High levels of citrulline (mM range) inhibit NG,NG-dimethylarginine dimethylaminohydrolase (DDAH), resulting in an increase in ADMA. ADMA, in turn, is a potent NOS inhibitor. Arginine concentrations can be modulated by the activity of arginases, which catalyze the formation of L-ornithine and urea from L-arginine. Dimethylarginine (DMA). *Enzyme names are in green blocks in italic.* (Adapted from Villanueva and Giulivi, 2010).

activity (Schulz *et al.*, 2009; Chen Z *et al.*, 2009). Site-specific phosphorylation also occurs at Ser114 and Ser615, but the functional consequences remain unclear (Schulz *et al.*, 2009).

Several upstream kinases which modulate eNOS activity have been identified, including protein kinase B (PKB/Akt), protein kinase A (PKA), protein kinase C (PKC), and Ca²⁺/calmodulin-dependent protein kinase (CaMK)II (Schulz *et al.*, 2009). 5' AMP-activated protein kinase (AMPK) has also been shown to enhance eNOS activity by direct phosphorylation at Ser1177 (Bradley *et al.*, 2010) and by promoting its association with heat shock protein 90 (HSP 90) (Schultz *et al.*, 2009).

Other findings suggest that trafficking of eNOS from plasmalemmal to intracellular structures is part of a physiological cycle highly sensitive to the state of cell activation (Rafikov *et al.*, 2011). The dynamic trafficking of eNOS between cell surface and intracellular compartments is supported in part by its close interaction with the scaffold protein caveolin (Parton RG *et al.*, 2013). In addition to regulating eNOS subcellular localization, the stable interaction with caveolin leads to the inhibition of eNOS enzyme activity in basal conditions (Chen Z *et al.*, 2012). Upon increases in intracellular calcium ([Ca²⁺]_i), Ca²⁺/calmodulin (CaM) displaces the inhibitory binding of caveolin to eNOS and allows enzyme activation (Kolluru GK *et al.*, 2010). Similarly, increasing vascular flow ("shear stress") and pressure in an *in situ* artery perfusion model rapidly leads to activation of caveolar eNOS with apparent eNOS dissociation from caveolin and association with calmodulin (Ando and Yamamoto, 2011).

This suggests a bimodal mechanism of regulation of NO production reflecting dynamic changes in the eNOS/caveolin and eNOS/CaM interactions (Kolluru GK *et al.*, 2010). However, the identification of both HSP 90 as a chaperone protein interacting with eNOS (Taipale *et al.*, 2010) and phosphorylation sites within eNOS sequence (Butt *et al.*, 2000; Bernier *et al.*, 2000; Michell *et al.*, 2001; Hill *et al.*, 2010) added more complexity to the post-translational regulation of eNOS. In the case of VEGF stimulation, both the interaction of eNOS with HSP 90 and its phosphorylation by PKB/Akt were shown to promote NO production in ECs (Koch and Claesson-Welsh, 2012). Interestingly, each of these regulatory processes, i.e. HSP 90 binding or PKB/Akt phosphorylation, seems to

work by increasing the “apparent” sensitivity of the enzyme to $\text{Ca}^{2+}/\text{CaM}$ (Balligand *et al.*, 2009). However, while the former promotes CaM association to eNOS (upon agonist-induced increase in $[\text{Ca}^{2+}]_i$) (Kolluru GK *et al.*, 2010), the latter appears to reduce CaM dissociation from activated eNOS (when $[\text{Ca}^{2+}]_i$ returns to basal levels) (Kolluru GK *et al.*, 2010; Moccia *et al.*, 2012; McCabe *et al.*, 2000).

1.2.2.1.2 The physiological effects of NO in the heart

NO-sGC- cyclic guanylyl monophosphate (cGMP) signalling

Once NO is released from its attachment to the ferric or ferrous ion within the haem group of NOS, it may readily diffuse from its point of biosynthesis and reach sGC in a variety of other cells. The sensitivity of sGC to NO is within the nanomolar range (Russwurm and Koesling, 2004; Rodríguez-Juárez and Aguirre, 2007; Hall CN and Garthwaite, 2009) and this property converts it into an undisputed primary physiological effector for NO. The mechanism by which sGC is activated by NO is complex and poorly understood (Cary *et al.*, 2006).

New knowledge concerning the regulatory pathways for gene expression activation governed by the cGMP–cyclic guanosine monophosphate kinase I (cGKI) has emerged, based on the seminal observation that cGKI is able to translocate to the nucleus (Casteel *et al.*, 2008; Pilz and Casteel, 2003) as well as an increasing list of physiological substrates phosphorylated by cGKI (Francis *et al.*, 2010), thus conferring a multifaceted role to this enzyme. The underlying mechanisms and potential relationships with the classical NO–cGMP pathway of cGKI, cyclic guanosine monophosphate kinase II (cGKII), need to be further elucidated (Martinez-Ruiz *et al.*, 2011). Signalling by cGMP is terminated through the action of phosphodiesterases (PDEs), a class of proteins composed of 11 known families in mammals and derived from 21 genes (Martinez-Ruiz *et al.*, 2011). Tissue and substrate specificities (for cGMP or cyclic adenosine monophosphate (cAMP)) are major determinants of their action and it is now well established that PDEs 5, 6, and 9 show high specificity for cGMP degradation (Martinez-Ruiz *et al.*, 2011) (see figure 1.9). After the significant scientific and social impact of the clinical use of PDE 5 inhibitors for erectile

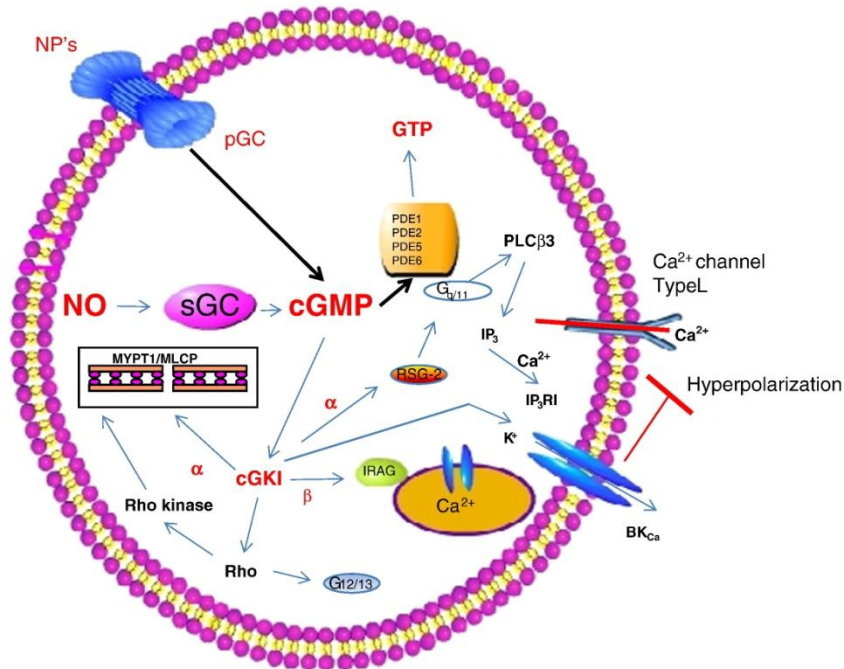


Figure 1.9: Classical mode of action of NO in vascular smooth muscle by activation of sGC and generation of cGMP (modified in part from Martínez-Ruiz *et al.*, 2011). Once this nucleotide is synthesized, a series of reactions triggered by the activation of cGMP-cGKI occurs, the final consequence being a decreased intracellular Ca²⁺ concentration. These reactions involve the participation of partner proteins such as IRAG, Rho, and Rho kinase and calcium channels. The decreased levels of Ca²⁺ result in the uncoupling of contractile proteins, myosin phosphatase target subunit 1 / myosin light-chain phosphatase (MYPT1/MLCP) and vascular relaxation. The cGMP signal is terminated by specific phosphodiesterases (PDEs) (Martínez-Ruiz *et al.*, 2011).

dysfunction, these enzymes have become major targets for therapeutic approaches (Wong ML *et al.*, 2006).

Effects on myocardial contractility: inotropic and lusitropic actions

Many diverse and often contradictory effects of NO or NO donors on myocardial function have been reported (Cotton JM *et al.*, 2002). Recently, though, it is believed that NO generally acts to fine tune and optimize cardiac pump function (Cotton JM *et al.*, 2002).

Studies have shown that low (sub-micromolar) concentrations of NO exert modest positive inotropic effects, which may serve to enhance basal cardiac function (Rastaldo *et al.*, 2007; Pavlovic *et al.*, 2013). Another study demonstrated a similar effect in normal human subjects undergoing cardiac catheterization, in whom intracoronary NOS inhibition with L-NMMA caused a small reduction in the maximal rate of left ventricular pressure development (LV dP/dt max), independent of changes in cardiac loading (Cotton JM *et al.*, 2001). An increasing body of data suggests that NO derived both from eNOS located in sarcolemmal caveolae and nNOS located probably in the sarcoplasmic reticulum (SR) of the cardiac myocyte may modulate central events of excitation–contraction coupling such as calcium influx through sarcolemmal L type channels and the release and re-uptake of calcium by the SR (Carnicer *et al.*, 2012; Nediani *et al.*, 2011). The precise physiological role of these effects remains unclear, but there is a clear suggestion of a fundamental autoregulatory role for NO in intra-cardiomyocyte calcium cycling (Cotton JM *et al.*, 2002).

Slightly higher concentrations of NO (but still within “physiological” ranges) enhance cardiomyocyte relaxation and diastolic function (Cotton JM *et al.*, 2002). A few studies showed that endothelium derived NO accelerates relaxation and reduces diastolic tone in a range of experimental preparations and species (Shah and MacCarthy, 2000; Rastaldo *et al.*, 2007; Pavlovic *et al.*, 2013). The underlying mechanism of these effects is thought to be a cGMP induced reduction in myofilament responsiveness to calcium (Rastaldo *et al.*, 2007; Pavlovic *et al.*, 2013; Layland *et al.*, 2002), an action that is also supported by studies conducted in anaesthetized pigs (Heusch *et al.*, 2000).

Similar to the effects on contractile function, NO generated locally within the myocardium also modulates basal heart rate (Cotton JM *et al.*, 2002). In particular, NO exerts biphasic effects on atrial firing rate and automaticity through modulation of the hyperpolarisation activated pacemaker current, I_f (Tamargo *et al.*, 2010). Low concentrations of NO donors increase the rate whereas higher concentrations are negative chronotropic (Cotton JM *et al.*, 2002). A final important effect of endothelium derived NO on basal cardiac function is the reversible inhibition of myocardial O_2 consumption, independent of contractile function, which has been demonstrated both *in vitro* (Ziolo *et al.*, 2008) and *in vivo*, in large animals (Heusch *et al.*, 2000). The underlying mechanism involves effects on the mitochondrial electron transport chain and may be at least partly cGMP independent. This action, like the others previously discussed, may be considered as potentially beneficial for global cardiac function (Cotton JM *et al.*, 2002).

Intra-cardiac NO generation is cyclical, with a vigorous rise around the time of early diastolic filling, and augmented by increased chamber stretch (preload) (Tousoulis *et al.*, 2012). It has therefore been suggested that mechanical stimuli (e.g. stretch and shear), whose qualitative and quantitative characteristics are determined largely by cardiac contractile properties and loading conditions, may serve to match contractile functions of the heart to altered workload on a beat-to-beat basis (Cotton JM *et al.*, 2002). As an example, experimental studies have shown that endogenous NO enhances the Frank-Starling response in the isolated heart (Angelone *et al.*, 2012). Furthermore, NO has been shown to play an important role in the stretch induced activation of cardiac muscle (Vila-Petrof *et al.*, 2001).

NO is also reported to modulate inotropic, chronotropic, and dromotropic responses to β adrenoceptor stimulation; low concentrations enhance and high concentrations reduce β adrenergic response (Collins and Rodrigo, 2010). NO also elicits both acute and chronic lusitropic myocardial effects (Bronzwaer and Paulus, 2008). Acute lusitropic effects of NO affect myocardial relaxation and diastolic distensibility, whereas chronic lusitropic effects of NO mainly influence myocardial diastolic distensibility (Bronzwaer and Paulus, 2008).

In mechanically stressed myocardium, high NO bioavailability also preserves LV diastolic function through chronic effects on calcium handling, cardiomyocyte hypertrophy, and

extracellular matrix deposition, as evident, respectively, from transgenic mice with cardiomyocyte-specific NOS1 overexpression subjected to transverse aortic constriction (Loyer *et al.*, 2008), from transgenic mice with cardiomyocyte-specific eNOS overexpression subjected to permanent coronary artery ligation (Shimokawa and Tsutsui, 2010) and from numerous experimental rat models chronically treated with NOS enhancers or NOS inhibitors (Bronzwaer and Paulus, 2008).

1.2.2.1.3 Metabolic effects of NO

NO does not only affect myocardial contractile function. Both endogenous and exogenous NO has been shown to exert metabolic effects on the myocardium (Brutsaert, 2003). Metabolic effects, such as decreased myocardial oxygen consumption (Brutsaert, 2003; Trochu *et al.*, 2000) the regulation of mitochondrial metabolism by direct inhibition of the respiratory chain (Stumpe *et al.*, 2001), as well as utilization of energy substrates by reducing myocardial glucose uptake (Tada *et al.*, 2000). These effects are suggestive of a putative cardioprotective mechanism for NO (Brutsaert, 2003). NO has also been shown to inhibit electron transfer in the mitochondria (Förstermann U and Sessa, 2012). In addition, NO has been shown to directly activate the mitochondrial KATP channels (Sasaki *et al.*, 2000), suggesting that NO might play a crucial role in what was regarded as the candidate end-effector of ischaemic preconditioning (IP)-protection. Furthermore, a possible role for NO derived from iNOS in the induction of apoptosis has been shown in neonatal mouse cardiomyocytes treated with the cytokine TNF- α (Song *et al.*, 2000).

1.2.2.1.4 NO in myocardial hypoxia

NO production during hypoxia/ischaemia

Most studies suggest that the production of NO increases during ischaemia, at least in the early stages (up to ± 30 min) (Shah & McCarthy, 2000). In one study, exercise has been

shown to protect against myocardial ischaemia, because of an increase in NO signalling (Calvert *et al.*, 2011). Another study reported that β_3 adrenoreceptor-stimulation by increased NOS, improves ischaemia/reperfusion injury (Aragón *et al.*, 2011). An important stimulus for the increase in NO production may be hypoxia (Beleslin-Čokić *et al.*, 2011). An augmented release of NO from coronary ECs contributes to hypoxic coronary vasodilatation (Crimi *et al.*, 2012). NO production by isolated cardiomyocytes was also increased by hypoxia (Obal *et al.*, 2012). The increase in NO production during ischaemia may serve to maintain coronary blood flow and myocardial function (Shah & McCarthy, 2000). Following prolonged severe ischaemia, however, the production of NO may decline (Yang G *et al.*, 2010).

Myocardial reperfusion / reoxygenation and beneficial effects of NO

Indirect NO-mediated improvement of contractile function can occur via (1) antiplatelet-adhesive and -aggregatory activity, leading to improvement in coronary blood flow (Mattapally and Banerjee, 2011); (2) decreased expression of adhesion molecules, such as P-selectin and intercellular adhesion molecule-1, on coronary ECs, resulting in decreased leukocyte adhesion (Hurd *et al.*, 2012); (3) prevention of the “no-reflow” phenomenon, whereby microvascular perfusion remains impaired, despite the re-establishment of epicardial coronary artery patency (Shah & McCarthy, 2000). Potential mechanisms by which NO may exert direct beneficial effects include (1) a reduction in O_2 demand, leading to improvement in O_2 supply-demand balance (Umbrello *et al.*, 2013); (2) reduction in myofilament responsiveness to Ca^{2+} (Jin CL *et al.*, 2013) and/or sarcolemmal Ca^{2+} influx (Kuster *et al.*, 2010), which would reduce the effects of Ca^{2+} overload; and (3) scavenging of ROS and thus a “cytoprotective” effect (Wink *et al.*, 2011).

Detrimental effects of NO during ischaemia-reperfusion

Several investigators have also reported detrimental effects of endogenous NO during ischaemia-reperfusion (Shah and McCarthy, 2000). For example, postconditioning

improved contractile function in the human myocardium by a NOS inhibitor or by a ROS scavenger, mercaptopropionylglycine (Lemoine *et al.*, 2010). In isolated rat hearts subjected to brief hypoxia at constant coronary flow, the addition of SNP at reoxygenation was detrimental, in marked contrast to addition of the drug during hypoxia (Shah and McCarthy, 2000).

1.2.2.1.5 NO in the heart – summary

In Summary:

- NO is one of the most important signalling molecules in the entire cardiovascular system;
- The main cellular source of NO is NOS (eNOS, iNOS and nNOS, all expressed in the cardiovascular system)
- NO has variable effects depending on, inter alia, NOS-isoform specific production, amount of NO released, experimental conditions, etc;
- In baseline physiological conditions, NO is predominantly eNOS-derived with biological effects such as maintenance of vascular homeostasis, anti-clotting and anti-inflammatory actions, cardiogenesis and maintenance of contractile function;
- In hypoxia and ischaemia, the role of NO becomes more variable.
- Mostly associated with protection, but can become harmful when NO reacts with O_2^- to form reactive and toxic free radicals, such as $OONO^-$, NO_2 , OH ;
- eNOS is an important source of hypoxia / ischaemia-induced increase in NO production via PI3K/PKB-stimulated phosphorylation at the serine 1177 residue.

(Mudau M, M.Sc Thesis, University of Stellenbosch, 2010)

1.2.2.2 Prostacyclin & Thromboxane A₂

Although NO is the best described endothelium-derived factor in the physiology and pathophysiology of endothelial function, it cannot explain all endothelium-dependent responses. Other endothelium-derived factors, such as prostacyclin (prostaglandin I₂, PGI₂) and thromboxane A₂ (TXA₂) also play an important role in maintenance of the vascular homeostasis (Fetalvero *et al.*, 2007).

PGI₂ and TXA₂ are products of the cyclooxygenase (COX) pathway and have earned considerable attention in cardiovascular research because of their distinct effects on vascular functions (Pecchi *et al.*, 2009; Belton *et al.*, 2000) (Figure 1.10).

PGI₂ is a major prostanoid generated by ECs, and is a potent vasodilator and an inhibitor of leukocyte adhesion and platelet aggregation. Therefore, PGI₂ is considered to be both anti-atherothrombotic and cardioprotective (Smith DD *et al.*, 2010). On the other hand, TXA₂ is a potent inducer of vasoconstriction, platelet activation, and platelet adhesion, and is a pro-atherogenic prostanoid. Since TXA₂ and PGI₂ exert opposing effects in the vasculature, their relative concentrations in the circulation and microenvironment are critical for the normal cardiovascular function and prevention of atherosclerotic progression (Smith DD *et al.*, 2010).

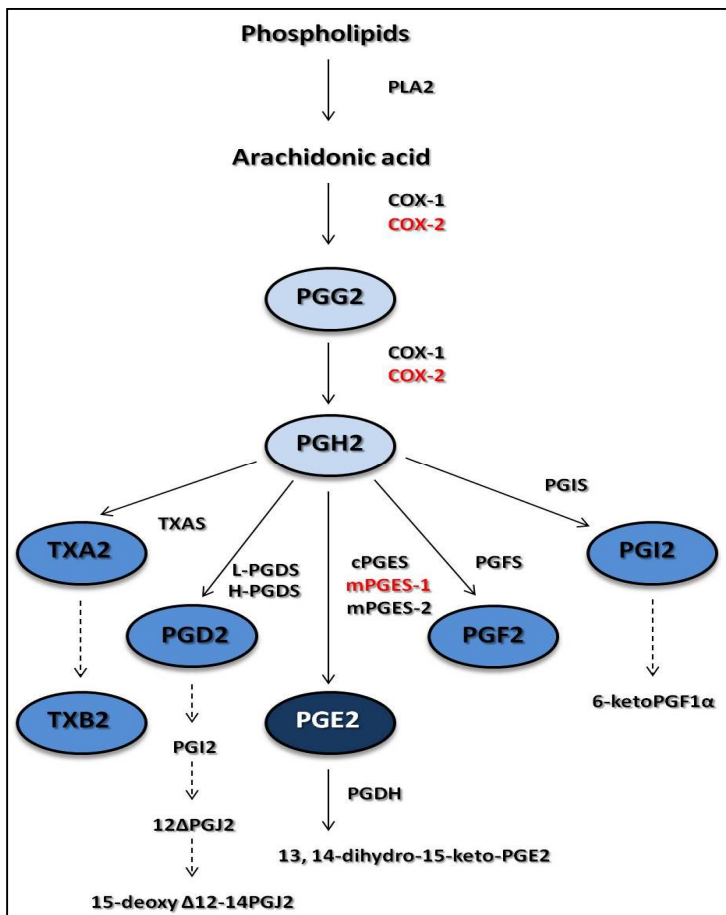


Figure 1.10: The COX pathways. Schematic representation of the prostanoids produced downstream of COX-1 and COX-2 enzymes (Pecchi *et al.*, 2009).

1.2.2.3 Endothelium-derived hyperpolarizing factor (EDHF)

Multiple molecular mechanisms regulate blood vessel relaxation, with NO well-established as the predominant mediator of endothelium-dependent vasorelaxation (NO was initially termed, EDRF (Murad F, 2006; Furchgott and Zawadzki, 1980; Ignarro *et al.*, 1987). Whereas NO acts by both cyclic GMP (cGMP)-dependent and cGMP-independent mechanisms to influence calcium disposition and sensitivity (Moncada S and Higgs, 2006), blood vessel relaxation and tone can also additionally be mediated by endothelium-dependent hyperpolarization (Feletou M and Vanhoutte, 2007; Cohen RA, 2005; Griffith TM, 2004). Numerous substances have been advanced as putative EDHFs, including arachidonic acid metabolites, PGI₂, epoxyeicosatrienoic acids (EETs) derived from cytochrome P450, lipoxygenase [12-(s)-hydroxyeicosatetraenoic acid (12-S-HETE)], ROS, hydrogen peroxide (H₂O₂), potassium ions (K⁺), vasoactive peptides, as well as NO itself (Feletou M and Vanhoutte, 2007; Cohen RA, 2005; Griffith TM, 2004; Liu *et al.*, 2011). It has also been suggested that EDHF function may be mediated through direct coupling between endothelial and smooth muscle cells by myoendothelial gap junctions composed of connexions (Feletou M and Vanhoutte, 2007; Cohen RA, 2005; Griffith TM, 2004).

Recently, hydrogen sulfide (H₂S) has been shown to be a major EDHF (Mustafa *et al.*, 2011), formed in vascular ECs from cysteine by cystathionine γ -lyase (CSE), which is calcium-calmodulin dependent (Yang G *et al.*, 2008). Whereas CSE appears to play a significant role in the cardiovascular system, two other enzymes have also been shown to generate H₂S in various tissues, namely cystathionine β -synthase (CBS) and 3-mercaptopyruvate sulfurtransferase (3-MST) (Mustafa *et al.*, 2011). In blood vessels however, CBS appears to play a negligible role in the production of H₂S (Zhao *et al.*, 2001), whereas the precise role of 3-MST has yet to be defined, despite its presence in vascular endothelium (Shibuya *et al.*, 2009). Acetylcholine-mediated blood vessel relaxation, however, is markedly reduced in CSE-deleted mice, which manifests as increased blood pressure comparable to levels in mice lacking eNOS (Yang G *et al.*, 2008; Huang PL *et al.*, 1995).

1.2.2.4 Endothelin-1 (ET-1)

The endothelins constitute a super family of peptides that are structurally similar to sarafotoxins found in snake venom (Bourque *et al.*, 2011). There are three distinct encoded isoforms (ET-1, ET-2, and ET-3), and although all isoforms are involved in vascular function (Barton *et al.*, 2008); ET-1 is the dominant isoform in the cardiovascular system and is therefore the most often studied (Bourque *et al.*, 2011). ET-1 is synthesized predominantly in vascular ECs, although it is also synthesized in vascular smooth muscle cells, extravascular tissues such as the spleen, pancreas, lung, and nervous system, and glomerular and epithelial cells within the kidney (Ruef *et al.*, 2001; Bourque *et al.*, 2011).

ET-1 exerts its functions by binding to G protein-coupled ET receptors, which are expressed in several tissues, including the myocardium, lung, pancreas, spleen, and nervous system, as well as in vascular tissues (Bourque *et al.*, 2011). Two receptors for endothelins, named ET_A and ET_B, have been identified (Bourque *et al.*, 2011). ET_A receptors are located within the vascular smooth muscle cells (VSMC), whereas ET_B receptors are located on both the endothelium as well as on VSMC (Bourque *et al.*, 2011). In the vasculature, ET_A receptors are made up of ET_{A1} and ET_{A2} subtypes, distinguished by their sensitivity to the endothelin receptor antagonist BQ-123; the BQ-123-sensitive ET_{A1} receptor is located in VSMC of most arteries and represents the dominant subtype (Iwasaki *et al.*, 2000), whereas the BQ-123-insensitive ET_{A2} receptor has been localized in human and rabbit saphenous veins (Nishiyama *et al.*, 1995; Sudjarwo *et al.*, 1994). ET_B receptors consist of ET_{B1} and ET_{B2} subtypes, and can be broadly distinguished by their endothelial and smooth muscle cell localization, respectively (Dashwood and Tsui, 2002; Haynes *et al.*, 1995; Masaki *et al.*, 1991). Binding of ET-1 to ET_A and ET_B receptors in VSMC results in vasoconstriction, whereas the predominant effect of ET-1 binding to ET_B receptors in the endothelium is increased NO and prostacyclin synthesis (Little *et al.*, 2008; Schiffrin, 2005). Whereas ET-1 binds both ET_A and ET_B receptors, evidence suggests ET-1₁₋₃₁ (Rossi *et al.*, 2002) selectively binds ET_A receptors (Mazzocchi *et al.*, 2000; Rebuffat *et al.*, 2001; D'Orleans-Juste P, 2006), although evidence that ET-1₁₋₃₁ binds ET_B receptors and mediates NO release also exists (Niwa Y *et al.*, 2000). Whether ET-1₁₋₃₂

preferentially binds one endothelin receptor over the other is not yet known (Bourque *et al.*, 2011).

1.2.2.5 Angiotensin II (Ang II)

Ang II is another endothelial-derived factor that regulates vascular function and structure. Ang II is the major bioactive peptide of the renin-angiotensin system (RAS) (Cat and Touyz, 2011). Ang II, produced systemically and in ECs, is a potent vasoactive peptide that also stimulates vascular smooth muscle cell growth, inflammation, and fibrosis through a myriad of signalling pathways (Touyz and Schiffrin, 2000; Mehta JL and Griendling, 2007; Lemarié and Schiffrin, 2010). Accordingly, Ang II plays an important physiological role in maintaining vascular tone by regulating immediate vasoconstriction, in addition to a pathophysiological role in CVDs such as hypertension, atherosclerosis, and heart failure, conditions that are associated with ED, vascular hyperreactivity, and structural remodelling (Cat and Touyz, 2011). Ang II exerts its diverse actions via two G protein-coupled receptors (GPCRs), namely Ang II type 1 receptors (AT1R) and type 2 receptors (AT2R) (Cat and Touyz, 2011). The AT1R mediates most of the pathophysiological actions of Ang II. AT2R is associated with antiproliferative, pro-apoptotic, and vasodilatory actions of Ang II and tends to counteract effects of the AT1R (Mehta JL and Griendling, 2007). Signalling pathways induced by Ang II/AT1R involve interactions with several heterotrimeric G proteins coupled to second messengers and cytosolic proteins, including phospholipase C (PLC), phospholipase A2 (PLA2), and phospholipase D (PLD) (Touyz and Schiffrin, 2000). In addition Ang II/AT1R regulates the activation of NADPH oxidase through the activation of many receptor and nonreceptor tyrosine kinases and serine threonine kinases, important in cell growth and hypertrophy (Cat and Touyz, 2011).

1.2.3 Endothelial heterogeneity, macrovascular vs. microvascular ECs and cardiac EC subtypes.

1.2.3.1 General endothelial heterogeneity

EC phenotypes are differentially regulated in space and time, giving rise to the phenomenon of “EC heterogeneity” (Aird WC, 2007a). Beyond the specification to arterial, venous, or lymphatic fate, it is currently recognized that ECs undergo further differentiation specific to the vascular bed or organ in which they reside (Atkins *et al.*, 2011). This phenotypic heterogeneity is the primary mechanism by which the endothelium carries out a myriad of vital functions, including control of microvascular permeability, vessel wall tone, coagulation and anticoagulation, inflammation, and angiogenesis (Aitsebaomo *et al.*, 2008; Aird WC, 2007a; Aird WC, 2007b). Endothelial heterogeneity is also responsible for the varied and diverse responses across differing vascular beds to pathological stimuli and disease states (Molema G, 2010; Davies *et al.*, 2010; Kwaan and Samama, 2010). The phenotypic heterogeneity of the endothelium of the various organ and vascular beds has been highly studied (Aitsebaomo *et al.*, 2005; Aird WC, 2007a; Aird WC, 2007b). Remarkably, despite these detailed observations, the molecular mechanisms of endothelial heterogeneity remain largely unknown (Atkins *et al.*, 2011). In recent years, the study of ECs in several vascular beds has made significant strides in elucidating some of these molecular mechanisms (Atkins *et al.*, 2011).

1.2.3.1.1 Structural Classification of Vascular Endothelium

Based on structural content, vascular endothelium can be classified into 3 main structural types: continuous, which is further subdivided into fenestrated or nonfenestrated, and discontinuous (or sinusoidal) (Aird WC, 2007a) (see figure 1.11).

Continuous Nonfenestrated

Continuous nonfenestrated endothelium is found predominantly in arteries, veins, and capillaries of the brain, skin, muscle, heart, and lung (Atkins *et al.*, 2011). Tight junctions and adherens junctions are the 2 main types of barrier forming intercellular junctions found in this type of endothelium (Dejana E, 2004; Bazzoni and Dejana, 2004). Their expression is variable across the endothelial tree, with higher expression in the continuous endothelium of arterioles compared to capillaries and venules (Atkins *et al.*, 2011). Molecules cross continuous nonfenestrated endothelium by the active process of transcytosis, which is mediated by specialized structures including caveolae and vesiculo-vacuolar organelles (Atkins *et al.*, 2011). Caveolae, flask-shaped, non-coated membrane invaginations (≈ 70 nm in diameter) that usually open to the luminal or abluminal side (Stan RV, 2005; Parton RG and Simons, 2007), are present in all types of endothelium, but have a particularly high expression in continuous nonfenestrated capillary ECs (Bendayan M, 2002). Caveolin-1 is the main structural component of caveolae and is regulated by distinct transcriptional mechanisms in ECs (Kathuria *et al.*, 2004). Vesiculo-vacuolar organelles also contain caveolin-1 and are focal collections of membrane bound vesicles of variable size that span the cytoplasm of the ECs (Dvorak AM *et al.*, 1996); they are mostly found in venules with continuous nonfenestrated endothelium (Dvorak AM and Feng, 2001).

Continuous Fenestrated

This class of ECs typically occurs at locations that are characterized by increased filtration or increased trans-endothelial transport and is found in capillaries of all exocrine and endocrine glands, digestive tract mucosa, and the kidney (e.g., glomeruli and a subpopulation of renal tubules) (Atkins *et al.*, 2011). Fenestrae are trans-cellular pores (≈ 70 nm in diameter) that extend through the full width of ECs and are thought to allow rapid exchange of molecules between the circulation and the surrounding tissue (Simionescu *et al.*, 1974). The majority of fenestrae contain a thin diaphragm across their opening that acts as a molecular filter (Atkins *et al.*, 2011). The type II membrane

glycoprotein plasmalemmal vesicle-associated protein-1 is currently the only molecular protein localized to the diaphragm (Stan *et al.*, 1999), and it has been discovered to be both necessary and sufficient for diaphragm formation in cultured ECs (Stan *et al.*, 2004; Ioannidou *et al.*, 2006). Other diaphragm-containing components of continuous endothelium include caveolae and transendothelial channels, which are patent pores spanning the ECs from the luminal to abluminal side (Stan RV, 2007). Compared with nonfenestrated endothelium, continuous fenestrated endothelium is more permeable to water and small solutes (Atkins *et al.*, 2011).

Discontinuous Fenestrated

This class of ECs is found in certain sinusoidal vascular beds, most notably the liver and bone marrow, which lack a well-formed basement membrane (Atkins *et al.*, 2011). Discontinuous fenestrated ECs are characterized by large heterogeneous fenestrae (100 to 200 nm in diameter) without diaphragms (Braet and Wisse, 2002). They have few caveolae and contain clathrin-coated pits and vesicles, which play an important role in receptor-mediated endocytosis (Atkins *et al.*, 2011).

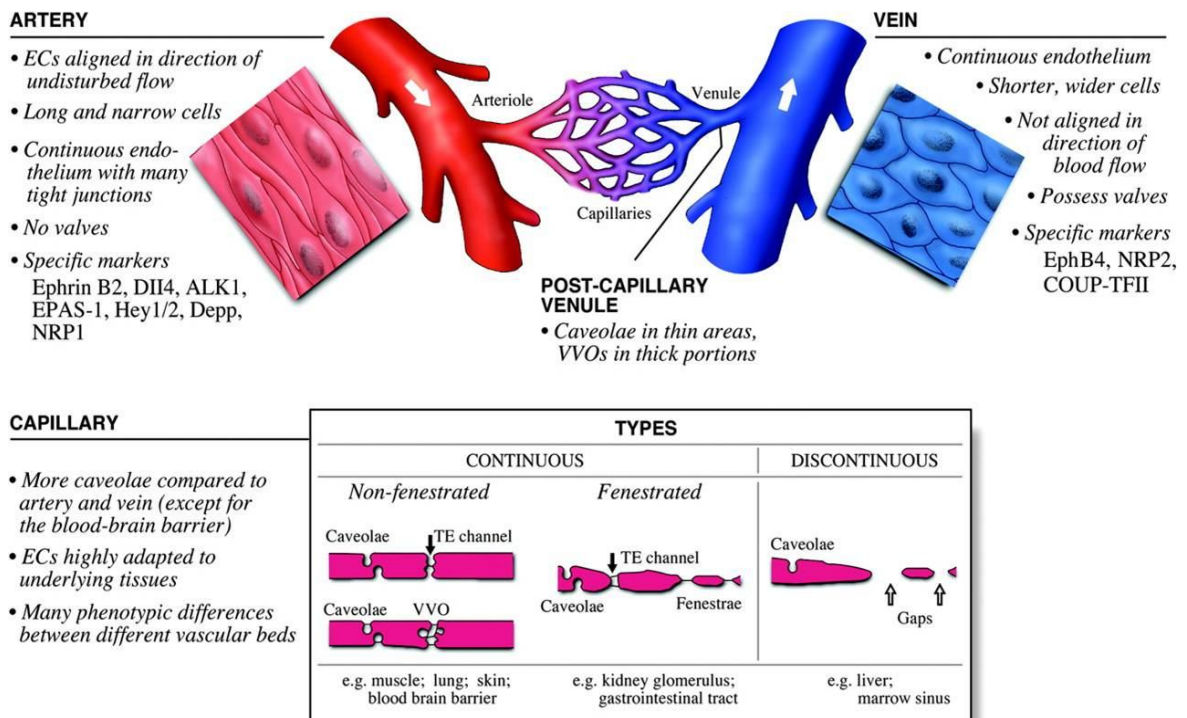


Figure 1.11: ECs in arteries, veins, and capillaries. Selected phenotypic differences between ECs in arteries, veins, postcapillary venules, and capillaries. ALK1 (activin-receptor-like kinase 1); Depp (decidual protein induced by progesterone); DII4 (delta-like 4); EPAS -1 (endothelial PAS domain protein 1); NRP1 (neuropilin 1); TE (transendothelial) and VVOs (vesiculo-vacuolar organelles) (Aird, 2007b).

1.2.3.2 Endothelial Heterogeneity in the Heart

ECs can have different effects on cardiac function, depending on their organization in the heart (Brutsaert, 2003). In the heart, ECs can be categorised based on their proximity and interaction with the cardiomyocytes (Strijdom and Lochner, 2009c). It is important to distinguish between the function of the cardiac ECs in the myocardial capillaries and at the endocardium (collectively referred to as cardiac endothelium) and the function of the coronary vascular endothelium in the major epicardial and smaller intramyocardial coronary arteries and veins (Brutsaert, 2003). ECs from larger coronary arteries, which constitute the coronary vascular endothelium (Figure 1.12), lie distant from cardiomyocytes (Strijdom and Lochner, 2009c). The vascular endothelium controls coronary artery function, by indirectly controlling coronary blood supply to the myocardium (Brutsaert, 2003).

Cardiac ECs in the myocardial capillaries (cardiac microvascular ECs: CMECs) and in the endocardial endothelium (EECs) are in close proximity to adjacent cardiomyocytes. The nature of the interactions between CMECs and EECs on the one hand and cardiomyocytes on the other, depends on intercellular distance and cell number ratio (Brutsaert, 2003). The cell number ratio, in turn, depends on the capillary-to-cardiomyocyte ratio and intercapillary distance (varies in species and cardiac sampling site) (Brutsaert, 2003). The distance between each CMEC and the closest cardiomyocyte is approximately 1 μ m. This strategic arrangement facilitates endothelial cell-to-cardiomyocyte paracrine signalling (Brutsaert, 2003). Although EECs and CMECs share common features in their effects on subjacent cardiomyocytes, these two cardiac EC types are, however, not identical. They differ with regard to developmental, morphological, and functional properties, the major difference probably resulting from the way in which they perceive and transmit signals and from their different hierarchic position and contribution within the overall endothelial system (Brutsaert, 2003) (see figure 1.13).

The close proximity between the CMECs and cardiomyocytes allow for bi-directional cellular communication and signalling between these cell types (Brutsaert, 2003). These direct effects include regulating metabolism, growth, contractility and rhythmicity in cardiomyocytes and are mediated by autocrine and paracrine secretion of substances

such as NO, ET-1, prostacyclins and a variety of growth factors (Brutsaert 2003; Hsieh *et al* 2006)(see figure 1.14).

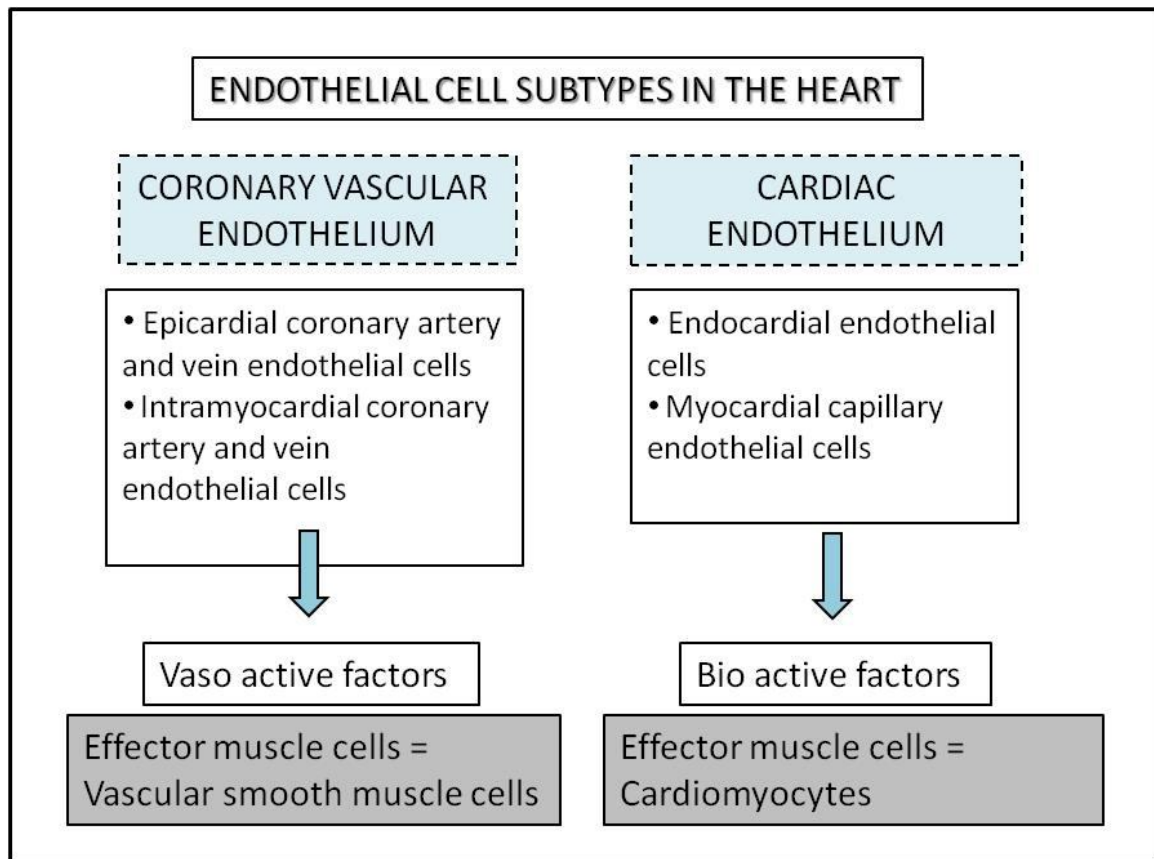


Figure 1.12: Classification of ECs in the heart. The classification is based on the proximity to, and direct paracrine influence on cardiomyocytes. Coronary vascular ECs are situated in the larger coronary arteries and veins, and have no direct effects on cardiomyocyte function. Their biological effects are similar to those of endothelium elsewhere in the body (maintenance of vascular homeostasis). Conversely, the cardiac ECs (endocardial ECs, EECs) and cardiac micro-vascular ECs (CMECs) have greater direct effects on cardiomyocyte function via the release of paracrine messengers such as NO (Strijdom and Lochner, 2009c).

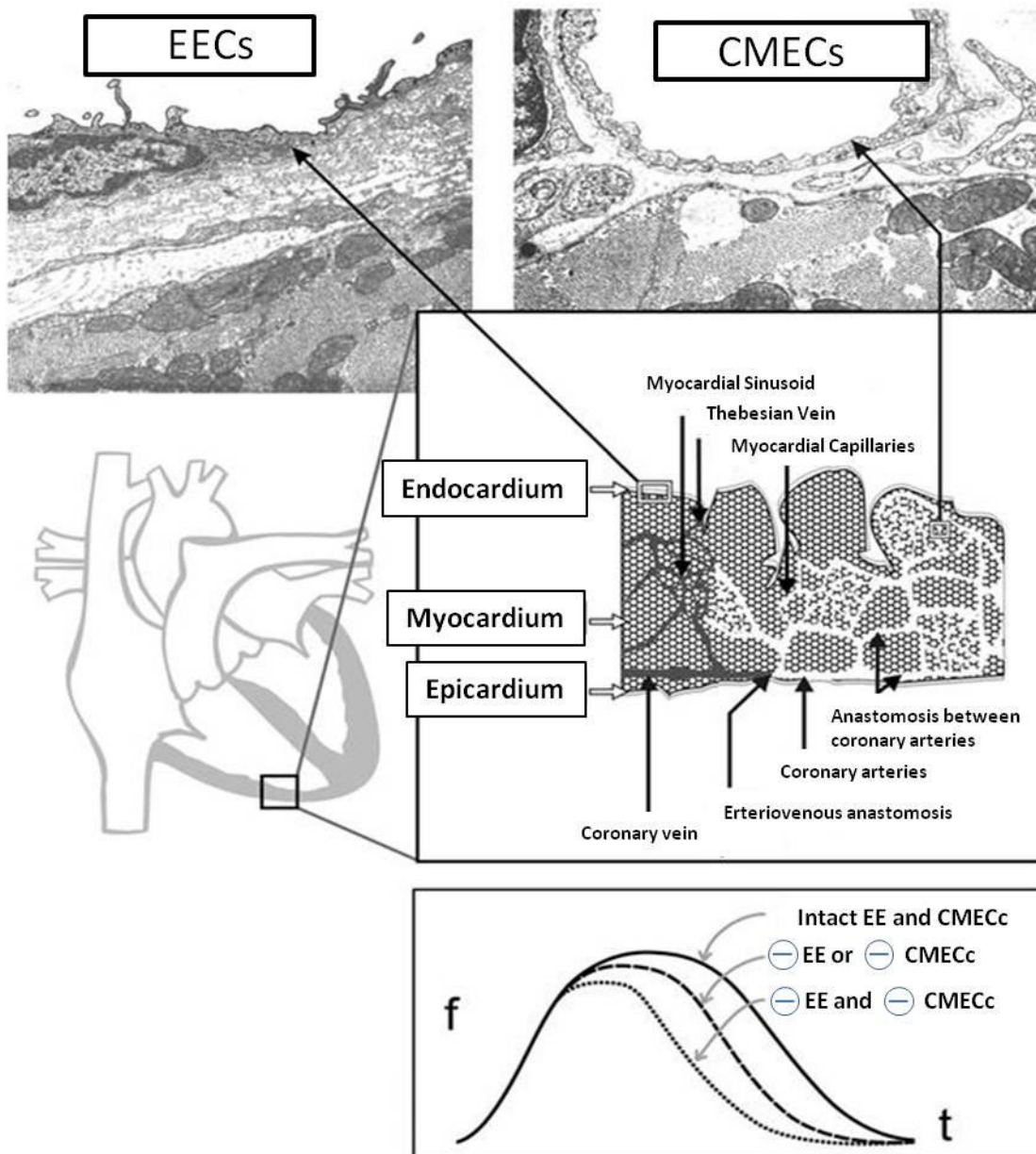


Figure 1.13: Cardiac ECs: Endocardial ECs (EECs) and cardiac microvascular ECs (CMECs), endothelium. The ventricular wall (inset) consists of the epicardium, the myocardium, and the endocardium. The endocardium includes a fibroelastic layer, a basement membrane, and a luminal layer of ECs, i.e., the EE [top left transmission electron microscopy (TEM) micrograph]. The distance between the CMECs (top right TEM micrograph) and cardiomyocytes is usually $<1 \mu\text{m}$; between EECs and cardiomyocytes, the distance ranges from $1 \mu\text{m}$ in small mammals to $>50 \mu\text{m}$ in humans. Analogous, and additive, myocardial actions of EECs and CMECs result in contractile twitch prolongation and increased peak

force development. The traces in the bottom panel represent isometric twitches (force, f vs. time, t traces) from isolated papillary muscles with intact EECs and CMECs, compared with twitches from muscles after selective EEC damage (-EE) by quick immersion of the papillary muscle in 0.5% Triton X-100 and to twitches from muscles with CMEC dysfunction (-VE) induced by a bolus injection of diluted Triton X-100 in a Langendorff heart before isolation of the papillary muscle. Endothelial damage or dysfunction induced premature relaxation and concomitantly decreased peak force development (modified from Brutsaert et al., 1998).

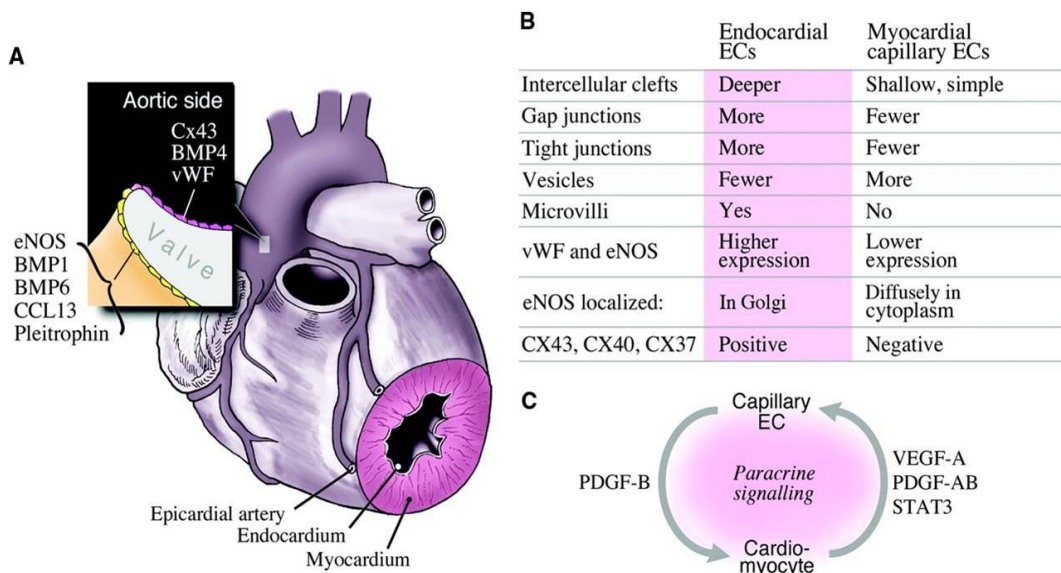


Figure 1.14: ECs in the heart. **A:** The three main endothelial compartments of the heart: the epicardial arteries, myocardial microvessels, and the endocardium (including valves) and selected side-specific differences in gene expression on aortic valve leaflets. **B:** Comparison of properties between EECs and CMECs. **C:** Examples of bidirectional crosstalk between CMECs and cardiomyocytes. VEGF and PDGF-AB are released by cardiomyocyte, whereas signal transducer and activator of transcription-3 (STAT3) is an intracellular transcription factor involved in regulating the expression of paracrine factors. BMP indicates bone morphogenetic protein (Aird, 2007b).

1.2.3.3 Cardiac microvascular endothelial cells (CMECs).

As mentioned previously, the endothelium in the heart is categorised into two subtypes, namely the coronary vascular endothelium and the cardiac endothelium (Strijdom and Lochner, 2009c). The coronary vascular endothelium constitutes the epicardial coronary arterial and venous ECs, and the intra-myocardial coronary arterial and venous ECs, whereas the cardiac endothelium constitutes the CMECs (> 90 % myocardial capillary derived) and EECs (Strijdom and Lochner, 2009c). Most cardiac endothelium-based studies employ ECs harvested from the larger blood vessels of the heart. Studies focusing on the properties and behaviour of myocardial capillaries and myocardial capillary-derived ECs (CMECs) under various physiological and pathophysiological conditions are few and far between, and their role in the context of particularly endothelial injury such as ED remains poorly understood.

Microvascular ECs lack vascular smooth muscle cells (VSMCs) and therefore the NO released by these EC subtypes is very unlikely to be involved in the regulation of vascular tone (Strijdom and Lochner, 2009c). Given the close proximity between CMECs and cardiomyocytes, the NO released from CMECs is likely to regulate the function and activity of underlying cardiomyocytes, in addition to maintaining integrity of the cardiac endothelium. Therefore, any injury to the CMECs and their subsequent response to it, could have a direct impact on the underlying cardiomyocyte and as a result, on myocardial function. For this reason, it is imperative that more studies are undertaken to investigate pathophysiological conditions (such as ED) in CMECs, and to explore the underlying cellular mechanisms.

1.3 Endothelial responses to harmful stimuli.

1.3.1 Vascular endothelium is a target of harmful stimuli.

The chronic presence of cardiovascular risk factors and resulting exposure to harmful circulating stimuli associated with these conditions, eventually overwhelm the defense mechanisms of the vascular endothelium, hence compromising its integrity and ultimately initiating ED (Deanfield *et al.*, 2007). For the purpose of this study, only some of these harmful stimuli will be discussed.

1.3.1.1 Tumour Necrosis factor alpha (TNF- α), Asymmetric dimethylarginine (ADMA), hypoxia, hyperglycaemia, oxidized-low density lipoprotein (LDL) and oxidative stress.

As mentioned previously, the location of the endothelium at the interface between circulating blood and the vessel wall endows upon it an obligatory role in vasoregulation, the provision of an anti-thrombotic surface facilitating laminar blood flow, and selective permeability (Limaye and Vades, 2007). As a natural consequence, its distinct location makes the endothelium a primary target of circulating harmful stimuli.

1.3.1.1.1 TNF- α :

TNF- α , a 17 kDa polypeptide, was originally discovered as a molecule released by macrophages in endotoxin exposed rabbits that resulted in hemorrhagic necrosis of experimental tumors (Carswell *et al.*, 1975). Now TNF- α is considered one of the most important cytokines and major effector of macrophage-mediated host defense and tissue injury, while also playing a crucial role in innate and adaptive immunity, cell proliferation, and apoptotic processes (Pober *et al.*, 2006).

Several mechanisms have been suggested for the induction/activation of NOS by TNF- α . Yoshizumi *et al.* (1993) showed that TNF- α markedly reduced mRNA levels of constitutive

(cNOS) in human umbilical vein ECs (HUVECs) in a dose- and time-dependent manner without changing the rate of cNOS gene transcription. Another study, however, suggested that TNF- α increases eNOS activity in HUVECs (De Palma *et al.*, 2006). Activation of eNOS by TNF- α requires activation of PKB/Akt, a known eNOS activator, via sphingosine-1-phosphate (Sph1P) receptor activation (Zhang H *et al.*, 2009). Sph1P receptor is activated by Sph1P, a sphingolipid involved in proliferation, survival, migration and differentiation of these cells, generated through neutral sphingomyelinase 2 (N-SMase2) and sphingosine kinase 1 (SK1) activation (De Palma *et al.*, 2006).

According to Zhang H *et al.* (2009), TNF- α -mediated activation of eNOS can lead to increased NO generation, which exerts protective effects on dendritic cell (DC) adhesion to endothelium induced by TNF- α itself. It has also been suggested that TNF- α may increase iNOS expression by activating nuclear factor κ B (NF- κ B) (Zhong L *et al.*, 1999). TNF- α -induced iNOS mRNA expression in microvascular ECs could be decreased by rooperol (a dicatechol from the South African plant *Hypoxis rooperi*) administration, which is an anti-inflammatory agent in the treatment of several inflammatory disorders (Bereta *et al.*, 1997). In HUVECs, the effect of TNF- α on iNOS expression was not affected by statin treatment, whereas reduced eNOS expression was reversed by rosuvastatin and ceruvastatin by inhibiting HMG-CoA (3-hydroxy-3-methylglutaryl-CoA) reductase and subsequent blocking of isoprenoid synthesis (Jantzen *et al.*, 2007).

Evidence suggests that TNF- α impairs endothelium-dependent and NO-mediated vasodilation in various vascular beds, e.g. mouse coronary arterioles (Gao *et al.*, 2007), rat coronary arterioles (Picchi *et al.*, 2006), cat carotid arteries (Aoki *et al.*, 1989) and bovine small coronary arteries (Ahmad *et al.*, 2002). Picchi *et al.*, (2006) demonstrated that ED in pre-diabetic metabolic syndrome is a result of the effects of TNF- α and the subsequent production of O₂⁻ (superoxide radical).

Myocardial I/R has been shown to increase the expression of TNF- α , which induced activation of XO (xanthine oxidase) and the production of O₂⁻, leading to coronary ED (Zhang *et al.*, 2006). Gao *et al.* (2007) showed that advanced glycation end-product (AGE)/receptor for AGEs (RAGE) and NF- κ B signalling play a pivotal role in elevating circulating and/or local vascular TNF- α production (Zhang *et al.*, 2009). The increased TNF- α

expression induces the production of ROS, leading to ED in Type 2 diabetes (Zhang *et al.*, 2009). Therefore, from the findings of these studies, it seems that ED associated with TNF- α in pathophysiological conditions is linked to excess production of ROS and a decrease in NO bioavailability (Zhang *et al.*, 2009).

Although some studies have shown that TNF- α induces increased NO, there are also studies where the opposite observation was made, and that this phenomenon is likely to be concentration (Chen TG *et al.*, 2011) and time (Tsou *et al.*, 2010) dependent in *in vitro* studies. According to some studies, TNF- α appears to decrease the bioavailability of NO by (i) diminishing the production of NO (Goodwin BL *et al.*, 2007; Picchi *et al.*, 2006; Ahmad *et al.*, 2002; Greenberg *et al.*, 1993), and (ii) enhancing the removal of NO (Gao *et al.*, 2007). Picchi *et al.* (2006) reported that the real-time production of NO in isolated coronary arteries from ZOF rats (Zucker Obese Fatty rats; a model of pre-diabetic metabolic syndrome) and acetylcholine (ACh)-induced NO production were significantly lower in ZOF rats compared with lean control rats. This result suggested that higher concentrations of circulating TNF- α and protein expression of TNF- α diminished NO bioavailability in ZOF rat coronary arteries via the decreased expression of eNOS (Figure 1.15).

Many studies have shown that the direct effects of TNF- α on eNOS are via down-regulating eNOS activation and expression and diminishing NO production in diverse vasculatures (Goodwin BL *et al.*, 2007; Picchi *et al.*, 2006; Ahmad *et al.*, 2002; Greenberg *et al.*, 1993). In addition to eNOS, other factors are also involved in regulating NO production, such as a functional citrulline/NO cycle (Xie *et al.*, 2000; Goodwin BL *et al.*, 2004; Hattori *et al.*, 1994; Husson *et al.*, 2003). The citrulline/NO cycle is regulated by ASS (argininosuccinate synthase) (Zhang *et al.*, 2009). NO is synthesized from the conversion of L-arginine to L-citrulline mediated by eNOS, and ASS catalyses the rate-limiting step in the arginine regeneration through the citrulline/NO cycle and appears to be co-coordinately regulated with eNOS activity (Oyadomari *et al.*, 2001)(Figure 1.15). Goodwin BL *et al.* (2007) have shown that TNF- α diminished the mRNA and protein expression of ASS in aortic ECs and directly resulted in the reduced production of NO. Gao and co-workers (Gao *et al.*, 2007; Picchi *et al.*, 2006) reported that TNF- α impaired

NO-mediated vasodilation in Type 2 diabetic coronary arterioles. A neutralizing antibody to TNF- α decreased the formation of ROS (O_2^- , $ONOO^-$ and H_2O_2) and improved NO-mediated vasodilation. TNF- α stimulates the endothelial generation of ROS by activation of NADPH oxidase, perhaps via the subunits gp91phox, NOX-1, p47phox and p22phox (Figure 1.15).

NO has been implicated as the major mediator of endothelium-dependent relaxation, but, as discussed previously, EDHF also plays an important role in regulating vascular tone and vasoreactivity, particularly in resistance blood vessels, where a small change in membrane potential causes a significant change in diameter (Feletou M and Vanhoutte, 2006). Type 2 diabetes impairs EDHF-mediated vasodilation (De Vriese *et al.*, 2000); however, the mechanisms have not been clearly elucidated. For example, the role of TNF- α in EDHF-mediated vascular dysfunction is controversial. Wimalasundera *et al.* (2003) reported that TNF- α did not inhibit EDHF-dependent vasodilation, whereas Gillham *et al.* (2008) observed a direct effect of TNF- α on EDHF-mediated vasodilation in human omental arteries by incubation of 1 nmol/l TNF- α for 1 or 2 hours. Their results showed that TNF- α impaired EDHF-mediated dilation. In addition, Kessler *et al.* (1999) found that TNF- α reduced EDHF synthesis with direct measurement of hyperpolarization in porcine coronary arteries, and Park *et al.* (2008) showed that EDHF-mediated dilation in coronary arterioles from Type 2 diabetic mice (dbTNF-/dbTNF-) was enhanced compared with Type 2 diabetic (db/db) mice. The possible mechanism of impaired EDHF-mediated vasodilation by TNF- α may be via epoxyeicosatrienoic acid (EETs), which is regarded as one of the candidate EDHF's. EETs are synthesized in the ECs from arachidonic acid (AA) through cytochrome P450 oxygenase (Zhang *et al.*, 2009). TNF- α down-regulated the protein expression of cytochrome P450 2C, which is the major family of cytochrome P450 mono-oxygenases in porcine aortic ECs (Kessler *et al.*, 1999) (Figure 1.15).

NO and ROS may play a dual role (i.e., inhibiting or promoting) in TNF- α -induced EC apoptosis (Xia *et al.*, 2006). Changes associated with endothelial apoptosis are embedded in a complex array of interdependent events that will be discussed in more detail below. These changes can affect many aspects of endothelial function, and may be directly linked to some manifestations of disease, such as atherosclerosis, allograft

vasculopathy, hypertension, congestive heart failure (CHF) and sepsis and associated syndromes (Stefanec, 2000).

Apoptotic ECs release interleukin 1 (IL-1) (Liew *et al.*, 2010; Dignat-George and Boulanger, 2011), which will have several important effects: (1) IL-1 may enhance apoptosis of ECs (Liew *et al.*, 2010); (2) it may enhance endocytosis of apoptotic bodies by surrounding ECs (Dignat-George and Boulanger, 2011) and (3) IL-1 activates neighboring ECs through the activation of nuclear factor κ B (NF κ B) (Grivennikov *et al.*, 2010; Partridge *et al.*, 2007; Meziani *et al.*, 2008). While activation of NF κ B may protect the EC from apoptosis (Mattson and Meffert, 2006) in an environment that is likely to be predominantly pro-apoptotic, it can also lead to the expression and release of adhesion molecules for inflammatory cells and production of pro-inflammatory cytokines (Zhang, 2008). Leukocytes may adhere, transmigrate, release proteases, cause additional endothelial injury and lead to the development of inflammatory changes in the vessel wall (Stefanec, 2000). Release of adhesion molecules prevents further leukocyte adherence (Gawaz *et al.*, 2005), but may at the same time cause leukocyte activation and lead to release of additional pro-inflammatory mediators or proteases (Ouedraogo *et al.*, 2007; Gawaz *et al.*, 2005), thereby giving rise to endothelial injury or apoptosis in nearby or distant endothelial surfaces. It has been suggested that mediators other than IL-1 participate in the above events (Stefanec, 2000), such as TNF- α .

Secretion of TNF- α by the endothelium has been demonstrated *in vitro* (Luan *et al.*, 2010). TNF- α plays a major role in inflammatory responses, causing apoptosis by signalling *via* the death receptors (Basuroy *et al.*, 2006). Signalling *via* "death receptors," such as the TNF- α receptor 1 (TNFR-1/CD120a), can trigger ECs to undergo apoptosis (Brouard *et al.*, 2002). Cross-linking of TNFR-1 leads to the recruitment of intra-cytoplasmic signal transduction molecules, e.g. TNF receptor-associated death domain (TRADD), Fas-associated death domain (FADD), and receptor-interacting protein (RIP) (Brouard *et al.*, 2002; Chen G and Goeddel, 2002). These molecules form the death-inducing signalling complex (DISC), which activates serine proteases, referred to as caspases (Thorburn, 2004). Caspase activation by DISC occurs via FADD-dependent recruitment and proximal catalytic cleavage/activation of pro-caspase-8 into the active form of caspase-8 (Brouard

et al., 2002; Reed, 2000), which activates additional pro-caspases into active caspases, e.g. caspase-3, that execute the terminal phase of apoptosis (Reed, 2000).

The mitochondrion plays a key role in the initiation and amplification of the apoptotic process (Norberg and Zhivotovsky, 2010). During apoptosis, it releases cytochrome c, which disrupts its electron transport chain. While normal oxidative phosphorylation loses some 1 to 5% of electrons to superoxide production, this percentage increases with loss of cytochrome c from the mitochondria of the apoptotic cell (Norberg and Zhivotovsky, 2010; Serviddio *et al.*, 2011). The freely diffusible NO and newly produced superoxide react to form peroxynitrite, itself a toxic and pro-apoptotic substance (Gregersen and Bross, 2010). NO is consumed in this reaction and is not available for its normal role in vasodilatation, inhibition of platelet aggregation, and prevention of endothelial apoptosis, as well as inhibition of vascular smooth muscle cell proliferation and leukocyte adhesion (Gregersen and Bross, 2010; Lamas, 2010; Pae *et al.*, 2010).

Normal anti-coagulant properties of vascular endothelium are lost during apoptosis (Stefanec, 2000). The surface of the apoptotic cell exhibits increased tissue factor pro-coagulant activity, as well as reduced surface thrombomodulin, heparan sulfate, and tissue factor pathway inhibitor expression (Aksu *et al.*, 2012). This leads to increased thrombin formation by both adherent and detached apoptotic ECs. Prostacyclin production is decreased during endothelial apoptosis (Levi and van der Poll, 2010). This might, apart from a reduced anti-apoptotic effect (Levi and van der Poll, 2010), lead to loss of inhibition of platelet activation (Levi and van der Poll, 2010). Both activated platelets and thrombin can enhance inflammatory and pro-apoptotic events through activation of leukocytes and ECs (Harlan, 2010; Jennings, 2009). Complement activation *via* the alternative pathway has been observed on apoptotic ECs (Chen W *et al.*, 2010). While this activation may enhance the clearance of apoptotic cells by phagocytes, it can also activate leukocytes and ECs, and mediate additional endothelial injury or apoptosis (Stefanec, 2000).

Adrenomedullin (vasodilation; Nishikimi *et al.*, 2011) and ET-1 (vasoconstriction; Thorin and Webb, 2010) levels are elevated in circumstances associated with endothelial equilibrium disturbance (Stefanec, 2000). Both were found to have an

autocrine/paracrine antiapoptotic effect on ECs (Nishikimi *et al.*, 2011; Thorin and Webb, 2010). Their secretion in circumstances associated with endothelial injury, activation, and apoptosis is controlled independently (Trimarchi, 2011), and may represent a mechanism that limits endothelial damage and enhances its recovery, while adjusting vascular tone and blood flow in the distribution of disturbed endothelial-derived vasomotor control.

It is clear from the above discussion that in the case of *in vitro* studies, the effects of TNF- α on NO production, ROS production and cell viability varies between different EC types, and is concentration and time-dependent. In view of this, data from various *in vitro* studies on the effects of TNF- α are often contradictory (please refer to Table 1.3 for a summary of the effects of different concentrations of TNF- α on ECs focusing on the NOS-NO biosynthesis pathway, oxidative stress and cell viability measurements). Therefore the exact mechanisms by which TNF- α exerts its effects at various time points and concentrations on different cell types, still remain unclear.

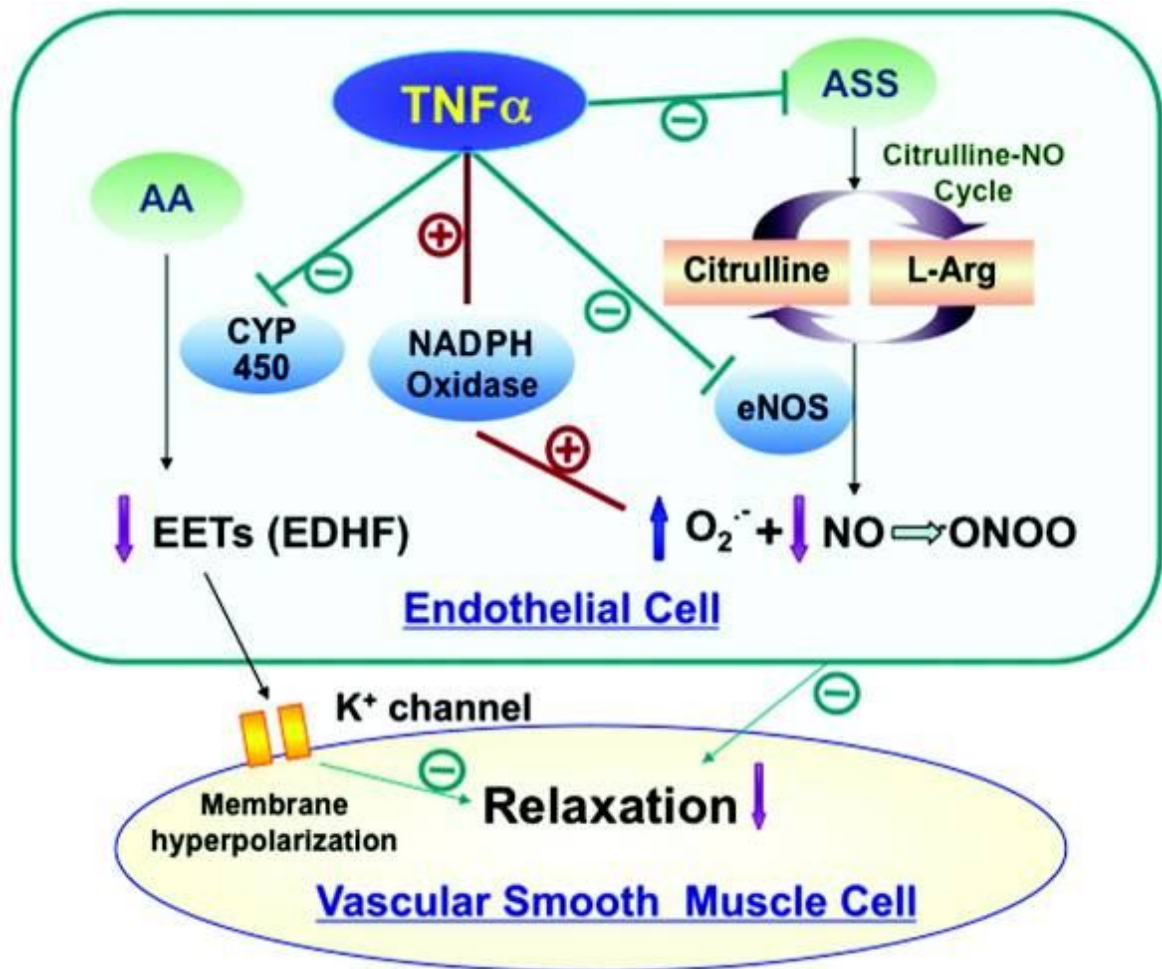


Figure 1.15: Role of TNF- α in ED. TNF- α reduces the production of NO through the inhibition of the enzyme expression of argininosuccinate synthase (ASS) and eNOS, and enhances the removal of NO through the increase in NADPH-dependent $O_2^{\cdot-}$ production to react with NO to form $ONOO^-$. As a consequence, TNF- α decreases the bioavailability of NO resulting in reduced induction of vascular smooth muscle relaxation. TNF- α also diminishes EETs, one of the candidate EDHFs, via the inhibition of cytochrome P450 (CYP 450) enzyme activity (Zhang *et al.*, 2009).

Table 1.3: Selection of *in vitro* EC studies investigating the effects of TNF- α stimulation.

TNF- α treatment	Cell / <i>in vitro</i> model	NOS-NO measurements	Oxidative stress	Viability	Reference
100 U / ml; 30 min	Coronary microvascular ECs	Not performed	\uparrow NADPH-oxidase (p47)	Not performed	Li C <i>et al.</i> , 2002, 2005
50 ng / ml; 0 – 60 min; max 6 hrs	HUVECs	NO measurements not performed; \uparrow phospho eNOS; \uparrow phospho PKB/Akt	Not performed	Not performed	De Palma <i>et al.</i> , 2006
5-10 ng / ml; 10 min	BAECs	\downarrow Nitrogen Oxide (NOx); \downarrow phospho eNOS; \downarrow phospho PKB/Akt (insulin and flow stimulated)	Not performed	Not performed	Kim HJ <i>et al.</i> , 2006a
300 U / ml; 1 h; max 4 hrs	HUVEC hybrid	Not performed	Superoxide / ROS levels unchanged	Not performed	Arai <i>et al.</i> , 1998
100 pg / ml; 48 hrs	BAECs	NO measurements not performed; \downarrow eNOS protein; \downarrow eNOS gene promoter activity; \downarrow NOS activity	Not performed	Not performed	Anderson <i>et al.</i> , 2004
0.1, 1, 10 ng / ml; 1 hr	HUVECs	Not performed	\uparrow Mitochondrial ROS	\uparrow Necrosis at 10 ng / ml TNF- α	Corda <i>et al.</i> , 2001
10 ng / ml; 16 hrs	Intrapulmonary arterial segments	NO measurements not performed; \uparrow eNOS staining (immunohistochemistry)	\uparrow superoxide levels (via \uparrow NADPH-oxidase activity); \uparrow nitrated protein staining	Not performed	Muzaffar <i>et al.</i> , 2004
40 ng / ml; 24 hrs	HUVEC (ECV304)	\uparrow Nitrites+Nitrates; eNOS measurements not performed	\uparrow H ₂ O ₂ ; \uparrow superoxide	\uparrow Apoptosis; \downarrow MTT	Wang P <i>et al.</i> , 1994
2 ng / ml; 8 hrs	Human coronary artery ECs	Unchanged nitrites+nitrates (Griess); unchanged eNOS expression	Not performed	Not performed	Jiang J <i>et al.</i> , 2010
40 ng / ml; 24 hrs	HUVEC (ECV304)	\uparrow nitrites+nitrates (Griess);	\uparrow ROS production	\uparrow Apoptosis;	Xia <i>et al.</i> , 2006

		↓eNOS expression; ↑iNOS expression	↑ Nitrotyrosine protein	↑ LDH release ↓ MTT staining	
5 – 1000 pg / ml; 24 hrs	HUVECs	Unchanged nitrites+nitrates (Griess); eNOS measurements not performed	↑Oxidative stress	Unchanged viability (trypan blue staining)	Scalera <i>et al.</i> , 2003
0.1 – 30 ng / ml; 18 hrs	HUVECs	NO measurements not performed; ↑ citrulline levels; eNOS measurements not performed	Not performed	Not performed	Radomski <i>et al.</i> , 1993
40 ng / ml; 24 hrs	HUVECs	↑Nitrites+Nitrates (Griess); eNOS measurements not performed	Not performed	↑ Apoptosis	Luo <i>et al.</i> , 2006
0.1 – 3 ng / ml; 4 – 24 hrs	HUVECs	NO measurements not performed; ↓cNOS mRNA	Not performed	Not performed	Yoshizumi <i>et al.</i> , 1993
50 ng / ml; 30 min – 24 hrs	Bovine pulmonary microvessel ECs	↓Nitrites (Griess) at 4 hrs; unchanged at 24 hrs; ↓eNOS protein at 24 hrs	Not performed	Unchanged viability (trypan blue staining)	Bove <i>et al.</i> , 2001
20 ng / ml; 1 – 24 hrs	HUVECs	Not performed	↑Superoxide ↑ Mitochondrial ROS	↑ ↓ Apoptosis depending on ROS source	Desphande <i>et al.</i> , 2000
0 – 50 ng / ml; 20 – 30 hrs	Bovine pulmonary artery ECs	Not performed	Not performed	↑ Apoptosis	Polunovsky <i>et al.</i> , 1994
10 ng / ml; 24 hrs	BAECs	↓eNOS mRNA and protein; ↓nitrite levels	Not performed	Not performed	Goodwin BL <i>et al.</i> , 2007
20 ng / ml; 24 hrs	HUVECs / BAECs	NO measurements not performed; ↓eNOS mRNA stability and protein	Not performed	Not performed	Yan <i>et al.</i> , 2008
60 000 U / ml	Microvascular and macrovascular ECs	↑Nitrites and ↑iNOS mRNA (TNF-α + Interferon-gamma; TNF-α + lipopolysaccharide	Not performed	Not performed	Geiger <i>et al.</i> , 1997

Table 1.4: Summary of the detrimental effects of TNF- α in the heart (Sack, 2002).

- The effect of TNF- α on cardiac contractile function has been shown to be both concentration- and time-dependent with a minimal threshold, seemingly required to induce a negative inotropic effect (Yokoyama T *et al.*, 1993).
- TNF- α expression and peptide production are up-regulated in the adult heart in response to pressure overload and in response to stretch in isolated cardiac myocytes (Kapadia *et al.*, 1997; Yokoyama T *et al.*, 1997). These hemodynamic loads elicit cardiomyocyte hypertrophy and extracellular matrix remodeling as phenotypic alterations that are thought to be adaptive responses in order to maintain normal cardiac contractility and homeostasis (Sack, 2002).
- The association of inflammation with atherosclerosis is now fairly well established (Mehta JL and Li, 1999; Ross, 1999) and the expression of pro-inflammatory cytokines such as TNF- α have been identified throughout the full spectrum of atherosclerotic development (Sack, 2002).
- The inflammatory reaction has been well documented in patients following percutaneous coronary intervention (Inoue *et al.*, 1999; Kamijikkoku *et al.*, 1998) and the expression of TNF- α has been shown to be elevated in restenotic lesions retrieved by arthroectomy (Clausell *et al.*, 1995).
- TNF- α is thought to play an integral role in the inflammatory reaction present in myocarditis (Feldman & McNamara, 2000; Satoh *et al.*, 2000; Seko *et al.*, 1997).
- Myocardial TNF- α production has been well documented during acute myocardial ischaemia with or without reperfusion (Irwin *et al.*, 1999; Meldrum DR *et al.*, 1998a; Meldrum DR *et al.*, 1998b).

Cardioprotective properties of TNF- α :

Apart from the detrimental effects of TNF- α , as described above, it was also shown in a study by Lecour *et al.* (2005) that TNF- α can protect the myocardium. It does so by mimicking classic ischaemic preconditioning (IPC) in a dose- and time-dependent manner, activating the signal transducer and activator of transcription-3 (STAT-3) signalling pathway (Lecour *et al.*, 2005).

1.3.1.1.2 Asymmetric dimethylarginine (ADMA):

ADMA was first described by Vallance *et al.* (1992a) as an endogenous inhibitor of NOS. Since then, the role of this molecule in the regulation of endothelial NO synthesis has increasingly attracted attention, especially as a novel cardiovascular risk factor (Böger RH, 2004). ADMA is found to be elevated in renal failure, CVD and diabetes mellitus (Böger, 2003b; Von Haehling *et al.*, 2010; Vallance *et al.*, 1992b). A low ratio of Arginine to ADMA (Arg/ADMA ratio) is also a marker of ED (Böger *et al.*, 2007). Prospective investigations of ADMA have highlighted its role as a predictor of CVD events or death in patients with established coronary artery disease (Krempf *et al.*, 2005; Lu *et al.*, 2003; Schnabel *et al.*, 2005), advanced renal failure (Zoccali *et al.*, 2001) or other high-risk conditions (Böger, 2006).

ADMA is released when methylated proteins are degraded into their amino acid components during hydrolytic protein turnover (see figure 1.16) (Böger *et al.*, 2003b). Enzymatic degradation of ADMA by dimethylarginine dimethylaminohydrolases (DDAH) has attracted much attention (Böger RH, 2004). DDAH degrades ADMA to dimethylamine and l-citrulline. DDAH activity is found in almost all tissues, with high activities in kidney and liver (Kimoto *et al.*, 1995). There are two allelic isoforms of this enzyme, DDAH-1 and DDAH-2, which show different tissue expression patterns (Leiper JM *et al.*, 1999). DDAH-1 is present in many tissues that also express neuronal NO synthase, whereas DDAH-2 is mainly present in vascular tissues that co-express eNOS (Leiper JM *et al.*, 1999). DDAH activity is reduced by oxidative stress induced by TNF- α or oxidized LDL in vitro (Ito *et al.*, 1999); moreover, it is modulated by S-nitrosylation (Leiper JM *et al.*, 2002).

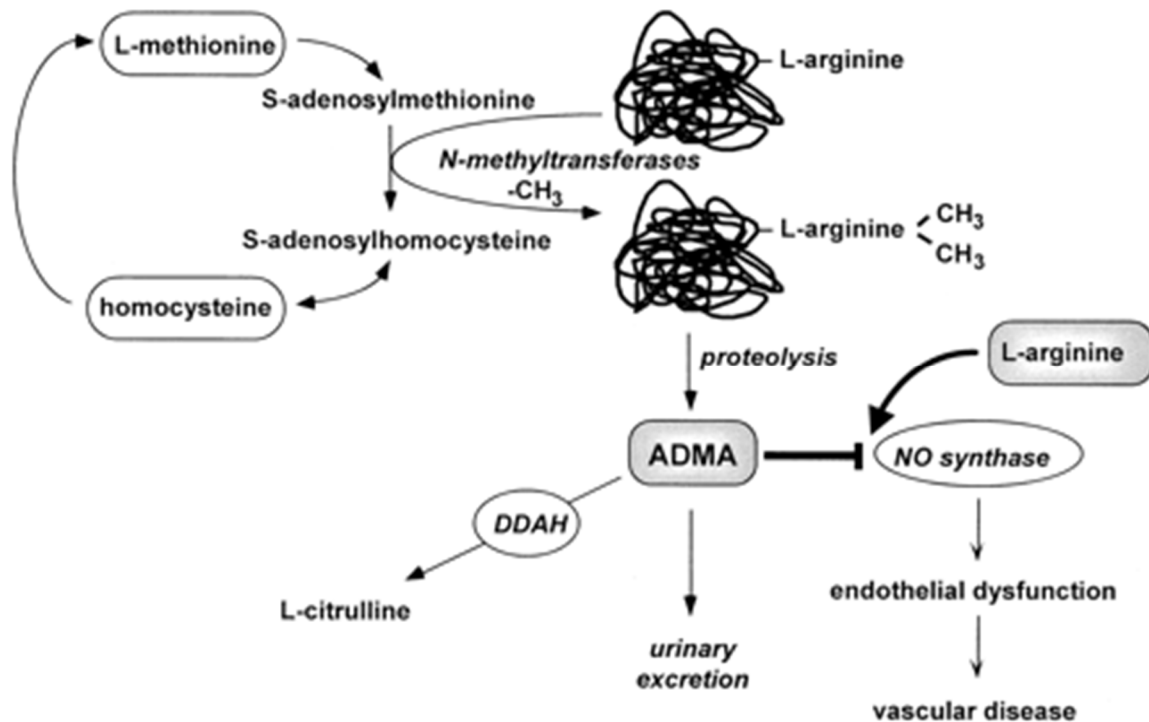


Figure 1.16: Schematic overview of biochemical pathways related to ADMA. Methylation of arginine residues within proteins or polypeptides occurs through N-methyltransferases, which utilize S-adenosylmethionine as a methyl group donor. After proteolytic breakdown of proteins, free ADMA is present in cytoplasm. It can also be detected circulating in human blood plasma. ADMA acts as an inhibitor of NOS by competing with the substrate of this enzyme, L-arginine, and causes ED and, subsequently, atherosclerosis. ADMA is eliminated from the body via urinary excretion and, alternatively, via metabolism by the enzyme DDAH to citrulline and dimethylamine (Böger RH, 2003a).

Targets of ADMA:

ADMA inhibits all 3 isoforms of NOS and is approximately equipotent with the pharmacological NOS inhibitor, L-NMMA (Vallance *et al.*, 1992a; MacAllister RJ *et al.*, 1994). In addition to blocking NO formation, L-NMMA treatment may uncouple NOS and lead to the generation of superoxide (Olken *et al.*, 1993; Pou *et al.*, 1999), and it is likely that ADMA can do the same.

Degradation of ADMA (The DDAHs):

Although symmetric dimethylarginine (SDMA) (the methylarginine that does not inhibit NOS) is eliminated almost entirely by renal excretion, ADMA and L-NMMA are extensively metabolized (McDermott, 1976; Ogawa T *et al.*, 1987). The major metabolic route is to citrulline and dimethylamine, a reaction catalyzed by DDAH (Ogawa T *et al.*, 1989; Kimoto *et al.*, 1995).

Cellular ADMA:

ADMA is generated within cells (Fickling SA *et al.*, 1993; Ueno *et al.*, 1992) and there is evidence that the cellular levels alter with pathophysiology (Vallance and Leiper, 2004). Although the precise concentration of ADMA within cells is unclear, ECs concentrate methylarginines so that if methylarginines are added to culture medium, the concentrations in the cell rise to approximately 5-fold higher than in surrounding medium (Bogle *et al.*, 1995). This concentration of methylarginines is probably attributable to transport by the arginine transport system referred to as the Y⁺ transporter (Bogle *et al.*, 1995). ECs express both protein arginine methyltransferases (PRMTs) and DDAHs (MacAllister RJ *et al.*, 1996) and inhibition of DDAH leads to significant accumulation of ADMA (MacAllister RJ *et al.*, 1996; Ito *et al.*, 1999; Ueda *et al.*, 2003). Furthermore, functional studies in vascular rings suggest that inhibition of DDAH produces changes in endothelial function consistent with substantial concentrations of ADMA in the vicinity of

eNOS (MacAllister RJ *et al.*, 1996). The overall output of ADMA from ECs presumably is a balance between rates of arginine methylation, rates of degradation of proteins containing methylated arginine, rates of metabolism of ADMA by DDAHs, and the rates of active extrusion from the cell (Vallance and Leiper, 2004). The relative importance of each component is not yet known, but the metabolic capacity of DDAH is high and it seems likely that DDAH activity will usually be the major determinant of overall ADMA levels within a cell.

ADMA is relatively stable and can diffuse between cells (Vallance and Leiper, 2004). The ADMA generated in one cell is capable of inhibiting NOS in another cell (Fickling SA *et al.*, 1999). This interaction has been clearly demonstrated for macrophages and ECs (Fickling SA *et al.*, 1999) and presumably may also occur for smooth muscle cells and ECs (Vallance and Leiper, 2004). This raises the possibility that ADMA provides a mechanism by which smooth muscle cells may signal to the endothelium (Vallance and Leiper, 2004).

Cardiovascular Effects of ADMA:

ADMA inhibits NOS and produces the effects expected of an isoform-nonspecific NOS inhibitor (Achan *et al.*, 2003; Kielstein *et al.*, 2004; Barba *et al.*, 2000). It elevates blood pressure, causes vasoconstriction, impairs endothelium-dependent relaxation, and increases EC adhesiveness (Vallance *et al.*, 1992b; Achan *et al.*, 2003; Boger *et al.*, 2000b). Extrapolation from other NOS inhibitors suggests that long-term exposure to ADMA would be expected to enhance atherogenesis and produce sustained hypertensive damage to end organs (Cayatte *et al.*, 1994; Naruse *et al.*, 1994).

In the heart, ADMA reduces heart rate and cardiac output, and other NOS inhibitors have similar effects (Achan *et al.*, 2003; Kielstein *et al.*, 2004). Left ventricular hypertrophy is also a feature of prolonged NOS inhibition (Vallance and Leiper, 2004).

ADMA also inhibits angiogenesis in animal models (Jang *et al.*, 2000). Furthermore, DDAH overexpression promotes angiogenic processes in cells in culture (Smith CI *et al.*, 2003) and in experimental tumors *in vivo* (Kostourou V *et al.*, 2002, 2003). DDAH

overexpression is also associated with an increase in vascular endothelial growth factor expression, and this seems to be important in promoting the angiogenesis (Smith CI *et al.*, 2003).

See table 1.5 for an overview of ADMA.

Table 1.5: ADMA in a nutshell (Vallance and Leiper, 2004).

Known	Not Known
ADMA is a competitive inhibitor of NOS	Whether endogenous ADMA concentrations increase sufficiently to inhibit NO production in vivo
ADMA is a product of protein turnover	Whether DDAH activity is the major determinant of ADMA levels in vivo
ADMA is metabolized by DDAH	Whether ADMA has a causal role in pathophysiology
ADMA is cleared by the kidney	Other than for renal failure, the data on changes with disease states are not consistent and the reason is not clear
Exogenous ADMA inhibits NO generation in tissue culture and organ bath experiments	
Infused ADMA reduces forearm blood flow in humans	
Infused ADMA reduces cardiac output and increases systemic vascular resistance in Humans	
Plasma ADMA concentration is increased in some disease states associated with ED and/or reduced NO production	

1.3.1.1.3 Hypoxia:

The metabolic and molecular changes in response to hypoxia/reoxygenation have been extensively investigated and reviewed, which has greatly contributed to our understanding of the pathophysiological modifications observed in organs subjected to ischaemia and reperfusion, including the heart (Michiels *et al.*, 2000). In view of their location at the inner lining of blood vessels, ECs are particularly and frequently exposed to variations in oxygen tension (Michiels *et al.*, 2000), and it is known that hypoxic conditions have profound effects on endothelial function (Michiels *et al.*, 2000).

Endothelial cell–neutrophil interactions (see figure 1.17):

One of the most pronounced effects of hypoxia on ECs is to increase EC adhesiveness for neutrophils (Nathan, 2006; Millar *et al.*, 2007). This phenomenon has been observed both *in vitro* and *in vivo* (Ploppa *et al.*, 2010) during hypoxia only, independent of subsequent reoxygenation.

In general, leukocyte emigration from the blood stream occurs through a sequential three-step process mediated by several adhesion molecules as well as chemoattractant/activator molecules (Muller, 2009). The initial rolling phase is mediated by selectins and consists in a slowing down of the leukocyte movement at the surface of the endothelium. Subsequently, firm adherence occurs via the interaction of the leukocyte β 2-integrins with ligands such as intercellular adhesion molecule-1 (ICAM-1). This binding requires activation of the integrins by exposure of the neutrophils to chemoattractant/activator molecules like interleukin-8 or platelet-activating factor (PAF) (Kumar SD *et al.*, 2011). Finally, transmigration through the endothelium occurs, triggered by a gradient of chemotactic factors (Williams *et al.*, 2011).

Some molecular basis for hypoxia-induced adherence of neutrophils to ECs has been untangled and the data obtained from human umbilical vein ECs (HUVECs) are summarized in Figure 1.17 (Michiels *et al.*, 2000). It follows the general pattern mentioned above and is the consequence of EC activation by hypoxia.

The hypoxia signalling cascade involves different pathways necessary for rapid cell activation or for the regulation of gene expression; it seems to be dependent on the cell type and varies according to the degree of hypoxia (Clerk *et al.*, 2007). In differentiated HUVEC exposed to oxygen deficiency, the initiating event of the EC activation is a decrease in the mitochondrial respiratory chain activity (Shimoda and Polak, 2007). A decrease in mitochondrial potential has been observed in liver sinusoidal ECs exposed to hypoxia (Alchera *et al.*, 2010). Moreover, direct inhibition of the respiratory chain in HUVECs also leads to enhanced neutrophil adherence (DiStasi and Ley, 2009).

Different second messengers may be responsible for the hypoxia-induced activation of ECs. Firstly, a reduction in cAMP concentration is observed in hypoxic ECs, which may be responsible for an increased vascular leakage (Kolluru GK *et al.*, 2008). Secondly, an increase in the cytosolic calcium concentration is observed in differentiated HUVECs (Østergaard *et al.*, 2007; Boisseau *et al.*, 2009). Calcium ion regulates the activity of various enzymes and is a mediator of signal transduction for thrombin, histamine or bradykinin stimulation in ECs. An elevated calcium concentration activates phospholipase A₂ in hypoxic ECs (Lambert *et al.*, 2006), leading to the synthesis of high amounts of prostaglandins (Farooqui and Horrocks, 2006). Increased PGI₂ release from bovine pulmonary artery ECs (El-Haroun *et al.*, 2008) and from HUVECs (Camacho *et al.*, 2011) and increased PGI₂, prostaglandin F_{2α} (PGF_{2α}), prostaglandin D₂ (PGD₂) and prostaglandin E₂ (PGE₂) release from HUVECs were indeed observed under hypoxia (Wang Y, 2010), while in some experimental models, a decrease was observed (Yang Y *et al.*, 2013). It was suggested by a review from Crosswhite and Sun (2010) that the hypoxia-induced synthesis of prostanoids also inhibits NO production via an autocrine negative feedback mechanism which could partially explain the frequently observed decrease of EDRF release by ECs in hypoxia. Mizukami *et al.* (2007) have demonstrated that hypoxia induces COX-2 expression via the activation of the NF-κB p65 transcription factor in human ECs. These data indicate that, under hypoxia, both COX and phospholipase A₂ activity increases, which could account for the increase in prostaglandin synthesis in ECs exposed to hypoxia.

Activation of phospholipase A₂ in hypoxic ECs not only allows a large release of prostaglandins but also the synthesis of PAF (Schildknecht and Ullrich, 2009; Goracci *et al.*, 2010). *In vivo* and *in vitro* studies showed that PAF is a neutrophil-activating agent promoting this adherence to the endothelium after hypoxia or ischaemia (Badimon *et al.*, 2012; Dumas *et al.*, 2012). Different structurally unrelated PAF antagonists as well as the inhibition of PAF synthesis by oleic acid indeed block neutrophil adherence to hypoxic ECs (Dumas *et al.*, 2012). According to a review by Clossé *et al.* (2010), hypoxia alone induces a calcium-dependent exocytosis of the Weibel–Palade bodies. As mentioned before, these organelles, typical of ECs, store the vWF. This exocytosis leads to the release of vWF and to the overexpression of P-selectin which then sustains neutrophil binding (Nurden, 2011). This explains why hypoxia-induced neutrophil adherence can be blocked by antibodies against P-selectin (Gleissner *et al.*, 2008; Millar *et al.*, 2007). In addition to PAF and P-selectin, the hypoxia-induced neutrophil adherence also requires the neutrophil β 2 integrin CD18 (Parmley *et al.*, 2007; Barletta *et al.*, 2012) as well as the endothelial ICAM-1 (DiStasi and Ley, 2009).

Neutrophils not only adhere but are also activated when in contact with hypoxic HUVECs (Gupta *et al.*, 2010). This activation is characterized by an increased cytosolic calcium concentration, by the release of high amounts of superoxide anion and by the synthesis of leukotriene B₄ (Nathan *et al.*, 2006). They are also sensitive to hypoxic conditions (Walmsley *et al.*, 2005). Hypoxia *per se* is able to increase CD18/CD11b expression at the surface of neutrophils, resulting in an enhanced adhesion to ECs (Uzel and Holland, 2012). On the other hand, hypoxia has been shown to decrease free radical production and cytokine synthesis by neutrophils in response to various stimuli (Victor *et al.*, 2005; Watt *et al.*, 2005). It must be noted that the contact of neutrophils with activated ECs not only results in adherence and activation but also in delayed apoptosis, thereby prolonging their useful life (Watt *et al.*, 2005). In conclusion, hypoxia *per se* is able to activate the ECs as well as to initiate all stages of recruitment, rolling, adhesion and activation of neutrophils in ischemic organs (Holyer, 2011).

Tissue remodeling:

The vascular tone is regulated under normal conditions through the release by ECs of both vasorelaxing molecules such as NO and prostacyclin and vasoconstricting agents like ET-1 (Sprague and Khalil, 2009).

Hypoxia differentially affects pro-vasodilation and pro-vasoconstriction molecules, which ultimately creates a condition favorable for the development of vasoconstriction (Li YSJ *et al.*, 2005). Indeed, the basal and agonist-stimulated release of pro-vasodilatation factors by ECs is quickly inhibited by hypoxia (Deanfield *et al.*, 2007) and NO production remains very low even after long periods of hypoxia (24–48 h) (Bertuglia and Giusti, 2005). This seems to be due to a decrease in eNOS expression (Jin HG *et al.*, 2006). Hypoxia generally enhances the release of ET-1 by ECs *in vitro* (Pak *et al.*, 2007); however, in other studies, a decrease was observed (Weigand *et al.*, 2006; Modesti *et al.*, 2006). *In vivo*, an increase in ET-1 circulating level was observed and this was correlated with an induction of ET-1 gene transcription in lungs (Whitman *et al.*, 2008).

The effect of hypoxia on the release of endothelial-released mitogenic molecules has previously been described (Shao *et al.*, 2011). PGF_{2α} and basic bFGF were identified as the pro-vascular smooth muscle mitogenic mediators (Shao *et al.*, 2011). bFGF seems to be released from intracellular stores by hypoxic ECs since there is no induction of its synthesis by hypoxia (Ahn *et al.*, 2008). Other mitogens, such as platelet-derived growth factor-B (PDGF-B), have also been detected in ECs subjected to sustained hypoxia (Ahn *et al.*, 2008). The presence of PDGF and of ET-1, which also has mitogenic properties for smooth muscle cells, contributes to the pro-proliferative activity present in conditioned media from ECs undergoing sustained hypoxia (Stenmark *et al.*, 2006). In conclusion, the increased production of these different mitogens combined with the suppression of endothelial NO synthase would be expected to accelerate smooth muscle cell growth and to induce vascular remodeling (Robertson *et al.*, 2012).

In addition to increase the release of growth factors, hypoxia stimulates the production of some extracellular matrix proteins, such as thrombospondin-1 in human ECs (Carmeliet, 2003). Thrombospondin-1 modulates smooth muscle cell proliferation and migration and

may be a negative regulator of angiogenesis (Carmeliet, 2003). Chronic *in vivo* hypoxic exposure indeed induces medial hypertrophy of pulmonary vessels (Stenmark *et al.*, 2005; Stenmark *et al.*, 2006). Cell proliferation and matrix deposition in hypoxia reflects an imbalance between pro-proliferative and anti-proliferative stimuli, most of them derived from the endothelium.

EC proliferation itself is also affected by hypoxia (Kiefer *et al.*, 2002). The most potent and specific mitogen for the ECs is vascular endothelial growth factor (VEGF) (Otrock *et al.*, 2007). It is known to initiate angiogenesis *in vivo* (Hicklin and Ellis, 2005). Its expression is upregulated by hypoxia in numerous cell types including ECs (Ferrara *et al.*, 2003). In addition, an increased expression of the VEGF receptor *Flt-1* (Ferrara *et al.*, 2003) and a functional upregulation of the VEGF receptor KDR or *Flk-1* by hypoxia (Ferrara *et al.*, 2003) have been reported in response to hypoxia, which can be responsible for the stronger VEGF-induced mitogenic response of hypoxic ECs compared to normoxia.

The release of all these cytokines and growth factors by hypoxic ECs is generally the result of a complex cascade of processes which ends with the activation of transcription factors (Michiels *et al.*, 2000), such as activator protein 1 (AP-1) (Bergman *et al.*, 2003), nuclear factor-interleukin-6 (NF-IL-6) (Haddad and Hisham, 2005), nuclear factor kappa beta (NF- κ B) (Haddad and Hisham, 2005) and Egr-1 (Lo *et al.*, 2001). However, the prototype of the transcription factors regulated by hypoxia is hypoxia inducible factor-1 (HIF-1) (Semenza GL, 2000). HIF-1 is a ubiquitous basic helix-loop-helix *Per Arnt Sim* (PAS) heterodimer which is activated by hypoxia (Olechnowicz and Peet, 2010). It is composed of the two subunits, HIF-1 α and HIF-1 β or aryl/hydrocarbon receptor nuclear translocator (ARNT), the former being upregulated by hypoxia (Qingdong and Costa, 2006).

Possible mechanisms of HIF-1 induction include protein stability and degradation by proteasome, phosphorylation, redox processes and HSP 90 binding regulating intracellular localization, or a combination of these mechanisms (Wenger, 2002; Bruick, 2003). Redox processes, for example involving H₂O₂, initiated by a postulated haem oxygen sensor have been proposed (Veal *et al.*, 2007). The mitochondrion, which generates ROS in higher amounts under hypoxic conditions, is another possible candidate (Kietzmann and Görlach, 2005).

It is therefore clear that hypoxia strongly affects the regulatory pathways of ECs as well as of smooth muscle cells, leading to the activation of several transcription factors and to the release of cytokines and growth factors. The end result is the formation of conditions favorable to vasoconstriction and proliferative activity, participating in the remodeling of the vascular wall (Rey and Semenza, 2010).

Physiological relevance:

The finding that the endothelial expression of some growth factors, cytokines as well as other genes is influenced by variations in oxygen concentration has physiological implications (Michiels *et al.*, 2000). Two main cascades of reactions have been characterized depending on the duration of the oxygen deficiency. Following acute hypoxia, ECs become activated and neutrophil adherence is observed (Granger DN and Senchenkova, 2010b). One consequence of this process is the development of a local inflammatory reaction in ischaemic organs which is worsened by reperfusion (reperfusion-injury) (Gourdin *et al.*, 2009). When chronic hypoxic conditions persist, the expression of growth factors, cytokines and pro-coagulation molecules is increased (Gourdin *et al.*, 2009). Several pathological conditions are known to be linked to hypoxic conditions of which three will be briefly discussed below.

Metabolic effects of hypoxia on ECs:

Hypoxia alters metabolic pathways in a number of ways, for instance, by inhibiting the oxygen-dependent process of mitochondrial oxidative phosphorylation (OXPHOS), hypoxia compromises ATP generation, thus placing a heavier reliance on glycolysis as an energy source (Denko, 2008; Frezza and Gottlieb, 2009). Increased glycolysis provides a rapid way to generate ATP albeit at the expense of large quantities of glucose, as reflected by raised lactic acid levels (Weljie and Jirik, 2011). The latter, in combination with the decreased ability of mitochondria to utilize protons in ATP generation, leads to intra-tumoural acidosis (Zhou J *et al.*, 2006). The events triggered by hypoxia depend to a large extent on the activity of the transcriptional regulator HIF-1 α and its partner HIF-1 β (Weljie and Jirik, 2011).

The HIF-1 α /HIF-1 β complex activates the transcription of multiple genes relevant to the “Warburg effect”, specifically, genes encoding glucose transporters and glycolytic pathway enzymes (Harris AL, 2002; Kim *et al.*, 2006b; Papandreou *et al.*, 2006). The phosphatidylinositol 3-kinase (PI3K) pathway via activation of PKB/Akt has also been implicated in the genesis of the “Warburg effect” by upregulating HIF-1 levels (Robey and Hay, 2009).

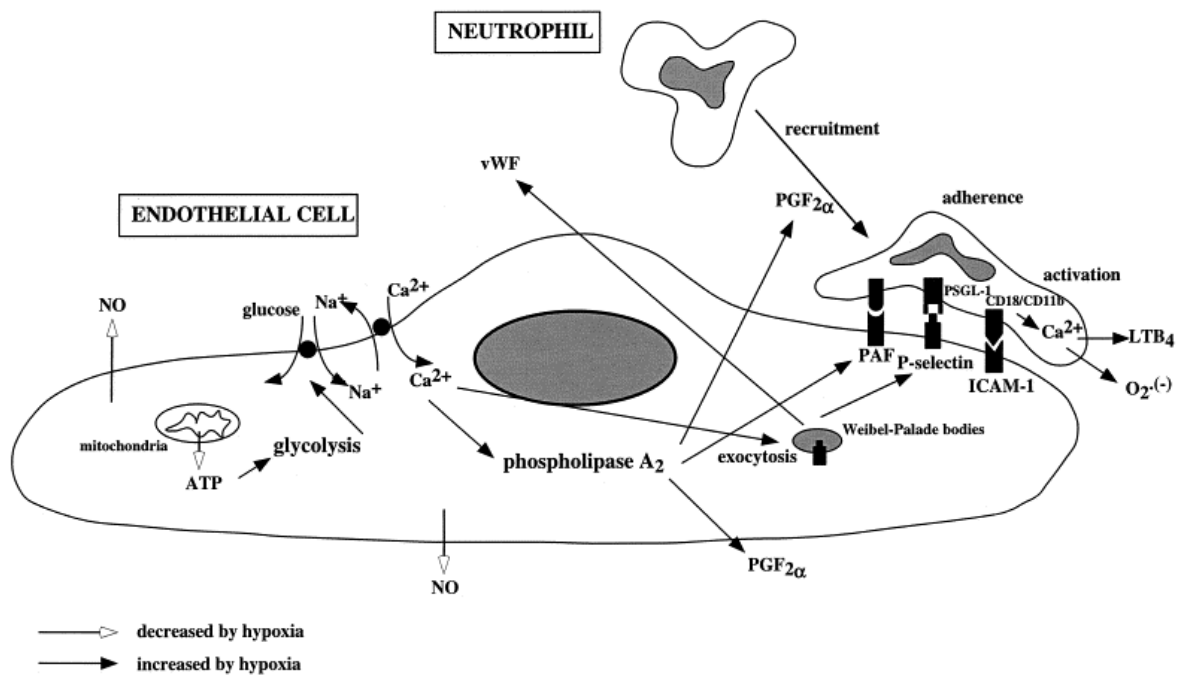


Figure 1.17: Metabolic and biochemical responses of ECs to hypoxia leading to their activation and to the adherence and activation of neutrophils. ICAM-1, intercellular adhesion molecule-1; LTB₄, leukotriene B₄; PAF, platelet-activating factor; PGF₂α, prostaglandin F₂α; PSGL-1, P-selectin glycoligand-1; vWF, von Willebrand factor.

Hypoxia as a cause of ED:

Previous studies have shown that exposure to chronic intermittent hypoxia (CIH) impairs endothelium-dependent vasodilation in the skeletal muscle and cerebral circulations (Phillips *et al.*, 2004; Tahawi *et al.*, 2001). In these studies there was strong evidence that a vascular decrease in NO bio-availability (Phillips *et al.*, 2004; Tahawi *et al.*, 2001) and increased O_2^- levels (Phillips *et al.*, 2006; Troncoso Brindeiro *et al.*, 2007) were possible underlying factors.

A decrease in NO bio-availability is considered to be the hallmark of ED (Imrie *et al.*, 2010). Increased scavenging of NO by O_2^- would be expected to decrease NO bio-availability, thereby impairing endothelium-dependent dilation (Marcus *et al.*, 2012). The mechanisms leading to CIH-induced stimulation of O_2^- production in vascular tissue are unknown; however, available evidence points to a role for the renin–angiotensin system (RAS) (Marcus *et al.*, 2012). Chronic infusion of Ang II elicits hypertension and ED by increasing O_2^- production from NADPH oxidase (Virdis *et al.*, 2011). Ang II-induced stimulation of O_2^- production from NADPH oxidase requires activation of the Ang II type-I receptor (AT1R) (Paravicini and Touyz, 2006). Circulating Ang II is increased in patients with obstructing sleep apnea (OSA) (Moller *et al.*, 2003) and experimental animals exposed to CIH (Yuan *et al.*, 2004).

Hypoxia modulates NOS activity and NO bio-availability:

Hypoxia may influence NO production, NO tissue concentration, and NOS expression by several mechanisms (Manukhina *et al.*, 2006): (i) limitation of NO production due to inadequate NOS substrate O_2 ; (ii) effect of O_2 on NOS feedback inhibition; (iii) modulation of NO bio-availability; (iv) induction of HIF-1 and other NOS transcription factors; (v) changes in intracellular Ca^{2+} concentration and Ca^{2+} influx; and (vi) induction of NOS-regulating heat shock proteins.

Acute, profound hypoxia can lead to decreased NO production by all three NOS isoforms (Weigand *et al.*, 2011). Less severe hypoxia, suppresses NO synthesis only moderately,

and this effect of hypoxia is blunted by increased Ca^{2+} influx, which activates Ca^{2+} /calmodulin-dependent NOS isoforms (Manukhina *et al.*, 2006). In severe hypoxia, Ca^{2+} activation of NOS cannot compensate for reduced O_2 availability, and NO deficiency may develop (Prabhakar and Semenza, 2012; Wagner *et al.*, 2013).

NO can bind to NOSFe^{2+} , forming a haem-NO complex ($\text{NOSFe}^{2+}\text{NO}$), which prevents the haem from binding O_2 and thus increases the apparent K_m for O_2 (Dweik, 2005). By this mechanism, NO feedback inhibits NOS, so that the enzyme functions at only a fraction of its catalytic capacity. During steady state NO synthesis, between ~70% and 90% of NOS exists as a ferrous-NO complex (Daff, 2010). Feedback inhibition of NOS by NO is modulated by O_2 concentration, since O_2 and NO compete for the haem iron (Daff, 2010). Furthermore, the rate of decay of the haem iron-NO complex is dependent on O_2 concentration; as O_2 concentration decreases, less NO is displaced by O_2 and NO production declines (Daff, 2010). As the haem-NO complex subsequently dissociates and then binds O_2 , the active enzyme (NOSFe^{3+}) is regenerated (Porasuphatana, 2001). The sensitivity of the ferrous-NO complex to O_2 influences the overall NOS response to O_2 . It is primarily by this mechanism, rather than the effect of O_2 as a substrate, that NOS produces NO in proportion to the O_2 concentration across the physiologic range (0–250 μM) (Tsai, 2010).

The response to chronic hypoxia also involves altered expression of NOS genes (Manukhina *et al.*, 2006). Some studies have demonstrated hypoxic down-regulation of eNOS expression in pulmonary ECs (Girgis *et al.*, 2003). Hypoxia reduced eNOS mRNA and/or protein in pulmonary artery ECs (Morrell *et al.*, 2009). These hypoxia effects were presumably due to both decreased transcription and destabilization of eNOS mRNA (Manukhina *et al.*, 2006). Similarly, other reports also demonstrated reduced eNOS expression in human umbilical vein and bovine aortic ECs exposed to low PO_2 (Prieto *et al.*, 2011; Chatterjee and Catravas, 2008). Reduced eNOS expression resulted from decreased eNOS mRNA stability and eNOS promoter activity (Morrell *et al.*, 2009). Post-translational regulation of iNOS by prolonged hypoxia was demonstrated in murine macrophages (Daniliuc *et al.*, 2003), in which 24-hr exposure to hypoxia (PO_2 23 ± 1.4 mm Hg) lowered iNOS activity but did not affect iNOS protein content. In these cells, hypoxia

disrupted interactions of iNOS with the cytoskeletal protein α -actinin 4, causing iNOS displacement from the submembranal regions, a location which may be important for normal iNOS activity (Daniliuc *et al.*, 2003).

Moderate hypoxia (4.8% O₂) can result in Ca²⁺ entering cells and activating eNOS (Ray, 2009). However, more prolonged hypoxia will terminate the Ca²⁺ entry and decrease NO synthesis (Rautureau and Schiffrin, 2012).

It is clear from the above discussion that hypoxia *per se* can be regarded as an important harmful stimulus to the vascular endothelium.

1.3.1.1.4 Hyperglycaemia:

Hyperglycaemia is the major causal factor in the development of ED in patients with diabetes mellitus (see figure 1.18) (De Vriese *et al.*, 2000). Clinical trials have identified hyperglycaemia as the key determinant in the development of chronic diabetic complications (Hadi and Al Suwaidi, 2007). The formation of advanced glycation end products (AGEs) is an important biochemical abnormality accompanying diabetes mellitus and inflammation in general (Hadi and Al Suwaidi, 2007). As can be seen in figure 1.18, it is proposed that the development of oxidative stress serves as a putative final pathway in the mechanism of hyperglycaemia-induced ED.

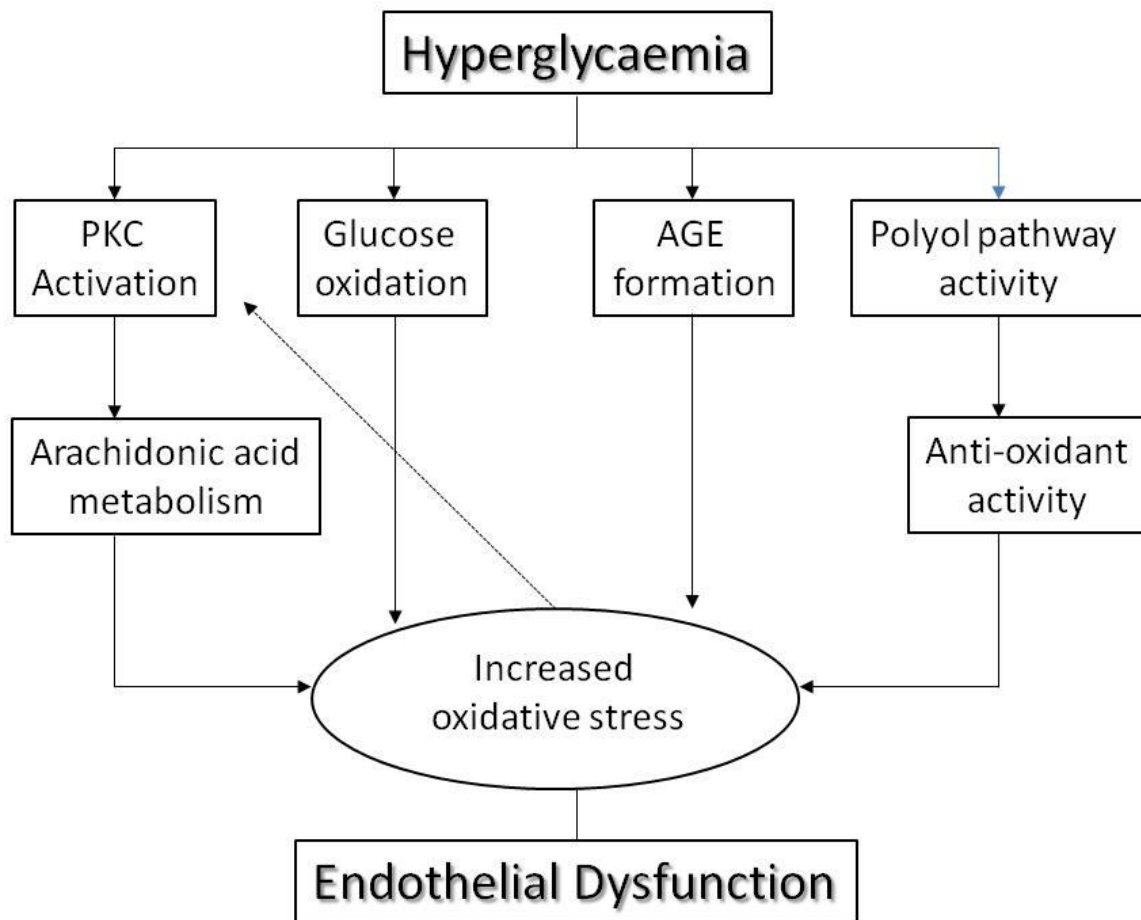


Figure 1.18: Pathophysiology of hyperglycaemia-induced ED (De Vriese *et al.*, 2000).

1.3.1.1.5 Oxidized low density lipoprotein (Ox-LDL):

Oxidation of low-density lipoproteins in the body has been associated with various pathological conditions, including atherosclerosis (Stroka *et al.*, 2012; Levitan *et al.*, 2010). Elevated oxidized low-density lipoproteins (ox-LDL) levels in the bloodstream have been identified as a risk factor for development of coronary artery disease and plaque formation (Berliner *et al.*, 2001; Diaz *et al.*, 1997; Holvoet P *et al.*, 2001; Holvoet P *et al.*, 1998; Toshima *et al.*, 2000). Exposure of the vascular endothelium to ox-LDL leads to EC injury and dysfunction, including disruption of cell–cell adhesion (Gardner *et al.*, 1999; Liao L and Granger, 1995), as well as impairment of NO release (Blair *et al.*, 1999).

Oxidized LDL and endothelial injury / ED:

Endothelial activation and/or dysfunction are widely accepted to be the earliest events in atherosclerosis (Li and Mehta, 2005). Ox-LDL is known to enhance the expression of pro-inflammatory genes, leading to monocyte recruitment to the vessel wall (Li and Mehta, 2000) and dysfunction of vascular ECs. LOX-1 activation by Ox-LDL causes endothelial changes that are characterized by activation NF- κ B through increased ROS, subsequent induction of adhesion molecules, and endothelial apoptosis (Chen M *et al.*, 2002). It is cytotoxic to ECs via the generation of free radicals (Cominacini *et al.*, 2000; Li and Mehta, 2000) and impairs NOS gene expression and its activity (Mehta JI *et al.*, 2001). Ox-LDL triggers activation of inflammatory signalling pathways, such as CD40/CD40L (Li *et al.*, 2003a), and increases gene expression and activity of matrix metalloproteinases (MMP-1 and -3) (Li *et al.*, 2003b) in ECs.

Oxidized LDL and its receptor LOX-1 in endothelium:

The biological effects of ox-LDL are mediated via its receptors. A number of scavenger receptors for ox-LDL, such as SR-A1/II, CD36, SR-B1, and CD68, have been identified on smooth muscle cells and monocytes/macrophages (Stephen *et al.*, 2010). However, these

receptors are not present on ECs in any significant amount (Stephen *et al.*, 2010). It has been suggested that vascular ECs in culture and *in vivo* internalize and degrade ox-LDL through a receptor-mediated pathway that does not involve the macrophage scavenger receptors (Kume *et al.*, 1991). Sawamura *et al.* (1997) first identified oxidized low-density lipoprotein receptor-1 (LOX-1) as a critical molecule that is responsible for ox-LDL uptake by ECs. Ox-LDL uptake via LOX-1 causes endothelial activation (Kita T, 1999). Furthermore, uptake of ox-LDL in ECs (internalization) and subsequent extrusion may be a mechanism by which ox-LDL is transported to the subendothelial region (Li and Mehta, 2005).

Experimental studies have shown that ox-LDL causes injury to ECs via activation of different signal transduction pathways such as those involving PKC and MAPK (Li and Mehta, 2005). Ren *et al.* (2000) suggested that PKC β may mediate ox-LDL-induced gene expression of plasminogen activator inhibitor-1 (PAI-1: serine protease inhibitor that functions as the principal inhibitor of tissue plasminogen activator and urokinase, the activators of plasminogen and hence fibrinolysis), while Li *et al.* (2003a) showed that ox-LDL induces the activation of PKC β , which plays an important role in the expression of matrix metalloproteinases (MMPs) and collagenase activity in ECs. Collectively, MMPs can degrade all components of the extracellular matrix (ECM), thereby influencing many important processes, such as cell proliferation, differentiation, migration, and death, as well as cell–cell interactions (Elkington *et al.*, 2005). In contrast, other PKC isoforms (α , δ and γ) did not change ox-LDL-induced MMP expression (Li and Mehta, 2005). Other studies (Li and Mehta, 2000a, b) showed that the activation of MAPK p42/44 plays a critical role in ox-LDL-induced gene expression of adhesion molecules, monocyte adhesion to ECs, and apoptosis. In addition, they found that the pathological effects of ox-LDL are mediated by its receptor LOX-1 in ECs. Cominacini *et al.*, (2000) observed that ox-LDL increases intracellular free radical generation and activates the pro-inflammatory transcription factor NF- κ B in bovine ECs. It is important to note that ox-LDL might activate different signalling pathways, which in turn interact with each other. These interactions may reflect the complicated cross-talk between intracellular signalling pathways induced by ox-LDL and other pro-atherogenic signals (Li and Mehta, 2005).

Ox-LDL and atherosclerosis:

The importance of ox-LDL in atherosclerosis was first established by employing the antioxidant probucol in atherosclerosis-prone hyperlipidaemic WHHL (The Watanabe heritable hyperlipidaemic) rabbits (Kita T *et al.*, 1987). This study showed the significance of the oxidative state in atherogenesis. A pro-oxidant state and formation of ox-LDL are potent mitogens for smooth muscle cells (Yang CM *et al.*, 2001). Furthermore, ox-LDL is taken up by the macrophages, which facilitates foam cell development (Yang CM *et al.*, 2001).

To elucidate the role of ox-LDL in plaque instability in coronary artery disease, Ehara *et al.* (2001) measured plasma ox-LDL levels in patients with acute myocardial infarction, unstable angina pectoris, and stable angina pectoris. Plasma ox-LDL levels in patients with acute myocardial infarction were higher than in patients with unstable or stable angina pectoris. Serum levels of total, HDL, and LDL cholesterol did not differ among different patient groups. Post-mortem studies of patients who died of acute myocardial infarction revealed that the culprit coronary lesion contained abundant macrophage-derived foam cells with distinct positivity for ox-LDL and its receptors. These results strongly suggested an important role for ox-LDL in the formation of plaque instability in human coronary atherosclerotic lesions. In addition, in another study, the same authors found that plasma ox-LDL levels were higher in patients with diabetes mellitus than in those without diabetes mellitus (Ehara *et al.*, 2002). In another study, soluble LOX-1 levels were shown to be significantly higher in the serum of patients with acute coronary syndrome than that of the control subjects (Hayashida *et al.*, 2005). Soluble LOX-1 may well become a future biomarker for early diagnosis of acute coronary syndrome (Hayashida *et al.*, 2005).

1.3.1.1.6 Oxidative stress:

Risk factors / diseases associated with oxidative stress:

Oxidative stress has been positively linked with CVD, since oxidation of LDL in the vascular endothelium is a precursor to plaque formation (Li JM and Mehta, 2005). Oxidative stress also plays a role in the ischaemic cascade due to oxygen reperfusion injury following hypoxia (Nijs *et al.*, 2006), which can result in stroke and myocardial infarction.

Cellular mechanisms of oxidative stress:

There are many ROS that play a central role in vascular physiology (Figure 1.19) and pathophysiology, the most important of which are NO, superoxide (O_2^-), hydrogen peroxide (H_2O_2) and peroxynitrite ($ONOO^-$) (Griendling KK and Fitzgerald, 2003). NO is normally produced by eNOS in the vasculature, but in inflammatory states, iNOS can be expressed in macrophages and smooth muscle cells (Griendling KK and Fitzgerald, 2003) as well as ECs (Zou *et al.*, 2004) and contribute to NO production.

Superoxide results from one electron reduction of oxygen by a variety of oxidases (Figure 1.19). When superoxide is produced together with NO (particularly when NO is generated in high amounts), the two molecules can rapidly react to form the highly reactive molecule, peroxynitrite (Griendling KK and Fitzgerald, 2003). Peroxynitrite is an important mediator of lipid peroxidation and protein nitration, including the oxidation of LDL, which has dramatic pro-atherogenic effects (Griendling KK and Fitzgerald, 2003). In the absence of immediately accessible NO, O_2^- is rapidly dismutated to the more stable H_2O_2 (by superoxide dismutase, SOD), which is then further converted to H_2O by either catalase or glutathione peroxidase (Griendling KK and Fitzgerald, 2003) (see figure 1.19). The effects of O_2^- and H_2O_2 on vascular function depend critically on the amounts produced. When formed in low amounts intracellularly, they can act as intracellular second messengers, modulating the function of biochemical pathways that mediate such responses as growth of vascular smooth muscle cells (VSMCs) and fibroblasts (Griendling KK and Fitzgerald, 2003). Higher amounts of ROS can cause DNA damage, significant toxicity, or even apoptosis, as demonstrated in ECs (Niwa K *et al.*, 2002) and smooth muscle cells (Deshpande *et al.*, 2002).

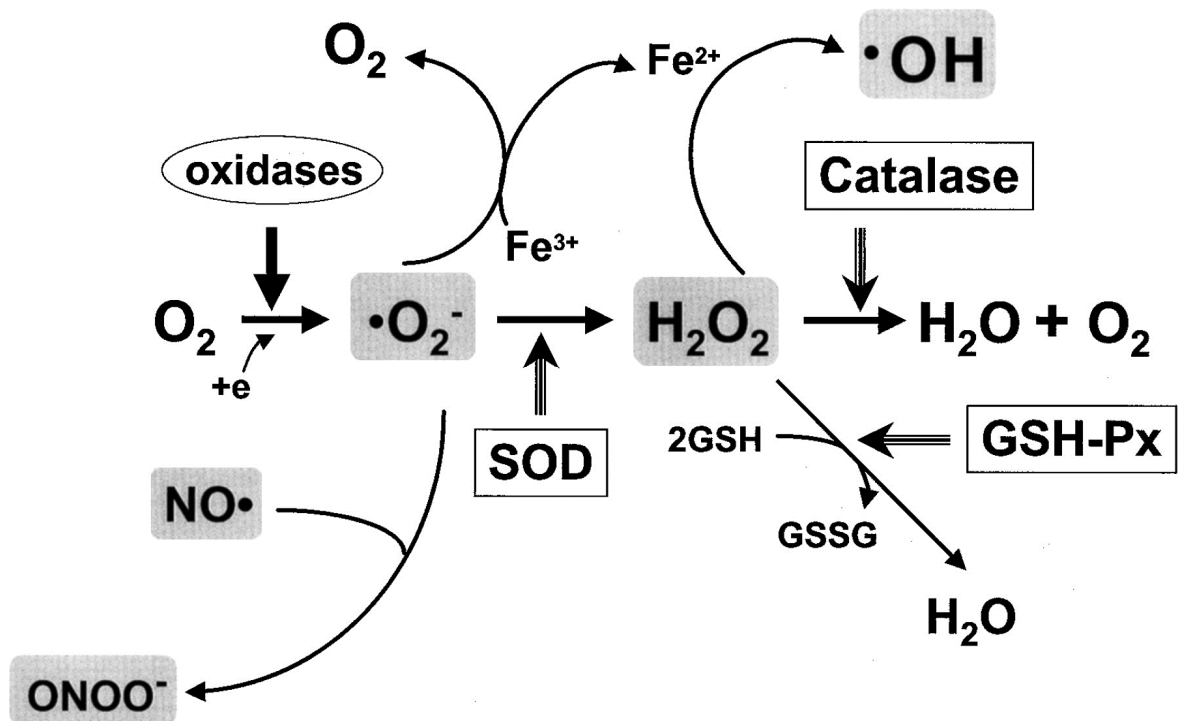


Figure 1.19: Vascular ROS. Highlighted in gray are some of the most important ROS in vascular cells. Oxidases convert oxygen to O_2^- , which is then dismutated to H_2O_2 by superoxide dismutase (SOD). H_2O_2 can be converted to H_2O by catalase or glutathione peroxidase (GSH-Px) or to hydroxyl radical ($\cdot OH$) after reaction with Fe^{2+} . In addition, O_2^- reacts rapidly with NO to form peroxynitrite (Griendling KK and Fitzgerald, 2003).

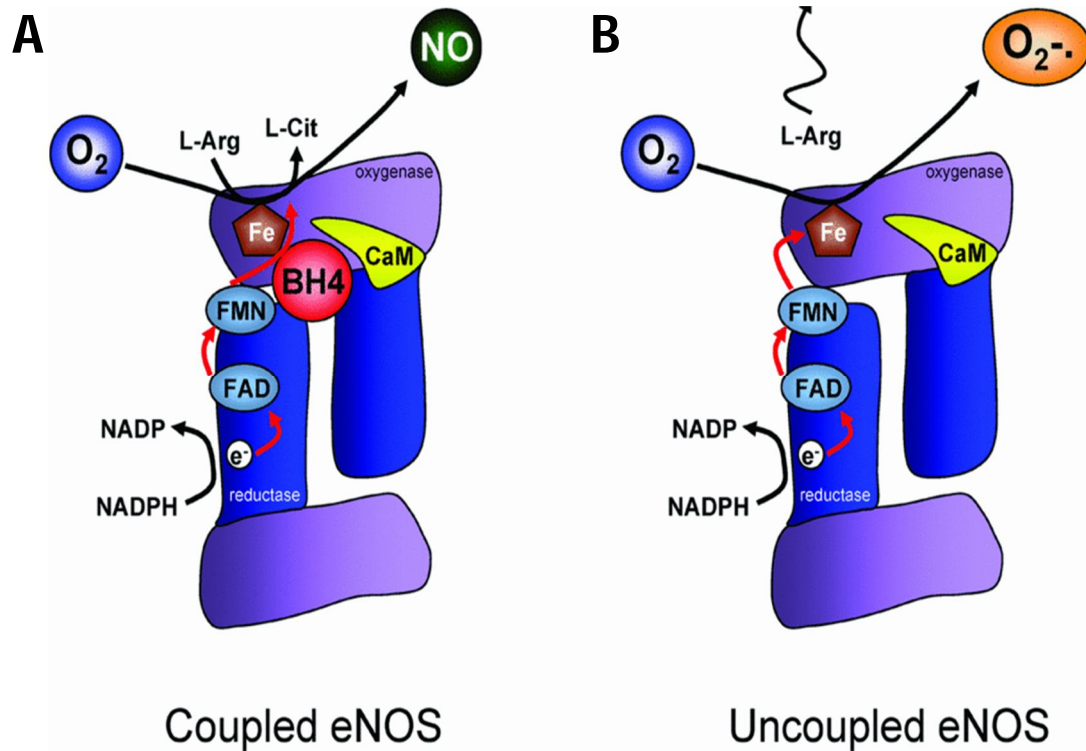


Figure 1.20: Coupled vs. uncoupled eNOS. **(A)** In healthy vascular endothelium, there is an increased BH₄ to BH₂ ratio. BH₄ binds to the ferrous-dioxygen domain in the oxygenase domain which results in a coupling reduction of molecular O₂ to L-arginine oxidation and synthesizes NO. **(B)** In diseased conditions, BH₄ is limited and becomes oxidized to BH₂ increasing the BH₂/BH₄ ratio to promote uncoupled eNOS. The electron transfer is uncoupled from L-arginine, the ferrous-dioxygen complex dissociates, and SO is produced from the oxygenase domain from molecular oxygen (Schmidt TS and Alp, 2007).

Cellular and Enzymatic Sources of ROS in the Vessel Wall:

ROS are derived from specific enzymatic or chemical reactions (Griendling KK and Fitzgerald, 2003). NO is produced in ECs by activation of eNOS during the normal functioning of the vessel wall. Vasodilator hormones raise intracellular Ca^{2+} , leading to an increase in eNOS activity and NO release (Bonomini *et al.*, 2012). Physical forces, such as shear stress, activate eNOS via PKA- or Akt-dependent phosphorylation (Balligand *et al.*, 2009). Pathophysiological expression of iNOS in both macrophages and vascular smooth muscle cells (VSMCs) elevates cytokine levels, resulting in localized inflammation (Sprague and Kahlil, 2009). This, in turn, results in production of NO in the absence of further stimuli (Sprague and Kahlil, 2009). Moreover, under some circumstances, eNOS becomes uncoupled and O_2^- is generated rather than NO (Yang Z *et al.*, 2006; Schmidt TS and Alp, 2007) (Figure 1.20). The NOS enzymes are thus potentially important sources of both NO and O_2^- , depending on the surrounding environment (Griendling KK and Fitzgerald, 2003).

Virtually all types of vascular cells produce O_2^- and H_2O_2 (Griendling KK *et al.*, 2000a). In addition to mitochondrial sources of ROS, O_2^- and/or H_2O_2 can also be generated by other sources (Figure 1.21) (Griendling KK and Fitzgerald, 2003). Two of the most important sources in bloodvessels under normal conditions are thought to be cytochrome P450 and the membrane-associated NADPH oxidase(s) (Rajagopalan *et al.*, 1996; Fleming *et al.*, 2001). A cytochrome P450 isozyme homologous to Cytochrome P450 2C9 (CYP 2C9) (an important cytochrome P450 enzyme with a major role in the oxidation of both xenobiotic and endogenous compounds) has been identified in coronary arteries and has been shown to produce O_2^- in response to bradykinin (Buttery *et al.*, 1996). NADPH oxidases, similar in structure to the neutrophil respiratory burst NADPH oxidase, but producing less O_2^- over a longer period of time, have been identified in vascular cells (Bedard and Krause, 2007). The endothelial, VSMC, and fibroblast enzymes are not identical, but have distinct subunit structures and mechanisms of regulation (Griendling KK *et al.*, 2000a).

NADPH oxidase proteins are major sources of ROS (Bedard and Krause, 2007; Brandes *et al.*, 2010; Lambeth, 2004). All NADPH oxidases contain a core subunit, termed NOX, which catalyzes the transfer of electrons from NADPH to molecular O_2 and leads to ROS generation. Five NOX isoforms (NOX1–5) have been identified, which form the basis of

distinct NADPH oxidases (Murdoch *et al.*, 2011). In the vasculature, NOX2 and NOX4 are expressed in the endothelium (Bedard and Krause, 2007).

All NOX enzymes utilize NADPH as an electron donor and catalyse the transfer of electrons to molecular oxygen to generate O_2^- and/or H_2O_2 (Sirker *et al.*, 2011). The enzymes require association with different subunits for their activation and also exhibit differences in activity (see figure 1.22, table 1.6). NOX2 and 4 bind to a smaller p22phox subunit, which is essential for enzyme activity (Von Löhneysen *et al.*, 2010). NOX2 is normally activated after cell stimulation by specific agonists (e.g. G-protein coupled receptor agonists such as Ang II, growth factors, cytokines and mechanical forces), which induce the association of regulatory subunits and activation of the enzyme (Sirker *et al.*, 2011). The cytosolic regulatory subunits for NOX2 are p47phox, p67phox, p40phox and Rac1 (Sirker *et al.*, 2011). However, NOX4 is constitutively active and does not require association with regulatory subunits, with regulation thought to occur mainly by changes in expression level (Sirker *et al.*, 2011) (see table 1.6). Furthermore, findings from several laboratories indicated that NOX4 predominantly generates H_2O_2 in contrast to NOX2, which generates O_2^- (Dikalov *et al.*, 2008; Martyn *et al.*, 2006; Serrander *et al.*, 2007). The biochemical basis for this property of NOX4 has recently been suggested to be related to the structure of its third extracytosolic loop, which differs significantly from those of NOX2 and contains a highly conserved histidine moiety which may prevent O_2^- release or may provide protons for O_2^- dismutation (Takac *et al.*, 2011). NOX2 (also known as gp91phox oxidase) was the first NADPH oxidase to be identified, being responsible for the phagocytic oxidative burst of neutrophils (Sirker *et al.*, 2011). Its neutrophil activity is important for non-specific host defence against microbial organisms and deficient activity of the oxidase results in chronic granulomatous disease (CGD), a condition in which affected children develop recurrent infections and inflammation (Holland, 2010). NOX2 has subsequently been found to be expressed at lower level in other inflammatory cells as well as in ECs, cardiomyocytes, fibroblasts and VSMC (Sirker *et al.*, 2011). NOX4 is reported to be expressed in all cardiovascular cell types although its *in vivo* level of expression in healthy cardiovascular tissues remains to be precisely defined (Sirker *et al.*, 2011).

Although the protein expression of p22phox largely depends on the presence of the NOX proteins, a link between the mRNA expression of the scaffolding protein and the ROS formation has been demonstrated (Brandes *et al.*, 2010). The mRNA expression of p22phox itself is redox sensitive as it is regulated by the transcription factors activator protein-1 (AP-1) (Brewer *et al.*, 2006) and NFκB (Cevik *et al.*, 2008). Antioxidants such as catalase (Manea A *et al.*, 2007) or red wine polyphenols (Manea A *et al.*, 2008) are able to counteract the induction of p22phox by stress-inducing signals such as Ang II or hypertension.

Ang II, tumor necrosis factor- α , thrombin, and PDGF α increase oxidase activity and raise intracellular levels of O_2^- and H_2O_2 in VSMCs (Griendling KK *et al.*, 2000a). Ang II and lactosylceramide activate the EC NADPH oxidase enzyme, whereas fibroblasts increase O_2^- production in response to Ang II, tumor necrosis factor- α , interleukin-1, and platelet-activating factor (Griendling KK *et al.*, 2000a). Physical forces, including cell stretch, laminar shear stress, and the disturbed oscillatory flow that occurs at branch points, are also potent activators of O_2^- production in ECs (Balligand *et al.*, 2009). There are two major mechanisms by which hormones and physical forces activate the NADPH oxidase: (1) acutely, whereby expressed enzyme is activated by phosphorylation, GTPase activity, and production of relevant lipid second messengers (Zafari *et al.*, 1999); and (2) chronically, when expression of rate-limiting subunits of the enzyme is induced, thereby providing higher levels of enzyme susceptible to activation (Lassègue *et al.*, 2001).

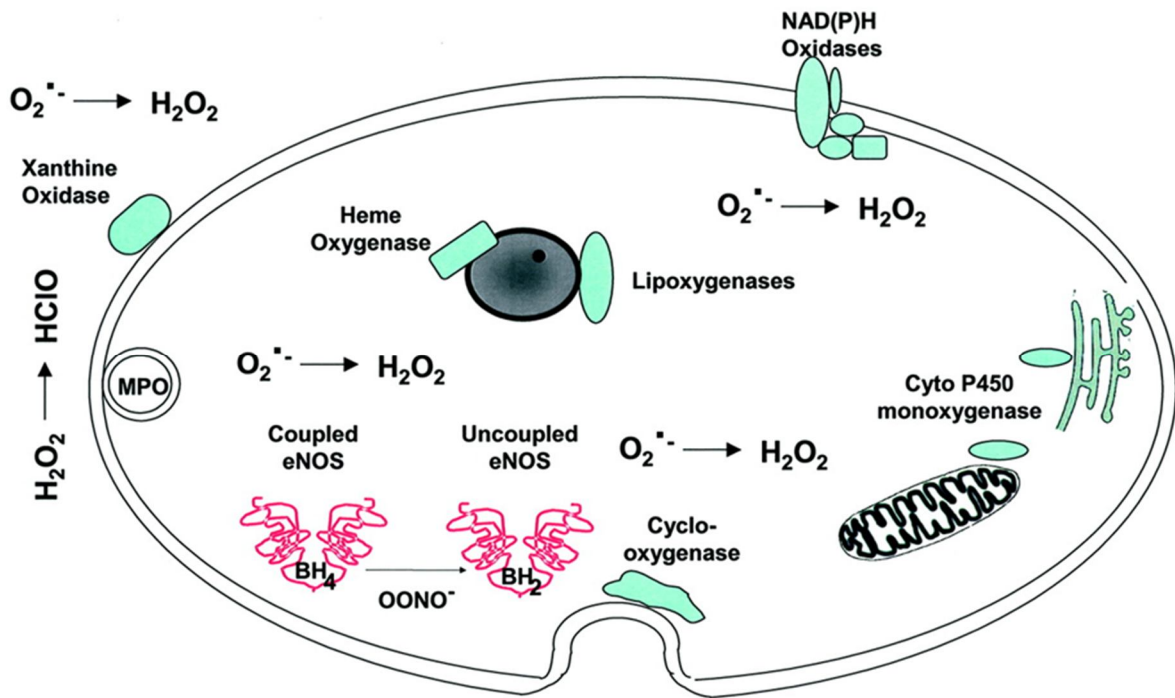


Figure 1.21: Potential sources of ROS in ECs. Many enzymes, including those in the mitochondrial electron transport chain, xanthine oxidase, COXs, lipoxygenases, myeloperoxidases, cytochrome P450 monooxygenase, uncoupled NOS, haem oxygenases, peroxidases, and NADPH oxidases, produce ROS. According to their location in the cell, these ROS are generated intracellularly, extracellularly, or in specific intracellular compartments (Griendling KK and Fitzgerald, 2003).

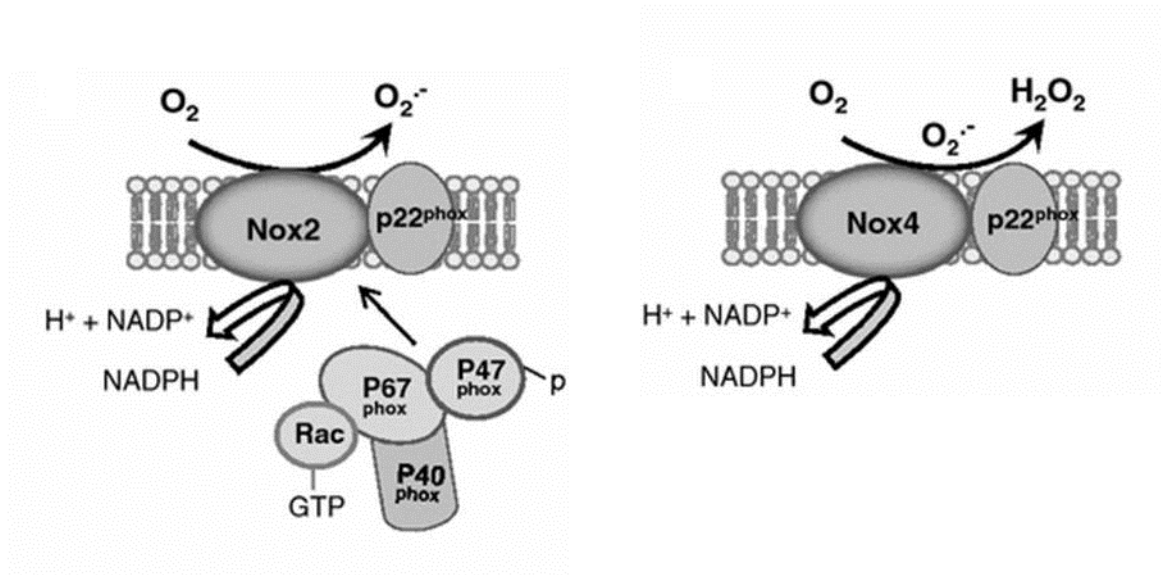


Figure 1.22: Schematic representation of NOX2 and NOX4 and oxidases. NOX2 requires association with cytosolic regulatory subunits for their activation, as indicated (Sirker *et al.*, 2011).

Table 1.6: The activity, regulation and expression of the main NOXs in the cardiovascular system (specifically the endothelium) (Sirker *et al.*, 2011).

	<i>NOX2</i>	<i>NOX4</i>
Constitutive activity	Absent or very low	High
Binding to p22phox essential for enzyme activity	Yes	Yes
Essential regulatory subunits	p67phox, p47phox, p40phox, Rac	None
Control	Post-translational modifications of regulatory subunits.	Transcriptional. Can be regulated by Poldip2.
Cell expression	Endothelial cells, cardiomyocytes, fibroblasts, human vascular smooth muscle, inflammatory cells.	Endothelial cells, cardiomyocytes, fibroblasts, vascular smooth muscle cells.

Biochemical Consequences of ROS Production in the Vessel Wall:

As noted above, ROS are involved in some of the most fundamental functions of the vessel wall (Griendling KK and Fitzgerald, 2003). NO is a critically important mediator of endothelium-dependent vasodilation, whereas O_2^- and H_2O_2 mediate VSMC growth, differentiation, and apoptosis (Griendling KK and Fitzgerald, 2003). The lipid peroxidation and protein nitration induced by $ONOO^-$ are some of the earliest atherogenic events (Pacher *et al.*, 2008). Because macrophages release ROS extracellularly, they activate matrix metalloproteinases (MMPs) MMP-2 and MMP-9 (Galis *et al.*, 1995; Rajagopalan *et al.*, 1996). Once activated, MMPs can degrade the collagen-based extracellular matrix, contributing to weakening of the fibrous cap and plaque rupture (Galis *et al.*, 1995). In VSMCs, ROS exert their effects via activation of specific intracellular signalling pathways and can profoundly influence both normal physiology and the course of vascular disease. Furthermore, it is becoming evident that stable products of ROS may also influence cellular function by adduction of signalling molecules or by serving as incidental ligands for both membrane and nuclear receptors in vascular cells (Griendling KK and Fitzgerald, 2003).

Just as NO mediates vasodilation by activating the VSMC guanylate cyclase, O_2^- and H_2O_2 can alter the activity of selected intracellular proteins. Unlike NO, no specific target for these ROS has been identified, nor has the identity of the actual reactive species been elucidated, although *in vitro* studies show that both O_2^- and H_2O_2 are able to inhibit protein phosphatases (Griendling KK and Fitzgerald, 2003). O_2^- and H_2O_2 or their products can modulate the activity of signalling pathways. For example, attenuation of agonist-induced ROS production by antisense inhibition of NADPH oxidase expression in VSMCs leads to reduction of Ang II-induced hypertrophy, platelet-derived product-stimulated tissue factor expression, and serum-induced growth (Görlach *et al.*, 2000; Ushio-Fukai *et al.*, 1996; Suh *et al.*, 1999). These effects appear to be mediated in part through activation of the c-Src, p38 mitogen-activated protein kinase, and the cell survival kinase (Akt) in the case of Ang II, and extracellular signal-regulated kinases in the case of PDGF (Touyz and Schiffrin, 2000). These signalling pathways, in turn, control gene expression (Griendling KK *et al.*, 2000b). In some cases, regulation of the gene is redox sensitive

because of the susceptibility of these upstream signalling pathways to ROS (Griendling KK *et al.*, 2000b). However, the affinity of certain transcription factors for their cognate DNA binding sites can also be directly modified by ROS, particularly nuclear factor- κ B and activator protein-1 (AP-1) transcription factors (Kunsch and Medford, 1999).

ROS regulate several general classes of genes, including adhesion molecules and chemotactic factors, antioxidant enzymes, and vasoactive substances (Griendling KK and Fitzgerald, 2003). Some of these are clearly an adaptive response, such as the induction of superoxide dismutase and catalase by H₂O₂ (Lu *et al.*, 1993). Upregulation of adhesion molecules (VCAM-1, intracellular adhesion molecule-1) and chemotactic molecules (monocyte chemoattractant protein-1) by oxidant-sensitive mechanisms is of particular relevance to vascular pathology (Kunsch and Medford, 1999). These molecules promote adhesion and migration of monocytes into the vessel wall. Conversely, transcriptional induction of adhesion molecules by cytokines is inhibited by NO donors in a cyclic guanosine monophosphate-independent manner (Spiecker *et al.*, 1998). These mechanisms combine to suppress adhesion molecule expression in the normal vessel wall and induce its expression in vasculopathies (Spiecker *et al.*, 1998).

1.3.1.2 Cardiovascular risk factors associated with harmful stimuli.

1.3.1.2.1 Diabetes mellitus (including insulin resistance and hyperglycaemia).

Both type 1 and type 2 diabetes are independent risk factors for the development of accelerated atherosclerosis, IHD and CVD in general (Esper *et al.*, 2006). Similarly, type 1 diabetes mellitus, insulin resistance and type 2 diabetes mellitus have been shown to be strongly associated with the development of ED (Potenza *et al.*, 2009). In fact, the temporal progression from insulin resistance to type 2 diabetes mellitus has been postulated to be mirrored by the progression of ED to atherosclerosis (Hsueh *et al.*, 2004). ED observed in diabetes mellitus is primarily attributable to (1) oxidative stress (increased O₂⁻ generation due to upregulated expression of NADPH oxidase), and (2) increased

formation of advanced glycation end-products (AGEs) (Guzik *et al.*, 2002; Avogaro *et al.*, 2008).

Hyperglycaemia, one of the main features of diabetes mellitus, results in non-enzymatic glycation of intracellular and extracellular proteins and lipids, which leads to the generation of AGEs. The latter subsequently accumulate in the vascular wall and reduce NO activity by quenching NO (Guzik *et al.*, 2002; Avogaro *et al.*, 2008). AGEs also bind to specific surface receptors, called receptors for AGEs (RAGE), which are expressed on cells such as monocytes, macrophages and VSMCs, resulting in the amplification of an inflammatory response (Guzik *et al.*, 2002; Avogaro *et al.*, 2008), increased vascular permeability and oxidative stress (Soldatos *et al.*, 2005). Hyperglycaemia is also known to activate PKC, which decreases eNOS activity, leading to reduced NO and increased ET-1 production (Avogaro *et al.*, 2008). In the setting of ED, endothelin receptor type B (ET_B) - mediated vasodilatory effects of ET-1 are blunted and therefore the vasoconstrictory state predominates (Versari *et al.*, 2009a). PKC also enhances the expression of adhesion molecules such as ICAM, VCAM and E-selectin (Avogaro *et al.*, 2008), which are associated with EC activation. ED has been reported to occur early in insulin resistance (Hsueh *et al.*, 2004). Often insulin resistance is associated with central adiposity and hence the metabolic syndrome, i.e. hypertriglyceridaemia, low high-density lipoprotein (HDL) levels, high low-density lipoprotein (LDL) levels and hypertension, all of which could potentially favour the development of ED and eventually atherogenesis (Hsueh *et al.*, 2004).

1.3.1.2.2 *Dyslipidaemia (including hypercholesterolaemia).*

Dyslipidaemia includes increased circulating lipids including cholesterol and triglycerides, a state which can predispose to ED (Mudau M *et al.*, 2012). Possible mechanisms underlying dyslipidaemia-induced ED include: (1) upregulation of NADPH oxidase, increased O₂⁻ production and oxidative stress (Furukawa *et al.*, 2004), (2) increased plasma levels of asymmetric dimethylarginine (ADMA) (Soldatos *et al.*, 2005), and (3) oxidation of LDL (Sawamura, 2004). As mentioned previously, ADMA is an endogenous inhibitor of eNOS and competes with L-arginine for the same binding site on eNOS, thus

resulting in eNOS uncoupling, increased O_2^- production and hence decreased NO production (Vallance *et al.*, 1992a). Plasma concentrations of ADMA have been reported to be increased in hypercholesterolaemia (Böger *et al.*, 1998; Böger *et al.*, 2003b), and this biomarker is considered to be both an indicator and risk factor of ED (Böger *et al.*, 1998). In addition to scavenging NO, excess O_2^- modifies LDL cholesterol to form ox-LDL, which plays a major role in the development of endothelial activation and atherogenesis (Zeibig *et al.*, 2011). Ox-LDL has been reported to promote ET-1 production (Boulanger *et al.*, 1992), expression of adhesion molecules and chemoattractants (Mallat and Tedgui, 2005), as well as VSMC migration and proliferation (Sawamura *et al.*, 2004). Furthermore, ox-LDL can be engulfed by macrophages forming foam cells which adhere to the vessel wall and contribute to the initiation of an atherosclerotic plaque (Sawamura *et al.*, 2004). Both LDL and ox-LDL have been shown to increase the activity of S-adenosylmethionine-dependent methyltransferases, which lead to the upregulation of ADMA synthesis (Böger *et al.*, 2000a). Thus, LDL and ox-LDL may be responsible for the increased plasma levels of ADMA in hypercholesterolaemia (Warnholtz *et al.*, 2001). LDL or ox-LDL can also upregulate caveolin-1 synthesis and consequently inhibit eNOS activity (Davignon *et al.*, 2004; Hamburg and Vita, 2005) (Figure 1.23).

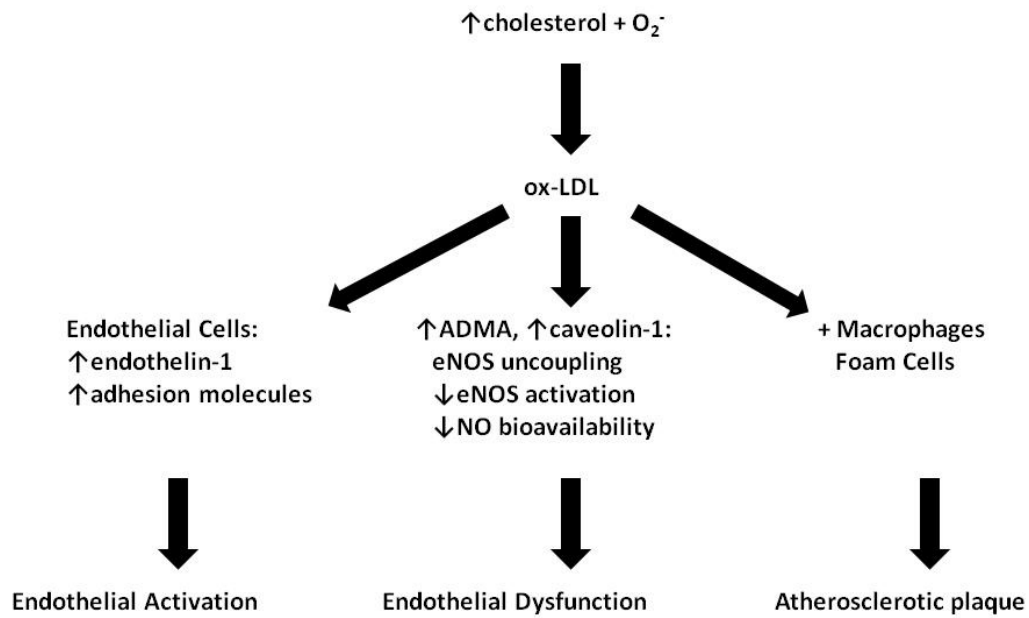


Figure 1.23: Pathophysiological effects and the interplay between increased plasma cholesterol and O_2^- levels, and EC responses (Mudau M *et al.*, 2012).

1.3.1.2.3 Hypertension

ED is a prominent underlying feature of hypertension (Bhatt *et al.*, 2011), and patients with hypertension have been shown to demonstrate reduced flow-mediated dilatation, characterized by blunted forearm blood flow in response to vasodilatory stimuli such as acetylcholine (Tang EH and Vanhoutte, 2010), which is known as the gold standard of clinical detection techniques of ED. Increased production of ROS and endothelial-derived contracting factors (EDCFs) such as ET-1, Ang II, PGH₂ and TXA₂, and decreased NO bioavailability are all observed in patients with hypertension (Versari *et al.*, 2009b; Tang EH and Vanhoutte, 2010). Shear stress is known to be one of the most important mechanisms of inducing NO-mediated vasodilation in both the micro- and microvasculature (Paniagua *et al.*, 2001; Hadi *et al.*, 2005). However, this response is reduced or absent in hypertensive patients (Paniagua *et al.*, 2001). In addition to this, Iaccarino *et al.* (2004) observed decreased PKB/Akt-dependent activation of eNOS in a model of spontaneously hypertensive rats (SHR). In another study, the role of oxidative stress and ED in the development of hypertension in spontaneously hypertensive rats was investigated (Bhatt *et al.*, 2011) and showed that early treatment with the antioxidant resveratrol was associated with reduced oxidative stress markers, improved endothelium-dependent vasodilatation and an attenuation in the development of hypertension in these animals.

1.3.1.2.4 Smoking

Tobacco smokers exhibit decreased NO bioavailability, increased levels of ox-LDL, and impaired flow-mediated vasodilation, all indicative of ED (Puranik *et al.*, 2003). Passive smoking has recently also been implicated in impairment of endothelial function (Puranik *et al.*, 2003; Barnoya and Glantz, 2005). It appears that the harmful effects of smoking on ECs are dose dependent and reversible upon smoking cessation (Puranik *et al.*, 2003). As with other CVD risk factors, oxidative stress appears to be the major mechanistic link between smoking and ED (Puranik *et al.*, 2003; Burke and FitzGerald, 2003). Cigarette smoke is rich in free radicals and directly delivers free radicals to the body (Valavanidis *et*

al., 2009). Besides being the supplier of free radicals, cigarette smoke facilitates endogenous release of ROS via activation of inflammatory cells (Burke and FitzGerald, 2003; Antoniadou *et al.*, 2008). Furthermore, smoking has been reported to decrease the levels of HDL cholesterol, which is known to have anti-ED and anti-atherosclerotic properties (Katusic, 2007).

1.3.1.2.5 Aging

One of the recognised predisposing factors of ED is increasing age (Katusic, 2007; Herrera MD *et al.*, 2010b). It is thought that the ability of ECs to produce NO is reduced with aging (Vanhoutte, 2002). Furthermore, some studies have reported reduced expression and activity of eNOS as well as decreased expression of a major downstream target molecule of NO, soluble guanylyl cyclase (sGC) in VSMCs, and its activity in older animals (Vanhoutte, 2002). In addition to the decreased NO production, other endothelial-derived relaxing factors (EDRFs) (prostacyclin and EDHF) are also reduced, while endothelial-derived contracting factors (EDCFs) such as ET-1 and COX-derived prostanoids, and ROS production are increased (Herrera MD *et al.*, 2010b; Vanhoutte, 2002). Plasma levels of ADMA are also known to rise with increased age (Vanhoutte, 2002). Another mechanism that could contribute to reduced NO levels in aging may be the increased activity of arginase I (Katusic, 2007; Herrera MD *et al.*, 2010b). Arginase I is an enzyme that catalyses conversion of L-arginine to L-ornithine and urea, and it thus competes with eNOS for L-arginine (Katusic, 2007). Therefore, the increased activity of this enzyme as observed with advancing age may result in uncoupling of eNOS, reduced NO production and as a result ED (Katusic, 2007; Herrera MD *et al.*, 2010b). The balance between EDRFs and EDCFs is lost with advancing age, establishing aging as a risk factor for the development of ED (Matsumoto *et al.*, 2007). Moreover, aging is often associated with co-morbid conditions such as diabetes, hypertension and hypercholesterolaemia, further exacerbating the risk of developing ED, atherosclerosis and ultimately CVDs (Herrera MD *et al.*, 2010b).

1.3.1.2.6 Other known factors that contribute to ED

Apart from the cardiovascular risk factors listed and discussed above, it is important to mention that there are several other known factors that also contribute to the development of ED. These factors are briefly listed below:

- Obesity and associated low grade inflammation
- Infectious diseases (e.g. HIV and elevated inflammatory markers)
- Hormonal influences (e.g. menopause, sex steroids)
- Arthritis
- Inflammatory bowel disease
- Genetic predisposition to ED

1.3.2 Early endothelial responses to harmful stimuli

Chronic exposure of the endothelium to cardiovascular risk factors and the harmful circulating stimuli associated with these conditions, will eventually overwhelm the defense mechanisms of the vascular endothelium, compromising its integrity and ultimately initiating endothelial activation, dysfunction and atherosclerosis (Deanfield *et al.*, 2007; Yang G *et al.*, 2010) (Figure 1.24).

1.3.2.1 Endothelial Activation

Endothelial activation refers to a specific change in the endothelial phenotype, characterized most notably by an increase in endothelial-leukocyte interactions and permeability, which is pivotal to inflammatory responses in both physiological and pathological settings (Alom-Ruiz *et al.*, 2008). It is also associated with the early stages of atherosclerosis and sepsis (Alom-Ruiz *et al.*, 2008). As a result of activation, the endothelium releases so-called Weibel–Palade bodies (López and Chen, 2009). Weibel–

Palade bodies, as mentioned previously, store and release two principal molecules, vWF and P-selectin, and thus play a dual role in hemostasis and inflammation (Babich *et al.*, 2008). An intact and healthy endothelium expresses various anticoagulants, such as tissue factor (TF) pathway inhibitor, thrombomodulin, endothelial protein C receptor, and heparin-like proteoglycans (Esmon CT and Esmon NL, 2011). In addition, ECs express the ectonucleotidase CD39/NTPDase1, which metabolizes the platelet agonist adenosine diphosphate (ADP). Finally, ECs also release the platelet inhibitors NO and prostacyclin (Watson, 2009; Atkinson *et al.*, 2006). However, activated ECs down regulate expression of the anticoagulant protein thrombomodulin, and up regulate expression of the procoagulant protein TF (Moore *et al.*, 2010). Endothelial activation also leads to the expression of various adhesion molecules on the surface of the endothelium, such as P-selectin, E-selectin, and vWF, that capture leukocytes, platelets, and microvesicles (MVs) (Ley *et al.*, 2007; Williams *et al.*, 2011; Pinsky *et al.*, 1996).

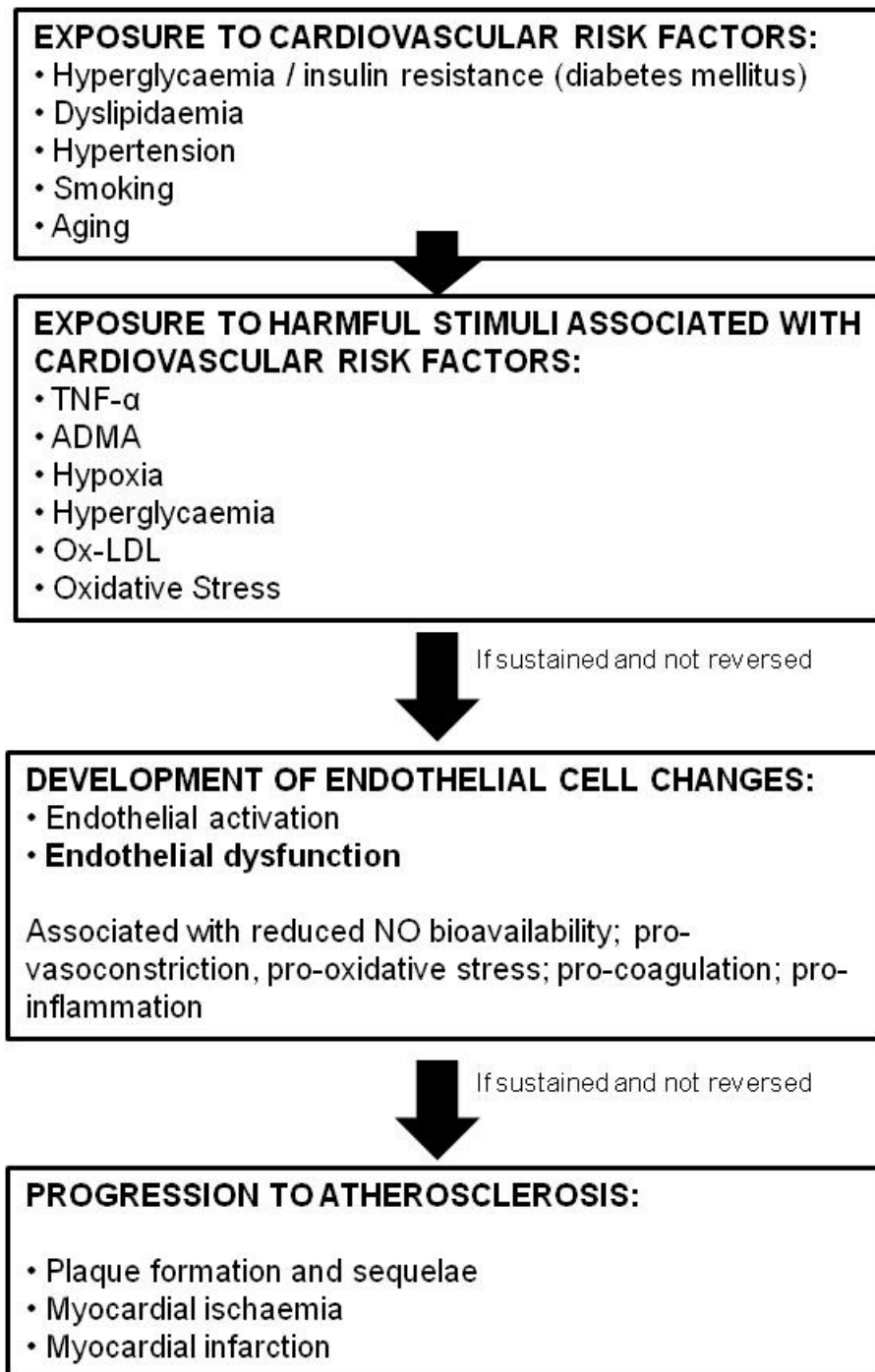


Figure 1.24: Exposure of ECs to cardiovascular risk factors and the resultant pathophysiological changes, i.e. endothelial activation and dysfunction, with progression to atherosclerosis if risk-factor exposure is sustained (adapted from Mudau M *et al.*, 2012).

1.3.2.2 Endothelial Dysfunction (ED)

1.3.2.2.1 Definition and features

Under physiologic conditions, endothelial stimulation induces the production and release of NO, which diffuses to surrounding tissue and cells and exerts its role in maintaining vascular homeostasis by relaxing vascular smooth muscle cells, and by preventing leukocyte adhesion and migration into the arterial wall, muscle cell proliferation, platelet adhesion and aggregation, and adhesion molecule expression (Luscher and Vanhoutte, 1990; Taddei *et al.*, 2003). However, under pathophysiological conditions (including the presence of cardiovascular risk factors and exposure to harmful circulating stimuli) the endothelium undergoes functional and structural changes leading to a loss of its protective role and transforming it into a pro-atherosclerotic structure (Luscher and Vanhoutte, 1990). The fundamental feature of ED is reduced NO bioavailability and can be the consequence of either reduced production by eNOS or an increased removal or scavenging by ROS (Luscher and Vanhoutte, 1990; Taddei *et al.*, 2003). Upon the reduction of NO bioavailability, ECs implement various physiological pathways in an attempt to compensate (Versari *et al.*, 2009b). For instance, endothelium-dependent vasodilation is still possible due to compensatory production and release of endothelium-derived vasodilators other than NO, such as endothelium-derived hyperpolarizing factors (EDHF) (Versari *et al.*, 2009b). Along with NO deficiency, a dysfunctioning endothelium also becomes the source of other substances and mediators that are detrimental to the arterial wall, including ET-1, tromboxane A₂, prostaglandin H₂, and ROS (Taddei *et al.*, 2003). ED, secondary to the harmful effects of cardiovascular risk factors, has been implicated in the pathogenesis of atherosclerosis and thrombosis, both for the loss of its protective capability and for the induction of pro-atherothrombotic mechanisms (Versari *et al.*, 2009b; Taddei *et al.*, 2003; Brunner *et al.*, 2005).

1.3.2.2.2 Proposed mechanisms of ED

According to the latest consensus in literature, oxidative stress appears to be the common underlying cellular mechanism for the development of ED in most, if not all, cardiovascular risk factor conditions (Mudau M *et al.*, 2012). In general, cardiovascular risk factors seem to be associated with upregulation of ROS sources, especially NADPH oxidase (Chhabra, 2009; Förstermann U and Munzel, 2006). Other sources of ROS such as xanthine oxidase, COX and mitochondria are also implicated (Guzik *et al.*, 2002). As described earlier, even eNOS can become a potential ROS generator when it is uncoupled (Förstermann U and Munzel, 2006).

Harmful effects of vascular oxidative stress include increasing VSMC proliferation (resulting in thickening of the vascular wall), EC apoptosis, and increased expression and activity of MMPs, which are involved in the establishment of an atherosclerotic plaque (Puranik and Celermajer, 2003). Oxidative stress comprises an imbalance in the rate of oxidant production and the levels of antioxidant activity (increased oxidant production vs. decreased anti-oxidant levels) (Pennathur and Heinecke, 2007). Under physiological conditions, the enzyme SOD regulates the levels of O_2^- (Landmesser U *et al.*, 2006). Increased O_2^- generation will overwhelm the defensive mechanisms of SOD, leaving O_2^- free to react with other molecules, especially NO, for which it has a greater affinity (Landmesser U *et al.*, 2006). In fact, the reaction between O_2^- and NO has been reported to occur much faster (rate constant = 6.7×10^9 m/s) than that of dismutation of O_2^- by SOD (rate constant = 2.0×10^9 m/s) (Huang PL, 2003). The reaction between O_2^- and NO leads to the generation of the highly reactive and harmful reactive nitrogen species (RNS), peroxynitrite ($ONOO^-$), which is one of the most potent inducers of ED (Yokoyama M, 2004).

High levels of peroxynitrite are cytotoxic, since essential cellular molecules such as DNA, lipids and proteins are exposed to oxidative damage (Mudau M *et al.*, 2012). In addition to being cytotoxic, peroxynitrite damages the eNOS structure (leading to eNOS uncoupling; see Figure 1.25, which further adds to the vicious cycle observed in ED (Kuzkaya, 2003) (Pacher *et al.*, 2007) (Figure 1.26). For a more detailed discussion of eNOS uncoupling, see section 1.3.2.2.2.1 below)

The development of inflammation is another commonly described mechanism of ED (Libby *et al.*, 2002). Under physiological conditions, the endothelium regulates vascular inflammation (including the expression of adhesion molecules and promotion of leukocyte adhesion) via the release of NO (Osto and Cosentino, 2010). It therefore follows that during ED, characterized by reduced NO levels sustained vascular inflammation will ensue, which is detrimental to the vascular system. However, several studies have reported that inflammation is not only a mechanistic consequence of ED, but also an inducer of ED; hence, inflammation is widely recognised as a risk factor for CVD (Libby *et al.*, 2002; Szmitko *et al.*, 2003). Furthermore, there seems to be a causal relationship between oxidative stress and inflammation (Madamanchi *et al.*, 2005). Oxidative stress may enhance vascular inflammation signalling pathways (Madamanchi *et al.*, 2005), and conversely inflammatory cells are known to be major sources of O_2^- (Clempus and Griendling, 2006). Inflammation is often associated with the overexpression of inflammatory cytokines such as tumour necrosis factor-alpha (TNF- α) and interleukin-1 (IL-1) (Blake and Ridker, 2001). These inflammatory cytokines in turn prompt ECs or macrophages to express adhesion molecules such as VCAM-1 and ICAM-1, MCP-1, interleukin-6 (IL-6) resulting in a state of endothelial activation, which is regarded by some as a precursor of ED (Blake and Ridker, 2001).

The role of TNF- α in ED has received considerable attention in recent years, and a causal link is now well established (Mudau M *et al.*, 2012). TNF- α has been reported to promote ROS formation via activation of NADPH oxidase and xanthine oxidase (Zhang W *et al.*, 2009). For example, Gao *et al.* (2007) reported that TNF- α induces ED via increased NADPH oxidase activity in coronary arterioles of mice with type 2 diabetes. In addition, TNF- α has been implicated in the downregulation of eNOS expression (and therefore decreased NO production) by accelerating eNOS mRNA degradation (Hamburg and Vita, 2005; Zhang W *et al.*, 2009; Stenvinkel, 2001). According to Zhang C *et al.*, (2006a) ED observed in myocardial ischaemia-reperfusion injury may be attributable to increased TNF- α expression via the enhancement of xanthine oxidase activity. TNF- α induces the gene expression of various inflammatory cytokines and chemokines, either dependently or independently of the activation of transcriptional factors, such as NF- κ B and AP-1. This TNF- α -mediated signalling initiates and accelerates atherogenesis, thrombosis, vascular

remodelling, vascular inflammation, endothelium apoptosis, vascular oxidative stress and impaired NO bioavailability, which contribute to the blunted vascular function. Dietary supplements and exercise have been previously shown to favourably reduce the risk of vascular dysfunction by inhibiting TNF- α production and (or) TNF- α -mediated signalling (Zhang H *et al.*, 2009).

Other harmful stimuli-induced mechanisms associated with the development of increased oxidative stress and decreased eNOS activation/eNOS uncoupling include activation of cholesterylester transport protein (CETP), downregulation of lipoprotein lipase, downregulation of peroxisome-proliferator activated receptor (PPAR), downregulation of PKA, activation of caveolin, activation of rho-kinase and downregulation of sphingosine-1-phosphate (Balakumar *et al.*, 2008).

Vasquez-Vivar *et al.* (2002) described the role of BH₄ in the balance between NO and O₂⁻ formation from eNOS. In the absence of BH₄, eNOS becomes uncoupled and cannot reach its normal NO-generating abilities (Rafikov *et al.*, 2011). Once eNOS becomes uncoupled due to decreased bioavailability of BH₄, the uncoupling process becomes self-propagating, since uncoupled eNOS generates O₂⁻, which will in turn oxidize the remaining BH₄ (Landmesser U *et al.*, 2003). As mentioned previously, O₂⁻ may react with NO, forming peroxynitrite (Beckman and Koppenol, 1996). The increased activity of enzymes such as NADPH oxidases ignites a cascade of ROS formation by producing O₂⁻ (Gielis *et al.*, 2011). Bursts of peroxynitrite generation oxidize BH₄ to BH₃, further increasing eNOS uncoupling, starting a bonfire of ROS production by eNOS (Gielis *et al.*, 2011), effectively bestowing upon eNOS the dubious role as a ROS-generating enzyme. The various reactions of peroxynitrite when occurring during the reaction of peroxynitrite with enzymes, macromolecules and lipids, have been shown to influence cellular functions. Peroxynitrite can also lead to irreversible nitration of tyrosine residues on other cellular proteins (Szabo, 2003), such as superoxide dismutase, cytoskeletal actin, neuronal tyrosine hydroxylase, cytochrome P450 and prostacyclin synthase (Greenacre and Ischiropoulos, 2001), causing impaired phosphorylation and enzymatic dysfunction (Kuzkaya *et al.*, 2003).

Importantly, elevated eNOS expression, without a parallel increase in BH₄, results in eNOS uncoupling because of an imbalance between the cofactor and the enzyme (Bendall *et al.*, 2005). Crabtree *et al.* (2009) investigated the stoichiometry of intracellular BH₄/eNOS interactions and demonstrated a striking linear relationship between eNOS activity and cellular BH₄ levels, with eNOS uncoupling occurring when the eNOS: BH₄ molar ratio exceeded 1. Increasing intracellular BH₂ concentrations in the presence of a constant eNOS: BH₄ ratio was sufficient to induce eNOS-dependent O₂⁻ production, indicating that eNOS/BH₄ reaction stoichiometry has a tandem role with the intracellular BH₄:BH₂ ratio (rather than absolute plasma concentrations of BH₄) in determining eNOS uncoupling, even when exogenous oxidative stress is absent (Crabtree *et al.*, 2009). In another study, Heiss *et al.* (2009) demonstrated that a decrease in BH₄ levels activated nuclear factor, erythroid derived 2 (NF-E2)-related factor, which leads to a reduction in eNOS protein levels in human ECs. Thus, the stoichiometric balance between BH₄ and eNOS is maintained, eNOS is kept in a coupled state, and ROS production is reduced. It was shown that murine ECs contain large amounts of dihydrofolate reductase (DHFR) and that reduction of DHFR activity by methotrexate, or genetic knockdown of DHFR by RNA interference, resulted in oxidation of BH₄ to BH₂ with subsequent eNOS uncoupling (Crabtree *et al.*, 2009). DHFR can regenerate BH₄ from BH₂ and preserve eNOS coupling by helping to maintain a better BH₄:BH₂ ratio, especially when both are scarce (Crabtree *et al.*, 2009).

The role of L-arginine (the main substrate of eNOS) in maintaining eNOS in a coupled state is not clear (Gielis *et al.*, 2011). It is unlikely that plasma L-arginine levels would fall below the critical concentration for eNOS activity in vivo, as the plasma level of L-arginine is 30 times higher than the eNOS (Crabtree *et al.*, 2009). In addition, L-arginine itself is recycled by the cell (Simon *et al.*, 2003). An increased intracellular breakdown by arginases, however, can lead to a very local, subcellular decrease in intracellular L-arginine (Bachetti *et al.*, 2004; Xu W *et al.*, 2004). As such, arginases, expressed in ECs can compete with eNOS for their shared substrate (L-arginine) (Bachetti *et al.*, 2004) and can therefore also have downregulating effects on eNOS (Xu W *et al.*, 2004). The endogenous eNOS inhibitor (ADMA) directly inhibits eNOS by competing with L-arginine for the same binding site; however, ADMA has also been shown to inhibit cellular L-arginine uptake by ECs

(Palm *et al.*, 2007). Therefore, a decreased L-arginine: ADMA ratio can result in reduced NO formation by eNOS (Böger, 2007). Indeed, Antoniadou *et al.* (2009) demonstrated a strong inverse association between serum ADMA and levels of eNOS dimer, in both human arteries and human veins. Furthermore, increased ADMA plasma concentrations are associated with oxidative stress within the vessels and the development of ED (Sydow and Munzel, 2003). From these findings, it appears that changes in ADMA concentrations, rather than changes in L-arginine levels, trigger eNOS uncoupling (Förstermann U and Munzel, 2006). The ZnS₄ cluster in the eNOS oxygenase domain, formed by a zinc ion and two cysteine residues from each monomer, is positioned equidistant from each haem group and is responsible for the maintenance of the integrity of the BH₄ binding site (Raman *et al.*, 1998). Mutation in this cluster prevents the binding of zinc, BH₄, or L-arginine and eliminates enzyme activity (Förstermann U and Munzel, 2006), suggesting that stabilization of the dimer interface by the zinc thiolate center is one of the keys for catalytic activity. Exposing the isolated eNOS enzyme to peroxynitrite, a by-product of the interaction between excessive NO and O₂⁻, leads to the oxidation of the zinc thiolate cluster, which uncouples eNOS (Förstermann U and Munzel, 2006). Recently, Chen W *et al.* (2010) demonstrated that the dimer stabilization induced by BH₄ does not require zinc occupancy in this thiolate cluster. Although peroxynitrite treatment induced loss of Zn binding and compromised eNOS activity, incubation with a zinc chelator did not alter eNOS activity (Chen W *et al.*, 2010).

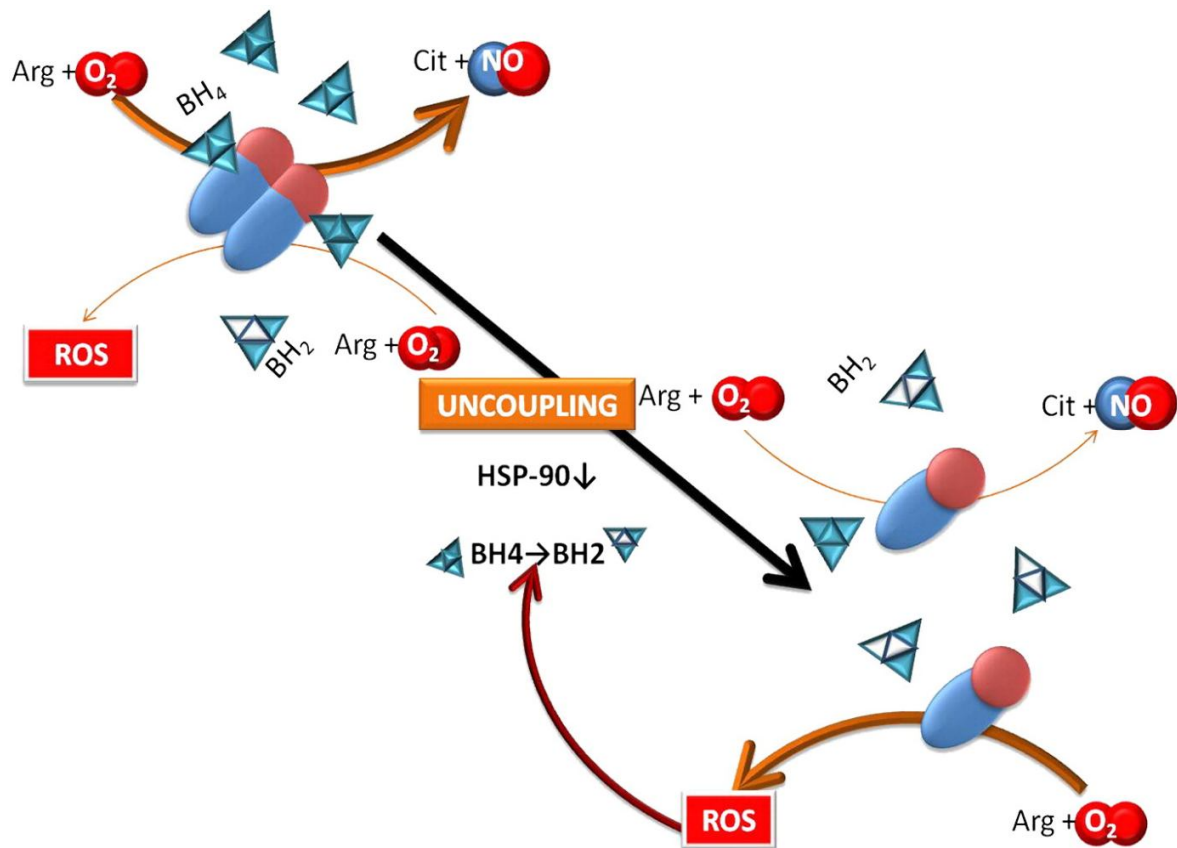


Figure 1.25: Schematic overview of eNOS uncoupling. In the presence of sufficient BH_4 , the eNOS dimer produces abundant amounts of NO (thick arrow) and a small fraction of ROS (thin arrow). BH_4 binds the oxygenase domain of eNOS and stabilizes the dimer. However, in absence of BH_4 , when there is more BH_4 oxidized to BH_2 , the eNOS dimer will uncouple into two monomers, which are less efficient in the production of NO and generate large amounts of ROS (thick arrow). ROS generated by uncoupled eNOS further oxidize BH_4 (Gielis *et al.*, 2011).

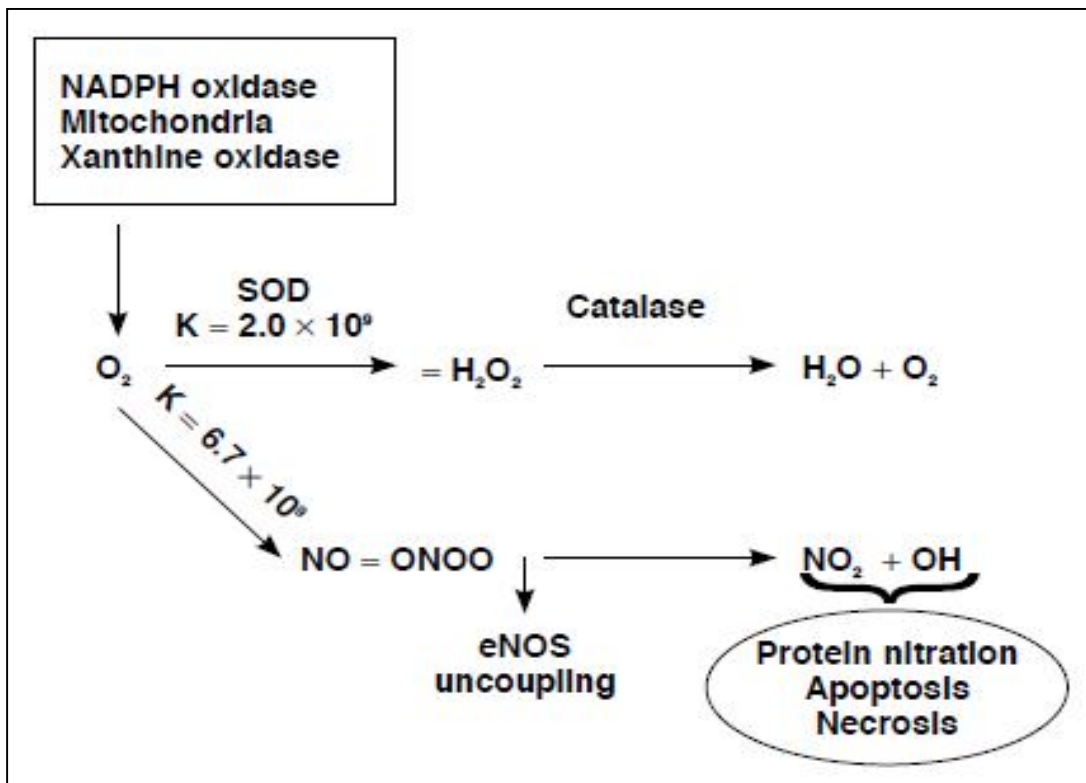


Figure 1.26: Oxidative and nitrosative stress. O_2^- anion (O_2^-) released from sources such as NADPH oxidase, mitochondria and xanthine oxidase is dismutated to hydrogen peroxide (H_2O_2) by superoxide dismutase (SOD), which is then converted to water and oxygen by catalase. However, O_2^- has a higher affinity for NO than SOD, and when NO is in excess, it preferentially combines with NO to produce peroxynitrite with various pathophysiological consequences (Mudau M *et al.*, 2012).

1.3.3 Progression to atherosclerosis

It is now widely recognised that deleterious alterations of endothelial physiology such as observed in ED, not only represent a key early step in the development of atherosclerosis, but are also involved in plaque progression and the occurrence of atherosclerotic complications (Kinlay and Ganz, 1997)(see figure 1.27). Although the association between cardiovascular risk factors and atherosclerotic disease is well documented, the mechanism by which these risk factors induce lesion formation and lead to events is not entirely defined (Chhabra, 2009). Given its strategic location, biological properties and barrier-like function, the EC layer is likely to serve as the 'missing link' between any given risk factor and its detrimental vascular effects (Halcox *et al.*, 2002). In fact, ED has previously been described as the *primum movens* ("first cause") of future cardiovascular complications (Bruyndonckx *et al.*, 2013).

Most, if not all risk factors that are related to atherosclerosis and cardiovascular morbidity and mortality, including traditional and nontraditional risk factors, are also found to be associated with ED (Cai and Harrison, 2000). Many of these risk factors, including dyslipidaemia, hypertension, diabetes and smoking are associated with overproduction of ROS and/or increased oxidative stress (Cai and Harrison, 2000)(Figure 32). By reacting with NO, ROS may reduce vascular NO bioavailability and promote cell damage (Tomasian *et al.*, 2000). Hence increased oxidative stress is considered a major mechanism involved in the pathogenesis of ED (Vogel *et al.*, 1998; Tomasian *et al.*, 2000; Quyyumi *et al.*, 1995).

The probability of developing ED increases with the number of risk factors present in an individual, but the potential to alter endothelial function may vary between risk factors (Celermajer *et al.*, 1994). Taken together, the status of endothelial function represents an integrated index of both the overall cardiovascular risk factor burden and the sum of all vasculoprotective factors in any given individual (Deedwania, 2000). Moreover, given its pivotal role in the atherogenic process, ED may be regarded as the "ultimate risk of the risk factors" indicating the existence of a specific pro-atherogenic vascular milieu which is associated with perfusion abnormalities and cardiovascular events (Bonetti *et al.*, 2003).

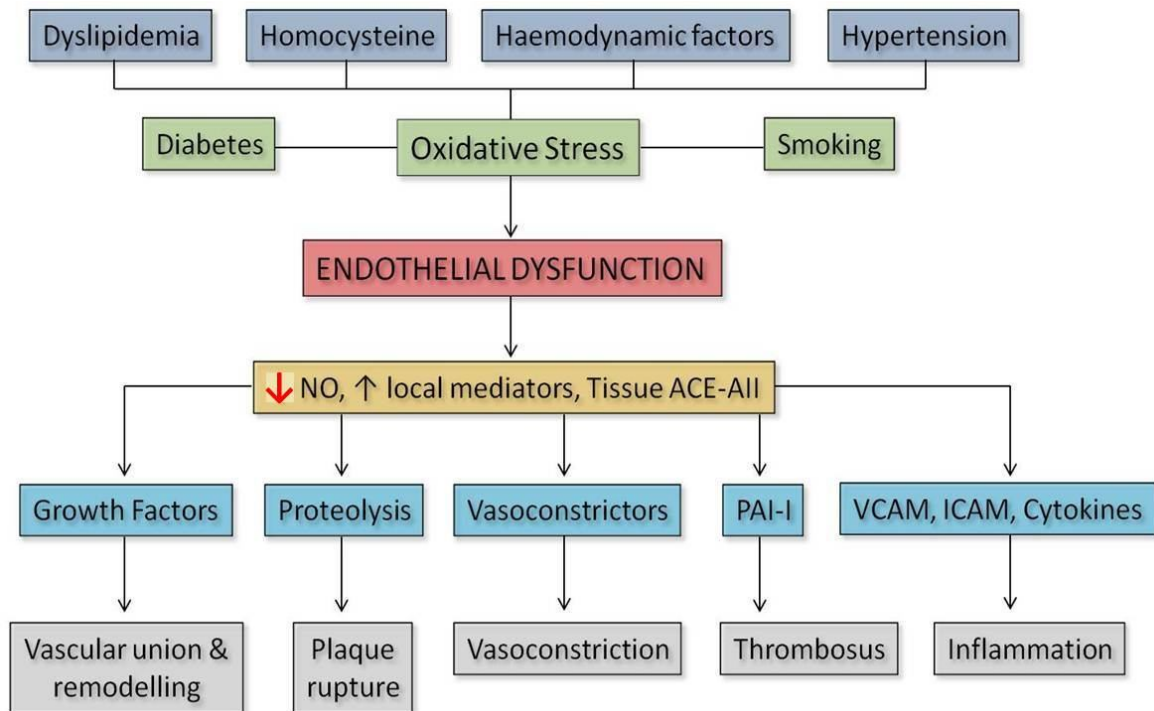


Figure 1.27: The central role of ED in the causation and progression of atherosclerosis. ED not only denotes impaired endothelial dependent vasodilatation, but also represents a state of endothelial activation which is characterized by a pro-inflammatory, proliferative and pro-coagulatory milieu that favours all stages of atherogenesis (Adapted from Chhabra, 2009).

1.3.4 Clinical relevance of endothelial function

The assessment of endothelial function may emerge as an integral adjuvant test for evaluation of the vulnerable patients at risk for future cardiovascular events (Lerman and Zeiher, 2005). In fact, the detection of ED can be a lifesaving clinical tool as ED is an early pathophysiological phenomenon and precursor of atherosclerosis. As such, ED is often regarded as both a predictor and surrogate marker of CVD, and therefore an important link between cardiovascular risk factors and disease (see figure 1.28). A few tests for evaluating endothelial function exist and will be discussed briefly below (Lekakis *et al.*, 2011; Deanfield *et al.*, 2007).

According to Deanfield *et al.*, (2007) such tests should be safe, noninvasive, reproducible, repeatable, cheap, and standardized between laboratories (see table 1.7). The results should also reflect the dynamic biology of the endothelium throughout the natural history of atherosclerotic disease, define subclinical disease processes, as well as provide prognostic information for risk stratification in the later clinical phase. No single test currently fulfills these requirements, and a panel of several tests is therefore needed to characterize the multiple facets of endothelial biology. Based on the above requirements, see table for a summary of current available tests and their advantages and disadvantages (Deanfield *et al.*, 2007).

Several pharmacological approaches have also been demonstrated to improve or reverse ED, although their effect is never selective and usually also target one or more traditional cardiovascular risk factors (Versari *et al.*, 2009b) (see table 1.7).

Lastly, but most important, the structural and functional integrity of the endothelium is crucial to maintain vascular homeostasis and prevent atherosclerosis. The endothelium is increasingly becoming a surrogate end point of the therapeutic approach to cardiovascular risk, as demonstrated by its inclusion among markers of organ damage in the latest European hypertension guidelines (Mancia *et al.*, 2007). Although ED is only considered a marker of cardiovascular risk, investing in the development of techniques to easily and noninvasively explore endothelial function at a low cost will improve the effectiveness of patients' cardiovascular therapy in the clinical setting tremendously.

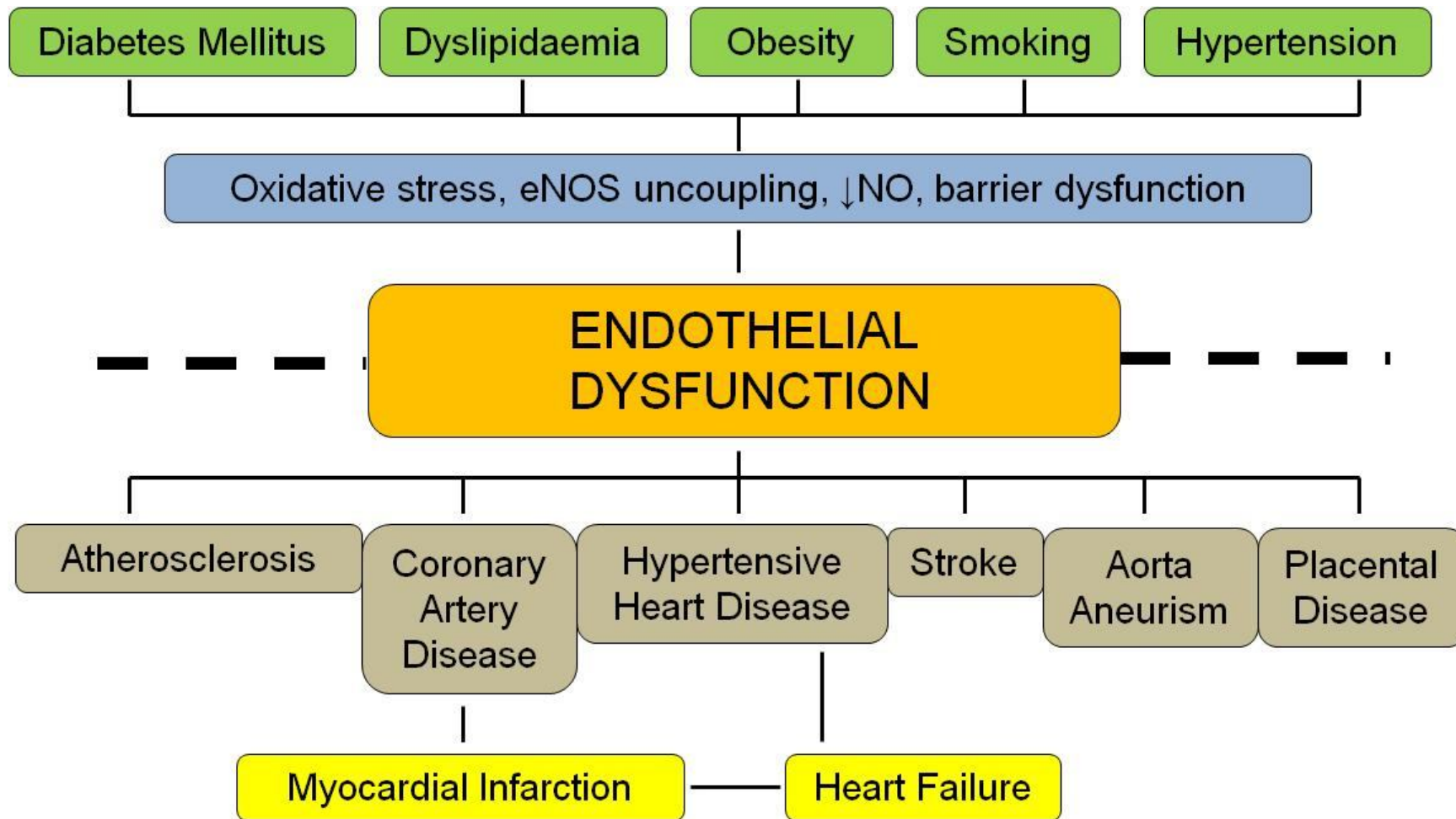


Figure 1.28: ED: the pathophysiological link between risk factors and CVD.

Table 1.7: Methods for Clinical Assessment of Endothelial Function (Deanfield *et al.*, 2007).

Technique (Outcomes measure)	Noninvasive	Repeatable	Reproducible*	Reflects Biology	Reversible	Predicts Outcome†
Cardiac catheterization (change in diameter, change in coronary blood flow)	-	-	+/-	+	+	+
Venous occlusion plethysmography (change in forearm blood flow)	-	+/-	+/-	+	+	+
Ultrasound FMD (change in brachial artery diameter): GOLD STANDARD	+	+	+/-	+	+	‡
PWA (change in augmentation index)	+	+	+/-	+	-	-
PCA (change in reflective index)	+	+	+/-	+	-	-
PAT (change in pulse amplitude)	+	+	+/-	+	-	-

+ indicates supportive evidence in literature; -, insufficient evidence; FMD, flow-mediated dilatation; PWA, pulse wave analysis; PCA, pulse contour analysis; and PAT, pulse amplitude tonometry.

*Reproducibility of PWA, PCA, and PAT has been less extensively investigated than FMD.

†Studies that link PWA, PCA, and PAT to outcome have not yet been reported.

‡ FMD is currently the gold standard for noninvasive assessment of conduit artery endothelial function because there is considerable clinical trial experience, validation, a firm link to biology, and association with cardiovascular events.

B. Motivation and Aims.**(i) Problem identification, rationale and motivation**

From the literature, it is clear that a healthy vascular endothelium is a prerequisite for a healthy cardiovascular system. It is now widely accepted that EC injury, particularly when it manifests as ED, is not only a mere predictor of future adverse cardiovascular events, but also a *reversible* precursor of atherosclerosis and its sequelae, so that early clinical intervention strategies can prevent atherogenesis and coronary artery disease. It is for this reason that there are currently numerous on-going clinical studies to determine the optimal diagnostic tools for clinical detection of ED, something that has eluded us until now. Important, however, is the fact that both basic scientists and clinicians have now come to realize the importance of early detection of ED.

The distinct location of cardiac microvascular ECs in the myocardial capillary network bestows upon them a unique role not only in the maintenance of cardiac vascular homeostasis, but also as regulators of myocardial function. Furthermore, the myocardial capillary network is regarded as the primary target of end-organ damage in the heart in conditions such as hypertension and diabetes mellitus. It is therefore surprising that so few EC-based studies have investigated and characterized this unique EC subtype, not only under baseline conditions, but also their response to the effects of harmful stimuli commonly associated with cardiovascular risk factors and disease. In our literature research, for example, we could only find one study that analysed the CMEC proteome with only 22 proteins being positively identified.

The main aim of this study was therefore to fill the gaps in literature by undertaking a comprehensive characterization of CMECs under baseline, unstimulated conditions, and after exposure to two physiologically and clinically relevant harmful stimuli. A wide variety of techniques was employed and many end-points, including morphology, function, viability, signal transduction events and large-scale protein expression patterns

were investigated. In the absence of any previous such wide-ranging studies on CMECs, I set out to establish and characterize *in vitro* models of EC injury in CMECs, with the objective to reproduce a classical model of ED

(ii) Aims of the study

In view of the fact that the purpose of the study was to characterize adult rat CMECs and their responses under baseline conditions and in conditions of injury induction, it was decided that this study would not be hypothesis-driven. Hence, the following aims were formulated:

Aim 1: Baseline characterization of commercially purchased primary CMEC cultures.

Previous attempts in our laboratory to harvest, isolate and culture CMECs from adult rat hearts proved to be technically difficult and the resulting cultures were frequently contaminated by other non-ECs. In view of this, we opted to purchase our cells commercially from a US-based company. The first aim of my study was therefore to validate the purity of the purchased CMECs, and comprehensively characterize the cells under normal, baseline conditions. The reduction in cellular NO levels is one of the gold standards used to detect EC injury / ED in vascular ECs. In view of this, the second part of this aim was to determine and compare the effect of treatment with a variety of potentially harmful stimuli often associated with cardiovascular risk factors and diseases on NO production in the CMECs.

Aim 2: Characterization and investigation of hypoxia-induced responses in CMECs.

Vascular ECs are frequently subjected to conditions of low PO₂ as a result of their strategic location at the interface between the vascular wall and circulating blood. Furthermore, hypoxia is a recognized risk factor for the development of ED. However, few

studies have investigated the effects of hypoxia on CMECs, and therefore the third aim of this study was to comprehensively characterize the responses of CMECs to hypoxia.

Aim 3: Characterization and investigation of TNF- α -induced responses in CMECs.

The development of systemic and local inflammation is associated with many cardiovascular risk factors and disease, including diabetes mellitus, obesity and atherosclerosis, and TNF- α is regarded as one of the primary pro-inflammatory cytokines mediating the harmful effects of inflammation. Vascular ECs are major targets of circulating TNF- α , which has been shown to induce ED in many *in vitro* and *in vivo* studies. In view of this, the third aim of the study was to comprehensively characterize the responses of the CMECs to TNF- α stimulation and establish whether ED could be induced.

CHAPTER TWO

Materials & Methods

The purpose of this chapter is to describe the general materials and methods used for the majority of experiments throughout the study. Whenever materials and methods were used that only applied to specific studies or experiments, descriptions will be supplied in the relevant results chapters.

2.1 Materials

2.1.1 General materials used

- *Life Technologies* (Carlsbad, California, USA): Attachment Factor (a sterile solution containing gelatin as an attachment factor for cell cultures); Trypsin (a solution containing 2.5 % trypsin) and Dihydroethidium (DHE).
- *Calbiochem* (San Diego, CA, USA): 4,5-diaminofluorescein-2/diacetate (DAF-2/DA).
- *Sigma-Aldrich* (St Louis, Mo, USA): Human recombinant tumor necrosis factor (TNF)- α ; Oleanolic Acid (OA); Asymmetric dimethyl-arginine (ADMA); Dihydrorhodamine-1, 2, 3 (DHR-123); 2', 7'-Dichlorofluorescein (DCF); 2,3-Dimethoxy-1,4-naphthoquinone (DMNQ); Diethylamine NONOate diethylammonium salt (DEA/NO).
- *Cell Signaling Technologies* (Beverly, MA, USA): Antibodies for the detection of: eNOS, phospho-eNOS (Ser 1177); PKB/Akt, phospho PKB/Akt (Ser 473); caveolin-1; heat shock protein 90 (HSP 90); cleaved caspase-3; cleaved poly (ADP-ribose) polymerase (PARP); and IK β .
- *Santa Cruz Biotechnologies* (Santa Cruz, CA, USA): Antibodies for the detection of: p22-phox, nitrotyrosine and iNOS antibodies.
- *Bio-Legend* (Biochem-Biotech) (San Diego, CA, USA): Alexa Fluor 647 Annexin V, Propidium iodide (PI) solution, Annexin V binding buffer and cell staining buffer.
- *AEC Amersham* (Buckinghamshire, UK): Enhanced chemiluminescence (ECL) detection reagent, ECL hyperfilm, and Horseradish peroxidase-linked anti-rabbit IgG.

- *Millipore* (Billerica, MA, USA): Polyvinylidene difluoride (PVDF) membrane (Immobilon™-P); authentic peroxyxynitrite.
- All other chemicals were of Analar grade and were purchased from Merck (methanol, standard salts for solutions and buffers, dimethyl sulfoxide (DMSO), etc).

2.2 Cardiac microvascular endothelial cells (CMECs)

Adult rat CMECs were purchased commercially from VEC technologies (Rensselaer, New York, USA). The microvascular endothelial cell harvesting technique employed by the company has previously been described (Nishida *et al.*, 1993; Piper *et al.*, 1990), and ensured the highest possible myocardial capillary-derived CMEC yield, precluding contamination by non-endothelial cells. Cells were received in 75 ml fibronectin coated tissue culture flasks and grown in microvascular endothelial growth medium (EGM) (Clonetics EGM-2MV; Lonza, Walkersville, MD) until they were fully confluent. The growth medium was supplemented with 10 % fetal bovine serum (FBS) (Highveld Biological, RSA), standard endothelial growth factors (vascular endothelial growth factor – VEGF, human epidermal growth factor – hEGF, human fibroblastic growth factor hFGF, long chain human insulin-like growth factor - R³-IGF-1), ascorbic acid, hydrocortisone and antibiotics (gentamicin and amphotericin B). The cells were grown in a tissue culture incubator (NuAire, Plymouth, USA) under standard atmospheric conditions: 21 % oxygen, 5 % carbon dioxide, 40-60 % humidity and temperature maintained at 37 °C. Confluent cells (cells evenly distributed and completely covering the growth surface of the flask) were removed from culture by the addition of pre-heated (37 °C) trypsin. Following addition of trypsin, the flasks were placed back into the incubator for a further five minutes to allow for trypsin-induced detachment of cells from the surface (this was verified by microscopic observation). When completely detached from the surface, the trypsin-cell mixture was collected, resuspended in growth medium and centrifuged at a 1000 rpm for 3 minutes at 4°C. After centrifugation, the trypsin-containing supernatant was aspirated and the cell pellets used to make cell stocks for future use. Briefly, pellets were carefully added to a cryo-vial containing “freezing” solution (90 % foetal bovine serum (FBS), 5 % growth medium and 5 % DMSO) and stored in liquid nitrogen.

2.2.1 Passaging procedure:

Cell pellets were removed from liquid nitrogen storage, seeded on 35 mm petri dishes and grown until enough petri dishes were available for experimentation. Briefly, the cell pellet-freezing solution mixtures were allowed to thaw, and the cell pellets then gently resuspended in the solution by a Pasteur pipette. Fresh growth medium was added to the freezing solution for enrichment, and cells subsequently seeded onto two 35 mm pre-coated (Attachment Factor) petri dishes. Cells were allowed to attach overnight, and the medium replaced with freshly prepared growth medium (supplemented with 10 % FBS) the next morning. Cells were allowed to grow to confluency, at which point they were trypsinised (as described above), resuspended in freshly prepared growth medium (10% FBS) and re-seeded to four pre-coated petri dishes in a 1:2 ratio. Passaging continued in a 1:2 ratio until sufficient petri dishes were available for experiments. With each passage the cells are labeled with the date and the number of passages done. This enabled us to (i) establish a time-frame for the growth of the cells from seeding to confluency and, (ii) ensure that the number of passages was closely monitored, as we previously established that culture purity begins to decline after 8 passages. See Figure 2.1 for a diagrammatic representation of the above procedures.

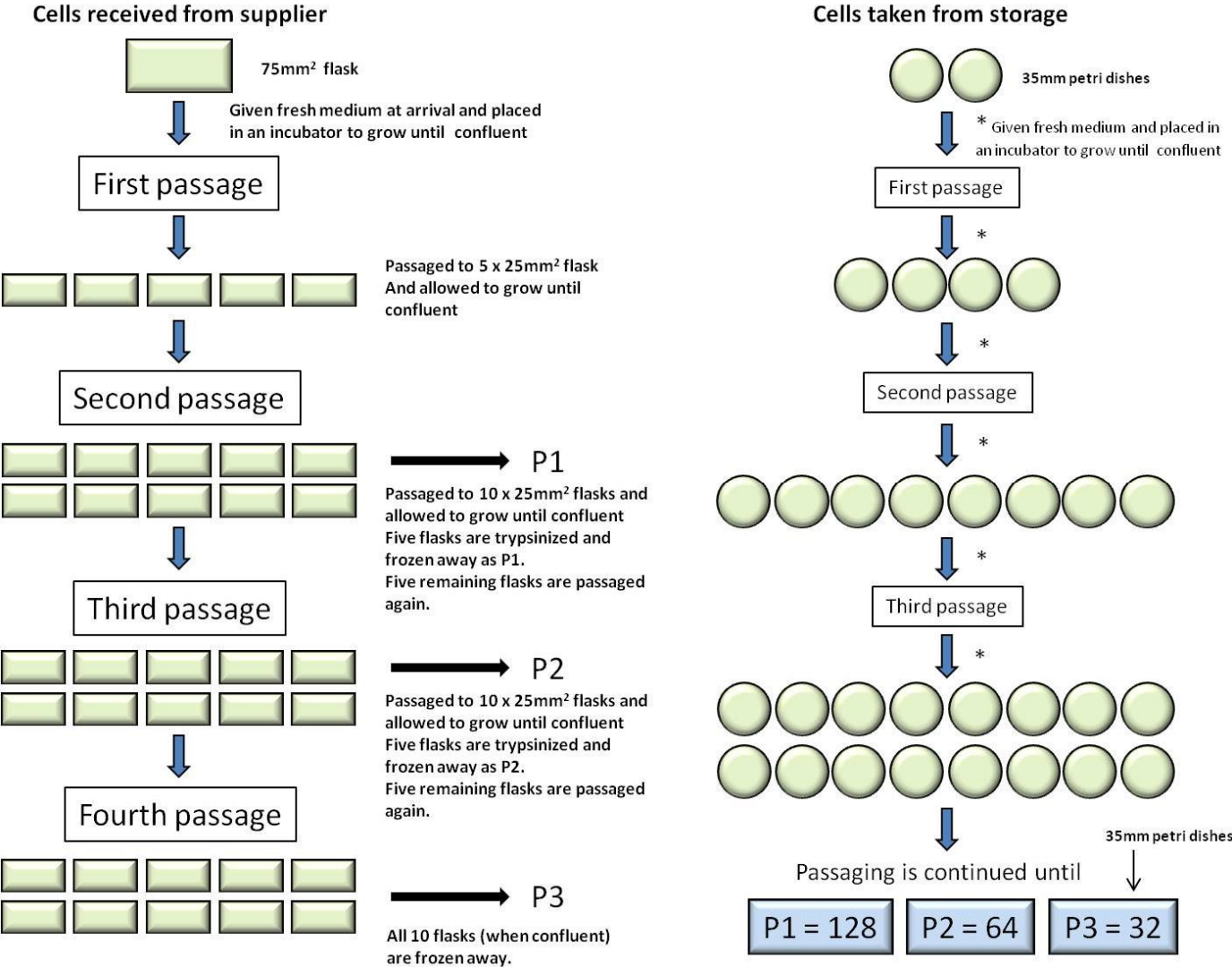


Figure 2.1: Procedure for passaging and labeling of cells.

All experiments were performed on cell cultures grown to confluency, thereby securing cell cycle arrest at the G0 phase as a result of cell-to-cell contact. Cell cycle arrest is known to cause cessation of any further cell proliferation (mitotic activity), thereby minimising possible cell cycle variability when evaluating experimental results (Viñals and Pouyssegur, 1999). Other cell-cycle synchronization protocols employed by researchers include roscovitine treatment and serum starvation (Cho *et al.*, 2005). Serum starvation protocols will be examined and discussed in more detail in Chapter 5 (characterization and investigation of TNF- α -induced responses in CMECs).

Subcultures of the 5th to 7th generations were used for experiments, as the cells were still morphologically and functionally viable, and passaging cells to these generations provided sufficient numbers of plates for statistically acceptable sample sizes. Petri dishes were randomly assigned to respective control and experimental groups. Specific experiments were repeated at least once or twice, and final sample sizes varied between $n = 6-12$ / experimental group.

2.3 **Methods**

2.3.1 General methods used in this study.

2.3.1.1 Flow cytometric analyses

Flow cytometric analyses of all fluorescent probes were performed on a Becton-Dickinson FACSCalibur flow cytometer (Franklin Lakes, NJ), located in the Stellenbosch University-BD Flow Cytometry Unit, Dept of Biomedical Sciences, Faculty of Medicine and Health Sciences. Fluorescence data were analyzed with Cellquest Pro[®] (version 5.2.1) software (Becton-Dickson and Co, San Jose, CA). All flow cytometry protocols were previously developed in our laboratory and published elsewhere (Strijdom *et al.*, 2004b and 2006). For all experiments, a total of 5 000-10 000 cells were routinely analyzed per sample. In order to ensure inter-sample consistency during the acquisition and analysis process of a specific experimental series, cell populations of control samples were gated according to their side scatter (cell granularity) and forward scatter (cell size), which excluded debris and non-

cellular particles from the analysis (Figure 2.3 A). The gate coordinates determined for control samples were retained and applied to all subsequent experimental samples in a particular flow cytometry session. Once gating has been completed, samples were analysed by measuring mean fluorescence intensity as obtained from a histogram (Figure 2.3 B). Unless stated otherwise, all flow cytometry data were expressed as: Mean fluorescence intensity as % of control (control adjusted to 100 %). The procedure as described above, applied for the majority of our fluorescence-based analyses.

Flow cytometers are able to analyze several thousand particles every second, in "real time," and can actively separate and isolate particles having specified properties. A flow cytometer is similar to a microscope, except that, instead of producing an image of the cell, flow cytometry offers "high-throughput" (for a large number of cells) automated quantification of set parameters. A flow cytometer has five main components (see figure 2.2):

- a flow cell - liquid stream (sheath fluid), which carries and aligns the cells so that they pass single file through the light beam for sensing
- a measuring system - commonly used are measurement of impedance (or conductivity) and optical systems - lamps (mercury, xenon); high-power water-cooled lasers (argon, krypton, dye laser); low-power air-cooled lasers (argon (488 nm), red-HeNe (633 nm), green-HeNe, HeCd (UV)); diode lasers (blue, green, red, violet) resulting in light signals
- a detector and Analogue-to-Digital Conversion (ADC) system - which generates forward scatter (FSC) and side scatter (SSC) as well as fluorescence signals from light into electrical signals that can be processed by a computer
- an amplification system - linear or logarithmic
- a computer for analysis of the signals.
- Channels: FL-1H: Excitation : 488 nm / emission: 530 nm (argon laser);
 FL-2H: Excitation: 488 nm / emission: 585 nm (argon laser);
 FL-3H: Excitation: 488 nm / emission: 670 nm (argon laser);
 FL-4H: Excitation: 635 nm / emission: 661 nm (red diode laser).

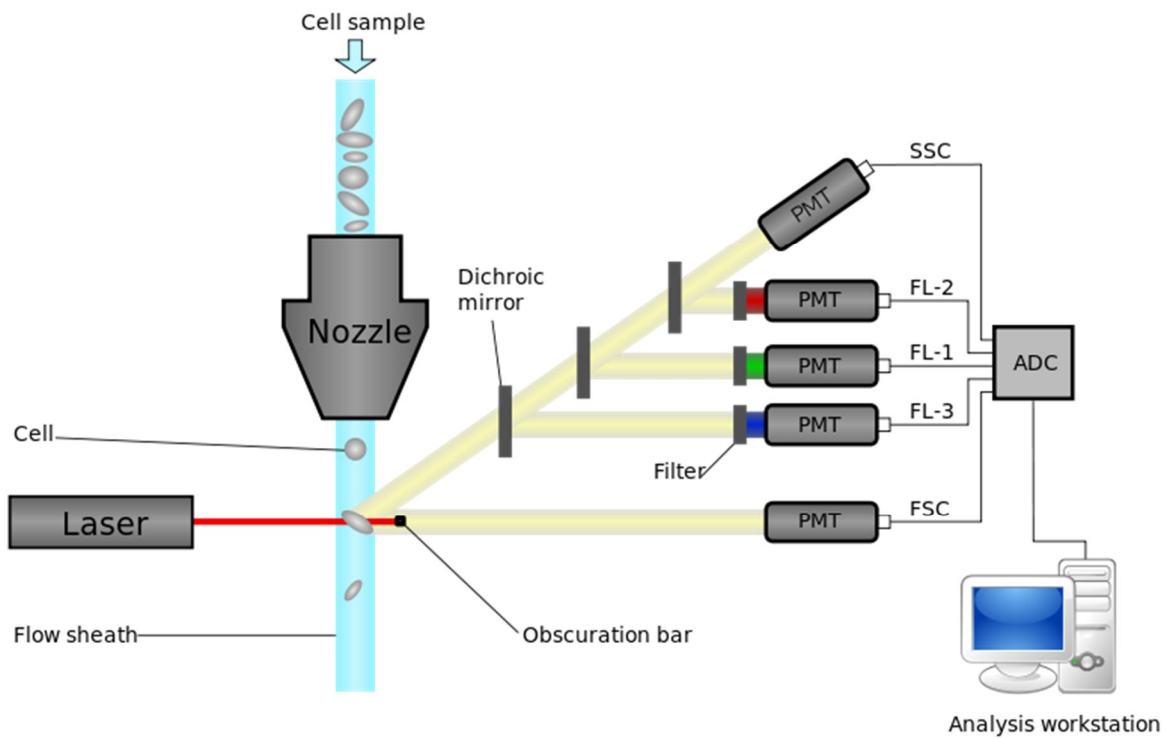


Figure 2.2: Schematic diagram of a flow cytometer, showing focusing of the fluid sheath, laser, optics (in simplified form, omitting focusing), photomultiplier tubes (PMTs), analogue-to-digital converter, and analysis workstation.

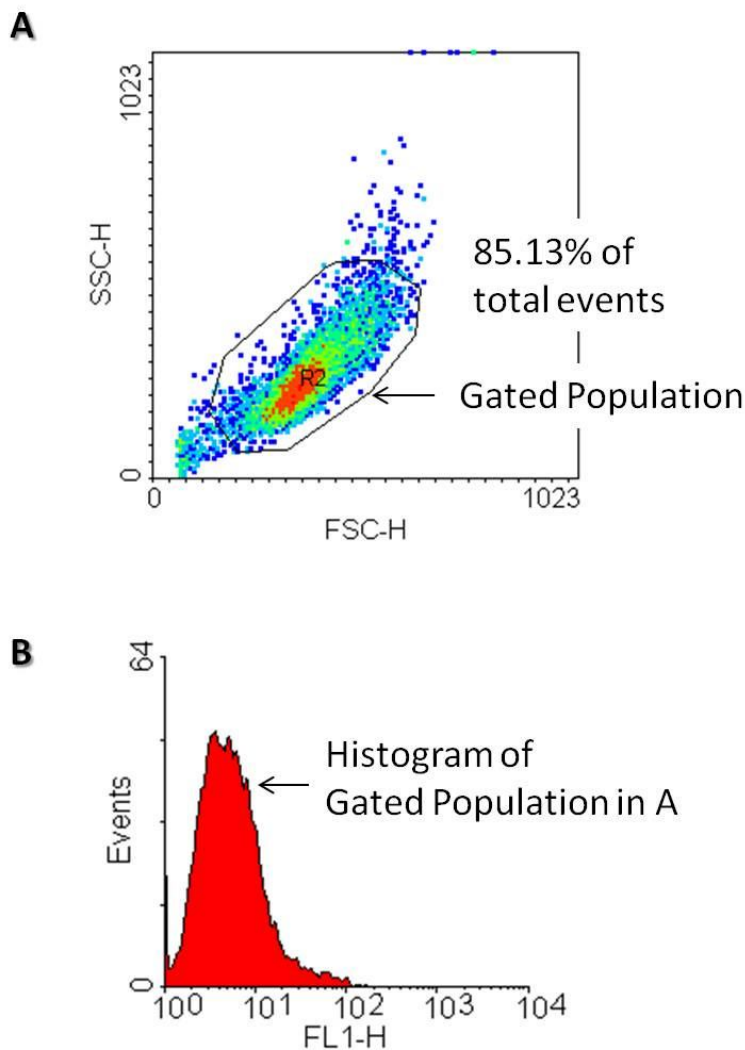


Figure 2.3: **A:** A representative density dot plot of a CMEC representative sample showing the forward scatter (FSC-H; X axis), which measures cell size, and side scatter (SSC-H; Y axis) which measures cell granularity. The population of interest subjected to analysis is selected by the gate (R1) as shown. The “warmer” the colour, the denser the population of cells. **B:** A representative histogram plot of a CMEC representative sample showing the FL1-H channel (FL1-H; X axis), which measures fluorescence intensity in the FL1-H channel, and number of events (Events; Y axis) which measures the number of cells counted. This histogram represents only the “gated” population in A.

2.3.1.1.1 Cell viability Measurements

For cell viability investigations, cells were removed from culture by trypsinisation, washed sequentially in staining and binding buffer (BioLegend) and subsequently treated with propidium iodide (PI; 5 μ M) and Annexin V conjugated with Alexa Fluor® 647 (5 μ M), incubated at room temperature in the dark for 15 min, and finally subjected to flow cytometric analysis. PI fluorescence was analysed in the FL2-H channel, and Annexin V in the FL4-H channel. Cell membrane permeability (loss of membrane integrity) grants the PI probe entrance into the cell which subsequently stains the nucleus. Therefore, cells demonstrating PI uptake and increased PI-fluorescence are deemed necrotic. Apoptotic cells are identified by increased fluorescence as a result of the binding of Annexin V to phosphatidylserine protein, which in viable cells is normally located on the internal surface of the plasma membrane, but translocates to the external surface of the plasma membrane during apoptosis. PI and Annexin V staining therefore distinguishes between cells undergoing necrosis and apoptosis respectively (Figure 2.4 and figure 2.5) (Wilkins *et al.*, 2002). The assay furthermore allows the investigator to measure necrosis and apoptosis simultaneously as shown in figure 2.6.

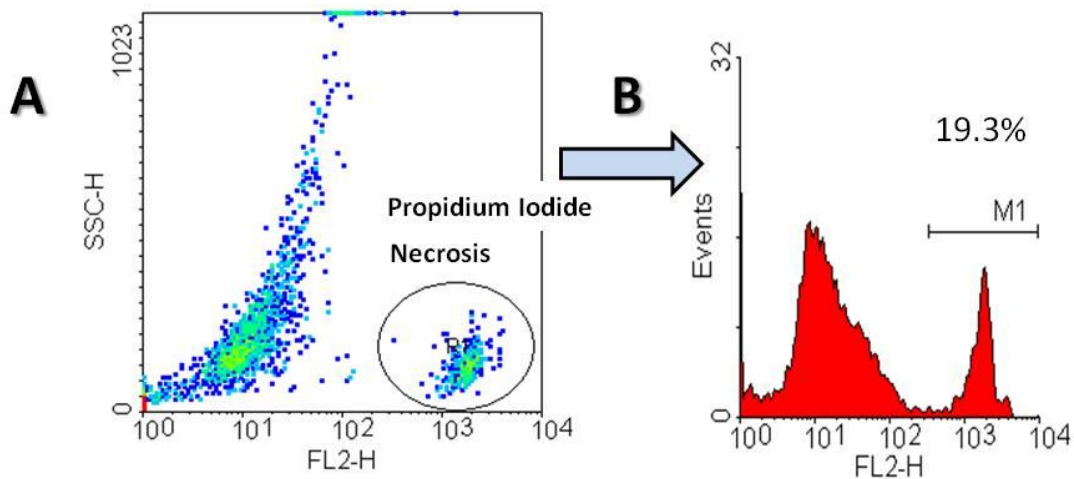


Figure 2.4: **A:** Density plot of a representative sample showing the sub-population of cell samples staining positively with PI (necrosis). **B:** Histogram plot, showing the corresponding PI fluorescence intensity. M1 refers to the % cells of the gated population (19.3%) that stained positively with PI.

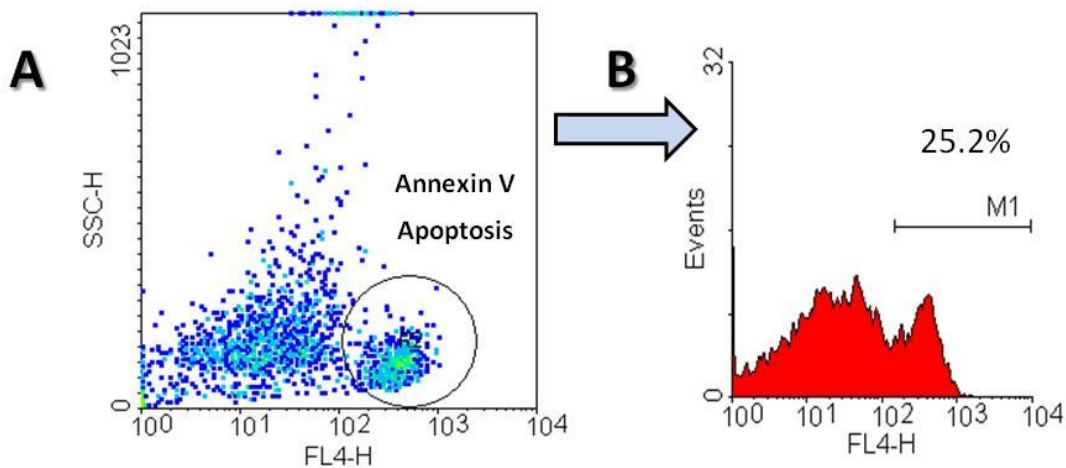


Figure 2.5: **A:** Density plot of a representative sample showing the sub-population of cell samples staining positively with Annexin V (apoptosis). **B:** Histogram plot, showing the corresponding Annexin V fluorescence intensity. M1 refers to the % cells of the gated population (25.2%) that stained positively with Annexin-V.

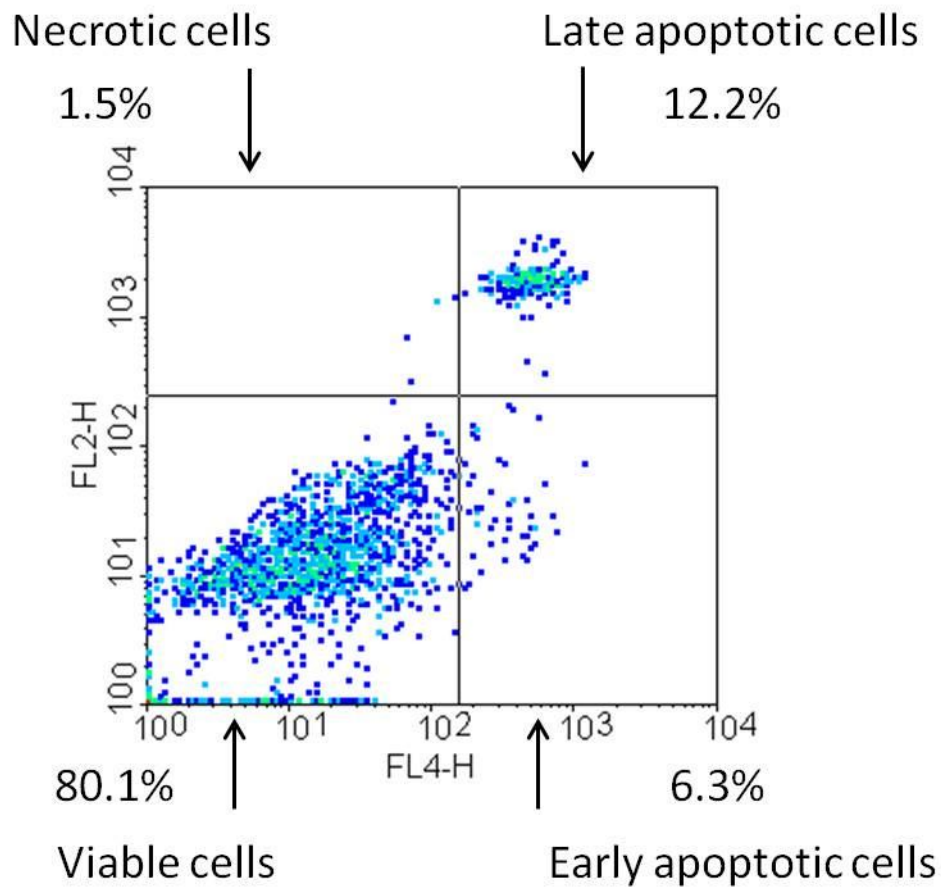


Figure 2.6 A density plot showing the simultaneous measurement of necrosis and apoptosis in one sample (PI measured in the FL2-H channel on the Y-axis and Annexin-V measured in the FL4-H channel on the X-axis), showing the percentage of viable (Left lower quadrant), early apoptotic (Right lower quadrant), late apoptotic (Right upper quadrant) and necrotic (Left upper quadrant) cells.

2.3.1.1.2 Nitric Oxide (NO) Measurements

Intracellular levels of NO were directly measured using flow cytometry-based procedure with the NO-specific DAF-2/DA fluorescent probe as previously developed in our laboratory and published elsewhere (Strijdom *et al* 2004b and 2006). Upon reacting with NO, DAF-2/DA is oxidized to diaminofluorescein-triazol (DAF-2T), which emits a green fluorescence analyzed in the FL1-H channel. At the end of the experiments, cells were washed with phosphate buffered saline (PBS) and incubated with 10 μ M DAF-2/DA at 37 °C for 3 hours. After 3 hours, DAF-2/DA was washed out, cells removed from culture by trypsinisation and resuspended in probe-free PBS for flow cytometric analysis.

The NO-specificity of the DAF-2/DA probe was regularly and randomly tested with the positive control NO donor, diethylamine NONOate diethylammonium salt (DEA/NO; 100 μ M) (from concentration determination studies in figure 2.8 A), which was administered to DAF-2/DA-containing cells at $t = 1$ h for 2 hours as shown in Figure 2.7.

As a standard procedure, all experiments included probe-free absolute control samples (to determine the autofluorescence of the cells) and DAF2/DA-containing control samples, in addition to the experimental samples containing DAF-2/DA. A significant increase in baseline fluorescence between absolute control samples and DAF-2/DA-containing samples confirmed that the DAF-2/DA uptake was sufficient (See figure 2.8B for a representative histogram depicting DAF-2/DA fluorescence).

CMECs exposed to 100 μ M DEA/NO (2 hours) showed a significant increase in DAF-2/DA mean fluorescence intensity (128.36 ± 5.75 % vs. 100 % control: $p < 0.05$) compared to untreated controls (see figure 2.8A). CMECs exposed to 500 μ M DEA/NO (2 hours), showed a significant increase in DAF-2/DA mean fluorescence intensity (120.46 ± 3.67 % vs. 100 % control: $p < 0.05$) compared to untreated controls (see figure 2.8A). CMECs exposed to 1mM DEA/NO (2 hours), showed a significant increase (191.06 ± 34.96 % vs. 100 % control: $p < 0.05$) in DAF-2/DA fluorescence compared to untreated controls (see figure 2.8A).

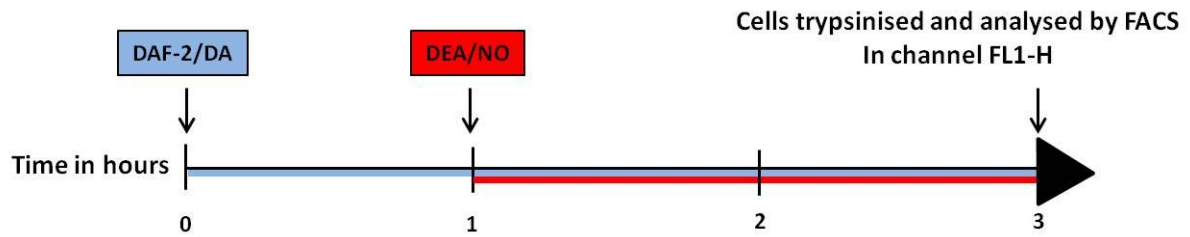


Figure 2.7: Positive control protocol with the NO donor, DEA/NO, to validate the NO-specificity of DAF-2/DA.

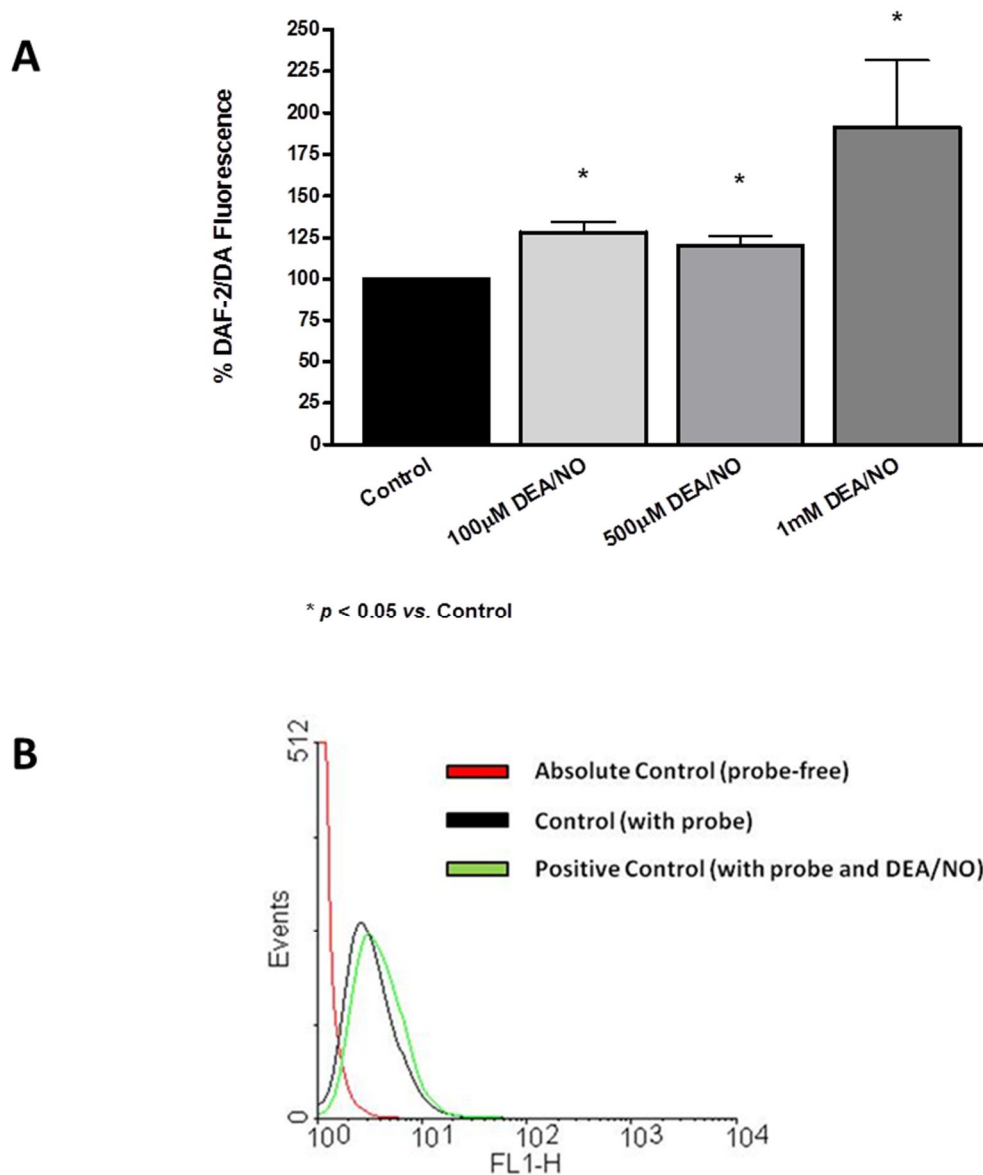


Figure 2.8: A: Measurement of DAF-2/DA fluorescence following treatment with increasing DEA/NO (100µM, 500µM & 1mM) concentrations for 30 minutes. Sample size: $n = 3 - 4$ / group.

B: Histogram showing mean fluorescence intensity measured in absolute control, DAF-2/DA-control and positive control (DEA/NO (100 µM) + DAF-2/DA) samples respectively (analyzed in the FL1-H channel).

2.3.1.1.3 ROS Measurements

ROS production in CMECs was measured with the following fluorescent probes: DHE (relatively specific for $O_2^{\cdot-}$) (Nazarewicz *et al.*, 2013), DHR-123 (ROS detection, previously shown to be sensitive for peroxynitrite and mitochondrial $O_2^{\cdot-}$) (Valez *et al.*, 2012; Tiede *et al.*, 2011) and DCF (sensitive for H_2O_2) (Rhee *et al.*, 2010).

DHE and DHR-123 protocols: After experimental treatment, cells were washed with PBS and treated with either $5\mu M$ DHE or $2\mu M$ DHR-123 in PBS and incubated at $37^\circ C$ for 3 hours as previously described (Navarro-Antolin *et al.*, 2001; Strijdom *et al.*, 2006). After 3 hours, probe-containing PBS was washed out and cells removed from culture by trypsinisation. Cells were resuspended in probe-free PBS and DHE and DHR-123 fluorescence was analyzed by flow cytometry in channels FL2-H and FL3-H respectively (Figure 2.10 B & 2.12 B). The specificity of the DHE and DHR-123 probes was regularly and randomly tested with positive control ROS donors, namely (i) 2, 3-dimethoxy-1, 4-naphthoquinone (DMNQ; $100\mu M$) (from concentration determination studies in figure 2.10 A), administered to DHE-containing cells at $t = 1h$ for 2 hours as shown in Figure 2.9, and (ii) authentic peroxynitrite ($ONOO^{\cdot-}$; $100\mu M$) (from concentration determination studies in figure 2.12 A) administered to DHR-123-containing cells at $t = 1h$ for 2 hours as shown in Figure 2.11.

DCF protocols: After experimental treatment, cells were washed with PBS and samples were treated with $10\mu M$ DCF and incubated at $37^\circ C$ for 60 minutes, after which probe-containing PBS was washed out and cells removed from culture by trypsinisation. Cells were resuspended in probe-free PBS and DCF fluorescence was analyzed by FACS in channel FL2-H (Figure 2.14 B). The specificity of the DCF probe was regularly and randomly tested with positive control ROS donor, namely H_2O_2 ($100\mu M$) (from concentration determination studies in figure 2.14 A), administered to DCF-containing cells at $t = 30\text{ min}$ for 30 minutes as shown in Figure 2.13.

CMECs exposed to $10\mu M$ DMNQ (2 hours) showed a significant increase in DHE mean fluorescence intensity ($156.13 \pm 10.01\%$ vs. 100% control: $p < 0.05$) compared to untreated controls (see figure 2.10A). CMECs exposed to $100\mu M$ DMNQ (2 hours), showed no change

in DHE mean fluorescence intensity (189.53 ± 10.09 % vs. 100 % control) compared to untreated controls (see figure 2.10A).

CMECs exposed to 100 μ M peroxynitrite (2 hours) showed a significant increase in DHR-123 mean fluorescence intensity (186.40 ± 1.35 % vs. 100 % control: $p < 0.05$) compared to untreated controls (see figure 2.12A). CMECs exposed to 500 μ M peroxynitrite (2 hours), showed a significant increase in DHR-123 mean fluorescence intensity (131.62 ± 12.51 % vs. 100 % control: $p < 0.05$) compared to untreated controls (see figure 2.12A). CMECs exposed to 1mM peroxynitrite (2 hours), showed no change in DHR-123 mean fluorescence intensity (104.03 ± 8.36 % vs. 100 % control) compared to untreated controls (see figure 2.12A).

CMECs exposed to 100 μ M H₂O₂ (30 minutes) showed a significant increase in DCF mean fluorescence intensity (397.74 ± 78.38 % vs. 100 % control: $p < 0.05$) compared to untreated controls (see figure 2.14A).

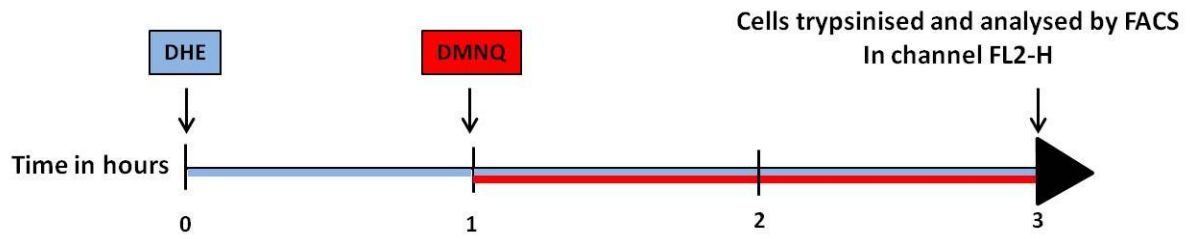


Figure 2.9: Positive control protocol with the O_2^- donor, DMNQ, to validate the relative O_2^- -specificity of DHE.

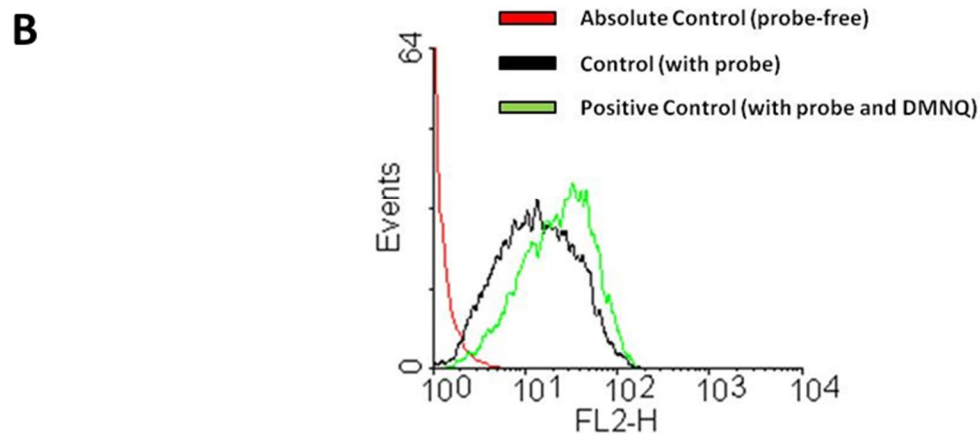
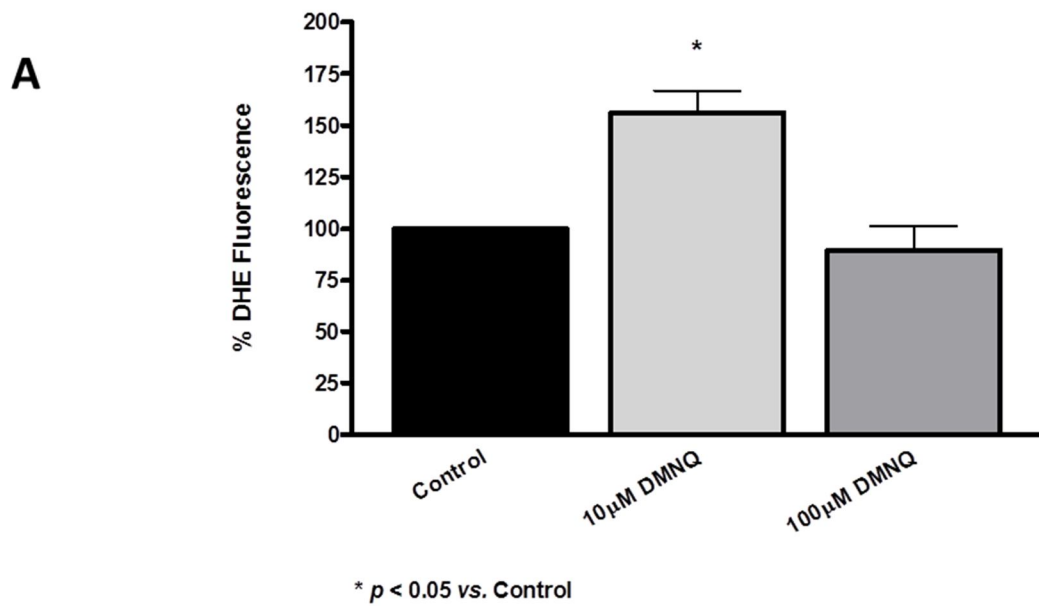


Figure 2.10: A: Measurement of DHE fluorescence following treatment with increasing DMNQ concentrations (10µM & 100µM) for 30 minutes. Sample size: $n = 3 - 4$ / group.

B: Histogram showing mean fluorescence intensity measured in absolute control, DHE-control and positive control (DMNQ (100 µM) + DHE) samples respectively (analysed in the FL2-H channel).

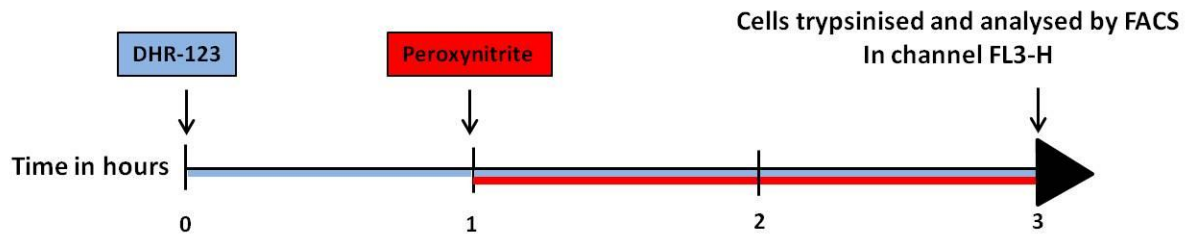


Figure 2.11: Positive control protocol with authentic peroxynitrite, to validate the relative peroxynitrite-specificity of DHR-123.

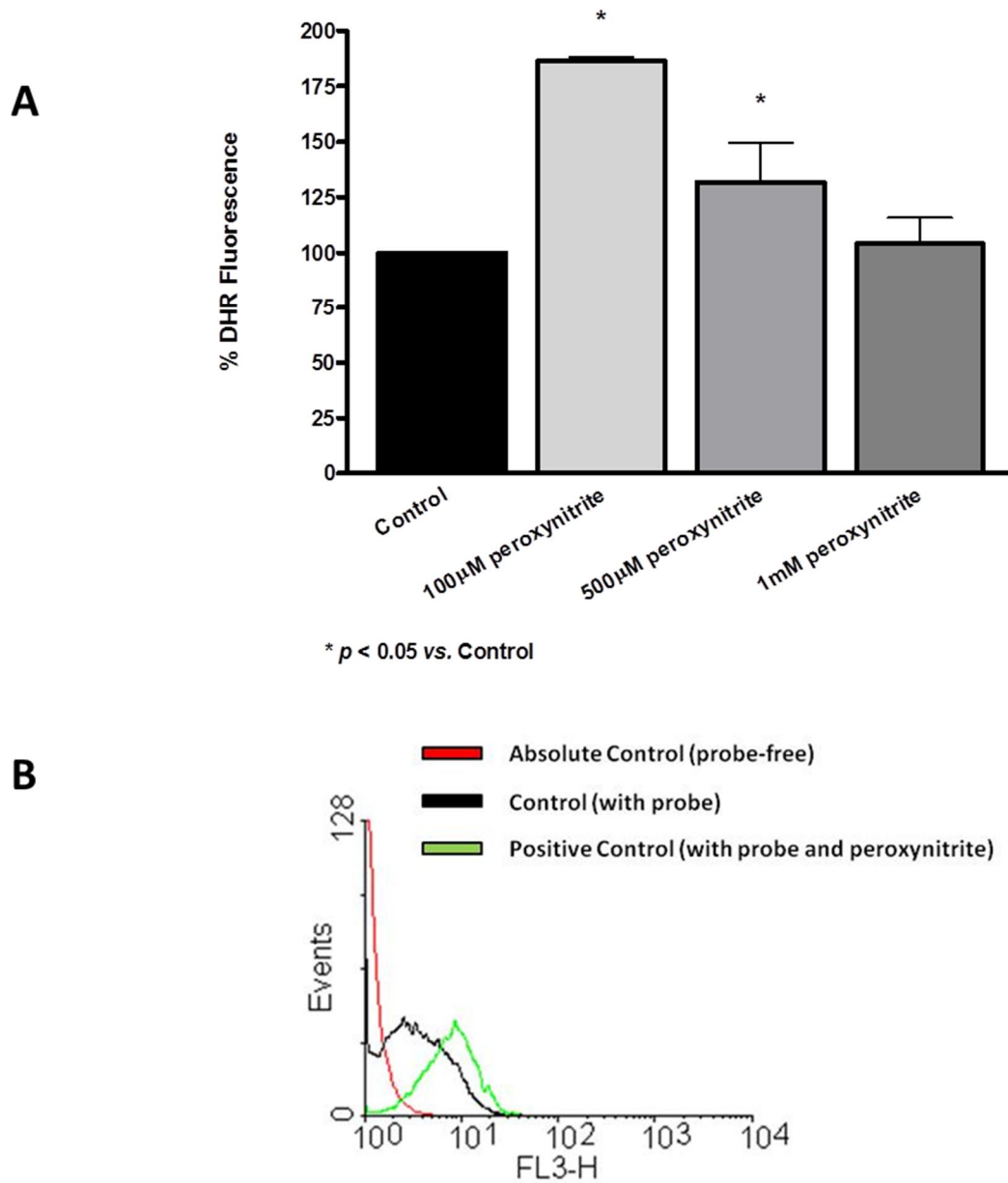


Figure 2.12: A: Measurement of DHR-123 fluorescence following treatment with increasing authentic peroxynitrite concentrations (100µM, 500µM & 1mM) for 30 minutes. Sample size: $n = 3 - 4$ / group.

B: Histogram showing mean fluorescence intensity measured in absolute control, DHR-123-control and positive control (ONOO⁻ (100 µM) + DHR-123) samples respectively (analysed in the FL3-H channel).

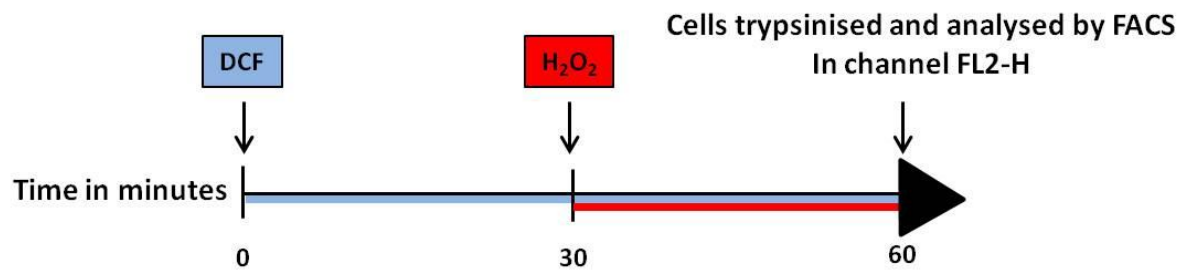


Figure 2.13: Positive control protocol with H₂O₂, to validate the relative H₂O₂-specificity of DCF.

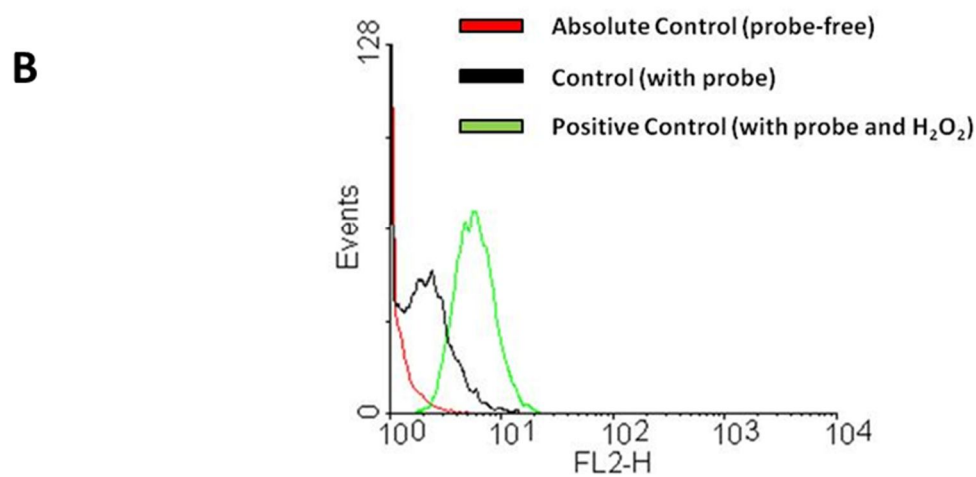
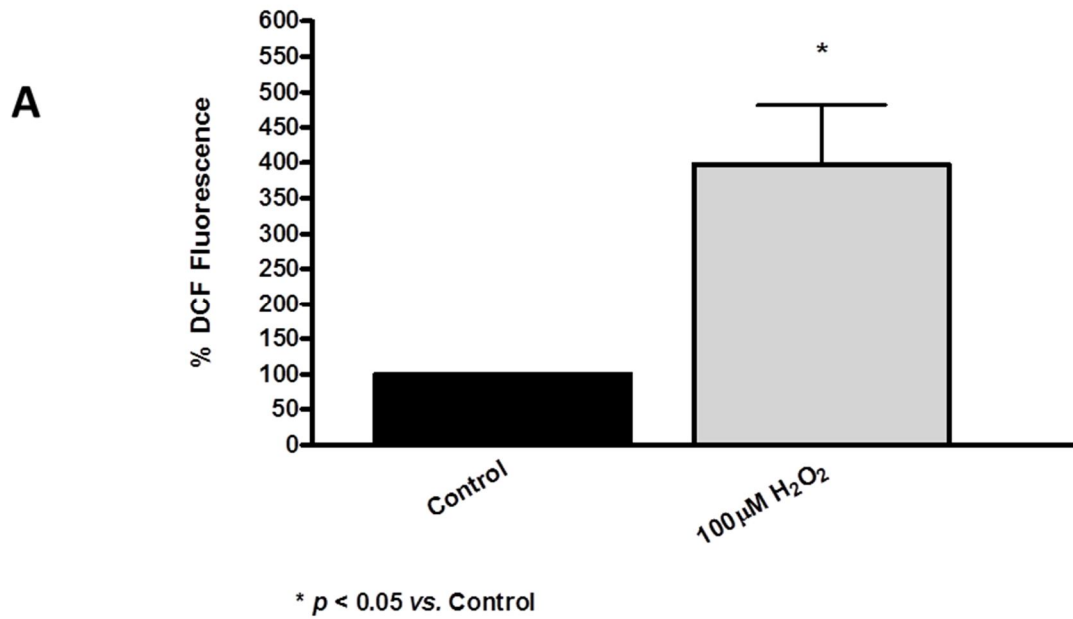


Figure 2.14: A: Measurement of DCF fluorescence following treatment with H_2O_2 (100 μM) for 30 minutes. Sample size: $n = 3 - 4$ / group.

B: Histogram showing mean fluorescence intensity measured in absolute control, DCF-control and positive control (H_2O_2 (100 μM) + DCF) samples respectively (analysed in the FL2-H channel).

2.3.1.2 Western blot analyses

NOS Signalling: Total and phosphorylated eNOS (1:1000 dilution; 10 – 20 minutes exposure) and PKB / Akt (1:1000 dilution; 5 – 10 minutes exposure) and total HSP 90 (1:1000 dilution; 3 – 5 minutes exposure), caveolin-1 (1:1000 dilution; 1 – 5 minutes exposure) and iNOS (1:200 dilution; 1 – 3 minutes exposure) were measured to investigate NOS signaling mechanisms.

Oxidative Stress: The membrane bound NADPH oxidase subunit, p22-phox (1:200 dilution; 3 – 5 minutes exposure), was used to measure nicotinamide adenine dinucleotide phosphate (NADPH) oxidase activity as previously described (Griendling KK *et al.*, 2000a).

Nitrosative Stress: The ability of the highly reactive NO-derived radical, ONOO⁻ (peroxynitrite) to nitrosylate tyrosine residues of cellular proteins and form nitrotyrosine, is an indication of nitrosative stress (Dalle-Donne *et al.*, 2005). Nitrotyrosine (1:500 dilution; 1 minute exposure) expression was therefore measured as a marker of nitrosative stress.

NFKB signalling: Activation of the NFKB pathway is usually an indication of a pro-inflammatory response (Ben-Neriah and Karin, 2011). Upon activation of this pathway, IKB α dislodges from the NFKB complex and undergoes proteasomal degradation; therefore, a reduction in IKB α protein levels is a marker of NFKB activation (Hoffmann A *et al.*, 2002). IKB α (1:1000 dilution; 5 – 10 minutes exposure) protein expression was therefore measured to investigate activity of the NFKB pathway.

Apoptosis: Cleaved caspase-3 (1:1000 dilution; 5 – 10 minutes exposure) and cleaved PARP (1:500 dilution; 5 - 10 minutes exposure) were measured to investigate apoptosis signalling.

Equal protein loading validation: β -tubulin (1:1000 dilution; 5 minute exposure) expression was measured to confirm equal protein loading in all samples.

General Western blotting protocol (see figures 2.15 & 2.16): To extract protein, CMECs from 140x tissue culture dishes representing 4th – 7th generation cells were pooled (10 culture dishes per sample to ensure that enough protein will be yielded) for a final total of 14 samples (each sample represented an experimental intervention). CMECs were removed

from culture by trypsinization, collected in 15 ml centrifugation tubes (centrifuged at 1000 rpm for 3 minutes) and resuspended in 1.5ml eppendorff tubes and centrifuged a final time at 1000 rpm for 3 minutes to form cell pellets. Zirconium oxide beads (bead size: 0.15 mm) were added to each cell pellet-containing tube, followed by addition of 800 μ l lysis buffer consisting of: 20 mM Tris; 1mM EGTA; 150 mM NaCl; 1mM β -glycerophosphate; 1 mM sodium orthovanadate; 2.5 mM tetra-sodium diphosphate; 1 mM PMSF; 0.1 % sodium dodecylsulfate (SDS); 10 μ g/ml aprotinin; 10 μ g/ml leupeptinin; 50 nM NaF and 1 % triton-X100. Following this, the cell pellets, zirconium beads and lysis buffer were homogenized in a Bullet Blender™ (Next Advance, Inc., NY, USA) at speed setting 5 for three cycles of 3-5 minutes each, with a resting period of 5 minutes in between. After homogenization, the tubes were centrifuged at 10 000 rpm for 10 minutes, the supernatant was collected (see Figure 2.17) and the protein content determined by the Bradford protein assay (Bradford, 1976). Based on the Bradford assay findings, a lysate was prepared containing Laemmli buffer (4% SDS, 20% glycerol, 10 % 2-mercaptoethanol, 0.004 % bromphenol blue and 0.125 M Tris HCl) (Laemmli, 1970) (making up half of the total lysate volume), lysis buffer and supernatant, which ensured a final protein content of 50 μ g/10 μ l per sample. Cell lysate proteins of equal amounts were subsequently loaded onto a 7.5 % (for eNOS and iNOS); 10 % (for PKB/Akt, nitrotyrosine, HSP 90, caveolin-1 and cleaved PARP, IK β α), 12 % (for p22-phox) and 15 % (for cleaved caspase-3) SDS-polyacrylamide gel and transferred onto PVDF membrane (Immobilon™-P, from Millipore). Non-specific binding sites on membranes were blocked with 5 % fat-free milk in Tris-buffered saline, 0.1 % tween-20 (Merck).

Following Western blotting, membranes were probed with the specific rabbit polyclonal primary antibodies (anti-eNOS, anti- PKB/Akt, anti-HSP 90, anti-caveolin-1, anti-cleaved caspase-3, anti-cleaved PARP and anti-IK β α), and (anti-p22-phox, anti-nitrotyrosine and anti-iNOS). The membranes were subsequently exposed to the secondary antibody, horseradish peroxidase-linked anti-rabbit IgG. The ECL™ system was employed to observe the immunoreactions. The same membranes were stripped of primary and secondary antibodies with 0.2M NaOH and re-probed (where applicable) for phosphorylated proteins with specific rabbit polyclonal primary antibodies (anti-phospho eNOS *ser 1177*, anti-phospho PKB/Akt *ser 474*). As the stripping method is known to be incomplete, it must be noted that there might still be residual binding of primary antibody with the total protein

left when membranes are re-probed for phosphorylated proteins. The method of first probing for total proteins, followed by stripping and subsequently probing for phosphorylated proteins is indeed flawed but is the optimized method for the current western blotting system that we are utilizing. All the membranes were then stripped again of primary and secondary antibodies with 0.2M NaOH and re-probed with specific rabbit polyclonal primary antibodies for expression of anti- β -tubulin. Films were analyzed by densitometry (UN-SCAN-IT, Silk Scientific, Orem, UT, USA). All Western blot data were expressed as a ratio of control with the number of control pixels adjusted to 1 (n = 3-4 / experimental group for all Western blot investigations).

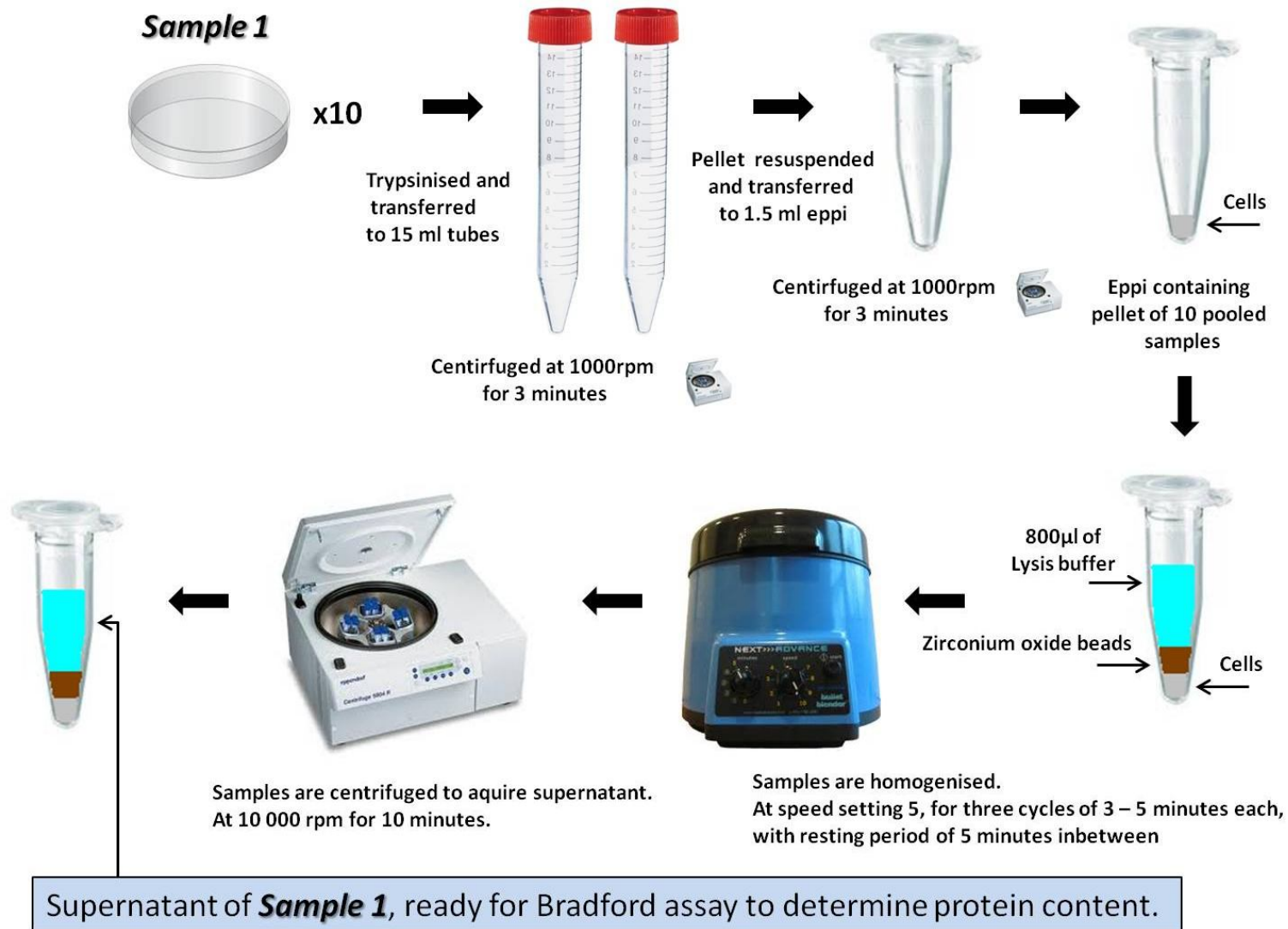
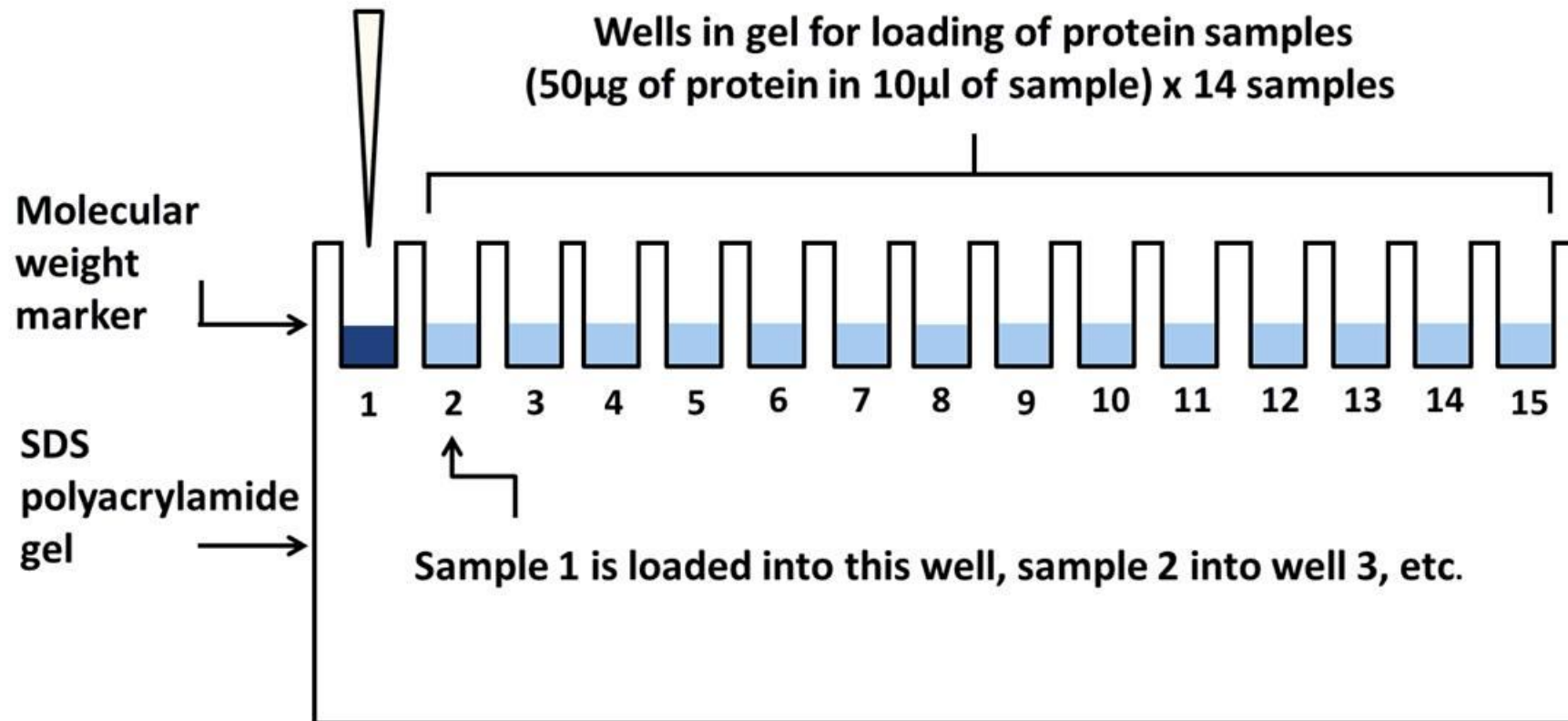


Figure 2.15: Protocol for sample preparation from cells to Bradford Assay.



First 3 wells (2-4) contain control samples (untreated cells) and the rest (5-15) contains experimental samples.

Figure 2.16: Example of a typical gel setup for a 14 sample western blot analyses.

2.3.1.3 Proteomics analyses (see Figure 2.17 for overview)

2.3.1.3.1 Protein isolation

Protein extraction was achieved by exactly the same method as described above for the Western blot analysis.

2.3.1.3.2 One dimensional sodium dodecyl sulfate polyacrylamide gel electrophoresis (1-D SDS-PAGE) followed by in-gel trypsin digestion.

Cell lysates of equal protein contents (50 µg / 10µl) were loaded onto a 7.5 % SDS-polyacrylamide gel and proteins separated by means of electrophoresis. The gel was then removed from the electrophoresis chamber and stained with 0.5% Coomassie Blue G-250 (Sigma Chemical Co, St Louis, MO, USA) (prepared in 50 % methanol / 10 % acetic acid) for approximately 5 minutes. The stain was discarded and the gel briefly rinsed with MilliQ water, after which it was unstained with 40 % HPLC grade methanol / 10 % acetic acid. The unstaining solution was replaced every 10 - 20 minutes until faint bands appeared, and continued until bands were clearly visible.

Each of the SDS-PAGE lanes was loaded with lysates from the respective experimental samples. In order to facilitate the trypsin digestion, each lane of the SDS-PAGE gel was further subdivided into 5 fractions, cut into smaller cubes and washed twice with water followed by 50 % (v / v) acetonitrile for 10 min. The acetonitrile was replaced with 50 mM ammonium bicarbonate and incubated for 10 min. This procedure was repeated two more times. All the gel pieces were then incubated in 100 % acetonitrile until they turned white, after which the gel pieces were dried *in vacuo*. Proteins were reduced with 10 mM DTT for 1 h at 57 °C. This was followed by brief washing steps of ammonium bicarbonate followed by 50 % acetonitrile before proteins were alkylated with 55 mM iodoacetamide for 1 h in the dark. Following alkylation, gel pieces were washed with ammonium bicarbonate for 10 min followed by 50 % acetonitrile for 20 min, before being dried *in vacuo*. The gel pieces were

digested with 100 μ l of 10 ng / μ l trypsin solution at 37 °C overnight. The resulting peptides were extracted twice with 70 % acetonitrile in 0.1 % formic acid for 30 min, and then dried and stored at -20 °C. Dried peptides were dissolved in 5 % acetonitrile in 0.1 % formic acid from which 10 μ l injections were prepared for nano-LC chromatography.

2.3.1.3.3 Filter Aided Sample Separation:

In some of the proteomics analyses, protein extraction was performed by means of an alternative method, namely the Filter Aided Sample Separation (FASP) method. For FASP, samples were dissolved in SDT lysis buffer (4 % SDS, 100 mM Tris-HCl pH 7.6, 0.1 M DTT (the latter was added freshly just before use)) to reach a final protein concentration of 600 μ g / ml. Following this, 400 μ l sample was mixed with 400 μ l UA buffer (8 M urea, 100 mM Tris-HCl, pH 8.5) and placed on the filter (Amicon Ultra 0.5 centrifugal filter, 10 kDa, Millipore, Ireland), and centrifuged for 40 min at 14 000 \times g. This was followed by the addition of 200 μ l UA and further centrifugation at 14 000 \times g for 40 min. The proteins were then alkylated by the addition of 100 μ l of 0.05 M iodoacetamide in UA, mixed and incubated for 5 min before centrifugation at 14 000 \times g for 30 min. This was followed by the addition of 100 μ l of UB (8 M urea, 0.1 M Tris-HCl pH 8.0), centrifugation for 30 min at 14 000 \times g, and the procedure repeated once. After centrifugation, 100 μ l of a 50 mM ammonium bicarbonate solution was added, centrifuged at 14 000 \times g for 30 min and repeated once.

Next, 40 μ l trypsin (Promega, Madison, WI, USA) was added and incubated at 37 °C for 17 hours in a wet chamber. The following morning the filter was placed in a clean Eppendorf tube and centrifuged for 40 min at 14 000 \times g, followed by the addition of 40 μ l 0.5 M NaCl solution and further centrifugation for 20 min at 14 000 \times g. Finally, the solution was acidified by the addition of 2.4 μ l formic acid (FA). The filtrate was desalted using C18 StageTips (Thermo Fischer Scientific, USA) according to the manufacturer's instructions. The desalted solution was dried *in vacuo* and stored at -20 °C. Dried peptides were dissolved in 5 % acetonitrile in 0.1 % FA from which 10 μ l injections were prepared for nano-LC chromatography.

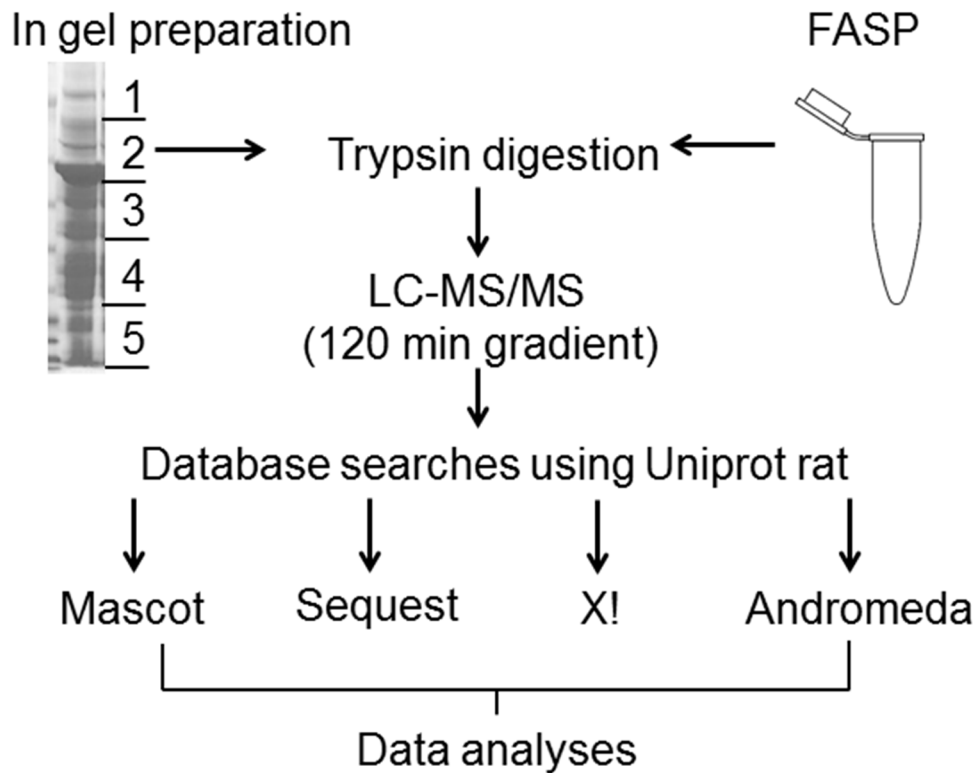


Figure 2.17: Workflow for identifying proteins in CMECs. An equal amount of protein (50 ug / 10 ul) was loaded onto the gel and 600 ng / μ l protein loaded for the FASP method respectively. The gel was stained using Coomassie blue and cut into 5 fractions for in-gel trypsin digestion. Peptides from the gel were extracted and prepared for LC-MS/MS. For those experiments in which proteins were separated and digested by the FASP method, proteins were trypsinised on the FASP membrane and subsequently extracted and prepared for LC-MS/MS. All MS/MS spectra were searched using Thermo Proteome Discoverer software (version 1.3) against in-house versions of Mascot, Sequest, X!tandem and Andromeda. For final data analyses, the identified proteins from all the search engines were combined to obtain a final list of proteins present in the CMEC proteome. (Diagram courtesy of Dr Salome Smit: Proteomics Unit, Central Analytical Facility, University of Stellenbosch).



Figure 2.18: **A:** The LTQ Orbitrap Velos mass spectrometer situated in the Proteomics Unit of the University of Stellenbosch (Thermo Fischer Scientific, USA). **B:** Nano-electrospray source. **C:** Nano-electrospray source magnified on screen.

2.3.1.3.4 Mass spectrometry (see Figure 2.18).

All mass spectrometry analyses were performed on a Thermo Scientific EASY-nLC II connected to a LTQ Orbitrap Velos mass spectrometer (Thermo Fischer Scientific, USA) equipped with a nano-electrospray source. For liquid chromatography, separation was performed on an EASY-Column pre-column (2 cm, ID 100 μm , 5 μm , C18), and then an EASY-column (10 cm, ID 75 μm , 3 μm , C18) with a flow rate of 300 nl / min. The gradient used was from 5-15 % B for 5 min, 15-35 % B for 90 min, 35-60 % B for 10 min, 60-80 % B for 5 min and kept at 80 % B for 10 min. Solvent A consisted of 100 % water in 0.1 % FA, and solvent B consisted of 100 % acetonitrile in 0.1 % FA.

The mass spectrometer was operated in data-dependent mode to automatically switch between Orbitrap-MS and LTQ-MS/MS acquisition. Data were acquired using the Xcaliber software package (Thermo Fischer Scientific, USA). The precursor ion scan MS spectra (m/z 400 – 2000) were acquired in the Orbitrap mode with resolution $R = 60000$ (number of accumulated ions: 1×10^6). The 20 most intense ions were isolated and fragmented in a linear ion trap (number of accumulated ions: 1.5×10^4) using collision-induced dissociation. The lock mass option (polydimethylcyclsiloxane; m/z 445.120025) enabled accurate mass measurements in both the MS and MS/MS modes. In data-dependent LC-MS/MS experiments, dynamic exclusion was applied with 60 s exclusion duration. Mass spectrometry conditions were as follows: 1.8 kV, capillary temperature of 250 $^{\circ}\text{C}$, with no sheath and auxiliary gas flow. The ion selection threshold was 500 counts for MS/MS and an activation Q-value of 0.25 and activation time of 10 ms were also applied for MS/MS.

2.3.1.3.5 Proteomic data analysis

Thermo Proteome Discoverer 1.3 software (Thermo Fischer Scientific, USA) was used to identify proteins via automated database searching (Mascot, Matrix Science, UK, and Sequest, Thermo Fischer Scientific, USA) of all tandem mass spectra against the UniProtTM rat database. Carbamidomethyl cysteine was set as fixed modification, and oxidized methionine, N-acetylation and deamidation (NQ) as variable modification. The precursor

mass tolerance was set to 10 ppm, and fragment mass tolerance set to 0.8 Da. Two missed tryptic cleavages were allowed. Proteins were considered positively identified when they were identified with at least 2 tryptic peptides per protein, a Mascot score threshold of 20, Sequest score threshold of 1.5 ($p < 0.05$), and a protein and peptide posterior error probability (PEP) of at least 0.01. Percolator (part of Mascot) was used for peptide validation with a maximum delta Cn of 0.5, and decoy database searches with a FDR of 0.02 and 0.05 with validation based on the q-value. Further protein identification was performed with the X!tandem search engine (Craig and Beavis, 2004) via the online UniProt rat database. Carbamidomethyl cysteine was set as fixed modification, and oxidized methionine, N-acetylation and deamidation (NQ) as variable modification. Proteins were considered positively identified when they were identified with p-score of more than 72 as determined by the X!tandem software. The false positive identification rate was calculated to be an average of 1.4 %. Andromeda's Maxquant 1.2.2.5 proteomics software package (Cox *et al.*, 2011) was used for protein identification with a protein and peptides PEP of at least 0.01 and 2 unique peptides per protein. For a diagrammatic representation of the SDS PAGE / in-gel trypsinization and filter-aided sample preparation (FASP) / in-solution trypsinization methods, mass spectrometry and data analysis.

Where indicated, differential protein regulation between two experimental groups were analysed by the Maxquant proteomics software package, and proteins were only considered differentially regulated with a protein and peptide PEP of 0.01, up or down regulation of ≥ 1.5 -fold and a p-value of $p < 0.05$.

2.3.1.3.6 Functional annotation analyses of proteins

Functional annotation analyses of the identified proteins in the CMECs were performed by submitting protein lists to the functional annotation tool of DAVID (The Database for Annotation, Visualization and Integrated Discovery) Bioinformatics Resources 6.7 (Huang DW *et al.*, 2009) The DAVID functional annotation tool allocates functionally related proteins from the submitted lists to specific Gene Ontology (GO) terms, and in this study, we were interested in the significantly represented GO terms determined by cellular

component, biological process and molecular function properties respectively. Another analysis tool offered by DAVID is the functional annotation cluster tool. Grouping functionally related GO terms into functional annotation clusters further assist in making sense of the proteome in terms of cellular functions and processes. In this regard, the P-value and fold enrichment of each annotation cluster indicate to which degree that cluster is overrepresented within the submitted dataset; clusters with p-values < 0.05 and larger fold-enrichments (≥ 1.5) are of particular interest when interpreting the data (Huang DW *et al.*, 2009).

2.4 **Statistical analyses**

All data in this dissertation are expressed as mean \pm standard error of the mean (SEM). Statistical analyses were performed with a Student's t-test (for comparison of two groups) or one-way analysis of variance (ANOVA) (with Bonferroni post-hoc test if $p < 0.05$; for comparison of more than 2 groups). Data achieving a p -value of < 0.05 were considered statistically significant. Graph Pad Prism[®] version 5.01 software was used for all analyses.

CHAPTER THREE

Characterization of primary CMEC cultures

3.1 Introduction

As mentioned previously, the distinct location of CMECs in the myocardial capillary network bestows upon them a unique role not only in the maintenance of vascular homeostasis, but also as regulators of myocardial function. Endothelial heterogeneity is particularly evident in specific organs such as the heart (Hendrickx *et al.*, 2004), where the myocardial capillaries and the endothelial cells that line them are regarded as primary targets of, and critical role-players in end-organ damage in the heart resulting from hypertension, diabetes mellitus and ischaemic heart disease (Lu L *et al.*, 2007). CMECs show distinct morphological and structural adaptations compared to other endothelial cell types, such as the expression of fewer tight and gap junctions, shallower intercellular clefts, no microvilli and relatively more caveolae and intracellular vesicles (Aird, 2007a). These adaptations suggest that CMECs form a rather leaky endothelial layer and are specialized to perform transcytosis-mediated transfer of materials (Aird, 2012). In view of the intimate CMEC-cardiomyocyte arrangement, cardiomyocytes are regarded as the primary cellular recipients of paracrine messengers secreted by CMECs, such as NO and endothelin-1. Therefore, CMECs are now recognized as important regulators of myocardial function (Brutsaert, 2003).

Despite the limited availability of data on CMEC structure and function, almost no information is available on the CMEC proteome. In the only previous proteomics-based study (partly) dedicated to rat coronary microvascular endothelial cells, a two-dimensional gel electrophoresis (2-DE) approach was followed, in which only 22 proteins were positively identified (Lu L *et al.*, 2007). The field of vascular proteomics has considerable shortcomings. Relative to other cell types, surprisingly little is known about the endothelial proteome in general, which is further confounded by the fact that 80% of all endothelial proteomic studies are conducted on one distinct endothelial cell type, viz. human umbilical venous endothelial cells (HUVECs) (Richardson *et al.*, 2010). The over reliance on HUVECs as a

research model does not consider the reality that endothelial cells show considerable structural and functional diversity across the vascular tree (Aird, 2007b), leaving other physiologically important endothelial cell subtypes, such as the CMECs, relatively under investigated (Mayr *et al.*, 2004).

Despite the fact that endothelial NO bio-availability is regarded as one of the gold standards in the assessment of endothelial cell function and health, surprisingly few studies utilise the direct measurement of intracellular NO-levels as an end-point when investigating the effects of harmful stimuli. Furthermore, findings are variable, often due to differences in experimental conditions, endothelial cell types used, and inconsistent concentrations and treatment times of harmful stimuli (see Table 1.3, Chapter 1 for variable *in vitro* effects of TNF- α on endothelial cells).

In summary, from the literature it is evident and surprising that so few endothelial cell-based studies have investigated and characterized CMECs, not only in view of their strategic location the myocardium, but also in view of their status as important role-players under physiological and pathophysiological conditions. Therefore, in this chapter we have set out to comprehensively characterize adult rat CMECs under baseline (unstimulated) conditions, and after exposure to a variety of harmful stimuli (using intracellular NO-levels as end-point).

3.2 **Specific Aims**

- To characterize the morphology and purity of the commercially purchased CMECs.
- To establish whether the CMECs express an array of selected proteins important for the purposes of this study.
- To characterize the baseline proteome of these cells.
- To examine the effects of various putative harmful stimuli on intracellular NO-levels in the CMECs.

3.3 Morphology, functional characterization and baseline protein expression of CMECs.

3.3.1 Morphology and functional characterization

In order to assess the morphology of the cells, they were photographed with a standard light microscope. A typical "cobblestone" monolayer morphology was observed, a distinct characteristic of cultured endothelial cells (Nishida *et al.*, 1993; Piper *et al.*, 1990) (see Figure 3.1). The presence of non-endothelial cells was negligible (on average, less than 10% of the total cell population was of non-endothelial origin). In addition, functional characterization was performed by measuring uptake of acetylated low density lipoprotein labeled with 1,1'-dioctadecyl-3,3',3'-tetramethylindo-carbocyanine perchlorate (Dil-ac-LDL)(Biomedical Technologies, Stoughton, MA, USA). This fluorescent probe is specific for endothelial cells (Nishida *et al.*, 1993; Piper *et al.*, 1990), and recognized as a marker of endothelial cell purity. Acetylated-low density lipoprotein (Ac-LDL) is taken up by endothelial cells *via* the "scavenger cell pathway" of LDL metabolism. Once a lipoprotein that contains Dil is taken up by a cell, the lipoprotein molecule is acted upon by lysosomal enzymes and the Dil accumulates in lysosomal membranes. Thus, cells that metabolize lipoproteins at different rates will accumulate varying amounts of Dil and endothelial cells are known to metabolise lipoproteins at a much higher rate than other cell types (Voyta *et al.*, 1984). Briefly, CMECs were incubated with 10 µg / ml Dil-ac-LDL at 37°C for 4 hours. The probe was subsequently washed out, and cells were removed from culture by trypsinisation, resuspended in PBS and the % fluorescent cells analyzed by flow cytometry in the FL2-H channel. A high fluorescence uptake (80 – 100 % of the total gated cell population) indicates endothelial cell purity, and no experiments were conducted on CMEC subcultures with < 80 % purity (see Figure 3.2). See Figure 3.3 for a fluorescence microphotograph of LDL-staining CMECs in culture.

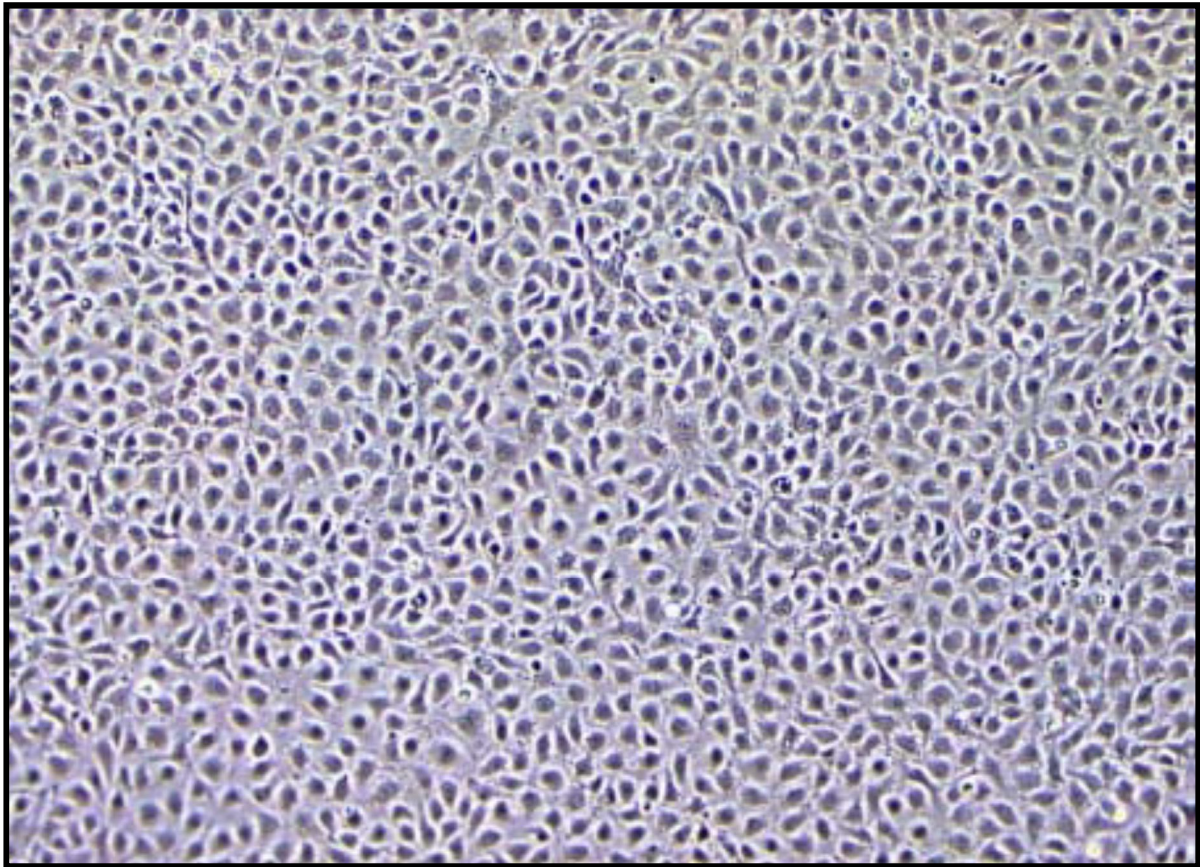


Figure 3.1: Validation of morphological appearance. Representative microphotograph (Carl Zeiss standard upright light microscope, West Germany) of a confluent CMEC culture (10x magnification) demonstrating a typical cobblestone appearance, commonly associated with endothelial cells in culture (Piper *et al.*, 1990; Nishida *et al.*, 1993)

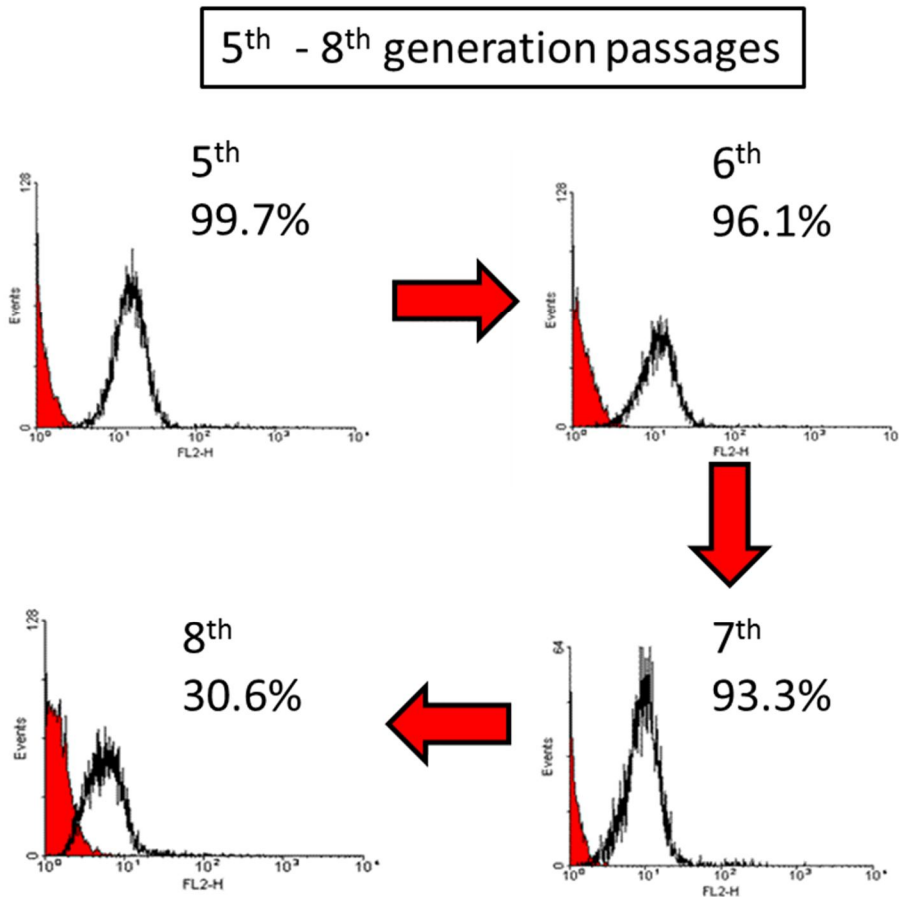


Figure 3.2: Flow cytometric analysis of the percentage cells staining positively for the Dil-ac-LDL fluorescent probe in cells from different culture generations. The red histogram represents autofluorescence (probe-free sample) and the black histogram the cells treated with Dil-ac-LDL. On average CMEC cultures demonstrated >93% positive staining.

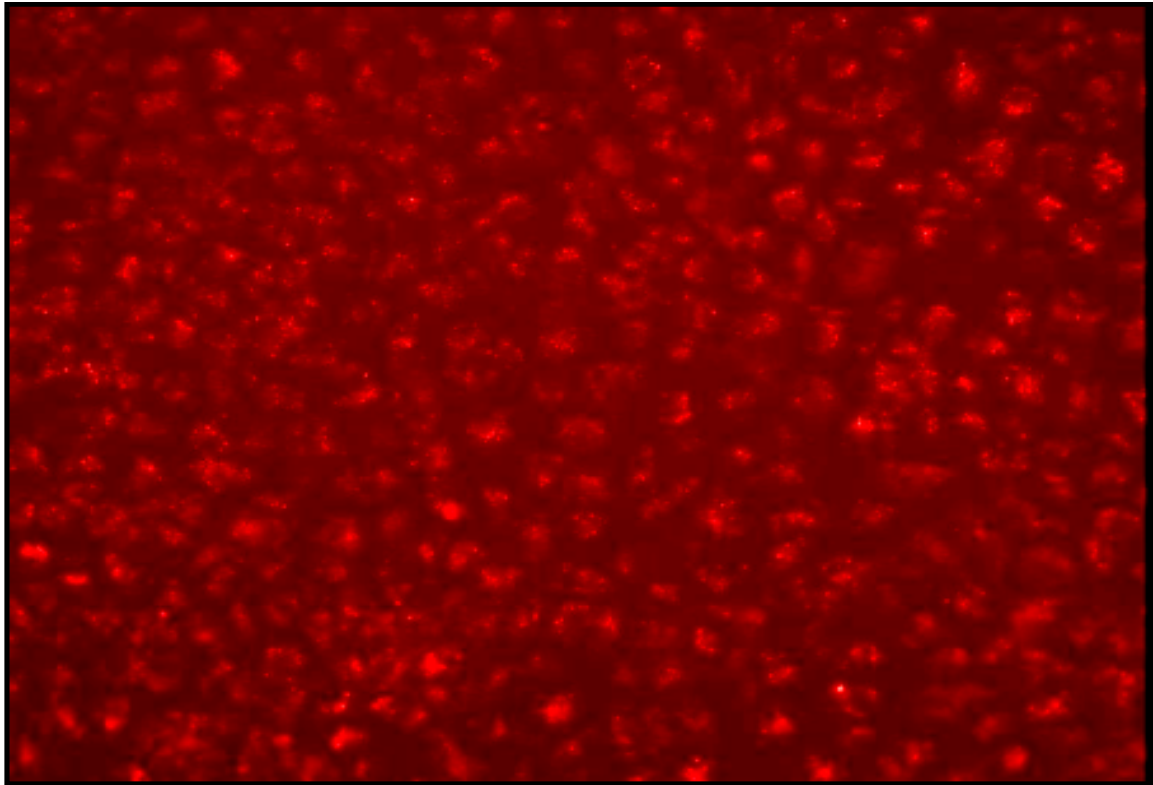


Figure 3.3: Validation of endothelial cell purity. Representative fluorescence microphotograph of LDL-staining CMECs in culture (20x magnification) clearly shows the bright red-staining endothelial cells that have taken up the fluorescently-labeled LDL (Olympus IX-81 inverted fluorescent microscope).

3.3.2 Expression of proteins involved with NOS-NO biosynthesis in CMECs.

In order to establish whether the CMECs express proteins that are crucial role-players in the NOS-NO biosynthesis pathway (an important end-point for the purposes of this study), we measured the expression of: eNOS, PKB/Akt, HSP 90, caveolin-1, iNOS and nNOS. Lysates of untreated samples were prepared (as previously described in chapter two) to yield a final protein content of 50µg / 10µl. These samples were subsequently loaded onto a 7.5% (for eNOS – 140 kDa, iNOS – 130 kDa, nNOS – 160 kDa, PKB/Akt – 58 kDa and HSP 90 – 90 kDa) and 12% (for Caveolin-1 – 20 kDa) SDS-polyacrylamide gel and transferred onto PVDF membrane (Immobilon™-P, from Millipore). Non-specific binding sites on membranes were blocked with 5 % fat-free milk in Tris-buffered saline, 0.1 % tween-20 (Merck).

Following Western blotting, membranes were probed with the specific rabbit polyclonal primary antibodies (anti-eNOS, anti-iNOS, anti-nNOS, anti-PKB/Akt, anti-HSP 90 and anti-caveolin-1). The membranes were subsequently exposed to the secondary antibody, horseradish peroxidase-linked anti-rabbit IgG. The ECLTM system was employed to observe the immunoreactions. We found that all the above proteins (eNOS, iNOS, nNOS, PKB/Akt, HSP 90 and caveolin-1), which all play central roles in endothelial cell NOS-NO signalling (Cortese-Krott *et al.*, 2011; Kuhr *et al.*, 2010; Basuroy *et al.*, 2011; Xu Q *et al.*, 2012; Briand *et al.*, 2011) were expressed in baseline CMECs (see Figure 3.4). The expression of nNOS is particularly interesting, as we are not aware of any previous studies that demonstrated the presence of this NOS isoform in CMECs. nNOS expression has previously been demonstrated in HUVECs (Chakrabarti *et al.*, 2012) and peri-microvascular nNOS-derived NO was found to play a role in vascular smooth muscle cell relaxation (Kavdia and Popel, 2004).

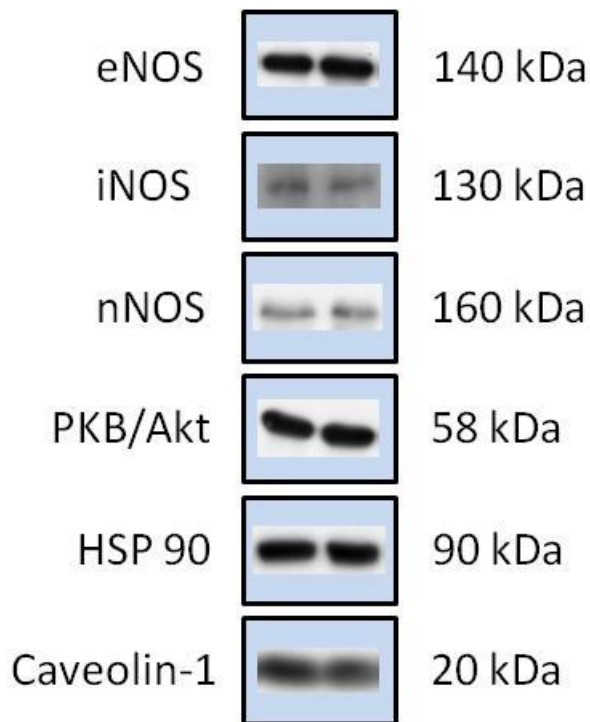


Figure 3.4: Total baseline expression of selected NOS-NO signalling proteins in the CMECs. In addition to the expression of all three of the main known NOS isoforms (eNOS, iNOS and nNOS) in the CMECs, we could also establish that HSP 90 and caveolin-1, both essential proteins associated with activation of eNOS, are expressed.

3.4 Comprehensive characterisation of the baseline CMEC proteome.

CMECs under baseline conditions were analysed by a method as previously described in chapter 2 (see figure 3.5 for an overview of the workflow followed). Following the identification of the proteins, the data were submitted to DAVID Bioinformatics Resources (version 6.7) for functional annotation analyses.

The SDS-PAGE gel method followed by LC-MS/MS identified a total of 1387 proteins and 13290 peptides in CMECs under baseline conditions (the complete list of identified proteins will be forwarded to the reviewers electronically). In order to optimize proteome coverage, four different search engines were consulted for protein identification. Mascot positively identified 801 proteins, whereas Sequest identified 1115 proteins (102 proteins unique to Sequest), X!tandem identified 747 proteins (29 proteins unique to X!tandem), and Maxquant identified 927 proteins (178 proteins unique to Maxquant).

Classification of the identified proteins according to molecular weight (Mr), showed that 73% of the proteins appeared in the 20-100 kDa range, with only 8% under the range of 20 kDa and 19% larger than 100 kDa. Classification based on the distribution of isoelectric point (pI) indicated that 10% of the proteins identified had a pI smaller than 5, and 5% had a pI larger than 11. The majority of the identified proteins had a pI between 5 and 8, which constituted 62% of the proteome. A total of 23% of the proteins fell in the 8-10 pI range. This is in contrast to a previous study on rat coronary microvascular endothelial cells that showed more spots in the alkaline pI range (Lu L *et al.*, 2007), and another 2-DE based study on HUVECs where more than 60% of the proteins were in the acidic pI range (Bruneel *et al.*, 2003). A possible explanation for this apparent inconsistency might be that MS based proteomic investigations such as the current study have no bias towards pI or Mr, whereas 2-D gel based approaches are constrained by the pH and Mr (Pietrogrande *et al.*, 2002; Smolka *et al.*, 2002; Roe and Griffin, 2006).

The proteome data succeeded in complementing the light microscopy and dil-ac-LDL uptake validations in characterizing the CMECs as vascular endothelial cells. For a list of 12 identified proteins, known to be predominantly or exclusively expressed in vascular endothelial cells, see Table 3.1. In an effort to place the proteomic findings of the present

study in a broader context, we investigated whether other proteomic-based endothelial cell studies in the literature had reported on, or identified the expression of identical or similar proteins. The results are summarized in Table 3.2. Next, we performed functional annotation analyses on the identified proteins in the baseline CMECs according to their expression in Gene Ontology (GO) terms (DAVID Bioinformatics Resources) (Huang DW *et al.*, 2009). We also analyzed the proteomic data by submitting the baseline CMEC protein list to the functional annotation cluster tool of DAVID, which groups functionally related GO terms in annotation clusters. The top 10 most enriched functional annotation clusters of the baseline CMEC proteome are shown in Figure 3.6.

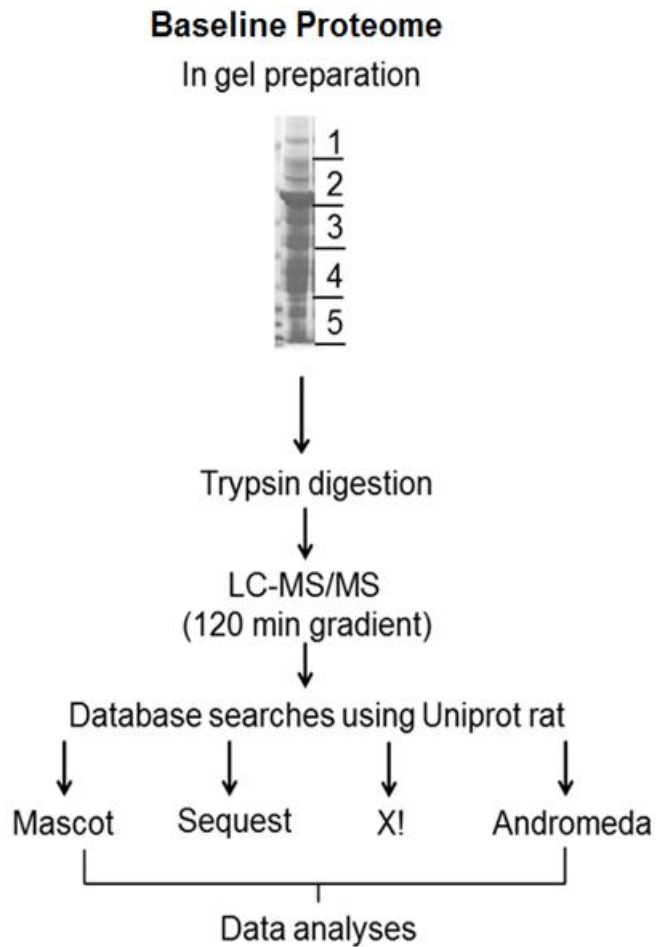


Figure 3.5: Workflow for identifying proteins in CMECs under baseline conditions. Protein extraction was performed by SDS-PAGE / in-gel trypsinisation. Proteins were separated by the Thermo Scientific EASY-nLC™ II nano-flow liquid chromatography system connected to a LTQ Orbitrap Velos™ mass spectrometer (Thermo Fischer Scientific, USA) equipped with a nano-electrospray source. Finally, proteins were identified by submitting protein lists to four different database search engines.

Table 3.1: List of identified proteins in the baseline CMEC proteome known to be predominantly expressed in vascular endothelial cells (the complete list of identified proteins is available on request).

Protein Identification	Accession Number
1. Angiopoetin-2	O35462
2. Angiotensin converting enzyme	P47820
3. Basal cell adhesion molecule	Q9ESS6
4. Caveolin-2	Q2IBC5
5. CD151 antigen (platelet-endothelial tetraspan antigen-3)	Q9QZA6
6. Endothelial cell-selective adhesion molecule	Q6AYD4
7. Endothelial protein C receptor	F1M7Q9
8. Intercellular adhesion molecule 2	Q6AXM6
9. Nitric oxide synthase	F1LQC7
10. Nitric oxide synthase, endothelial	Q62600
11. Platelet-endothelial cell adhesion molecule	Q3SWT0
12. von Willebrand factor	F1M957

Table 3.2: Comparison of selected proteins identified in the baseline CMECs of the present study with those identified in other studies performed on similar or other endothelial cell types.

Protein Name	CMECs	CorMECs	BMECs	CAECs	AECs
1. Glyceraldehyde-3-phosphate dehydrogenase	+	+	+	-	-
2. Alpha-enolase	+	-	-	+	-
3. ATP synthase subunit beta, mitochondrial	+	-	-	-	+
4. ATPase, H ⁺ transporting	+	-	-	-	+
5. Chaperonin subunit 8 (Theta)	+	+	+	-	-
6. Chloride intracellular channel protein 4	+	+	+	-	-
7. Cytosol aminopeptidase	+	+	+	-	-
8. Fructose-bisphosphate aldolase A	+	-	-	+	+
9. Macrophage-capping protein	+	+	+	-	-
10. Ornithine aminotransferase, mitochondrial	+	+	+	-	-
11. PDZ and LIM domain protein 1	+	+	+	-	-

12. Peptidyl-prolyl cis-trans isomerase A; cyclophilin A	+	-	-	+	+
13. Peptidyl-prolyl cis-trans isomerase D	+	+	+	-	-
14. Peroxiredoxin-2	+	-	-	-	+
15. Prohibitin	+	-	-	+	-
16. Spectrin alpha chain	+	-	-	-	+
17. Stress-induced-phosphoprotein 1	+	-	-	-	+
18. Succinyl-CoA:3-ketoacid-coenzyme A transferase 1, mitochondrial	+	-	-	-	+
19. Vesicle amine transport protein 1 homolog	+	+	+	-	-
20. Vesicle-associated membrane protein-associated protein A	+	+	+	-	-
21. Vesicle-associated membrane protein-associated protein B	+	+	+	-	-
22. Vimentin	+	-	-	+	+

CMECs: CMECs of the present study; CorMECs: Coronary microvascular endothelial cells from Lu L *et al.* (2007); BMECs: Brain microvascular endothelial cells (Lu L *et al.*, 2007); CAECs: Coronary artery endothelial cells (Yu *et al.*, 2004); AECs: Aorta endothelial cells (Almofti *et al.*, 2006).
 + Positively identified and reported; --- Not identified and / or reported.

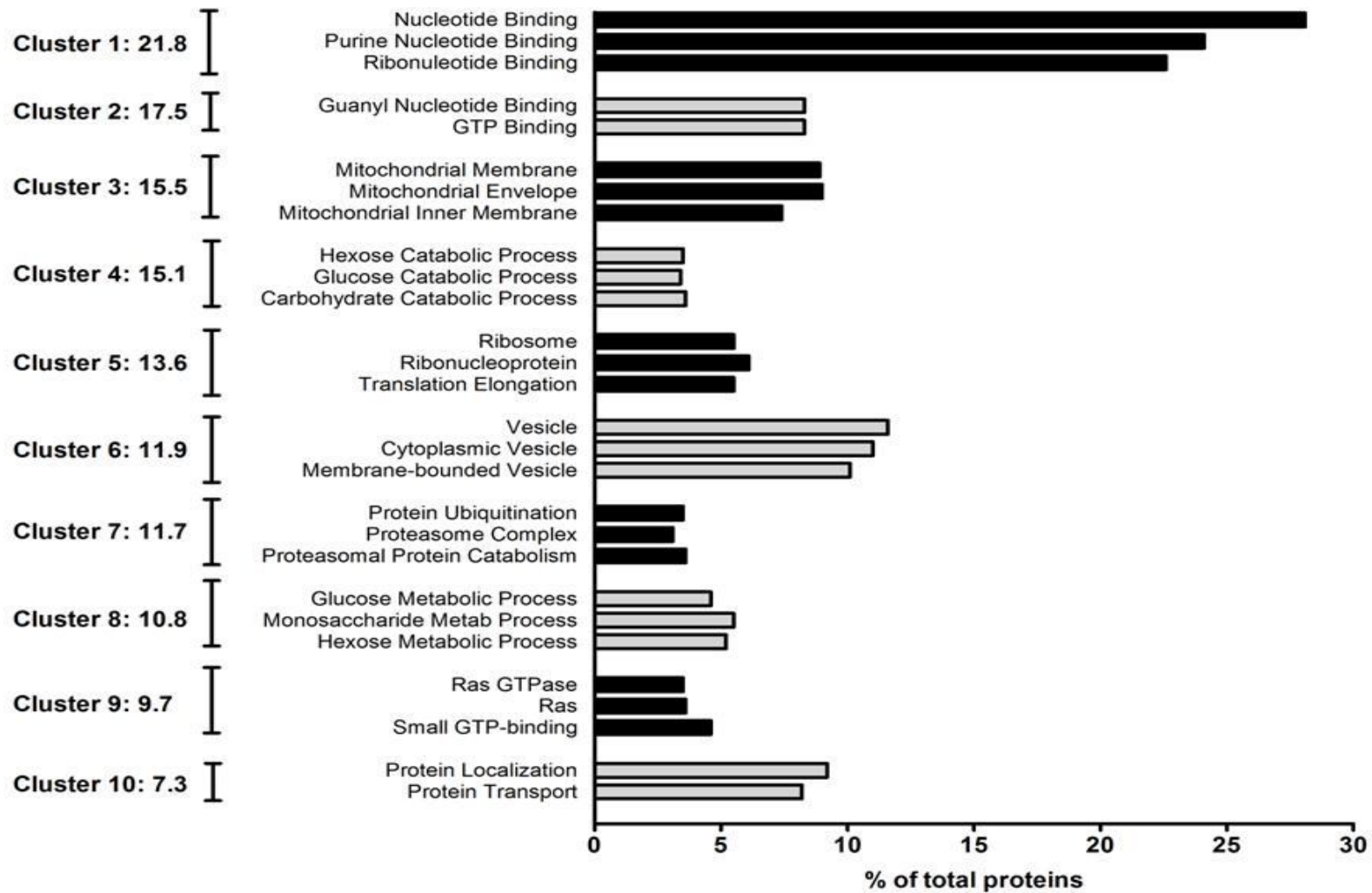


Figure 3.6: Functional annotation analysis (DAVID Bioinformatics) of the proteins identified in baseline CMECs showing the top 10 most enriched annotation clusters with their respective enrichment scores and GO terms.

3.5 The effect of various harmful stimuli on the NO production of CMECs – FACS analysis.

As part of our endeavours to characterise the CMECs, we investigated the response of the CMECs to several harmful stimuli commonly associated with cardiovascular risk factors or disease states. As end-point, we measured the intracellular NO-production in the CMECs. These experiments were performed as part of our initial baseline pilot studies to optimise the use of the DAF-2/DA probe, the measurement of DAF-2/DA fluorescence by flow cytometry, and finally also to assist in selecting which stimuli will eventually be comprehensively studied in the later chapters of this dissertation.

In these initial pilot studies, CMECs were treated for 24 hours with angiotensin II (100 nM), high glucose concentration (25 mM), hypoxia ($O_2 < 0.6\%$), ox-LDL (40 $\mu\text{g}/\text{ml}$), ADMA (500 M), and TNF- α (5 ng / ml and 20 ng / ml).

Interestingly, treatment with angiotensin II, glucose, hypoxia and ox-LDL induced significant increases in NO production after 24 hours. Conversely, ADMA and TNF- α (20 ng / ml) treatment resulted in a significant decrease in NO production, whereas TNF- α (5 ng / ml) had no effect on NO-production.

CMECs exposed to: 100 μM DEA/NO (2 hours) showed a significant increase ($128.36 \pm 5.75\%$ vs. 100 % control: $p < 0.05$); 100 nM Angiotensin II (24 hours) showed a significant increase ($109.68 \pm 4.67\%$ vs. 100 % control: $p < 0.05$); 25 mM glucose (24 hours) showed a significant increase ($114.42 \pm 5.59\%$ vs. 100 % control: $p < 0.05$); $< 0.6\%$ O_2 (24 hours) showed a significant increase ($144.09 \pm 11.60\%$ vs. 100 % control: $p < 0.05$); 40 $\mu\text{g}/\text{ml}$ oxidized-LDL (24 hours) showed a significant increase ($128.82 \pm 4.99\%$ vs. 100 % control: $p < 0.05$); 500 μM ADMA (24 hours) showed a significant decrease ($88.47 \pm 2.25\%$ vs. 100 % control: $p < 0.05$); 5 ng / ml TNF- α (24 hours) showed no change ($100.71 \pm 5.04\%$ vs. 100 % control: $p < 0.05$) and 20 ng / ml TNF- α (24 hours) showed a significant decrease ($74.02 \pm 1.61\%$ vs. 100 % control: $p < 0.05$) in DAF-2/DA fluorescence compared to untreated or normoxic controls (see figure 3.7).

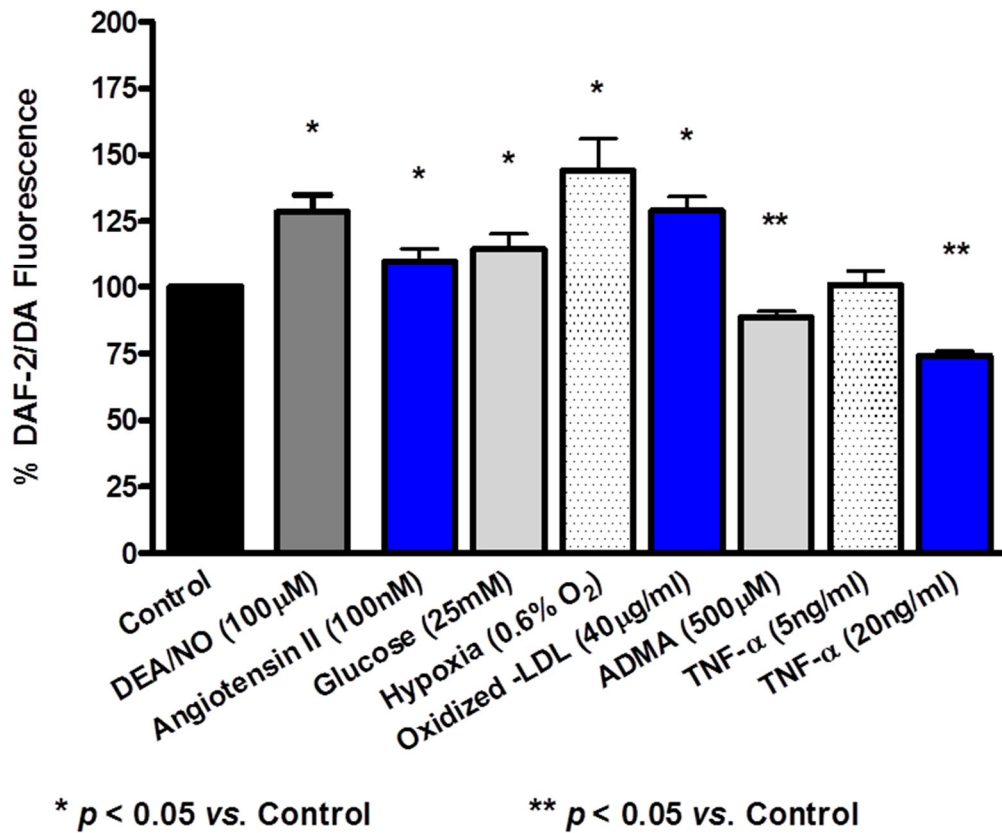


Figure 3.7: Intracellular NO-levels measured by the mean fluorescence intensity of DAF-2/DA (expressed as a percentage of control; control = 100%). DEA/NO was used as a positive control for DAF-2/DA. A significant increase is indicated as * and a significant decrease as **. The samples sizes varied between $n = 6 - 33$ per group.

3.6 **Discussion**

3.6.1 **Characterization of the morphology, culture specificity and expression of critical proteins involved with NOS-NO biosynthesis in CMECs.**

Previous studies have characterized vascular endothelial cells in terms of morphology, by observing that the cultured cells grow as a single layer and adopt a “cobble-stone” appearance (Nishida *et al.*, 1993). Using a standard light microscope with a 10x magnification, we confirmed that the CMECs demonstrate the typical cobble-stone appearance (see figure 3.1). Other studies have also verified the “purity” of endothelial cell cultures by staining with the fluorescent probe, Dil-Ac-LDL. Positive staining has been confirmed by fluorescent microscopy (Scheller *et al.*, 2012; Ma, 2012) or by flow cytometric analysis of Dil-ac-LDL fluorescence with flow cytometry (Eggermann *et al.*, 2003; Von Ballmoos *et al.*, 2010). We were able to show that the CMECs stained positively for Dil-ac-LDL, by fluorescent microscopy (figure 3.3) and flow cytometric analysis, which indicated that the percentage positively staining cells was > 90 % up to the 7th generation (see figure 3.2).

In a separate series of experiments, we showed that the CMECs expressed baseline proteins commonly associated with endothelial cell NOS-NO signalling, namely all three NOS isoforms: eNOS (Liu G *et al.*, 2012), iNOS (Raphael *et al.*, 2010) and nNOS (Chakrabarti *et al.*, 2012), as well as HSP 90 (Desjardins *et al.*, 2012) and caveolin-1 (Malan *et al.*, 2013), and PKB/Akt, one of the major upstream activators of eNOS (Fournier *et al.*, 2012) (see figure 3.4). Other researchers have also shown that eNOS (Scheller *et al.*, 2012; Zhang P *et al.*, 2011), HSP 90 (Dib *et al.*, 2012; Miwa *et al.*, 2013), caveolin-1 (Davalos *et al.*, 2010; Jagielska *et al.*, 2012), iNOS (Siamwala *et al.*, 2010; Namdar *et al.*, 2012) and PKB/Akt (Strijdom *et al.*, 2009b; Wang L *et al.*, 2012) are expressed in CMECs. The expression of nNOS has been shown in various cell types, namely neurons (Chao *et al.*, 1996; Vizzard *et al.*, 1994), myocytes (Silvagno *et al.*, 1996; Gath *et al.*, 1997), epithelial cells (North *et al.*, 1994; Asano *et al.*, 1994), Macula densa cells (Schricker *et al.*, 1996; Wang Y *et al.*, 1997), mast cells (Shimizu *et al.*, 1997), gonadotrophs and folliculostellate cells (Ceccatelli *et al.*, 1993; Iwai *et al.*, 1995) as well as neutrophils (Wallerath *et al.*, 1997). Expression of nNOS in endothelial cells have also been shown, namely in HUVECs (Chakrabarti *et al.*, 2012). However, although

nNOS is clearly expressed in other endothelial cell types (e.g. HUVECs) and non-endothelial cell types, the expression of nNOS has, as far as we are aware, not previously been demonstrated in CMECs; therefore this appears to be a novel finding.

3.6.2 The CMEC proteome under baseline conditions.

At least 12 proteins, known to be predominantly or exclusively expressed in vascular endothelial cells (Table 3.1), were identified in the CMECs. These proteins are associated with a wide range of endothelial-specific functions: endothelial cell adhesion (basal cell adhesion molecule, endothelial cell-selective adhesion molecule, intercellular adhesion molecule and CD151 antigen / platelet-endothelial cell adhesion molecule); angiogenesis (angiopoietin-2); angiotensin biosynthesis (angiotensin converting enzyme, ACE); nitric oxide synthesis (endothelial nitric oxide synthase, nitric oxide synthase and caveolin) and blood coagulation (endothelial protein C receptor and von Willebrand factor). The identification of these proteins serves to demonstrate the value of proteomics in complementing more traditional endothelial cell purity validation techniques (morphological light microscopic appearance and dil-ac-LDL uptake: Figures 3.1, 3.2 and 3.3).

Next, we attempted to contextualize our proteomic data by undertaking a review of the literature to compare our findings with those of proteomics-based studies on other vascular endothelial cell types (Table 3.2). Twenty-two proteins with a relatively wide range of functions were randomly selected from our protein list and compared to lists of identified proteins in rat coronary microvascular endothelial cells (Lu L *et al.*, 2007), rat brain microvascular endothelial cells (Lu L *et al.*, 2007), human coronary artery endothelial cells (Yu *et al.*, 2004), and rat aortic endothelial cells (Almofti *et al.*, 2006). Approximately 50 % of the selected proteins in our study were also identified and reported in the rat coronary microvascular endothelial cell and rat brain microvascular endothelial cell study (Lu L *et al.*, 2007), suggesting a significant similarity in the protein expression between the CMECs and the other two microvascular endothelial cell types. Of the selected proteins in our study, ~23 % was identified and reported in a study on human coronary arterial endothelial cells

(Yu *et al.*, 2004), and ~ 41 % in a study performed on rat aortic endothelial cells (Almofti *et al.*, 2006).

In order to gain a better understanding of how the 1387 identified proteins are functionally linked, the protein list was submitted to the functional annotation tool of DAVID Bioinformatics System (Huang DW and Lempicki, 2009). The cytosolic component (GO term: 0005829) represented the highest % protein count (28.4 %; p-value: 2.6×10^{-58} ; 3.2 fold enrichment), whereas 9.4 % of the total identified proteins was associated with the membrane component (GO term: 0005624; p-value: 3.6×10^{-5} ; 1.6 fold enrichment), which is higher than previously reported in brain microvascular endothelial cells (5 %) (Pottiez *et al.*, 2010), but lower than in corneal endothelial cells (~28 %) (Dyrlund *et al.*, 2012).

One of the outstanding features of the cellular component analysis was the high representation of mitochondrial cellular component proteins (GO term: 0005739; 23.3 % protein count; p-value = 2.1×10^{-28} ; 2.3 fold enrichment) in our cells. We were unable to find any other endothelial-based study reporting anything similar. In fact, our findings closely resembled the % mitochondrial protein count in muscle cells as previously shown in human skeletal muscle cells (~22 %) (Hojlund *et al.*, 2008). The highly enriched mitochondrial protein component is remarkable in view of the fact that mitochondrial proteins on average make up only 5 % - 10 % of total cellular proteins (Hojlund *et al.*, 2008; Rabilloud, 2008) and that endothelial mitochondria comprise 5 %, 10 % and 11 % of the total endothelial cell volume in the liver (Blouin *et al.*, 1977), rat aortic endothelial cells (Ungvari *et al.*, 2008), and metabolically active blood-brain barrier endothelial cells (Kluge *et al.*, 2013) respectively. When we applied functional annotation cluster analysis (Figure 3.5), the mitochondrial membrane and mitochondrial inner membrane proteins collectively represent the third most enriched cluster in the CMECs (enrichment score: 15.5). These findings suggest that the CMECs seem to be quite distinct with regards their mitochondrial abundance compared to other endothelial cell types. A representative fluorescence microphotograph of MitotrackerTM -stained cells, demonstrating mitochondrial abundance in the CMECs is shown in Figure 3.8.

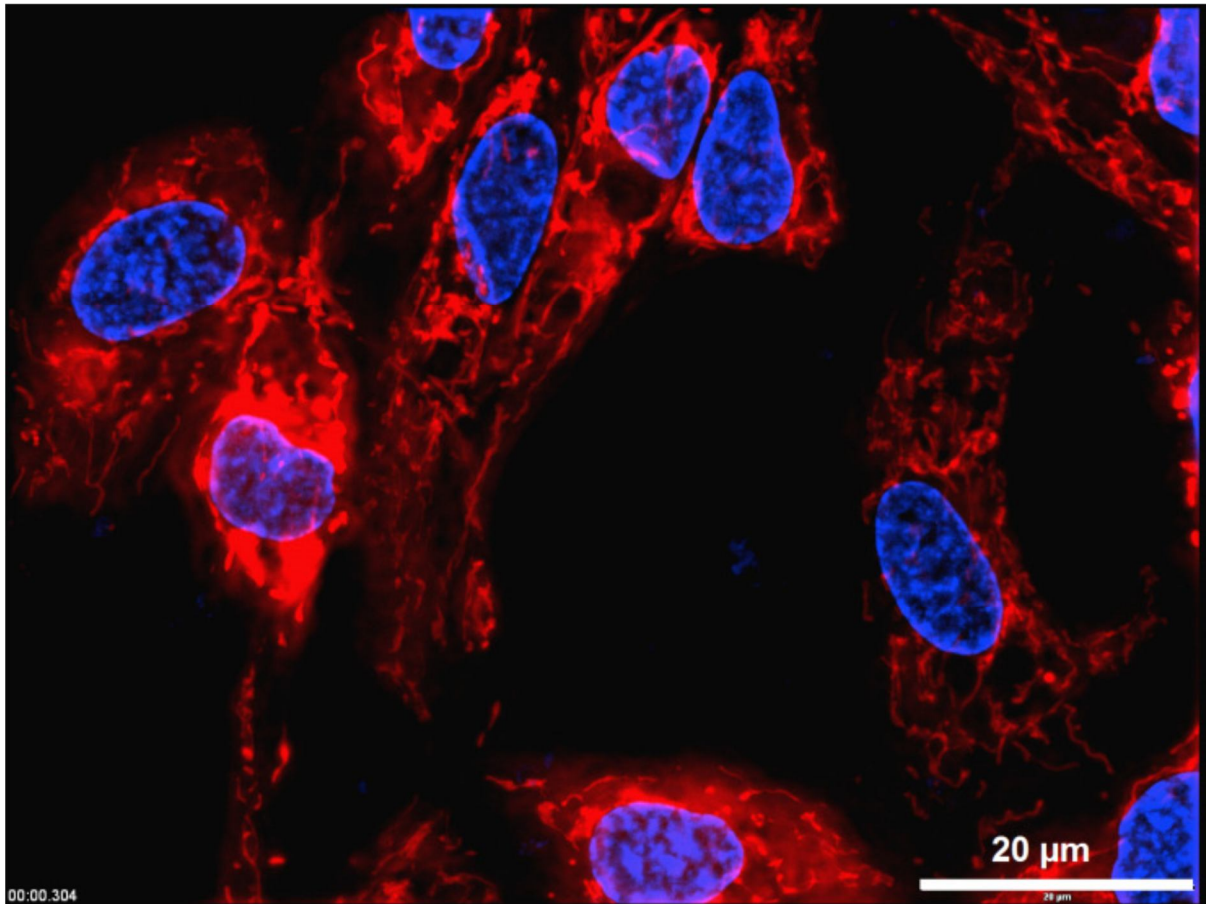


Figure 3.8: Mitochondrial abundance (structures stained bright red) in CMECs stained with MitoTracker™ Red (Olympus IX81 inverted fluorescent microscope, Olympus GMBH, Hamburg, Germany).

Interestingly, the highly enriched mitochondrial cellular component cluster was not matched by classical ATP-generating mitochondrial processes and functions such as the tricarboxylic acid cycle (TCA cycle; cluster no. 12; enrichment score 6.7; not shown), fatty acid oxidation (cluster no. 47; enrichment score: 2.1; not shown) and ATP synthesis coupled proton transport (cluster no. 51; enrichment score: 2.0; not shown). The relatively low representation of these energy generating mitochondrial functions may be due to the fact that endothelial mitochondria are generally not regarded as the primary source of cellular ATP, rather they are thought to act as sensors in cellular signalling responses, sensors of local oxygen levels, sources of NO and ROS, and regulators of Ca²⁺ homeostasis (Kluge et al., 2013; Davidson and Duchon, 2007). In fact, glycolytic metabolism has previously been shown to be the predominant source of endothelial cellular energy, supplying between 75 % and 99 % of endothelial ATP in aortic and coronary microvascular endothelial cells respectively (Davidson and Duchon, 2007; Culic *et al.*, 1997; Spahr *et al.*, 1989; Mertens *et al.*, 1990). These reports are supported by our own annotation cluster data. The clusters containing glycolytic processes such as carbohydrate catabolism, glucose catabolism and hexose catabolism (cluster no. 4; enrichment score: 15.1; Figure 3.5), and glucose metabolism, monosaccharide metabolism and hexose metabolism (cluster no. 8; enrichment score: 10.8; Figure 3.5) were significantly more enriched than mitochondrial energy metabolism processes.

Vesicles and related cellular component GO terms occupied the 6th most enriched functional annotation cluster in the CMECs (enrichment score: 11.9; Figure 3.5), and proteins associated with vesicles (GO term: 0031982) represented 11.6 % of the total identified proteins (p-value: 3.7 x 10⁻¹³; fold enrichment: 2.3). Furthermore, the biological process of vesicle-mediated transport achieved a 7.5 % protein count (GO term: 0016192; p-value: 2.6 x 10⁻⁹; fold enrichment: 2.4), similar to previous observations in neurons (~7.5 % protein count and fold enrichment: 3) (Estrada-Bernal *et al.*, 2012). The high degree of enrichment associated with vesicles and vesicular transport in our cells is not unexpected, as CMECs are known to express a greater abundance of vesicles than other cardiac endothelial types (Brutsaert, 2003; Aird, 2007a). In addition to vesicles, capillary endothelial cells express high concentrations of caveolae (Benyadan, 2002; Aird, 2007), which facilitates the process of vesicle-mediated transcytosis via vesiculo-vacuolar organelles (VVOs) (Benyadan,

2002). Cardiac capillary endothelial cells are particularly enriched with VVOs. Indeed, our own analyses showed that both vacuoles (GO term: 0005773; protein count: 2.7 %; p-value: 0.03; fold enrichment: 1.7) and caveolae (GO term: 0005901; protein count: 1.2 %; p-value: 0.02; fold enrichment: 2.7) featured as enriched cellular components in the CMECs.

The functional annotation cluster comprising the Ras superfamily of small GTPases also featured prominently in the CMEC proteome (cluster no. 9; enrichment score: 9.7; Figure 3.5). More than 25 proteins belonging to the Ras superfamily were identified, including members of the Ras, Rho and Rab subfamilies. Rab GTPases are primarily involved with the regulation of vesicular transport (Wennerberg *et al.*, 2005), and it came as no surprise that Rab proteins were particularly well represented in the CMECs (18 Rab proteins were identified out of 61 known Rab proteins (Wennerberg *et al.*, 2005). The Rho GTPases are known to regulate cell adhesion and microvascular permeability (Spindler *et al.*, 2010), and our cells expressed prominent Rho subfamily proteins, including Rac2, Cdc42, RhoC and RhoG, as well as several proteins associated with Rho-signalling (e.g. Rho-associated protein kinase 2, Rho GTPase-activating protein and Rho GDP-dissociation inhibitor).

In addition to the above, the full range of cellular protein metabolism, from translation, protein transport and localization to protein breakdown by proteasomal processes was well represented in the baseline CMEC proteome (See Figure 3.6).

3.6.3 The effect of various harmful stimuli on the NO production of CMECs (FACS analysis).

In a series of initial pilot studies to characterise the CMECs with regards to their response to a variety of harmful stimuli, we exposed the cells to angiotensin II, high glucose concentrations, hypoxia, oxidised LDL, ADMA and TNF- α , and measured the response in terms of intracellular NO-production. These are all factors that have previously been shown to reduce endothelial NO bio-availability and hence induce endothelial dysfunction. In view of this, we assessed the CMEC responses to 24 h treatment with the stimuli by the measurement of intracellular NO-production.

3.6.3.1 Angiotensin II (100 nM for 24 hours):

Elevated angiotensin II levels have been observed in patients with atherosclerotic risk factors, including hypertension, diabetes, and renal dysfunction (Cai *et al.*, 2003, Harrison DG *et al.*, 2003a). It has also been shown to mediate endothelial dysfunction and promote vascular inflammation and atherogenesis (Harrison DG *et al.*, 2003b; Arruda *et al.*, 2005; Kunieda *et al.*, 2006).

According to a study by Hill-Kapturczak *et al.*, (1999), addition of physiological concentrations of angiotensin II (10^{-8} M) caused a rapid release of NO from porcine pulmonary artery endothelial cells (PPAEs). This angiotensin II-stimulated NO release from PPAE cells required extracellular L-arginine and was inhibited by L-nitro-arginine methyl ester. In another study, the same cell line as above was treated with 100nM of angiotensin II for 1 minute, 15 minutes and 8 hours (Li JM *et al.*, 2007a). They showed an increase in MAPK activation, which led to an angiotensin receptor type 2-dependant increase in eNOS expression in PAECs. In a study by Saito *et al.* (1996), cultured bovine endothelial cells were treated with 10^{-7} M angiotensin II and this led to an increase in NO_x production. Lastly, another study also reported an increase in NO in a microvascular endothelial cell type, thus supporting our findings (Bayraktutan and Ülker, 2003). They treated rat coronary microvascular endothelial cells (rCMECs) with different dosages of angiotensin II (1 – $10\mu\text{mol/l}$) and found an enhancement in NO release. All the above studies support our finding of increased NO in CMECs after 24 hour treatment with angiotensin II (see figure 3.7).

In contrast to the above mentioned studies, another study found that treatment of BAECs with angiotensin II (200nM) treatment was associated with increased cellular O_2^- production and decreased endothelial NO bio-availability (Doughan *et al.*, 2008). Also, Chapulsky and Cai (2005) found in BAECs that endothelial NADPH-oxidase-derived H_2O_2 down-regulates dihydrofolate reductase (DHFR) expression in response to angiotensin II, resulting in tetrahydrobiopterin (H_4B) deficiency and uncoupling of eNOS. Lastly, a study by Desideri *et al.* (2003) showed that angiotensin II increased NADPH-oxidase activity in HUVECs, promoted ROS generation, reduced NOS activity, increased NO breakdown and consequently impaired NO availability in these cells.

From the above discussion, we speculate that the decrease in NO that was found in some of the studies, was possibly due to an overproduction of O_2^- , which would lead to it binding to available NO (forming OONO⁻). Any excess NO that is produced is thus being “mopped up” by the large amounts of O_2^- produced under these circumstances in the cells (Pacher *et al.*, 2007).

In our hands, *in vitro* treatment with angiotensin II also led to an increase in NO production. This might be explained by the activation of the angiotensin receptor type 2 (ATR2), which could lead to activation and phosphorylation of the PI3K - PKB/Akt signalling pathway (Herrera MD and Garvin, 2010a), which is the opposite of the NO decreasing effect of angiotensin receptor type 1 (ATR1) stimulation (Desideri *et al.*, 2003). PKB/Akt can then in turn phosphorylate eNOS at Ser1177 and subsequently lead to an increased production in NO (Herrera MD and Garvin, 2010a). Further exploration of the mechanisms underlying the increased NO production did not fall within the scope of the pilot studies.

3.6.3.2 *In vitro* simulation with hyperglycaemia: Glucose (25 mM for 24 hours):

Hyperglycaemia is one of the main characteristic features of type 1 and 2 diabetes and plays a pivotal role in diabetes-associated microvascular complications. Although hyperglycaemia also contributes to the occurrence and progression of macrovascular disease, other factors such as dyslipidaemia, hyperinsulinaemia, and adipose-tissue-derived factors play a more dominant role. A mutual interaction between these factors and endothelial dysfunction occurs during the progression of the disease (Bakker *et al.*, 2009).

Our finding that high glucose levels (25 mM) resulted in increased NO production after 24 hours (see figure 3.7), was supported by a previous study on human aortic endothelial cells (HAECs) in which exposure to high glucose increased eNOS gene and protein expression, and NO release (Cosentino *et al.*, 1997). This was also shown in cultured retinal endothelial cells, where treatment with high glucose (25 mM), lead to an increase in expression and activity of eNOS compared to normal glucose (5 mM) treated cells (El-Remessy *et al.*, 2003). A study by Sobrevia *et al.* (1996) showed that exposure to elevated glucose was associated with a

selective stimulation of L-arginine transport (system y^+), which was paralleled by an increase in basal release of NO.

In contrast to these findings, other groups demonstrated reduced basal NO production in response to high glucose, with a concomitant reduction in eNOS expression in human coronary artery endothelial cells (HAECs) and bovine aortic endothelial cells (BAECs) (Ding *et al.*, 2000; Du *et al.*, 2001). In a study by Salt *et al.* (2003) it was demonstrated that insulin-stimulated NO production was abolished in HAECs cultured in 25 mmol / l glucose and they hypothesized that this inhibition of insulin-stimulated NO production was a consequence of reduced expression or activity of insulin signalling proteins.

The increase in NO that was observed in our experiments might be explained by either the selective stimulation of L-arginine transport as in one of the above supporting studies (Sobrevia *et al.*, 1996) or an upregulation of eNOS (Cosentino *et al.*, 1997; El-Remessy *et al.*, 2003). Chronic exposure to high levels of glucose is also associated with a marked increase of O_2^- production and will lead to an imbalance between NO and O_2^- (Ding *et al.*, 2000) and while the levels of NO produced outweighs the levels of O_2^- produced (as might be the case in our study), NO production will not be negatively affected. However increased NO production in aorta endothelial cells reported by Cosentino *et al.* (1997), for example, was coupled with an even greater increase in generation of O_2^- when the exposure to high glucose levels was prolonged, which eventually led to the inactivation of NO. Further exploration of the underlying mechanisms did not fall within the scope of the initial pilot studies.

3.6.3.3 Hypoxia ($O_2 < 0.6\%$)

The response of the CMECs to hypoxia is addressed in detail in the next chapter.

3.6.3.4 Oxidised-LDL (40 µg / ml for 24 hours):

As mentioned before, atherosclerosis is the accumulation of cholesterol and other lipids in the artery and numerous studies have demonstrated that ox-LDL causes endothelial dysfunction and accelerates atherosclerosis (Wong WT *et al.*, 2011). Ox-LDL stimulates endothelium to secrete MCP-1, which induces filtration and entrapment of ox-LDL into the sub-endothelial space, leading to differentiation of monocytes into “foam” macrophage (Tabata *et al.*, 2003). Ox-LDL is also capable of inducing proliferation and migration of vascular smooth muscle cells by increasing the expression of platelet-derived growth factor (Taguchi *et al.*, 2000). Ox-LDL may enhance the pro-coagulant activity of endothelium, which may easily lead to thrombosis and finally atherosclerosis (Ann and Paul, 2001). Lastly, another possible effect is that ox-LDL activates G1 protein-coupled scavenger receptors, which will in turn deactivate the l-arginine pathway and reduce the activity of NO synthase (Tanner *et al.*, 1991).

Functionally, the vascular release of NO is abnormal in the setting of hypercholesterolaemia (Jin RC and Loscalzo, 2010). The mechanisms underlying this abnormality are likely multifactorial (Ramasamy *et al.*, 1998). Studies of vessels from animals with short-term hypercholesterolaemia showed that endothelial production of NO was not suppressed, but paradoxically increased (Minor *et al.*, 1990). It has also been shown that oxidized LDL can increase eNOS mRNA levels in low concentrations and decrease the eNOS expression at high concentrations (Hirata *et al.*, 1995). In the latter study, bovine aortic endothelial cells (BAECs) were treated for up to 24 hours with ox-LDL at low concentrations (10 µg / ml) and high concentrations (100 µg / ml). Some researchers proposed that lysophosphatidyl choline (LPC) in ox-LDL can increase eNOS expression in endothelial cells in a dose-dependent fashion (Minor *et al.*, 1990; Zembowicz *et al.*, 1995). Another important component of ox-LDL is 13-HPODE (13-hydroperoxyoctadecadienoate) (Jiang X *et al.*, 2012). The major polyunsaturated fatty acid present in LDL is linoleic acid which is converted to oxidized linoleic acid during the atherosclerotic process (Egert *et al.*, 2009). 13-HPODE has potent biological effects that include the induction of interleukin-1 and VCAM-1 expression (Qin *et al.*, 2013). Minor *et al.* (1990) hypothesized that HPODE is a candidate molecule which might mediate the effect of oxidized LDL on increased NO production. One of the

mechanisms by which HPODE might increase nitric oxide production is by up-regulating the eNOS gene expression in atherosclerotic vessels (Minor *et al.*, 1990).

In contrast to the up-regulation of eNOS-NO biosynthesis found in the above mentioned studies, Liao JK *et al.*, (1995) reported that oxidized-LDL (0 – 100 µg / ml) caused a time- and concentration-dependent decrease in steady-state eNOS mRNA and enzyme activity in human endothelial cells. This downregulation was found to occur principally at the posttranscriptional level, resulting in a reduction in eNOS mRNA half-life from 36 to 10 hours. Very high levels of native LDL were found to decrease eNOS mRNA expression (Vidal *et al.*, 1998). Other previous studies also showed that ox-LDL impairs the release of NO from endothelial cells (Chin *et al.*, 1992; Kugiyama *et al.*, 1990). Ox-LDL promotes the recruitment of inflammatory cells to the vessel wall, which may increase local production of ROS leading to the inactivation of NO (Granger D *et al.*, 2010a). There is evidence that ox-LDL and products of lipid peroxidation can react with NO directly and eliminate its biological activity (Chin *et al.*, 1992; O'Donnell *et al.*, 1999). Ox-LDL was also shown to decrease eNOS protein levels in endothelial cells (Liao JK *et al.*, 1995), thus potentially decreasing production of NO. Finally, products of lipid peroxidation, including lysophosphatidylcholine, may interfere with signal transduction and receptor-dependent stimulation of NOS activity (Kugiyama *et al.*, 1990; Keaney *et al.*, 1996) and with activation of guanylyl cyclase (Schmidt K *et al.*, 1992).

Finally, in a study by Grafè *et al.* (1998), cardiac microvascular and macrovascular ECs were isolated from human hearts and treated with ox-LDL to show that these cell types respond differently to ox-LDL. Briefly, they speculate that the preferential localization of atherosclerotic lesions in the macrovasculature may in part be due to a higher susceptibility of macrovascular (than microvascular) endothelial cells to ox-LDL. The relatively reduced susceptibility of microvascular endothelial cells to the NO-lowering effects of ox-LDL could be a further explanation for our observations.

3.6.3.5 ADMA (500 μ M for 24 hours):

As mentioned above, ADMA is an endogenous inhibitor of NOS produced by endothelial cells (Anderssohn *et al.*, 2010). ADMA has been associated with impaired endothelial function in humans (Juonala *et al.*, 2007), and clinical evidence suggests that serum ADMA may be a novel cardiovascular risk factor (Maas *et al.*, 2007; Schnabel *et al.*, 2005).

A recent study assessed the effects of ADMA treatment (0 – 500 μ M) on HUVECs and it was shown that ADMA treatment up to 10 μ M had no effects on nitrite and nitrate levels. However, above this concentration, nitrite and nitrite/nitrate accumulation was significantly decreased by ADMA (Mohan and Fung, 2012). In another study, it was suggested that ADMA increases oxidative stress by uncoupling of NOS (Pritchard *et al.*, 1995). In this situation optimal electron flow within the two catalytic domains of NOS is impaired and molecular oxygen becomes the sole electron acceptor and NOS generates O_2^- radicals (Pritchard *et al.*, 1995). Böger *et al.* (2000a, b) showed that ADMA concentration dependently increases O_2^- production by cultured human endothelial cells. In another study the same group presented data where the inhibition of NOS by ADMA decreases NO production in HUVECs (Bode-Böger *et al.*, 2005). All the above studies support the significant decrease in intracellular NO levels observed in the CMECs after 24 hours of treatment with ADMA (500 μ M), which is to be expected given the fact that ADMA inhibits NO production (see figure 3.7).

3.6.3.6 TNF- α (5 ng / ml and 20 ng / ml for 24 hours):

The response of the CMECs to TNF- α is addressed in detail in chapter five.

3.7 Conclusion

In this chapter, we supplied a characterisation of adult rat CMECs under baseline conditions. Apart from the morphological and fluorescence-labeled validation of cell purity, we demonstrated that the CMECs express an array of signalling proteins essential in the NOS-NO biosynthesis pathway. Additionally, we also showed that iNOS, and interestingly, nNOS were expressed, indicating that these cells express the full battery of the principal NOS isoforms. The western blotting measurements of some selected proteins related to the generation of NO were important for the purposes of this study, as changes in the NOS-NO biosynthesis pathway would form an integral end-point for the rest of our investigations.

The most novel aspect of this chapter was the comprehensive characterisation of the baseline CMEC proteome. We are only aware of one study in the literature that partially reported on the baseline proteome of CMECs, in which 22 proteins were positively identified. All in all, 1387 proteins were identified in our CMECs. Therefore, to our knowledge, this study is the most extensive documentation of any mammalian CMEC proteome to date and represents a novel addition to existing vascular proteomic databases. An outstanding feature of the baseline CMEC proteome was the surprisingly high enrichment of mitochondrial proteins, mainly those denoted as cellular component proteins. There is no evidence in the literature of previous studies reporting on similar observations in any other vascular endothelial cell type. The uniquely high abundance of mitochondrial proteins observed in our CMECs (protein count as % of total proteins: ~ 23%) may point to a distinct role for their mitochondria, which was apparently not related to ATP synthesis under baseline conditions. CMECs participate in an important functional and regulatory cross-talk with cardiomyocytes, and given the frequent exposure of the myocardial capillary endothelium to varying degrees of oxygen tension, it is possible that the mitochondria of CMECs have a particularly important role as the oxygen sensors of the myocardium. Such an essential function would conceivably require high numbers of mitochondria. The high enrichment of vesicle proteins in my view serves as confirmation of the role of CMECs in capillary transcytosis. The high enrichment of RAS signalling proteins (25 Ras GTPase proteins, and 18 Rab proteins), most likely supplies support for the involvement of vesicular transport and finally, the high enrichment of glycolytic proteins,

confirms previous observations in other endothelial cell types that glycolysis is the main energy source in these cell types.

In the final section of this chapter, we show the results of some of my very initial pilot studies in which we evaluated the CMECs with regard to their response to various harmful stimuli commonly associated with cardiovascular risk factors and disease states. By subjecting these cells to the various stimuli as listed in figure 3.7 and assessing intracellular NO production as an endpoint, we were given a very basic “snapshot” of CMEC responses to 24 hour exposure to these stimuli. Interestingly, almost all of the stimuli seemed to have an increasing effect on the NO production of these cells (except for ADMA and TNF- α at 20 ng / ml). Initially we expected that these substances would reduce the NO bio-availability and therefore assist in providing us with an *in vitro* model for endothelial dysfunction. However, as will become evident in later chapters, endothelial cell injury and responses suggestive of dysfunction are not necessarily marked by reduced NO production, at least not within the time-frames of our *in vitro* experiments. Although various other pilot studies (many of them not included) were conducted in order to assist me in selecting the harmful stimuli on which we would focus in the rest of this dissertation, the initial NO-production investigations were a good starting point, and helped us to optimise the fluorescent probe – FACS analysis technique in the CMECs.

After some contemplation, we decided to focus on hypoxia and TNF- α treatment as the injury-inducing models of choice. These will be described in detail in the following chapters.

CHAPTER FOUR

Characterization and investigation of hypoxia-induced responses in CMECs

4.1 Introduction

The metabolic and molecular changes in response to hypoxia have been extensively investigated and reviewed and have largely contributed towards the knowledge of the pathophysiological events in organs subjected to hypoxia, including the heart (Michiels *et al.*, 2000). As discussed in detail in chapter one (page 60), endothelial cells (ECs) are, due to their location, frequently exposed to variations in oxygen tension (Michiels *et al.*, 2000). It has been shown that hypoxic conditions indeed have profound effects on endothelial function (Tang N *et al.*, 2004; Deanfield *et al.*, 2007).

Previous studies have shown that exposure to chronic intermittent hypoxia impairs endothelium-dependent vasodilation in the skeletal muscle and cerebral circulations (Phillips *et al.*, 2004; Tahawi *et al.*, 2001). These studies strongly suggested that a vascular decrease in NO bio-availability (Phillips *et al.*, 2004; Tahawi *et al.*, 2001) and increased O_2^- levels (Phillips *et al.*, 2006; Troncoso Brindeiro *et al.*, 2007) were possible underlying factors. As mentioned before, a decrease in NO bio-availability is considered to be the hallmark of ED (Imrie *et al.*, 2010). The decrease in NO bio-availability observed in many previous endothelial cell-based studies could be due to a few processes, such as an increase in scavenging of NO by O_2^- (Marcus *et al.*, 2012). Hypoxia may influence NO production, NO tissue concentration, and NOS expression in variable manners by several mechanisms (Manukhina *et al.*, 2006). These mechanisms include: (i) limitation of NO production due to reduced O_2 levels (O_2 is an essential requirement for NOS-mediated conversion of L-arginine to NO); (ii) effect of O_2 on NOS feedback inhibition; (iii) modulation of NO bio-availability; (iv) induction of HIF-1 and other NOS transcription factors; (v) changes in intracellular Ca^{2+} concentration and Ca^{2+} influx; and (vi) induction of NOS-regulating heat shock proteins. Exposure to hypoxia can indeed lead to a decrease in NO production by all three NOS isoforms (Weigand *et al.*, 2011).

The response to hypoxia also involves altered expression of NOS genes (Manukhina *et al.*, 2006). Some studies have demonstrated hypoxic down-regulation of eNOS expression in pulmonary endothelial cells (Girgis *et al.*, 2003). Others showed that hypoxia reduced eNOS mRNA and/or protein in pulmonary artery endothelial cells (Morrell *et al.*, 2009). In another endothelial cell study investigating the effects of 24 hours hypoxia, it was found that the transcription of eNOS in HUVECs exposed to hypoxia (< 1% O₂) was significantly repressed (Fish *et al.*; 2010). Conversely, previous studies from our own group demonstrated significant increases in the expression of eNOS in hypoxic CMECs, which was accompanied by increased NO-production (Strijdom *et al.*; 2006). In the same study by Strijdom *et al.* (2006), it was further shown that iNOS-specific inhibition did not alter hypoxia-induced NO-production, thereby excluding increased iNOS activity as a possible source of NO. From the above it is clear that the available data on hypoxia-induced changes in endothelial cells are not always consistent, particularly with regard to NOS-NO biosynthesis. In view of this, we aimed in this chapter to comprehensively characterise the CMECs and their responses to hypoxia.

For the purposes of this chapter, we aimed to establish a hypoxic protocol that could induce significant, but not lethal injury in the CMECs. One of the novel aspects of this chapter were the proteomic analysis studies, in order to explore global protein expression and differential protein regulation patterns. A careful review of the literature has revealed that there is no evidence of studies in which large-scale differential protein regulation in hypoxic CMECs has been investigated. This is an important gap that has to be addressed in order to fully understand how this distinct endothelial cell subtype responds to hypoxia on subcellular, molecular level. Overall, it is evident from the literature that the relatively few studies have investigated CMECs in the context of hypoxia, which is a gap that we have attempted to fill in this chapter.

4.2 **Methods**

CMECs were cultured and grown as described previously (page 111). The **first part** of this chapter describes the establishment and validation of the hypoxia protocol. The CMECs were exposed to a 6, 18 and 24 hours hypoxia by lowering the atmospheric O₂ (0.6 % O₂, 5 % CO₂, balance: N₂, 40-60 % humidity, incubation temperature: 37 °C) in a multi-gas tissue culture incubator (Sanyo Biomedical, Japan). After conducting pilot studies, we found that at 1 % O₂ there was no change in cell viability (as measured by PI and Annexin V) compared to normoxic samples (data not shown). We therefore set the O₂ at 0.6 % (which was the lowest O₂ concentration achievable with the incubator) and found that this concentration succeeded in inducing a significant reduction in cell viability; hence, the rest of the investigations were performed at 0.6 % O₂. Control, normoxic CMECs were incubated under standard atmospheric conditions for 6, 18 and 24 hours (21 % O₂, 5 % CO₂, 40-60 % humidity, incubation temperature: 37 °C) (see figure 4.1 for hypoxia protocol). Validation of hypoxia-induced reduction in cell viability was performed by flow cytometric analysis of the % propidium iodide-staining (necrosis) and annexin-V-staining (apoptosis) cells using a commercially available kit (Alexa Fluor® 647 Annexin V conjugate / propidium iodide; BioLegend, San Diego, CA, USA) as described in chapter 2. We also validated the induction of a hypoxic state by performing western blot analysis of HIF-1 α expression (an important protein marker of hypoxia) in CMECs exposed to 24 hours of hypoxia.

In the **second part of the study**, we explored the NO-synthesis response of the CMECs to 24 hours of hypoxia by investigating the eNOS-NO biosynthesis pathway. This was achieved by measuring the expression of eNOS protein by western blotting and intracellular NO production with DAF-2/DA (as described in chapter 2, page 121). Furthermore, we were interested in whether oxidative stress was induced in the hypoxic CMECs. In this regard, we investigated whether the hypoxia protocol (24 hours) resulted in an increase in ROS generation. We chose to measure ROS production by FACS analysis of dihydrorhodamine-123 (DHR-123; Sigma Chemical Co, St Louis, MO, USA) mean fluorescence intensity. The DHR-123 fluorophore has previously been shown to localise in mitochondria and fluoresce when oxidized (Tiede *et al.*, 2011), and could therefore be an indicator of mitochondrial ROS formation. However, we and others have demonstrated that DHR-123 was also sensitive for

peroxynitrite (ONOO⁻) (Strijdom *et al.*, 2009c; Navarro-Antolin *et al.*, 2001). Furthermore, we were interested to establish whether hypoxia had any regulatory effects on the activity of the superoxide producing NADPH-oxidase enzyme by measuring the expression of p22 phox (a surrogate marker of NADPH-oxidase activity) with western blotting. In the final set of investigations in this part of the chapter, we determined whether the 24 hours hypoxia protocol induced nitrosative stress by measuring the expression of nitrotyrosine.

In the **third part** of the chapter, the CMEC proteome was comprehensively investigated in terms of large-scale protein expression and differential regulation patterns after subjecting CMECs to a 24 hour hypoxia protocol as described above. Preparation of samples for proteomics analysis was performed by the filter-aided sample preparation (FASP) technique followed by in-solution trypsinisation (described in detail in chapter 2, page 138). A total of 3 samples were prepared for normoxic and hypoxic groups respectively. See figure 4.2 for an overview of the workflow followed for proteomic analyses of hypoxic CMECs. Data analysis (including functional annotation analyses of proteins) of proteomics results, were performed as described in chapter 2 (page 141). Where indicated, differential protein regulation between control, normoxic and hypoxic samples was analysed by the Maxquant proteomics software package, and proteins were only considered differentially regulated with a protein and peptide PEP of 0.01, up or down regulation of ≥ 1.5 -fold and a p-value of $p < 0.05$.

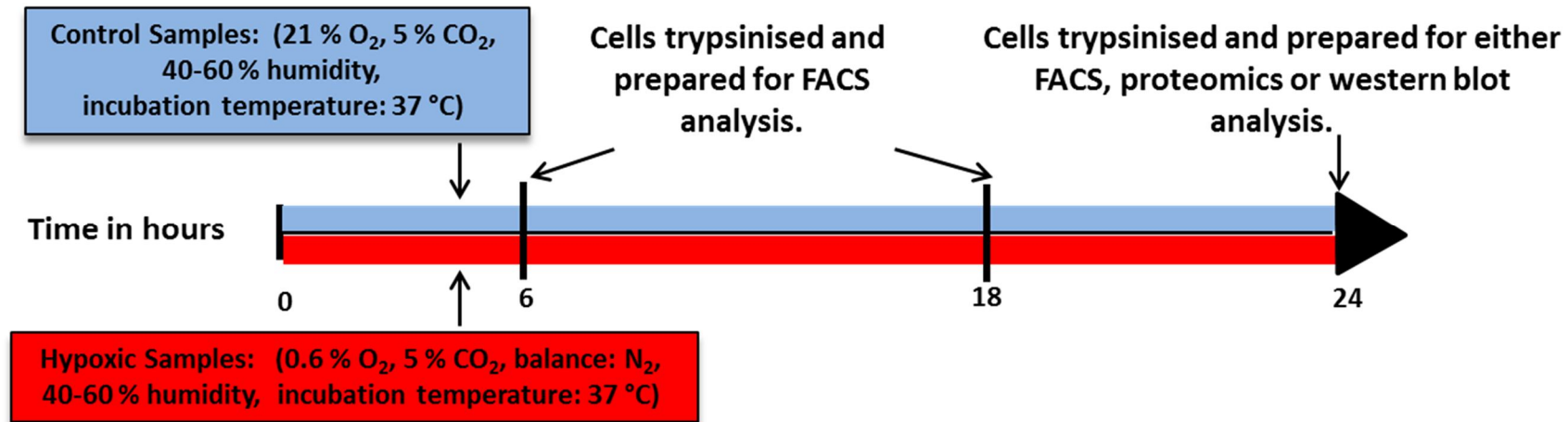


Figure 4.1: The hypoxia protocol. Cells were incubated at either 0.6 % O₂ (hypoxic samples) or at 21 % O₂ (control, normoxic samples) for 6, 18 and 24 hours respectively. The 6 and 18 hour timepoints were only used to investigate cell viability, and all other investigations were based on samples exposed to 24 hour hypoxia.

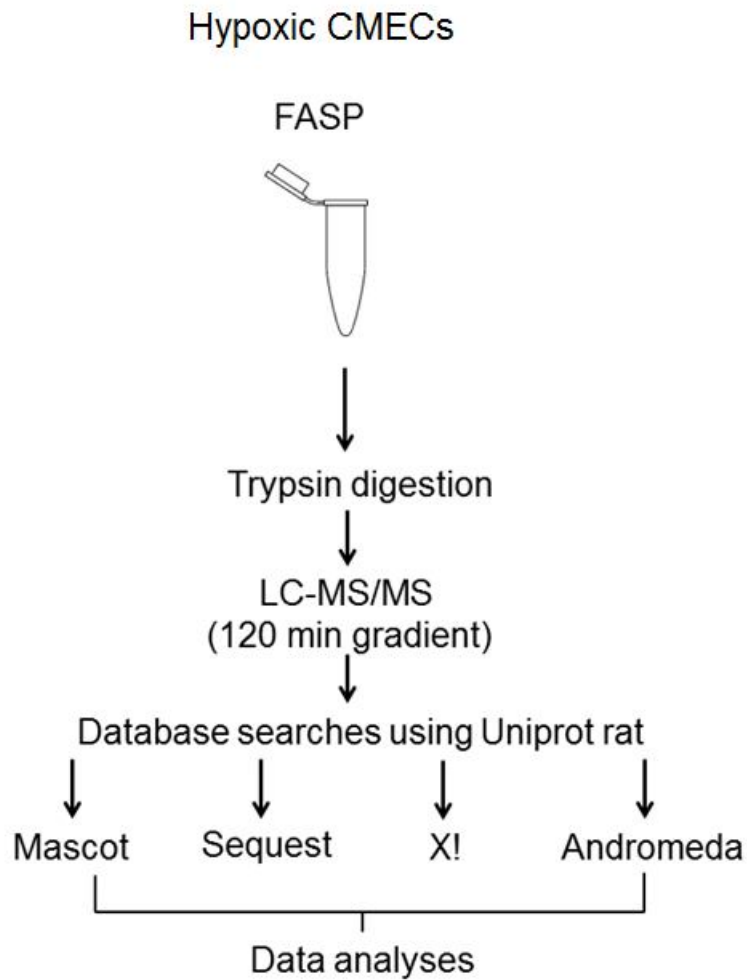


Figure 4.2: Workflow for proteomic analyses of CMECs under hypoxic conditions. The proteins were trypsinized on the FASP membrane and then extracted and prepared for LC-MS/MS. All MS/MS spectra were searched using Thermo Proteome Discoverer software (version 1.3) against in-house versions of Mascot, Sequest, X!tandem and Andromeda. For final data analyses, the identified proteins from all the search engines were combined to obtain a final list of proteins present in the hypoxic CMEC proteome.

4.3 **Results**

4.3.1 **Validation of the hypoxia protocol.**

CMECs exposed to hypoxia ($O_2 < 0.6\%$), showed a decrease at 6 hours ($56.01 \pm 5.40\%$ vs. 100 % control: $p < 0.05$), no change at 18 hours ($109.25 \pm 2.85\%$ vs. 100 % control: $p < 0.05$) and an increase at 24 hours ($190.33 \pm 5.25\%$ vs. 100 % control: $p < 0.05$) in the % propidium iodide (PI) staining cells (measuring necrosis) (see figure 4.3), compared to normoxic controls. CMECs exposed to hypoxia ($O_2 < 0.6\%$), showed a decrease at 6 hours ($46.05 \pm 1.55\%$ vs. 100 % control: $p < 0.05$), an increase at 18 ($174.59 \pm 8.06\%$ vs. 100 % control: $p < 0.05$) as well as 24 hours ($370.16 \pm 5.97\%$ vs. 100 % control: $p < 0.05$) in the % Annexin V staining cells (measuring apoptosis) (see figure 4.4), compared to normoxic controls. In view of these pilot time-response studies, we continued with the 24 hour protocol for all subsequent investigations. In order to contextualise the necrosis and apoptosis results of the CMECs, we conducted separate experiments to compare the necrotic and apoptotic responses of the CMECs to those observed in another cardiac-derived cell line (H9C2 myoblasts). Results showed an increase in necrosis in hypoxic CMECs ($162.34 \pm 30.09\%$ vs. 100 % control: $p < 0.05$) as well as in the H9C2 myoblasts ($228.99 \pm 9.19\%$ vs. 100 % control: $p < 0.05$) compared to control CMECs (see figure 4.5). Results also showed an increase in apoptosis in hypoxic CMECs ($219.41 \pm 31.75\%$ vs. 100 % control: $p < 0.05$) as well as in hypoxic H9C2 myoblasts ($601.79 \pm 45.39\%$ vs. 100 % control: $p < 0.05$) compared to controls. The necrosis observed in the H9C2 myoblasts was significantly more than in the CMECs ($219.41 \pm 31.75\%$ vs. $601.79 \pm 45.39\%$: $p < 0.05$) (see figure 4.6). Exposing CMECs to 24 hours of hypoxia led to a significant increase (1.33 ± 0.07 vs. 1.00 control: $p < 0.05$) (see figure 4.7) in the expression of HIF-1 α , compared to normoxic controls. The demonstration of HIF-1 α stabilisation (i.e. increased expression) is a critical molecular validating marker of hypoxia, in addition to the fluorescence-based markers (PI and Annexin-V) described earlier with regard to necrosis and apoptosis.

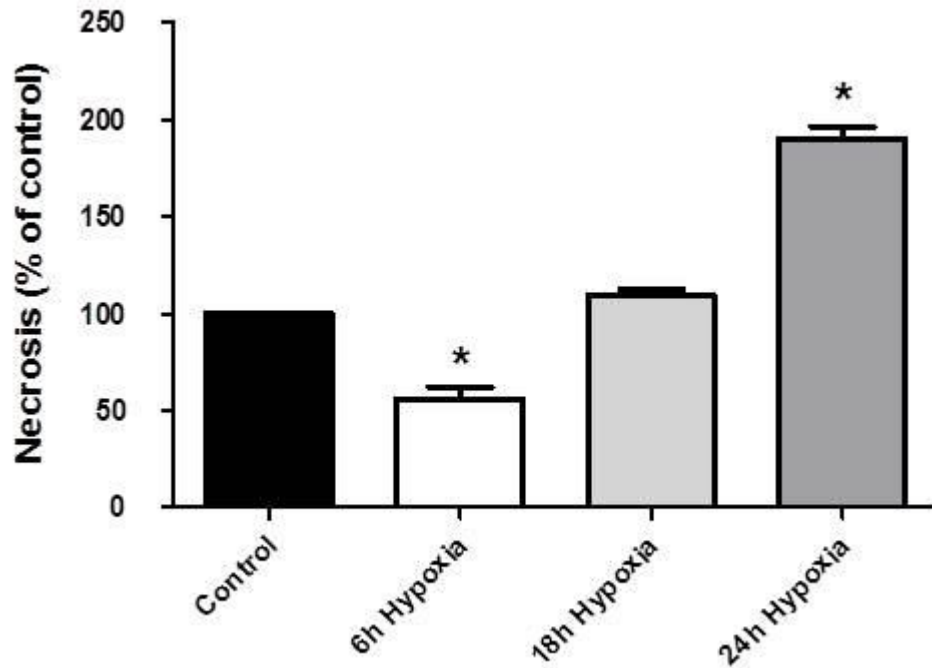


Figure 4.3: Hypoxia time-response studies with necrosis expressed as % PI staining cells (expressed as a percentage of control; control = 100%). Sample size: n = 4 - 6 / group.

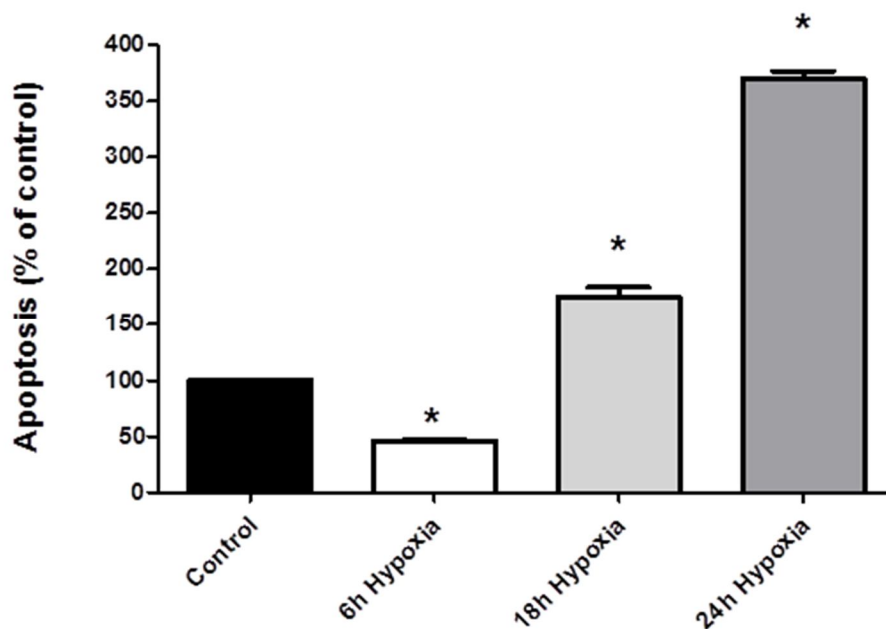
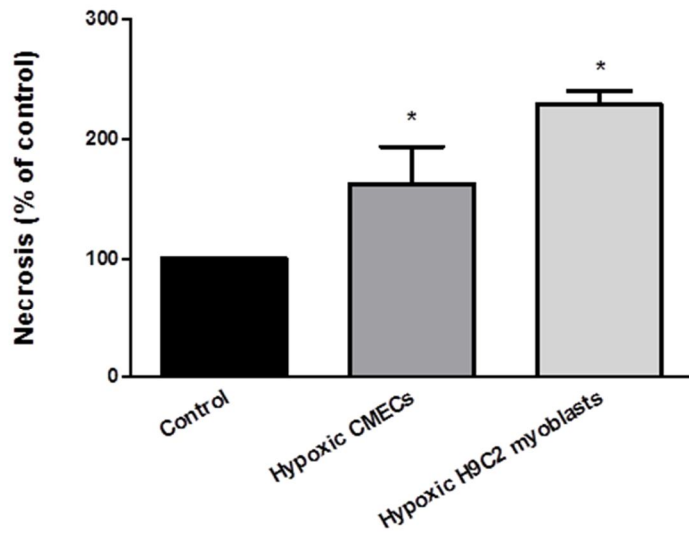
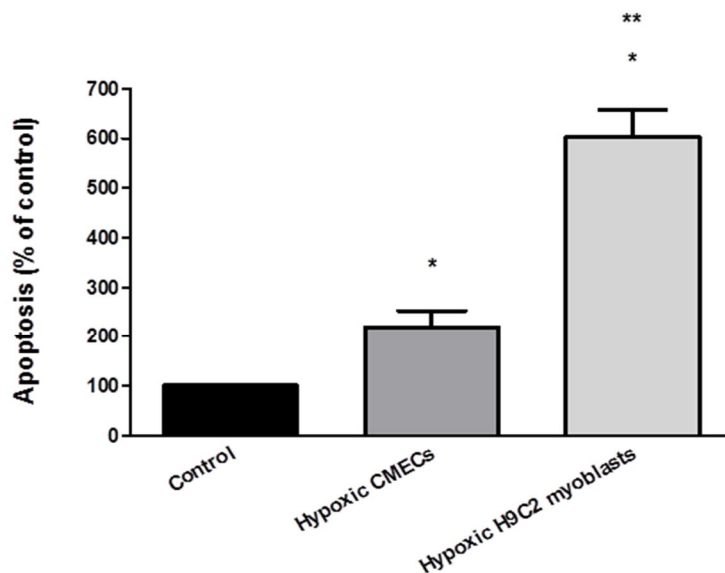


Figure 4.4: Hypoxia time-response studies with apoptosis expressed as % Annexin V staining cells (expressed as a percentage of control; control = 100%). Sample size: n = 4 - 6 / group.



* $p < 0.05$ vs. Control

Figure 4.5: Necrosis in hypoxic CMECs compared to hypoxic H9C2 myoblasts at 24 hours with necrosis expressed as % PI staining cells (expressed as a percentage of control; control = 100%). Sample size: $n = 10 - 14$ / group.



* $p < 0.05$ vs. Control ** $p < 0.05$ vs. hypoxic CMECs

Figure 4.6: Apoptosis in hypoxic CMECs compared to hypoxic H9C2 myoblasts at 24 hours with apoptosis expressed as % Annexin V staining cells (expressed as a percentage of control; control = 100%). Sample size: $n = 10 - 14$ / group.

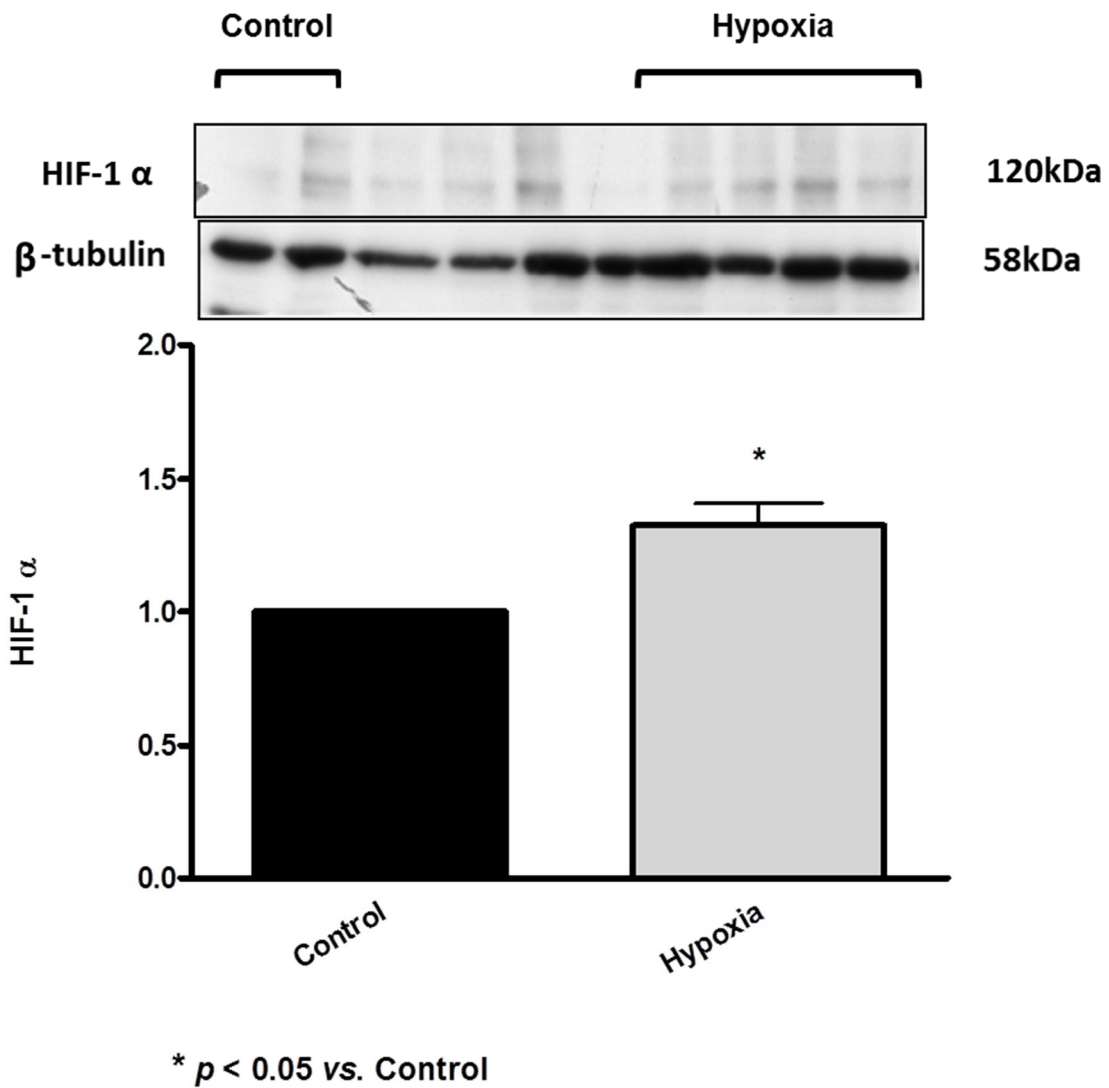


Figure 4.7: HIF-1 α expression in hypoxic CMECs. Representative western blot of CMECs exposed to 24h hypoxia shows a significant increase in HIF-1 α expression compared to normoxic control, serving as a final validation of our hypoxia-inducing protocol. β -tubulin was used to validate equal protein loading. All data were expressed as a ratio of control with control adjusted to 1 (please refer to page 134, chapter 2). Sample size: $n = 4$ / group.

4.3.2 eNOS-NO biosynthesis; oxidative stress; nitrosative stress:

Exposing CMECs to 24 hours of hypoxia led to a significant increase (1.79 ± 0.03 vs. 1.00 control: $p < 0.05$) (see figure 4.8) in the expression of eNOS, compared to normoxic controls. The hypoxia-induced up-regulation of eNOS expression was accompanied by an increase in mean DAF-2/DA mean fluorescence intensity (144.26 ± 11.78 % vs. 100 % control: $p < 0.05$) (see figure 4.9). CMECs exposed to hypoxia showed an increase in mean DHR-123 fluorescence intensity (129.88 ± 3.23 % vs. 100 % control: $p < 0.05$) (see figure 4.10). Exposing CMECs to 24 hours of hypoxia led to a significant decrease (0.55 ± 0.05 vs. 1.00 control: $p < 0.05$) (see figure 4.11) in the expression of p22 phox, compared to normoxic controls. Exposing CMECs to 24 hours of hypoxia led to a significant increase (1.52 ± 0.08 vs. 1.00 control: $p < 0.05$) (see figure 4.12) in the expression of nitrotyrosine, compared to normoxic controls.

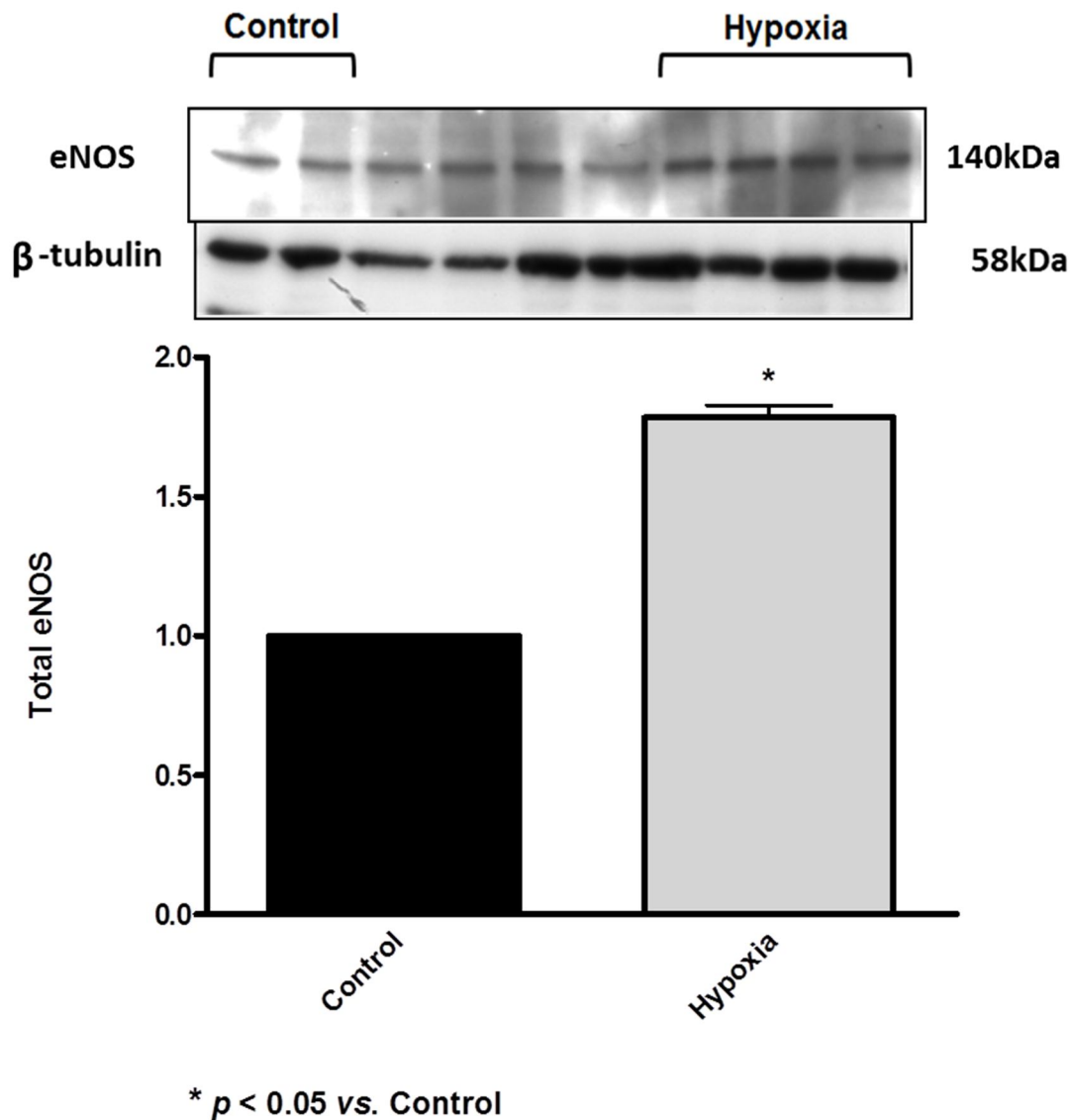
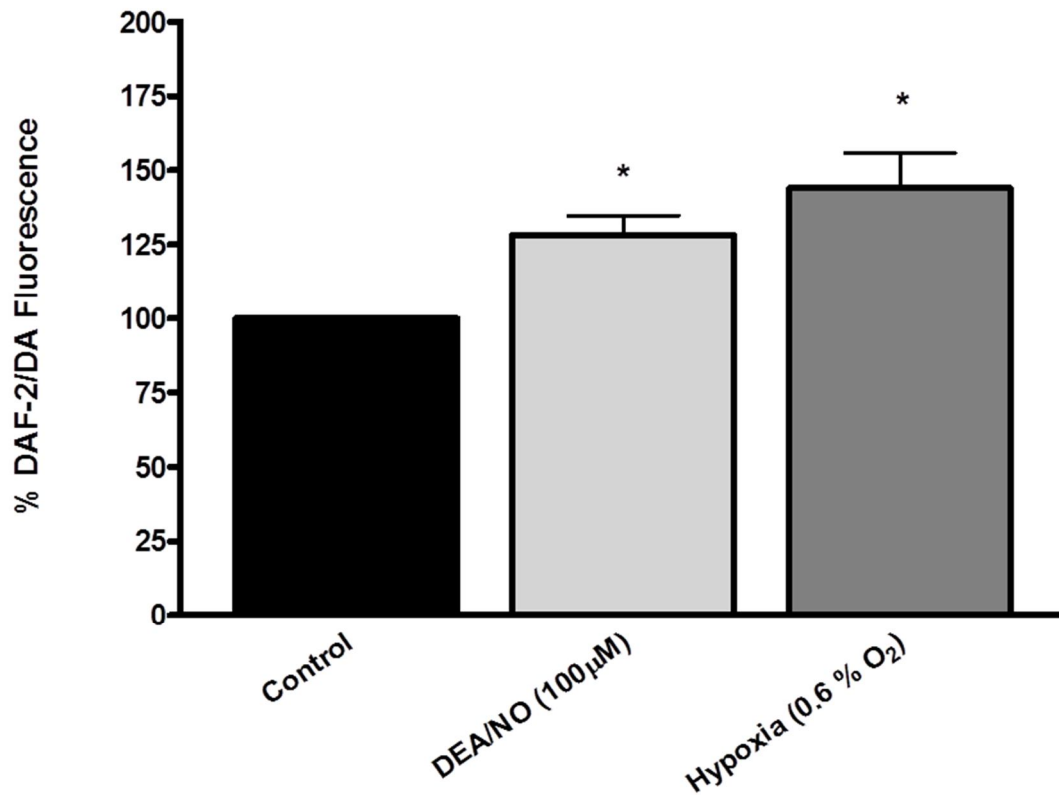


Figure 4.8: Total eNOS expression in hypoxic CMECs. Representative western blot of CMECs exposed to 24h hypoxia shows a significant increase in eNOS expression compared to normoxic control. β-tubulin was used to validate equal protein loading. All data were expressed as a ratio of control with control adjusted to 1 (please refer to page 134, chapter 2). Sample size: n = 4 / group.



* $p < 0.05$ vs. Control

Figure 4.9: Hypoxia-induced (24 hours hypoxia) increase in NO production measured as mean 4,5-diaminofluorescein-2/diacetate (DAF-2/DA) fluorescence intensity expressed as percentage of control. Diethylamine NONOate diethylammonium salt (DEA/NO; 100 μM) was used as positive control (see figure 2.7, page 122 for DEA/NO protocol). Sample size: $n = 5 - 33$ / group.

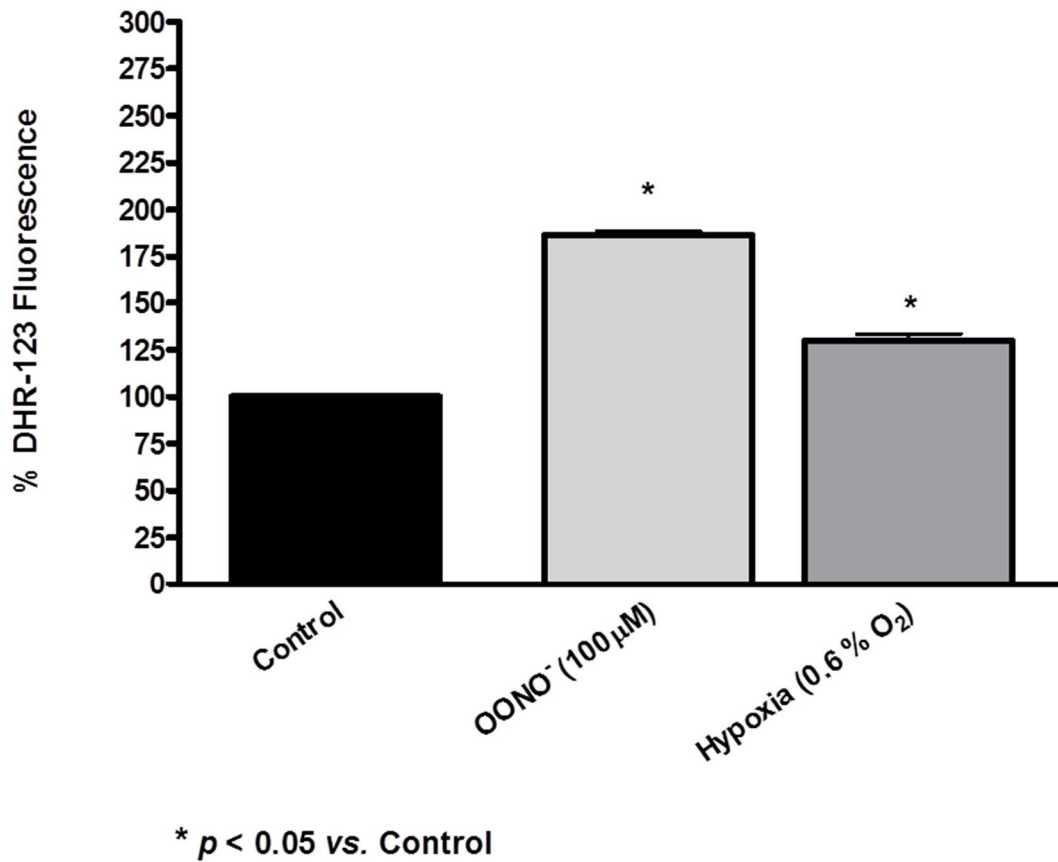


Figure 4.10: Hypoxia-induced cell injury (24 hours hypoxia) demonstrated by increased oxidative stress measured as % dihydrorhodamine-123 (DHR-123) mean fluorescence intensity of control. Authentic peroxynitrite (ONOO⁻) was used as positive control (see figure 2.11, page 128 for ONOO⁻ protocol). Sample size: $n = 4 - 11$ / group.

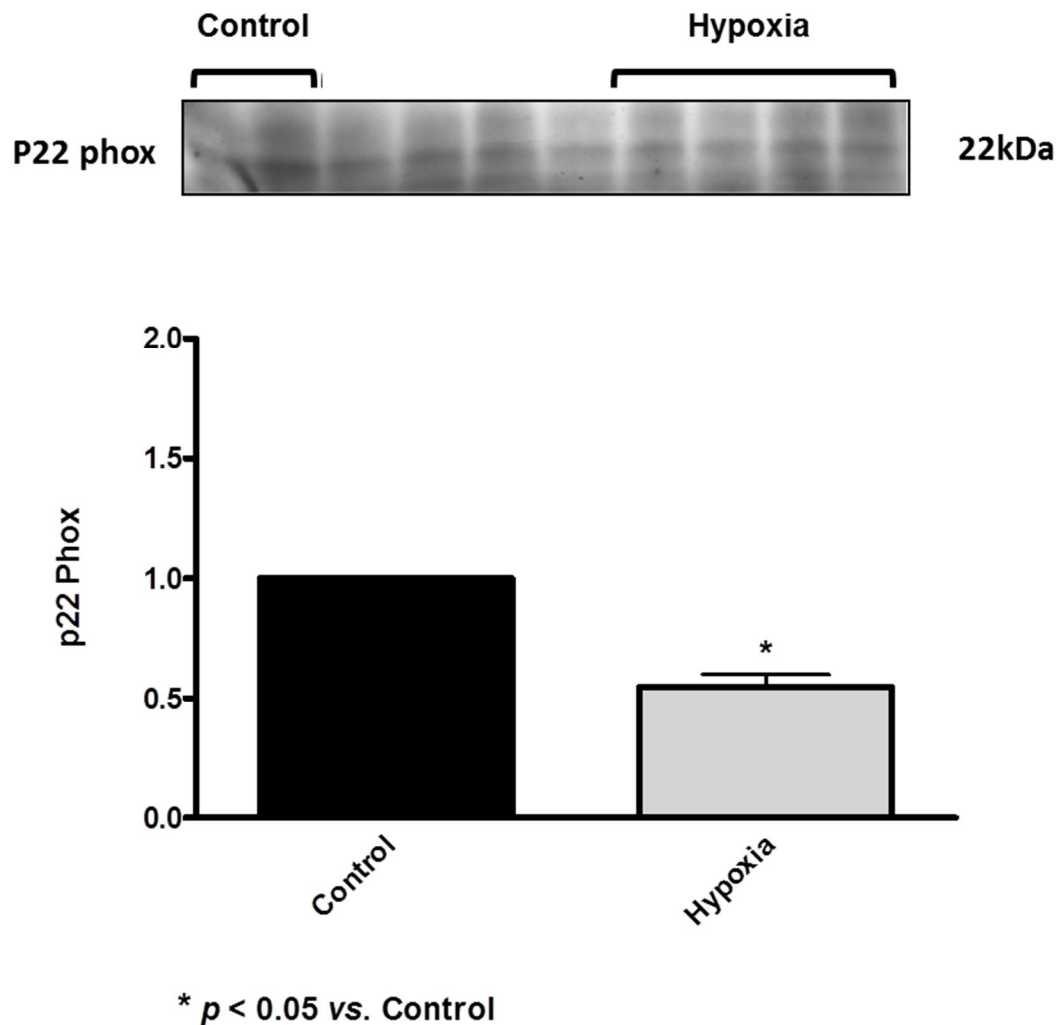


Figure 4.11: P22 phox expression in hypoxic CMECs. Representative western blot of CMECs exposed to 24h hypoxia shows a significant decrease in p22 phox expression compared to normoxic control. All data were expressed as a ratio of control with control adjusted to 1 (please refer to page 134, chapter 2). Sample size: n = 4 / group.

Note: due to unforeseen circumstances at the time of this set of western blot analysis, we were unable to perform β -tubulin expression; however, the original Bradford protein determinations were used as confirmation of equal protein content in each sample.

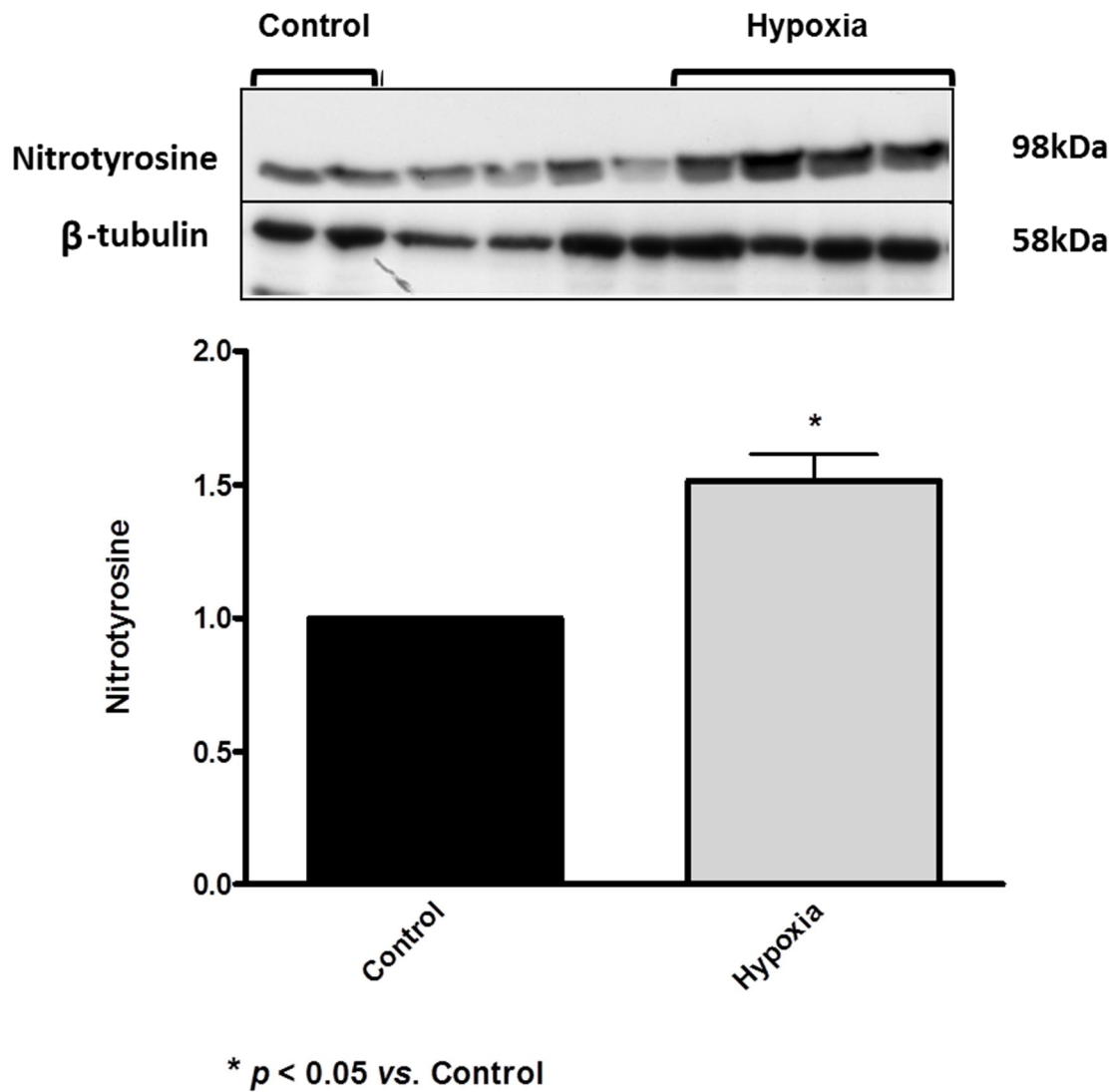


Figure 4.12: Nitrotyrosine expression in hypoxic CMECs. Representative western blot of CMECs exposed to 24h hypoxia shows a significant increase in nitrotyrosine expression compared to normoxic control. β -tubulin was used to validate equal protein loading. All data were expressed as a ratio of control with control adjusted to 1 (please refer to page 134, chapter 2). Sample size: $n = 4 - 6$ / group.

4.3.3 Proteomic analyses

Proteomic analysis by Maxquant software revealed that there were 67 proteins uniquely identified in hypoxic CMECs only (not detected in normoxic, control CMECs), and 10 significantly up regulated proteins (≥ 1.5 -fold) in hypoxic CMECs relative to normoxic control cells as per the predetermined minimum criteria for protein regulation (Table 4.1). Conversely, 2 proteins were identified in control CMECs only (no detection in hypoxic CMECs), and 9 proteins in the hypoxic CMECs were ≥ 1.5 -fold down regulated compared to normoxic control (Table 4.2). For a complete list of the differentially regulated proteins in hypoxia, please refer to supplementary data files that will be supplied electronically. Next, we submitted the list of the strongly represented proteins in hypoxic CMECs, i.e. proteins identified in hypoxia only samples ($n = 67$) plus proteins significantly upregulated by hypoxia ($n = 10$) to the DAVID functional annotation analysis tool. Figure 4.13 shows the highly enriched functional annotation clusters in hypoxic CMECs.

Table 4.1: List of hypoxia-induced up regulated proteins in CMECs (≥ 1.5 -fold).

Protein Name	Accession	Function*	Fold regulation	p-value
1. Alpha-enolase	P04764	Glycolytic enzyme; hypoxia tolerance	↑4.9-fold	0.01
2. Glyceraldehyde-3-phosphate dehydrogenase	P04797	Glycolytic enzyme; apoptosis	↑3.9-fold	0.03
3. Pyruvate kinase isozymes M1/M2	P11980	Glycolytic enzyme; interaction with hypoxia inducible factor (HIF1A) via EGLN3 under hypoxic conditions leads to hypoxia-induced promotion of transcription activity	↑3.4-fold	0.02
4. Moesin	O35763	Connects cytoskeleton to cell membrane; cell adhesion	↑2.9-fold	0.005
5. L-lactate dehydrogenase A chain	P04642	Conversion of pyruvate to lactate under low oxygen conditions	↑2.2-fold	0.0004
6. ATP synthase subunit alpha, mitochondrial	P15999	ATP synthesis	↑1.9-fold	0.04
7. Phosphoglycerate kinase 1	P16617	Glycolytic enzyme	↑1.8-fold	0.04
8. Elongation factor 2	P05197	Protein biosynthesis	↑1.7-fold	0.015
9. Transforming protein RhoA	P61589	Actin cytoskeleton organisation	↑1.6-fold	0.04
10. Eukaryotic initiation factor 4A-II	Q5RK11	Protein biosynthesis	↑1.6-fold	0.03

*All protein functions were obtained from the UniProt database (<http://www.uniprot.org/>).

Table 4.2: List of hypoxia-induced down regulated proteins in CMECs (≥ 1.5 -fold).

Protein Name	Accession	Function*	Fold regulation	p-value
1. Heterogeneous nuclear ribonucleoprotein M	Q62826	mRNA processing and splicing	↓9.6-fold	0.01
2. Superoxide dismutase [Cu-Zn]	P07632	Anti-oxidant	↓7.7-fold	0.003
3. D6.1A protein	O55158	Multi-pass membrane protein; mediator of protein glycosylation and signal transduction; inhibitory regulation of coagulation	↓5.7-fold	0.03
4. Granulins	P23785	Cytokine activity; possibly pro-inflammatory; cell growth and proliferation	↓5.1-fold	0.01
5. Aldose reductase	P07943	Oxidoreductase activity; NADPH-dependent reduction reactions	↓2.6-fold	0.03
6. Transketolase	P50137	Connects pentose-phosphate pathway with glycolysis; biosynthesis of NADPH	↓2.3-fold	0.04
7. Tropomyosin alpha-3 chain	Q63610	Actin cytoskeleton stabilization	↓2.3-fold	0.03
8. Macrophage-capping protein	Q6AYC4	Actin capping; controls actin-based motility	↓2.1-fold	0.04
9. Dihydropyrimidinase-related protein 2	P47942	Cytoskeleton organization	↓2-fold	0.04

*All protein functions were obtained from the UniProt database (<http://www.uniprot.org/>).

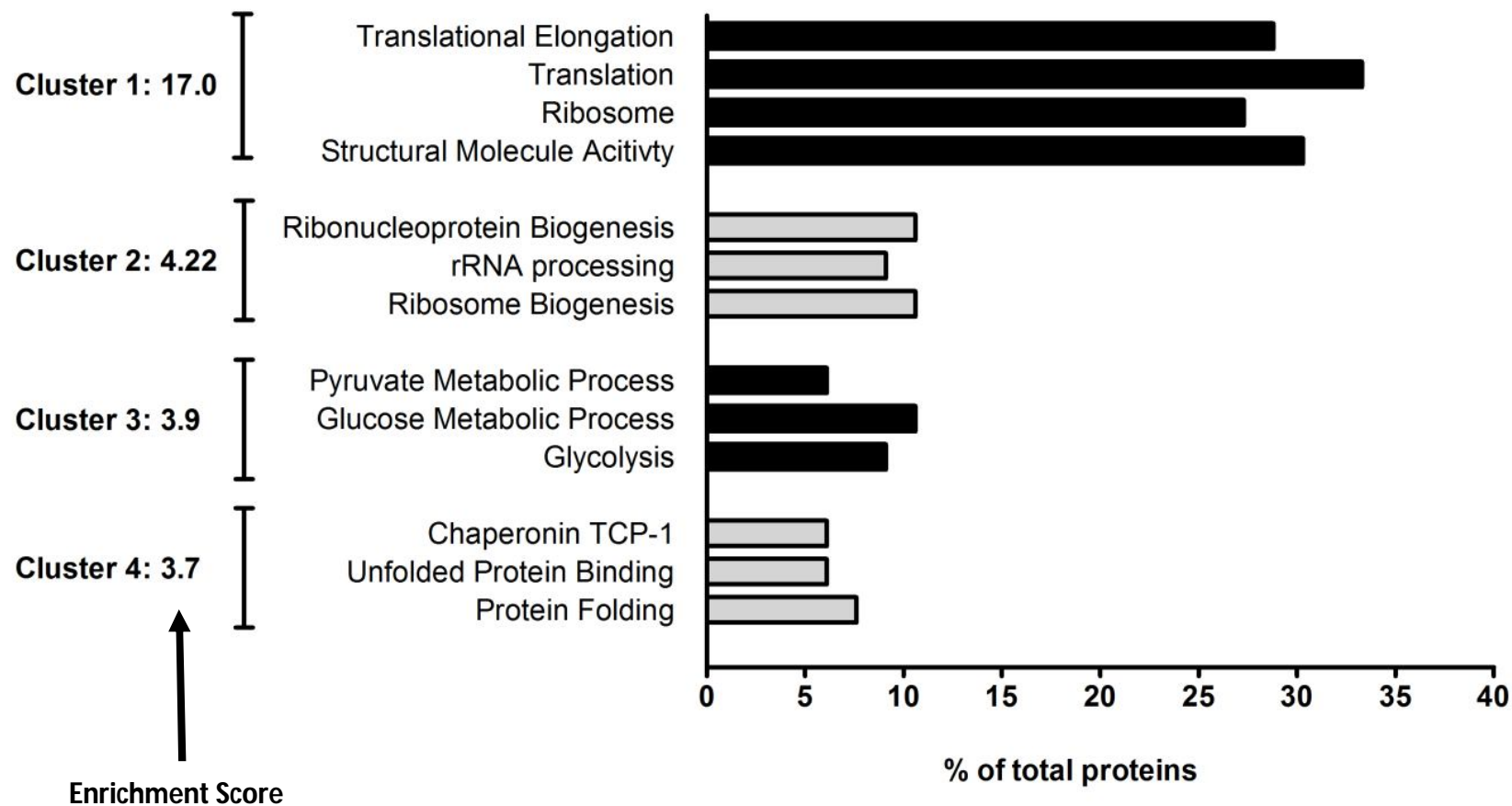


Figure 4.13: Functional annotation clusters of strongly represented proteins in hypoxic CMECs. Strongly represented proteins ($n = 77$) are defined as significantly upregulated proteins ($n = 10$) plus proteins identified in hypoxic CMECs only ($n = 67$). The top 4 most enriched annotation clusters associated with strongly represented proteins are shown with their respective enrichment scores and GO terms.

4.4 **Discussion**

In view of their unique location and direct exposure to circulating blood, endothelial cells are often subjected to conditions of low PO₂ (Graven KK and Farber, 1998), which could impair vascular homeostasis and, in the case of the cardiac microvasculature, impact on the viability and function of underlying cardiomyocytes.

In this chapter we aimed to investigate the response of the CMECs to 24 hours hypoxia, by lowering the O₂ concentration in the incubator to < 0.6 %. We decided not to manipulate the growth medium, e.g. lowering the FBS concentration, or adding factors that inhibit mitochondrial function. In this way, we ensured that the changes and responses observed were exclusively a result of the reduced atmospheric O₂ concentration.

4.4.1 **Validation of hypoxia-inducing protocol.**

Historically, cell death by hypoxia was believed to manifest as necrosis (Wolle *et al.*, 1995). However, other studies were also able to show the existence of hypoxia-induced apoptosis (Shostak *et al.*, 1997; Muschel *et al.*, 1995). Cell responses to hypoxia depend on the severity and the duration of the decreased oxygen availability but also on the cell type. A study by Hall JL *et al.* (2001), showed no significant change in the percentage of apoptotic nuclei at 6 or 18 hours in either calf pulmonary artery endothelial cells (CPAEs) or HUVECs, suggesting that the decrease in redox factor-1 (Ref-1) protein expression precedes the induction of apoptosis. This study also demonstrated that the transient up regulation of Ref-1 significantly inhibited hypoxia-mediated endothelial cell apoptosis (Hall JL *et al.*, 2001). However, after exposure to 24 hours of hypoxia, they showed an increase in apoptosis in both these cells types. The data obtained from the above studies support our own 24 hours hypoxia findings. The finding in our study that 6 hours of hypoxia seemed to be anti-apoptotic and anti-necrotic, was not surprising, as was also shown in one of the above studies, where Ref-1 was significantly upregulated after 6 hours of hypoxia and which subsequently led to the inhibition of apoptosis (Hall JL *et al.*, 2001). The reduction in apoptosis and necrosis observed at shorter periods of hypoxia may be due to an initial

protective / adaptive response by the endothelial cells. To place the relative resistance of the CMECs to hypoxia in context, we compared their apoptotic and necrotic responses to the same hypoxia protocol in another cardiac cell line, H9C2 myoblasts (see figures 4.5 & 4.6), and it was clear that the CMECs were more resistant. Indeed, endothelial cells are known to be quite resistant to hypoxic injury, as was shown in a study that subjected HUVECs to hypoxia, where apoptosis was only evident after prolonged hypoxic exposure (48 hours) (Graven KK and Farber, 1998). This phenomenon was also demonstrated in coronary endothelial cells where mitochondrial oxygen consumption only started to decrease when the PO₂ was < 3 mm Hg, and ATP levels remained constant at PO₂ levels as low as 0.1 mm Hg (Mertens *et al.*, 1990).

Numerous previous studies have found HIF-1 expression to be increased as a result of *in vitro* exposure of endothelial cells (Manalo *et al.*, 2005), cardiac endothelial cells (Sano *et al.*, 2007) and specifically CMECs (Li J *et al.*, 2011) to hypoxia. In our study, exposure of CMECs to 24 hours hypoxia also resulted in a significant increase (see figure 4.7) in the expression of HIF-1 α , compared to normoxic controls, thereby further validating our hypoxia-inducing protocol. It was suggested by many researchers that the mitochondria are a likely site of oxygen sensing, which results in downstream HIF-1 α induction. In a study by Guzy and Schumacker (2006) it was proposed that the electron transport chain acts as an O₂ sensor by releasing ROS in response to hypoxia. The ROS released during hypoxia acted as signalling agents that triggered diverse functional responses, including activation of gene expression through the stabilization of HIF-1 α .

The physiological implications of HIF-1 α up-regulation will be discussed in more detail in Section 4.4.3.

4.4.2 eNOS-NO biosynthesis, oxidative stress and nitrosative stress:

We showed that 24 hours hypoxia induced an up-regulation of eNOS, the most important NOS isoform in endothelial cells, accompanied by an increase in intracellular NO-production. The demonstration of increased eNOS expression could serve as an indication that the 24

hours hypoxia protocol induced activation of the PKB/Akt – eNOS – NO pathway in CMECs as previously shown by Strijdom *et al.* (2009b). Other endothelial cell-based studies also demonstrated increased production in NO in BAECs exposed to 24 hours of hypoxia (Min *et al.*, 2006). Hoffmann A *et al.* (2001), observed up-regulation of the eNOS gene in porcine aortic endothelial cells (PAEC) after exposing them to 6 – 24 hours of hypoxia. In a study in bovine aortic endothelial cells (BAECs) it was shown that the amount of eNOS mRNA increases to almost twice the basal levels after only 6 hours of hypoxia (Arnet *et al.*, 1996). In another study on cerebral endothelial cells, it was shown that hypoxia leads to an increase in the expression of iNOS, which subsequently produces high amounts of NO (Xu J *et al.*, 2000). Another study also showed an increase in eNOS protein (after 2 hours of hypoxia) in two porcine endothelial cell lines derived from different coronary artery vascular beds (Justice *et al.*, 2000). Conversely, a study performed on human aortic endothelial cells showed that 24 hours hypoxia resulted in a decrease in NO production (due to a down-regulation of eNOS) (Olszewska-Pazdrak *et al.*, 2009). However, overall, there seems to be general consensus in the literature that myocardial tissue responds to hypoxia by increasing eNOS-NO biosynthesis. In a review by Massion *et al.* (2003), it was stated that both myocardial eNOS and iNOS are up-regulated after exposure to hypoxia, and that eNOS is induced by both acute and chronic hypoxia exposure. This was confirmed in other review papers on the topic (Shah and MacCarthy, 2000; Kolář and Ošťádal, 2004). Our findings are therefore in line with reports in the literature, both with regards to myocardial tissue as a whole and with regards to vascular endothelium.

The development of oxidative stress in hypoxia is an important, if seemingly counterintuitive response observed in most cell types. One of the major sources of increased ROS production in hypoxic cells are the mitochondria, and it is now widely accepted that mitochondrial ROS generation during hypoxia may serve as a signalling system which eventually leads to the induction of HIF-1 (Guzy *et al.*, 2006). In vascular endothelial cells, NADPH-oxidase has traditionally been viewed as one of the major ROS generating systems; however, the role of endothelial mitochondrial ROS generation has recently become a focus of attention (Zhang M *et al.*, 2006). Endothelial mitochondria have been shown to respond to hypoxia by increased ROS production (Zhang M *et al.*, 2006; Pearlstein *et al.*, 2002), and our own data with the mitochondrial ROS-sensitive fluorophore, DHR-123, appear to confirm these

findings. There are also several reports in the literature of hypoxia-induced ROS increases that are not necessarily derived from mitochondria. In a study by Ali *et al.* (1999) performed on HUVECs, it was shown that ROS production was significantly increased after 24 hours of hypoxia, and another study, also found increased levels of mitochondrial ROS in CMECs, at 4 hours hypoxia (Liu Y *et al.*, 2011). Increased ROS generation can occur after only 10-30 minutes of hypoxia in both HUVECs and PAECs) (Shen Y *et al.*, 2013; Abdallah *et al.*, 2007). Studies where endothelial cells were exposed to longer periods of hypoxia also showed increased ROS. For instance, HUVECs exposed to 6 hours of hypoxia led to a significant increase in 2',7'- dichlorofluorescein (DCF) and dihydroethidium (DHE) fluorescence indicating increased ROS production (Pearlstein *et al.*, 2002). Exposing BAECs to 18 hours of hypoxia also increased ROS production significantly in these cells (Walford *et al.*, 2004).

In order to further explore the oxidative stress response of the CMECs to hypoxia, we measured the expression of p22 phox, which is a surrogate marker of NADPH-oxidase activity (Griendling KK *et al.*, 2000a). Interestingly, we found a significant down-regulation of p22 phox, which is suggestive of reduced NADPH-oxidase activation. This finding is contradictory to most other studies that found increased NADPH-oxidase activation after exposure to hypoxia. In a study performed on rats exposed to 17 days of hypoxia, an increase in p22 phox was found in Leydig cells isolated from the testes of rats exposed to hypoxia (Zhang GL *et al.*, 2013). Lastly, a study by Rathore *et al.* (2008) also showed an increase in p22 phox after hypoxia in pulmonary artery smooth muscle cells (PASMCs). It is not clear why the CMECs responded by reduced activation of NADPH-oxidase in our hands. It could possibly be a response unique to this endothelial cell type; furthermore, it could also be suggestive of a less important role for the NADPH-oxidase system as a source of ROS in our cells. Despite the significant increase in DHR-123 fluorescence, we could not show increased fluorescence when using the general intracellular O_2^- probe, dihydro-ethidium (DHE) (see figure 4.14), which further supports the p22 phox / NADPH-oxidase findings. It has to be borne in mind that our protocol took a snapshot view of intracellular responses at 24 hours. It is possible that this chosen time-point may have missed an earlier transient increase in O_2^- generation which was not detected by the DHE probe at 24 hours.

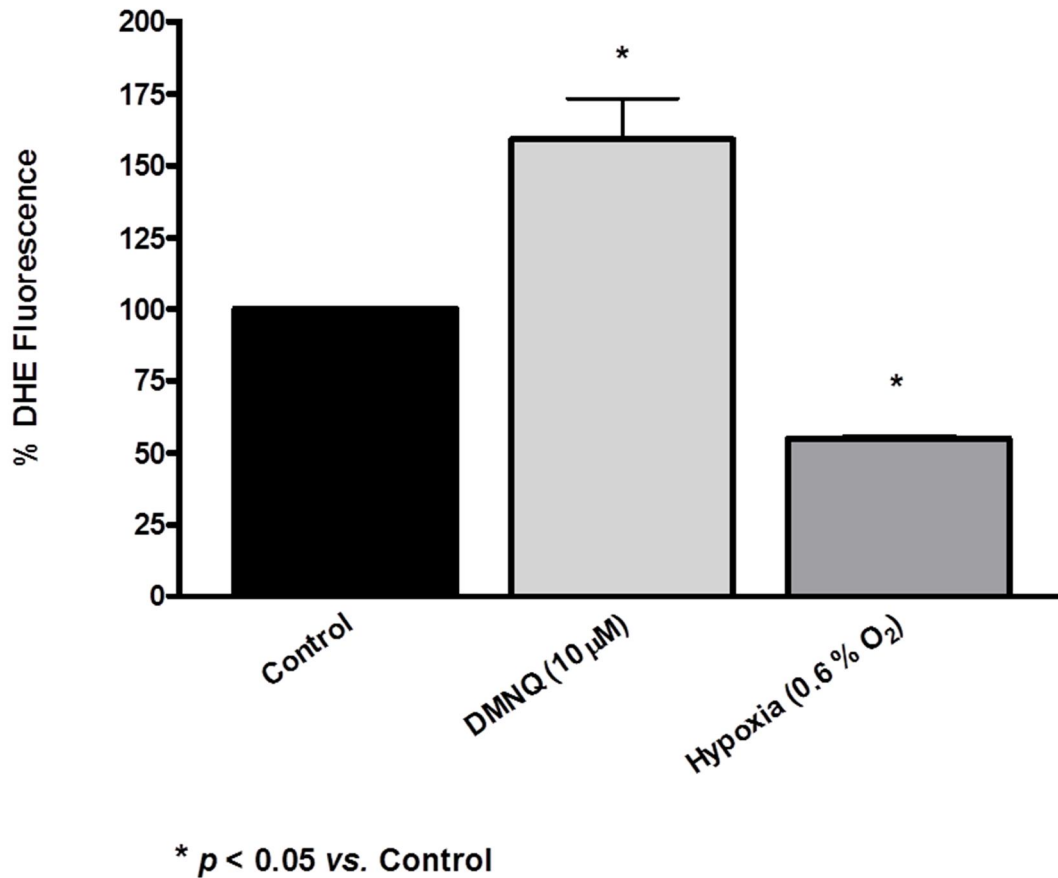


Figure 4.14: Hypoxia-induced cell injury (24 hours hypoxia) was not demonstrated by decreased oxidative stress measured as % dihydroethidium (DHE) mean fluorescence intensity of control. 2, 3-Dimethoxy-1,4-naphthoquinone (DMNQ, 100µM) was used as positive control. Please refer to figure 2.9 (page 126) for complete protocol. Sample size: n = 6 - 10 / group.

Finally, we investigated whether hypoxia would alter the nitrosative stress status in the cells. Nitrotyrosine, a known marker of nitrosative stress (Dalle-Donne *et al.*, 2005), was measured by western blotting, and our data showed a significant increase in nitrotyrosine levels, indicative of the development of nitrosative stress. This was also shown in a study on cerebral endothelial cells, where hypoxia led to an increase in the expression of nitrotyrosine (Xu J *et al.*, 2000). Demiryürek *et al.* (2000) also found increased levels of nitrotyrosine in sections from rat lungs subjected to hypoxia. Lastly, a study performed on 12-day-old rat pups, cerebral hypoxia–ischemia induced a transient increase nitrotyrosine (Van den Tweel *et al.*, 2005). From a thorough literature search, it appears that most studies demonstrating an increase in nitrotyrosine due to hypoxia, are performed on brain tissue, as elevated levels of nitrotyrosine after hypoxia in the brain is strongly associated with brain injury. As far as we are aware, this is the first study to show an increase in nitrosative stress in hypoxic CMECs.

4.4.3 Proteomics analysis

4.4.3.1 The CMEC proteome under hypoxic conditions: Up regulated and strongly represented proteins

A total of 10 up regulated proteins were identified in the hypoxic CMECs using strict criteria (fold- up regulation ≥ 1.5 and $p < 0.05$), half of which was glycolytic enzymes (alpha enolase, glyceraldehyde-3-phosphate dehydrogenase (GAPDH), pyruvate kinase, phosphoglycerate kinase and L-lactate dehydrogenase (LDH)) (Table 4.1). Our findings are similar to those of a 2-D gel proteomics-based study of brain microvascular endothelial cells exposed to 24h hypoxia, in which 10 glycolytic enzymes were up regulated, including all of those identified in the CMECs (Haseloff *et al.*, 2006). In another study, the coronary effluent collected from human hearts after 60 min global ischaemia was analyzed (Li J *et al.*, 2011), and several glycolytic proteins were shown to be up regulated, including LDH and GAPDH. GAPDH was one of the first glycolytic enzymes whose expression was shown to be up regulated by hypoxia in endothelial cells (Graven KK *et al.*, 1993); since then several other studies have reported hypoxia-induced up regulation of glycolytic enzymes (Haseloff *et al.*, 2006). The

gene promoters of many glycolytic enzymes, including alpha enolase and LDH, contain hypoxia response elements with binding sites for hypoxia inducible factor-1 (HIF-1) (Semenza GL *et al.*, 1996), which could lead to activation of gene transcription and explain the increased expression of these enzymes under hypoxic conditions. HIF-1 α stabilization in endothelial cells is known to happen at very low O₂ concentrations; in fact, a study on HUVECs showed that HIF-1 α expression only appeared at 0.5 % O₂ (Quintero *et al.*, 2006). Although the CMECs showed some low grade HIF-1 α expression at normal O₂ concentrations, western blotting analysis demonstrated significant increased expression in the hypoxic CMECs (Figure 4.7), which could help explain the up regulation of several glycolytic enzymes.

In addition to the 10 up regulated proteins, 67 unique proteins were detected in hypoxia samples, but not in normoxic control samples (please refer to electronic supporting data). Therefore, a total of 77 strongly represented hypoxia-induced proteins were identified, which were submitted to DAVID Bioinformatic Systems for functional annotation analyses. The top four most enriched annotation clusters, with which the strongly represented proteins associated, are shown in Figure 4.9. The up regulated expression of individual glycolytic enzymes discussed above is further underscored by the fact that the functional annotation cluster of glycolysis achieved the third highest enrichment in the hypoxic proteome (Cluster 3; enrichment score: 3.9). In addition, the GO term of glycolysis (GO term: 0006096) was particularly enriched (9.1 % protein count; p-value: 2.9 x 10⁻⁶; fold enrichment: 26), as was glucose metabolism (GO term: 0006006; 10.6% protein count; p-value: 2.5 x 10⁻⁴; fold enrichment: 7.8). As mentioned earlier, endothelial cells are primarily glycolysis-driven for their metabolic needs, so the high enrichment of glycolysis and related processes under the stress-inducing condition of low PO₂ comes as no surprise.

Rather unexpectedly, the mitochondrial proton-transporting ATP synthase complex (GO term: 0005753) was 27-fold enriched (4.5 % protein count; p-value: 0.005), and mitochondrial oxidative phosphorylation (GO term: 0006119) was 8.2-fold enriched (4.6 % protein count; p-value: 0.04) in the hypoxic CMEC proteome. Furthermore, both ATP synthase gamma chain and ATP synthase subunit b, mitochondrial were detected in hypoxic CMECs only (please refer to electronic supporting data). These findings suggest that the

hypoxic CMECs were to some degree responding by significant up regulation of proteins involved with mitochondrial oxidative phosphorylation and ATP generation. This is surprising for two reasons; first, mitochondria are not the primary energy source in endothelial cells regardless of the oxygen levels (Davidson and Duchon, 2007), and second, all metazoan cells respond to hypoxia by attenuating mitochondrial ATP-generation via oxidative phosphorylation (Semenza GL, 2011; Solaini *et al.*, 2010). Furthermore, there seems to be consensus in the literature that ATP synthase activity is inhibited in conditions of hypoxia; however, the exact regulation of ATP synthase in hypoxia remains to be elucidated (Solaini *et al.*, 2010).

The paradoxical and disproportionate overexpression of mitochondrial oxidative phosphorylation and ATP synthesis proteins may merely reflect a transient compensatory stress response by the mitochondria. However, it may also be the result of hypoxia-induced protein dysregulation, which, when regarded in conjunction with the increased mitochondrial ROS production, could suggest the development of mitochondrial dysfunction. It has to be borne in mind that the high enrichment of these proteins does not necessarily account for increased mitochondrial oxidative phosphorylation and ATP synthase activity. The mitochondrial protein regulation data observed in the hypoxic CMECs are intriguing, and warrant further investigations.

Overall, the 77 strongly represented proteins in hypoxic CMECs associated most significantly with the biological process cluster that includes translation, translation elongation, ribosomes and structural molecule activity (Cluster 1; enrichment score: 17; Figure 4.7). Furthermore, functional annotation analysis of the GO terms describing translation (GO:0006412; 33 % protein count; p-value: 6.4×10^{-16} ; fold enrichment: 10) and translation elongation (GO:0006414; 29 % protein count; p-value: 2.4×10^{-24} ; fold enrichment: 39) featured prominently in the hypoxic cells. Increased regulation of translation is an adaptive cellular response to hypoxia traditionally observed in solid tumours, which is to a large extent mediated by the family of HIF-1 transcription factors (Van den Beucken *et al.*, 2006). HIF-1 leads to the transcriptional activation of several genes involved with, among others, anaerobic glycolysis and angiogenesis (Van den Beucken *et al.*, 2006). Our data suggest that the hypoxic CMECs responded in a similar fashion, as observed by increased HIF-1 α and

glycolytic enzyme expression. Increased translation regulatory activity during hypoxia is, however, not exclusively a function of HIF-1 α (Van den Beucken *et al.*, 2006; Liu L and Simon, 2004). It has for example previously been reported that hypoxia increases the expression of the eukaryotic initiation factor eIF4E (eukaryotic translation initiation factor 4E) - binding protein (4E-BP) (Hidalgo *et al.*, 2012), and attenuates the activity of eukaryotic elongation factor-2 (eEF-2) (Liu L *et al.*, 2006), both of which result in reduced overall gene translation in the cell. Interestingly, our proteomic data showed a 1.7-fold up regulation of elongation factor-2 and 1.6-fold up regulation of eukaryotic initiation factor 4A-II (Table 4.1); in addition, elongation factor 1-gamma and eukaryotic translation initiation factor 5A-1 were detected in hypoxic CMECs only, with no detection in normoxic cells (please refer to electronic supporting data). It therefore appears as if the CMECs responded to hypoxia by a net increase in processes leading to protein biosynthesis, which seems to contradict previous reports in literature (Van den Beucken *et al.*, 2006; Liu L and Simon, 2004; Wouters *et al.*, 2005; Chen Z *et al.*, 2013).

Increased heat shock protein 90 (HSP 90) expression has been shown to be an important hypoxia-induced response in endothelial cells, both on mRNA level (Polotsky *et al.*, 2012), as well as protein level (Presley *et al.*, 2008). In the latter study (bovine aortic endothelial cells), hypoxia induced HSP 90 and eNOS expression, leading to increased HSP 90-eNOS binding and subsequent activation of eNOS. A protective response in the hypoxic cells is thus triggered via increased eNOS-derived NO production, which inhibits mitochondrial respiration and ultimately reduces cellular oxygen demand (Presley *et al.*, 2008). Our proteomic data, however, showed that HSP 90 expression was not up regulated in the hypoxic CMECs (Figure 4.15 A) and this observation was validated by subsequent Western blotting of HSP 90 (0.95 ± 0.02 vs. 1.00 control: $p < 0.05$) (See figure 4.15 B). Despite the absence of HSP 90 up regulation, we have previously shown that 24h hypoxia induced activation of the PKB/Akt – eNOS – NO pathway in CMECs (Strijdom *et al.*, 2009b), and in the current study, eNOS was significantly up regulated in hypoxic cells, which was accompanied by increased NO levels (see figure 4.6). It therefore seems that the hypoxic CMECs are able to increase eNOS-derived NO biosynthesis via a mechanism that apparently does not require HSP 90 induction.

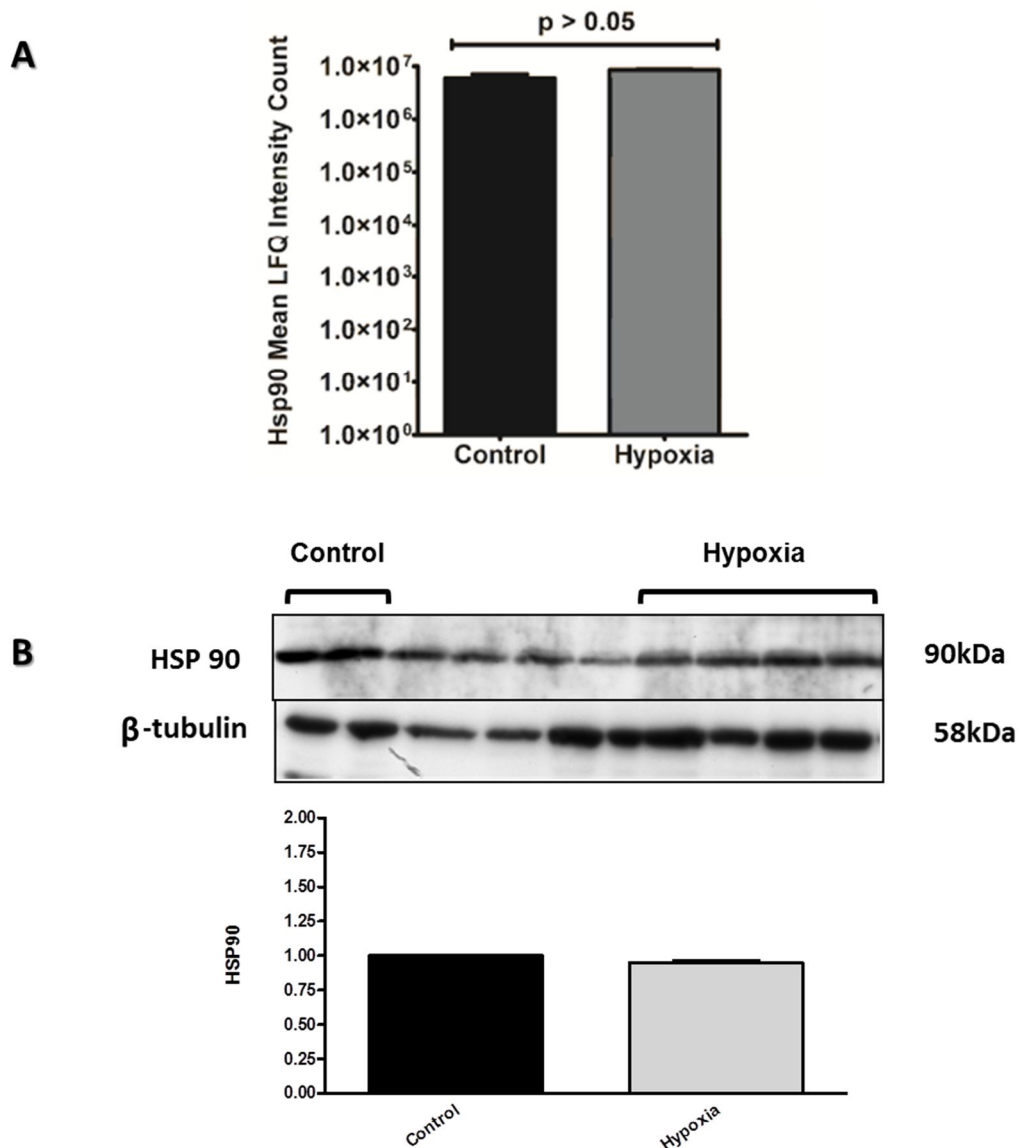


Figure 4.15: A: Proteomic analysis with the Maxquant software package revealed that hypoxia had no significant effect on the mean LFT intensity count of heatshock protein-90 (HSP 90) beta (Accession No: P34058), which was independently validated by Western blot analysis of HSP 90 α/β expression (see figure 4.15B below). Sample size: n = 3 / group.

B: Total HSP 90 expression in hypoxic CMECs. Representative western blot of CMECs exposed to 24 hours hypoxia shows no change in HSP90 expression compared to normoxic control. β -tubulin was used to validate equal protein loading. All data were expressed as a ratio of control with control adjusted to 1 (please refer to page 134, chapter 2). Sample size: n = 4 / group.

4.4.3.2 The CMEC proteome under hypoxic conditions: Down regulated proteins

An outstanding feature of the down regulated proteins (Table 4.2) was the manner in which the hypoxic CMECs responded with regard to anti-oxidant systems. Superoxide dismutase [Cu-Zn] (SOD 1) was the second most significantly down regulated protein in the hypoxic CMECs. Hypoxia-induced SOD 1 suppression has previously been shown by proteomic analysis of hypoxic rat renal tissue (Son *et al.*, 2008), and in hearts of rats subjected to chronic hypoxia (Zhou W *et al.*, 2012). In addition, aldose reductase and transketolase, both associated with NADPH function and biosynthesis, were also down regulated in our cells. NADPH is regarded as a critical regulator of cellular antioxidant systems, including the glutathione system, catalase and SOD (Stanton, 2012; Santos *et al.*, 2011). Interestingly, a proteomics-based study on hypoxic brain capillary endothelial cells found a 15-fold up regulation of the spot intensity of transketolase (Haseloff *et al.*, 2006), which is in contrast to our own data (2.3-fold down regulation; Table 4.2); The profound up regulation of transketolase in the brain capillary endothelial study was, however, not matched by increased activity of the enzyme (Stempien-Otero *et al.*, 1999). In addition to the down regulation of major anti-oxidant systems in our cells, we observed increased mitochondrial ROS production (Figure 4.5). On the other hand, separate experiments conducted on hypoxic CMECs showed a significant down regulation of p22-phox (0.55 ± 0.05 vs. 1.00 control: $p < 0.05$) (an indicator of NADPH-oxidase activity; see Figure 4.11), pointing to possible reduced NADPH-oxidase-derived ROS production. In summary, our data suggests that the hypoxic CMECs responded in an apparent contrasting fashion with regard to redox regulation; however, on the balance there seemed to be a net drive towards the development of oxidative stress, mainly as a result of reduced anti-oxidant systems such as SOD 1 and increased mitochondrial ROS levels.

Three of the nine significantly down regulated proteins observed in the hypoxic CMECs (tropomyosin, macrophage capping-protein and dihydropyrimidinase-related protein) are known to have regulatory effects on cytoskeleton organization and stabilization (Table 4.2), which could possibly suggest a disruption of the actin cytoskeleton and by extension, indicate early signs of barrier dysfunction (Dudek and Garcia, 2001). On the other hand, the cytoskeletal proteins, catenin-delta (involved with adherens junction organisation and cell

adhesion), and capping protein (actin filament) muscle Z-line, beta (involved with actin cytoskeleton organisation) were strongly represented in hypoxic cells with no detection in normoxic cells (please refer to electronic supporting data). It therefore seems that the response of the hypoxic CMECs was variable in this regard, similar to observations made in a study on hypoxic brain capillary endothelial cells in which 7 cytoskeletal proteins were differentially regulated, with 3 up regulated and 4 down regulated respectively (Stempien-Otero *et al.*, 1999). Another family of cytoskeletal proteins, the β -tubulins, has previously been shown to be regulated by hypoxia (Saussede-Aim and Dumontet, 2009; Raspaglio *et al.*, 2008); however, our proteomic data showed that the expression of β -tubulin remained unchanged, which was subsequently validated by western blotting (Figure 4.16A & B).

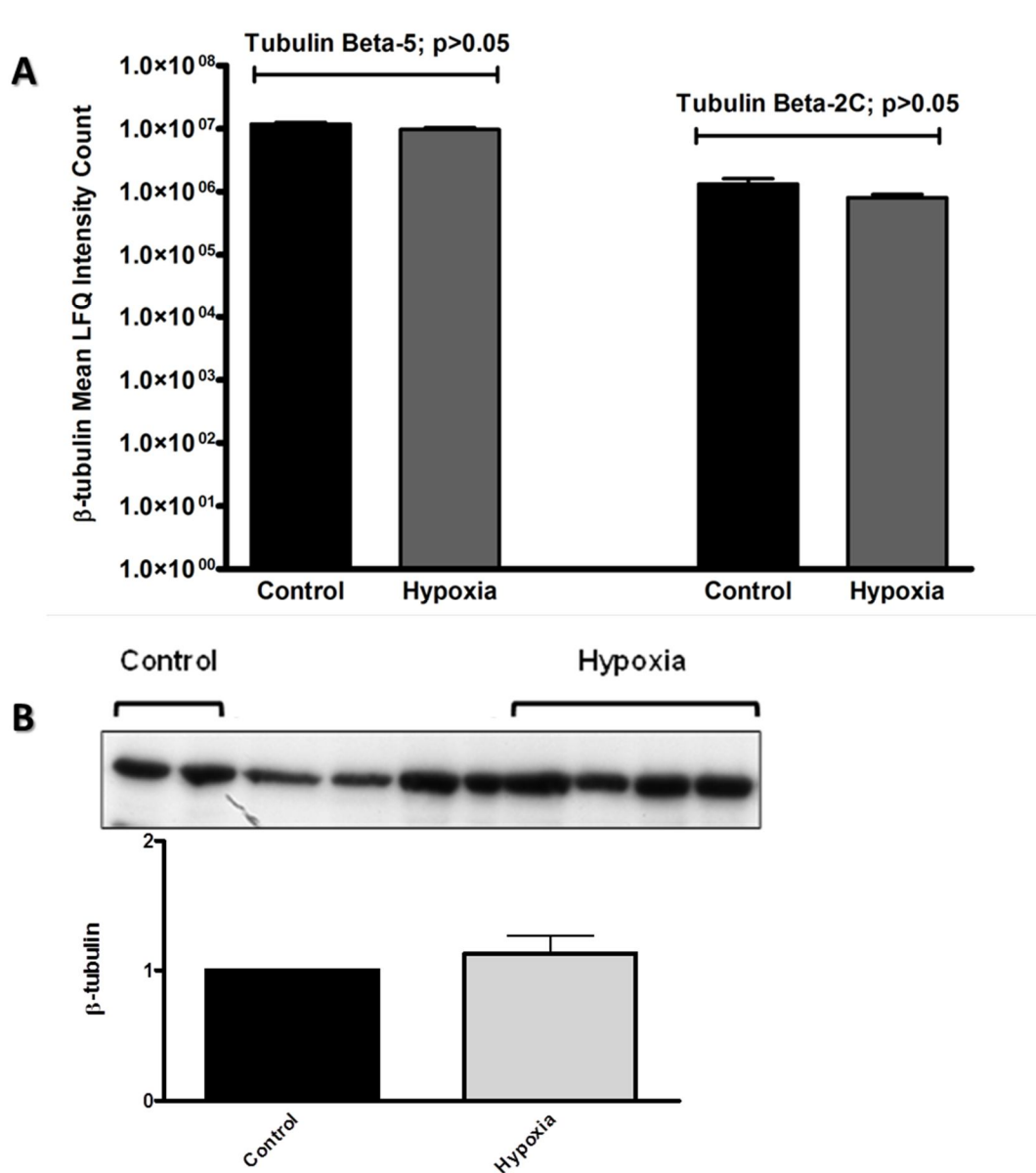


Figure 4.16: A: Maxquant analysis showed no significant changes in the mean LFT intensity count of either tubulin beta-5 (Accession No: P69897) or tubulin beta-2C (Accession No: Q6P9T8) in hypoxic CMECs, which was independently validated by Western blot analysis of HSP 90 α/β expression (see figure 4.16 (B) below). Sample size: $n = 3$ / group.

B: Total β -tubulin expression in hypoxic CMECs. Representative western blot of CMECs exposed to 24 hours hypoxia shows no change in β -tubulin expression compared to normoxic control. All data were expressed as a ratio of control with control adjusted to 1 (please refer to page 134, chapter 2). Sample size: $n = 4$ / group.

4.5 **Conclusion**

In conclusion, the findings of this chapter are novel in that no previous studies have characterised the hypoxic response in CMECs in an equally comprehensive manner. We approached the studies in this chapter by making use of various endpoints, protocols and techniques. A combination of cutting edge technology was applied, from fluorophore-FACS analysis assays to an extensive proteomic analysis. We investigated intracellular events, (including the measurement of nitric oxide and ROS), important endothelial signalling proteins and large-scale differential protein regulation. The following findings are in our view of particular interest:

- Validation of cellular hypoxia by demonstrating increased HIF-1 α expression (regarded by many as the most sensitive marker of cellular hypoxia), necrosis and apoptosis. This was achieved, despite what many would regard as a “mild” hypoxic insult (i.e. no manipulation of the growth medium composition to artificially enhance the injurious effects); hence, the cellular responses are exclusively due to the lowering of atmospheric O₂ concentrations. When the injury observed in the CMECs was contextualised by subjecting a different cardiac-derived cell line (H9C2 myoblasts) to the same hypoxia protocol, it was interesting to note that the CMECs were relatively more resistant to the injury-inducing effects of the hypoxic insult. These observations confirm the widely held notion that vascular endothelial cells are often notoriously resistant to hypoxia, which makes sense from a physiological point of view, since these cells form the inner lining of blood vessels where they are often exposed to low oxygen tension, particularly in the capillary networks of the body.
- Demonstration of an up-regulation of the eNOS-NO biosynthesis pathway. This finding is in agreement with various previous studies, not only in other vascular endothelial cell types, but also in the myocardium at large. These results furthermore confirm previous studies from our own laboratory on the same cell type, which showed a major role for the PKB/Akt-eNOS pathway. The eNOS-NO data appear to suggest that the CMECs were not yet switching to a dysfunctional state, at least not at the 24 hour time-point. In separate experiments (data not shown), it was

interesting to observe that the increased trends were still present at 48 hours hypoxia.

- Oxidative stress: The various endpoints used to assess the overall oxidative stress status of the hypoxic CMECs revealed an interesting, if conflicting picture. On the one hand, DHR-123 fluorescence indicated increased ROS production, probably derived from the mitochondria (although the DHR-123 probe has also been shown to have some sensitivity for peroxynitrite species). This was accompanied by a concomitant reduction in important anti-oxidant systems in the cells, most notably an almost 8-fold downregulation of SOD1. On the other hand, NADPH-oxidase activity as measured by p22 phox expression was significantly reduced, accompanied by decreased O_2^- levels as measured by the DHE probe. And finally, we demonstrated a clear increase in cellular nitrosative stress by observing elevated levels of nitrotyrosine. Clearly, the cells' overall oxidative stress status was quite fluid at 24 hours of hypoxia. On the whole, however, it is our belief that a pro-oxidative and pro-nitrosative stress scenario had developed at 24 hours, as is evident by the large down-regulation of SOD-1, accompanied by increases in DHR-123 fluorescence and nitrotyrosine expression.
- The response of mitochondrial protein regulation as demonstrated by our proteomic analysis was intriguing. Particularly the up-regulation of proteins involved with oxidative phosphorylation and mitochondrial ATP synthase are seemingly counterintuitive, as hypoxia is generally accepted to down-regulate aerobic energy metabolic processes. However, despite the novelty of these findings, it must be borne in mind that up-regulation of protein expression does not necessarily signify increased functional activity. In the absence of functional data, it can be speculated that there was at least some early signs of dysregulation of these mitochondrial proteins at play, at least at the 24 hour snapshot view.
- The significant enrichment of glycolysis and up-regulation of several glycolytic enzymes as shown in the proteomic data came as no surprise, and served to confirm that the CMECs behave in a similar fashion to most other eukaryotic cells when facing a hypoxic insult. Despite the fact that these data were not surprising, it does not reduce the significance and novelty of these findings as ours is the first study to demonstrate this phenomenon in CMECs.

- The significant enrichment of translational processes such as elongation and initiation are interesting and somewhat contradictory to studies on other cell types in the literature, which usually describe an overall down-regulation of protein biosynthetic processes during hypoxia. It is not clear why our cells responded in this fashion, and the absence of any previous similar studies on CMECs further complicates our ability to place our findings in perspective. We therefore speculate that this phenomenon could merely be a transient observation at the 24 hour time-point, or it could indeed be a response unique to our endothelial cell type. The effect of HIF-1 α stabilisation and resulting increased transcriptional activity of HIF- α target genes could also be a contributing factor in this regard.

Note: *Some parts of this chapter were submitted to the International Journal of Proteomics for publication in September 2013. The manuscript was under review at the time of submitting this dissertation.*

Below is a cartoon summarising the most significant cellular responses observed in the hypoxic CMECs:

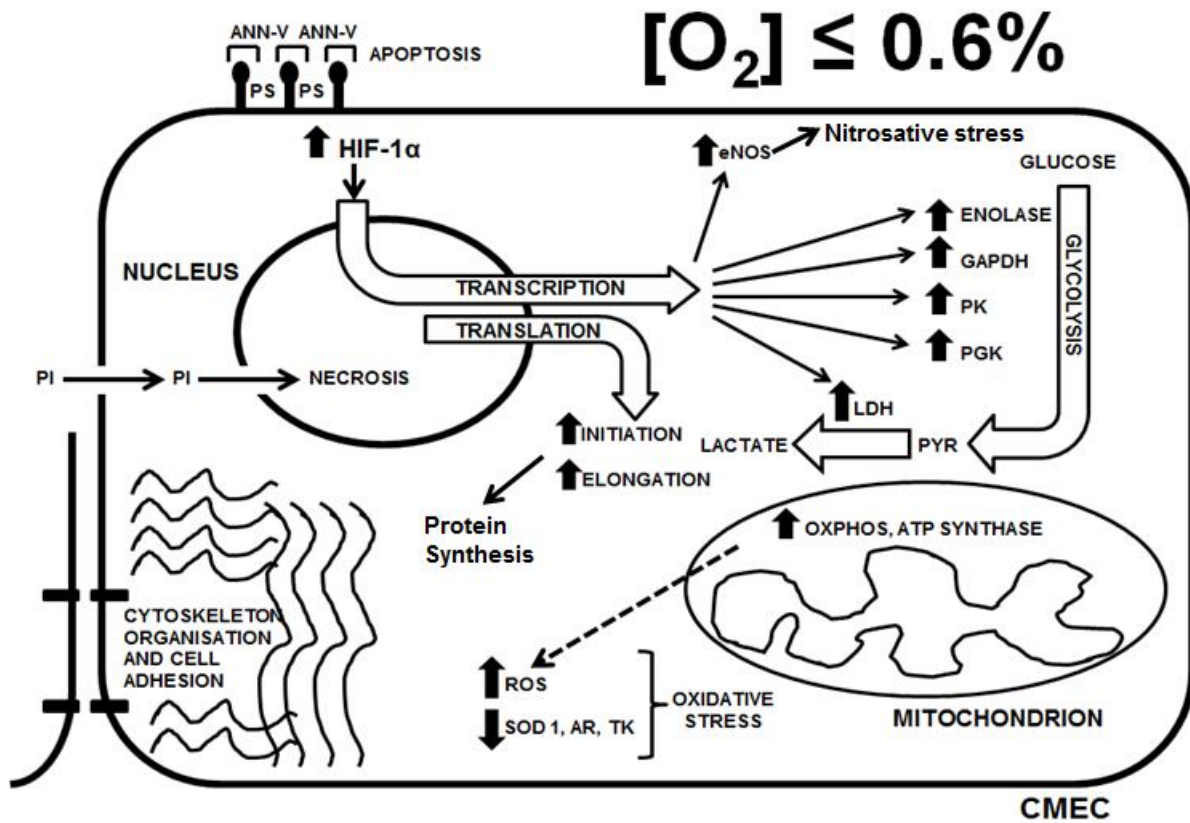


Figure 4.17: A cartoon depicting the major findings in the hypoxic CMECs.

CHAPTER FIVE

TNF- α -induced responses in CMECs: Baseline investigations

5.1 Introduction

TNF- α has been shown to induce a wide range of intracellular mechanisms and effects in the vascular endothelium, which seem to be strongly dose- and time-dependent (please refer to table 1.3, page 51, chapter 1). One of the most prominent and biologically important pathways in endothelial cells is the eNOS-NO biosynthesis pathway. This pathway captures the essence of vascular endothelial function, namely to maintain and regulate the dilatory state of the vasculature and thereby securing effective perfusion to the body. The eNOS-derived generation of NO is physiologically very closely related to the intracellular levels of ROS, and a fine balance exists between the generation of NO (and activity of eNOS) on the one hand, and the generation of ROS on the other. It should therefore come as no surprise that one of the primary objectives of this study was to comprehensively investigate the eNOS-NO biosynthesis pathway and the relative oxidative stress status of our endothelial cells when exposed to TNF- α administration. In this chapter, we will provide data obtained from several experiments in which we attempted to systematically evoke responses from our cells under different conditions.

5.1.1 TNF- α induces a down-regulation of NOS-NO biosynthesis

Evidence from the literature suggests that TNF- α can impair endothelium-dependent and NO-mediated vasodilation in various vascular beds, e.g. mouse coronary arterioles (Gao *et al.*, 2007), rat coronary arterioles (Picchi *et al.*, 2006) and bovine small coronary arteries (Ahmad *et al.*, 2002). Picchi *et al.* (2006) demonstrated that endothelial dysfunction in pre-diabetic metabolic syndrome is both a result of the effects of TNF- α and subsequent production of O₂⁻. Gao *et al.* (2007) showed that AGE (advanced glycation end-product)/RAGE (receptor for AGEs) and nuclear factor κ B (NF- κ B) signalling play a pivotal

role in elevating circulating and/or local vascular TNF- α production. The increased TNF- α expression induces the production of ROS, leading to endothelial dysfunction in Type 2 diabetes. Endothelial dysfunction associated with TNF- α in pathophysiological conditions are linked to excess production of ROS and a decrease in NO bioavailability (Zhang W *et al.*, 2009).

TNF- α appears to decrease the bioavailability of NO by (i) diminishing the production of NO (Goodwin BL *et al.*, 2007; Picchi *et al.*, 2006; Ahmad *et al.*, 2002; Greenberg *et al.*, 1993), and (ii) enhancing the removal of NO (Gao *et al.*, 2007). Picchi *et al.* (2006) reported that the real-time production of NO in isolated coronary arteries from ZOF rats (Zucker Obese Fatty rats; a model of pre-diabetic metabolic syndrome) and ACh (acetylcholine)-induced NO production were significantly lower in ZOF rats compared with the lean control rats. These findings suggested that higher concentrations of circulating and protein expression of TNF- α diminished NO bioavailability in ZOF rat coronary arteries via the decreased expression of eNOS. Many studies have shown that the direct effects of TNF- α on eNOS are via down-regulating eNOS expression and diminishing NO production in diverse vasculatures (Goodwin BL *et al.*, 2007; De Palma *et al.*, 2006; Picchi *et al.*, 2006; Gao *et al.*, 2007). In addition to eNOS, other factors are also involved in regulating NO production, and one of those factors is a functional citrulline/NO cycle (Xie *et al.*, 2000; Hattori *et al.*, 1994; Husson *et al.*, 2003). The citrulline/NO cycle is regulated by ASS (argininosuccinate synthase). NO is synthesized from the conversion of L-arginine into L-citrulline mediated by eNOS, and ASS catalyses the rate-limiting step in the arginine regeneration through the citrulline/NO cycle and appears to be co-ordinately regulated with eNOS activity (Oyadomari *et al.*, 2001). Goodwin BL *et al.* (2007) showed that TNF- α diminished the mRNA and protein expression of ASS in aortic ECs and directly resulted in the reduced production of NO. Gao *et al.*, 2007 and Picchi *et al.*, 2006) reported that TNF- α impaired NO-mediated vasodilation in Type 2 diabetic coronary arterioles by stimulating the endothelial generation of ROS via activation of NADPH oxidase. When a neutralizing antibody to TNF- α was administered, the formation of ROS (O_2^- , $ONOO^-$ and H_2O_2) was decreased and NO-mediated vasodilation improved.

5.1.2 TNF- α induces an up-regulation of NOS-NO biosynthesis

Contrary to the above studies, others have demonstrated opposite effects of TNF- α on the NOS-NO pathway. Several mechanisms have been suggested for the induction/activation of NOS by TNF- α . Yoshizumi *et al.* (1993) demonstrated that TNF- α markedly reduced mRNA levels of eNOS in HUVECs in a dose- and time-dependent manner without changing the rate of eNOS gene transcription. TNF- α appeared to decrease eNOS mRNA levels by increasing the rate of mRNA degradation. Another study, however, suggested that TNF- α increases eNOS activity in HUVECs (De Palma *et al.*, 2006). Activation of eNOS by TNF- α requires activation of PKB/Akt (protein kinase B), a known eNOS activator, via Sph1P (sphingosine-1-phosphate) receptor activation. Sph1P receptor is activated by Sph1P, a sphingolipid involved in proliferation, survival, migration and differentiation of these cells, generated through N-SMase2 (neutral sphingomyelinase 2) and SK1 (sphingosine kinase 1) activation (De Palma *et al.*, 2006).

TNF- α mediated activation of eNOS is accompanied by increased NO generation, which exerts protective effects on DC (dendritic cell) adhesion to endothelium induced by TNF- α itself. It has also been suggested that TNF- α may increase iNOS expression by activating NF- κ B (Zhong L *et al.*, 1999). TNF- α -induced iNOS mRNA expression in microvascular ECs could be decreased by rooperol (a dicatechol from the South African plant *Hypoxis rooperi*) administration, which is an anti-inflammatory agent in the treatment of several inflammatory disorders (Bereta *et al.*, 1997). In HUVECs, the effect of TNF- α on iNOS expression was not affected by statin treatment, whereas reduced eNOS expression was reversed by rosuvastatin and ceruvastatin by inhibiting HMG-CoA (3-hydroxy-3-methylglutaryl-CoA) reductase and subsequent blocking of isoprenoid synthesis (Jantzen *et al.*, 2007).

From the above literature review, it is quite clear that the effects of TNF- α are indeed time-, dose- and even cell type-dependent. It is also interesting to note that the responses can in fact be in direct opposition to each other (down-regulation of eNOS-NO vs. up-regulation of eNOS-NO). Please refer to table 1.3 in chapter 1 (page 51) for a summary of TNF- α treatment studies performed at various time points, concentrations, endothelial cell types and endpoints measured, which further confirms the above statement.

5.2 **Specific Aims**

For the purposes of this chapter, our approach was based on three essential research questions:

- What is the effect of the TNF- α concentration administered to the CMECs?
- What is the effect of short term TNF- α incubation time on the CMEC responses?
- What is the effect of modifying the serum content of the growth medium on the CMEC responses to TNF- α treatment?

5.3 **Methods**

5.3.1 **The effects of different TNF- α concentrations.**

CMECs were cultured and grown as described in chapter two (page 111). CMECs were treated with 3 different concentrations of TNF- α (0.5 ng /ml, 5 ng /ml and 20 ng / ml) for 24 hours (see figure 5.1 for the protocol). The respective TNF- α concentrations and periods of treatment were selected based on an extensive literature research performed on previous *in vitro* endothelial cell studies (please refer to table 1.3, page 51). It was our intention to choose three different concentrations, ranging from low to high. After each of these respective treatments, cells were stained with: (i) propidium iodide (PI) (no analysis for 0.5 ng / ml at 48 hours); (ii) Annexin V (as described on page 118 in chapter 2) (no analysis for 0.5 ng / ml at 48 hours) to measure cell viability; (iii) DAF-2/DA (as described on page 121, chapter 2) to measure NO; (iv) dihydroethium (DHE), 2', 7'-dichlorofluorescein (DCF) (as described on page 124, chapter 2) to measure oxidative stress; and (v) dihydrorhodamine-1, 2, 3 (DHR-123) (as described on page 124, chapter 2) to measure oxidative and nitrosative stress by means of flow cytometric analysis. Positive controls were incorporated for NO (as described on page 121, chapter 2) and oxidative stress measurements (as described on page 124, chapter 2) (refer to figure 5.1 for complete protocol). The mean fluorescence intensity (expressed as % of control) of each of the above fluorescent probes was compared with that

of the TNF- α treated samples to determine the effect of TNF- α at different concentrations (24 hours treatment).

In a separate series, cells were either treated with 0.5 ng / ml, 5 ng / ml and 20 ng /ml TNF- α for 24 hours or with 5 ng / ml TNF- α for 24 and 48 hours and subsequently prepared for western blot analysis (as described on page 132 – 134 in chapter two, see figures 2.15 & 2.16) (see figure 5.1 for treatment protocol). The expression and activation of the following proteins were investigated (please refer to chapter 2, page 132 for the concentration and exposure time of each protein):

NOS Signalling: Total and phosphorylated eNOS and PKB / Akt, and total HSP 90 and caveolin-1 were measured to investigate NOS signalling mechanisms.

Oxidative Stress: The membrane bound NADPH oxidase subunit, p22-phox, was used to measure nicotinamide adenine dinucleotide phosphate (NADPH) oxidase activity as previously described (Griendling KK *et al.*, 2000a).

Nitrosative Stress: The ability of the highly reactive NO-derived radical, ONOO- (peroxynitrite) to nitrosylate tyrosine residues of cellular proteins and form nitrotyrosine, is an indication of nitrosative stress (Dalle-Donne *et al.*, 2005). Nitrotyrosine expression was therefore measured as a marker of nitrosative stress.

NF- κ B signalling: Activation of the NF- κ B pathway is usually an indication of a pro-inflammatory response (Ben-Neriah and Karin, 2011), and a prominent intracellular pathway known to be induced by TNF- α . Upon activation of this pathway, IK β dislodges from the NF- κ B complex and undergoes proteasomal degradation; therefore, a reduction in IK β protein levels is a marker of NF- κ B activation (Hoffmann A *et al.*, 2002). IK β protein expression was therefore measured to investigate activity of the NFK β pathway.

Equal protein loading validation: β -tubulin expression was measured to confirm equal protein loading in all samples.

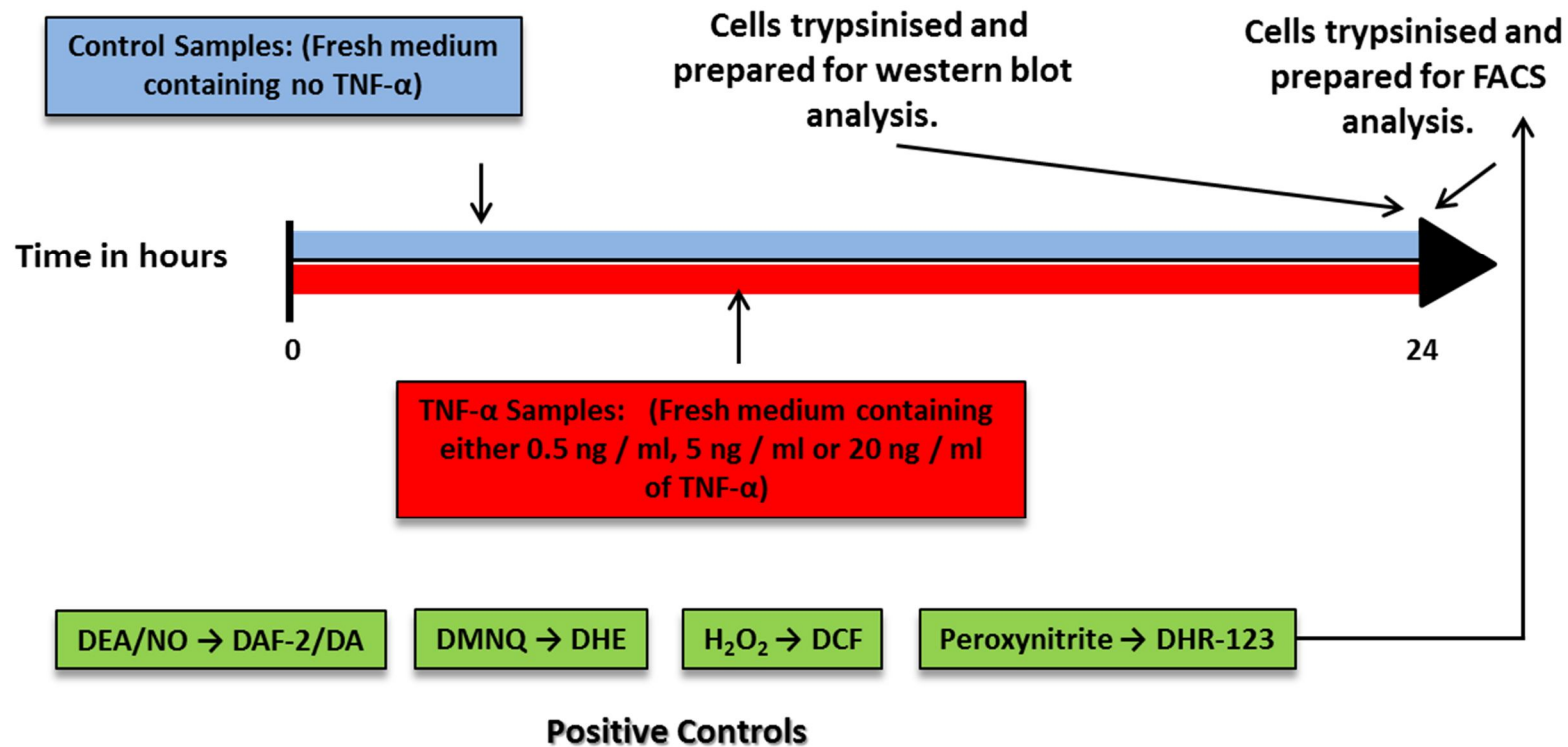


Figure 5.1: Protocol for treatment of CMECs with 0.5 ng / ml, 5 ng / ml or 20 ng / ml (24 hours) for subsequent FACS and western blot analyses.

5.3.2 Short term treatment of CMECs with TNF- α (20 ng / ml) for 30 minutes.

In order to assess whether the measurements at the end of the standard 24 hour TNF- α treatment protocol might have failed to detect important intracellular responses at early time-points, we conducted a separate series of experiments in which the CMECs were treated with TNF- α for 30 minutes. From the literature, it is apparent that many authors evaluated TNF- α -effects at early time points, such as 10 minutes (Kim HJ *et al.*, 2006a), 30 minutes (Li C *et al.*, 2002, 2005; Bove *et al.* 2001) and 1 hour (De Palma *et al.*, 2006; Corda *et al.*, 2001). CMECs were cultured and grown as described in chapter two (page 111) and treated with TNF- α (20 ng / ml) for 30 minutes (see figure 5.3 for the protocol). In order to contextualise the TNF- α data, we included experiments in which CMECs were treated with another known harmful stimulus, ox-LDL (40 μ M) for 30 minutes. After each of these respective treatments, cells were removed from culture by trypsinisation and subsequently treated with DAF-2/DA to measure NO, and DHE, DCF and DHR-123 to measure oxidative/nitrosative stress by means of flow cytometric analysis. Positive controls were used for NO (as described on page 121, chapter 2) and oxidative stress measurements (as described on page 124, chapter 2) (refer to figure 5.2 for complete protocol). The mean fluorescence intensity (expressed as % of control) was determined for each of the fluorescent probes as previously described.

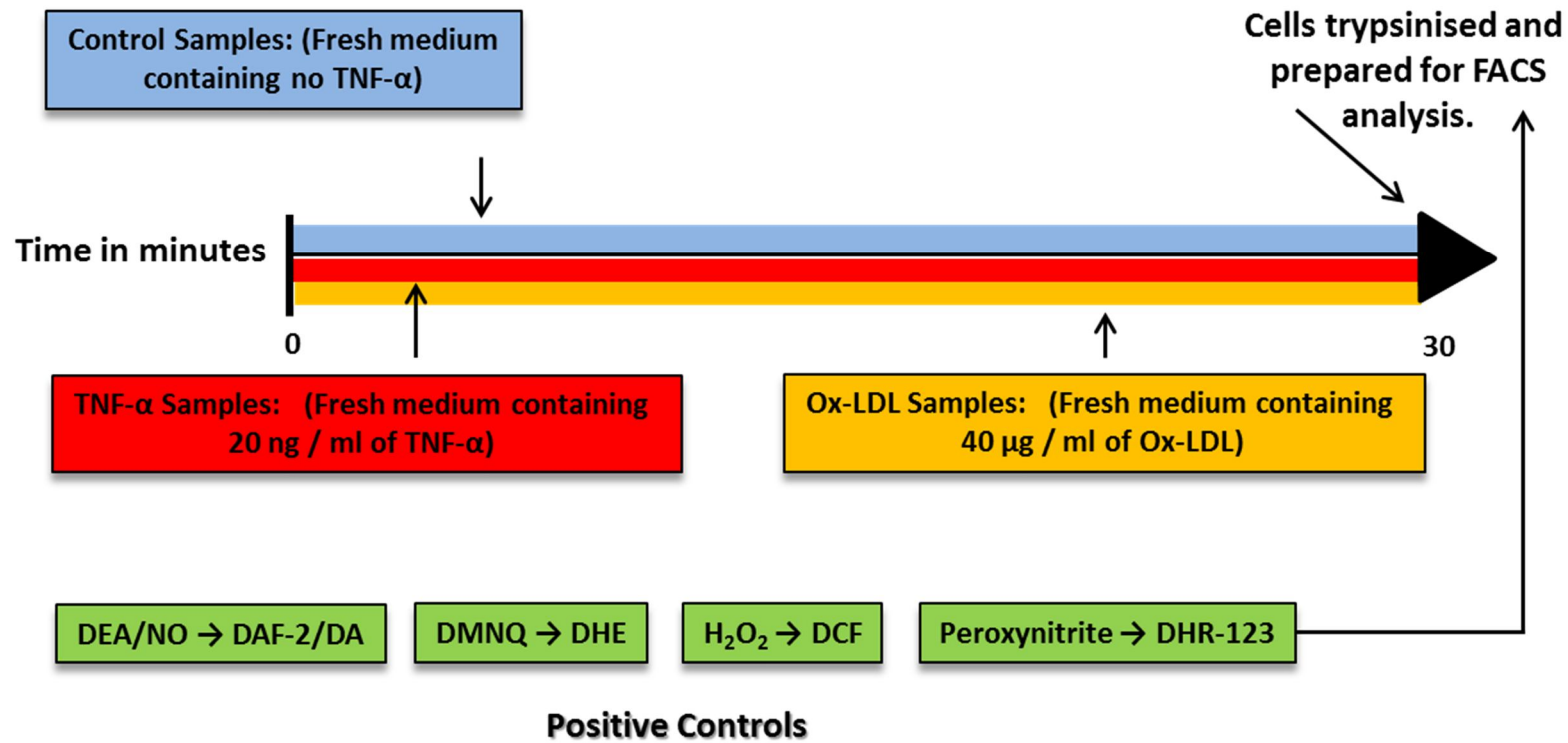


Figure 5.2: Protocol for treatment of CMECs with 20 ng / ml TNF- α and Ox-LDL (40 μ g / ml) for 30 minutes for subsequent FACS analysis NO production, oxidative stress and nitrosative stress.

5.3.3 Investigating the effects of modification of the serum content of growth medium on ROS production.

From the literature, it appears that many authors prefer to investigate oxidative stress in cell models that were incubated in either low serum or serum-free growth medium (Ago *et al.*, 2004; Li JM *et al.*, 2007b; Monaghan-Benson and Burrige, 2009) The rationale for this intervention is apparently to stimulate the ROS-producing enzyme systems in the cells and thereby remove the possible masking effects that normal or high serum-containing growth medium may exert on ROS production in cells. The NADPH-oxidase enzyme, one of the major ROS generators in endothelial cells, has for example been shown to be up-regulated by, *inter alia*, nutrient deprivation (Li H *et al.*, 2008). Furthermore, we almost consistently, with very few exceptions, found that my TNF- α -treated CMECs either responded with no changes in ROS generation, or even reduced ROS generation, which contradicts what is generally published in the literature. In view of this, we performed a separate series of experiments in which the foetal bovine serum (FBS) concentration of the growth medium was reduced in order to evaluate the effects of serum reduction and deprivation on superoxide production. CMECs were treated with TNF- α (20 ng / ml) in medium containing either 0, 5 or 10 % serum for 24 hours (see figure 5.3 for the protocol). After each of these respective treatments, cells were removed from culture by trypsinisation and subsequently treated with dihydroethium (DHE) (as described on page 124, chapter 2) to measure oxidative stress by means of flow cytometric analysis. Positive controls were also included (as described on page 124, chapter 2) (refer to figure 5.3 for complete protocol).

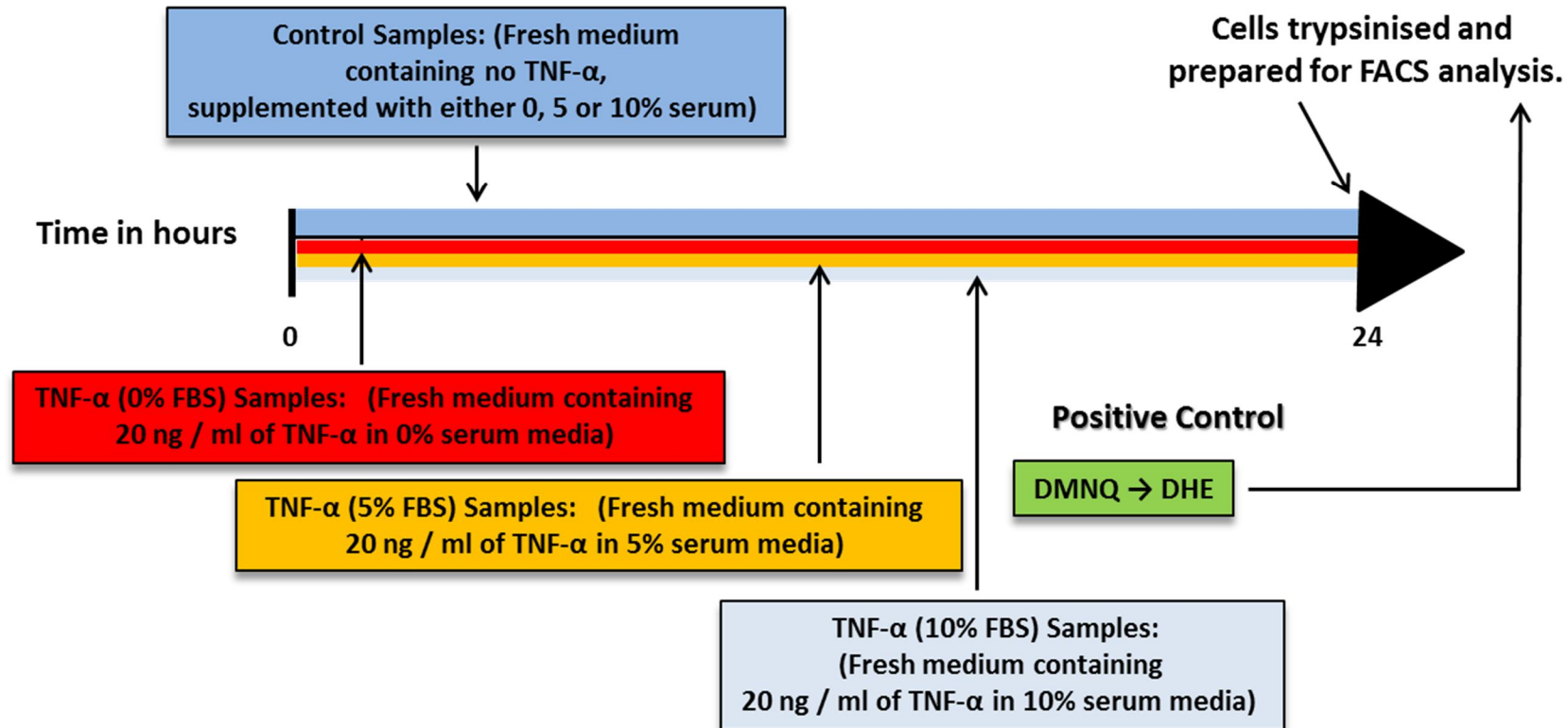


Figure 5.3: Protocol for treatment of CMECs with 20 ng / ml TNF- α for 24 hours in medium supplemented with either 0, 5 or 10 % foetal bovine serum (FBS) for subsequent FACS analysis of superoxide production (DHE fluorescence).

5.4 **Results**

5.4.1 **The effects of different TNF- α concentrations: 0.5, 5 and 20 ng / ml.**

5.4.1.1 **Cell viability measurements (FACS analysis).**

CMECs exposed to TNF- α (0.5 ng / ml for 24 hours), showed no change (87.62 ± 7.22 % vs. 100 % control: $p < 0.05$) in propidium iodide (PI) fluorescence (measuring necrosis) (see figure 5.4), compared to untreated controls. Similarly, CMECs exposed to TNF- α (0.5 ng / ml for 24 hours), showed no change (116.57 ± 19.72 % vs. 100 % control: $p < 0.05$) in Annexin V fluorescence (measuring apoptosis) (see figure 5.5), compared to untreated controls. When increasing the TNF- α concentration to 5 ng / ml, CMECs showed a decrease (77.65 ± 6.58 % vs. 100 % control: $p < 0.05$) in PI fluorescence (see figure 5.4), and a decrease (66.18 ± 5.21 % vs. 100 % control: $p < 0.05$) in Annexin V fluorescence (see figure 5.5), compared to the untreated controls respectively. When a relatively high concentration of TNF- α was administered to the cells (20 ng / ml for 24 hours), there was a decrease in both PI fluorescence (50.36 ± 6.48 % vs. 100 % control: $p < 0.05$) (see figure 5.4) and Annexin V fluorescence (79.59 ± 6.22 % vs. 100 % control: $p < 0.05$) (see figure 5.5), compared to untreated controls respectively.

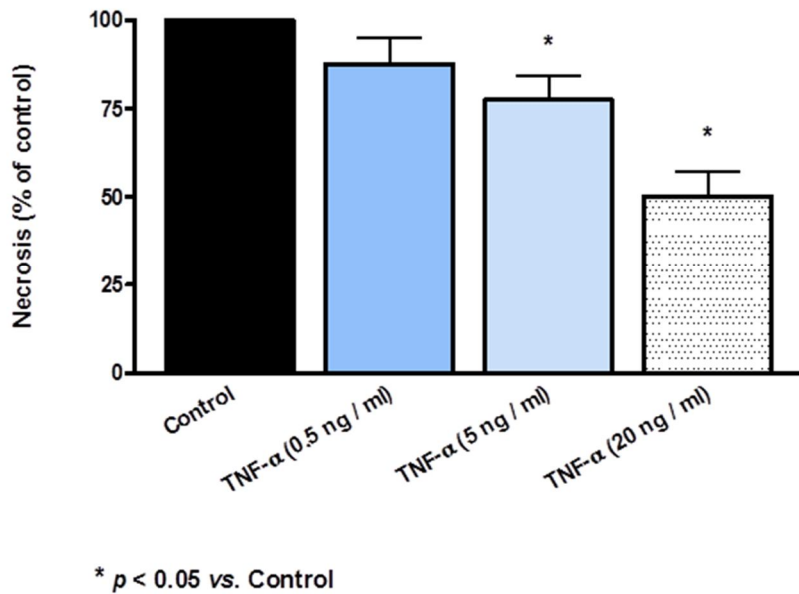


Figure 5.4: TNF- α effects on necrosis at different concentrations (0.5, 5 and 20 ng / ml for 24 hours). Necrosis expressed as % PI stained cells (as a percentage of control; control = 100 %). Sample size: $n = 4 - 6$ / group.

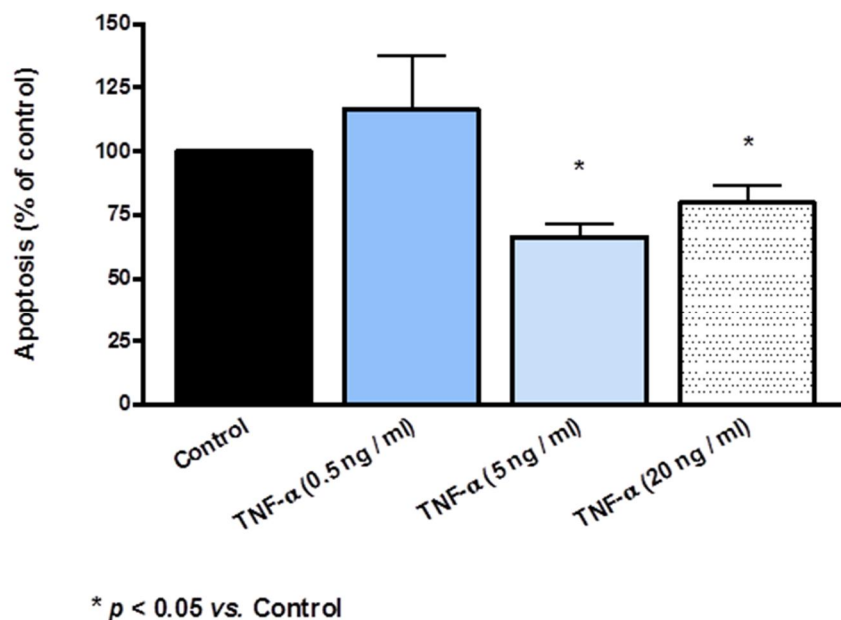


Figure 5.5: TNF- α effects on apoptosis at different concentrations (0.5, 5 and 20 ng / ml for 24 hours). Apoptosis expressed as % Annexin V stained cells (as a percentage of control; control = 100 %). Sample size: $n = 4 - 6$ / group.

5.4.1.2 NO production measurements (FACS analysis).

CMECs exposed to 0.5 ng /ml TNF- α (24 hours) showed a significant decrease in DAF-2/DA mean fluorescence intensity (81.24 ± 2.78 % vs. 100 % control: $p < 0.05$) compared to untreated controls (see figure 5.6). CMECs exposed to 5 ng / ml TNF- α (24 hours), showed no change (100.71 ± 5.04 % vs. 100 % control: $p < 0.05$) in DAF-2/DA fluorescence (see figure 5.6), compared to untreated controls. CMECs exposed to 20 ng / ml TNF- α (24 hours), showed a significant decrease (74.02 ± 1.61 % vs. 100 % control: $p < 0.05$) in DAF-2/DA fluorescence (see figure 5.6), compared to untreated controls.

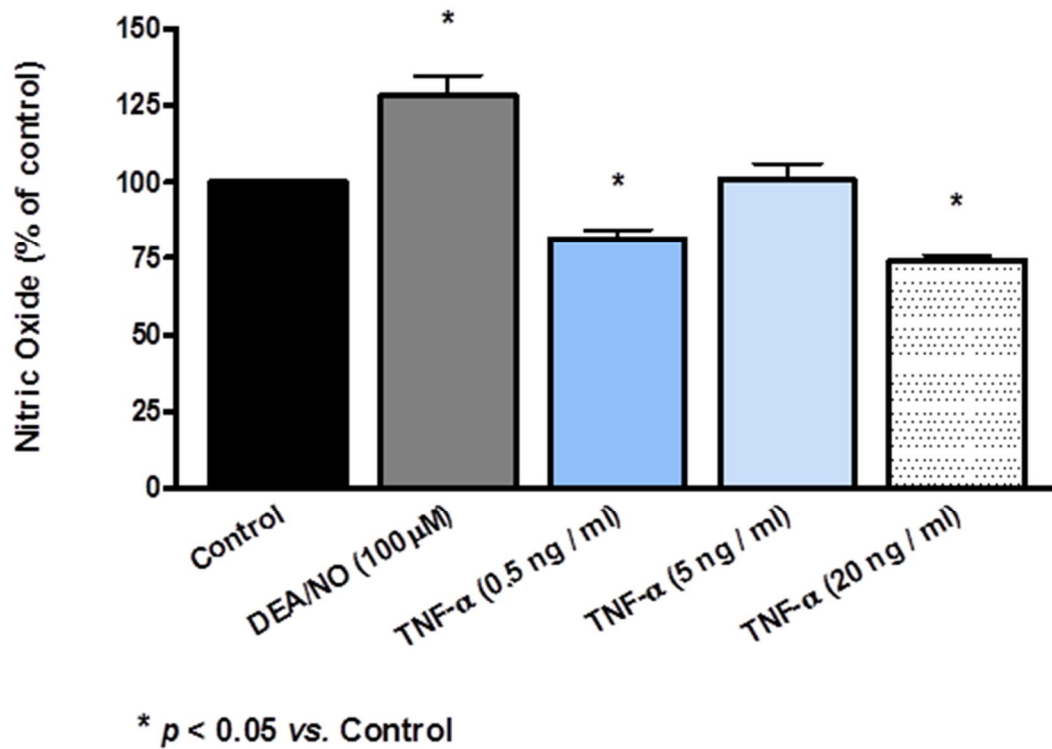


Figure 5.6: TNF- α effects on mean DAF-2/DA fluorescence at different concentrations (0.5, 5 and 20 ng / ml for 24 hours). Data presented as % DAF-2/DA fluorescence (expressed as a percentage of control; control = 100%). The NO-donor, DEA/NO (100 μ M) was used as a positive control. Sample size: n = 4 – 6 / group.

5.4.1.3 Reactive oxygen species measurements (FACS analysis)

5.4.1.3.1 TNF- α 0.5 ng/ml for 24 hours

Dihydroethidium (DHE) fluorescence (sensitive for O₂⁻): A decrease in mean DHE fluorescence was observed: 71.86 ± 4.21 % vs. 100 % control: $p < 0.05$ (see figure 5.7).

2', 7'-dichlorofluorescein (DCF) fluorescence (sensitive for H₂O₂): A decrease in mean DCF fluorescence was observed: 46.22 ± 2.00 % vs. 100 % control: $p < 0.05$ (see figure 5.8).

Dihydrorhodamine-123 (DHR-123) fluorescence (sensitive for mitochondrial ROS and peroxynitrite): No changes were observed in mean DHR-123 fluorescence: 95.15 ± 2.41 % vs. 100 % control) (see figure 5.9).

5.4.1.3.2 TNF- α 5 ng/ml for 24 hours

Dihydroethidium (DHE) fluorescence (sensitive for O₂⁻): A decrease in mean DHE fluorescence was observed: 83.39 ± 2.37 % vs. 100 % control: $p < 0.05$ (see figure 5.7).

2', 7'-dichlorofluorescein (DCF) fluorescence (sensitive for H₂O₂): A decrease in mean DCF fluorescence was observed: 69.89 ± 3.72 % vs. 100 % control: $p < 0.05$ (see figure 5.8).

Dihydrorhodamine-123 (DHR-123) fluorescence (sensitive for mitochondrial ROS and peroxynitrite): A decrease in mean DHR-123 fluorescence was observed: 85.54 ± 2.11 % vs. 100 % control: $p < 0.05$ (see figure 5.9).

5.4.1.3.3 TNF- α 20 ng/ml for 24 hours

Dihydroethidium (DHE) fluorescence (sensitive for O₂): A decrease in mean DHE fluorescence was observed: 80.55 ± 2.53 % vs. 100 % control: $p < 0.05$ (see figure 5.7).

2', 7'-dichlorofluorescein (DCF) fluorescence (sensitive for H₂O₂): An increase in mean DCF fluorescence was observed: 113.72 ± 2.88 % vs. 100 % control: $p < 0.05$ (see figure 5.8).

Dihydrorhodamine-123 (DHR-123) fluorescence (sensitive for mitochondrial ROS and peroxynitrite): A decrease in mean DHR-123 fluorescence was observed: 71.91 ± 1.01 % vs. 100 % control: $p < 0.05$ (see figure 5.9).

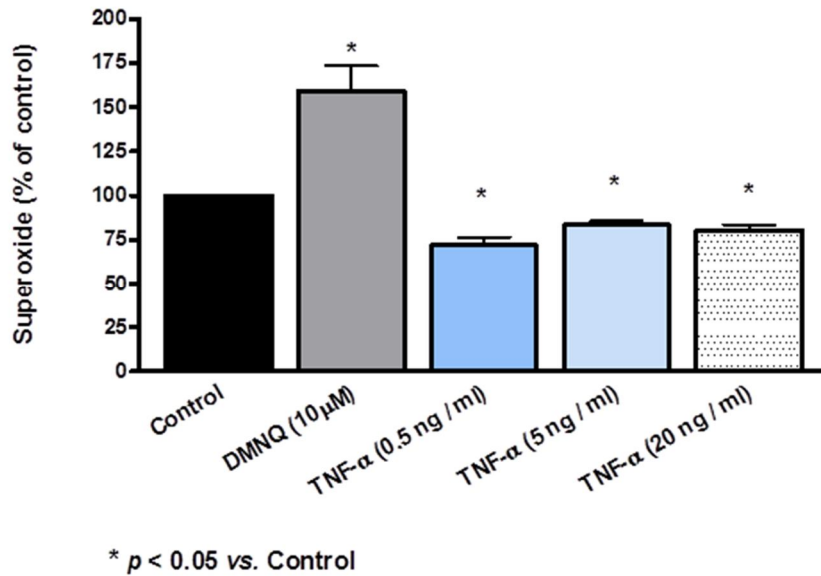


Figure 5.7: TNF- α effects on mean DHE fluorescence at different concentrations (0.5, 5 and 20 ng / ml for 24 hours). Data presented as % DHE fluorescence (expressed as a percentage of control; control = 100%). DMNQ (10µM) was used as a positive control. Sample size: n = 4 – 6 / group.

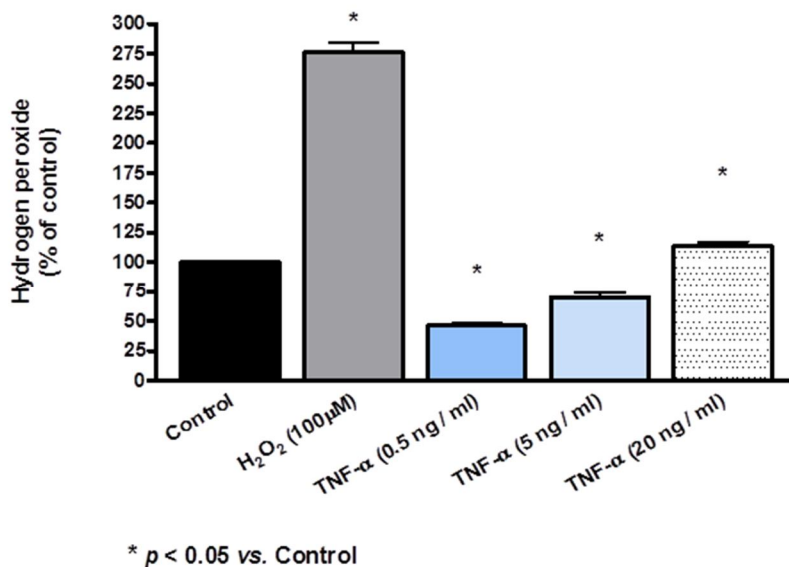


Figure 5.8: TNF- α effects on mean DCF fluorescence at different concentrations (0.5, 5 and 20 ng / ml for 24 hours). Data presented as % DCF fluorescence (expressed as a percentage of control; control = 100%). H₂O₂ (100µM) was used as a positive control. Sample size: n = 4 – 6 / group.

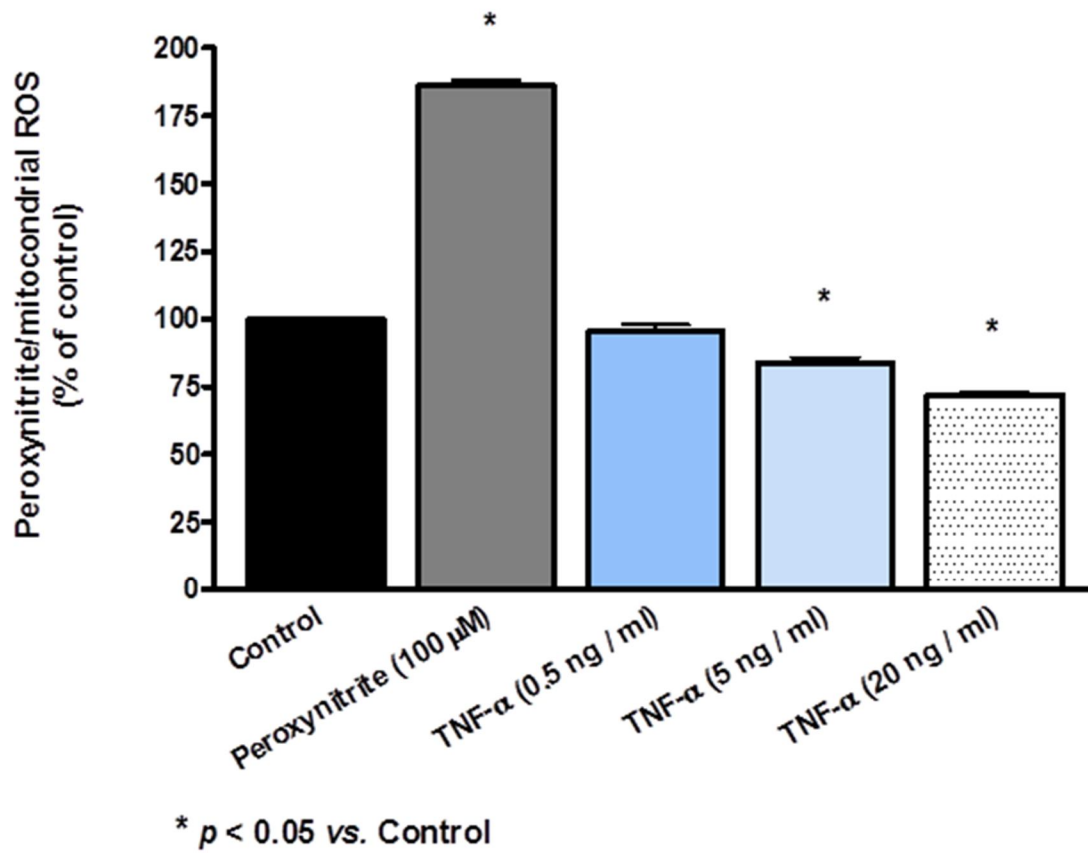


Figure 5.9: TNF- α effects on mean DHR-123 fluorescence at different concentrations (0.5, 5 and 20 ng / ml for 24 hours). Data presented as % DHR-123 fluorescence (expressed as a percentage of control; control = 100%). Authentic peroxynitrite (100µM) was used as a positive control. Sample size: n = 4 – 6 / group.

5.4.1.4 Western blot analysis of eNOS signalling:

5.4.1.4.1 eNOS

5.4.1.4.1.1 TNF- α 0.5 ng /ml for 24 hours

Phosphorylated eNOS: A decrease in phospho eNOS was observed: 0.58 ± 0.04 vs. 1.00 control: $p < 0.05$ (see figure 5.10).

Total eNOS: An increase in total eNOS was observed: 1.45 ± 0.12 vs. 1.00 control: $p < 0.05$ (see figure 5.11).

Phospho eNOS expressed as a ratio of total eNOS: A decrease in the ratio of phospho / total eNOS was observed: 0.41 ± 0.04 vs. 1.00 control: $p < 0.05$ (see figure 5.12).

5.4.1.4.1.2 TNF- α 5 ng /ml for 24 hours

Phosphorylated eNOS: A decrease in phospho eNOS was observed: 0.67 ± 0.08 vs. 1.00 control: $p < 0.05$ (see figure 5.10).

Total eNOS: An increase in total eNOS was observed: 1.74 ± 0.36 vs. 1.00 control: $p < 0.05$ (see figure 5.11).

Phospho eNOS expressed as a ratio of total eNOS: A decrease in the ratio of phospho / total eNOS was observed: 0.42 ± 0.05 vs. 1.00 control: $p < 0.05$ (see figure 5.12).

5.4.1.4.1.3 TNF- α 20 ng/ml for 24 hours

Phosphorylated eNOS: A decrease in phospho eNOS was observed: 0.50 ± 0.02 vs. 1.00 control: $p < 0.05$ (see figure 5.10).

Total eNOS: An increase in total eNOS was observed: 2.73 ± 0.12 vs. 1.00 control: $p < 0.05$ (see figure 5.11).

Phospho eNOS expressed as a ratio of total eNOS: A decrease in the ratio of phospho / total eNOS was observed: 0.19 ± 0.01 vs. 1.00 control: $p < 0.05$ (see figure 5.12).

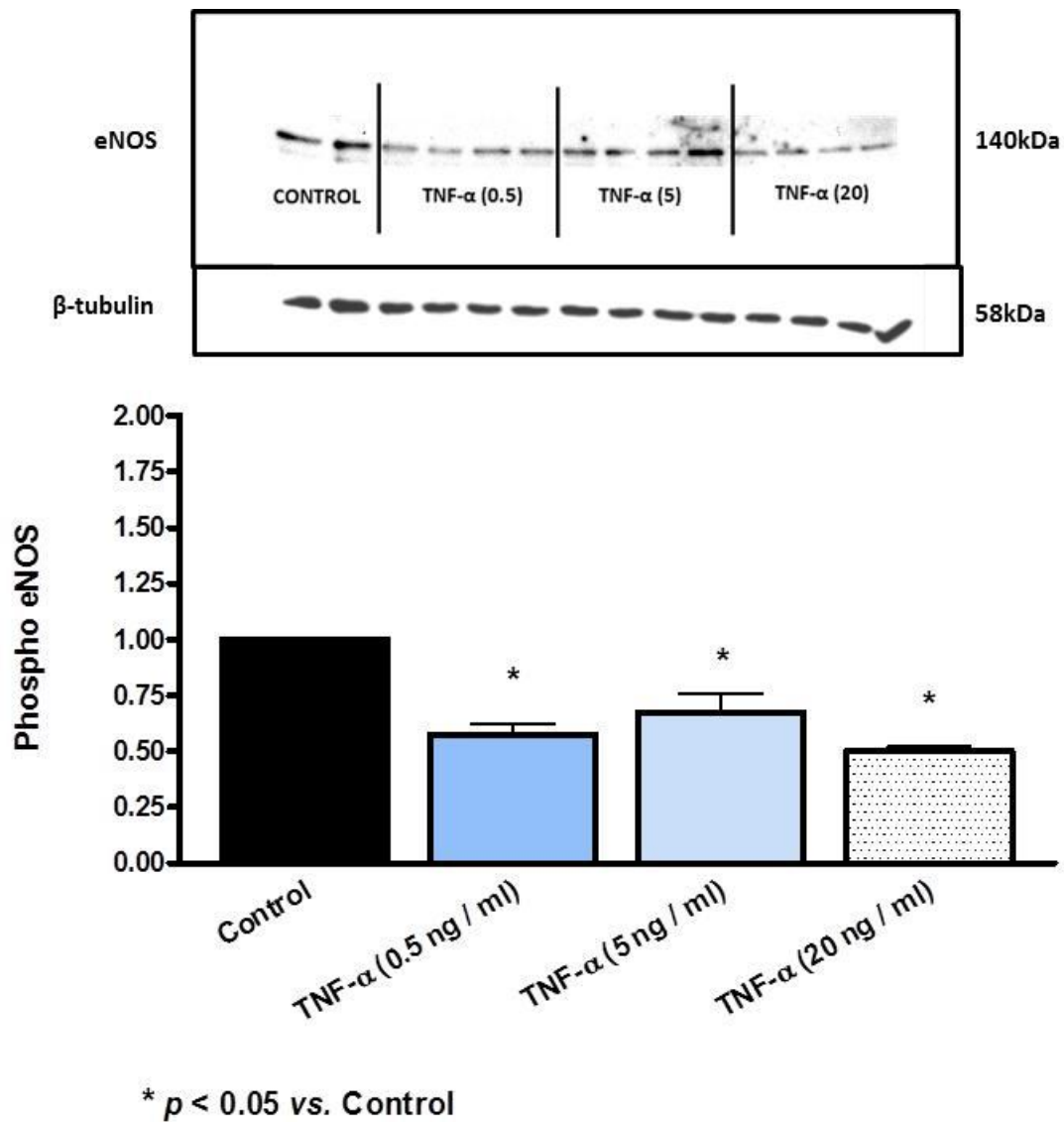


Figure 5.10: TNF- α effects on phosphorylated eNOS (phospho Ser 1177) at different concentrations (0.5, 5 and 20 ng / ml for 24 hours). Phosphorylated eNOS is expressed as a ratio of control; control adjusted to 1 (please refer to page 134, chapter 2). Sample size: n = 4 / group.

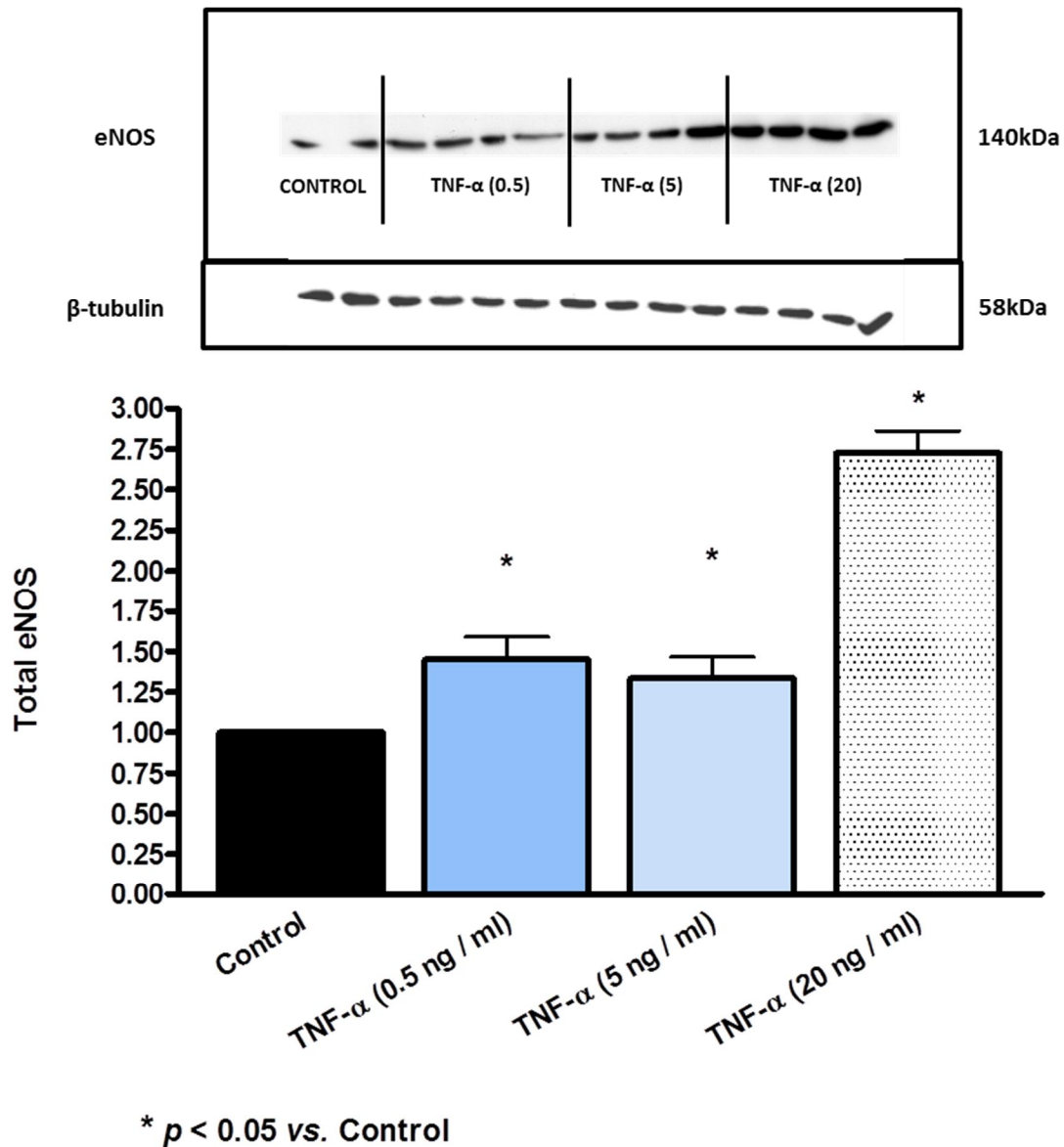


Figure 5.11: TNF- α effects on total eNOS expression at different concentrations (0.5, 5 and 20 ng / ml for 24 hours). Total eNOS expression is expressed as a ratio of control; control adjusted to 1 (please refer to page 134, chapter 2). Sample size: $n = 4$ / group.

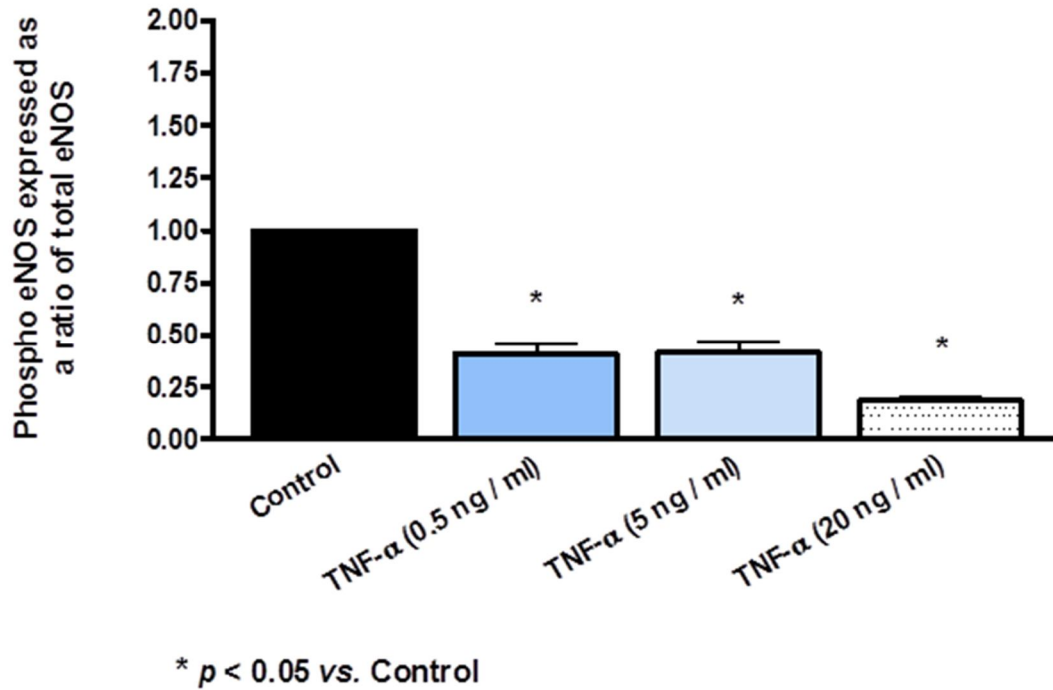


Figure 5.12: TNF- α effects on the phosphorylated eNOS / total eNOS expression at different concentrations (0.5, 5 and 20 ng / ml for 24 hours). Phospho / Total eNOS levels are expressed as a ratio of control; control adjusted to 1 (please refer to page 134, chapter 2). Sample size: $n = 4$ / group.

5.4.1.4.2 PKB/Akt

5.4.1.4.2.1 TNF- α 0.5 ng/ml for 24 hours

Phosphorylated PKB/Akt: A decrease in phospho PKB/Akt was observed: 0.42 ± 0.05 vs. 1.00 control: $p < 0.05$ (see figure 5.13).

Total PKB/Akt: A decrease in total PKB/Akt was observed: 0.51 ± 0.08 vs. 1.00 control: $p < 0.05$ (see figure 5.14).

Phospho PKB/Akt expressed as a ratio of total PKB/Akt: No change in the ratio of phospho / total PKB/Akt was observed: 0.88 ± 0.12 vs. 1.00 control) (see figure 5.15).

5.4.1.4.2.2 TNF- α 5 ng/ml for 24 hours

Phosphorylated PKB/Akt: No change in phospho PKB/Akt was observed: 0.82 ± 0.09 vs. 1.00 control) (see figure 5.13).

Total PKB/Akt: A decrease in total PKB/Akt was observed: 0.59 ± 0.06 vs. 1.00 control: $p < 0.05$ (see figure 5.14).

Phospho PKB/Akt expressed as a ratio of total PKB/Akt: No change in the ratio of phospho / total PKB/Akt was observed: 1.48 ± 0.25 vs. 1.00 control) (see figure 5.15).

5.4.1.4.2.3 TNF- α 20 ng/ml for 24 hours

Phosphorylated PKB/Akt: A decrease in phospho PKB/Akt was observed: 0.39 ± 0.03 vs. 1.00 control: $p < 0.05$ (see figure 5.13).

Total PKB/Akt: A decrease in total PKB/Akt was observed: 0.71 ± 0.01 vs. 1.00 control: $p < 0.05$ (see figure 5.14).

Phospho PKB/Akt expressed as a ratio of total PKB/Akt: A decrease in the ratio of phospho / total PKB/Akt was observed: 0.55 ± 0.03 vs. 1.00 control: $p < 0.05$ (see figure 5.15).

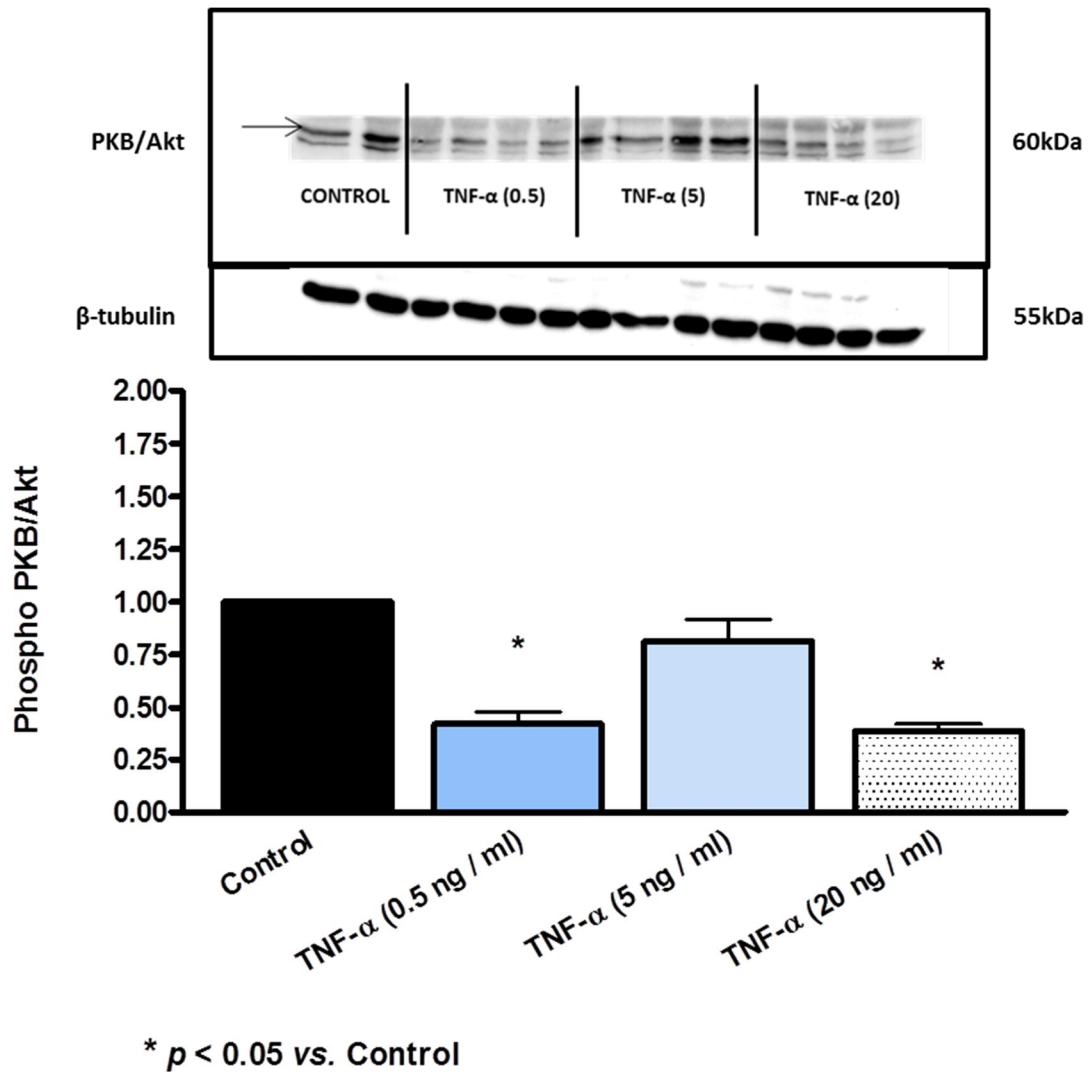


Figure 5.13: TNF- α effects on phosphorylated PKB/Akt (phospho Ser 473) at different concentrations (0.5, 5 and 20 ng / ml for 24 hours). Phosphorylated PKB/Akt is expressed as a ratio of control; control adjusted to 1 (please refer to page 134, chapter 2). Sample size: $n = 4$ / group.

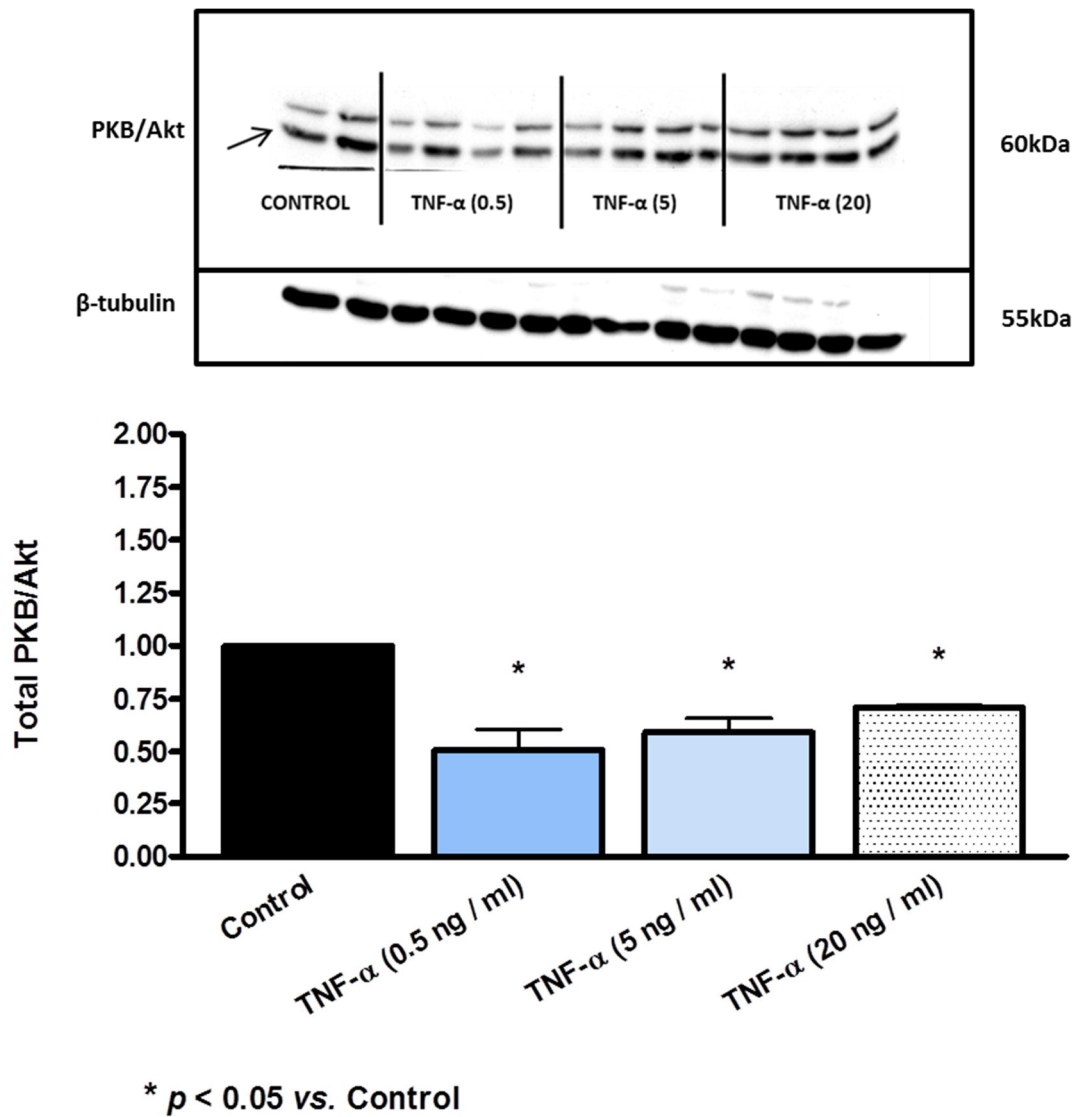


Figure 5.14: TNF- α effects on total PKB/Akt expression at different concentrations (0.5, 5 and 20 ng / ml for 24 hours). Total PKB/Akt expression is expressed as a ratio of control; control adjusted to 1 (please refer to page 134, chapter 2). Sample size: $n = 4$ / group.

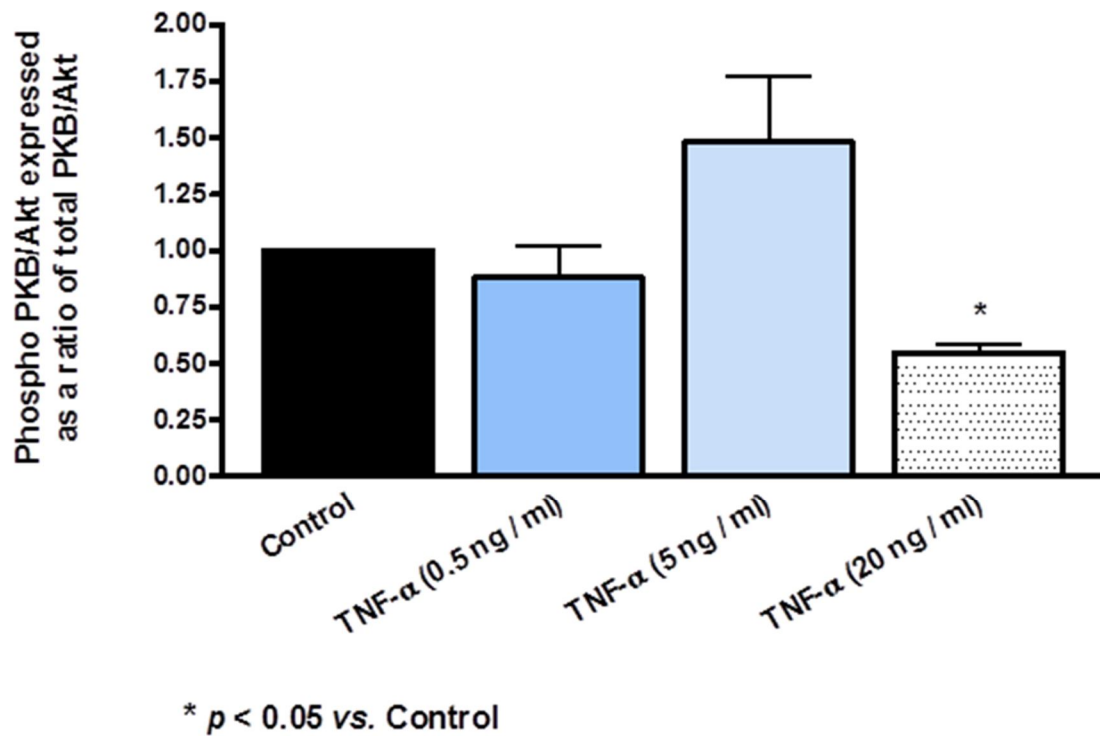


Figure 5.15: TNF- α effects on the phosphorylated PKB/Akt / total PKB/Akt expression at different concentrations (0.5, 5 and 20 ng / ml for 24 hours). Phospho / Total PKB/Akt levels are expressed as a ratio of control; control adjusted to 1 (please refer to page 134, chapter 2). Sample size: $n = 4$ / group.

5.4.1.4.3 HSP 905.4.1.4.3.1 TNF- α 0.5 ng /ml for 24 hours

HSP 90: A decrease in HSP 90 was observed: 0.70 ± 0.04 vs. 1.00 control: $p < 0.05$ (see figure 5.16).

5.4.1.4.3.2 TNF- α 5 ng /ml for 24 hours

HSP 90: A decrease in HSP 90 was observed: 0.64 ± 0.06 vs. 1.00 control: $p < 0.05$ (see figure 5.16).

5.4.1.4.3.3 TNF- α 20 ng /ml for 24 hours

HSP 90: A decrease in HSP 90 was observed: 0.79 ± 0.02 vs. 1.00 control: $p < 0.05$ (see figure 5.16).

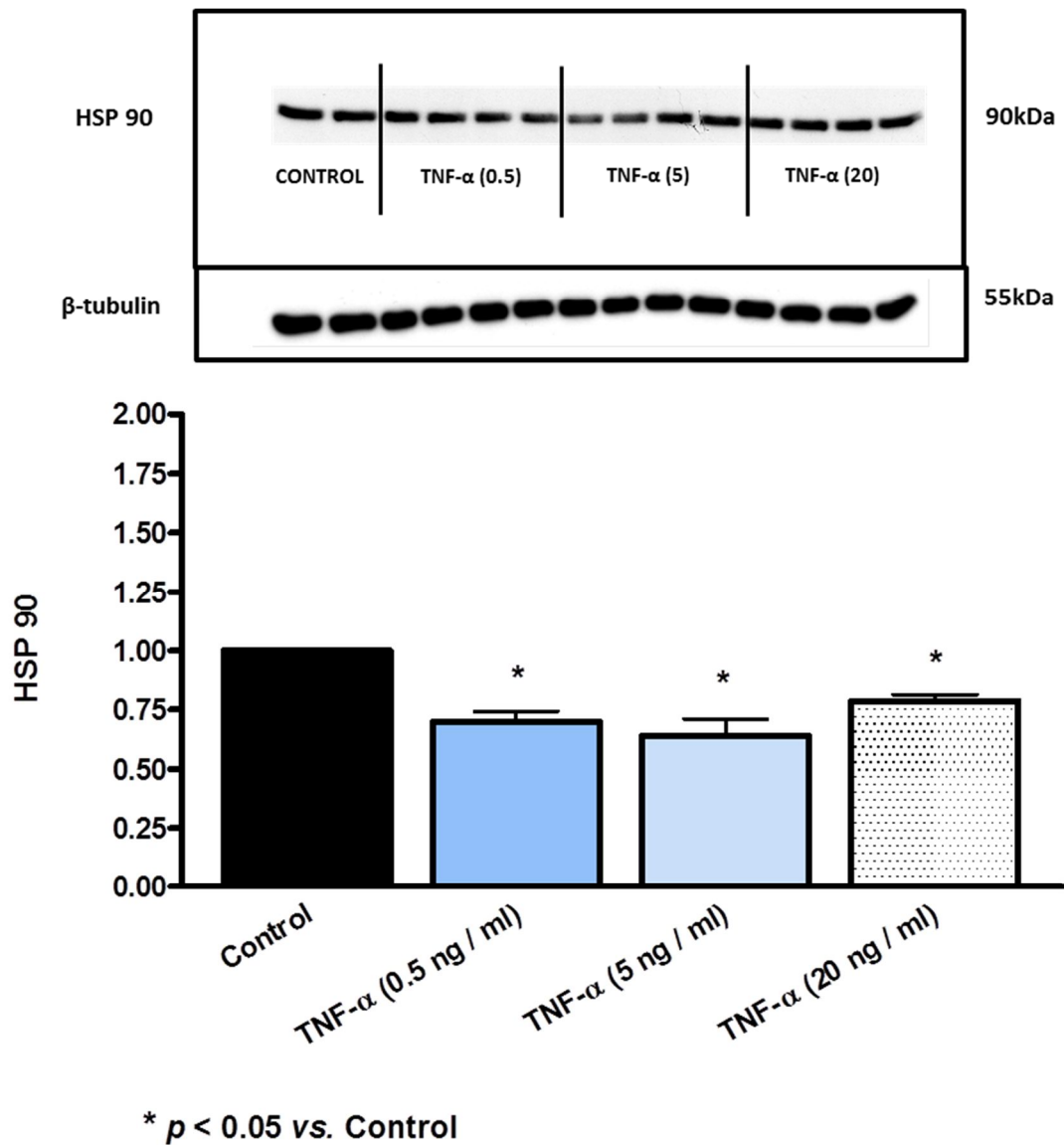


Figure 5.16: TNF- α effects on total HSP 90 expression at different concentrations (0.5, 5 and 20 ng / ml for 24 hours). Total HSP 90 expression is expressed as a ratio of control; control adjusted to 1 (please refer to page 134, chapter 2). Sample size: $n = 4$ / group.

5.4.1.4.4 Caveolin-1

5.4.1.4.4.1 TNF- α 0.5 ng/ml for 24 hours

Caveolin-1: No change in caveolin-1 was observed: 0.89 ± 0.12 vs. 1.00 control) (see figure 5.17).

5.4.1.4.4.2 TNF- α 5 ng/ml for 24 hours

Caveolin-1: A decrease in caveolin-1 was observed: 0.72 ± 0.05 vs. 1.00 control: $p < 0.05$ (see figure 5.17).

5.4.1.4.4.3 TNF- α 20 ng/ml for 24 hours

Caveolin-1: No change in caveolin-1 was observed: 0.92 ± 0.11 vs. 1.00 control) (see figure 5.17).

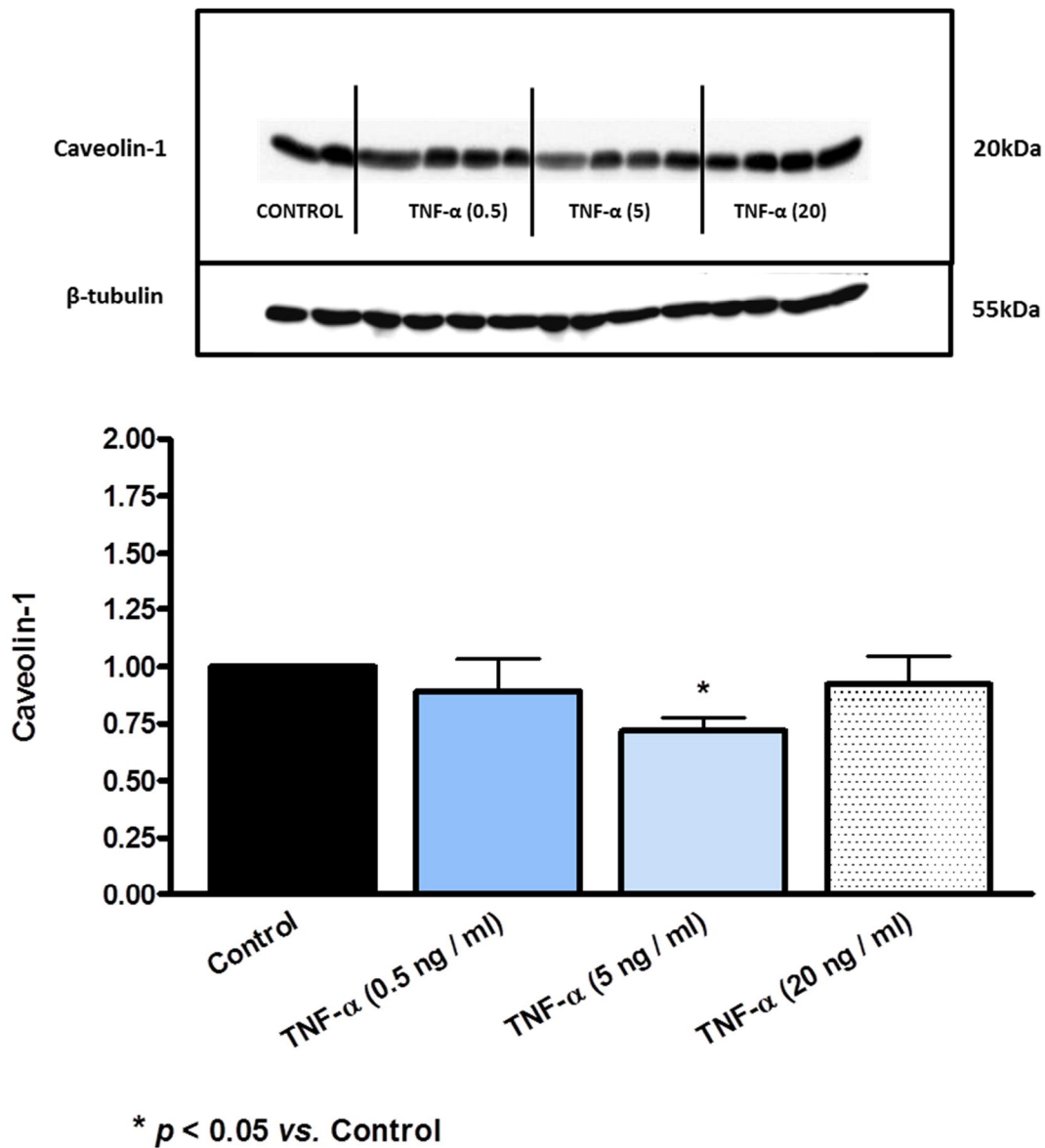


Figure 5.17: TNF- α effects on total caveolin-1 expression at different concentrations (0.5, 5 and 20 ng / ml for 24 hours). Total caveolin-1 expression is expressed as a ratio of control; control adjusted to 1 (please refer to page 134, chapter 2). Sample size: $n = 4$ / group.

5.4.1.5 Western blot analysis of proteins associated with oxidative stress: p22-phox:

5.4.1.5.1 TNF- α 0.5 ng /ml for 24 hours

P22 phox: No change in p22 phox was observed: 1.01 ± 0.01 vs. 1.00 control) (see figure 5.18).

5.4.1.5.2 TNF- α 5 ng /ml for 24 hours

P22 phox: An increase in p22 phox was observed: 1.25 ± 0.08 vs. 1.00 control: $p < 0.05$ (see figure 5.18).

5.4.1.5.3 TNF- α 20 ng /ml for 24 hours

P22 phox: An increase in p22 phox was observed: 1.34 ± 0.11 vs. 1.00 control: $p < 0.05$ (see figure 5.18).

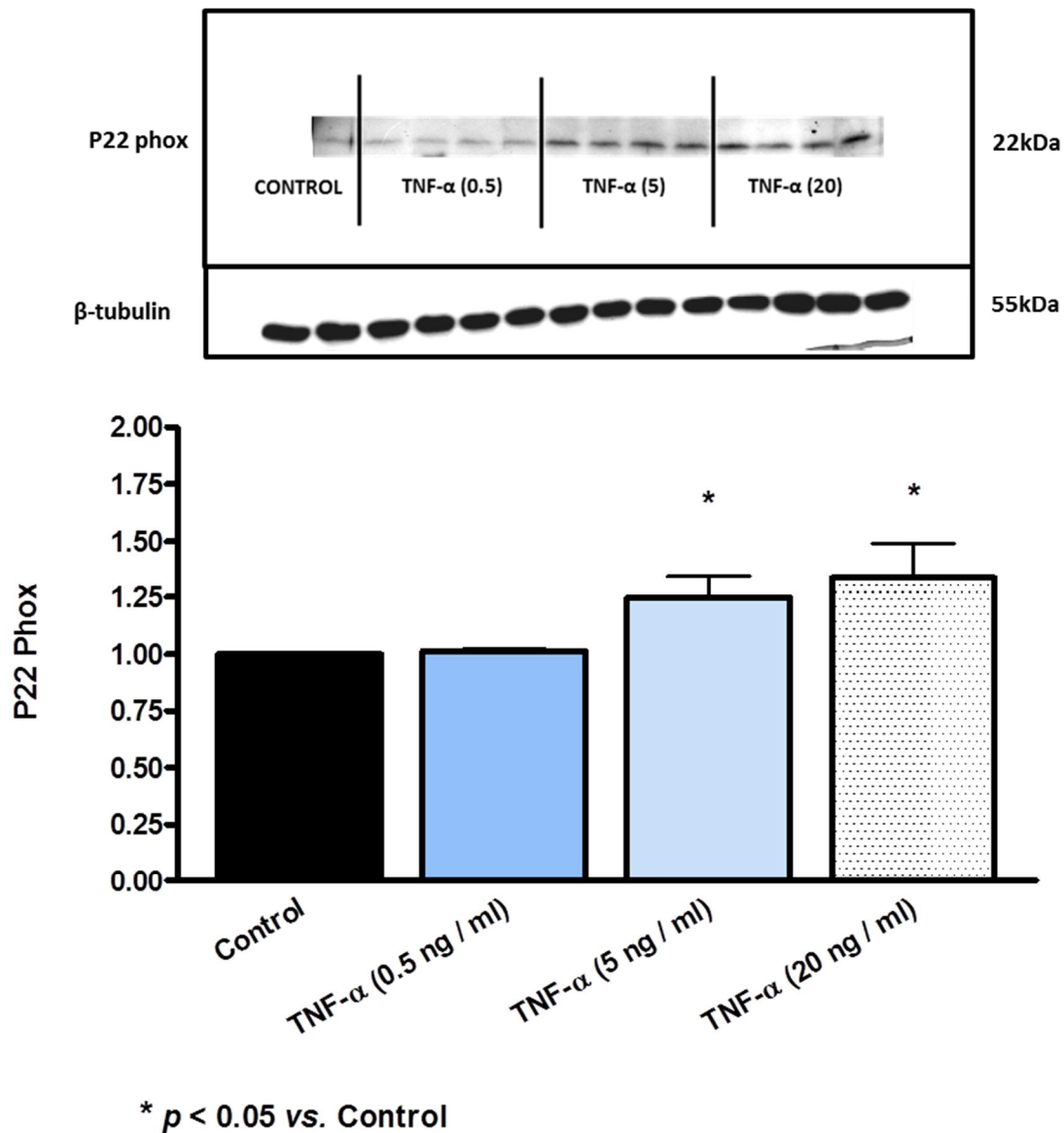


Figure 5.18: TNF- α effects on total p22-phox expression at different concentrations (0.5, 5 and 20 ng / ml for 24 hours). Total p22-phox expression is expressed as a ratio of control; control adjusted to 1 (please refer to page 134, chapter 2). Sample size: $n = 4$ / group.

5.4.1.6 Western blot analysis of proteins associated with nitrosative stress: nitrotyrosine:

5.4.1.6.1 TNF- α 0.5 ng/ml for 24 hours

Nitrotyrosine: No change in nitrotyrosine was observed: 0.99 ± 0.05 vs. 1.00 control) (see figure 5.19).

5.4.1.6.1 TNF- α 5 ng/ml for 24 hours

Nitrotyrosine: A decrease in nitrotyrosine was observed: 0.87 ± 0.04 vs. 1.00 control: $p < 0.05$ (see figure 5.19).

5.4.1.6.1 TNF- α 20 ng/ml for 24 hours

Nitrotyrosine: No change in nitrotyrosine was observed: 0.91 ± 0.07 vs. 1.00 control) (see figure 5.19).

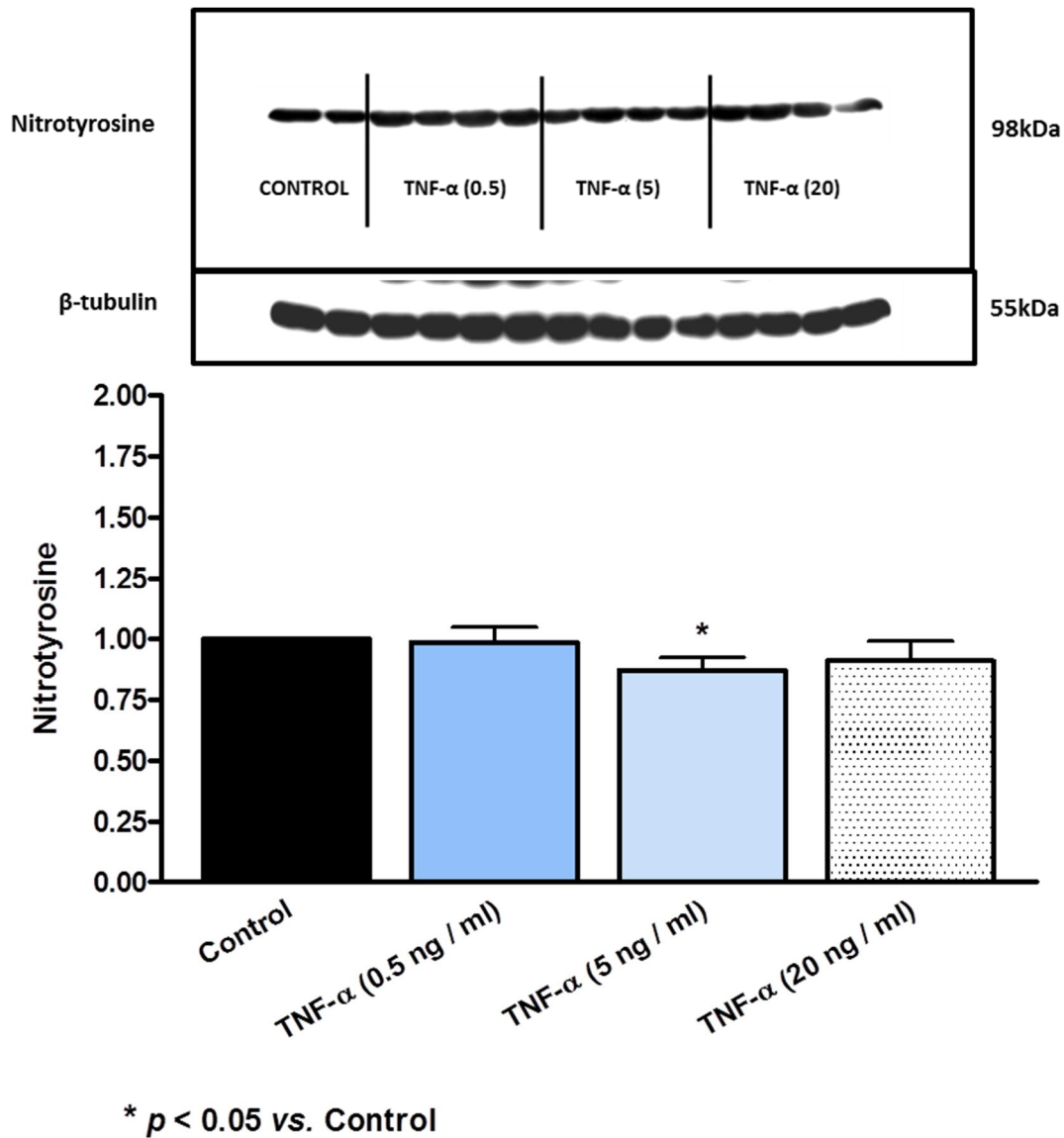


Figure 5.19: TNF- α effects on nitrotyrosine expression at different concentrations (0.5, 5 and 20 ng / ml for 24 hours). Nitrotyrosine expression is expressed as a ratio of control; control adjusted to 1 (please refer to page 134, chapter 2). Sample size: $n = 4$ / group.

5.4.1.7 Western blot analysis of proteins associated with NF- κ B signalling: IK β - α :

5.4.1.7.1 TNF- α 0.5 ng /ml for 24 hours

Total IK β α : A decrease in total IK β α was observed: 0.78 ± 0.02 vs. 1.00 control: $p < 0.05$ (see figure 5.20).

5.4.1.7.2 TNF- α 5 ng /ml for 24 hours

Total IK β α : A decrease in total IK β α was observed: 0.74 ± 0.02 vs. 1.00 control: $p < 0.05$ (see figure 5.20).

5.4.1.7.3 TNF- α 20 ng /ml for 24 hours

Total IK β α : A decrease in total IK β α was observed: 0.50 ± 0.01 vs. 1.00 control: $p < 0.05$ (see figure 5.20).

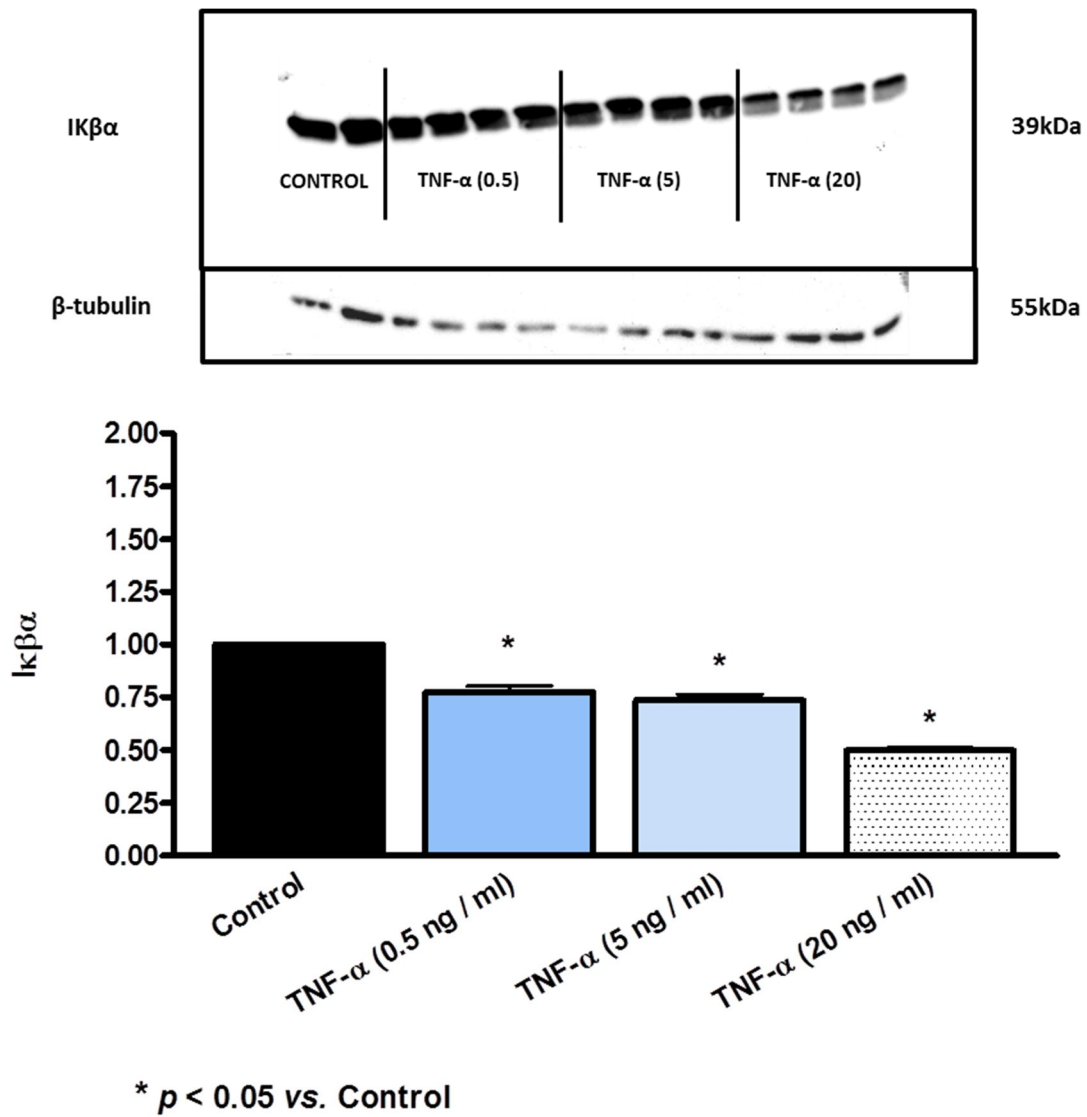


Figure 5.20: TNF- α effects on I κ B- α expression at different concentrations (0.5, 5 and 20 ng / ml for 24 hours). I κ B- α expression is expressed as a ratio of control; control adjusted to 1 (please refer to page 134, chapter 2). Sample size: $n = 4$ / group.

5.4.2 The effects of short term treatment with TNF- α (20 ng / ml): 30 minutes

5.4.2.1 *NO production measurements (FACS analysis).*

CMECs exposed to TNF- α (20 ng / ml for 30 minutes), showed a significant decrease (89.85 ± 2.19 % vs. 100 % control: $p < 0.05$) in mean DAF-2/DA fluorescence compared to untreated controls (see figure 5.21). In order to contextualise the TNF- α data, we included experiments in which the CMECs were exposed to another harmful stimulus, ox-LDL (40 μ g / ml for 30 minutes). Data showed unchanged mean DAF-2/DA fluorescence intensity: 97.07 ± 3.37 % vs. 100 % control: $p < 0.05$ (see figure 5.21).

5.4.2.2 *ROS measurements (FACS analysis).*

CMECs exposed to TNF- α (20 ng / ml for 30 minutes), showed no change in mean DHE fluorescence intensity (97.38 ± 4.04 % vs. 100 % control) (see figure 5.22). CMECs exposed to TNF- α (20 ng / ml for 30 minutes), showed no change in mean DCF fluorescence intensity (92.99 ± 3.25 % vs. 100 % control) (see figure 5.23). CMECs exposed to TNF- α (20 ng / ml for 30 minutes), showed no change in mean DHR-123 fluorescence intensity (106.16 ± 3.55 % vs. 100 % control) (see figure 5.24). CMECs exposed to Ox-LDL (40 μ g / ml for 30 minutes), showed an increase in mean DHE fluorescence intensity (116.11 ± 4.73 % vs. 100 % control: $p < 0.05$); a decrease in mean DCF fluorescence intensity (90.73 ± 0.39 % vs. 100 % control: $p < 0.05$); and no change in mean DHR-123 fluorescence intensity (100.77 ± 3.77 % vs. 100 % control) respectively (see figures 5.22 – 5.24).

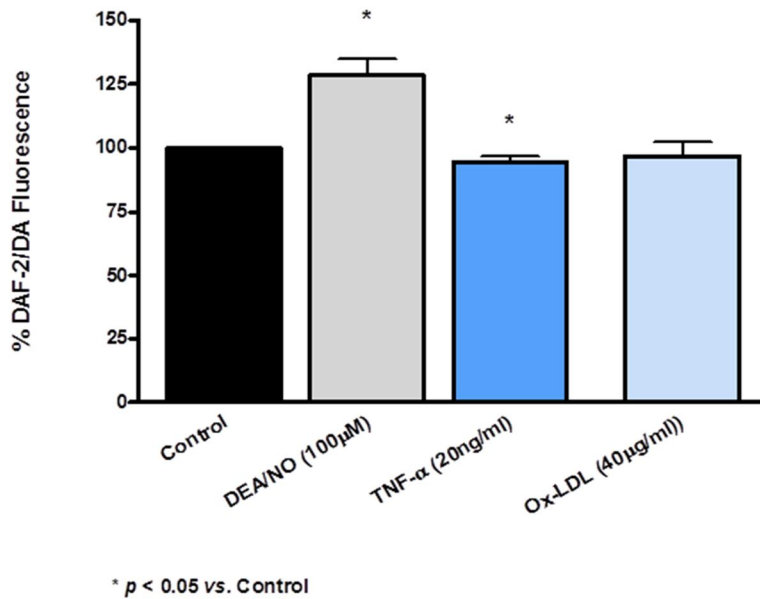


Figure 5.21: Effects of TNF- α (20 ng / ml) and Ox-LDL (40 μ g / ml) on mean DAF-2/DA fluorescence intensity for 30 minutes. DAF-2/DA fluorescence expressed as a percentage of control; control = 100%. DEA/NO (100 μ M) was used as a positive control. Sample size: n = 4 – 6 / group.

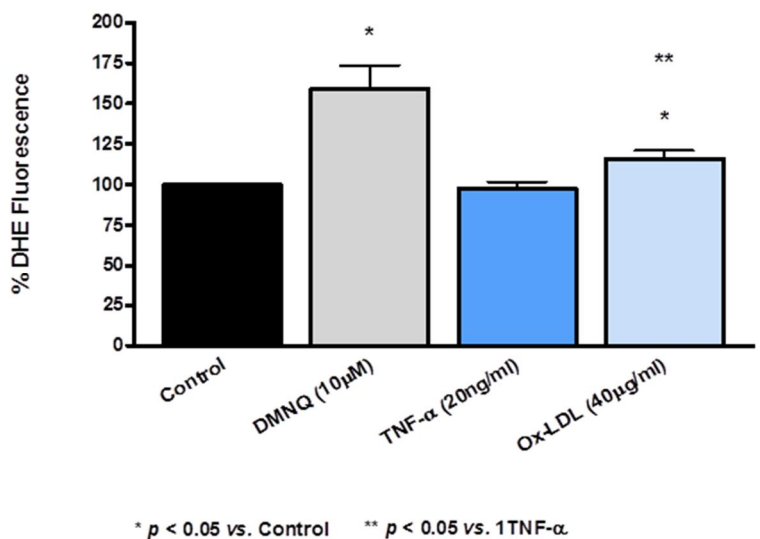


Figure 5.22: Effects of TNF- α (20 ng / ml) and Ox-LDL (40 μ g / ml) on mean DHE fluorescence intensity for 30 minutes. DHE fluorescence expressed as a percentage of control; control = 100%. DMNQ (10 μ M) was used as a positive control. Sample size: n = 4 – 6 / group.

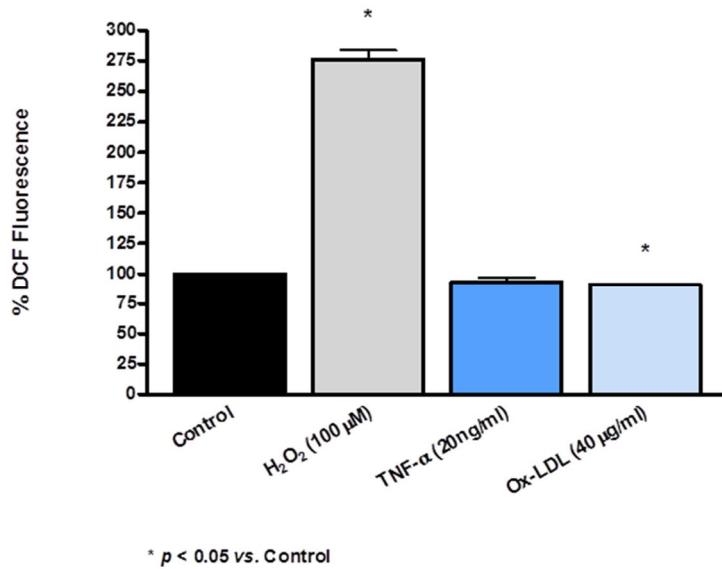


Figure 5.23: Effects of TNF- α (20 ng / ml) and Ox-LDL (40 μ g / ml) on mean DCF fluorescence intensity for 30 minutes. DCF fluorescence expressed as a percentage of control; control = 100%. H₂O₂ (100 μ M) was used as a positive control. Sample size: n = 4 – 6 / group.

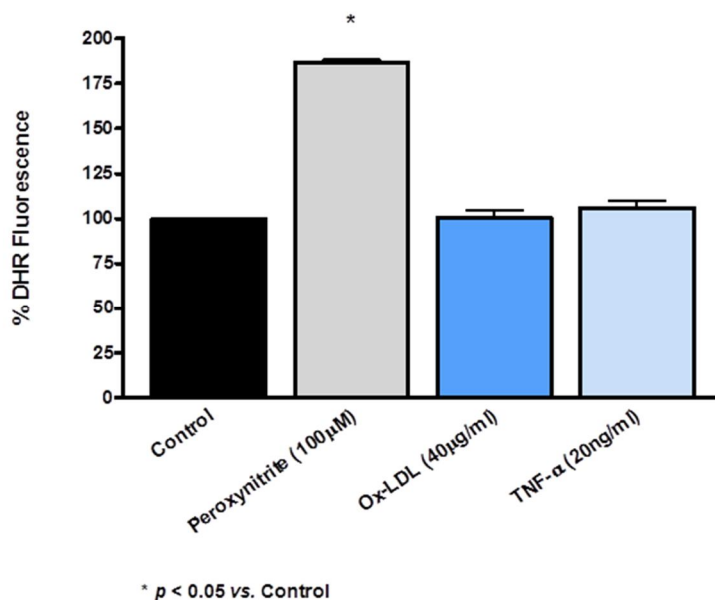
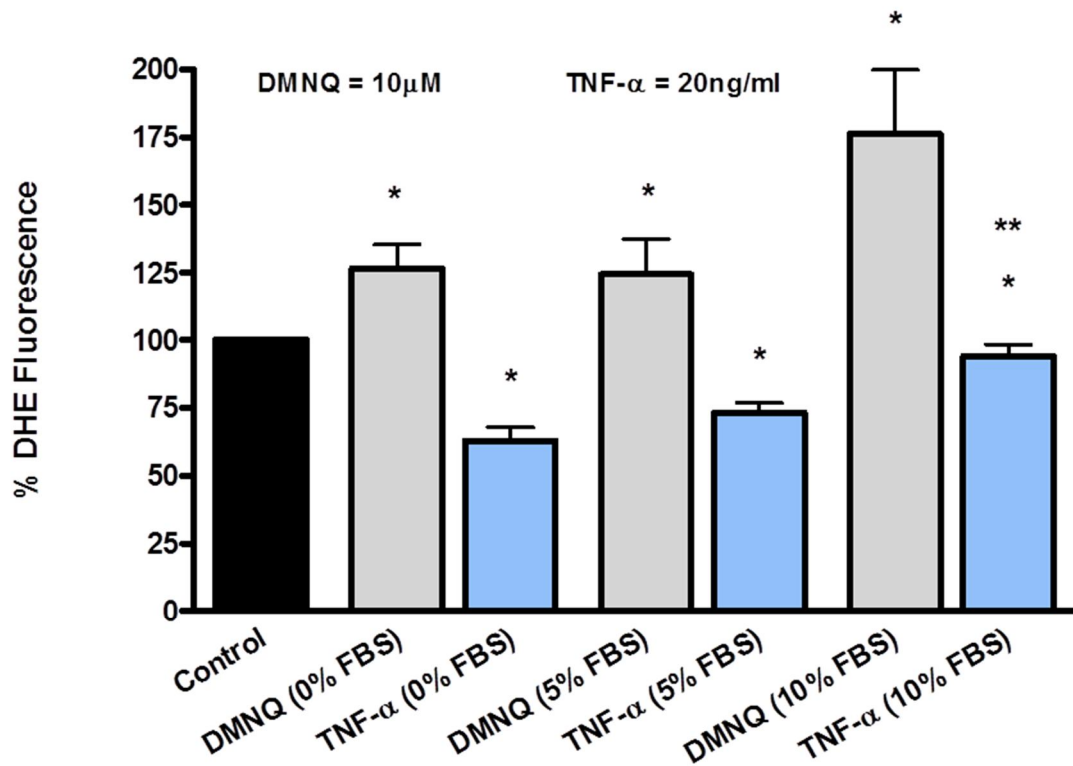


Figure 5.24: Effects of TNF- α (20 ng / ml) and Ox-LDL (40 μ g / ml) on mean DHR-123 fluorescence intensity for 30 minutes. DHR-123 fluorescence expressed as a percentage of control; control = 100%. Authentic peroxynitrite (100 μ M) was used as a positive control. Sample size: n = 4 – 6 / group.

5.4.3 The effects of reduced serum content in growth medium on superoxide production in CMECs treated with TNF- α (20 ng / ml): 24 hours

CMECs exposed to TNF- α (20 ng / ml for 24 hours) (**growth medium = 0 % serum**), showed a significant decrease in mean DHE fluorescence intensity (62.77 ± 4.41 % vs. 100 % control: $p < 0.05$). CMECs exposed to TNF- α (20 ng / ml for 24 hours) (**growth medium = 5 % serum**), showed a significant decrease in mean DHE fluorescence intensity (73.21 ± 3.07 % vs. 100 % control: $p < 0.05$). When CMECs were exposed to TNF- α (20 ng / ml for 24 hours) in 10% serum-containing growth medium, a significant decrease in mean DHE fluorescence intensity was again observed (93.98 ± 3.78 % vs. 100 % control: $p < 0.05$). See figure 5.25 for a graphical representation of the data.



* $p < 0.05$ vs. Control

** $p < 0.05$ vs. TNF- α (0% FBS) & TNF- α (5% FBS)

Figure 5.25: Effects of growth media with different serum contents (0%, 5% and 10% FBS) on mean DHE fluorescence intensity in CMECs treated with TNF- α (20 ng / ml) for 24 hours. DHE fluorescence expressed as a percentage of control; control = 100%. Data presented as DHE fluorescence expressed as a percentage of control; control = 100%). DMNQ (10 μ M) was used as a positive control. Sample size: $n = 4 - 6$ / group.

5.5 **Discussion**

5.5.1 **The effects of different TNF- α concentrations: 0.5, 5 and 20 ng / ml (24 hours)**

24 hours treatment with the lowest concentration of TNF- α administered in this series of experiments (0.5 ng / ml), had no effect on apoptosis (as measured by Annexin V fluorescence) or necrosis (propidium iodide staining), although the two higher concentrations (5 and 20 ng / ml) seemed to be both anti-necrotic and anti-apoptotic (see figures 5.4 & 5.5). In contrast to our findings, other studies found both an increase in necrosis as well as apoptosis, with TNF- α concentrations ranging from 10 – 50 ng / ml and treatment periods ranging from 1 – 30 hours (Corda *et al.*, 2001; Wang P *et al.*, 1994; Luo *et al.*, 2006; Polunovsky *et al.*, 1994). In support of our findings, a study performed on HUVECs treated with 20 ng /ml TNF- α for 1-24 hours also found a decrease in apoptosis (Desphande *et al.*, 2000). The apoptosis data are interesting, as TNF- α is often considered in the literature to be a pro-apoptotic agent (Van den Oever *et al.*, 2010; Ji *et al.*, 2003; Stefanec, 2000). However, a closer inspection of the multitude of pathways that are switched on by TNF-binding to its receptors indicate that TNF- α can equally lead to pro-apoptotic and anti-apoptotic effects even within the same signal transduction pathway (Gaur and Aggarwal, 2003; Li H and Lin, 2008; Chen G and Goeddel, 2002). In further support of our Annexin V data, we performed subsequent measurements of cleaved caspase-3 expression, which was also down-regulated (see Chapter 6).

TNF- α regulates eNOS expression and/or activity, which exerts direct effects on NO production. Many studies have shown that TNF- α significantly decreased eNOS expression in ECs (Zhang J *et al.*, 1997; Goodwin BL *et al.*, 2007; Xia *et al.*, 2006; Seidel *et al.*, 2006), and down-regulated eNOS expression with reduced NO production in diverse vasculatures (Goodwin BL *et al.*, 2007; Gao *et al.*, 2007; Picchi *et al.*, 2006). However, in our hands eNOS expression was increased at all three concentrations (namely 0.5, 5 and 20 ng / ml) (see figure 5.11). The activation of eNOS (serine 1177 phosphorylation), however, was significantly decreased by all three TNF- α concentrations (figure 5.10), a trend that was even more pronounced when the relative phosphorylated eNOS / total eNOS was calculated

(figure 5.12). TNF- α -induced reduction of phosphorylated eNOS was previously also shown in BAECs (Kim HJ *et al.*, 2006a; see Table 1.3).

PKB/Akt is a major upstream activator of eNOS (Manning and Cantley, 2007), and for this reason, we included measurements of PKB/Akt in our experiments. Whereas PKB/Akt expression was down-regulated at all three TNF- α concentrations, activated PKB/Akt (phosphorylated PKB/Akt at serine 473) was decreased at 0.5 ng / ml and 20 ng / ml TNF- α (figures 5.14 & 5.13 respectively), and the relative activation of PKB/Akt (phosphorylated PKB/Akt / total PKB/Akt) was only decreased at 20 ng / ml (figure 5.15). In contrast to our findings, studies that investigated the effects of TNF- α -treatment in endothelial cells (De Palma *et al.*, 2006) and in cardiomyocytes (Hiroaka *et al.*, 2001) showed increased levels of phosphorylated PKB/Akt. However, in support of our findings, a study by Kim F *et al.* (2001) showed that fluid shear stress (FSS) increased phosphorylation of PKB/Akt at Serine 473 in BAECs, but that brief pretreatment with TNF- α (10 ng / ml) before FSS stimulation led to decreased levels of phosphorylation of Serine 473 in PKB/Akt.

Another protein that is closely involved with the eNOS-NO biosynthesis pathway, is HSP 90. HSP 90 is a chaperone protein that plays an important role in post-translational activation of eNOS by increasing eNOS sensitivity to Ca²⁺/calmodulin via HSP 90 – eNOS interaction (Balligand *et al.*, 2009). In addition to the decreased eNOS activation and general trends of PKB/Akt down-regulation, we also found decreased HSP 90 expression (see figure 5.16), which is further indicative of a generalised down-regulation of the PKB/Akt-HSP 90-eNOS enzyme complex. The fact that we did not observe an increase in caveolin-1 at any of three concentrations of TNF- α (see figure 5.17), in fact a decreased expression was found at TNF- α 5 ng / ml, does not fit well with the scenario described above as caveolin-1 is known to inhibit the activity of NOS (Bucci *et al.*, 2000). In view of the overall down-regulated eNOS activity seen in the CMECs, we would have expected caveolin-1 expression to increase, as was shown in a study on BAECs treated with TNF- α (0.5 ng / ml) (Wang L *et al.* 2008).

In human aortic ECs treated with TNF- α for 8 hours, in addition to observing a down-regulation of eNOS expression, the authors found an induction in the mRNA expression of the inducible NOS isoform, iNOS. (MacNaul and Hutchinson, 1993). TNF- α -induced increased expression of iNOS has also been observed in other endothelial cells studies (Chen X *et al.*,

2008; Bereta *et al.*, 1997; Zhang C *et al.*, 2006b). In view of this, in a separate series of investigations, we investigated whether TNF- α (20 ng / ml; 24 hours) would increase iNOS expression in our cells. Our results showed a significant increase in iNOS expression (see figure 5.27). As far as we are aware, this is a novel finding in this cell type.

Most other studies measured the breakdown products of NO as an indication of NO production following TNF- α treatment. In our study, we made use of a direct intracellular and NO-specific measurement assay by FACS analysis of DAF-2/DA fluorescence. Regardless of the method used, a few studies found similar decreases in NO as observed in our study with the 0.5 and 20 ng / ml TNF- α concentrations (Bove *et al.*, 2001; Goodwin BL *et al.*, 2007; Kim HJ *et al.*, 2006a). In order to investigate whether how the TNF- α -induced NO results in the CMECs compared with a different endothelial cell line, we employed a separate series of experiments where we subjected rat aortic endothelial cells (AECs) to TNF- α treatment. Generally, the overall trends were similar between the two cell lines, although it was interesting to note that at TNF- α 5 ng / ml, the NO-production in the AECs was significantly more reduced than in the CMECs and that TNF- α (20 ng / ml) did not exert any effects in the AECs whereas the CMECs responded with a reduction in NO production (see figure 5.28). In order to investigate whether the NO-lowering effects observed in the CMECs at a TNF- α concentration of 20 ng / ml (24 hours) were reversible, we pre-treated the cells with oleanolic acid (OA), a known inducer of the eNOS-NO pathway (Rodriguez-Rodriguez *et al.*, 2008). We pre-administered OA at a concentration of 40 μ g / ml, followed by TNF- α (20 ng / ml) for 24 hours (following the same protocol as described in section 5.3.1). The results showed that pre-treatment with OA abolished the NO-lowering effects of TNF- α , suggesting that the TNF- α effects on NO production were indeed reversible. (see figure 5.26).

In view of the attenuation of NO-production observed in both the CMECs and AECs at 5 ng / ml TNF- α , a fellow postgraduate student in our research group investigated whether pre-treatment with 5 ng /ml TNF- α would negatively affect acetylcholine-induced vasorelaxation in isolated rat aortic ring segments. The data showed attenuation in aortic relaxation, which is indicative of endothelial dysfunction (see figure 5.29).

Collectively, therefore, the investigations so far suggest that TNF- α treatment was able to induce a dysfunctional state in our cells, as is evident from the down-regulation of the eNOS-NO biosynthesis pathway, and further supported by the functional data obtained in the aortic ring segments.

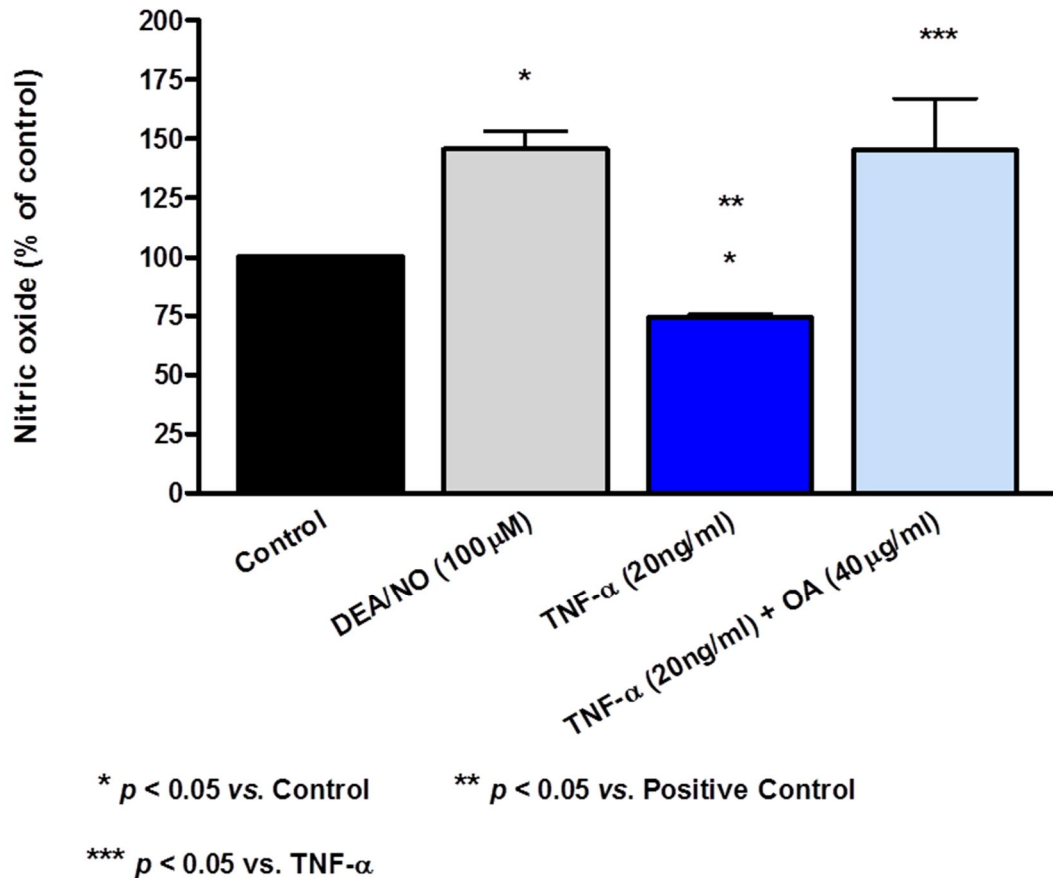


Figure 5.26: The effects of 40 µg / ml OA pre-treatment on the mean DAF-2/DA fluorescence intensity in TNF- α -treated CMECs (20 ng / ml; 24 hours). Data presented as % DAF-2/DA fluorescence (expressed as a percentage of control; control = 100%). The NO-donor, DEA/NO (100µM) was used as a positive control. Sample size: n = 4 – 6 / group.

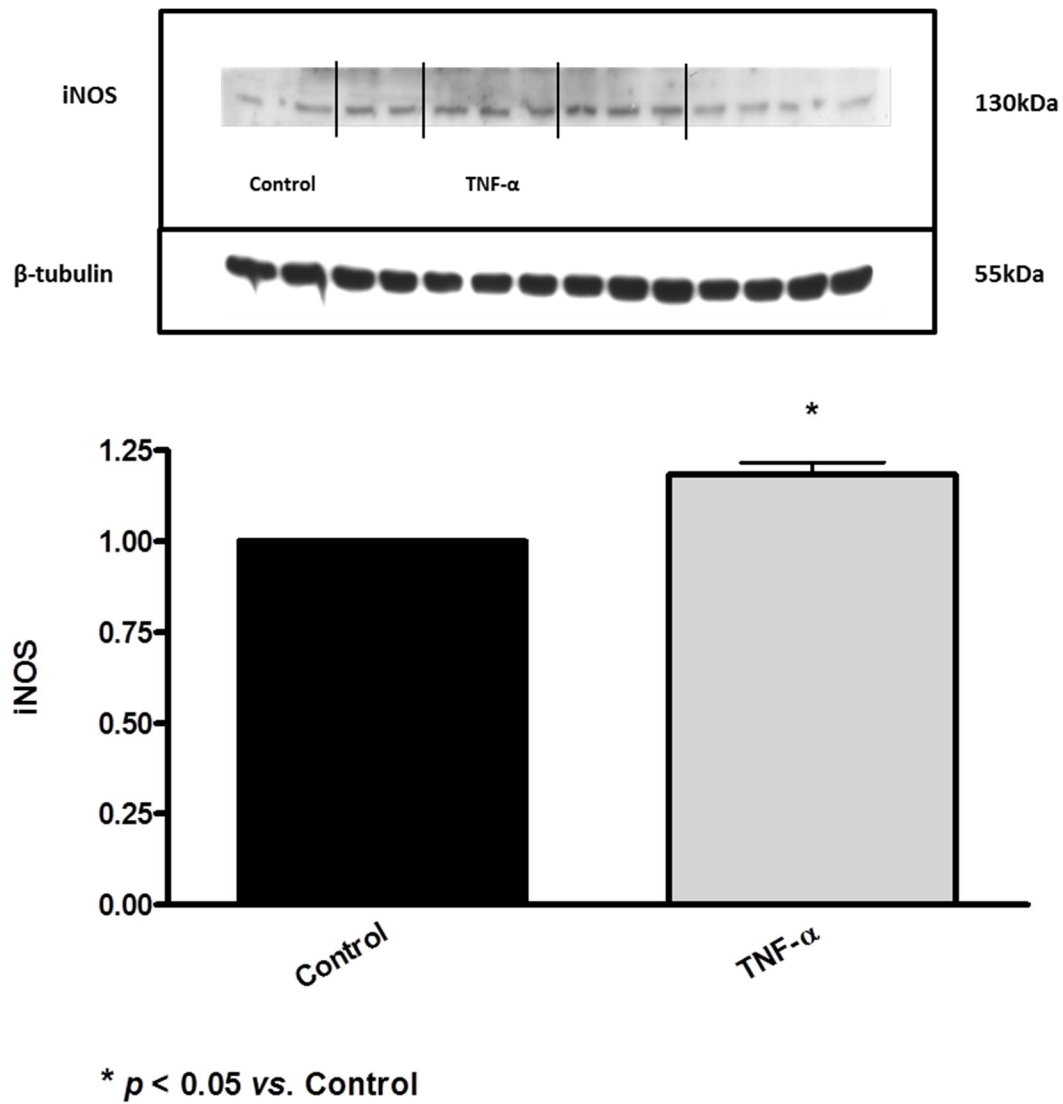


Figure 5.27: The effects of 20 ng / ml TNF- α on iNOS expression. iNOS expression is expressed as a ratio of control; control adjusted to 1 (please refer to page 134, chapter 2). Sample size: n = 4 / group.

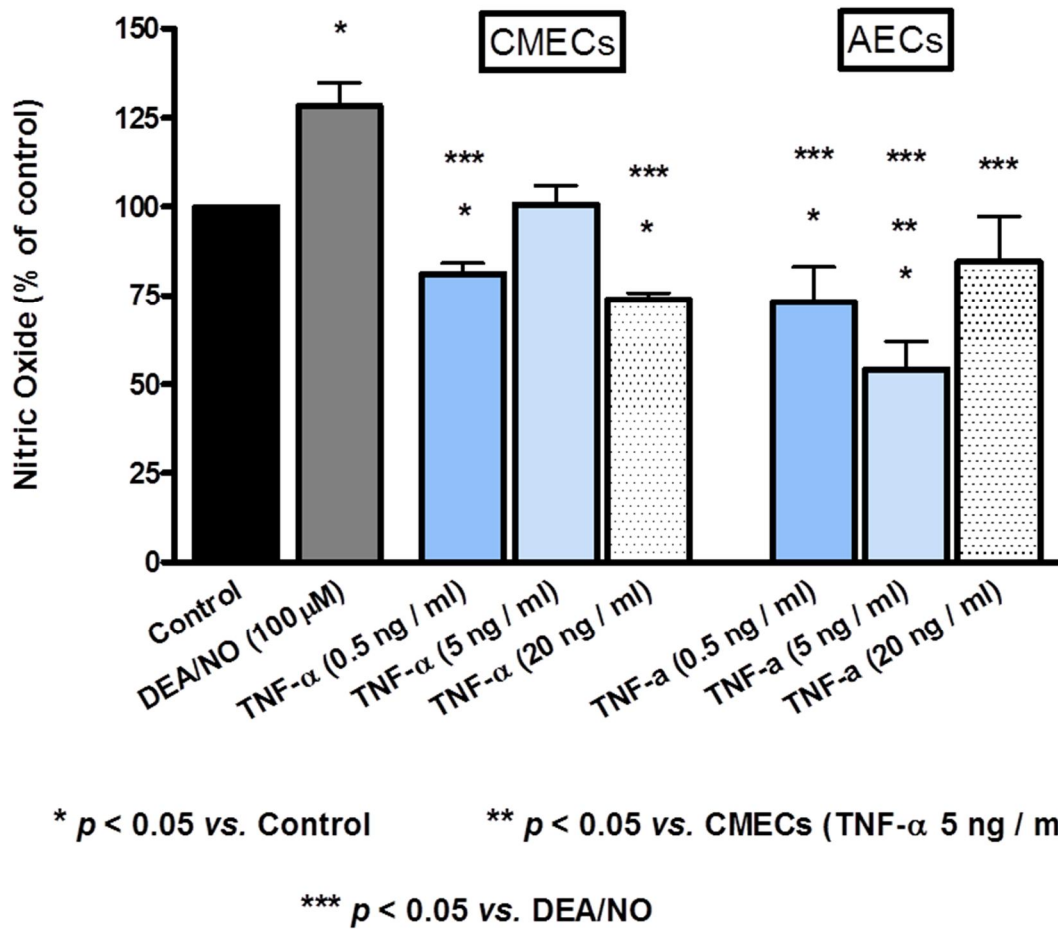


Figure 5.28: TNF- α effects on mean DAF-2/DA fluorescence at different concentrations (0.5, 5 and 20 ng / ml for 24 hours) in CMECs and AECs. Data presented as % DAF-2/DA fluorescence (expressed as a percentage of control; control = 100%). The NO-donor, DEA/NO (100 μ M) was used as a positive control. Sample size: $n = 4 - 6$ / group. (Graph courtesy of Mashudu Mudau).

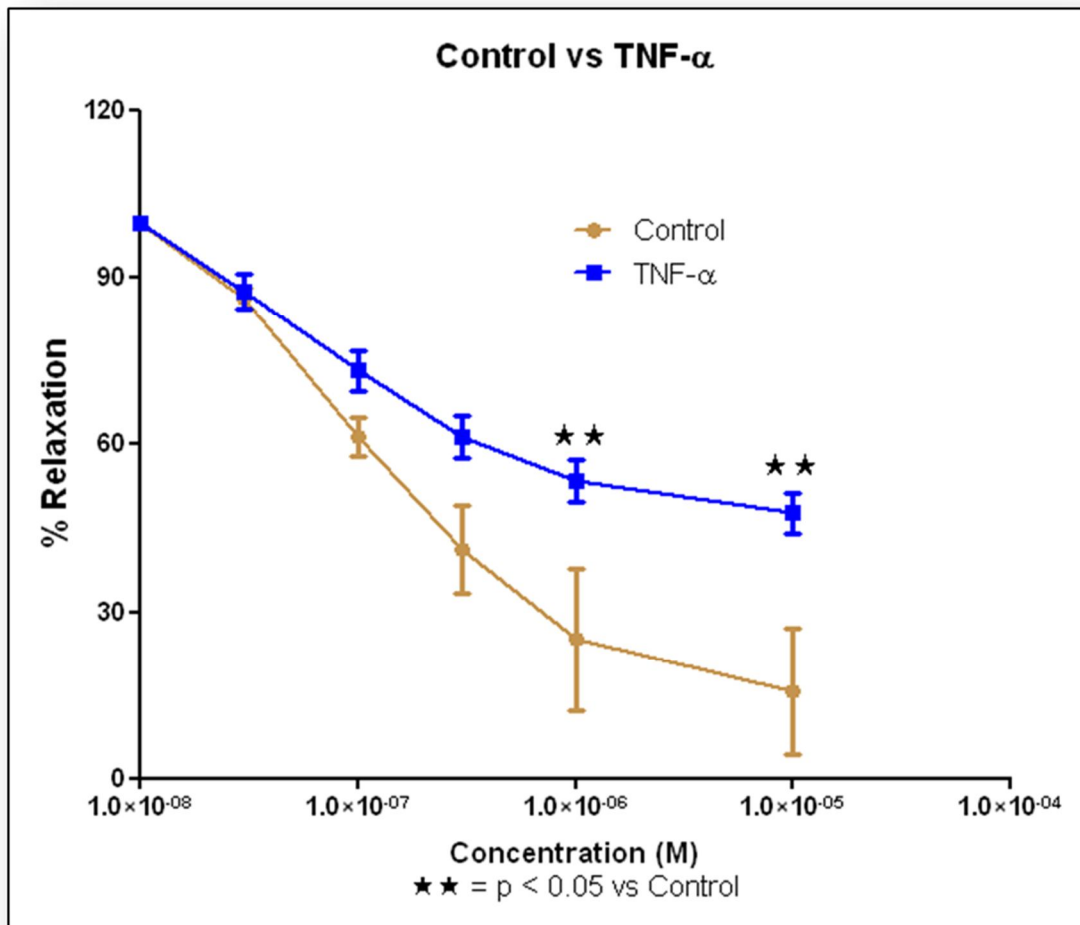


Figure 5.29: Acetylcholine-induced aortic ring relaxation. Rings were pre-contracted with phenylephrine, followed by treatment with 10 ng / ml TNF- α for 30 minutes and finally accumulative acetylcholine administrations to induce endothelial- and NO-dependent vasorelaxation. Data are expressed as % relaxation of maximum pre-contraction. Sample size: n = 4 – 6 / group. (Experiments and figure courtesy of Dirk Loubser, MSc Study).

TNF- α is often associated with increased ROS production in endothelial cells (for review, see: Chen W *et al.*, 2008). TNF- α was shown to induce O₂⁻ production in neutrophils and ECs, reportedly via CAPK (ceramide-activated protein kinase), NADPH oxidase (Sorescu and Griending, 2002), XO (Downey *et al.*, 1991), and NOS (Pritchard *et al.*, 1995; Cai and Harrison DG, 2000). With the exception of a modest increase in DCF fluorescence at TNF- α 20 ng / ml, all the other fluorescent probe results demonstrated an overall reduction in ROS generation following TNF- α treatment (see figures 5.7 – 5.9). This was surprising and difficult to explain in view of the overwhelming evidence in the literature to the contrary, albeit it mainly in other endothelial cell types. We will discuss our strategies to further investigate this phenomenon in the next sections. We further assessed the oxidative stress status of the cells by measuring the expression of p22 phox. As mentioned previously, p22 phox is regarded as a marker of NADPH-oxidase activity, which has been suggested to be the principal source of O₂⁻ production in several animal models of vascular disease (Warnholtz *et al.*, 1999). In endothelial cells, NADPH oxidase activation has been shown to occur in response to TNF- α (Frey *et al.*, 2002). Our p22 phox data were suggestive of a TNF- α dose-dependent increase in NADPH-oxidase-derived oxidative stress (see figure 5.18).

Confirmation of NF- κ B activation: TNF- α is known to induce the transcription of NF- κ B, which regulates the expression of genes involved in inflammation, oxidative stress and endothelial dysfunction (Dela Paz *et al.*, 2007; Rimbach *et al.*, 2000; Kumar A *et al.*, 2004). TNF- α initiates the signalling cascades via IKK α and IKK β (Zhang H *et al.*, 2009). Following TNF- α binding to its receptor 1, the NF- κ B inhibitory protein IKB α is phosphorylated, ubiquitinated and degraded by the proteasome, thus releasing NF-KB to translocate into the nucleus (Zhang H *et al.*, 2009). In our study, we found a dose-dependent decrease in IKB α (see figure 5.20) which is an indication of increased NF-KB activation and an ensuing inflammatory response. Although we did not specifically investigate the association between the NF-KB activation and increased iNOS expression in our CMECs, it is quite possible that the iNOS induction was a result of NF- κ B activation, as iNOS is a known gene target of the activated NF- κ B transcription factor (Aktan, 2004). Furthermore, the activation of NF- κ B may also partly explain the anti-apoptotic findings discussed earlier, as activation of the TNF- α - TNF Receptor 1 – NF-KB pathway is considered by many to inhibit apoptosis (Chen G *et al.*, 2002).

5.5.2 Short term treatment of CMECs with TNF- α (20 ng / ml) for 30 minutes.

An overview of the literature demonstrates that the effects that TNF- α are time-dependent, in addition to being concentration-dependent (Yoshimi *et al.*, 1993; Li C *et al.*, 2002; Li YSJ *et al.*, 2005; Polunovsky *et al.*, 1994; Yan *et al.*, 2008). Whereas some studies have shown an increase in NO production after 24 hours (Wang P *et al.*, 1994; Xia *et al.*, 2006) others showed a decrease in NO after shorter periods of treatment (10 minutes and 1 hours) (Kim HJ *et al.*, 2006; Corda *et al.*, 2001). Furthermore, as mentioned in the previous section, our 24 hour TNF- α data showed a general trend of reduced ROS production, which is contrary to most reports in the literature. Therefore, in the light of this fact, we were interested to determine whether a shorter treatment time would perhaps reveal an early burst of ROS generation which could have been missed at 24 hours. Our data showed that, overall, NO production and ROS production as measured by our various fluorescent probes followed similar trends to the 24 hour findings when exposed to 30 minutes of TNF- α treatment (figures 5.6 – 9 and figures 5.21 - 24).

5.5.3 The effects of reduced serum content in growth medium on superoxide production in CMECs treated with TNF- α (20 ng / ml): 24 hours

Serum reduction or starvation is widely used as a method to induce cell cycle arrest in order to ensure that all cells in a specific tissue culture dish are synchronized (Chen M *et al.*, 2012), similar to the effects achieved when allowing cells to grow to confluency. However, many studies have implemented the method of serum starvation not for the above purpose, but because it is believed that the presence or the amount of serum in the culture medium can “mask” the effect of treatment on oxidative stress or superoxide production in *in vitro* experiments (Tey *et al.*, 2010; Lee SB *et al.*, 2005). Therefore, many studies that measured superoxide production *in vitro*, implemented the serum starvation protocol by either reducing the amount of serum in the medium or culturing the cells in serum-free medium. In the present study, cells that were serum deprived (0% and 5 % FBS-containing growth media) and treated with TNF- α (20 ng / ml) for 24 hours, showed similar decreasing trends in DHE fluorescence than observed in the normal serum-containing medium (10% FBS)

investigations (see figure 5.25). These results show that reducing the serum content, or even removing it completely from the growth medium had no effect on the trends observed with the ROS data in cells incubated with 10% serum-containing growth media. Our data contradict the findings of previous studies conducted on other endothelial cell types. In a study by Basuroy *et al.* (2006), cerebral microvessel endothelial cells (CMVECs) were serum starved (0.1% FBS) overnight and subsequently treated with 15 ng / ml TNF- α for 3 – 6 hours. They found an increase in ROS formation detected by Rh123 and ethidium fluorescence microscopy. In another study, HUVECs were serum starved for 2 hours and treated with 10 ng / ml TNF- α for 8 hours (Szotowska *et al.*, 2007). They found increased ROS levels as was indicated by a lucigenin chemiluminescence assay. An increase in ROS production, as measured by DCF fluorescence, was also found in a study where serum starved HUVECs were treated with 10 ng / ml TNF- α for 1 hour (Lee SJ *et al.*, 2011). In conclusion, our serum reduction experiments suggest that, in our hands, the CMECs did not respond to TNF- α treatment with higher ROS production (as measured by DHE fluorescence) compared to CMECs incubated in normal (10%) serum-containing growth medium. It therefore appears that a possible increase in ROS production was not masked by our choice of 10% FBS enriched growth medium.

5.6 **Conclusion**

In conclusion and as far as we are aware, the findings of this chapter are novel in that no previous studies have characterised the responses to TNF- α treatment at different concentrations and time-points in CMECs in an equally comprehensive manner. We approached the studies in this chapter by making use of various concentrations of TNF- α as well as “short-term” vs. “long-term” treatments. Another factor, namely the amount of serum present in the growth medium was also investigated as a possible contributor to some puzzling results we found in earlier parts of the study, particularly with regard to the surprising observations in the ROS production experiments. Various endpoints were measured to address the different effects of TNF- α on the CMECs. Again (as in the previous chapter), we investigated various intracellular parameters as well as important endothelial

signalling proteins. In our view, the following findings are the most important of this chapter:

- eNOS-NO biosynthesis: As was indicated by many other previous studies, we found an overall down-regulation of the eNOS-NO biosynthesis pathway in a dose-dependent manner, as indicated by the down-regulation of eNOS activity as well as its chaperone HSP 90. This was further supported by the decrease in NO production at 0.5ng / ml and 20 ng / ml, in spite of the modest increase in iNOS expression. Because of the strong link between TNF- α and vascular endothelial dysfunction, these findings come as no surprise, and are in general agreement with the literature. Short-term treatment with the highest concentration of TNF- α had the same effect as long-term treatment (a decrease in NO production). Our data were well supported by additional experiments in which we compared the effects of TNF- α treatment on NO production in the CMECs with a different endothelial cell line (AECs), and we could also demonstrate the probable dysfunctional effect of TNF- α in isolated aortic ring segments.
- ROS production and oxidative stress: The ROS production in TNF- α -treated CMECs was thoroughly investigated, and we made use of no less than three independent probes (DHE, DCF and DHR-123). Surprisingly, the fluorescent probe results pointed to an oxidative- and nitrosative stress free scenario. On the other hand, we also measured NADPH-oxidase activity, which did indeed show concentration-dependent increases (p22 phox expression), whereas nitrotyrosine expression (an important marker of nitrosative stress), was reduced. For these reasons, we found it necessary to re-investigate the ROS production in our cells after TNF- α treatment in two different scenarios. Firstly, with reduced serum in the media, as we speculated that the normal presence (10 %) of serum might be “masking” the effects of TNF- α on ROS production. Secondly, we investigated the effect of TNF- α on ROS production at a shorter incubation time (30 minutes) as the initial ROS production response might have already been lost at 24 hours. Despite all these efforts, the findings remained the same, leading us to speculate, in our hands, the CMECs seemingly did not respond to TNF- α by increasing intracellular ROS production as measured by our chosen fluorescent probes.

CHAPTER SIX

A characterization and investigation of TNF- α -induced responses in CMECs: A proteomic analysis.

6.1 Introduction

As previously shown in chapter 4, the technique of proteomics allows for large-scale characterization and analysis of protein expression and regulation in cells in response to certain experimental manipulations (Anderson and Anderson, 1998). As such, data obtained from proteomic analysis can add valuable insights into protein pathways and mechanisms induced by experimental interventions. Relatively few papers have been published in the field of vascular endothelial proteomics, which is surprising given the importance of endothelial cells in cardiovascular physiology and pathology (Richardson *et al.*, 2010). More particularly, there is a lack of data available on proteomic characterization and regulation in TNF- α stimulated endothelial cells with only a few studies that have exclusively focused on this aspect (Ma *et al.*, 2006; Freed and Greene, 2010). As mentioned before, CMECs are an endothelial cell phenotype found mainly in myocardial capillaries where they participate in an intimate interaction with surrounding cardiomyocytes (Brutsaert, 2003). Consequently, CMECs are regarded as important regulators of myocardial function via the actions of various secretory products such as NO and endothelin-1. CMECs are a distinct member of the vascular endothelial cell family in terms of location, structure, function and role in end-organ myocardial pathology such as ischaemic heart disease (Aird, 2007a). However, there is limited information available on the total protein expression and regulation patterns in this endothelial cell subtype, both with regard to normal and TNF- α stimulated cells. The importance of comprehensively investigating the large-scale protein expression patterns in the context of TNF- α stimulation lies in the fact that many cardiovascular risk factors (e.g. diabetes mellitus and obesity) and cardiovascular diseases (e.g. atherosclerosis and heart failure) have been shown to be associated with a pro-inflammatory environment and thus elevated circulating TNF- α levels (Dandona *et al.*, 2005; Lau *et al.*, 2005; Bruunsgaard *et al.*, 2000; Torre-Amione *et al.*, 1996). One of the primary targets of the actions of harmful

circulating TNF- α is the vascular endothelium. A thorough literature review has revealed that very few proteomics-based studies have been conducted on the effects of TNF- α stimulation, not only in the context of vascular endothelium in general, but more specifically in the context of CMECs. Therefore, in this chapter, we investigated and analysed the CMEC proteome following treatment with TNF- α . With the help of an on-line functional annotation analysis software program, we were able to make observations in terms of protein networks, clusters and pathways that were either strongly represented in the TNF- α -treated cells, or those that were down-regulated. We supplemented the proteomics data with directed additional investigations to further validate the findings.

6.2 **Methods**

For the purposes of the proteomics studies, we decided to treat the cells with 5 ng / ml TNF- α for 24 hours. The rationale behind this decision was mainly determined by the fact that we observed sufficient changes in the flow cytometry and western blot endpoints at this concentration and treatment time. Furthermore, due to budgetary constraints, we did not have the luxury of submitting samples for 0.5, 5 and 20 ng/ml TNF- α treatments. Initially, before we commenced with the main proteomic studies (performed by Dr Salome Smit of the Proteomics Unit of Stellenbosch University), we approached Applied Biomics (San Francisco, USA) to perform a small series of pilot analyses on untreated control and TNF- α (5 ng / ml; 24 hours) treated CMECs. Cells were prepared by performing a protein extraction of TNF- α treated and untreated (control) samples as described in chapter 2 (page 131). A total of 3 samples were prepared for control, untreated and TNF- α treated groups respectively. A protein content of 50 μ g / ml was used as final protein concentration. Protein was subsequently precipitated by adding 1 volume of protein solution to 9 volumes of cold ethanol (100 %). It was then mixed and kept for at least 60 minutes at -20°C . Following the precipitation of the proteins, the suspension was centrifuged for 15 minutes at 4°C in a microcentrifuge at maximum speed (15000 g). The supernatant was carefully discharged and the pellet retained and dried. The pellet was resuspended in ethanol (100 %) and couriered (at room temperature) to Applied Biomics for analysis. The company performed 2-dimensional differential gel electrophoresis (2D-DIGE) from which the spots of interest were

selected. Our instructions to Applied Biomics were to investigate the top differentially regulated (up- or down-regulated) phospho-proteins in the TNF- α samples compared to untreated controls.

Following the pilot studies, we approached the Proteomics Unit of Stellenbosch University to perform the main proteomic analyses on our samples (untreated control CMECs vs. TNF- α -treated CMECs; TNF- α : 5 ng / ml for 24 hours). Preparation of samples for proteomics analysis was performed by one dimensional SDS-PAGE, followed by in gel trypsin digestion (as described in chapter 2, page 135). Thermo Proteome Discoverer 1.3 (Thermo Scientific, Bremen, Germany) was used to identify proteins via automated database searching (Mascot, Matrix Science, London, UK, and Sequest) of all tandem mass spectra against the Uniprot rat database. For the determination of proteins that were only present in either the treated or untreated sample the protein had to be detected in 2 of the 3 replicates but absent in all 3 replicates from the other sample. For protein regulation, SIEVE 1.3 (Thermo Scientific, Bremen, Germany) and Maxquant Proteomics software packages were used. Proteins were only considered differentially regulated with a protein and peptide PEP of 0.01, up or down regulation of ≥ 1.5 -fold and a p-value of $p < 0.05$. These strict criteria were used to ensure that differences in abundance are real and not due to parent ions that had not been detected due to random fluctuations during MS/MS data-dependent acquisition. See figure 5.3 for overview of the proteomic procedures followed in the TNF- α investigations. Data analysis (including functional annotation analyses of proteins) of proteomics results, were performed as described in chapter 2 (page 139).

Additional investigations (e.g. western blots, FACS analyses and fluorescence microscopy) were performed based on standard methods described previously in this dissertation to further support and validate the proteomics findings.

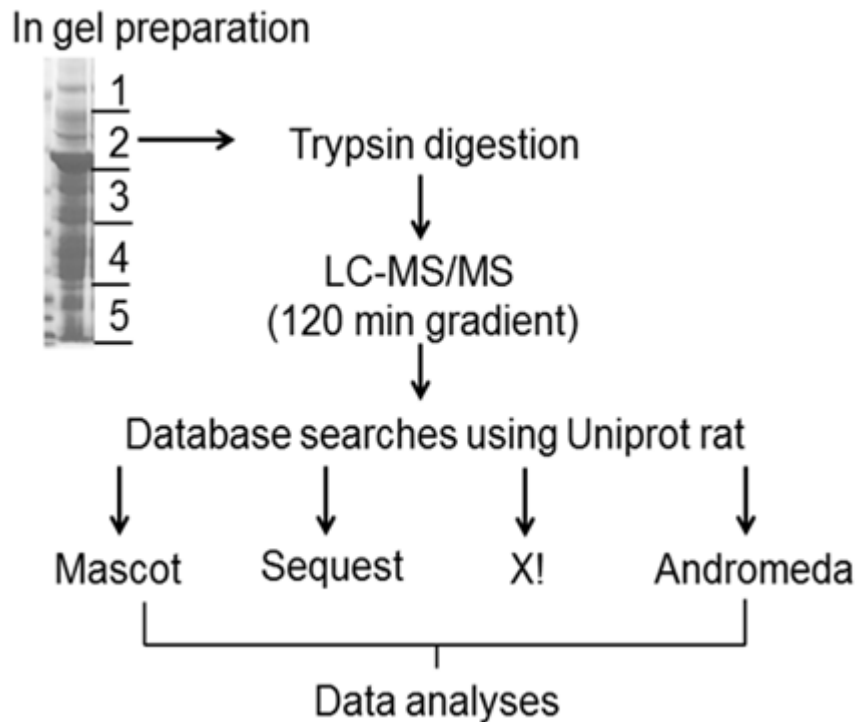


Figure 6.1: Workflow for the proteomic analyses of untreated, control and TNF- α -treated (TNF- α : 5 ng / ml for 24 hours) samples. An equal amount of protein (50 ug / 10 ul) was loaded onto the SDS-PAGE gel. The gel was stained using Coomassie blue and cut into 5 fractions for in-gel trypsin digestion. Peptides from the gel were extracted and prepared for LC-MS/MS. All MS/MS spectra were searched using Thermo Proteome Discoverer software (version 1.3) against in-house versions of Mascot, Sequest, X!tandem and Andromeda. For final data analyses, the identified proteins from all the search engines were combined to obtain a final list of proteins present in the TNF- α treated CMEC proteome. Sample sizes were as follows: Control, untreated: n = 3 and TNF- α treatment: n = 3.

6.3 **Results**

6.3.1 **Pilot studies: 2D-DIGE-phosphoproteomics (Applied Biomics)**

A photograph of the 2D-gel with the full proteome of untreated, control CMECs is shown in figure 6.2. The top high confidence, differentially regulated phospho-proteins in the TNF- α -treated samples, as analysed by Applied Biomics, are shown in Table 6.1. Of note is the pronounced upregulation of heterogeneous nuclear ribonucleoprotein K (hnRNP K) and the downregulation of HSP 90 (see table 6.1 and figure 6.3).

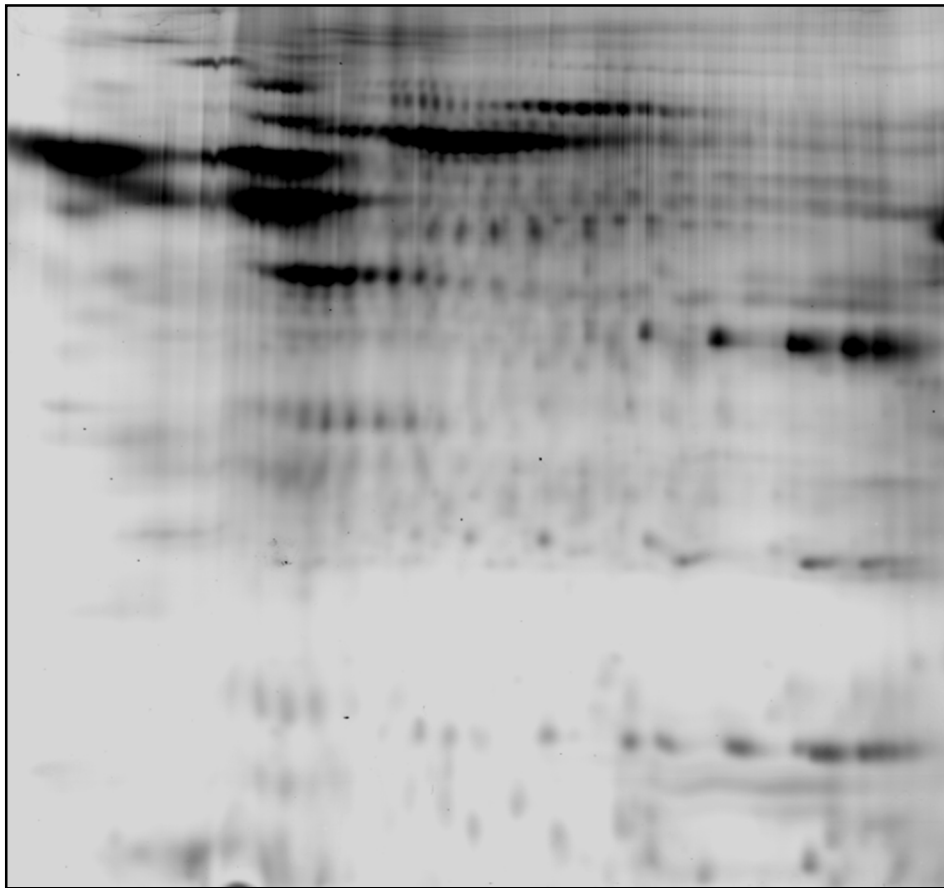


Figure 6.2: A two dimensional gel from Applied Biomics, from which differentially regulated spots were eventually selected for further analysis.

Table 6.1: High confidence differentially expressed phosphorylated proteins in TNF- α treated (5 ng/ml; 24 h) CMECs as determined by 2-D DIGE.

Protein identity	Fold Regulation
Heterogeneous nuclear ribonucleoprotein K, isoform CRA_b [<i>Rattus norvegicus</i>]	↑1.9-fold
Profilin [<i>Rattus norvegicus</i>]	↑ 1.7-fold
Beta-actin [<i>Rattus norvegicus</i>]	↑ 1.6-fold
Ras-related protein Rab-23 [<i>Rattus norvegicus</i>]	↑ 1.6-fold
Zinc finger protein 347 [<i>Rattus norvegicus</i>]	↑ 1.6-fold
Heat shock protein HSP 90-alpha [<i>Rattus norvegicus</i>]	↓ 1.6-fold

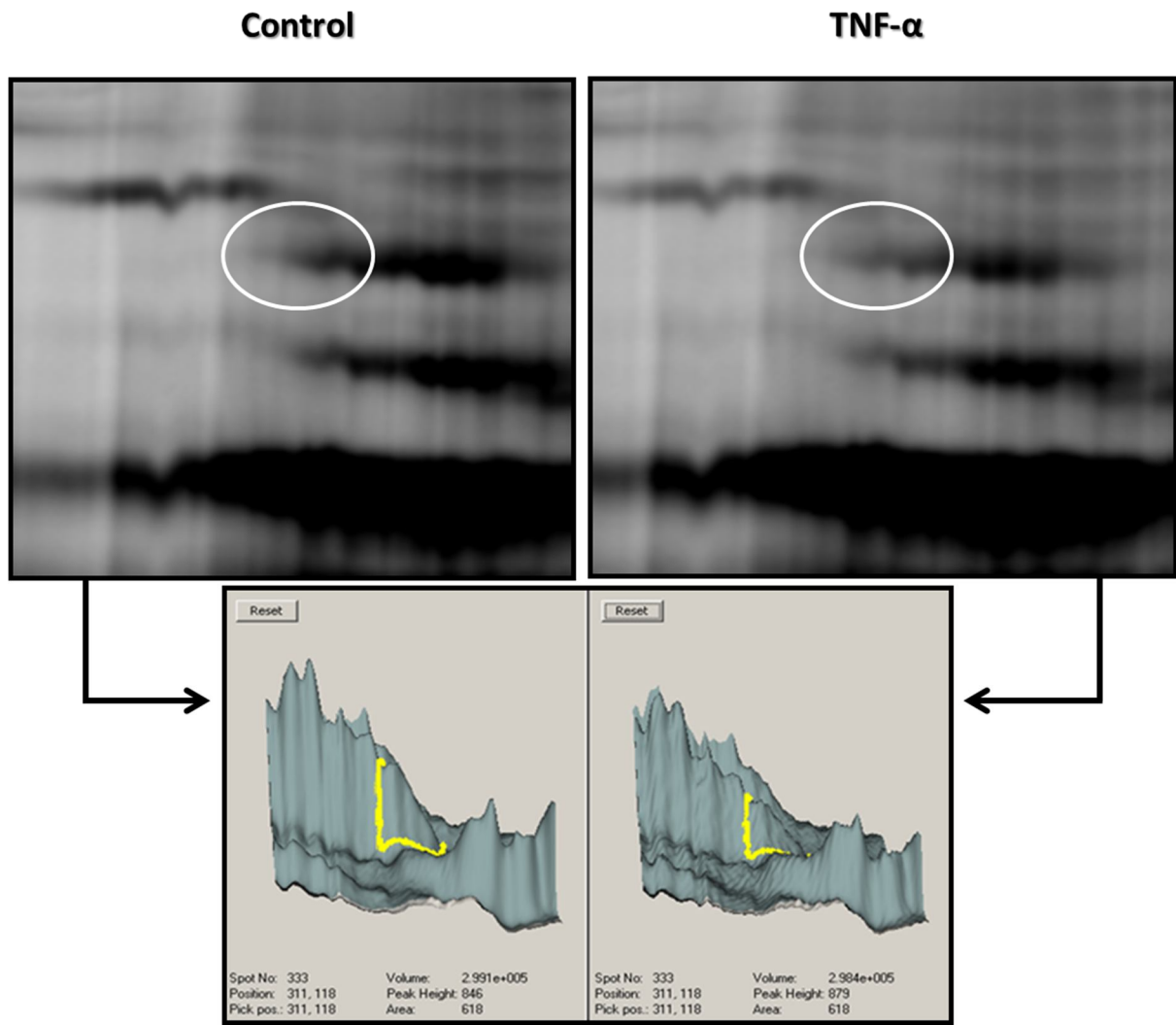


Figure 6.3: The location of the HSP 90-alpha spot indicated on the 2D gel showing reduction in abundance between control (left) and TNF- α -treated (right) samples. Below are the in-gel image analyses of the control and TNF- α HSP 90-alpha spots showing a graphical representation of their 3-dimensional characteristics. Subsequent calculations indicated that the protein was down-regulated by 1.6-fold.

6.3.2 Large-scale protein expression and regulation analyses: Main Study:

Collectively, the Maxquant and SIEVE search engines identified a total of 232 unique proteins that were detected in TNF- α -treated cells only, and not detected in control samples. See Table 6.2 for a selected list of proteins that were detected in TNF- α -treated samples only. Furthermore, the search engines detected a total of 83 proteins that were significantly up-regulated (≥ 1.5 -fold) in TNF- α -treated samples vs. control (see Table 6.3 for a selected list of up-regulated proteins). Conversely, 72 proteins were uniquely expressed in control CMECs only, and whose detection was subsequently lost when cells were treated with TNF- α ; furthermore, 153 proteins were significantly down-regulated (≥ 1.5 -fold) in TNF- α -treated samples. The complete lists of differentially expressed proteins will be supplied electronically.

Clearly, it is impossible to give a complete description of the changes we observed in the expression and regulation of individual proteins. However, some interesting results, which have bearing on the aims of this chapter and dissertation will be listed here and discussed later:

- **Similarities with Applied Biomics 2D-DIGE-proteomics analysis:** HSP 90- α was 5.8-fold and HSP 90- β 4.2-fold down-regulated respectively in TNF- α -treated CMECs (See Table 6.4), which follows the same trend observed in the Applied Biomics data (HSP-90 alpha: 1.6 down-regulation; see figure 6.3).
- **Validation of TNF- α -signalling:** TNF-R1 Death Associated Protein (TRADD) and NF- κ B were expressed only in TNF- α -treated cells, and not untreated control cells (See Table 6.2).
- **Regulation of apoptosis:** Bid (pro-apoptotic; in TNF- α -treated cells only), PEA-15 (anti-apoptotic; in TNF- α -treated cells only), BOK (pro-apoptotic; in TNF- α -treated cells only), metadherin (anti-apoptotic; in TNF- α -treated cells only), and gelsolin (anti-apoptotic; 43-fold down-regulation). See Tables 6.2 – 6.4.
- **Proteins involved with oxidative stress status:** Park-7 (anti-oxidant; in TNF- α cells only), SOD-2, mitochondrial (anti-oxidant; 2-fold up-regulation), SOD-1 (anti-oxidant; 2.4-fold down-regulation). See Tables 6.2-6.4.

- **Mitochondrial proteins:** Acetyl transferase component of pyruvate dehydrogenase (3-fold up-regulation), carnitine-acylcarnitine carrier protein (3-fold up-regulation), acyl CoA dehydrogenase (5-fold up-regulation), isocitrate dehydrogenase (in TNF- α -treated cells only), ADP/ATP translocase 2 (7.6-fold up-regulation), cytochrome C1 (2-fold up-regulation), electron transfer flavoprotein (2-fold up-regulation), VDAC-1 (2-fold up-regulation), cytochrome C oxidase (in TNF- α -treated cells only) and glycerol-3-phosphate dehydrogenase (in TNF- α -treated cells only). See Tables 6.2-6.4.
- **Proteins involved with inflammatory / immune response:** RT1 class I histocompatibility antigen (in TNF- α -treated cells only), complement C4 (2.2-fold up-regulation), intercellular adhesion molecule 1 (7.2-fold up-regulation), interferon-induced guanylate-binding protein 2 (6.9-fold up-regulation), interleukin 1 family (in TNF- α -treated cells only), and prostaglandin E synthase 3 (1.58-fold up-regulation). See Tables 6.2-6.4.

It is customary to validate proteomic analysis data by reproducing the trends observed in differentially regulated proteins with an alternative measurement technique. We chose to validate the down-regulation of HSP 90, as shown by both Applied Biomics (see figure 6.3) and by the Proteomics Unit of Stellenbosch University (see Table 6.4) by performing western blot analysis of HSP 90 in control and TNF- α -treated cells. The western blot results also showed a significant down-regulation as shown in figure 6.4).

Table 6.2: Selected list of strongly represented proteins (detected in TNF- α samples only)

Accession Number	Protein IDs
Q5U318	Astrocytic phosphoprotein PEA-15
Q6QI09	ATP synthase gamma chain
P31399	ATP synthase subunit d, mitochondrial
Q792S6	Bcl-2-related ovarian killer protein (BOK)
Q9JLT6	BH3-interacting domain death agonist (BID)
P05503	Cytochrome c oxidase subunit 1
P10888	Cytochrome c oxidase subunit 4 isoform 1, mitochondrial
P04904	Glutathione S-transferase alpha-3
P24473	Glutathione S-transferase kappa 1
D3ZGW4	Glutathione S-transferase Mu 1
P35571	Glycerol-3-phosphate dehydrogenase, mitochondrial
D4A1I2	Interleukin 1 family, member 6 (Predicted)
P41565	Isocitrate dehydrogenase [NAD] subunit gamma 1, mitochondrial
F1LQ51	Jak1
Q5U2Z4	Nuclear factor of kappa light polypeptide gene enhancer in B-cells 2, p49/p100
D3ZVI9	Parkinson disease 7 domain containing 1 (PARK-7)
D3ZGX7	Metadherin
P16391	RT1 class I histocompatibility antigen, AA alpha chain
D3Z8V9	Signal transducer and activator of transcription 3 (Stat3)
D3ZZC5	TNFRSF1A-associated via death domain (Tradd)

Table 6.3: Selected list of strongly represented proteins (up-regulated in TNF- α samples)

Accession No	Protein Name	Fold Up-Regulation	p-value
Q09073	ADP/ATP translocase 2	7.6	0.001
P08649	Complement C4	2.2	0.03
D3ZFQ8	Cytochrome c_1	1.8	9.6×10^{-9}
P08461	Acetyltransferase component of pyruvate dehydrogenase complex, mitochondrial	2.8	0.04
P13803	Electron transfer flavoprotein subunit alpha_ mitochondrial	1.6	9.9×10^{-20}
P63245	RACK-1; Guanine nucleotide-binding protein subunit beta-2-like 1	2.7	0.01
Q00238	Intercellular adhesion molecule 1	7.2	0.01
Q63663	Interferon-induced guanylate-binding protein 2	6.9	0.0005
P97521	Mitochondrial carnitine /acylcarnitine carrier protein	2.7	0.04
O35244	Peroxiredoxin_6	2.0	9.9×10^{-20}
P83868	Prostaglandin E synthase 3	1.58	0.0004
P07895	Superoxide dismutase [Mn], mitochondrial; SOD-2	2.0	0.0005
P45953	Acyl-CoA dehydrogenase, mitochondrial	5.1	0.02
Q9Z2L0	Voltage-dependent anion-selective channel protein 1 (VDAC-1)	1.6	3.3×10^{-16}

Table 6.4: Selected list of underrepresented proteins (down-regulated in TNF- α samples)

Accession No	Protein Name	Fold Down-Regulation	p-value
Q68FP1	Gelsolin	42.9	7.6×10^{-12}
P04906	Glutathione S-transferase P	2.6	9.9×10^{-20}
P30713	Glutathione S-transferase theta-2	1.5	0.03
P82995	Heat shock protein HSP 90-alpha	5.8	0.008
P34058	Heat shock protein HSP 90-beta	42.1	9×10^{-11}
Q9R063	Peroxiredoxin-5-mitochondrial	2.0	0.0002
P35704	Peroxiredoxin-2	5.6	7.7×10^{-13}
O35244	Peroxiredoxin-6	11.5	9.9×10^{-20}
P07632	Superoxide dismutase [Cu_Zn]; SOD-1	2.4	5×10^{-9}

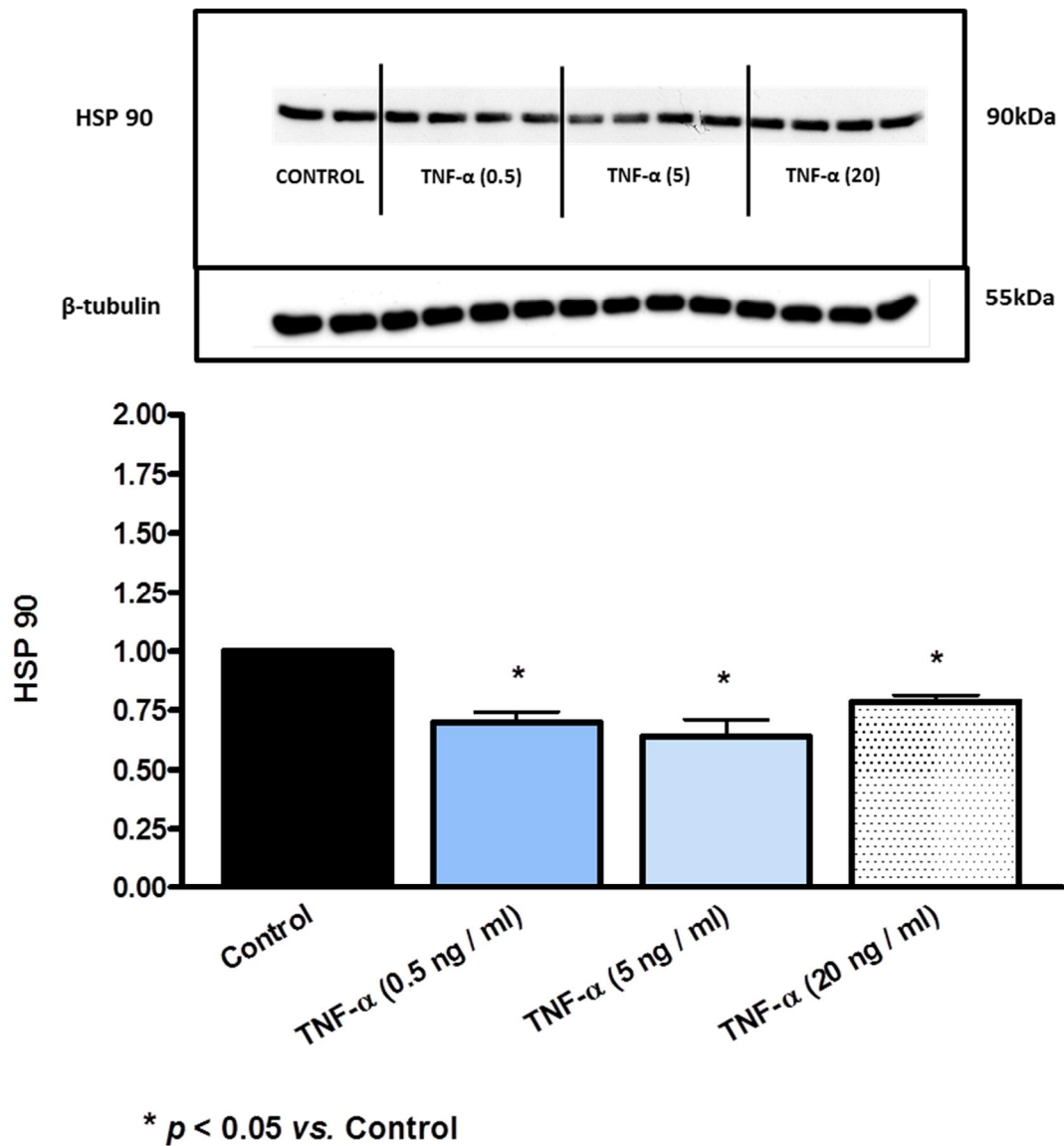


Figure 6.4: A western blot analysis of CMECs treated with 0.5, 5 and 20 ng / ml TNF- α for 24 hours, showing a decrease in HSP 90 expression when compared to control. Data expressed as a ratio of control; control adjusted to 1 (please refer to page 134, chapter 2). Sample size: $n = 4$ / group.

Next, we submitted the list of the **strongly represented** proteins in TNF- α -treated CMECs, i.e. proteins identified only in TNF- α -treated samples ($n = 232$ proteins) plus proteins significantly upregulated by TNF- α ($n = 83$) to the DAVID functional annotation analysis tool in order to gain insight into the functional processes and pathways with which the strongly represented proteins were associated. See Tables 6.2, 6.3 and 6.4 for the cellular components, biological processes and molecular functions respectively associated with the strongly represented proteins. Similarly, we submitted the list of **underrepresented proteins** in TNF- α -treated CMECs, i.e. proteins that were identified in control samples, but whose detection was lost in TNF- α -treated samples ($n=72$) and proteins that were significantly down-regulated in TNF- α samples ($n=153$) for functional annotation analysis. See Tables 6.5, 6.6 and 6.7 for the cellular components, biological components and molecular functions respectively associated with the underrepresented proteins. The most prominent findings from the functional annotation analyses are as follows:

Strongly represented proteins in TNF- α -treated CMECs: From the *cellular component analyses* (Table 6.5) it is clear that mitochondrial proteins were well represented and highly enriched. Cytoskeletal and proteasomal proteins were also well represented. The *biological processes analyses* (Table 6.6) revealed a high enrichment and representation of translation, protein transport and proteasomal degradation. Furthermore proteins involved with responses to oxidative stress, ROS, glutathione metabolism and oxidation-reduction reactions were highly enriched, as were the processes of nitric oxide biosynthesis and apoptosis. In the *molecular functions* category (Table 6.7), anti-oxidant and oxido-reductase activity featured prominently, as did glutathione peroxidase activity.

Underrepresented proteins in TNF- α -treated CMECs: Proteins involved with *cellular components* that were highly enriched included actin cytoskeletal proteins and ribosomal proteins (Table 6.8). In the *biological processes* category (Table 6.9), cytoskeleton organisation, proteasomal catabolic processes, vesicle-mediated transport and cell cycle were enriched. Ribosomal biogenesis also featured prominently, as did glutathione metabolism. Interestingly, glutathione metabolism was equally enriched in the strongly represented and underrepresented category, pointing to an equal “gain” and “loss” of proteins involved with this aspect of anti-oxidant activity with TNF- α -treatment. Glycolysis

was also highly enriched, despite the modest number of proteins associated with this process. With regard to the *molecular function analyses* (Table 6.10), ribosome binding was significantly enriched. Structural molecule activity also featured prominently. Interestingly, peroxiredoxin (a ubiquitous anti-oxidant system) activity was very highly enriched in the underrepresented protein list, as was GTP-ase activity.

Table 6.5: Cellular components associated with TNF- α -induced up regulated proteins and proteins detected only in TNF- α stimulated cells.

CELLULAR COMPONENT (GO TERMS)	NUMBER OF PROTEINS	P-VALUE	FOLD ENRICHMENT
1. Cytosol	50	8×10^{-13}	3.0
2. Mitochondrion	51	1×10^{-11}	2.7
3. Mitochondrial inner membrane	19	2×10^{-7}	4.5
4. Mitochondrial matrix	13	0.00001	5.0
5. Cytoskeleton	28	0.0006	2.0
6. Proteasome complex	6	0.001	7.5
7. Cytoplasmic membrane-bounded vesicle	16	0.01	2.0
8. Internal side of the plasma membrane	8	0.01	3.3
9. Extrinsic to membrane / peripheral membrane proteins	10	0.04	2.2
10. Mitochondrial nucleoid (mitochondrial DNA)	4	0.009	9.3

Table 6.6: Biological processes associated with TNF- α -induced up regulated proteins and proteins detected only in TNF- α stimulated cells.

BIOLOGICAL PROCESS (GO TERMS)	NUMBER OF PROTEINS	P-VALUE	FOLD ENRICHMENT
1. Protein transport	21	0.00006	2.77
2. Translation	18	0.00008	3.05
3. Coenzyme metabolism	10	0.0004	4.5
4. Glutathione metabolism	5	0.0006	12.5
5. Response to oxidative stress	10	0.0009	4.0
6. Response to reactive oxygen species	7	0.002	5.5
7. Response to hydrogen peroxide	6	0.004	5.8
8. Mitochondrial organisation and biogenesis	8	0.001	5.1
9. Mitochondrial transport	5	0.004	7.7
10. Apoptosis	14	0.005	2.5
11. Regulation of nitric oxide biosynthesis	4	0.006	10.7
12. Inhibition of cellular protein metabolism	8	0.008	3.5
13. Mitochondrial membrane organization	4	0.009	9.0
14. Oxidation reduction process	17	0.01	2.0
15. Intermediary metabolism	9	0.02	2.7
16. Nicotinamide metabolism	4	0.02	6.9
17. Immune system development	9	0.03	2.5
18. Regulation of protein ubiquitination	5	0.03	6.3
19. Oxidoreduction coenzyme metabolic process	4	0.03	5.6
20. Proteasomal protein catabolic process	5	0.03	4.4

Table 6.7: Molecular functions associated with TNF- α -induced up regulated proteins and proteins detected only in TNF- α stimulated cells.

MOLECULAR FUNCTION (GO TERMS)	NUMBER OF PROTEINS	P-VALUE	FOLD ENRICHMENT
1. Antioxidant activity	6	0.0003	9.9
2. Nucleotide binding	46	0.0003	1.7
3. Oxidoreductase activity, acting on peroxide as acceptor	5	0.0006	12.7
4. Unfolded protein binding	6	0.005	5.3
5. Glutathione peroxidase activity	3	0.01	19.4
6. Protein kinase binding	8	0.01	3.2
7. Coenzyme binding (acyl-CoA; FAD; FMN; NAD; NADP)	9	0.01	2.8
8. Lipid binding	11	0.03	2.2
9. Phospholipid binding	6	0.04	3.1
10. GTP-ase activity	5	0.04	3.6

Table 6.8: Cellular components associated with TNF- α -induced down regulated proteins and proteins detected only in control (untreated) cells.

CELLULAR COMPONENT (GO TERMS)	NUMBER OF PROTEINS	P-VALUE	FOLD ENRICHMENT
1. Cytosol	50	8×10^{-15}	3.3
2. Cytoskeleton	42	3×10^{-12}	3.3
3. Non-membrane-bounded organelle	58	5×10^{-11}	2.4
4. Intermediate filament: cytoskeleton	10	0.00001	7.2
5. Ribosomal subunit	9	0.00001	8.1
6. Actin cytoskeleton	13	0.00002	4.6
7. Cytoplasmic membrane-bounded vesicle	20	0.00006	2.9
8. Proteasome complex	7	0.00008	9.7
9. Protein-RNA (ribonucleoprotein) complex	16	0.003	2.4
10. Ribosome	12	0.005	2.7

Table 6.9: Biological processes associated with TNF- α -induced down regulated proteins and proteins detected only in control (untreated) cells

BIOLOGICAL PROCESS (GO TERMS)	NUMBER OF PROTEINS	P-VALUE	FOLD ENRICHMENT
1. Cytoskeleton organization	21	0.0000001	5.0
2. Regulation of protein ubiquitination	9	0.000006	8.9
3. Protein transport	20	0.00001	3.1
4. Proteasomal protein catabolic process	8	0.00004	8.5
5. Translation	16	0.0001	3.3
6. Cell cycle	16	0.0002	3.0
7. Regulation of protein metabolism	15	0.0003	3.2
8. Activation of enzyme activity	15	0.0005	3.0
9. Vesicle-mediated transport	14	0.001	2.8
10. Protein catabolic process	12	0.001	3.2
11. Ribosome biogenesis	6	0.004	5.8
12. Response to reactive oxygen species	6	0.004	5.7
13. Glutathione metabolism	4	0.004	12.1
14. Small GTPase mediated signal transduction	9	0.004	3.5
15. Cell redox homeostasis	5	0.006	7.0
16. Oxidation reduction	15	0.009	2.1
17. Regulation of apoptosis	16	0.01	2.1
18. Response to hydrogen peroxide	5	0.01	5.8
19. Cellular homeostasis	12	0.01	2.3
20. Glycolysis	4	0.01	7.8

Table 6.10: Molecular functions associated with TNF- α -induced down regulated proteins and proteins detected only in control (untreated) cells.

MOLECULAR FUNCTION (GO TERMS)	NUMBER OF PROTEINS	P-VALUE	FOLD ENRICHMENT
1. Structural molecule activity	27	6×10^{-9}	3.8
2. GTP-ase activity	11	3×10^{-7}	9.1
3. Nucleotide binding	48	1×10^{-6}	2.0
4. Cytoskeleton protein binding	15	0.0003	3.1
5. Ribosome binding	4	0.0008	20.0
6. Structural component of ribosome	12	0.001	3.3
7. Peroxiredoxin activity	3	0.003	34.8
8. ATP binding	27	0.004	1.8
9. RNA binding	13	0.008	2.4
10. Antioxidant activity	4	0.02	7.6

6.4 **Discussion**

6.4.1 **Pilot Studies: Applied Biomics**

In this series of investigations, we subjected our control and TNF- α stimulated CMECs (5 ng / ml; 24h) to a 2D-DIGE-based proteomic analysis. In Table 6.1 those phosphorylated proteins that demonstrated the greatest degree of differential expression are highlighted. For the purposes of this chapter, we will only discuss the up-regulation of heterogeneous nuclear ribonucleoprotein K, isoform CRA_b (HnRNP K), which showed the greatest up-regulation in the TNF- α -treated cells (1.9-fold increase). In a previous study on cultured cell lines, hnRNP K was responsible for repression of the pro-apoptotic Bcl-x_s isoform of Bcl-x (Revil *et al.*, 2009). It is therefore possible that the significant upregulation of hnRNP K formed part of a pro-survival (anti-apoptotic) phenotype elicited in our TNF- α stimulated CMECs. The down-regulation of HSP 90 will be discussed later, as this was also observed in the analyses conducted at our university's proteomics unit.

6.4.2 **The main study: Proteomic analysis of TNF-alpha (5 ng / ml) treated CMECs (performed at the Proteomics Unit, Stellenbosch University).**

Two protein identification and quantification software packages were used to analyse the control and TNF- α -treated proteomes, namely *MaxQuant* (<http://www.maxquant.org/>) and *Sieve* (http://www.thermo.com/eThermo/CMA/PDFs/Various/File_53659.pdf). Maxquant software identified a total of 1102 proteins and Sieve a total of 1511 proteins. Collectively, there were 232 proteins that were identified in TNF- α -treated samples only, and 83 proteins that were up-regulated in TNF- α -treated samples compared to control. Conversely, there were 72 proteins detected only in control samples and 153 down-regulated proteins in TNF- α -treated samples vs. control. As a comparison, in one of only a few studies that comprehensively analysed the proteome in TNF- α -treated endothelial cells, Ma *et al.* (2006) treated HUVECs with 25 ng / ml TNF- α for 18 hours. There were 1243 ± 48 protein spots on the 2D-gel map. Differential analysis showed 21 protein spots that were different in

intensity including 9 expression increased protein spots and 11 expression decreased protein spots following TNF- α stimulation (Ma *et al.*, 2006).

In order to simplify the discussion, the differentially regulated proteins in TNF- α -treated CMECs are categorised as either "*strongly represented proteins*" or "*underrepresented proteins*". Strongly represented proteins refer to those identified proteins that were unique to the TNF- α -treated CMECs, i.e. they were not detected in untreated control samples. Proteins that were significantly up-regulated (≥ 1.5 -fold; $p < 0.05$) in TNF- α -treated cells were also included in the strongly represented protein category. The underrepresented protein category was made up of proteins that were detected in control CMECs, but whose detection was lost in the TNF- α -treated cells as well as proteins that were significantly down-regulated (≥ 1.5 -fold; $p < 0.05$) in TNF- α -treated cells. For reference, please see Tables 6.2 – 6.4 for selected lists of differentially regulated proteins identified in the CMECs. Complete lists of all the differentially regulated proteins will be supplied electronically.

TNF- α -signalling: Activated TNF- α receptor 1 (TNFR1) recruits TNFR1-associated death domain protein (TRADD), which in turn triggers two opposite signalling pathways leading to caspase activation for apoptosis induction and NF- κ B activation for anti-apoptotic, pro-inflammatory protein upregulation (Wang Y *et al.*, 2000) (see figure 6.5). TRADD as well as NF- κ B were strongly represented in our TNF- α treated CMECs (see Table 6.2) and this suggests that both the classical TNF- α – TNF receptor 1 – TRADD and TNF- α – TNF- α receptor 1 - NF- κ B pathways were induced by exogenous TNF- α administration in our CMECs. As shown in Chapter 5, we investigated the induction of the NF- κ B pathway by measuring the expression of the NF- κ B inhibiting protein, I κ B- α (surrogate marker of NF- κ B activation), and the western blot results showed a significant down-regulation of I κ B- α , indicative of proteasomal degradation and hence NF- κ B activation (see figure 6.5).

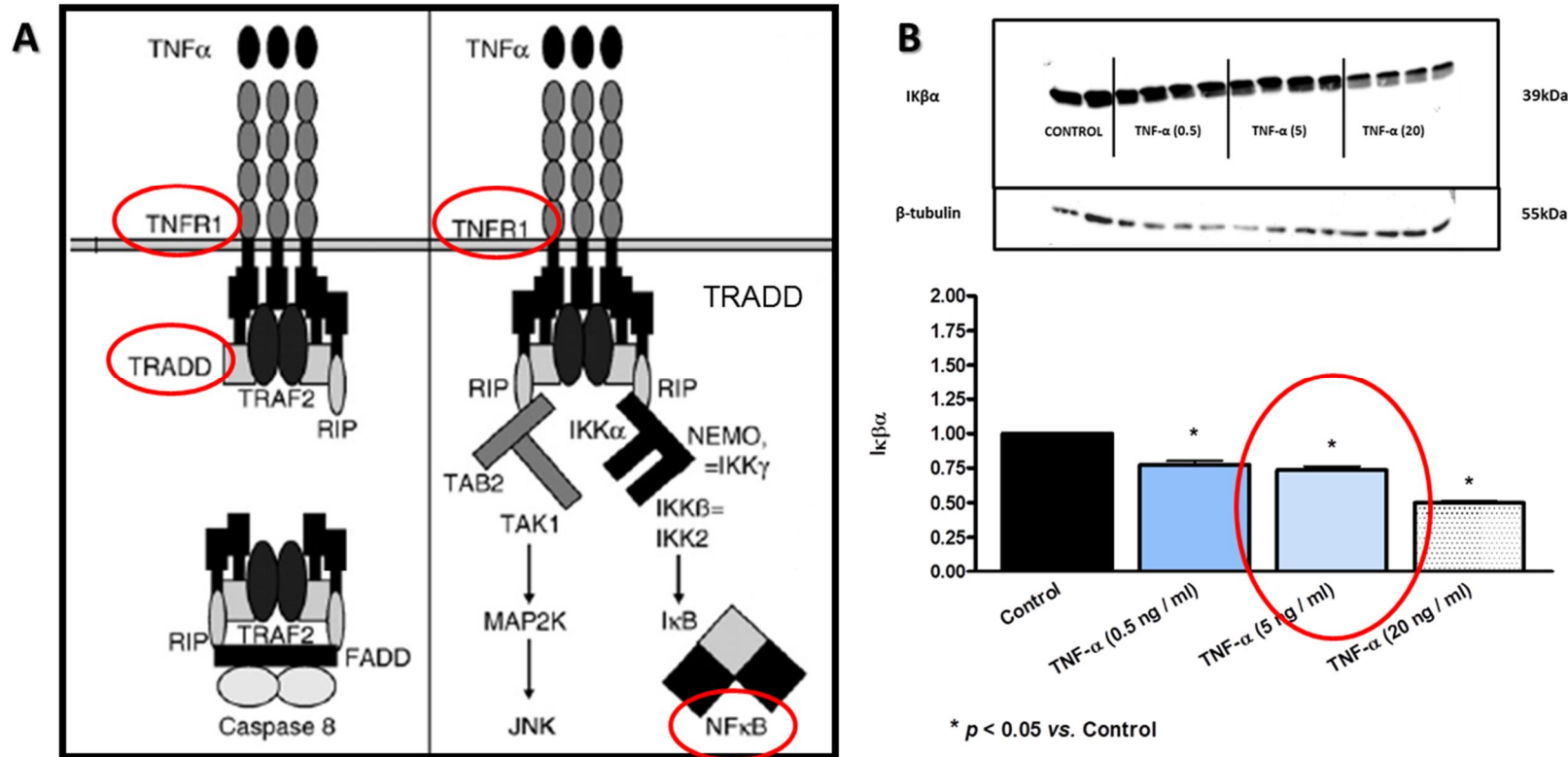


Figure 6.5: A: Classical signalling pathways of TNF-α receptor type 1 (TNFR1), showing activation of TRADD and NF-κβ (Corda *et al.*, 2001).

B: Western blot analysis of CMECs treated with 5 ng / ml TNF-α for 24 hours, showing a decrease in IKβα expression when compared to control. Data were expressed as a ratio of control with control adjusted to 1 (please refer to page 134, chapter 2). Sample size: n = 4 / group.

Apoptosis: The apoptotic regulation that ensued from the intracellular TNF- α -signalling revealed a mixed picture, including evidence of the induction of both pro-apoptotic and anti-apoptotic pathways. This phenomenon is not surprising, in view of the fact that activation of the TNF- α receptor 1 complex can give rise to apoptosis (via TRADD) and anti-apoptosis (via NF- κ B). Activation of the TNF- α receptor 1 – TRADD complex can give rise to a signalling pathway that eventually activates caspase-8, which in turn activates (cleaves) caspase-3 leading to the induction of apoptosis (see figure 6.6). The proteomic data showed that astrocytic phosphoprotein PEA-15 (PEA-15), which is a known inhibitor of TNF-R1-mediated caspase 8 activity, was strongly represented in TNF- α treated CMECs (see Table 6.2). The inhibition of caspase 8 was further validated by western blot analysis of cleaved caspase-3 (downstream target of caspase-8). Results showed that cleaved caspase-3 expression was significantly down-regulated in the TNF- α -treated CMECs (see figure 6.7). In contrast to our findings, another study found a significant increase in caspase-3 activity in TNF- α treated (10 ng / ml for 12 hours) rat vascular endothelial cells (Freed and Greene, 2010). In summary, our findings indicate that although TRADD was up-regulated, the caspase-8 – caspase-3 pathway appeared to be down-regulated, possibly by the actions of PEA-15. Another example of an anti-apoptotic effect elicited by TNF- α -treatment was the strong representation of metadherin (see Table 6.2). On the other hand, the proteomic data showed that other pro-apoptotic proteins were strongly represented in the TNF- α -treated samples. Examples of such proteins included BH3-interacting domain death agonist (BID) and Bcl-2-related ovarian killer protein (BOK) (see Table 6.5). BID is involved with a pro-apoptotic signalling cascade leading to the release of cytochrome C from mitochondria (see figure 6.8). BOK is also thought to mediate apoptosis via mitochondrial release of cytochrome C (Rodriguez *et al.*, 2006). Finally, the proteomic data showed a significant underrepresentation of the anti-apoptotic protein, gelsolin (~ 43-fold down-regulation; see Table 6.4). With regard to functional annotation analyses, TNF- α -treatment induced a strong representation of 14 proteins associated with the biological process of apoptosis (2.5-fold enrichment; $p = 0.005$) (Table 6.6), whereas 16 proteins associated with apoptosis regulation were underrepresented in the TNF- α cells (2.1-fold enrichment; $p = 0.01$) (Table 6.9), which suggests a small trend in favour of increased apoptosis.

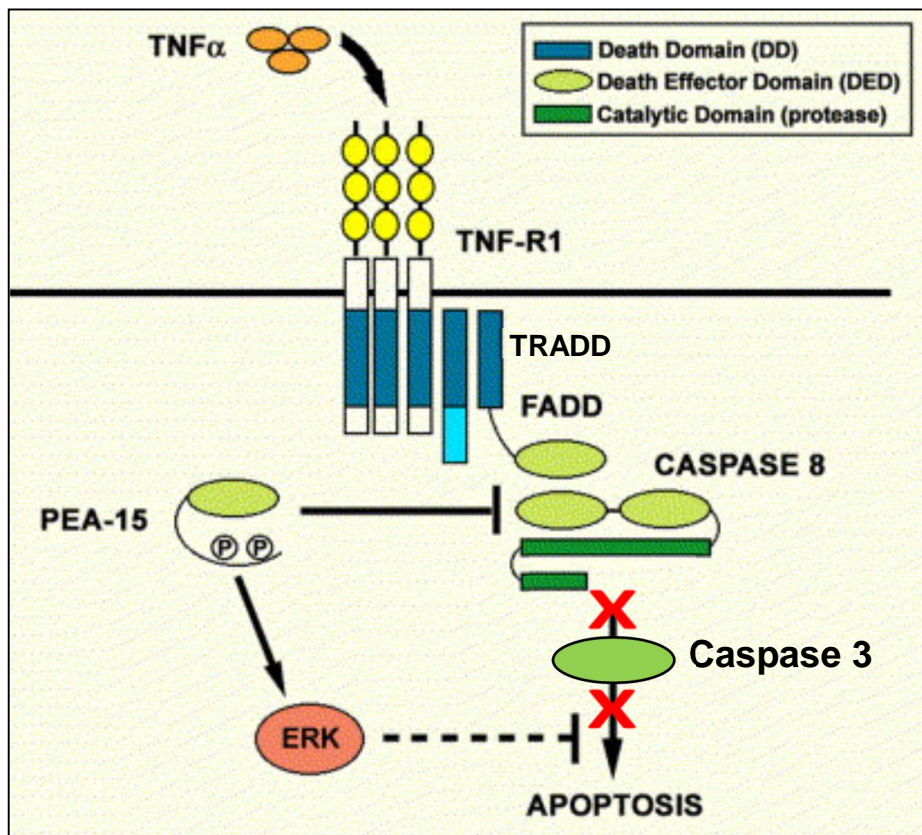


Figure 6.6: PEA-15 regulates TNF- α -induced apoptosis. PEA-15 participates in the formation of the death inducing signalling complex (DISC) (formed by the receptor, FADD and caspase-8), where it may bind to FADD and/or pro-caspase-8, blocking the activation of the caspase 8, further leading to inactivation of caspase 3 and decreased apoptosis (adapted from Renault *et al.*, 2003).

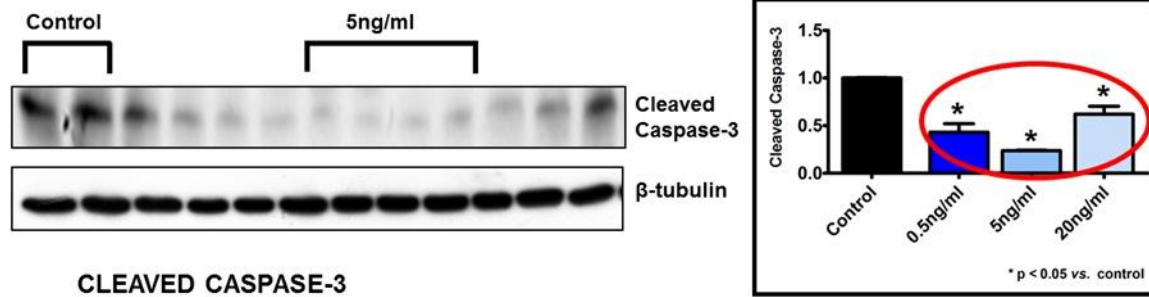


Figure 6.7: Western blot analysis of TNF- α treated (5 ng / ml for 24 hours) CMECs, showing a decrease in cleaved caspase-3 when compared to control. Data were expressed as a ratio of control with control adjusted to 1 (please refer to page 134, chapter 2). Sample size: n = 4 / group.

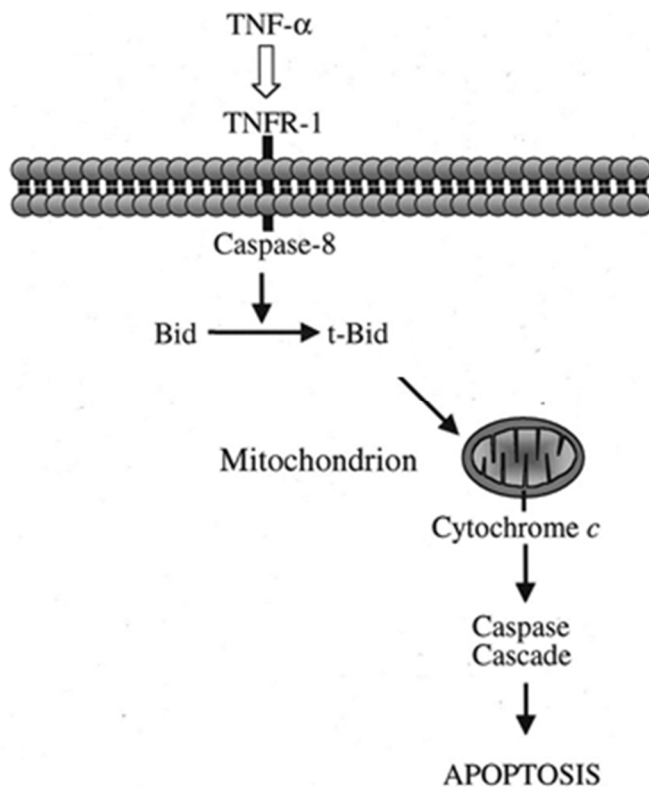


Figure 6.8: The BID pro-apoptotic signalling pathway activated by TNF- α -TNF R1 activation. (adapted from Guicciardi *et al.*, 2005).

Oxidative stress: According to the literature, exposure of vascular endothelial cells to TNF- α is generally associated with increased oxidative stress (Chen *W et al.*, 2008). However, in our hands, the oxidative stress response of the CMECs to TNF- α was similarly mixed as was the case with the apoptosis response. Proteomic data showed significant up-regulation of two major anti-oxidant systems, namely Parkinson disease 7 domain containing 1 (PARK-7), which was detected in TNF- α -treated samples only (Table 6.2) and mitochondrial superoxide dismutase [Mn] (also known as SOD-2), which was 2-fold up-regulated (Table 6.3). Park 7 functions as a redox-sensitive chaperone or as a sensor for oxidative stress (Bonifati *et al.*, 2003). Our SOD-2 data are supported by the findings of a previous study by Franzén *et al.* (2003), in which HUVECs were treated with 250 U/ ml TNF- α for up to 7 hours; this study demonstrated a 3.5-fold upregulation of SOD2. On the other hand, the other SOD isoform, superoxide dismutase [Cu_Zn] (SOD-1) was underrepresented showing a 2.4-fold down-regulation in TNF- α -treated cells (Table 6.4). In order to supplement our proteomic data, the oxidative stress response in TNF- α -treated CMECs was further investigated by western blot analysis of p22-phox (marker of NADPH-oxidase activity; see Chapter 5). The results showed a significant up-regulation in the expression of this protein, indicative of TNF- α -induced NADPH-oxidase activation. Interestingly, as was extensively discussed in Chapter 5, increased NADPH-oxidase activity did not result in the detection of increased DHE, DCF or DHR-123 sensitive ROS generation, either at 30 minutes or 24 hours of TNF- α -treatment.

Although the lack of increased intracellular ROS levels could be explained by experimental and protocol related reasons, this could also be the result of an anti-oxidant processes and functions in the cells that were, on balance, perhaps slightly more enriched in the overrepresented protein category than in the underrepresented protein category (compare Tables 6.6 and 6.7 with Tables 6.9 and 6.10). Finally, in our supplementary investigations, we evaluated whether there was any increased mitochondrial ROS generation in response to TNF- α -treatment. This phenomenon has previously been described (Corda *et al.*, 2001; Figure 6.9). In this series of experiments, we treated CMECs with 5 ng / ml TNF- α for 24 hours, followed by incubation with MitoTracker Green to localise the mitochondria (Figure 6.10 A and B: top panels). This was followed by incubation with MitoTracker Red, a mitochondrial ROS-sensitive fluorophore (Figure 6.10 C and D: bottom panels). From the photographs, it is clear that the mitochondria of TNF- α -treated cells stained significantly

more than the untreated, control samples, which indicated increased mitochondrial ROS production in the TNF- α cells. In summary, clearly the TNF- α cells sensed oxidative stress, which is evident from the overrepresented anti-oxidant proteins and systems, which could possibly explain why our general ROS probes were unable to record increased ROS generation. However, conversely, there were also a few anti-oxidant proteins and systems that were down-regulated; furthermore, we detected significant increases in NADPH-oxidase activity as well as mitochondrial ROS generation. Clearly, the oxidative stress status and the cellular responses were still in flux at the 24 hour time period.

When one considers the functional annotation data, several **biological processes** involved with oxidative stress and the response to oxidative stress were strongly represented in TNF- α -treated cells, including: glutathione metabolism (5 proteins, 12.5-fold enrichment, $p = 0.0006$); response to oxidative stress (10 proteins, 4-fold enrichment, $p = 0.0009$); response to reactive oxygen species (7 proteins, 5.5-fold enrichment, $p = 0.002$); response to hydrogen peroxide (6 proteins, 5.8-fold enrichment, $p = 0.004$) and oxidation reduction process (17 proteins, 2-fold enrichment, $p = 0.01$) (Table 6.6). With regard to **molecular functions** associated with strongly represented proteins, antioxidant activity featured prominently (6 proteins, 9.9-fold enrichment, $p = 0.0003$), as well as oxidoreductase activity acting on peroxide as acceptor (5 proteins, 12.7-fold enrichment, $p = 0.0006$) and glutathione peroxidase activity (3 proteins, 19.4-fold enrichment, $p = 0.01$) (Table 6.7). In the underrepresented category, the **biological process** of response to reactive oxygen species featured prominently (6 proteins, 5.7-fold enrichment, $p = 0.004$), as did glutathione metabolism (4 proteins, 12.2-fold enrichment, $p = 0.004$), cell redox homeostasis (5 proteins, 7-fold enrichment, $p = 0.006$), oxidation reduction (15 proteins, 2.1-fold enrichment, $p = 0.009$) and response to hydrogen peroxide (5 proteins, 5.8-fold enrichment, $p = 0.01$) (Table 6.9). Underrepresented proteins associated with the following **molecular functions**: peroxiredoxin activity (3 proteins, 34.8-fold enrichment, $p = 0.003$) and antioxidant activity (4 proteins, 7.6-fold enrichment, $p = 0.02$) (Table 6.10). On the whole, the functional annotation data suggest a modest trend in favour of antioxidant responses.

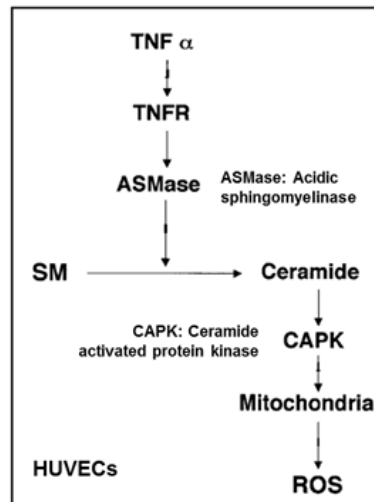


Figure 6.9: The proposed mechanism of TNF- α -induced mitochondrial ROS production (Corda *et al.*, 2001).

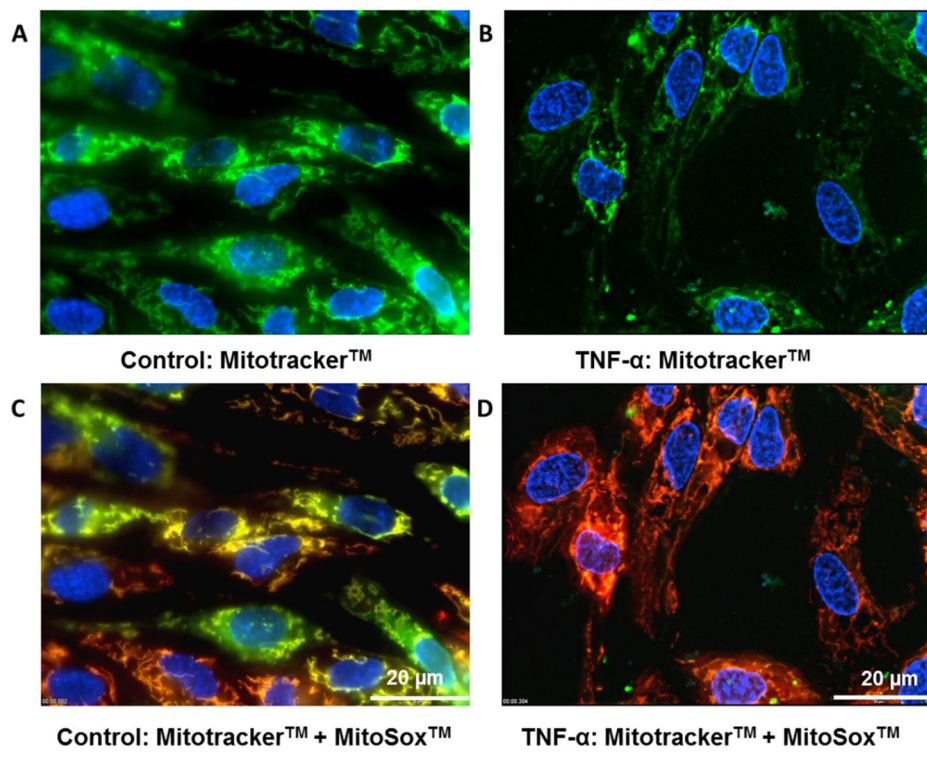


Figure 6.10: Fluorescence microscopy (Olympus IX-81 inverted fluorescent microscope, with CellR imaging software) of CMECs stained with MitoTracker Green to identify the mitochondria (Panels A and B: control and TNF- α -treated cells respectively), followed by addition of mitochondrial ROS-sensitive MitoSox, detecting mitochondrial ROS production (red stain) (Panels C and D: control and TNF- α -treated cells respectively).

HSP 90: As previously mentioned, HSP 90 acts as a scaffold protein, presenting substrates such as eNOS to PKB/Akt for phosphorylation (Brazil *et al.*, 2002); therefore, HSP 90 plays an integral role in the activation of eNOS via phosphorylation at the serine 1177 residue. Although the treatment with TNF- α 5 ng / ml for 24 hours did not change DAF-2/DA fluorescence (See Chapter 5), both the lower (0.5 ng / ml) and higher (20 ng / ml) concentrations decreased DAF-2/DA fluorescence (intracellular NO production). Furthermore, a reduction in the relative activation of eNOS was observed in TNF- α -treated cells (Chapter 5). From the proteomic data (Figure 6.3 and Table 6.4), and subsequent western blot analysis (Figure 6.4), it is clear that there was a significant down-regulation of HSP 90 in the TNF- α -treated cells, which could be one of the mechanisms underlying the reduction observed in the eNOS-NO biosynthesis pathway.

Unfortunately, as the reader will appreciate, it is an impossible task to discuss all the proteomic data and functional annotation analyses in detail here. We have attempted to focus on those responses that are of importance to this dissertation as whole.

6.5 Conclusions

In conclusion, the findings of this chapter are novel in that no previous studies have characterised the TNF- α stimulated response in CMECs in an equally comprehensive manner. We approached the study in this chapter by investigating large-scale differential protein regulation, intracellular events, and important endothelial signalling proteins. The results suggest that, in our hands, TNF- α treatment induced a state of relative flux at 24 hours, with some subtle signs of endothelial dysfunction and oxidative stress. We have attempted to somehow summarise the most important findings (in our view) in figure 6.11.

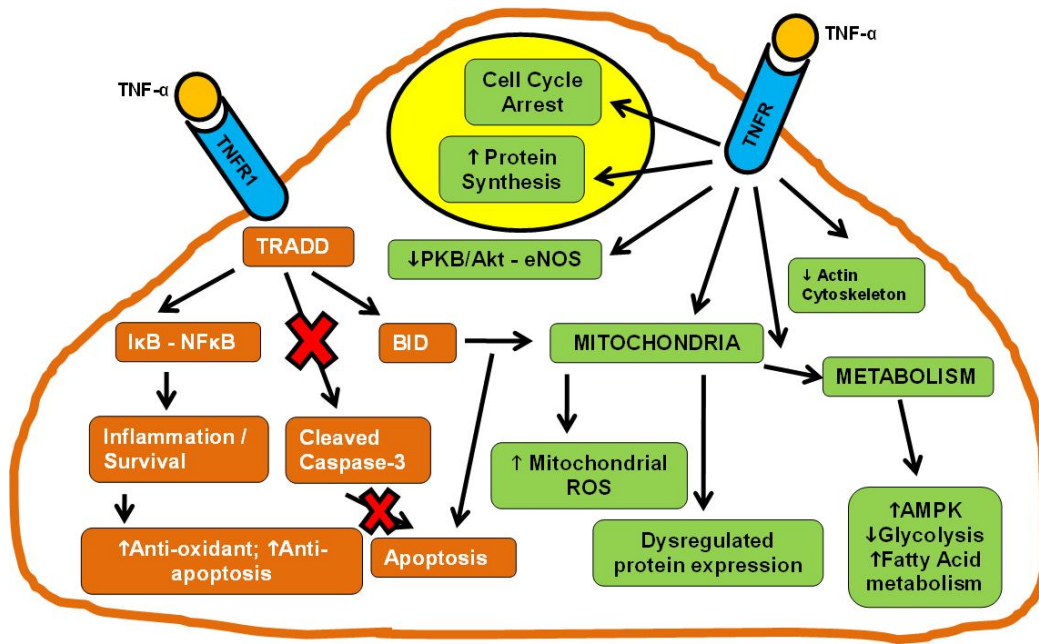


Figure 6.11: A cartoon depicting the summary of the most significant intracellular events in TNF- α -treated CMECs based on the results in this chapter. Generally, the proteomic data suggested that the TNF- α – TNFR1 – TRADD and TNF- α – TNFR1 – NF- κ B pathways were activated. This resulted in the activation of both pro-apoptotic the one hand, and pro-survival / pro-inflammatory / anti-apoptotic mechanisms on the other. Supplementary investigations showed a down-regulation of cleaved caspase-3, which suggests that the TRADD - caspase-3 pathway was attenuated, possibly via PEA 15. Mitochondrial-derived apoptosis may have been induced via the BID system. The response to oxidative stress was mixed, with some antioxidant systems strongly represented in the TNF- α cells, whereas others were underrepresented. TNF- α induced a strong up-regulation of mitochondrial proteins (51 in total), which was associated with induction of AMP-kinase and increased fatty acid metabolism and reduced glycolysis. Other responses as suggested by the proteomic data included decreased actin cytoskeleton organisation and cell cycle arrest. Taken together with the findings of Chapter 5, it appears as if a modest state of endothelial dysfunction was induced (decreased eNOS activity), together with increased oxidative stress which elicited an antioxidant response in the cells; however, outspoken apoptosis had not yet been established at 24 hours treatment. (*Adapted from: Strijdom H, Genis A, Smit S. Cardiac microvascular endothelial cells: characterization of total protein expression and responses to TNF- α . Paper presented at the SA / UK cardiovascular meeting; UCT; August 2012*).

CHAPTER SEVEN

Investigating the role of the TNF receptors and subsequent signalling events.

7.1 Introduction

In view of the interesting results in the previous chapter, where the proteomic analyses and supplementary western blot data suggested a role for TNFR1 – TRADD – NF- κ B pathway activation in our exogenously TNF- α -treated CMECs, we aimed to further tease out the respective roles of TNFR1 and TNFR2 in this chapter by making use of commercially available TNFR1- and TNFR2-blockers. From the literature, it is clear that very few vascular endothelial cell studies have investigated the respective roles of TNFR1 and TNFR2 in cells exposed to exogenous TNF- α -treatment. Certainly, we found no studies performed on CMECs. Therefore, all the data contained in this chapter are novel, particularly with regard to the end-points we chose to investigate.

TNF exerts its function by binding to and signalling via two distinct receptors (Hijdra *et al.*, 2012; Chandrasekharan *et al.*, 2007). TNFR1 (CD120a) is constitutively expressed, albeit it at relatively low levels, on nearly all nucleated cell types (Vandenabeele *et al.*, 1995), including endothelial cells (Kneilling *et al.*, 2009). TNFR2 (CD120b) is inducible and expressed by cells of myeloid lineage, peripheral T cells and alveolar lymphocytes and macrophages (Ye *et al.*, 2001; Faustman *et al.*, 2010; Kieszko *et al.*, 2007). As most information regarding TNF signalling is derived from TNFR1, the role of TNFR2 is likely underestimated (Naudé *et al.*, 2001).

7.1.1 TNFR1

Upon contact with their ligand, TNF receptors also form trimers, their tips fitting into the grooves formed between TNF monomers. This binding causes a conformational change to occur in the receptor, leading to the dissociation of the inhibitory protein SODD from the

intracellular death domain. This dissociation enables the adaptor protein TRADD to bind to the death domain, serving as a platform for subsequent protein binding. Following TRADD binding, three pathways can be initiated (Wajant *et al.*, 2003; Chen G *et al.*, 2002) (please refer to figure 7.1 for a complete signalling pathway of TNFR1).

7.1.1.1 Activation of NF- κ B.

Tumor necrosis factor receptor type 1-associated DEATH domain protein (TRADD) recruits TNF receptor-associated factor 2 (TRAF2) and receptor-interacting protein (RIP) (So *et al.*, 2011). TRAF2 in turn recruits the multicomponent protein kinase I κ B kinase (IKK), enabling the serine-threonine kinase RIP to activate it. An inhibitory protein, I κ B α , that normally binds to NF- κ B and inhibits its translocation (Morgan and Liu, 2010), is phosphorylated by IKK and subsequently degraded, releasing NF- κ B. NF- κ B is a heterodimeric transcription factor that translocates to the nucleus and mediates the transcription of a vast array of proteins involved in cell survival and proliferation, inflammatory response, and anti-apoptotic factors (Ghosh *et al.*, 2012).

7.1.1.2 Activation of the MAPK pathways.

Of the three major MAPK cascades, TNF induces a strong activation of the stress-related c-Jun N-terminal kinase (JNK) family, evokes a moderate response from p38-MAPK, and is responsible for minimal activation of the classical extracellular signal-regulated kinases (ERKs) (Crisafulli *et al.*, 2009). JNK translocates to the nucleus and activates transcription factors such as c-Jun and ATF2 (Walczynski *et al.*, 2013). The JNK pathway is involved in cell differentiation, proliferation, and is generally pro-apoptotic (Bogoyevitch *et al.*, 2010).

7.1.1.3 Induction of death signalling.

Like all death-domain-containing members of the TNFR superfamily, TNFR1 is involved in death signalling (Gaur et al., 2003). However, TNF-induced cell death plays only a minor role compared to its overwhelming functions in the inflammatory process. Its death-inducing capability is weak compared to other family members (such as Fas), and often masked by the anti-apoptotic effects of NF- κ B (Walczak, 2011). Nevertheless, TRADD binds Fas-Associated protein with Death Domain (FADD), which then recruits the cysteine protease caspase-8 (Ikner and Ashkenazi, 2011). A high concentration of caspase-8 induces its autoproteolytic activation and subsequent cleaving of downstream executioners caspase-3 and caspase-7, triggering the apoptotic demise of the cell (Ikner and Ashkenazi, 2011).

The myriad and often-conflicting effects mediated by the above pathways indicate the existence of extensive cross-talk. Factors, such as cell type, concurrent stimulation with other cytokines or the amount of ROS generated can shift the balance in favor of one pathway or another. Such complicated signalling ensures that, whenever TNF is released, various cells with vastly diverse functions and conditions can all respond appropriately to inflammation (Locksley *et al.*, 2001; Bouwmeester *et al.*, 2004).

7.1.2. TNFR2

TNFR2 is readily cleaved by the metalloprotease TNF- α converting enzyme (TACE) into its soluble shed form which is still capable of TNF binding, rapidly altering the number of functional TNFR2 receptors that can signal their proliferative or apoptotic actions (Pennica *et al.*, 1992; Porteu and Hieblot, 1994; Higuchi and Aggarwal, 1994). Although regulation of TNFR protein expression is not restricted purely to TNFR2 (Manna and Aggarwal, 1998), generally the more restrictive tissue distribution of TNFR2 and the flexible TNFR2 protein regulation suggest a physiological role for TNFR2 regulation in modulating TNF-responsiveness (MacEwan, 2002). TNFRs form homotrimers upon activation by TNF without the assembly of receptor heterotrimers (Moosmayer *et al.*, 1994), however the TNFR1 : TNFR2 protein ratio has been found to be important in the way a cell predetermines its TNF

response (Medvedev *et al.*, 1996; Declercq *et al.*, 1998; Baxter *et al.*, 1999). Deletion of TNFR2 in transgenic mice has uncovered that this receptor subtype is important in low dose TNF-induced lethality (Erickson *et al.*, 1994). In addition to a role in thymocyte proliferation (Grell *et al.*, 1998), TNFR2 plays an important role in models of cerebral malaria and microvascular endothelial cell damage (Lucas R *et al.*, 1997a, b; 1998). Langerhans cell migration was depressed in mice lacking TNFR2 (Wang B *et al.*, 1996), whereas TNFR2 plays a critical role in multiorgan inflammation (Douni and Kollias, 1998). Clearly, TNFR2 has a role in certain tissues and diseased states, but the validity of direct comparisons between TNFR-null transgenic mice and normal cells and tissues which ubiquitously express TNFRs at altering TNFR1 : TNFR2 ratios, has to be considered when analysing the physiological role of TNFR1 and TNFR2 (MacEwan, 2002). Please see figure 7.1 for a complete signalling pathway of TNFR2.

It has also been shown that endothelial cells express a third TNF- α receptor, known as the lymphotoxin- β receptor (LTBR). This receptor is known to play an important role in the inflammatory responses of these cells (Pablos *et al.*, 2005; Madge *et al.*, 2008); however, it is not as extensively described in the literature as TNFR1 and TNFR2. For the purposes of this chapter, we only focused on the two receptors described above (TNFR1 & TNFR2).

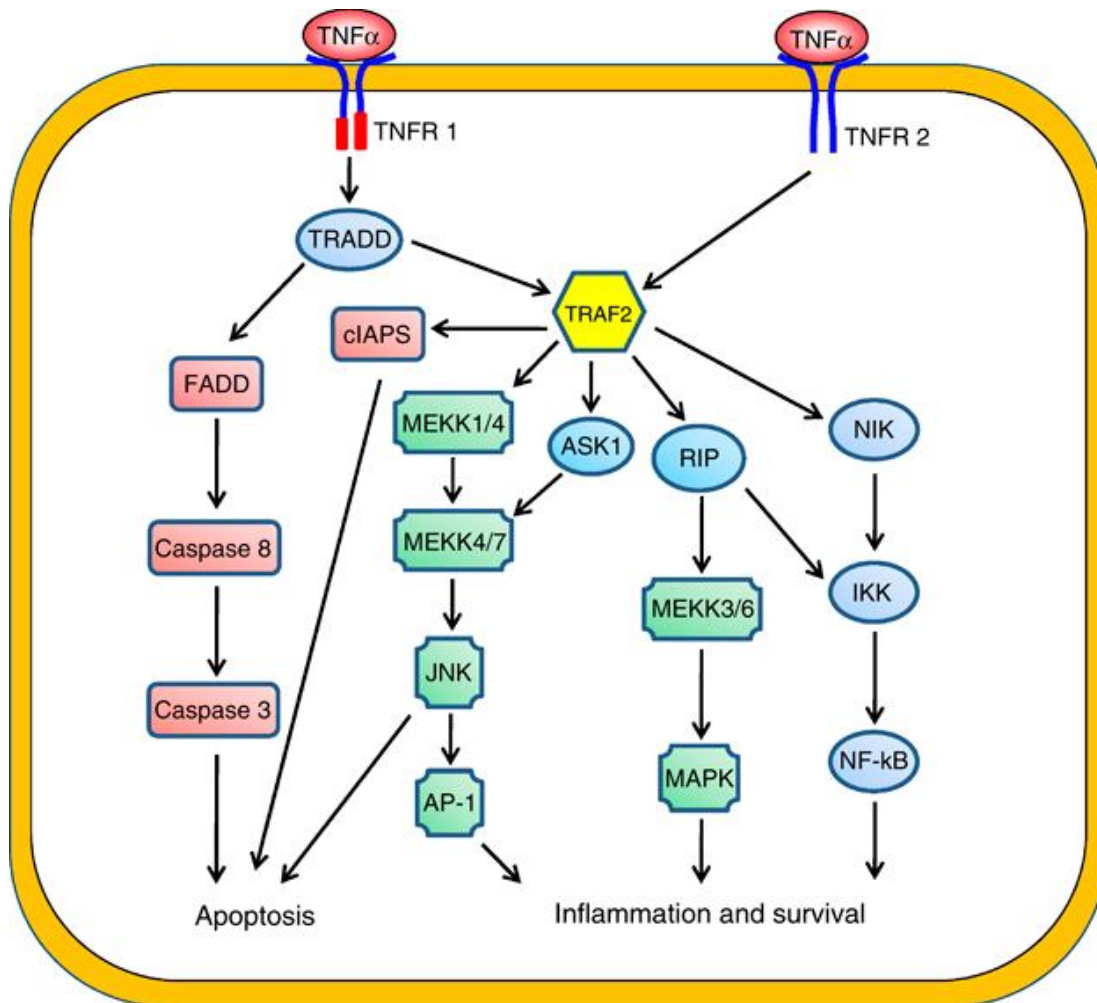


Figure 7.1: The downstream signalling pathways of TNF- α and TNFR1 and TNFR2. It is proposed that the downstream effects of activation of both receptors can activate different pathways to induce apoptosis, cell survival or inflammation. (Adapted from Wu and Zhou, 2010).

7.2 **Methods**

In order to determine the respective roles of TNFR1 and TNFR2 in TNF- α -treated CMECs, we purchased human TNF RI / TNFRSF1A (TNF- α receptor blocker 1 – TRB1) and TNF RII / TNFRSF1B (TNF- α receptor blocker 2 – TRB2) polyclonal (Goat IgG) antibodies from R&D Systems Inc. (Minneapolis, MN 55413, USA). CMECs were pre-treated with either 1 μ g / ml of TRB1 or TRB2 or TRB1+TRB2 for 30 minutes and then subsequently treated with TNF- α (20 ng / ml) for a further 30 minutes (see figure 7.2 for complete protocol). We have chosen to use 30 minutes as incubation time, as pilot studies with the receptor blockers performed at 24 hours treatment showed inconclusive results. Previous studies that investigated the effects of these specific antibodies, used concentrations of TNF RI / TNFRSF1A and TNF RII / TNFRSF1B ranging from 0 – 10 μ g / ml (Cooper *et al.*, 2007; Hase *et al.*, 2004). The datasheet from both products recommended a concentration of 1 μ g / ml and after conducting dose-response studies (data not shown) we decided to use the recommended concentration. After treatment, the cells were removed from culture by trypsinisation and prepared for subsequent western blot analysis (as described on page 132 – 134 in chapter two, see figures 2.15 & 2.16) (see figure 7.2 – 7.4 for treatment protocols). The expression and activation of the following proteins were investigated (please refer to chapter 2, page 132 for the concentration and exposure time of each protein):

NOS Signalling: Total and phosphorylated eNOS and PKB / Akt, and total HSP 90, caveolin-1 and iNOS were measured to investigate NOS signalling mechanisms.

Oxidative Stress: The membrane bound NADPH oxidase subunit, p22-phox, was used to measure nicotinamide adenine dinucleotide phosphate (NADPH) oxidase activity as previously described (Griendling KK *et al.*, 2000a).

Nitrosative Stress: The ability of the highly reactive NO-derived radical, ONOO⁻ (peroxynitrite) to nitrosylate tyrosine residues of cellular proteins and form nitrotyrosine, is an indication of nitrosative stress (Dalle-Donne *et al.*, 2005). Nitrotyrosine expression was therefore measured as a marker of nitrosative stress.

NFK β signalling: Activation of the NFK β pathway is usually an indication of a pro-inflammatory response (Ben-Neriah and Karin, 2011). Upon activation of this pathway, IK β α dislodges from the NFK β complex and undergoes proteasomal degradation; therefore, a reduction in IK β α protein levels is a marker of NFK β activation (Hoffmann A *et al.*, 2002). IK β α protein expression was therefore measured to investigate activity of the NFK β pathway.

Apoptosis: Cleaved caspase-3 and cleaved PARP were measured to investigate apoptosis signalling.

Equal protein loading validation: β -tubulin expression was measured to confirm equal protein loading in all samples.

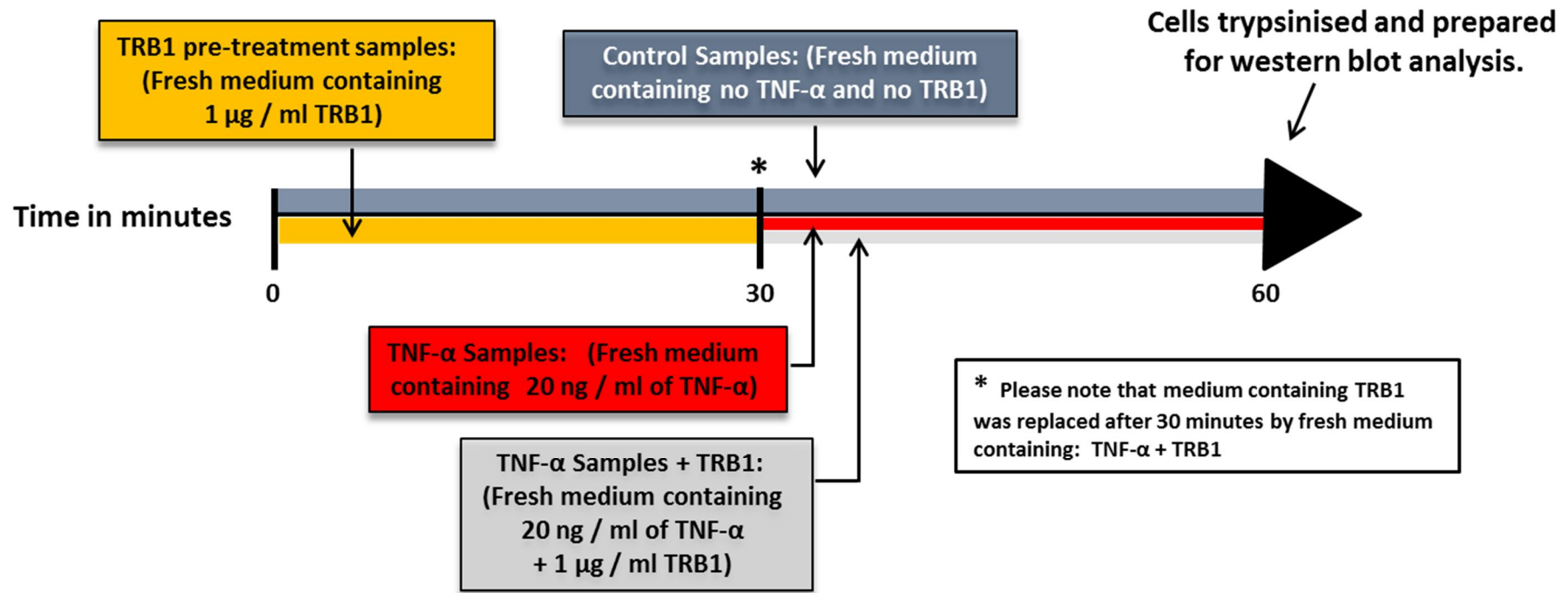


Figure 7.2: Protocol for treatment of CMECs with 20 ng / ml TNF- α with or without 1 µg / ml of TRB1 for 30 minutes for subsequent western blot analysis.

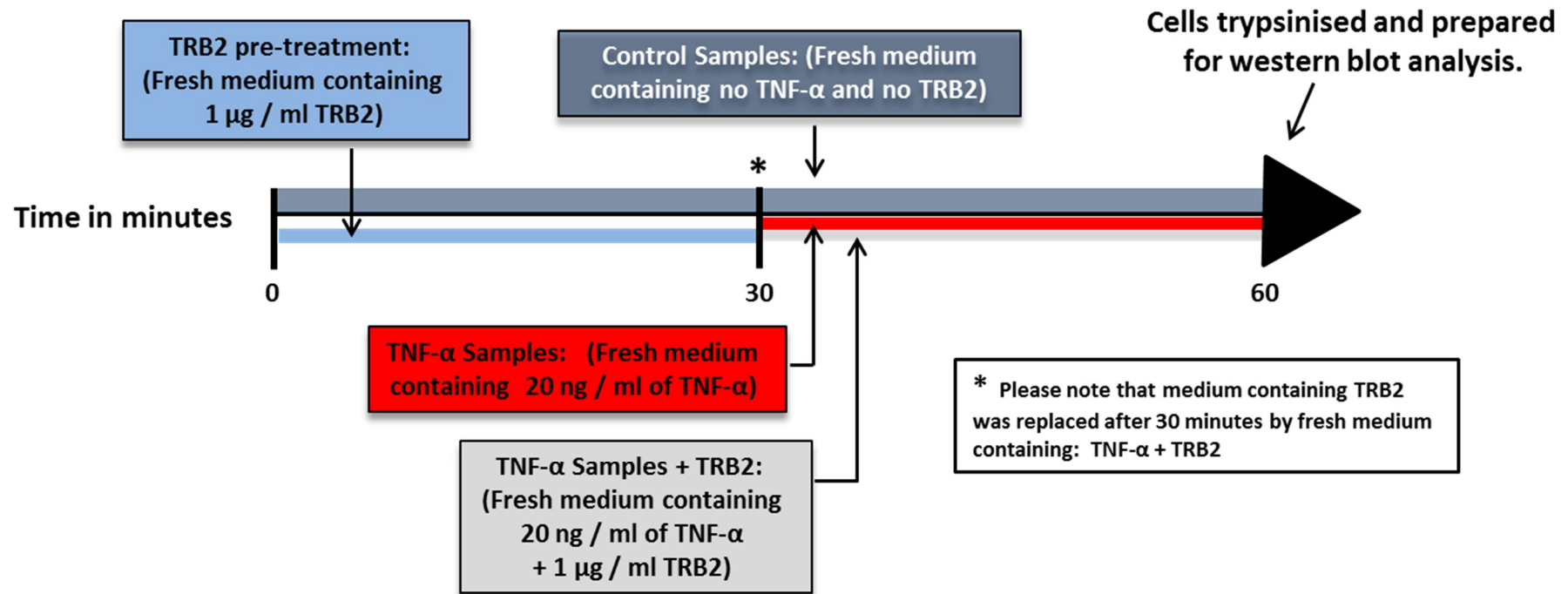


Figure 7.3: Protocol for treatment of CMECs with 20 ng / ml TNF-α with or without 1 µg / ml of TRB2 for 30 minutes for subsequent western blot analysis.

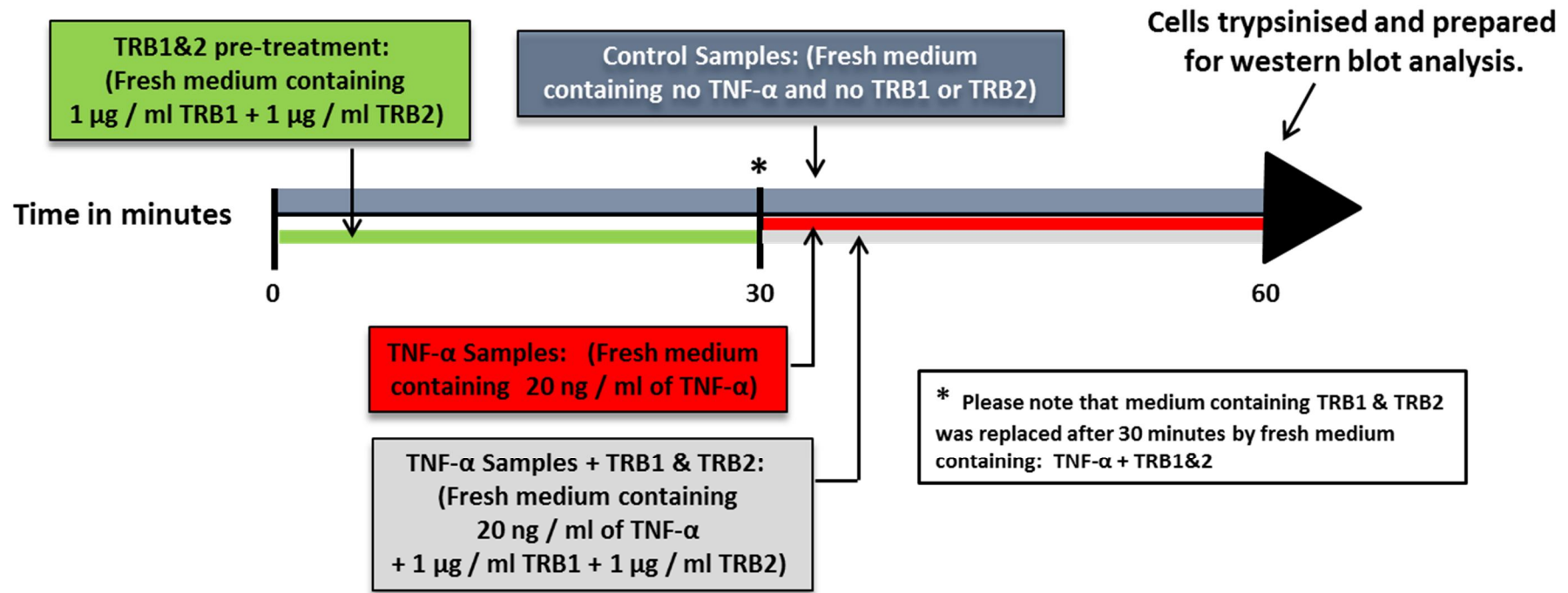


Figure 7.4: Protocol for treatment of CMECs with 20 ng / ml TNF- α with or without 1 µg / ml of TRB2 and 1 µg / ml of TRB2 for 30 minutes for subsequent western blot analysis.

7.3 **Results**

7.3.1 **NOS signalling:**

eNOS

Exposing CMECs to 30 minutes of TNF- α (20 ng / ml) led to unchanged phosphorylated eNOS levels (0.98 ± 0.05 vs. 1.00 control) (see figure 7.5), unchanged total eNOS expression (0.92 ± 0.02 vs. 1.00 control) (see figure 7.6), and unchanged phosphorylated / total eNOS ratios (1.07 ± 0.05 vs. 1.00 control) (see figure 7.7) respectively.

TNFR1 blockade: Exposing CMECs to 30 minutes of TNF- α (20 ng / ml) + TRB1 (1 μ g / ml) led to decreased phosphorylated eNOS levels (0.78 ± 0.01 vs. 1.00 control: $p < 0.05$) (see figure 7.5), decreased total eNOS expression (0.74 ± 0.02 vs. 1.00 control: $p < 0.05$) (see figure 7.6), and unchanged phosphorylated / total eNOS ratios (1.06 ± 0.05 vs. 1.00 control) (see figure 7.7) respectively.

TNFR2 blockade: Exposing CMECs to 30 minutes of TNF- α (20 ng / ml) + TRB2 (1 μ g / ml) led to unchanged phosphorylated eNOS levels (0.65 ± 0.13 vs. 1.00 control) (see figure 7.5), decreased total eNOS expression (0.66 ± 0.06 vs. 1.00 control: $p < 0.05$) (see figure 7.6), and unchanged phosphorylated / total eNOS ratios (0.99 ± 0.18 vs. 1.00 control) (see figure 7.7) respectively.

TNFR1 + TNFR2 blockade: Exposing CMECs to 30 minutes of TNF- α (20 ng / ml) + TRB1&2 (1 μ g / ml) led to decreased phosphorylated eNOS levels (0.10 ± 0.03 vs. 1.00 control: $p < 0.05$) (see figure 7.5), decreased total eNOS expression (0.56 ± 0.02 vs. 1.00 control: $p < 0.05$) (see figure 7.6), and decreased phosphorylated / total eNOS ratios (0.17 ± 0.06 vs. 1.00 control: $p < 0.05$) (see figure 7.7) respectively.

When the different groups were compared to each other, it was evident that blocking **both** TNFR1 and TNFR2 resulted in outspoken decreases (~ 80%) in the relative activation of eNOS (phospho / total eNOS ratio) vs. TNFR1 only or TNFR2 only blockade (see Figure 7.7).

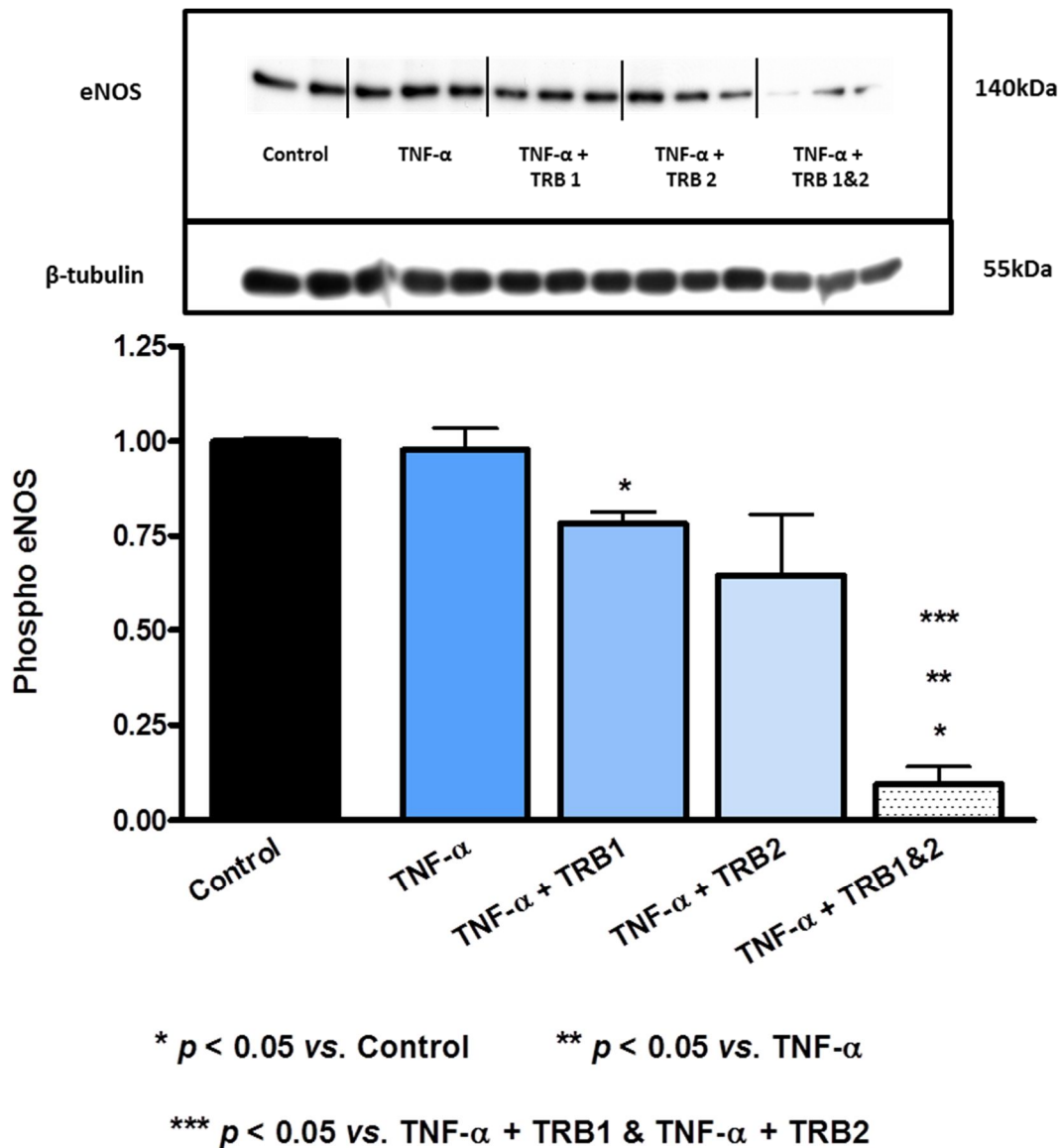


Figure 7.5: The effects of TNF- α receptor blockade (1 μ g / ml) on phosphorylated eNOS in TNF- α (20 ng / ml)-treated CMECs. Data are represented as phosphorylated eNOS (expressed as a ratio of control; control = 1). β -tubulin was used to validate equal protein loading. All data were expressed as a ratio of control with control adjusted to 1 (please refer to page 134, chapter 2). Sample size: $n = 3$ / group.

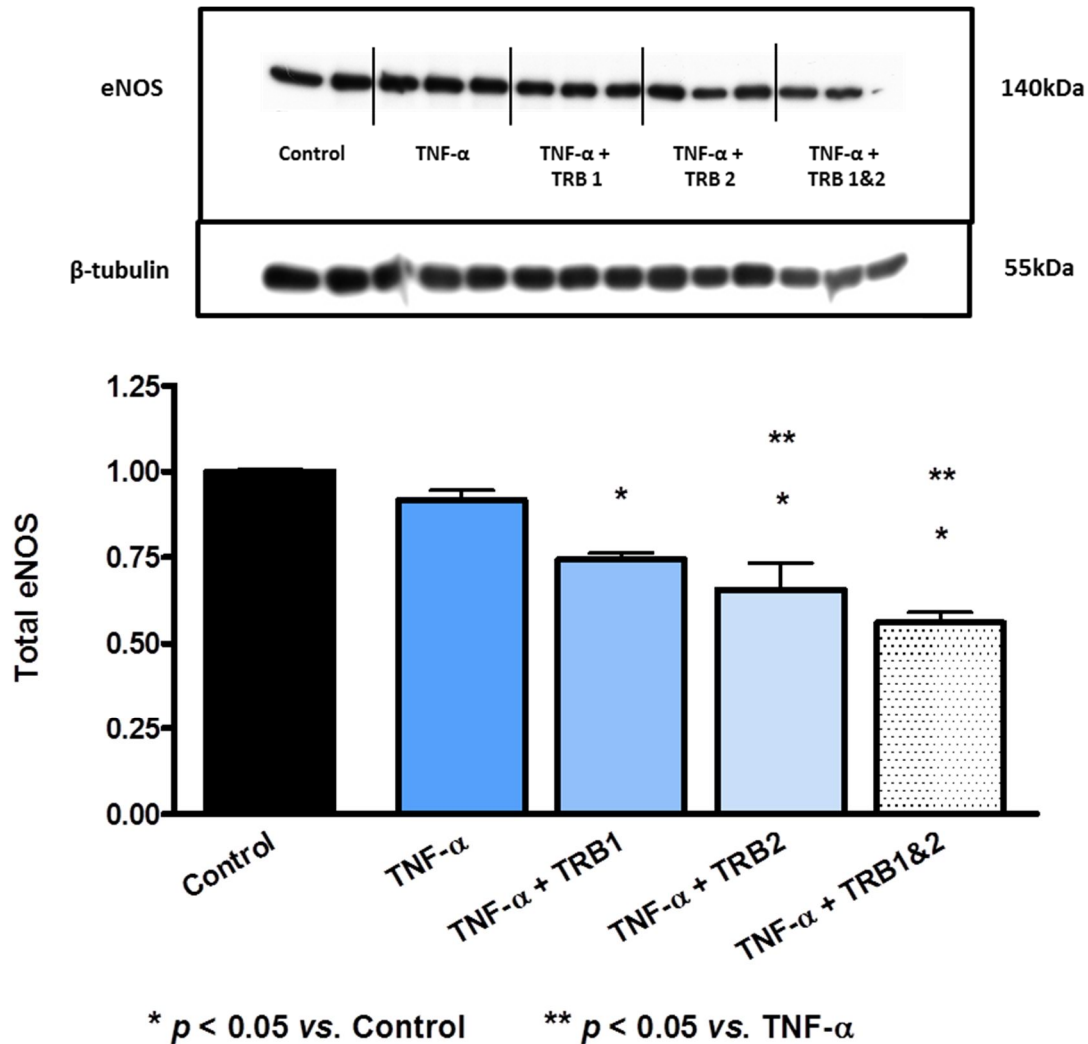


Figure 7.6: The effects of TNF- α receptor blockade (1 μ g / ml) on total eNOS expression in TNF- α (20 ng / ml)-treated CMECs. Data are represented as total eNOS (expressed as a ratio of control; control = 1). β -tubulin was used to validate equal protein loading. All data were expressed as a ratio of control with control adjusted to 1 (please refer to page 134, chapter 2). Sample size: n = 3 / group.

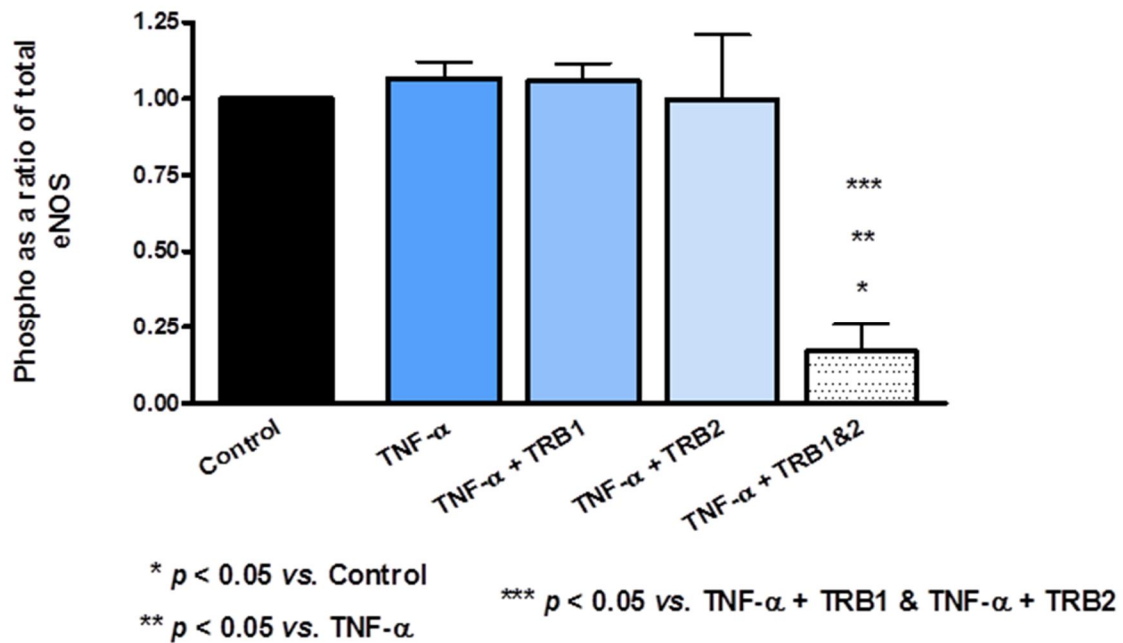


Figure 7.7: The effects of TNF- α receptor blockade (1 μ g / ml) on phosphorylated / total eNOS ratios in TNF- α (20 ng / ml)-treated CMECs. Data are represented as phosphorylated eNOS / total eNOS (expressed as a ratio of control; control = 1). All data were expressed as a ratio of control with control adjusted to 1 (please refer to page 134, chapter 2). Sample size: $n = 3$ / group.

PKB/Akt

Exposing CMECs to 30 minutes of TNF- α (20 ng / ml) led to unchanged phosphorylated PKB/Akt levels (1.00 ± 0.07 vs. 1.00 control) (see figure 7.8), unchanged total PKB/Akt expression (0.88 ± 0.04 vs. 1.00 control) (see figure 7.9), and increased phosphorylated / total PKB/Akt ratios (1.30 ± 0.03 vs. 1.00 control: $p < 0.05$) (see figure 7.10) respectively.

TNFR1 blockade: Exposing CMECs to 30 minutes of TNF- α (20 ng / ml) + TRB1 (1 μ g / ml) led to unchanged phosphorylated PKB/Akt levels (1.10 ± 0.03 vs. 1.00 control) (see figure 7.8), unchanged total PKB/Akt expression (0.88 ± 0.01 vs. 1.00 control) (see figure 7.9), and increased phosphorylated / total PKB/Akt ratios (1.25 ± 0.05 vs. 1.00 control: $p < 0.05$) (see figure 7.10) respectively.

TNFR2 blockade: Exposing CMECs to 30 minutes of TNF- α (20 ng / ml) + TRB2 (1 μ g / ml) led to unchanged phosphorylated PKB/Akt levels (0.96 ± 0.07 vs. 1.00 control) (see figure 7.8), unchanged total PKB/Akt expression (0.85 ± 0.04 vs. 1.00 control) (see figure 7.9), and unchanged phosphorylated / total PKB/Akt ratios (1.13 ± 0.03 vs. 1.00 control) (see figure 7.10) respectively.

TNFR1 + TNFR2 blockade: Exposing CMECs to 30 minutes of TNF- α (20 ng / ml) + TRB1&2 (1 μ g / ml) led to unchanged phosphorylated PKB/Akt levels (0.96 ± 0.03 vs. 1.00 control) (see figure 7.8), unchanged total PKB/Akt expression (0.91 ± 0.06 vs. 1.00 control) (see figure 7.9), and unchanged phosphorylated / total PKB/Akt ratios (1.07 ± 0.03 vs. 1.00 control) (see figure 7.10) respectively.

When the different groups were compared to each other, it was evident that blocking **both** TNFR1 and TNFR2 resulted in a modest, but significant decrease in the relative activation of PKB/Akt (phospho / total PKB/Akt) vs. the TNF- α -treated group, but not vs. TNFR1 only or TNFR2 only blockade (see Figure 7.10).

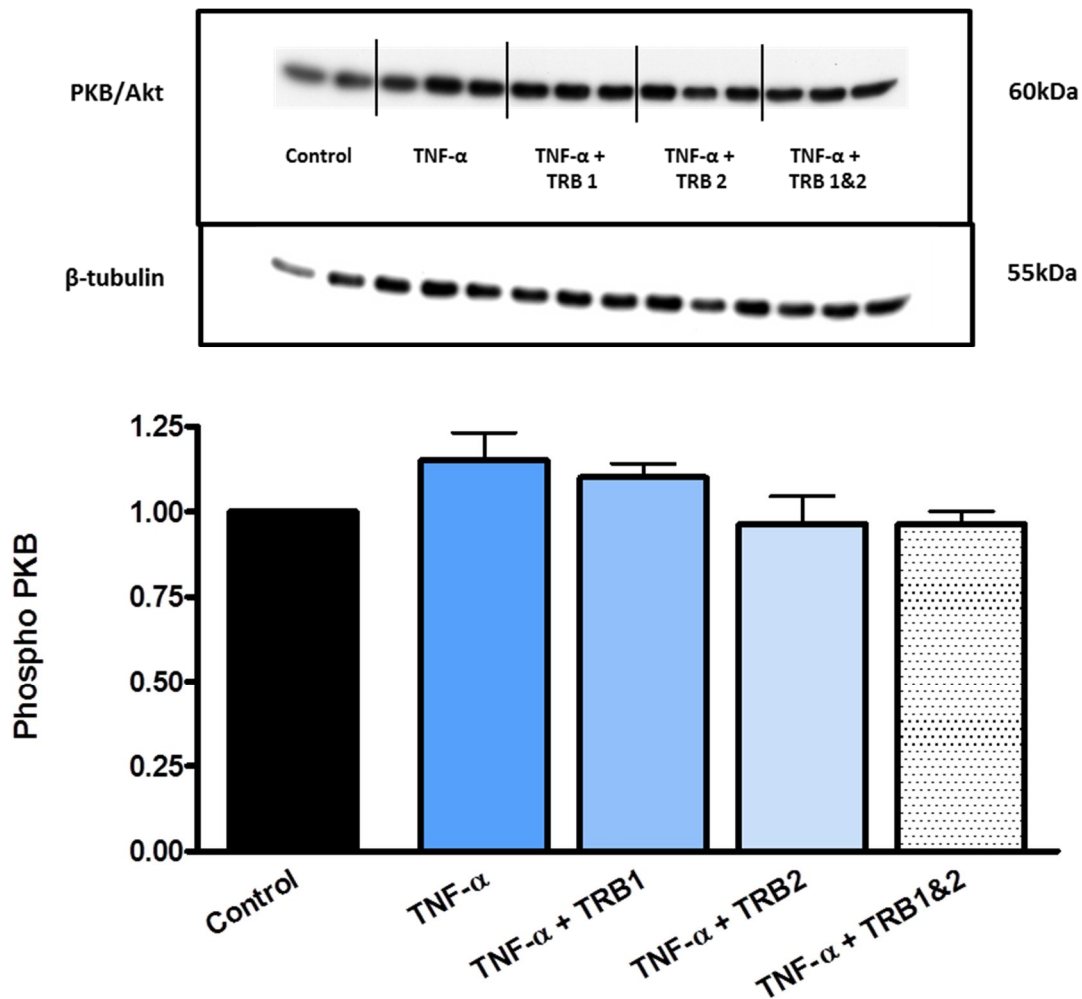


Figure 7.8: The effects of TNF- α receptor blockade (1 μ g / ml) on phosphorylated PKB/Akt in TNF- α (20 ng / ml)-treated CMECs. Data are represented as phosphorylated PKB/Akt (expressed as a ratio of control; control = 1). β -tubulin was used to validate equal protein loading. All data were expressed as a ratio of control with control adjusted to 1 (please refer to page 134, chapter 2). Sample size: n = 3 / group.

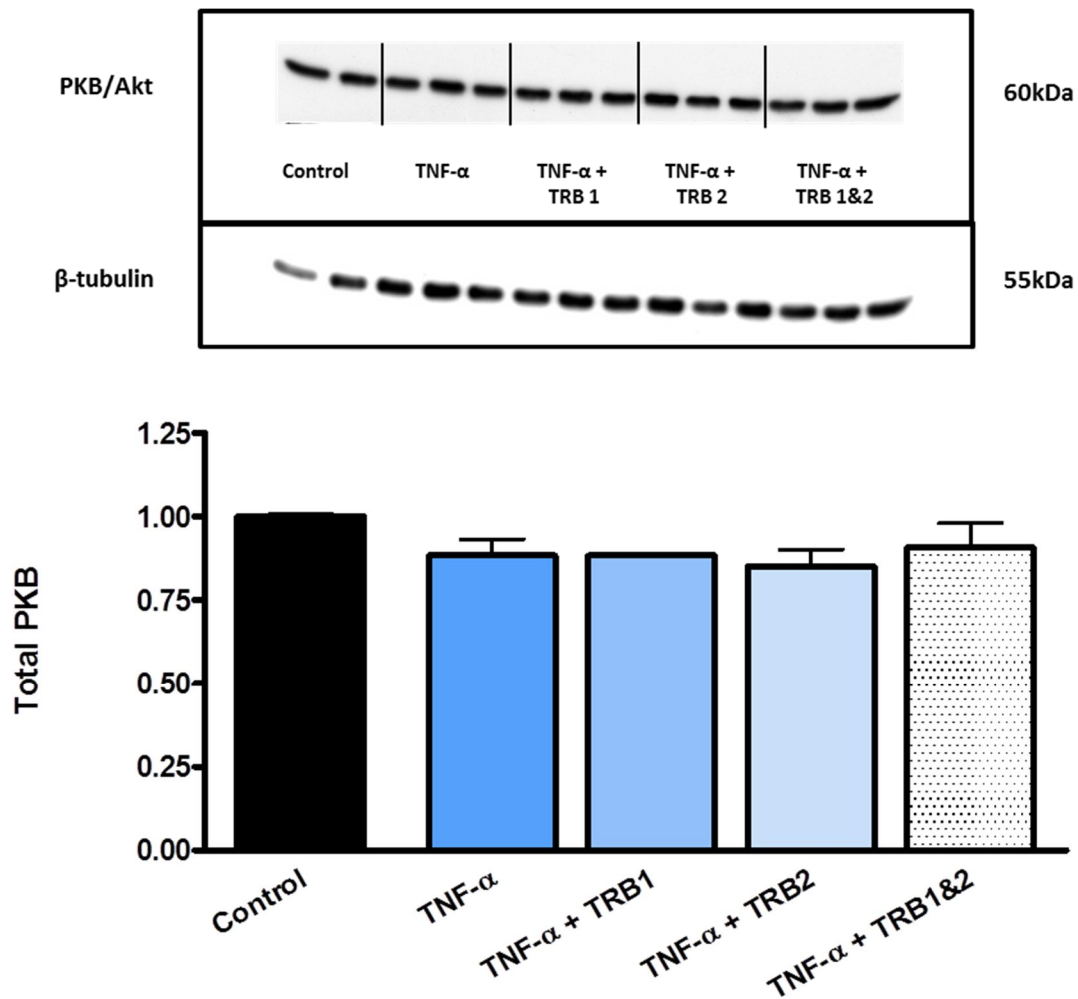


Figure 7.9: The effects of TNF- α receptor blockade (1 μ g / ml) on total PKB/Akt expression in TNF- α (20 ng / ml)-treated CMECs. Data are represented as total PKB/Akt (expressed as a ratio of control; control = 1). β -tubulin was used to validate equal protein loading. All data were expressed as a ratio of control with control adjusted to 1 (please refer to page 134, chapter 2). Sample size: n = 3 / group.

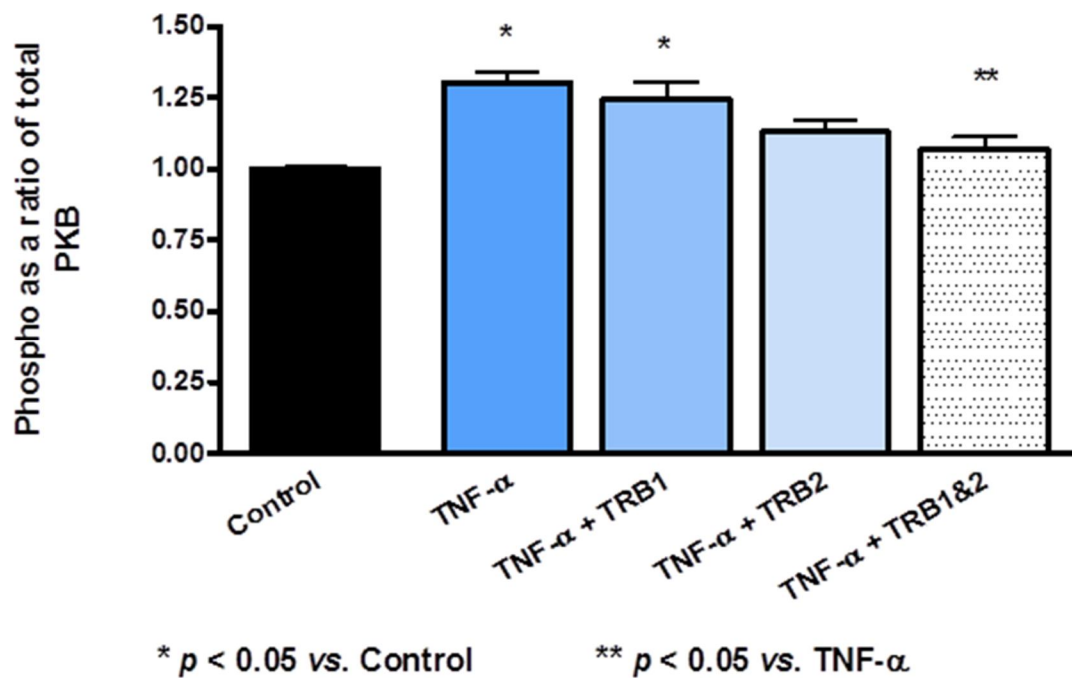


Figure 7.10: The effects of TNF- α receptor blockade (1 μ g / ml) on phosphorylated / total PKB/Akt ratios in TNF- α (20 ng / ml)-treated CMECs. Data are represented as phosphorylated PKB/Akt / total PKB/Akt (expressed as a ratio of control; control = 1). All data were expressed as a ratio of control with control adjusted to 1 (please refer to page 134, chapter 2). Sample size: n = 3 / group.

HSP 90

Exposing CMECs to 30 minutes of TNF- α (20 ng / ml) led to unchanged HSP 90 expression levels (1.05 ± 0.05 vs. 1.00 control) (see figure 7.11).

TNFR1 blockade: Exposing CMECs to 30 minutes of TNF- α (20 ng / ml) + TRB1 (1 μ g / ml) led to unchanged HSP 90 expression levels (0.91 ± 0.06 vs. 1.00 control) (see figure 7.11).

TNFR2 blockade: Exposing CMECs to 30 minutes of TNF- α (20 ng / ml) + TRB2 (1 μ g / ml) led to decreased HSP 90 expression levels (0.64 ± 0.04 vs. 1.00 control: $p < 0.05$) (see figure 7.11).

TNFR1 + TNFR2 blockade: Exposing CMECs to 30 minutes of TNF- α (20 ng / ml) + TRB1 & 2 (1 μ g / ml) led to decreased HSP 90 expression levels (0.68 ± 0.05 vs. 1.00 control: $p < 0.05$) (see figure 7.11).

When the different groups were compared with each other, it was evident that blockade of TNFR2 resulted in a significant decrease in HSP 90 expression compared to TNF- α -treated groups as well as groups in which TNFR1 was blocked. Blockade of both TNFR1 and TNFR2 significantly decreased HSP 90 expression when compared to TNF-treated cells. See Figure 7.11.

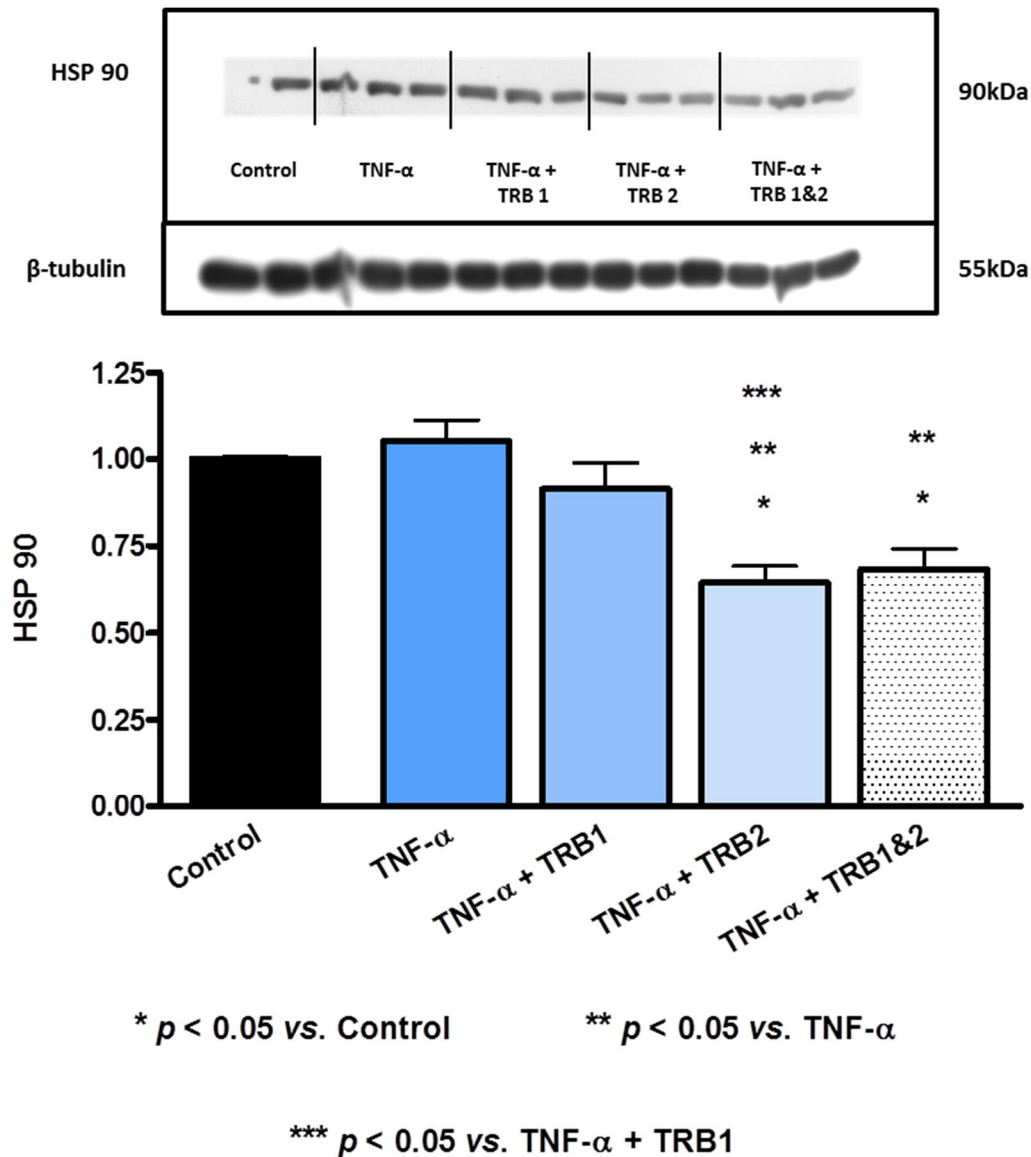


Figure 7.11: The effects of TNF- α receptor blockade (1 μ g / ml) on HSP 90 expression in TNF- α (20 ng / ml)-treated CMECs. Data are represented as HSP 90 expression (expressed as a ratio of control; control = 1). β -tubulin was used to validate equal protein loading. All data were expressed as a ratio of control with control adjusted to 1 (please refer to page 134, chapter 2). Sample size: n = 3 / group.

Caveolin-1

Exposing CMECs to 30 minutes of TNF- α (20 ng / ml) led to unchanged caveolin-1 expression levels (0.83 ± 0.06 vs. 1.00 control) (see figure 7.12).

TNFR1 blockade: Exposing CMECs to 30 minutes of TNF- α (20 ng / ml) + TRB1 (1 μ g / ml) led to decreased caveolin-1 expression levels (0.67 ± 0.04 vs. 1.00 control: $p < 0.05$) (see figure 7.12).

TNFR2 blockade: Exposing CMECs to 30 minutes of TNF- α (20 ng / ml) + TRB2 (1 μ g / ml) led to unchanged caveolin-1 expression levels (0.86 ± 0.04 vs. 1.00 control) (see figure 7.12).

TNFR1 + TNFR2 blockade: Exposing CMECs to 30 minutes of TNF- α (20 ng / ml) + TRB1 & 2 (1 μ g / ml) led to unchanged caveolin-1 expression levels (1.02 ± 0.11 vs. 1.00 control) (see figure 7.12).

When the different groups were compared with each other, it was evident that the TNF- α -treated cells in which TNFR1 was blocked was the only group in which the expression of caveolin-1 was significantly decreased vs. control, but not vs. any of the other groups (see Figure 7.12).

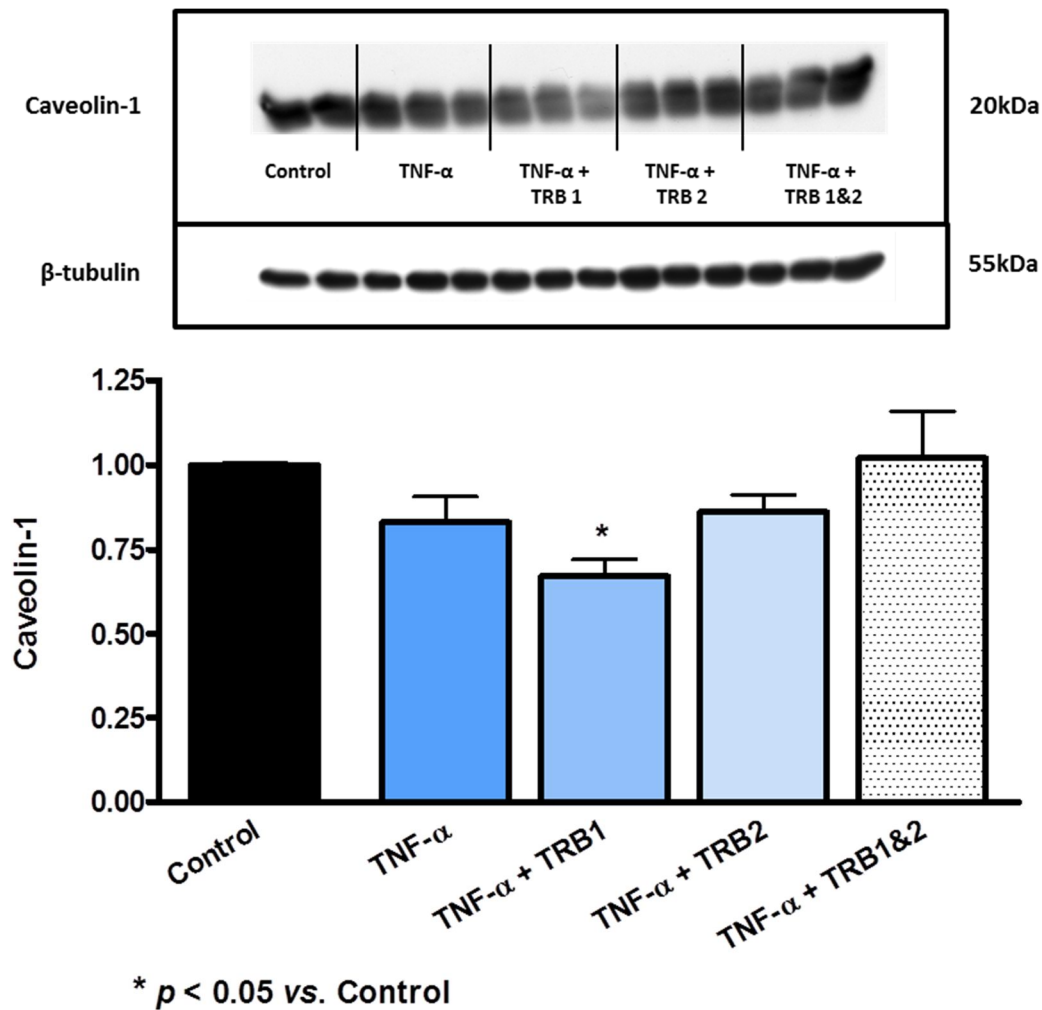


Figure 7.12: The effects of TNF- α receptor blockade (1 μ g / ml) on caveolin-1 expression in TNF- α (20 ng / ml)-treated CMECs. Data are represented as caveolin-1 expression (expressed as a ratio of control; control = 1). β -tubulin was used to validate equal protein loading. All data were expressed as a ratio of control with control adjusted to 1 (please refer to page 134, chapter 2). Sample size: $n = 3$ / group.

iNOS

Exposing CMECs to 30 minutes of TNF- α (20 ng / ml) led to increased iNOS expression levels (1.32 ± 0.08 vs. 1.00 control: $p < 0.05$) (see figure 7.13).

TNFR1 blockade: Exposing CMECs to 30 minutes of TNF- α (20 ng / ml) + TRB1 (1 μ g / ml) led to unchanged iNOS expression levels (1.27 ± 0.08 vs. 1.00 control) (see figure 7.13).

TNFR2 blockade: Exposing CMECs to 30 minutes of TNF- α (20 ng / ml) + TRB2 (1 μ g / ml) led to unchanged iNOS expression levels (0.94 ± 0.12 vs. 1.00 control) (see figure 7.13).

TNFR1 + TNFR2 blockade: Exposing CMECs to 30 minutes of TNF- α (20 ng / ml) + TRB1 & 2 (1 μ g / ml) led to decreased iNOS expression levels (0.42 ± 0.05 vs. 1.00 control: $p < 0.05$) (see figure 7.13).

When the different groups were compared with each other, it was evident that the TNF- α -treated cells in which both TNFR1 + TNFR2 were blocked resulted in outspoken down-regulation of iNOS expression compared to all the other groups. Also noticeable was the up-regulation of iNOS in the TNF- α treated group (without blockers) (see Figure 7.13).

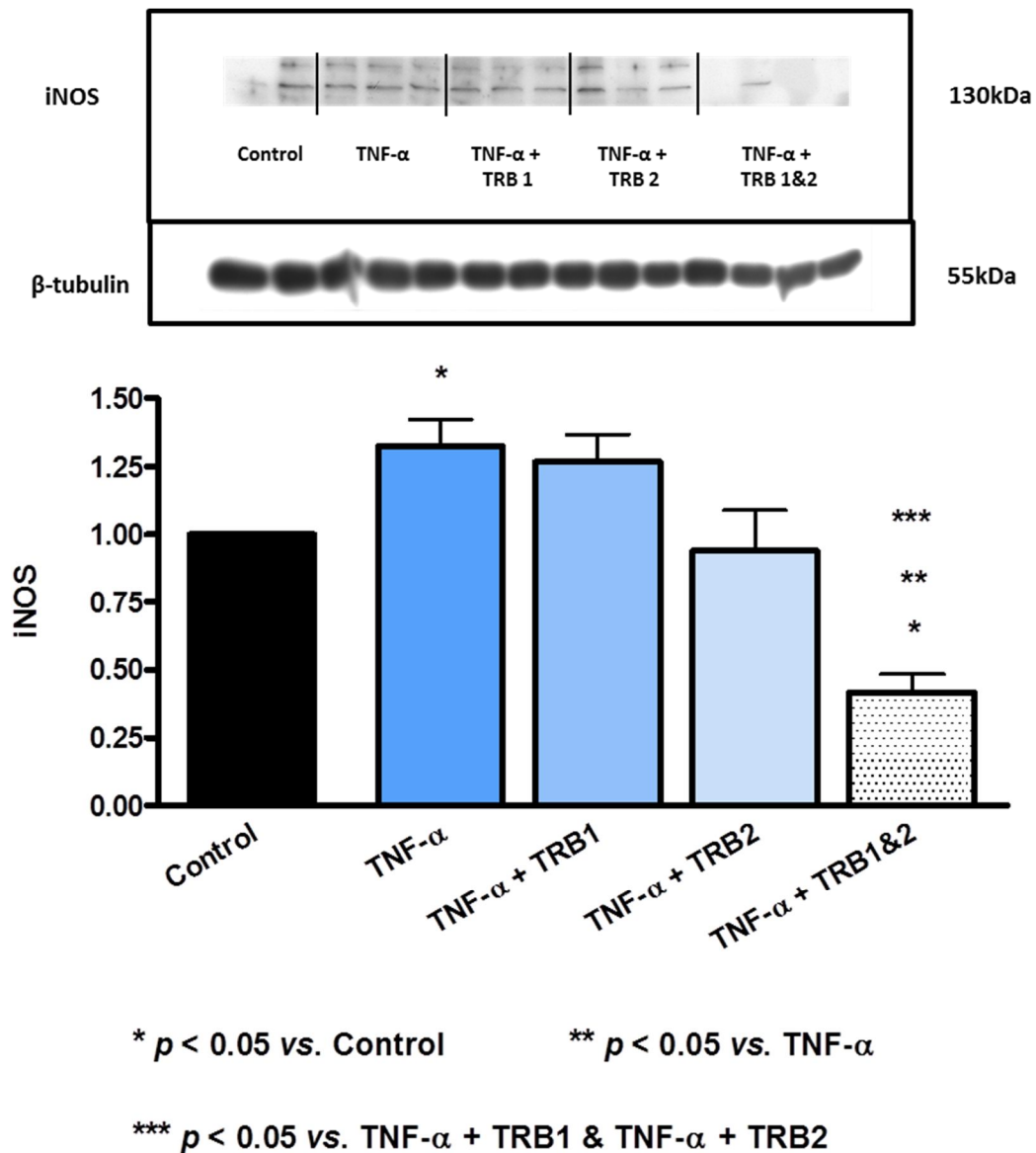


Figure 7.13: The effects of TNF- α receptor blockade (1 μ g / ml) on iNOS expression in TNF- α (20 ng / ml)-treated CMECs. Data are represented as iNOS expression (expressed as a ratio of control; control = 1). β -tubulin was used to validate equal protein loading. All data were expressed as a ratio of control with control adjusted to 1 (please refer to page 134, chapter 2). Sample size: n = 3 / group.

7.3.2 Western blot analysis of oxidative stress: p22 phox

Exposing CMECs to 30 minutes of TNF- α (20 ng / ml) led to increased p22 phox expression levels (1.55 ± 0.07 vs. 1.00 control: $p < 0.05$) (see figure 7.14).

TNFR1 blockade: Exposing CMECs to 30 minutes of TNF- α (20 ng / ml) + TRB1 (1 μ g / ml) led to increased p22 phox expression levels (1.89 ± 0.12 vs. 1.00 control: $p < 0.05$) (see figure 7.14).

TNFR2 blockade: Exposing CMECs to 30 minutes of TNF- α (20 ng / ml) + TRB2 (1 μ g / ml) led to increased p22 phox expression levels (1.71 ± 0.12 vs. 1.00 control: $p < 0.05$) (see figure 7.14).

TNFR1 + TNFR2 blockade: Exposing CMECs to 30 minutes of TNF- α (20 ng / ml) + TRB1 & 2 (1 μ g / ml) led to unchanged p22 phox expression levels (1.41 ± 0.18 vs. 1.00 control) (see figure 7.14).

When the different groups were compared with each other, it was evident that the up-regulation of p22 phox by TNF- α could not be reversed by TNFR1 blockade only or by TNFR2 blockade only. However, when both receptors were blocked, the significant increase in expression compared to untreated control CMECs was partially reversed (see Figure 7.14).

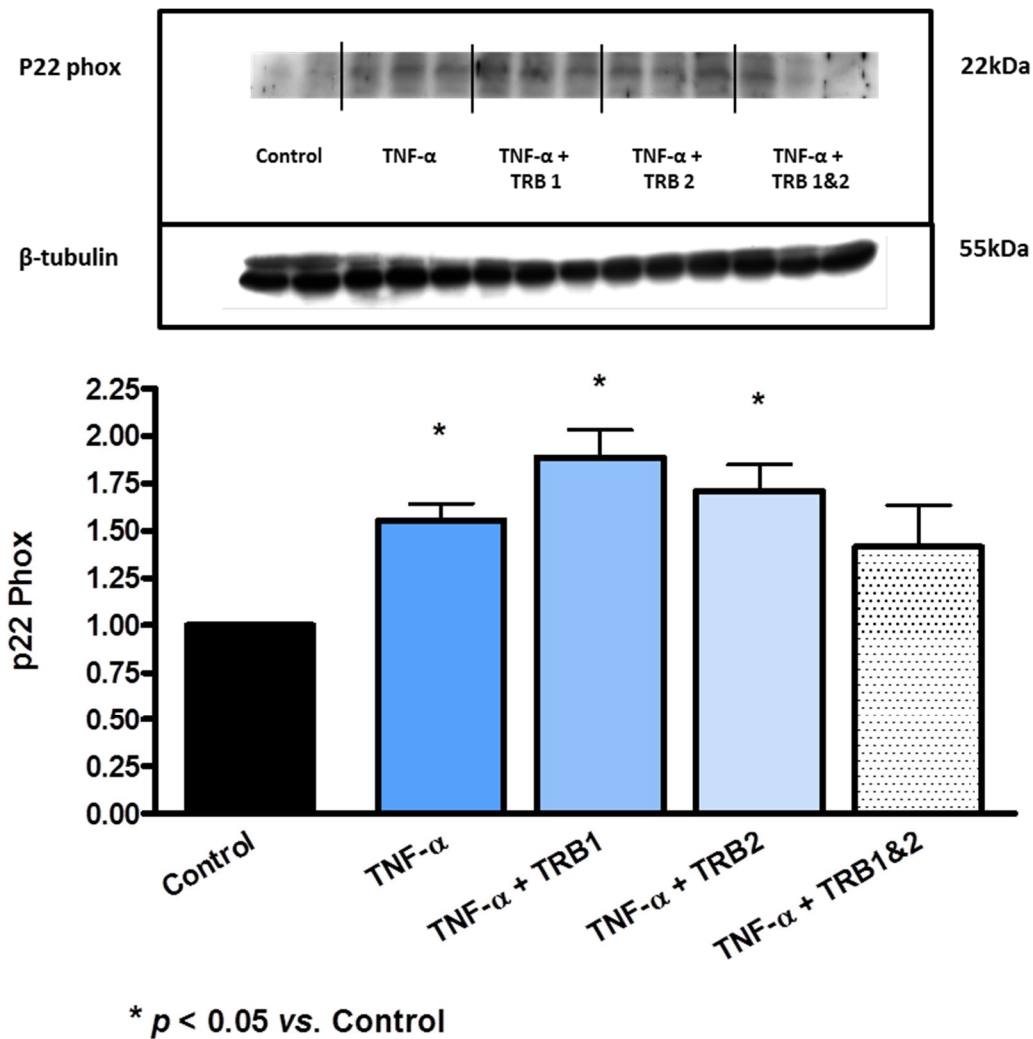


Figure 7.14: The effects of TNF- α receptor blockade (1 μ g / ml) on p22 phox expression in TNF- α (20 ng / ml)-treated CMECs. Data are represented as p22 phox expression (expressed as a ratio of control; control = 1). β -tubulin was used to validate equal protein loading. All data were expressed as a ratio of control with control adjusted to 1 (please refer to page 134, chapter 2). Sample size: n = 3 / group.

7.3.3 Western blot analysis of nitrosative stress: nitrotyrosine

Exposing CMECs to 30 minutes of TNF- α (20 ng / ml) led to unchanged nitrotyrosine expression levels (0.97 ± 0.03 vs. 1.00 control) (see figure 7.15).

TNFR1 blockade: Exposing CMECs to 30 minutes of TNF- α (20 ng / ml) + TRB1 (1 μ g / ml) led to unchanged nitrotyrosine expression levels (0.93 ± 0.01 vs. 1.00 control) (see figure 7.15).

TNFR2 blockade: Exposing CMECs to 30 minutes of TNF- α (20 ng / ml) + TRB2 (1 μ g / ml) led to decreased nitrotyrosine expression levels (0.70 ± 0.02 vs. 1.00 control: $p < 0.05$) (see figure 7.15).

TNFR1 + TNFR2 blockade: Exposing CMECs to 30 minutes of TNF- α (20 ng / ml) + TRB1 & 2 (1 μ g / ml) led to unchanged nitrotyrosine expression levels (0.93 ± 0.04 vs. 1.00 control) (see figure 7.15).

When the different groups were compared with each other, it was evident that the TNF- α -treated cells in which TNFR2 was blocked resulted in a significant down-regulation of nitrotyrosine expression compared to all the other groups (see Figure 7.15).

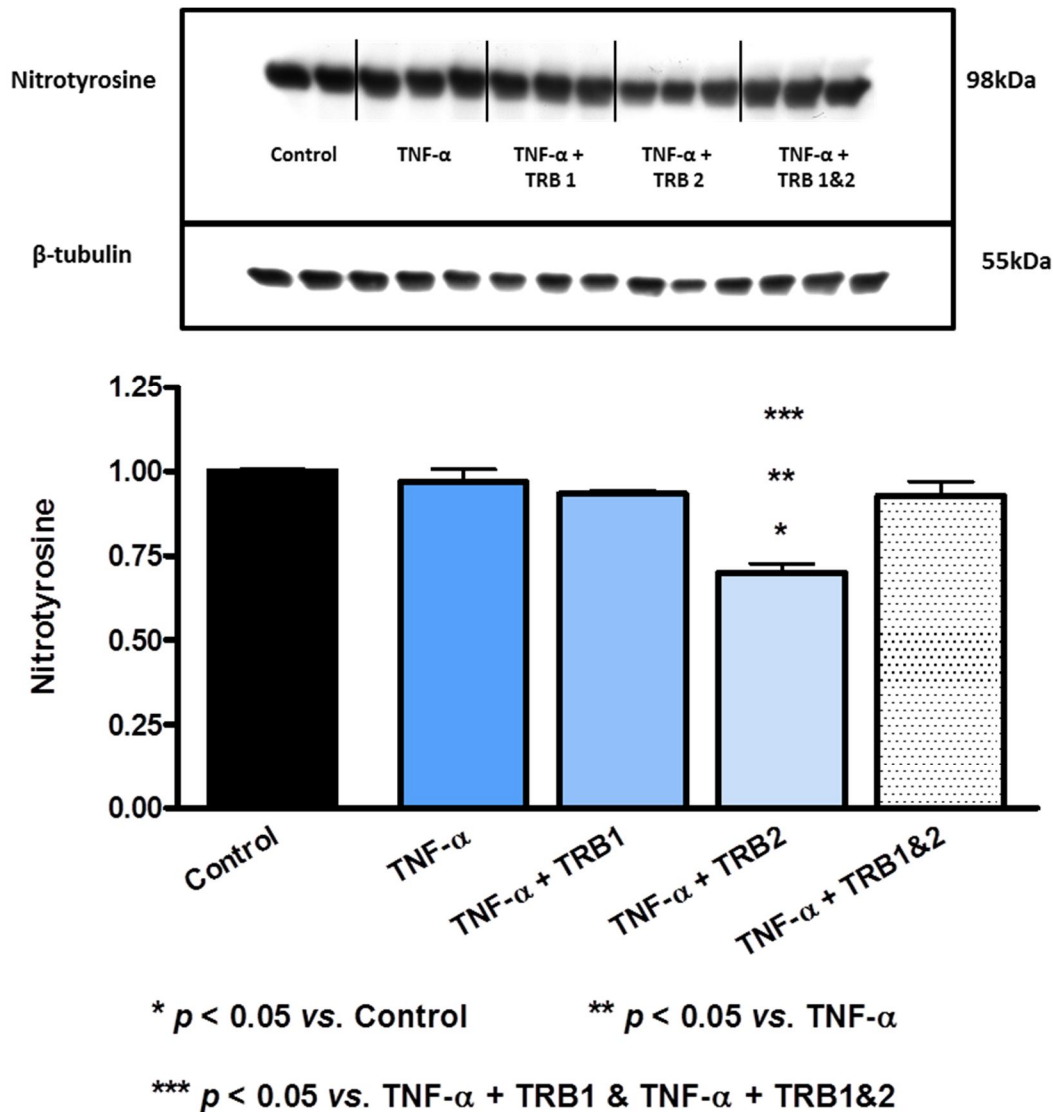


Figure 7.15: The effects of TNF- α receptor blockade (1 μ g / ml) on nitrotyrosine expression in TNF- α (20 ng / ml)-treated CMECs. Data are represented as nitrotyrosine expression (expressed as a ratio of control; control = 1). β -tubulin was used to validate equal protein loading. All data were expressed as a ratio of control with control adjusted to 1 (please refer to page 134, chapter 2). Sample size: n = 3 / group.

7.3.4 Western blot analysis of NFκB signalling: IKβα

Exposing CMECs to 30 minutes of TNF-α (20 ng / ml) led to unchanged IKβα expression levels (0.99 ± 0.08 vs. 1.00 control) (see figure 7.16).

TNFR1 blockade: Exposing CMECs to 30 minutes of TNF-α (20 ng / ml) + TRB1 (1 μg / ml) led to unchanged IKβα expression levels (1.16 ± 0.03 vs. 1.00 control) (see figure 7.16).

TNFR2 blockade: Exposing CMECs to 30 minutes of TNF-α (20 ng / ml) + TRB2 (1 μg / ml) led to unchanged IKβα expression levels (1.20 ± 0.10 vs. 1.00 control) (see figure 7.16).

TNFR1 + TNFR2 blockade: Exposing CMECs to 30 minutes of TNF-α (20 ng / ml) + TRB1 & 2 (1 μg / ml) led to increased IKβα expression levels (1.56 ± 0.03 vs. 1.00 control: $p < 0.05$) (see figure 7.16).

When the different groups were compared with each other, it was interesting to note that TNF-α did not achieve reduction in IKβα expression as observed with 24 hour treatment investigations previously discussed in this dissertation. However, it was that the TNF-α-treated cells in which both TNFR1 + TNFR2 were blocked resulted in a significant up-regulation of IKβα expression compared to all the other groups, except the TNFR2 blockade group (see Figure 7.16).

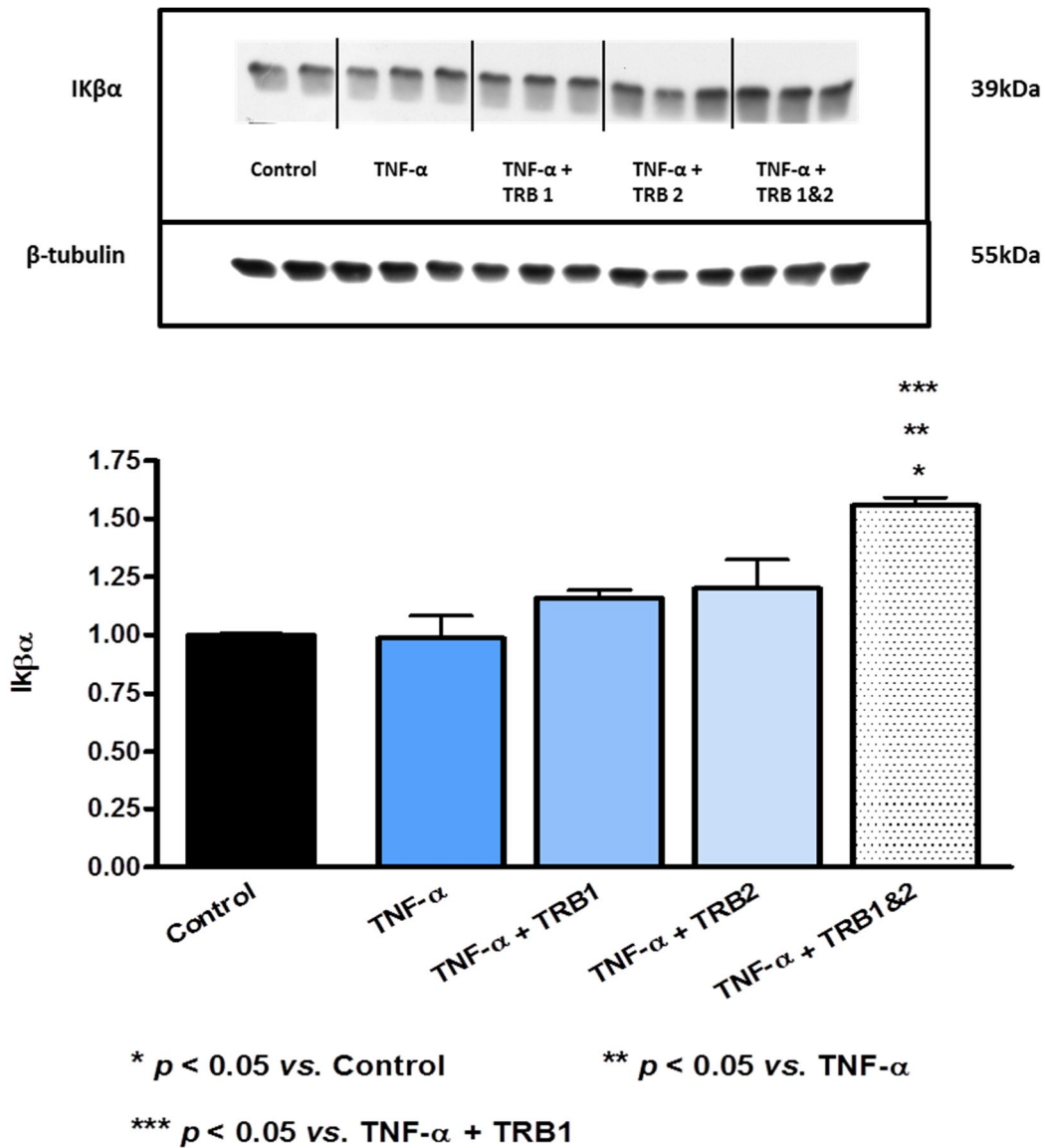


Figure 7.16: The effects of TNF- α receptor blockade (1 μg / ml) on IK $\beta\alpha$ expression in TNF- α (20 ng / ml)-treated CMECs. Data are represented as IK $\beta\alpha$ expression (expressed as a ratio of control; control = 1). β -tubulin was used to validate equal protein loading. All data were expressed as a ratio of control with control adjusted to 1 (please refer to page 134, chapter 2). Sample size: $n = 3$ / group.

7.3.5 Western blot analysis of apoptosis signalling:

Cleaved Caspase-3

Exposing CMECs to 30 minutes of TNF- α (20 ng / ml) led to increased cleaved caspase-3 expression levels (1.48 ± 0.11 vs. 1.00 control: $p < 0.05$) (see figure 7.17).

TNFR1 blockade: Exposing CMECs to 30 minutes of TNF- α (20 ng / ml) + TRB1 (1 μ g / ml) led to unchanged cleaved caspase-3 expression levels (1.16 ± 0.10 vs. 1.00 control) (see figure 7.17).

TNFR2 blockade: Exposing CMECs to 30 minutes of TNF- α (20 ng / ml) + TRB2 (1 μ g / ml) led to decreased cleaved caspase-3 expression levels (0.58 ± 0.21 vs. 1.00 control: $p < 0.05$) (see figure 7.17).

TNFR1 + TNFR2 blockade: Exposing CMECs to 30 minutes of TNF- α (20 ng / ml) + TRB1 & 2 (1 μ g / ml) led to decreased cleaved caspase-3 expression levels (0.78 ± 0.04 vs. 1.00 control: $p < 0.05$) (see figure 7.17).

When the different groups were compared with each other, it was interesting to note that TNF- α significantly increased cleaved caspase-3 levels at this time point, something that was not observed in the 24 hours experiments (see Chapter 6). Furthermore, all three blockade scenarios succeeded in either partially or completely reversing the effects of TNF- α treatment. In fact, TNFR2 blockade alone and TNFR1 + TNFR2 blockade resulted in a significant reduction in cleaved caspase-3 levels compared to untreated controls and TNF- α treated cells (without blockers). Additionally, TNFR1 + TNFR2 blockade resulted in a significant reduction in cleaved caspase-3 levels compared to the TNFR1 blockade group (see Figure 7.17).

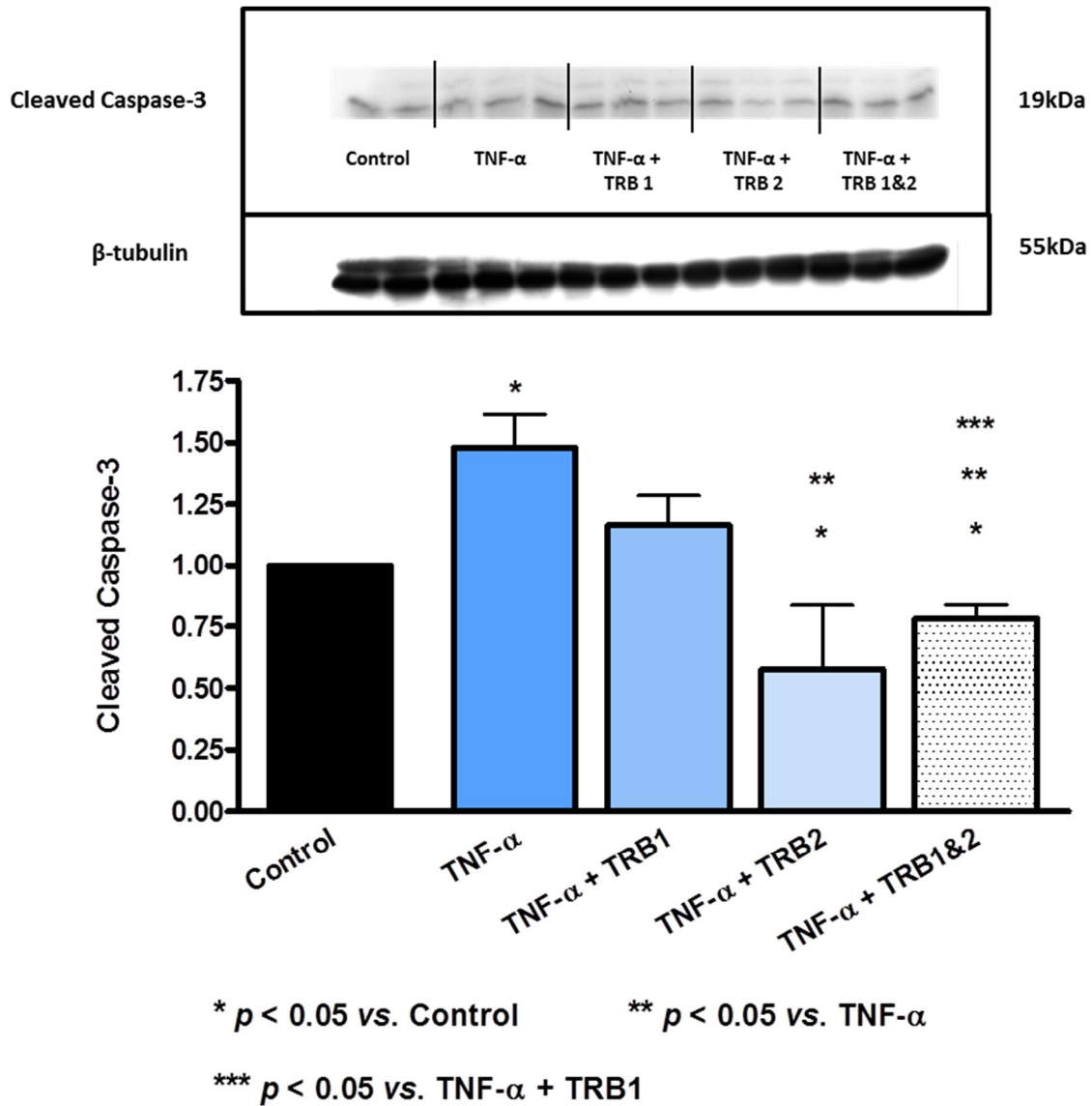


Figure 7.17: The effects of TNF- α receptor blockade (1 μ g / ml) on cleaved caspase-3 expression in TNF- α (20 ng / ml)-treated CMECs. Data are represented as cleaved caspase-3 expression (expressed as a ratio of control; control = 1). β -tubulin was used to validate equal protein loading. All data were expressed as a ratio of control with control adjusted to 1 (please refer to page 134, chapter 2). Sample size: $n = 3$ / group.

Cleaved PARP

Exposing CMECs to 30 minutes of TNF- α (20 ng / ml) led to increased cleaved PARP expression levels (1.33 ± 0.07 vs. 1.00 control: $p < 0.05$) (see figure 7.18).

TNFR1 blockade: Exposing CMECs to 30 minutes of TNF- α (20 ng / ml) + TRB1 (1 μ g / ml) led to increased cleaved PARP expression levels (1.33 ± 0.07 vs. 1.00 control: $p < 0.05$) (see figure 7.18).

TNFR2 blockade: Exposing CMECs to 30 minutes of TNF- α (20 ng / ml) + TRB2 (1 μ g / ml) led to increased cleaved PARP expression levels (1.33 ± 0.07 vs. 1.00 control: $p < 0.05$) (see figure 7.18).

TNFR1 + TNFR2 blockade: Exposing CMECs to 30 minutes of TNF- α (20 ng / ml) + TRB1 & 2 (1 μ g / ml) led to increased cleaved PARP expression levels (1.78 ± 0.04 vs. 1.00 control: $p < 0.05$) (see figure 7.18).

Exposing CMECs to 24 hours of TNF- α (20 ng / ml) + TRB1 & 2 (1 μ g / ml) led to a significant increase (1.33 ± 0.07 vs. 1.00 control: $p < 0.05$) (see figure 7.18) in the expression of cleaved PARP compared to untreated controls.

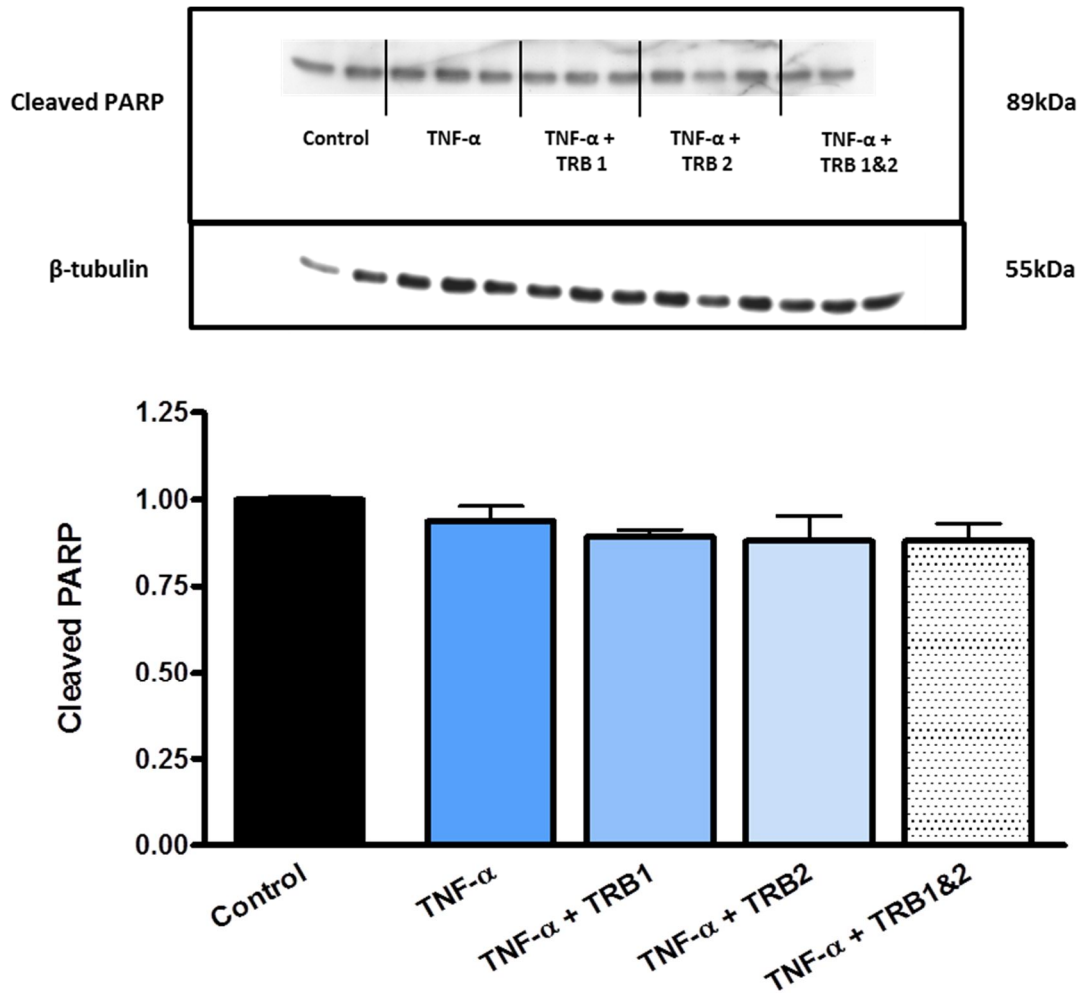


Figure 7.18: The effects of TNF- α receptor blockade (1 μ g / ml) on cleaved PARP expression in TNF- α (20 ng / ml)-treated CMECs. Data are represented as cleaved PARP expression (expressed as a ratio of control; control = 1). β -tubulin was used to validate equal protein loading. All data were expressed as a ratio of control with control adjusted to 1 (please refer to page 134, chapter 2). Sample size: n = 3 / group.

7.4 **Discussion**

A thorough literature search has revealed that there is a lack of studies that have investigated the intracellular effects (endpoints: NOS, oxidative and nitrosative stress, NF- κ B, and apoptosis signalling) of exogenous TNF- α treatment in the context of pharmacological TNF receptor blockade in endothelial cells. In the light of this, we will discuss a few studies that have investigated the effects of the TNF- α receptors in different scenarios.

To determine the effects of anti-receptor antagonistic antibodies, human umbilical vein endothelial cells (HUVECs) were pretreated for 1 hour in the absence or presence of the appropriate antibody, before the addition of TNF- α (50 ng / ml) for 4 to 24 hours (Paleolog *et al.*, 1994). They found the following: Anti-p55 (TNFR1) and anti-p75 (TNFR2) receptor antibodies inhibited endothelial adhesion molecule expression and cytokine release to different degrees; anti-p55 receptor agonistic antibody increased release of cytokines and adhesion molecule expression on endothelial cells; anti-p55 agonist Htr-9 inhibits endothelial cell proliferation and endothelial cell responses to lymphotoxin are significantly inhibited by anti-p55 but not by anti-p75 antibody. Interestingly, another study investigated the involvement of both receptors in the activation of endothelial cells by TNF- α (Slowik *et al.*, 1993). They blocked HUVECs 2 hours prior to treatment with 6 ng / ml TNF- α for another 4 hours and concluded from their results that contrary to Mackay *et al.* (1993), both receptors are involved in endothelial cell activation.

In a study on cardiac myocytes, cells were exposed to pre-treatment with anti-TNFR1 and anti-TNFR2 for 30 minutes to neutralize the receptors and then subsequently treated for a further 30 minutes with 25 ng / ml TNF- α , a clear role for the TNFR2 was shown in cardiac pathology (Defer *et al.*, 2007). Their results characterized a TNFR2-dependent signalling and illustrated the close interplay between TNFR1 and TNFR2 pathways in cardiac myocytes. Although apparently predominant, TNFR1-dependent responses were under the yoke of TNFR2, acting as a critical limiting factor.

In the present study, the pre-treatment of CMECs with 1 μ g / ml of either TRB1 or TRB2 or the combination and subsequent treatment with TNF- α (20 ng / ml) for a further 30 minutes, yielded quite interesting and novel results and will be discussed below.

NOS signalling: We (see Chapter 5) and others (Gao *et al.*, 2007; Picchi *et al.*, 2006; Ahmad *et al.*, 2002) have previously shown that TNF- α can impair NO- production. Therefore, the effects of TNF receptor blockade was also investigated with regard to its possible effects on NOS-NO biosynthesis. Treatment of CMECs with TNF- α alone had no effect on eNOS expression or phosphorylation, despite a relative increase in PKB/Akt activation. TNF- α treatment, however, did result in an increase in iNOS expression. Blocking of either TNFR1 alone or TNFR2 alone had no effect on relative eNOS activation and iNOS expression in TNF- α -treated cells; however, when both TNFR1 and TNFR2 were blocked, eNOS activation was profoundly decreased, even compared to untreated control groups. Blockade of both TNFR1 and TNFR2 also significantly decreased iNOS expression. The large reduction in eNOS activation was accompanied by a reduction in HSP 90 (which is required for eNOS phosphorylation). These data are interesting, as it suggests that *both* TNFR1 and TNFR2 are required for eNOS activation, not only in the context of exogenous TNF- α -treatment, but possibly also for baseline, physiological levels of activated eNOS. Alternatively, although we could not substantiate this from evidence in the literature, it is theoretically possible that the exogenously administered TNF- α may have exerted non-receptor mediated effects on eNOS activation. Although we did not investigate this, it would be interesting to perform the double blockade experiments on normal, untreated cells to further unravel this phenomenon. Our data therefore also suggest that crosstalk between the two receptors is present in the regulation of NOS signalling. Interestingly, although some of the respective treatments had an effect on some of the key role-players in NOS-signalling (HSP 90 and caveolin-1) as well as one of the upstream activators of eNOS, it did not have any effect on eNOS. For instance, with TNF- α treatment only, PKB/Akt was upregulated, but eNOS unchanged (see figure 7.19A). Blocking TNFR1 also upregulated PKB/Akt and downregulated caveolin-1, but eNOS remained unchanged (see figure 7.19B). Blocking TNFR2 decreased HSP 90, but eNOS remained unchanged (see figure 7.19C). See figures 7.19 (A-D) for a schematic representation of the findings of the NOS signalling investigations.

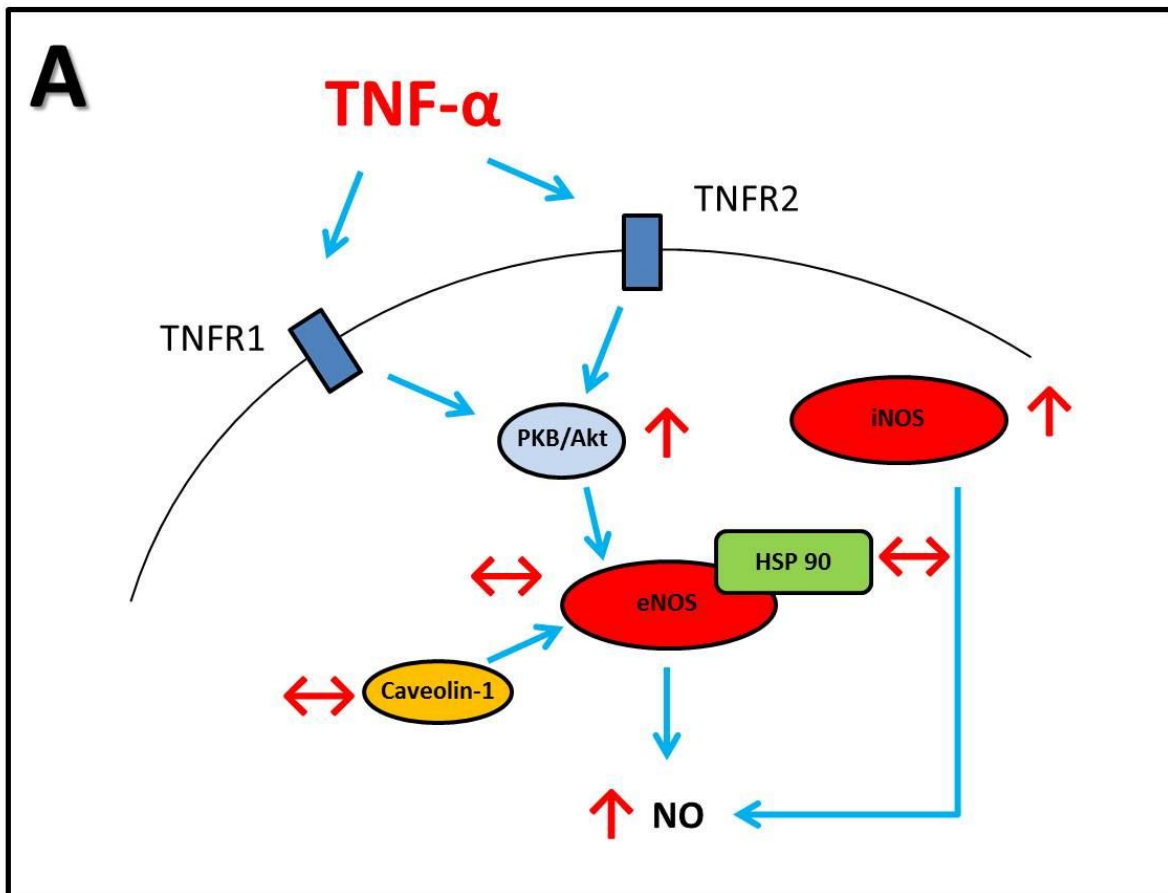


Figure 7.19: Simplified schematic overview of:

A: TNF- α NOS-signalling.

Note: Red letters indicate treatment, blue arrows indicate active pathways and black arrows indicate inactive pathways.

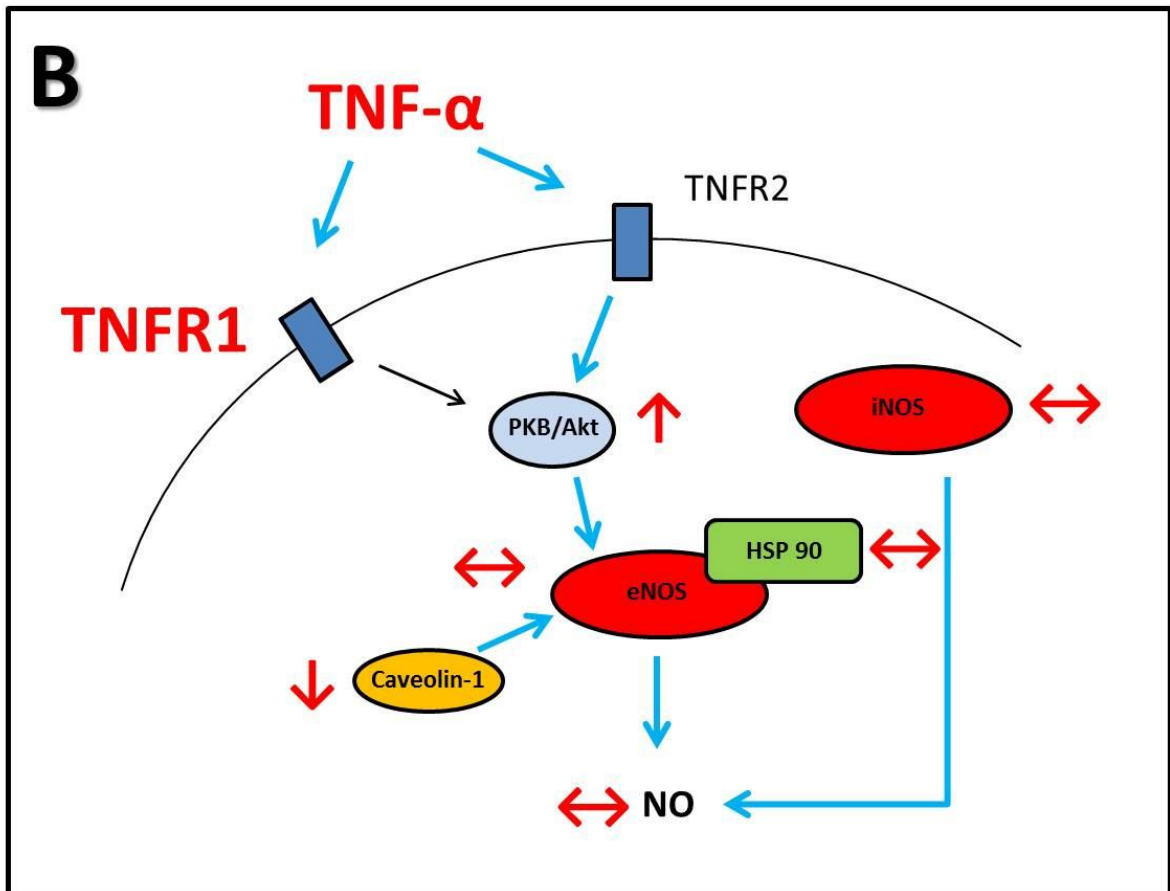


Figure 7.19: Simplified schematic overview of:

B: TNF- α + TRB1 NOS-signalling.

Note: Red letters indicate treatment, blue arrows indicate active pathways and black arrows indicate inactive pathways.

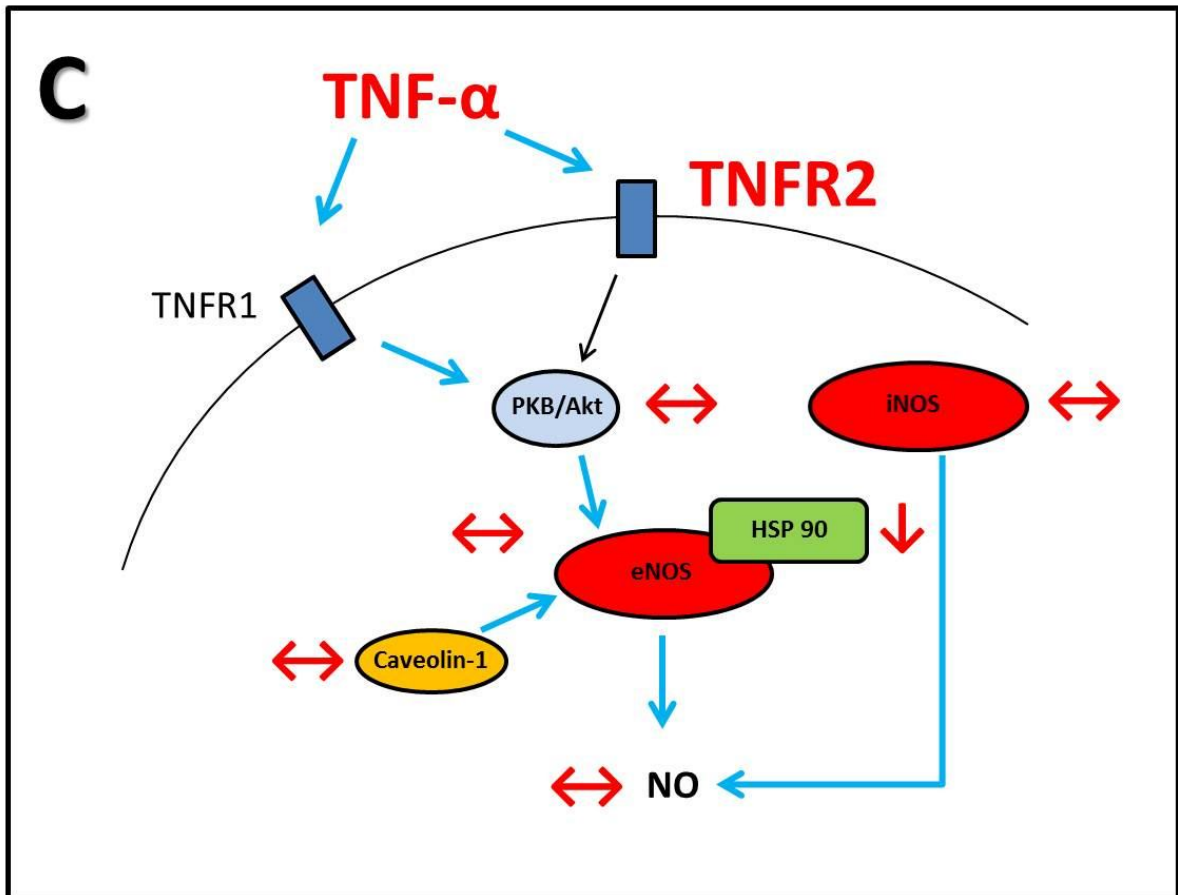


Figure 7.19: Simplified schematic overview of:

C: TNF- α + TRB2 NOS-signalling.

Note: Red letters indicate treatment, blue arrows indicate active pathways and black arrows indicate inactive pathways.

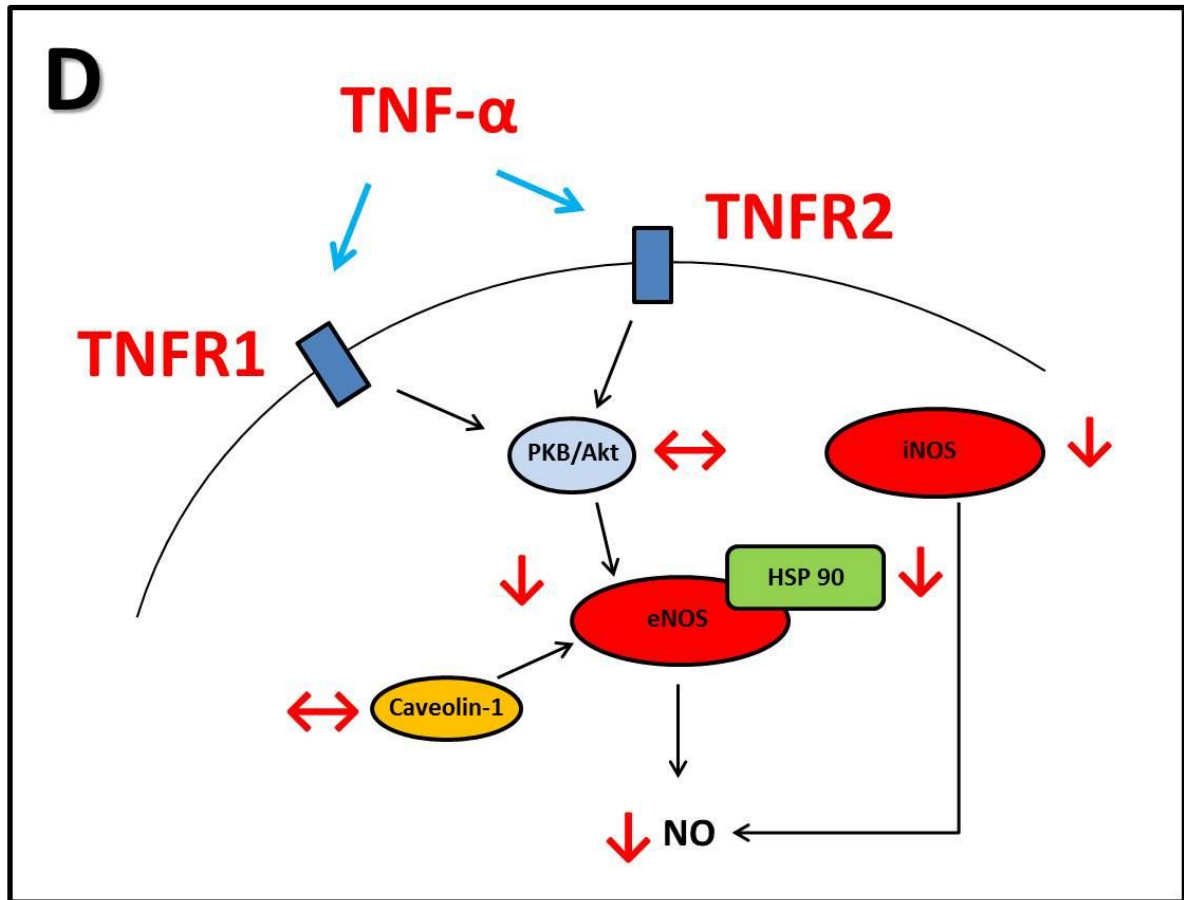


Figure 7.19: Simplified schematic overview of:

D: TNF- α + TRB1 & 2 NOS-signalling.

Note: Red letters indicate treatment, blue arrows indicate active pathways and black arrows indicate inactive pathways.

Oxidative / nitrosative stress: TNF- α is often associated with increased ROS production in endothelial cells (Chen W *et al.*, 2008). In light of this fact, we also set out to investigate the effects of TNF receptor blockade with regard to its possible effects on ROS production. CMECs treated with TNF- α caused an increase in p22 phox expression, but had no effect on nitrotyrosine expression (see figure 7.20A). In view of the significant increase in p22 phox, we assume that some degree of oxidative stress had been induced. From the data it is evident that either TNFR1 or TNFR2 leads to TNF- α -induced up-regulation of p22 phox, but when both receptors are simultaneously blocked, the increased TNF- α -induced expression of p22 phox is lost (figure 7.20B & C). These results are again suggestive of crosstalk between the two receptor systems. With regard to nitrotyrosine expression, the data showed that nitrosative stress was not induced in any of the groups. See figures 7.20 (A-D) for a schematic representation of the findings of the oxidative / nitrosative stress investigations.

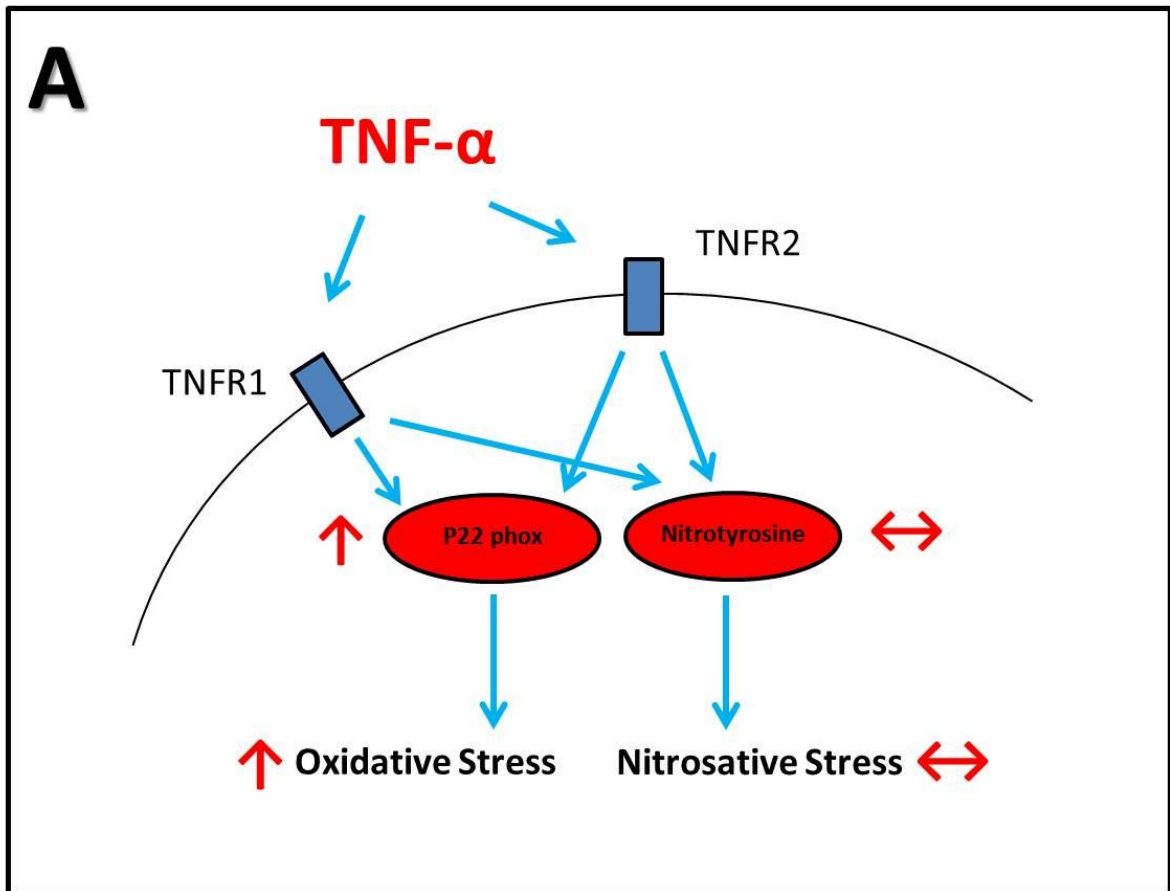


Figure 7.20: Simplified schematic overview of:

A: TNF- α oxidative/nitrosative stress-signalling.

Note: Red letters indicate treatment, blue arrows indicate active pathways and black arrows indicate inactive pathways.

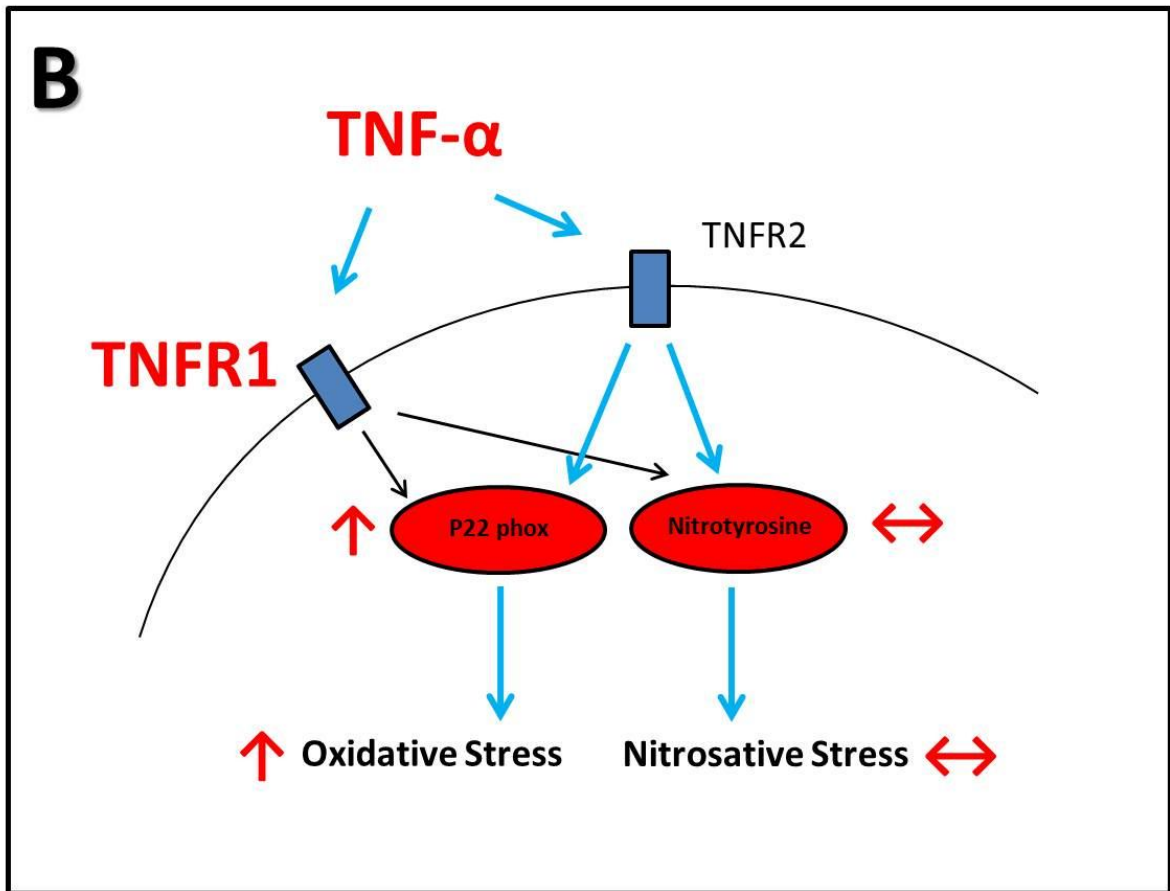


Figure 7.20: Simplified schematic overview of:

B: TNF- α + TRB1 oxidative/nitrosative stress-signalling.

Note: Red letters indicate treatment, blue arrows indicate active pathways and black arrows indicate inactive pathways.

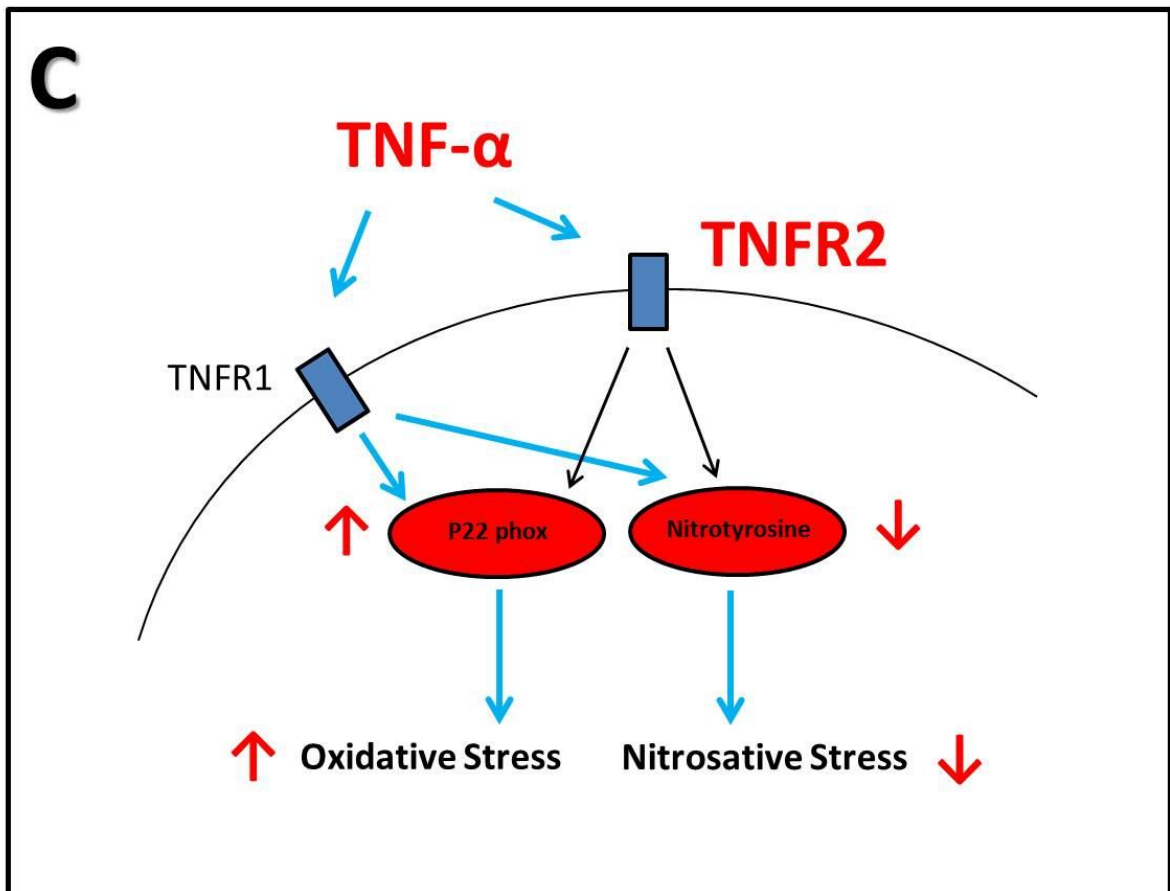


Figure 7.20: Simplified schematic overview of:

C: TNF- α + TRB2 oxidative/nitrosative stress-signalling.

Note: Red letters indicate treatment, blue arrows indicate active pathways and black arrows indicate inactive pathways.

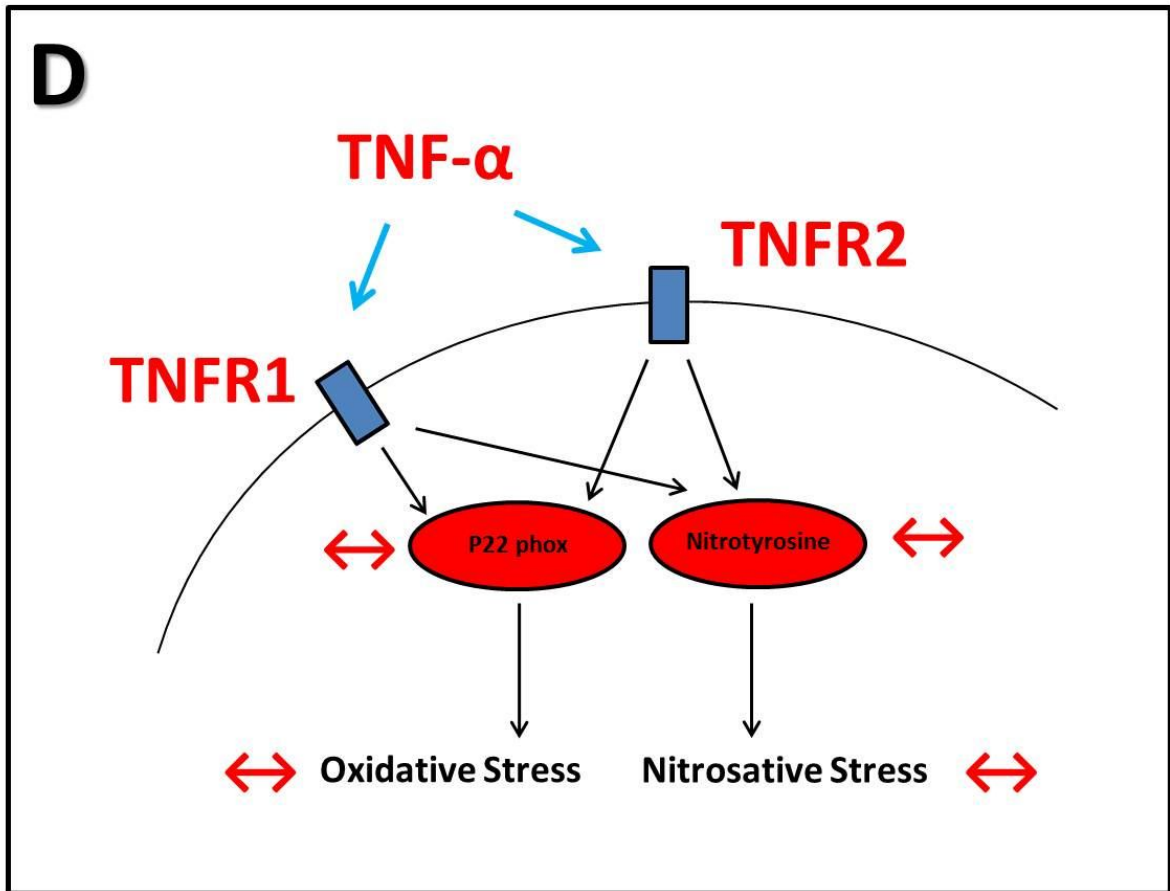


Figure 7.20: Simplified schematic overview of:

D: TNF- α + TRB1 & 2 oxidative/nitrosative stress-signalling.

Note: Red letters indicate treatment, blue arrows indicate active pathways and black arrows indicate inactive pathways.

NF- κ B signalling: According to the literature, a reduction in IK β α protein levels is a marker of NF- κ B activation (Hoffmann *et al.*, 2002). Therefore, it was important for us to investigate the effects of TNF receptor blockade with regard to its possible effects on NF- κ B activation. Interestingly, TNF- α (20 ng / ml) treatment did not result in decreased IK β α (as was seen in chapter 5 with the same concentration), although the duration of treatment seems to be an important factor here (see figure 7.21A). In view of this, we assume that TNF- α in this experimental scenario did not lead to NF- κ B activation. From the data it is evident that blockade of both receptors (TRB1+TRB2), led to a significant increase in IK β α protein levels, where blocking of either had no effect (see figure 7.21B & C) and from this we assume that both receptors are required for NF- κ B activation (see figure 7.21D). Therefore, we can assume that TNF- α probably elicits its pro-inflammatory effects through both receptors. See figures 7.21 (A–D) for a schematic representation of the findings of the IK β α signalling investigations.

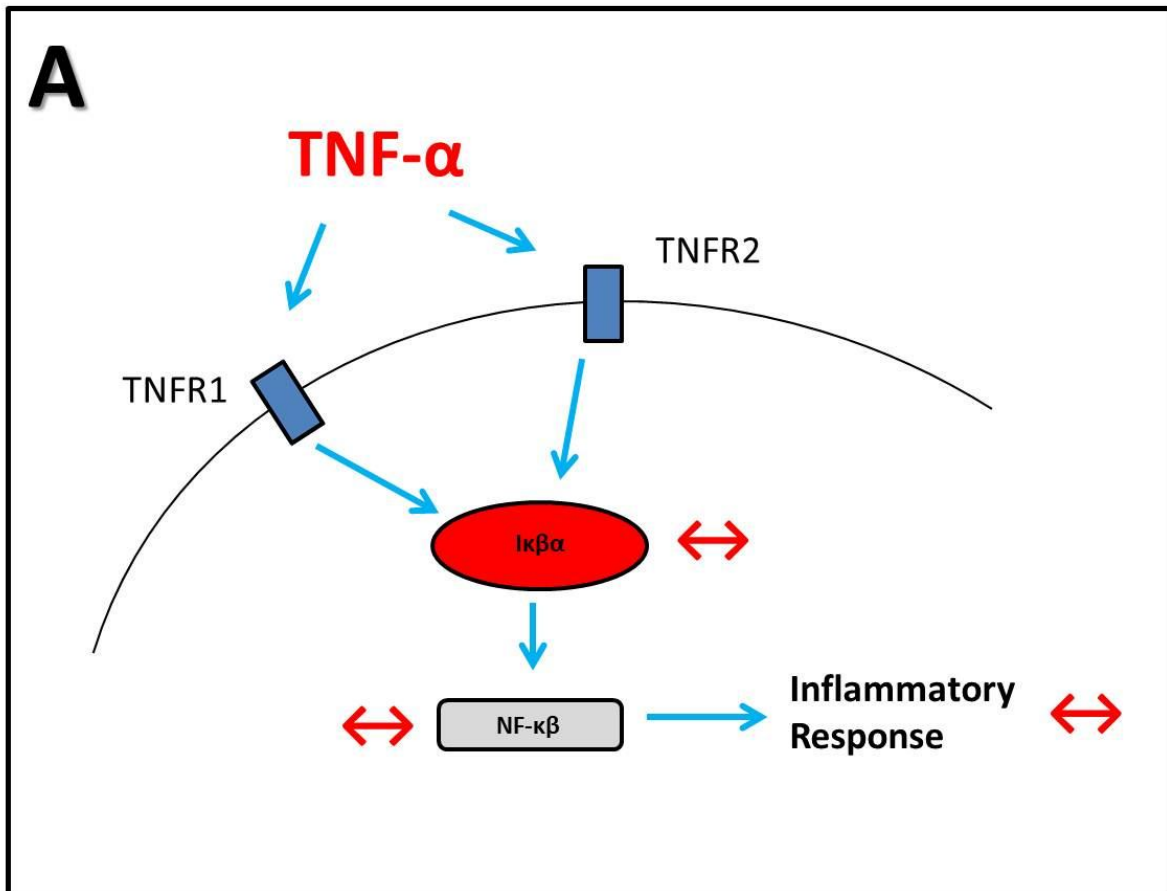


Figure 7.21: Simplified schematic overview of:

A: TNF- α I κ B α -signalling.

Note: Red letters indicate treatment, blue arrows indicate active pathways and black arrows indicate inactive pathways.

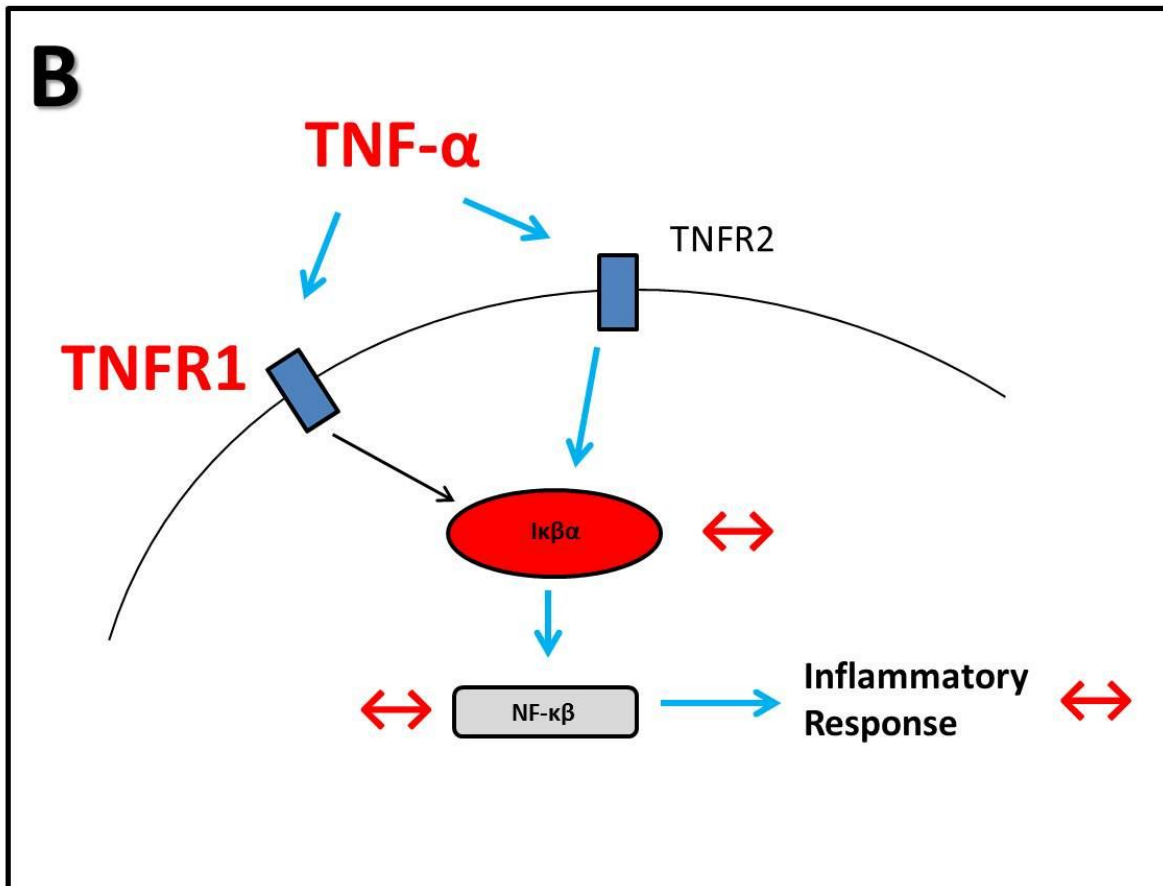


Figure 7.21: Simplified schematic overview of:

B: TNF- α + TRB1 IK β α -signalling.

Note: Red letters indicate treatment, blue arrows indicate active pathways and black arrows indicate inactive pathways.

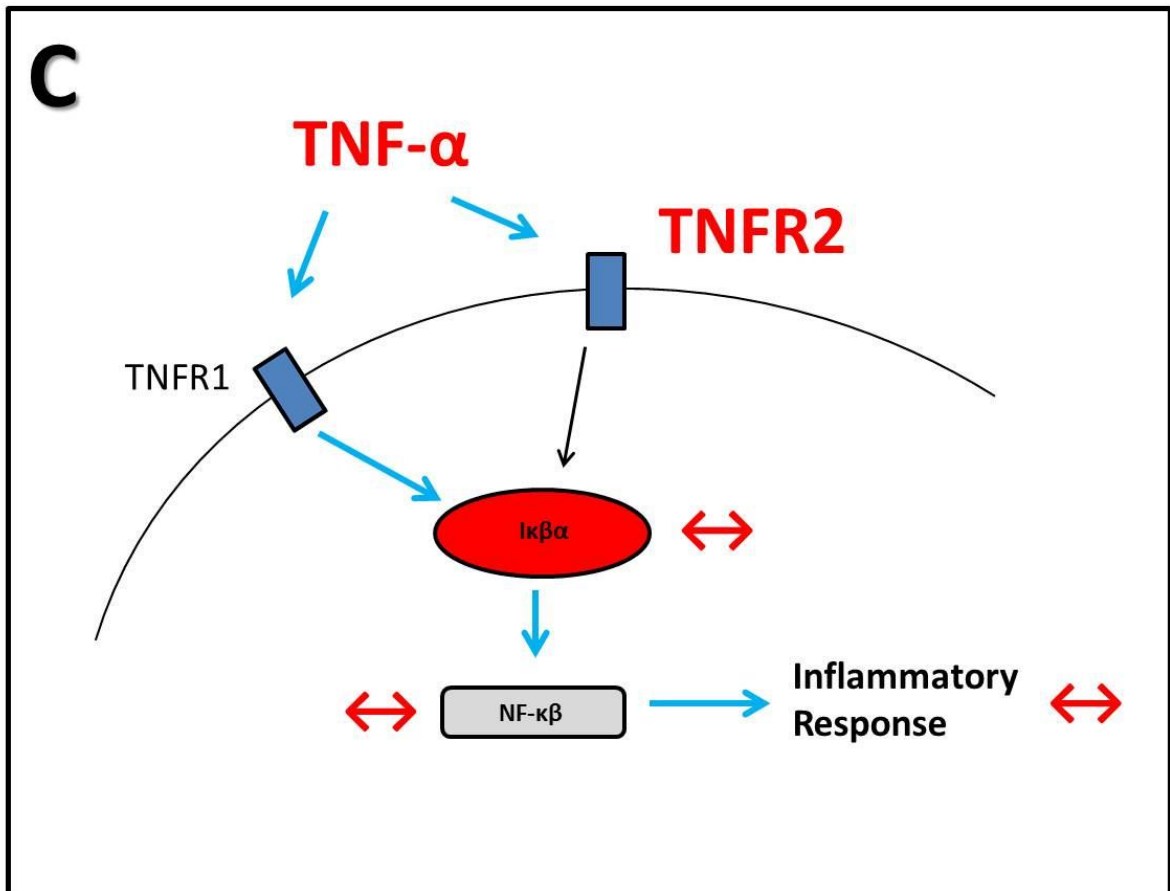


Figure 7.21: Simplified schematic overview of:

C: TNF- α + TRB2 IK β α -signalling.

Note: Red letters indicate treatment, blue arrows indicate active pathways and black arrows indicate inactive pathways.

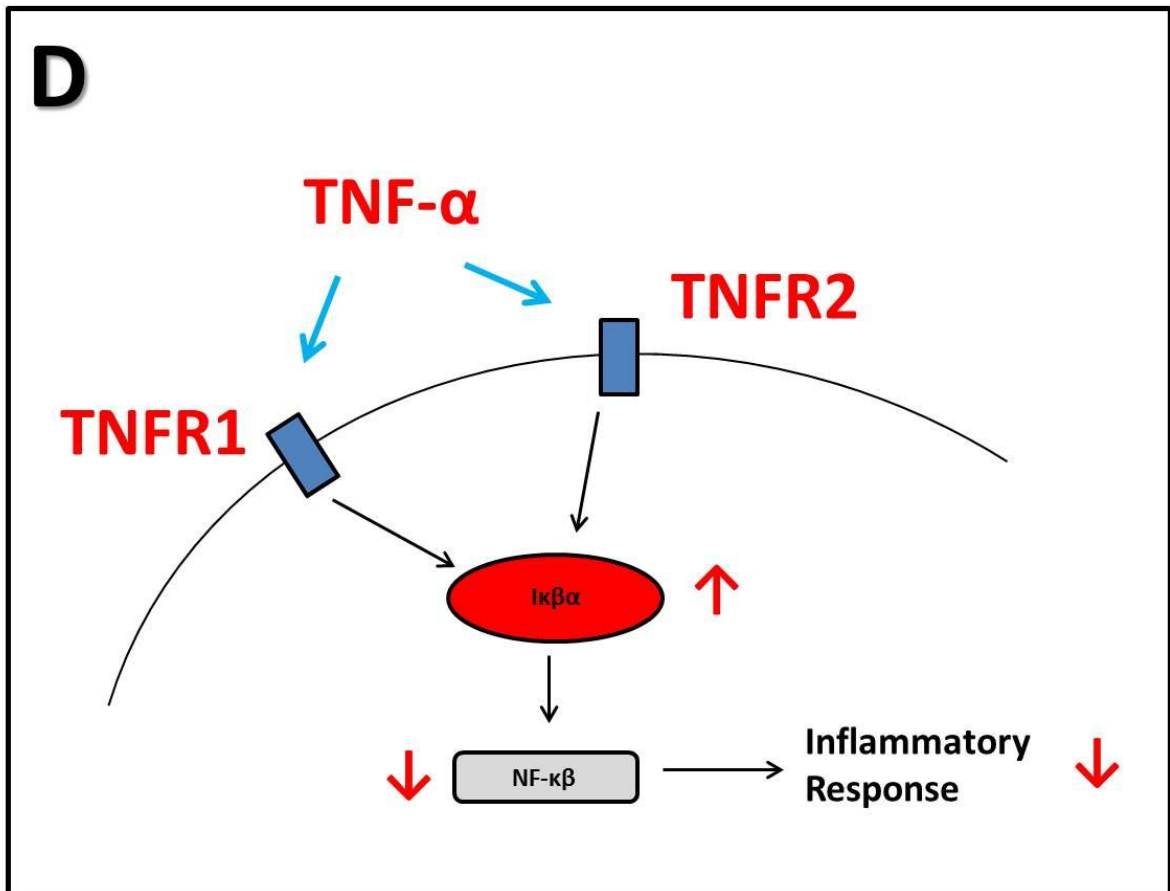


Figure 7.21: Simplified schematic overview of:

D: TNF- α + TRB1 & 2 IK β α -signalling.

Note: Red letters indicate treatment, blue arrows indicate active pathways and black arrows indicate inactive pathways.

Apoptosis: According to many studies in the literature, apoptosis is often a consequence of TNF- α induced effects. Therefore, as has been the case throughout the chapters dealing with TNF- α in this dissertation, the effects of TNF receptor blockade was also investigated with regard to its possible effects on apoptosis. CMECs treated with TNF- α caused an increase in cleaved caspase-3, but had no effect on cleaved PARP (see figure 7.22). In view of the significant increase in cleaved caspase-3, it is sufficient for the purposes of the present chapter to assume that some degree of apoptosis had been induced. From the data it is evident that both TNFR1 and TNFR2 are required for the induction of the caspase-3 apoptosis pathway, since all three blockade scenarios (see figure 7.22B, C & D) resulted in either a partial attenuation (TRB1 alone), or in fact a complete reversal (TRB2 alone and TRB1+TRB2; almost signifying an anti-apoptotic response) of the TNF- α effects. Our data therefore suggest that crosstalk between the two receptor systems is present in the regulation of caspase-3. Interestingly, none of the respective treatments had any effects on baseline cleaved PARP levels, indicating that, in our hands, this branch of apoptosis was not involved. See figures 7.22 (A–D) for a schematic representation of the findings of the apoptosis investigations.

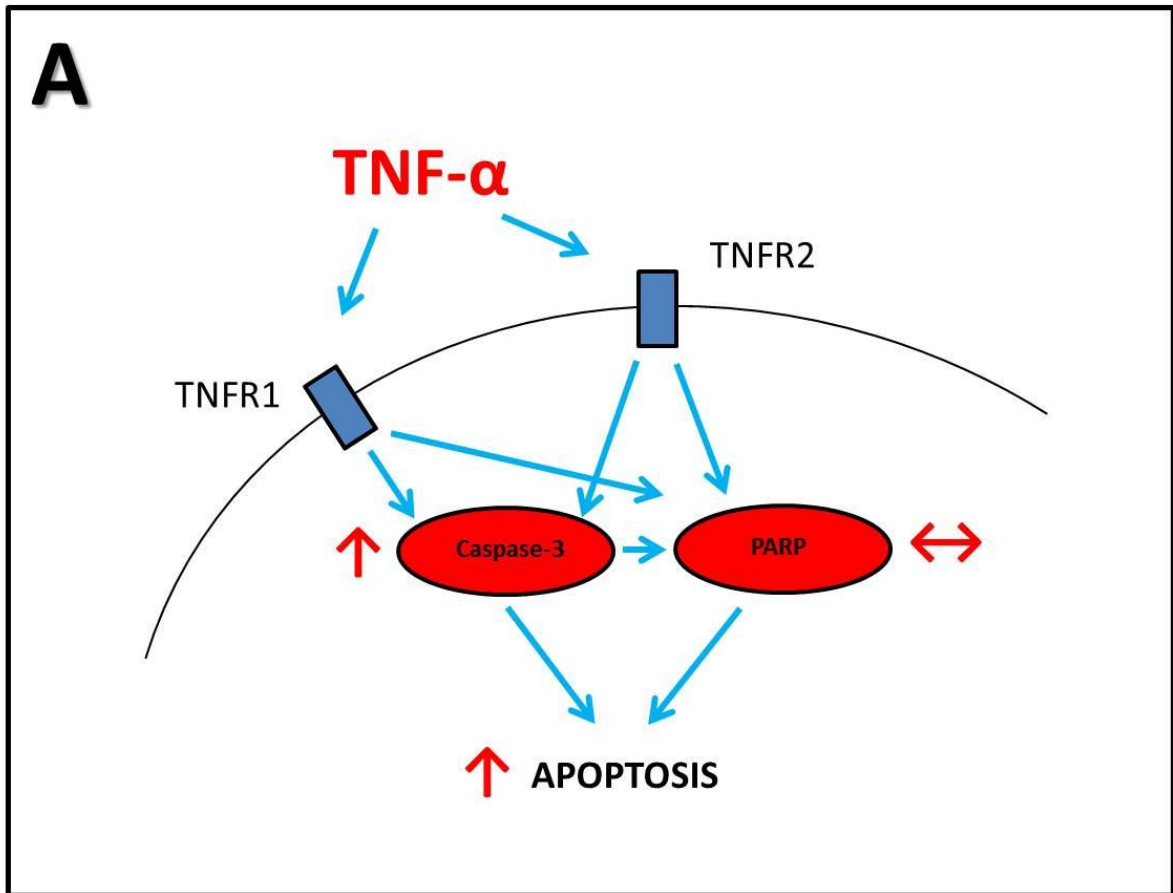


Figure 7.22: Simplified schematic overview of:

A: TNF- α apoptosis-signalling.

Note: Red letters indicate treatment, blue arrows indicate active pathways and black arrows indicate inactive pathways.

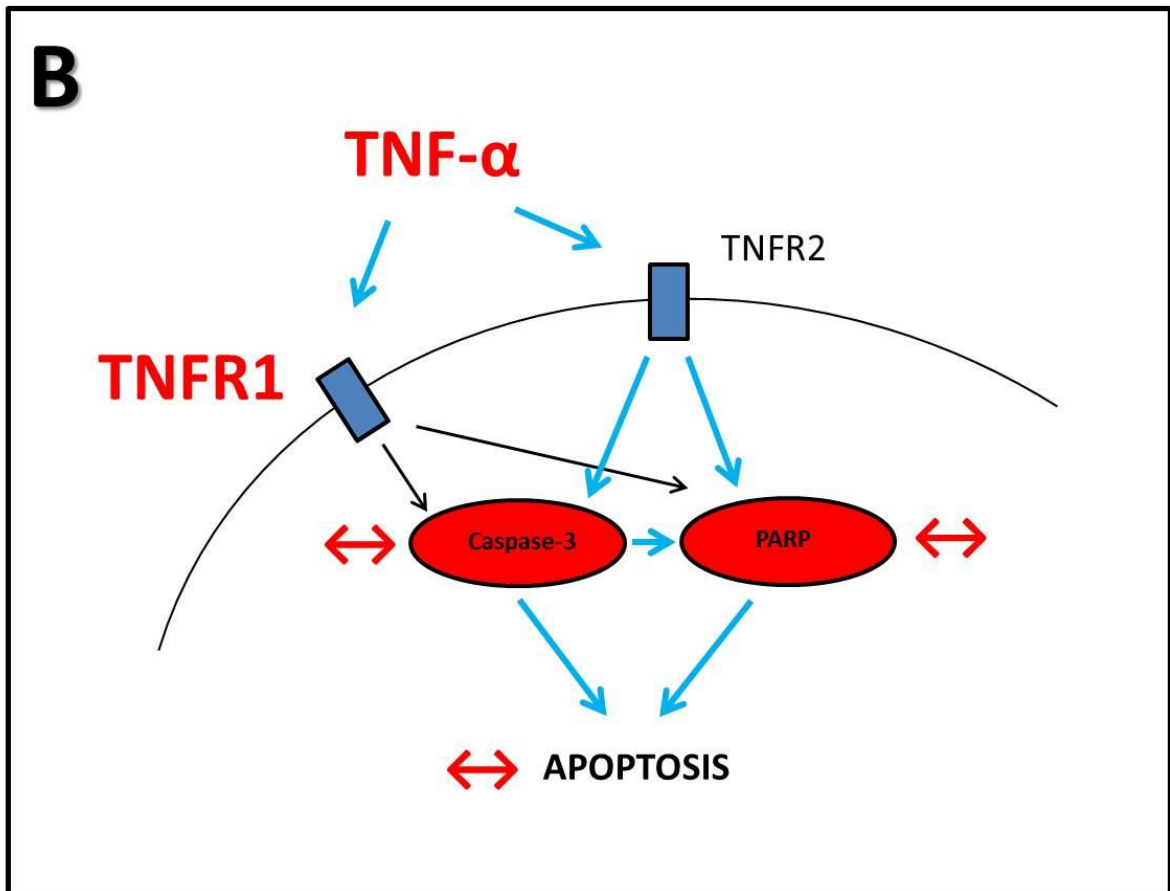


Figure 7.22: Simplified schematic overview of:

B: TNF- α + TRB1 apoptosis-signalling.

Note: Red letters indicate treatment, blue arrows indicate active pathways and black arrows indicate inactive pathways.

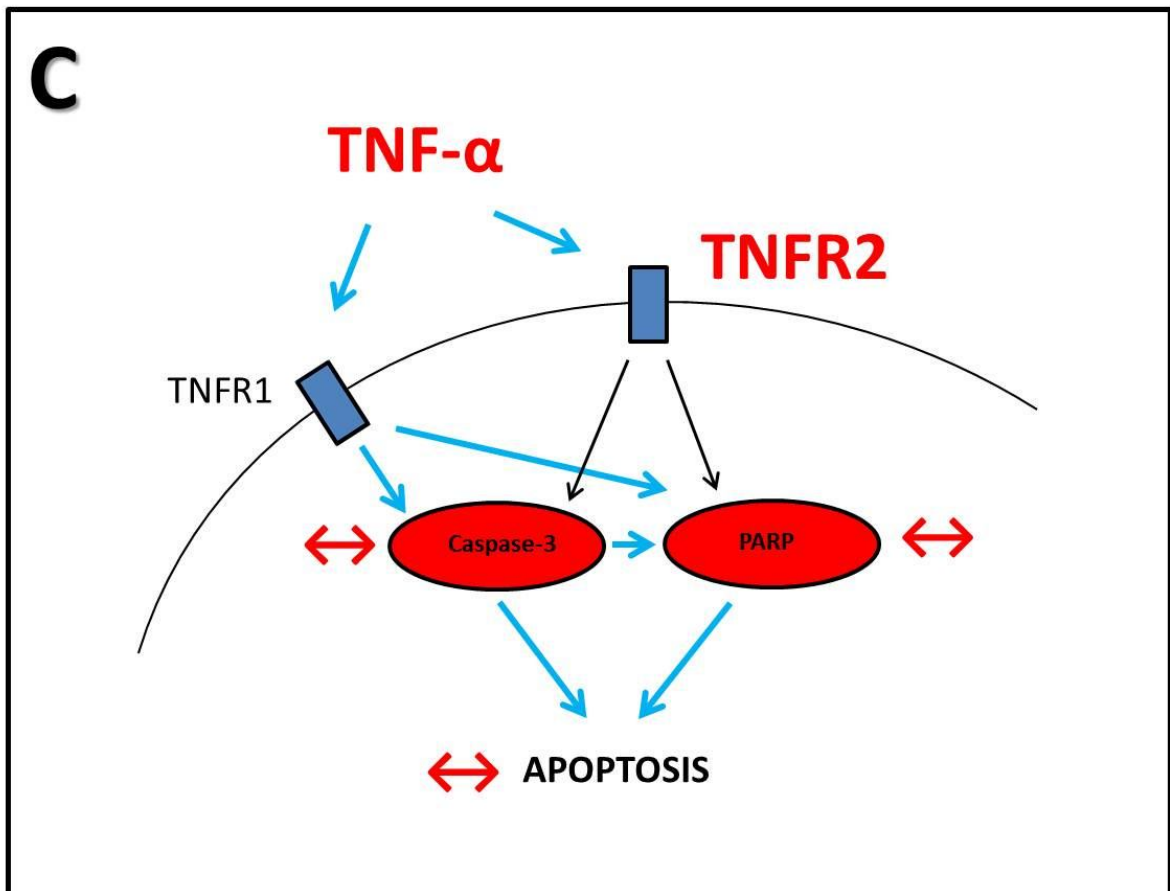


Figure 7.22: Simplified schematic overview of:

C: TNF- α + TRB2 apoptosis-signalling.

Note: Red letters indicate treatment, blue arrows indicate active pathways and black arrows indicate inactive pathways.

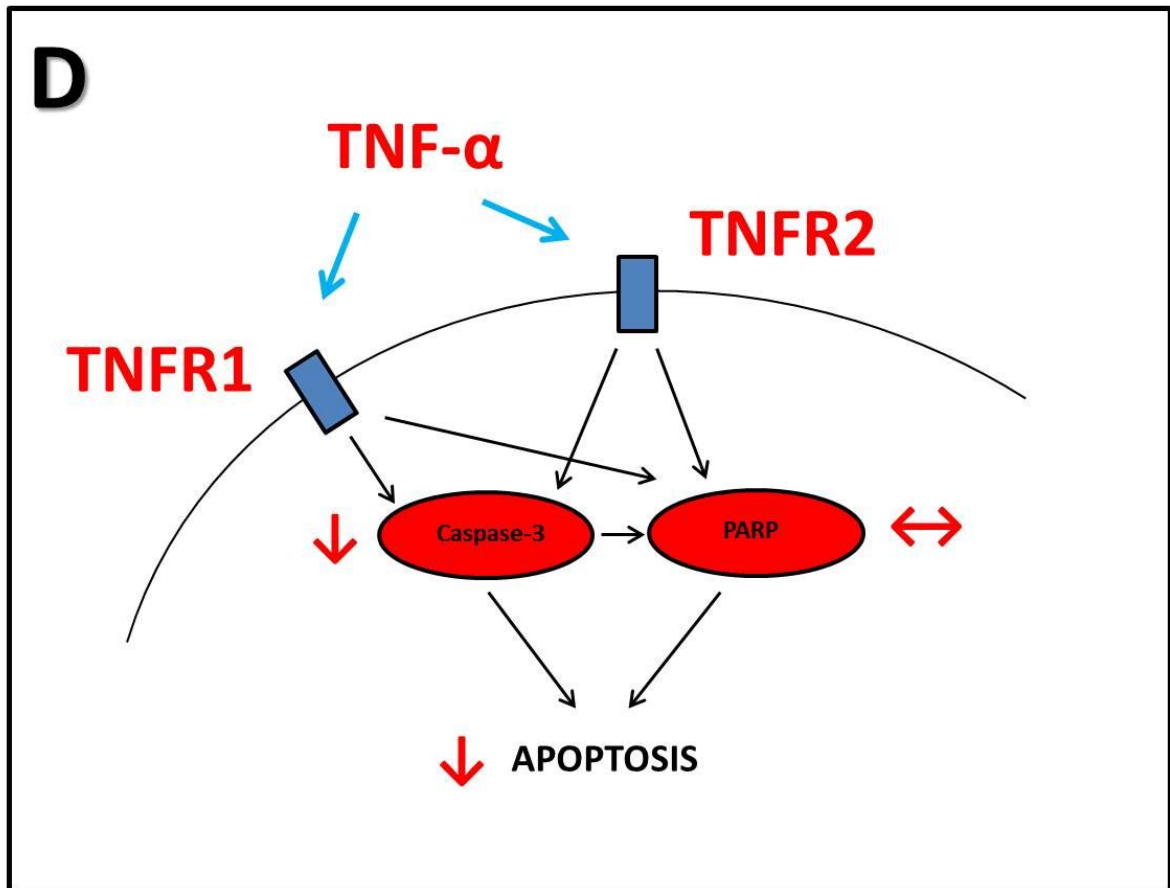


Figure 7.22: Simplified schematic overview of:

D: TNF- α + TRB1 & 2 apoptosis-signalling.

Note: Red letters indicate treatment, blue arrows indicate active pathways and black arrows indicate inactive pathways.

When reviewing the above results, it is important to bear in mind that there are also soluble forms of both TNF- α receptors (which represent the extracellular portions of membrane-associated TNF receptors and are probably shed from them by proteolytic partition) (Diez-Ruiz et al., 1995). The existence of soluble TNF receptors provides a new insight into the regulation of TNF- α function since they may act as antagonists or inhibitors for endogenous TNF- α , serve as binding proteins to carry endogenously produced TNF- α out of the site of production and may stabilize or even enhance the effects of TNF- α (Diez-Ruiz *et al.*, 1995). However, the antibodies that were used in this study to block the effects of the two TNF receptors are also sensitive for the soluble forms of these receptors (TNFRSF1A for TNFR1 and TNFRSF1B for TNFR2) (Cooper *et al.*, 2007; Hase *et al.*, 2005) (see page 303).

7.5 **Conclusion**

In conclusion, the findings of this chapter are novel in that no previous studies have characterised the effects of the TNF- α receptors in conjunction with exogenous TNF- α treatment in CMECs. We approached the study in this chapter by making use of western blot analysis to draw a clear picture of how the treatment used in this chapter will affect the various important signalling events present in endothelial cells. We therefore investigated intracellular events, (including the measurement of nitric oxide and ROS) and as mentioned important endothelial signalling proteins. See figures 7.19 – 7.22 for a schematic summary of events.

- It did not come as a surprise to find that TNF- α indeed increased cleaved caspase-3 and seemed to exert pro-apoptotic effects. Interestingly, we could not observe this at 24 hours TNF- α treatment (see previous chapters), which therefore suggests that the pro-apoptotic response, at least where caspase-3 is involved, is an early event. When we blocked the different TNF- α receptors, we found that TNFR1 led to a decrease in cleaved caspase-3 and thus have a partial attenuating effect on TNF- α induced apoptosis (this is a surprising finding as the receptor type 1 is usually referred to as the “death-receptor”) and that TNFR2 seemed to have no effect on apoptosis. Interestingly, blocking both receptors almost seemed to have an anti-apoptotic effect.

- Our data also demonstrated that TNF- α treatment alone had no effect on the relative activation of eNOS. This finding is not in agreement with various previous studies, among others also my own data as presented in previous chapters. However, it must be noted that in this chapter, the cells were only treated for 30 minutes and not 24 hours. Interestingly, TNF- α , at this shorter period of treatment, upregulated iNOS, which we also found to be the case at 24 hours (see chapter 5, page 261). Blocking of the two receptors individually, although they had effects on key components of eNOS-activation (such as PKB/Akt, HSP 90 or caveolin-1) had no overall effect on eNOS activity, and neither did these interventions have any effects on iNOS expression. Interestingly, blocking both receptors simultaneously seemed to profoundly suppress eNOS activation below baseline levels. This interesting finding opens itself up for some interesting speculative scenarios: Are both receptors required for baseline activation of eNOS (regardless of the presence of exogenous TNF- α)? Does the exogenously administered TNF- α exert direct down-regulating effects on eNOS activation via a non-receptor mediated process when both receptors are not available for binding? Unfortunately, time and resources did not allow for a further investigation of this observation; however, it is certainly something that should be explored, starting with a simple investigation of the effect of TNFR1 and TNFR2 blockade on control (i.e. baseline, untreated) CMECs. In similar fashion and equally intriguing, blocking of both receptors also decreased iNOS expression below baseline levels .

- Oxidative / nitrosative stress: When CMECs were treated with TNF- α only, an upregulation in p22 phox was observed, which is not unexpected, and in agreement with our findings at 24 hours TNF- α treatment in previous chapters. This treatment, however, had no effects on nitrosative stress as measured by nitrotyrosine expression. Blocking TNFR1 only caused an increase in p22 phox expression. This is contradictory to popular belief, since there is an assumption in many studies that the TNF- α receptor 2 is usually not involved with oxidative stress (Shen HM and Pervaiz, 2006). The only receptor that stayed true to its reputation as the “bad” receptor was receptor type 1, because when we blocked type 2, we also observed an increase in p22 phox expression. Interestingly, in this blockade scenario, we found a decrease in nitrotyrosine expression. Not surprisingly, when both receptors were blocked, the TNF- α -induced up-regulation of p22 phox was abolished, which

again speaks in favour of TNFR1-TNFR2 crosstalk. It is important to note that from the data it is clear that both receptors are involved in the up-regulation of p22 phox.

- NF- κ B activation: Treatment of CMECs for only 30 minutes did not seem to lead to NF- κ B activation as was the case for 24 hours treatment (as shown in chapter 5). Interestingly, when both receptors were blocked, a decrease in NF- κ B activity was observed, suggesting a role for both receptors in NF- κ B activity. As previously mentioned in section 7.1.1.1, it is known in the literature that NF- κ B mediates the transcription of a vast array of proteins involved in cell survival and proliferation, inflammatory response, and anti-apoptotic factors (Ghosh *et al.*, 2012).

7.6 Limitations

Please note that the observations made and conclusions drawn were based on one technique of investigation only (western blot analysis) and simply based on this alone. The researchers do recognize the immense complexity of TNF- α signalling and the oversimplifying of the findings was aimed at creating an understanding of the results.

We also acknowledge the limitations of using pharmacological inhibitors to explore the role of receptors, as the researcher can never assume that the inhibitors are 100% specific.

Lastly, due to time and logistical constraints, we were unable to include experiments investigating the effects of the receptor blockers on untreated, control groups. We are aware that this would have added value to the study, and will include control groups in future studies.

CHAPTER EIGHT

Final Conclusions

The original aim of this study was to investigate the responses of cardiac microvascular endothelial cells to various harmful stimuli, specifically paying focused and detailed attention to underlying mechanisms. The rationale behind this overall aim was the fact that vascular endothelial cells, by virtue of their location at the inner lining of blood vessels, are often the very first targets of harmful stimuli associated with cardiovascular risk factors and diseases. The choice of the specific endothelial cell type was mainly motivated by the fact that relatively little research has been performed on CMECs. It was anticipated, therefore, that this PhD study would add value and novel findings to existing literature. The first logical step was to perform a comprehensive characterisation of the cells under baseline, untreated conditions, on which we reported in Chapter 3. Once the baseline investigations were completed, we decided to focus on two important and clinically relevant harmful stimuli. In Chapter 4, we described the responses of CMECs to hypoxia. The relevance of hypoxia lies in the fact that capillary-derived endothelial cells such as the CMECs are frequently exposed to conditions of low oxygen supply. Furthermore, during a cardiac ischaemic event, it is conceivable that the CMECs represent the “first line of defense” of the myocardium during hypoxia. In Chapters 5-7 the focus shifted to creating an *in vitro* inflammatory microenvironment by treating the cells with one of the most important pro-inflammatory cytokines, TNF- α , and to explore the cellular responses to this insult. Inflammation, and therefore high circulating TNF- α levels, are important features of many cardiovascular risk factors and diseases such as diabetes mellitus, obesity, ischaemic heart disease / atherosclerosis and heart failure to name but a few.

All the experiments performed in these chapters were achieved by making use of previously established and several new techniques not previously used in our research group, accompanied by the measurement of various endpoints in order to generate a comprehensive view of the mechanisms of the responses of CMECs to the above two stimuli. All in all, this study incorporated the following cutting edge techniques:

- Fluorescence-based flow cytometry assays for the detection of various intracellular molecules and species;
- Western blotting measurements;
- Proteomics;
- Light microscopy and fluorescence microscopy

Chapter 3: Here, we wanted to gain information on the CMECs under baseline conditions, before embarking on the investigation into the responses of these cells to harmful stimuli. Indeed, the fact that 1387 proteins were identified in the CMECs represented the most extensive documentation of any mammalian CMEC proteome to date and a novel addition to existing vascular proteomic databases.

Chapter 4: It was important and necessary to investigate the CMECs in the context of hypoxia, as vascular endothelial cells are frequently exposed to low levels of PO₂ as well as the fact that hypoxia is considered to be an independent risk factor for the development of endothelial dysfunction. Again, we made use of proteomic analysis to offer a comprehensive overview of the response of these cells subjected to hypoxia and the findings provided a novel addition to the study. The CMECs responded by a general up-regulation of the eNOS-NO biosynthesis pathway. At 24 hours hypoxia, it seemed that these cells were still largely resistant to hypoxic damage. Although the intracellular ROS measurements were somewhat contradictory, the strong down-regulation of SOD1, accompanied by an increase in DHR123 fluorescence did point towards a general state of oxidative- and nitrosative stress in the CMECs after 24 hours of hypoxia. The proteomics results in Chapter 4 also provided further confirmation of adaptations in energy metabolism that one would expect in hypoxic endothelial cells, such as the significant enrichment of glycolysis and up-regulation of several glycolytic enzymes. However, the findings with regard to the changes in mitochondrial proteins were not that easy to explain, and further research into these phenomena is indicated.

Chapters 5-7: In the remaining chapters, we investigated the responses of CMECs to exogenously administered TNF- α . Several different experimental protocols and interventions, such as pharmacological blockade of TNF- α receptors were implemented to rule out certain scenarios and narrow down the possible explanations for the findings. In

Chapter 5, we showed that exogenous TNF- α -treatment induced an adaptive response in the cells, often signified by contradictory trends, yet, overall it is our belief that the observed effects were an indication that the cells were in a transitional state from being “functional” to “dysfunctional”, with early signs of oxidative and nitrosative stress and the activation of pathways that would conceivably result in a pro-inflammatory phenotype. In the final chapter, we were interested in the respective roles of the two TNF- α receptors. The so-called “death-receptor”, TNFR 1, stayed true to its reputation and we found several indications of damage when TNFR 2 was blocked. However, TNF- α -binding to TNFR 2 (in the presence of TNFR1 blockade), widely considered to be the “good” receptor, also caused an increase in oxidative stress in our CMECs. The results obtained from blocking either one of the two receptors or both, led us to believe that both receptors are involved (to varying degrees) in the responses observed, with crosstalk between the two receptor-mediated downstream pathways presumably taking place.

In summary, the findings of this study supplied a comprehensive, novel insight into the cells that line the microvasculature of the myocardium, which are to a great extent under-researched in the field of ischaemic heart disease (IHD) and endothelial dysfunction (ED). As originally stated in the introduction, the prevalence of heart disease, and ischaemic heart disease in particular, is rising and remains one of the top causes of morbidity and mortality world-wide. In view of the pivotal role of the vascular endothelium in the development of cardiovascular disease, as well as the fact that endothelial dysfunction is regarded as an early, potentially reversible predictor of future adverse cardiac events, it is imperative that we continue investigating the endothelium, and its responses to the various risk factors that ultimately lead to its functional demise. In this dissertation, we comprehensively investigated the responses of adult rat CMECs to two major harmful stimuli typically associated with the development of cardiovascular disease, namely hypoxia and TNF- α . We chose this cell type in view of the fact that it is generally neglected in the literature, yet at the same time, located within the cardiac muscle, which potentially renders it very important in the development of ischaemic heart disease. The findings of my investigations were mixed: some results were in agreement with existing data in the literature, others contradicted the literature and yet others were novel. As with every research model, ours also had its limitations, but we firmly believe that this dissertation will form an important

part of the growing puzzle of understanding the role of endothelial cells in cardiovascular disease.

Shortcomings of the present study:

In hindsight, the following aspects would have added more value and depth to the present study, but due to time and cost restraints, these aspects were not addressed in the present study.

- Supplementing the proteomics data with more extensive western blot analysis (as was done in chapter 5 with the TNF- α results). The hypoxic data was obtained much earlier in the study and it was only towards the latter part of the study that we started to investigate a larger array of proteins with western blot analysis (including cleaved caspase-3, PARP and IK β α).
- The up-regulation of mitochondrial proteins in hypoxic CMECs was somewhat counterintuitive, as hypoxia is generally accepted to down-regulate aerobic energy metabolic processes. We did mention that the up-regulation of proteins does not necessarily mean that the activity was increased. The lack of functional data on the CMEC mitochondria in this chapter was a shortcoming; however, future investigations could address this, as time and project funding did not allow for this in the current PhD study.
- The proteomic data obtained from the 24 hour hypoxia experiments were also contradictory in terms of the significant enrichment of translational processes such as elongation and initiation. For the same reasons explained previously, we were not able to further investigate this aspect.
- The work on the TNF- α receptor blockers was performed exclusively with western blot analyses, which, in hindsight, left several questions unanswered in view of the very interesting findings. The exclusion of control groups for the receptor blockers (without TNF- α) is also a limitation, as this would have added value to the data in that chapter. However, these investigations were performed towards the end of the

PhD study and if allowed more time, we would have liked to conduct more comprehensive investigations, such as proteomic analyses.

- Other shortcomings include the fact that for the largest part of this study, we focused on one endothelial cell type, which of course was the aim of the PhD. Although we tried to show some comparative data by including aortic endothelial cells in Chapter 5, if time and funding allowed, we would have preferred to do this more often throughout the study.
- Lastly, in a study performed on a rat cardiac cell line, it is important to mention that the assumptions are made that:
 - a. rat cells behave similarly to human cells under normal as well as pathological conditions,
 - b. the in vitro environment corresponds well with the in vivo environment and
 - c. experiments performed on cell lines that have undergone several passages have the limitation of only using the “stronger” surviving cells and not necessarily those that were included in the primary cells and this may skew results.

Future directions

As a direct and indirect consequence of the findings of this dissertation, we plan to conduct the following future studies:

- (i) Further investigations into the role of the mitochondrial proteins in hypoxia, in view of the interesting mitochondrial expression data obtained in Chapter 4. Experiments could include phospho-proteomic analyses, as well as other more function-directed studies such as mitochondrial respiration (with Oxygraph),
- (ii) Expansion of the TNFR antibody experiments to complement the western blot data obtained in Chapter 7, which could include proteomics and other intracellular end-points,
- (iii) Inclusion of a different vascular endothelial cell type for comparative purposes,
- (iv) Inclusion of *ex vivo* functional investigations (e.g. aortic vascular tissue),

(v) Inclusion of animal models in which the effects of cardiovascular risk factors (e.g. obesity and insulin resistance) on vascular endothelial function can be investigated,

(vi) Development of endothelial cell harvesting techniques so that researchers in our research group can create our own primary endothelial cell cultures from healthy and diseased animals.

Outputs that resulted directly or indirectly from this study:

1. Peer-reviewed journal publications:

Manuscript currently under review: Strijdom H, **Genis A**, Van Rensburg S, Westcott C, Mudau M, Van Vuuren D, Smit S. Novel characterization of the rat cardiac microvascular endothelial proteome and its regulation by hypoxia. *Int J Proteomics* 2013.

Mudau M, **Genis A**, Lochner A, Strijdom H. Endothelial Dysfunction – the early predictor of atherosclerosis. *Cardiovasc J Africa* 2012; 23(4): 222-231.

2. Published Peer-reviewed Conference Abstracts:

Genis A, Strijdom H, Westcott C, Mudau M. Signalling responses in cardiac microvascular endothelial cells, following treatment with high dosage of TNF-alpha, with or without co-treatment with Oleanolic Acid. *International Union of Physiological Sciences, Birmingham, UK*. 2013.

Strijdom H, Smit S, Westcott C, **Genis A**. Proteomic characterization of cardiac endothelial cell responses to TNF-alpha, hypoxia and asymmetric dimethylarginine (ADMA) stimulation. *SA Heart*. 2012.

Strijdom H, Mudau M, Westcott C, **Genis A**. Tumor necrosis factor (TNF)- α : towards a model of endothelial dysfunction. *Scientific Research and Essays*. 2012.

Genis A, Mudau M, Westcott C, Strijdom H. Evidence of pro-survival responses in TNF- α stimulated microvascular endothelial cells. *Scientific Research and Essays*. 2012.

Genis A, Westcott C, Mudau M, Strijdom H. Effect of low-dose TNF- α administration on oxidative/nitrosative stress: the Akt/eNOS/NO pathway and viability in cardiac endothelial cells. *Atherosclerosis (Suppl.)*. 2011.

Strijdom H, Westcott C, Mudau M, **Genis A**. Microvascular endothelial cell responses to inflammatory stimulation. *SA Heart*. 2011.

Genis A, Westcott C, Mudau M, Strijdom H. Tumor necrosis factor (TNF)- α induces endothelial dysfunction (ED) in cultured cardiac microvascular Endothelial Cells (CMECs) by downregulation of the PKB/Akt-eNOS signaling pathway. *J Mol Cell Cardiol*. 2010.

Genis A, Mudau E, Lochner A, Strijdom H. A novel model of Endothelial Dysfunction (ED) in cultured cardiac microvascular endothelial cells (CMECs). *SA Heart*. 2009.

3. Conference outputs:

Genis A, Westcott C, Strijdom H, Lochner A. Evidence of pro-survival responses in TNF- α stimulated microvascular endothelial cells. *Physiology Society of Southern Africa Annual Congress*. 2011. **Winner of poster competition.**

Genis A, Strijdom H, Westcott C, Mudau M. Microvascular endothelial cell adaptive responses following TNF-stimulation. *Annual Research Day, Faculty of Health Sciences, Stellenbosch University*. 2011.

Van Rensburg S, Strijdom H, Westcott C, Mudau M, **Genis A**. The role of tumour necrosis factor alpha (TNF- α) and hypoxia in microvascular endothelial cells. *Annual Research Day, Faculty of Health Sciences, Stellenbosch University*. 2011.

Van Rensburg S, Strijdom H, Westcott C, Mudau M, **Genis A**. Tumor necrosis factor alpha (TNF- α) and hypoxia: towards a model of endothelial dysfunction. *Physiology Society of*

Southern Africa Annual Congress. 2011. **Selected to be presented in the Wyndham competition.**

Genis A, Mudau M, Lochner A, Strijdom H. Tumor necrosis factor (TNF)-alpha induces endothelial dysfunction (ED) in cultured Cardiac Microvascular Endothelial Cells (CMECs), by downregulation of the PKB/Akt signalling pathway. *Society of International Heart Research, World Congress, Kyoto, Japan. J Mol Cell Cardiol.* 2010; 48 (5, S1): S94.

Genis A, Strijdom H, Westcott C, Mudau M. An In Vitro Model of Endothelial Dysfunction in Cultured Cardiac Microvascular Endothelial Cells (CMEC). *Physiology Society of Southern Africa, Annual Congress*. 2009.

Genis A, Mudau E, Lochner A, Strijdom H. A Novel Model of Endothelial Dysfunction (ED) in Cultured Cardiac Microvascular Endothelial Cells (CMECs). *SA Heart*. 2009. **Winner of poster competition in the Basic Sciences category.**

4. Other outputs:

Honours degrees of students I supervised:

Sam van Rensburg: graduated 2012.

Charlize van Nieuwenhuizen: graduates end 2013.

Invited Commentary by the International Atherosclerosis Society:

Strijdom H, **Genis A**. When traditional and non-traditional cardiovascular risk factors target the vascular endothelium: A double blow to the burden of disease in South Africa. *International Atherosclerosis Society* May 2013;

<http://www.athero.org/commentaries/comm1135.asp>.

References:

Abdallah Y, Gligorievski D, Kasseckert SA, Dieterich L, Schäfer M, Kuhlmann CR, Noll T, Sauer H, Piper HM and Schäfer C. The role of poly(ADP-ribose) polymerase (PARP) in the autonomous proliferative response of endothelial cells to hypoxia. *Cardiovasc Res.* 2007; 73 (3): 568-574.

Achan V, Broadhead M, Malaki M, Whitley G, Leiper J, MacAllister R & Vallance P. Asymmetric dimethylarginine causes hypertension and cardiac dysfunction in humans and is actively metabolised by dimethylarginine dimethylaminohydrolase. *Arterioscler. Thromb. Vasc. Biol.* 2003; 23: 1455-1459.

Ago T, Kitazono T, Ooboshi H, Iyama T, Han YH, Takada Y, Wakisaka M, Ibayashi S, Utsumi H and Iida M. Nox4 as the major catalytic component of an endothelial NAD (P) H oxidase. *Circulation.* 2004; 109 (2): 227-233.

Ahmad M, Zhang Y, Papharalambus C and Alexander RW. Role of isoprenylcysteine carboxyl methyltransferase in tumor necrosis factor- α stimulation of expression of vascular cell adhesion molecule-1 in endothelial cells. *Arterioscler. Thromb. Vasc. Biol.* 2002; 22: 759-764.

Ahn A, Frishman WH, Gutwein A, Passeri J and Nelson M. Therapeutic Angiogenesis: A New Treatment Approach for Ischemic Heart Disease-Part I. *Cardiology in Review.* 2008; 16 (4): 163-171.

Aird WC . Review: Phenotypic Heterogeneity of the Endothelium. I: Structure, functions and mechanisms. *Circulation Research.* 2007a; 100: 174-190.

Aird WC. Reviews: Phenotypic Heterogeneity of the Endothelium. II. Representative Vascular Beds. *Circulation Research.* 2007b; 100: 174-190.

Aird WC. Endothelial cell heterogeneity. *Cold Spring Harb. Perspect. Med.* 2012; 2: a006429.

Aitsebaomo J, Portbury AL, Schisler JC, Patterson C. Brothers and sisters: molecular insights into arterial-venous heterogeneity. *Circ Res.* 2008; 103: 929-939.

Aksu K, Donmez A and Keser G. Inflammation-induced thrombosis: mechanisms, disease associations and management. *Current pharmaceutical design.* 2012; 18 (11): 1478-1493.

Aktan F. iNOS-mediated nitric oxide production and its regulation. *Life sciences.* 2004; 75 (6): 639-653.

Alchera E, Dal Ponte C, Imarisio C, Albano E and Carini R. Molecular mechanisms of liver preconditioning. *World J Gastroenterol.* 2010; 16(48): 6058-6067.

Ali MH, Schlidt SA, Chandel NS, Hynes KL, Schumacker PT and Gewertz BL. Endothelial permeability and IL-6 production during hypoxia: role of ROS in signal transduction. *American Journal of Physiology - Lung Cellular and Molecular Physiology.* 1999; 9 (277): L1057-L1065.

Almofti MR, Huang Z, Yang P, Rui Y and Yang P. Proteomic analysis of rat aorta during atherosclerosis induced by high cholesterol diet and injection of vitamin D3. *Clinical and Experimental Pharmacology and Physiology.* 2006; 33: 305-309.

- Alom-Ruiz SP, Anilkumar N, Shah AM. Reactive oxygen species and endothelial activation. *Antioxid Redox Signal*. 2008; 10(6): 1089-100.
- Anderson NL and Anderson NG. Proteome and proteomics: new technologies, new concepts, and new words. *Electrophoresis*. 1998; 19 (11): 1853-1861.
- Anderssohn M, Schwedhelm E, Lüneburg N, Vasan RS and Böger RH. Review article: Asymmetric dimethylarginine as a mediator of vascular dysfunction and a marker of cardiovascular disease and mortality: an intriguing interaction with diabetes mellitus. *Diabetes and Vascular Disease Research*. 2010; 7 (2): 105-118.
- Ando J and Yamamoto K. Effects of Shear Stress and Stretch on Endothelial Function. *Antioxidants & Redox Signaling*. 2011; 15(5): 1389-1403.
- Angelone T, Gattuso A, Imbrogno S, Mazza R and Tota B. Nitrite is a positive modulator of the Frank-Starling response in the vertebrate heart. *American Journal of Physiology-Regulatory, Integrative and Comparative Physiology*. 2012; 302 (11): R1271-R1281.
- Ann M and Paul H. Oxidized LDL and HDL: antagonist in atherosclerosis. *FASEB J*. 2001; 15: 2073–2084.
- Antoniades C, Shirodaria C, Leeson P, Antonopoulos A, Warrick N, Van-Assche T, Cunnington C, Tousoulis D, Pillai R, Ratnatunga C, Stefanadis C and Channon KM. Association of plasma asymmetrical dimethylarginine (ADMA) with elevated vascular superoxide production and endothelial nitric oxide synthase uncoupling: implications for endothelial function in human atherosclerosis. *Eur. Heart J*. 2009; 30: 1142–1150.
- Antoniades C, Tousoulis D, Stefanadis C. Smoking in Asians: it doesn't stop at vascular endothelium. *Int J Cardiol* 2008; 128: 151–153.
- Aoki N, Siegfried M and Lefer AM. Anti-EDRF effect of tumor necrosis factor in isolated, perfused cat carotid arteries. *Am. J. Physiol*. 1989; 256: H1509–H1512.
- Aragón JP, Condit ME, Bhushan S, Predmore BL, Patel SS, Grinsfelder DB, Gundewar S *et al*. Beta3-adrenoreceptor stimulation ameliorates myocardial ischemia-reperfusion injury via endothelial nitric oxide synthase and neuronal nitric oxide synthase activation. *Journal of the American College of Cardiology*. 2011; 58 (25): 2683-2691.
- Arai T, Kelly SA, Brengman ML, Takano M, Smith EH, *et al*. Ambient but not incremental oxidant generation effects intercellular adhesion molecule 1 induction by tumour necrosis factor alpha in endothelium. *Biochem J*. 1998; 331(Pt 3): 853–861.
- Arnet UA, McMillan A, Dinerman JL, Ballermann B and Lowenstein CJ. Regulation of Endothelial Nitric-oxide Synthase during Hypoxia. *Journal of Biological Chemistry*. 1996; 271: 15069-15073.
- Arruda RM, Peotta VA, Meyrelles SS and Vasquez EC. Evaluation of vascular function in apolipoprotein E knockout mice with angiotensin-dependent renovascular hypertension. *Hypertension*. 2005; 46: 932–936.

Asano K, Chee CB, Gaston B, Lilly CM, Gerard C, Drazen JM and Stamler JS. Constitutive and inducible nitric oxide synthase gene expression, regulation, and activity in human lung epithelial cells. *Proc. Natl. Acad. Sci. USA*. 1994; 91: 10089–10093.

Atkins GB, Jain MK and Hamik A. ATVB in Focus: Vascular Cell Lineage Determination and Differentiation . Endothelial Differentiation. Molecular Mechanisms of Specification and Heterogeneity. *Arteriosclerosis, Thrombosis, and Vascular Biology*. 2011; 31: 1476-1484.

Atkinson B, Dwyer K, Enjyoji K, Robson SC. Ecto-nucleotidases of the CD39/NTPDase family modulate platelet activation and thrombus formation: Potential as therapeutic targets. *Blood Cells Mol Dis*. 2006; 36(2): 217–222.

Avogaro A, de Kreutzenberg S, Fadini G. Endothelial dysfunction: causes and consequences in patients with diabetes mellitus. *Diabetes Res Clin Pract*. 2008; 82: S94–S101.

Babich V, Meli A, Knipe L, Dempster JE, Skehel P, Hannah MJ and Carter T. Selective release of molecules from Weibel-Palade bodies during a lingering kiss. *Blood*. 2008; 111: 5282-5290.

Baccari MC, Traini C, Garella R, Cipriani G and Vannucchi MG. Relaxin exerts two opposite effects on mechanical activity and nitric oxide synthase expression in the mouse colon. *AJP – Endo*. 2012; 303 (9): E1142-E1150.

Bachetti T, Comini L, Francolini G, Bastianon D, Valetti B, Cadei M, Grigolato P, Suzuki H, Finazzi D, Albertini A, Curello S and Ferrari R. Arginase pathway in human endothelial cells in pathophysiological conditions. *J. Mol. Cell. Cardiol*. 2004; 37: 515–523.

Badimon L, Padró T and Vilahur G. Atherosclerosis, platelets and thrombosis in acute ischaemic heart disease. *European Heart Journal: Acute Cardiovascular Care*. 2012; 1: 60-74.

Bakker W, Eringa EC, Sipkema P and van Hinsbergh VWM. Endothelial dysfunction and diabetes: roles of hyperglycemia, impaired insulin signaling and obesity. *Cell and tissue research*. 2009; 335 (1): 165-189.

Balakumar P, Kaur T, Singh M. Potential target sites to modulate vascular endothelial dysfunction: current perspectives and future directions. *Toxicology*. 2008; 245(1–2): 49–64.

Balligand JL, Feron O and Dessy C. eNOS activation by physical forces: from short-term regulation of contraction to chronic remodeling of cardiovascular tissues. *Physiol. Rev*. 2009; 89: 481–534.

Barba G, Vallance P, Strazzullo P, MacAllister RJ. Effects of sodium intake on the pressor and renal responses of nitric oxide synthesis inhibition in normotensive individuals with different sodium sensitivity. *J Hypertens*. 2000; 18: 615–621.

Barletta KE, Ley K and Mehrad B. ATVB in Focus: The Role of Adenosine in Response to Vascular Inflammation. Regulation of Neutrophil Function by Adenosine. *Arteriosclerosis, Thrombosis, and Vascular Biology*. 2012; 32: 856-864.

Barnoya J, Glantz SA. Cardiovascular effects of secondhand smoke: nearly as large as smoking. *Circulation* 2005; 111: 2684–2698.

- Barton M, Yanagisawa M. Endothelin: 20 years from discovery to therapy. *Can J Physiol Pharmacol*. 2008; 86: 485–498.
- Basuroy S, Bhattacharya S, Tcheranova D, Qu Y, Regan RF, Leffler CW and Parfenova H. HO-2 provides endogenous protection against oxidative stress and apoptosis caused by TNF- α in cerebral vascular endothelial cells. *Am J Physiol Cell Physiol*. 2006; 291 (5): C897-C908.
- Basuroy S, Tcheranova D, Bhattacharya S, Leffler CW and Parfenova H. Nox4 NADPH oxidase-derived reactive oxygen species, via endogenous carbon monoxide, promote survival of brain endothelial cells during TNF- α -induced apoptosis. *American Journal of Physiology-Cell Physiology*. 2011; 300 (2): C256-C265.
- Baxter GT, Kuo RC, Jupp OJ, Vandenabeele P and MacEwan DJ. Tumor necrosis factor- α mediates both apoptotic cell death and cell proliferation in a human hematopoietic cell line dependent on mitotic activity and receptor subtype expression. *J. Biol. Chem*. 1999; 274: 9539 - 9547.
- Bayraktutan U and Ülker S. Effects of Angiotensin II on Nitric Oxide Generation in Proliferating and Quiescent Rat Coronary Microvascular Endothelial Cells. *Hypertens Res*. 2003; 26: 749–757.
- Bazzoni G, Dejana E. Endothelial cell-to-cell junctions: molecular organization and role in vascular homeostasis. *Physiol Rev*. 2004; 84: 869–901.
- Beckman JS, Koppenol WH. Nitric oxide, superoxide, and peroxynitrite: the good, the bad, and ugly. *Am. J. Physiol*. 1996; 271: C1424–C1437.
- Bedard K and Krause KH. The NOX Family of ROS-Generating NADPH Oxidases: Physiology and Pathophysiology. *Physiol Rev*. 2007; 87 (1): 245-313.
- Beleslin-Cokic BB, Cokic VP, Yu X, Weksler BB, Schechter AN and Noguchi CT. Erythropoietin and hypoxia stimulate erythropoietin receptor and nitric oxide production by endothelial cells. *Blood*. 2004; 104 (7): 2073-2080.
- Belton O, Byrne D, Kearney D, Leahy A, Fitzgerald DJ. Cyclooxygenase-1 and -2 -dependent prostacyclin formation in patients with atherosclerosis. *Circulation* 2000; 102: 840-845.
- Bendall JK, Alp NJ, Warrick N, Cai S, Adlam D, Rockett K, Yokoyama M, Kawashima S and Channon KM. Stoichiometric relationships between endothelial tetrahydrobiopterin, endothelial NO synthase (eNOS) activity, and eNOS coupling in vivo: insights from transgenic mice with endothelial-targeted GTP cyclohydrolase 1 and eNOS overexpression. *Circ. Res*. 2005; 97: 864–871; 2005.
- Bendayan M. Morphological and cytochemical aspects of capillary permeability. *Microsc Res Tech*. 2002; 57: 327–349.
- Ben-Neriah Y and Karin M. Inflammation meets cancer, with NF- κ B as the matchmaker. *Nature Immunology*. 2011; 12: 715–723.
- Bereta J, Bereta M, Allison AC, Kruger PB and Koj A. Inhibitory effect of di-catechol rooperol on VCAM-1 and iNOS expression in cytokine-stimulated endothelium. *Life Sci*. 1997; 60: 325–334.

Bergman, Marina R., Sunfa Cheng, Norman Honbo, Lucia Piacentini, Joel S. Karliner, and David H. Lovett. A functional activating protein 1 (AP-1) site regulates matrix metalloproteinase 2 (MMP-2) transcription by cardiac cells through interactions with JunB-Fra1 and JunB-FosB heterodimers. *Biochemical Journal*. 2003; 369 (Pt 3): 485.

Berliner JA, Subbanagounder G, Leitinger N, Watson AD, Vora D. Evidence for a role of phospholipid oxidation products in atherogenesis. *Trends in Cardiovascular Medicine*. 2001; 11: 142–147.

Bernier SG, Haldar S, Michel T. Bradykinin-regulated Interactions of the Mitogen-activated Protein Kinase Pathway with the Endothelial Nitric-oxide Synthase. *J. Biol. Chem*. 2000; 275: 30707–30715.

Bertuglia S and Giusti A. Microvascular Oxygenation and Oxidative Stress During Postischemic Reperfusion. Oxygen Transport to Tissue XXVI. *Advances in Experimental Medicine and Biology*. 2005; 566: 23-29.

Bhatt SR, Lokhandwala MF, Banday AA. Resveratrol prevents endothelial nitric oxide synthase uncoupling and attenuates development of hypertension in spontaneously hypertensive rats. *Eur J Pharmacol*. 2011; 667(1-3): 258–264.

Binglan Y, Mohd S, Egorina EM, Sovershaev MA, Raheer MJ, Lei C, Wu MX, Bloch KD and Zapol WM. Endothelial dysfunction enhances vasoconstriction due to scavenging of nitric oxide by a hemoglobin-based oxygen carrier. *Anesthesiology*. 2010; 112 (3): 586-594.

Blair A, Shaul PW, Yuhanna IS, Conrad PA, Smart EJ. Oxidized low density lipoprotein displaces endothelial nitric-oxide synthase (eNOS) from plasmalemmal caveolae and impairs eNOS activation. *Journal of Biological Chemistry*. 1999; 274: 32512–32519.

Blake GJ, Ridker PM. Novel clinical markers of vascular wall inflammation. *Circ Res* 2001; 89: 763–771.

Blouin A, Bolender RP, Weibel ER. Distribution of organelles and membranes between hepatocytes and nonhepatocytes in the rat liver parenchyma: a stereological study. *The Journal of Cell Biology*. 1977; 72: 441-455.

Bode-Böger SM, Scalera F and Martens-Lobenhoffer J. Asymmetric dimethylarginine (ADMA) accelerates cell senescence. *Vasc Med*. 2005; 10: S65.

Böger RH, Bode-Böger S, Szuba A, et al. Asymmetric dimethylarginine (ADMA): a novel risk factor for endothelial dysfunction, its role in hypercholesterolemia. *Circulation*. 1998; 98: 1842–1847.

Böger RH, Bode-Boger SM, Tsao PS, Lin PS, Chan JR, Cooke JP. An endogenous inhibitor of nitric oxide synthase regulates endothelial adhesiveness for monocytes. *J Am Coll Cardiol*. 2000a; 36: 2287–2295.

Böger RH, Sydow K, Borlak J, Thum T, Lenzen H, Schubert B, Tsikas D, Bode-Böger SM. Molecular Medicine. LDL Cholesterol Upregulates Synthesis of Asymmetrical Dimethylarginine in Human Endothelial Cells. Involvement of S-Adenosylmethionine-Dependent Methyltransferases. *Circulation Research*. 2000b; 87: 99-105.

Böger RH, Vallance P, Cooke JP. Asymmetric dimethylarginine (ADMA): a key regulator of nitric oxide synthase. *Atherosclerosis*. Suppl 2003a; 4: 1–3.

Böger RH. The emerging role of ADMA as a novel cardiovascular risk factor. *Cardiovasc. Res.* 2003b; 59: 824-833.

Böger RH. Asymmetric dimethylarginine, an endogenous inhibitor of nitric oxide synthase, explains the "L-arginine paradox" and acts as a novel cardiovascular risk factor. *J Nutr.* 2004; (10 Suppl): 2842S-2847S.

Böger RH. Asymmetric dimethylarginine (ADMA): a novel risk marker in cardiovascular medicine and beyond. *Ann Med.* 2006; 38: 126–136.

Böger RH. The Pharmacodynamics of L-Arginine1–3. *J. Nutr.* 2007; 137 (6): 1650S-1655S.

Bogle RG, MacAllister RJ, Whitley GS, Vallance P. Induction of NG-monomethyl-L-arginine uptake: a mechanism for differential inhibitor of NO synthases? *Am J Physiol.* 1995; 269: C750–756.

Bogoyevitch MA, Ngoei KRW, Zhao TT, Yeap YYC and Ng DCH. c-Jun N-terminal kinase (JNK) signaling: recent advances and challenges. *Biochimica et Biophysica Acta (BBA)-Proteins and Proteomics.* 2010; 1804 (3): 463-475.

Boisseau MR, Pruvost A, Renard M, Clossé C, Belloc F, Seigneur M and Maurel A. Effect of buflomedil on the neutrophil-endothelial cell interaction under inflammatory and hypoxia conditions. *Pathophysiology of Haemostasis and Thrombosis.* 2009; 26 (4): 182-188.

Bonetti PO, Lerman LO, Lerman A. Endothelial dysfunction: a marker of atherosclerotic risk. *Atheroscler Thromb Vasc Biol.* 2003 Feb; 23(2): 168-75.

Bonifati V, Rizzu P, Squitieri F, Krieger E, Vanacore N, Van Swieten JC, Brice A et al. DJ-1 (PARK7), a novel gene for autosomal recessive, early onset parkinsonism. *Neurological Sciences.* 2003; 24 (3): 159-160.

Bonomini M, Giardinelli A, Morabito C, Di Silvestre S, Di Cesare M, et al. Calcimimetic R-568 and Its Enantiomer S-568 Increase Nitric Oxide Release in Human Endothelial Cells. *PLoS ONE.* 2012; 7(1): e30682.

Boulanger CM, Tanner FC, Bea ML, et al. Oxidized low density lipoproteins induce mRNA expression and release of endothelin from human and porcine endothelium. *Circ Res.* 1992; 70: 1191–1197.

Bourque SL, Davidge ST and Adams MA. Review. The interaction between endothelin-1 and nitric oxide in the vasculature: new perspectives. *AJP - Regu Physiol.* 2011; 300 (6): R1288-R1295.

Bouwmeester T, Bauch A, Ruffner H et al. A physical and functional map of the human TNF-alpha/NF-kappa B signal transduction pathway. *Nat Cell Biol.* 2004; 6:97–105.

Bove K, Neumann P, Gertzberg N, Johnson A. Role of eNOS-derived NO in mediating TNF-induced endothelial barrier dysfunction. *Am J Physiol Lung Cell Mol Physiol.* 2001; 280: L914–922.

- Brábek J, Mierke CT, Rösel D, Veselý P and Fabry B. The role of the tissue microenvironment in the regulation of cancer cell motility and invasion. *Cell Communication and Signaling*. 2010; 8:22.
- Bradford, M. A Rapid and Sensitive Method for the Quantitation of Microgram Quantities of Protein Utilizing the Principle of Protein-Dye Binding. *Anal. Biochem*. 1976; 72: 248-254.
- Bradley EA, Eringa EC, Stehouwer CDA, Korstjens I, van Nieuw Amerongen GP, Musters R, Sipkema P, Clark MG and Rattigan S. Activation of AMP-activated protein kinase by 5-aminoimidazole-4-carboxamide-1- β -D-ribofuranoside in the muscle microcirculation increases nitric oxide synthesis and microvascular perfusion. *Arteriosclerosis, Thrombosis, and Vascular Biology*. 2010; 30 (6): 1137-1142.
- Braet F and Wisse E. Structural and functional aspects of liver sinusoidal endothelial cell fenestrae: a review. *Comp Hepatol*. 2002; 1: 1.
- Brandes RP, Weissmann N, Schröder K. NADPH oxidases in cardiovascular disease. *Free Radic Biol Med*. 2010; 49:687–706.
- Bratt JM, Franzi LM, Linderholm AL, Last MS, Kenyon NJ and Last JA. Arginase enzymes in isolated airways from normal and nitric oxide synthase 2-knockout mice exposed to ovalbumin. *Toxicol. Appl. Pharmacol*. 2009; 234: 273–280.
- Bratt JM, Franzi LM, Linderholm AL, O’Roark EM, Kenyon NJ and Last JA. Arginase inhibition in airways from normal and nitric oxide synthase 2-knockout mice exposed to ovalbumin. *Toxicol. Appl. Pharmacol*. 2010; 242: 1–8.
- Brazil DP, Park J and Hemmings BA. PKB binding proteins: getting in on the Akt. *Cell*. 2002; 111 (3): 293-303.
- Brewer AC, Sparks EC and Shah AM. Transcriptional regulation of the NADPH oxidase isoform, Nox1, in colon epithelial cells: role of GATA-binding factor(s). *Free Radic. Biol. Med*. 2006; 40: 260–274.
- Briand N, Le Lay S, Sessa WS, Ferré P and Dugail I. Distinct roles of endothelial and adipocyte caveolin-1 in macrophage infiltration and adipose tissue metabolic activity. *Diabetes*. 2011; 60 (2): 448-453.
- Bronzwaer JGF and Paulus WJ. Nitric oxide: the missing lusitrope in failing myocardium. *European Heart Journal*. 2008; doi:10.1093/eurheartj/ehn393.
- Brouard S, Berberat PO, Tobiasch E, Seldon MP, Bach FH and Soares MP. Heme oxygenase-1-derived carbon monoxide requires the activation of transcription factor NF-kappa B to protect endothelial cells from tumor necrosis factor-alpha-mediated apoptosis. *J Biol Chem*. 2002; 277: 17950–17961.
- Bruckdorfer R. The basics about nitric oxide. *Mol Aspect Med*. 2005 ; 26:3-31.
- Bruick RK. Oxygen sensing in the hypoxic response pathway: regulation of the hypoxia-inducible transcription factor. *Genes & development*. 2003; 17 (21): 2614-2623.

Bruneel A, Labas V, Mailloux A, Sharma S, Vinh J, Vaubourdolle M and Baudin B. Proteomic study of human umbilical vein endothelial cells in culture. *Proteomics*. 2003; 3 (5): 714-723.

Brunner H, Cockcroft JR, Deanfield J, Donald A, Ferrannini E, Halcox J, Kiowski W, Luscher TF, Mancina G, Natali A, Oliver JJ, Pessina AC, Rizzoni D, Rossi GP, Salvetti A, Spieker LE, Taddei S, Webb DJ. Endothelial function and dysfunction. Part II: Association with cardiovascular risk factors and diseases: a statement by the Working Group on Endothelins and Endothelial Factors of the European Society of Hypertension. *J Hypertens* 2005; 23:233–246.

Brutsaert DL, Franssen P, Andries LJ, De Keulenaer GW, Sys SU. Cardiac endothelium and myocardial function. *Cardiovasc Res*. 1998; 38: 281–290.

Brutsaert DL. Cardiac Endothelial-Myocardial Signaling: Its Role in Cardiac Growth, Contractile Performance, and Rhythmicity *Physiol Rev*. 2003; 83 (1): 59-115.

Brunnsgaard H, Skinhøj P, Pedersen AN, Schroll M and Pedersen BK. Ageing, tumour necrosis factor- α (TNF- α) and atherosclerosis. *Clinical & Experimental Immunology*. 2000; 121 (2): 255-260.

Bruyndonckx L, Radtke T, Eser P, Vrints CJ, Ramet J, Wilhelm M and Conraads VM. Methodological considerations and practical recommendations for the application of peripheral arterial tonometry in children and adolescents. *International journal of cardiology*. 2013.

Bryan NS, Bian K and Murad F. Discovery of the nitric oxide signaling pathway and targets for drug development. *Front Biosci*. 2009; 14: 1-18.

Bucci M, Gratton JP, Rudic RD, Acevedo L, Roviezzo F, Cirino G and Sessa WC. In vivo delivery of the caveolin-1 scaffolding domain inhibits nitric oxide synthesis and reduces inflammation. *Nat. Med*. 2000; 6: 1362–1367.

Burke A, FitzGerald GA. Oxidative stress and smoking-induced vascular injury. *Progr Cardiovasc Dis*. 2003; 46: 79–90.

Buskila Y and Amitai Y. Astrocytic iNOS-Dependent Enhancement of Synaptic Release in Mouse Neocortex. *AJP - JN Physiol*. 2010; 103 (3): 1322-1328.

Butt E, Bernhardt M, Smolenski A, Kotsonis P, Frohlich LG, Sickmann A, Meyer HE, Lohmann SM, Schmidt HH. Endothelial nitric-oxide synthase (Type III) is activated and becomes calcium independent upon phosphorylation by cyclic nucleotide-dependent protein kinases. *J. Biol. Chem*. 2000; 275: 5179–5187.

Buttery LD, Springall DR, Chester AH, et al. Inducible nitric oxide synthase is present within human atherosclerotic lesions and promotes the formation and activity of peroxynitrite. *Lab Invest*. 1996; 75: 77– 85.

Cai H and Harrison DG. Endothelial dysfunction in cardiovascular disease: the role of oxidative stress. *Circ Res*. 2000; 87(10): 840-4.

Cai H, Li Z, Dikalov S, Holland SM, Hwang J, Jo H, Dudley SC Jr and Harrison DG. NAD(P)H oxidase-derived hydrogen peroxide mediates endothelial nitric oxide production in response to angiotensin II. *J Biol Chem*. 2002; 277: 48311-48317.

- Cai H, Griendling KK and Harrison DG. The vascular NAD (P) H oxidases as therapeutic targets in cardiovascular diseases. *Trends in pharmacological sciences*. 2003; 24 (9): 471-478.
- Calcerrada P, Peluffo G and Radi R. Nitric Oxide-Derived Oxidants with a Focus on Peroxynitrite: *Molecular Targets, Cellular Responses and Therapeutic Implications*. 2011; 17 (35): 3905-3932.
- Calvert JW, Condit ME, Aragón JP, Nicholson CK, Moody BF, Hood RL, Sindler AL *et al*. Exercise Protects Against Myocardial Ischemia–Reperfusion Injury via Stimulation of β 3-Adrenergic Receptors and Increased Nitric Oxide Signaling: Role of Nitrite and Nitrosothiols Novelty and Significance. *Circulation research*. 2011; 108 (12): 1448-1458.
- Camacho M, Rodríguez C, Guadall A, Alcolea S, Orriols M, Escudero JR, Martínez-González J and Vila L. Hypoxia upregulates PGI-synthase and increases PGI2 release in human vascular cells exposed to inflammatory stimuli. *Journal of lipid research*. 2011; 52 (4): 720-731.
- Carmeliet P. Angiogenesis in health and disease. *Nature medicine*. 2003; 9.6: 653-660.
- Carnicer R, Crabtree MJ, Sivakumaran V, Casadei B and Kass DA. Nitric oxide synthases in heart failure. *Antioxidants & Redox Signaling*. 2012.
- Carswell EA, Old LJ, Kassel RL, *et al*. An endotoxin-induced serum factor that causes necrosis of tumors. *Proc Natl Acad Sci U S A*. 1975; 72: 3666–3670.
- Cary SP, Winger JA, Derbyshire ER and Marletta MA. Nitric oxide signaling: no longer simply on or off. *Trends Biochem. Sci*. 2006; 31: 231–239.
- Casteel DE, Zhang T, Zhuang S and Pilz RB. cGMP-dependent protein kinase anchoring by IRAG regulates its nuclear translocation and transcriptional activity. *Cell. Signal*. 2008; 20: 1392–1399.
- Cat AND and Touyz RM. Cell Signaling of Angiotensin II on Vascular Tone: Novel Mechanisms. *Curr Hypertens Rep*. 2011; 13: 122–128.
- Cayatte AJ, Palacino JJ, Horten K, Cohen RA. Chronic inhibition of nitric oxide production accelerates neointima formation and impairs endothelial function in hypercholesterolemic rabbits. *Arterioscler Thromb*. 1994; 14: 753–759.
- Ceccatelli S, Hulting AL, Zhang X, Gustafsson L, Villar M and Hokfelt T. Nitric oxide synthase in the rat anterior pituitary gland and the role of nitric oxide in regulation of luteinizing hormone secretion. *Proc. Natl. Acad. Sci. USA*. 1993; 90: 11292–11296.
- Celermajer DS, Sorensen KE, Bull C, *et al*. Endothelium-dependent dilation in the systemic arteries of asymptomatic subjects relates to coronary risk factors and their interaction. *J Am Coll Cardiol*. 1994; 24(6): 1468-74.
- Cevik MO, Katsuyama M, Kanda S, Kaneko T, Iwata K, Ibi M, Matsuno K, Takechi T, Cui W, Sasaki M and Yabe-Nishimura C. The AP-1 site is essential for the promoter activity of NOX1/NADPH oxidase, a vascular superoxide-producing enzyme: Possible involvement of the ERK1/2-JunB pathway. *Biochem. Biophys. Res. Commun*. 2008; 374: 351–355.

- Chhabra A, Verma A and Mehta K. Tissue transglutaminase promotes or suppresses tumors depending on cell context. *Anticancer research*. 2009; 29 (6): 1909-1919.
- Chakrabarti S, Chan CK, Jiang Y and Davidge ST. Neuronal nitric oxide synthase regulates endothelial inflammation. *J Leukoc Biol*. 2012; 91(6): 947-56.
- Chapulsky K and Cai H. Endothelial dihydrofolate reductase: Critical for nitric oxide bioavailability and role in angiotensin II uncoupling of endothelial nitric oxide synthase. *PNAS*. 2005; 102 (25): 9056–9061.
- Chan SY and Loscalzo J. Endothelial Regulation of Pulmonary Vascular Tone. *Textbook of Pulmonary Vascular Disease*. 2011, Part 1, 167-195.
- Chandrasekharan UM, Siemionow M, Unsal M, Yang L, Poptic E, Bohn J, Ozer K et al. Tumor necrosis factor α (TNF- α) receptor-II is required for TNF- α -induced leukocyte-endothelial interaction in vivo. *Blood*. 2007; 109 (5): 1938-1944.
- Chao DS, Hwang PM, Huang F and Bredt DS. Localization of neuronal nitric oxide synthase. *Methods Enzymol*. 1996; 268: 488–496.
- Chatterjee A and Catravas JD. Endothelial nitric oxide (NO) and its pathophysiologic regulation. *Vascular pharmacology*. 2008; 49 (4): 134-140.
- Chen G and Goeddel DV. TNF-R1 Signaling: A Beautiful Pathway. *Science*. 2002; 296 (5573): 1634-1635.
- Chen M , Masaki T and Sawamura T. LOX-1, the receptor for oxidized low-density lipoprotein identified from endothelial cells: implications in endothelial dysfunction and atherosclerosis. *Pharmacology & therapeutics*. 2002; 95 (1): 89-100.
- Chen X, Andresen BT, Hill M, Zhang J, Booth F, Zhang C. Role of reactive oxygen species in tumor necrosis factor-alpha induced endothelial dysfunction. *Curr Hypertens Rev* 2008; 4(4): 245-255.
- Chen Z, Peng I, Sun W, Su M, Hsu P, Fu Y, Zhu Y, DeFea K, Pan S, Tsai M and Shyy JY. AMP-Activated Protein Kinase Functionally Phosphorylates Endothelial Nitric Oxide Synthase Ser633. *Circulation Research*. 2009; 104: 496-505.
- Chen W, Druhan LJ, Chen CA, Hemann C, Chen YR, Berka V, Tsai AL and Zweier JL. Peroxynitrite induces destruction of the tetrahydrobiopterin and heme in endothelial nitric oxide synthase: transition from reversible to irreversible enzyme inhibition. *Biochemistry*. 2010; 49: 3129–3137.
- Chen F, Pandey D, Chadli A, Catravas JD, Chen T and Fulton DJR. Hsp90 regulates NADPH oxidase activity and is necessary for superoxide but not hydrogen peroxide production. *Antioxidants & redox signalling*. 2011; 14 (11): 2107-2119.
- Chen TG, Zhong ZY, Sun GF, Zhou YX and Zhao Y. Effects of tumour necrosis factor-alpha on activity and nitric oxide synthase of endothelial progenitor cells from peripheral blood. *Cell Prolif.*, 2011, 44, 352–359.

- Chen M, Huang J, Yang X, Liu B, Zhang W, Huang L, Deng F et al. Serum starvation induced cell cycle synchronization facilitates human somatic cells reprogramming. *PLoS one*. 2012; 7 (4): e28203.
- Chen Z, Bakhshi FR, Shajahan AN, Sharma T, Mao M, Trane A, Bernatchez P, van Nieuw GP, Bonini MG, Skidgel AI, Malika AB and Minshalla RD. Signaling. Nitric oxide-dependent Src activation and resultant caveolin-1 phosphorylation promote eNOS/caveolin-1 binding and eNOS inhibition. *Mol. Biol. Cell*. 2012; 23 (7): 1388-1398.
- Chen Z, Lai TC, Jan YH, Lin FM, Wang WC, Xiao H, Wang YT, Sun W, Cui X, Li YS, Fang T, Zhao H, Padmanabhan C, Sun R, Wang DL, Jin H, Chau GY, Huang HD, Hsiao M and Shyy JY. Hypoxia-responsive miRNAs target argonaute 1 to promote angiogenesis. *J. Clin. Invest*. 2013; 123 (3): 1057-67.
- Chhabra N. Endothelial dysfunction – A predictor of atherosclerosis. *Internet J Med Update* 2009; 4(1): 33–41.
- Chin JH, Azhar S, Hoffman BB. Inactivation of endothelial derived relaxing factor by oxidized lipoproteins. *J Clin Invest*. 1992; 89: 10-18.
- Cho SR, Ock SA, Yoo JG, Choe SY and Rho GJ. Effects of Confluent, Roscovitine Treatment and Serum Starvation on the Cell-cycle Synchronization of Bovine Foetal Fibroblasts. *Reproduction in Domestic Animals*. 2005; 40 (2): 171-176.
- Choi D, Hwang K-C, Lee K-Y, Kim Y-H. Ischemic heart disease: current treatments and future. *J Contr Release* 2009; 140: 194-202.
- Clempus RE and Griendling KK. Reactive oxygen species signaling in vascular smooth muscle cells. *Cardiovascular Research*. 2006; 71: 216 – 225.
- Clerk A, Cullingford TE, Fuller SJ, Giraldo A, Markou T, Pikkarainen S and Sugden PH. Signaling pathways mediating cardiac myocyte gene expression in physiological and stress responses. *Journal of cellular physiology*. 2007; 212 (2): 311-322.
- Closse C, Seigneur M, Renard M, Pruvost A, Dumain P, Belloc F and Boisseau MR. Influence of hypoxia and hypoxia-reoxygenation on endothelial P-selectin expression. *Pathophysiology of Haemostasis and Thrombosis*. 2010; 26 (4): 177-181.
- Cohen W, Hnasko R, Schubert W and Lisanti MP. Role of caveolae and caveolins in health and disease. *Physiol. Rev*. 2004; 84: 1341–1379.
- Cohen RA. The endothelium-derived hyperpolarizing factor puzzle: a mechanism without a mediator? *Circulation*. 2005; 111: 724–727.
- Collins HE and Rodrigo GC. Inotropic Response of Cardiac Ventricular Myocytes to β -Adrenergic Stimulation With Isoproterenol Exhibits Diurnal Variation Involvement of Nitric Oxide. *Circulation research*. 2010; 106 (7): 1244-1252.
- Cominacini L, Pasini AF, Garbin U, Davoli A, Tosetti ML, Campagnola M, et al. Oxidized low density lipoprotein (ox-LDL) binding to ox-LDL receptor-1 in endothelial cells induces the activation of NF-

kappaB through an increased production of intracellular reactive oxygen species. *J Biol Chem* 2000; 28(275): 12633–8.

Conner SD and Schmid SL. Regulated portals of entry into the cell. *Nature*. 2003; 6; 422 (6927): 37-44.

Cooper RD, Daniel-Issakani S, Ding R, Gururaja TL, Huang J, Kinoshita T, Masuda ES, McLaughlin J, Payan DG, Singh R, Yung S, Zhou X. A class of small molecules that inhibit TNFalpha-induced survival and death pathways via prevention of interactions between TNFalphaRI, TRADD, and RIP1. *Chem. Biol.* 2007 14: 1105-18.

Corda S, Laplace C, Vicaut E, et al. Rapid reactive oxygen species production by mitochondria in endothelial cells exposed to tumor necrosis factor-alpha is mediated by ceramide. *Am J Respir Cell Mol Biol.* 2001; 24: 762–768.

Corrado E, Rizzo M, Coppola G, Muratori I, Carella M and Novo S. Endothelial dysfunction and carotid lesions are strong predictors of clinical events in patients with early stages of atherosclerosis: a 24-month follow-up study. *Coronary Artery Disease.* 2008; 19 (3): 139-144.

Cortese-Krott, Miriam M., Roberto Sansone, Sivatharsini Sivarajah, Ana Rodriguez-Mateos, Gunter G. Kuhnle, Thomas Krenz, Christoph Krisp et al. Decreased Expression and Activity of Red Cell eNOS Correlate With Endothelial Dysfunction in Humans. *Free Radical Biology and Medicine.* 2011; 51: S157.

Cosentino F, Hishikawa K, Katusic ZS and Lüscher TF. High glucose increases nitric oxide synthase expression and superoxide anion generation in human aortic endothelial cells. *Circulation.* 1997; 96 (1): 25-28.

Cotton JM, Kearney MT, MacCarthy PA, et al. Effects of nitric oxide synthase inhibition on basal function and the force-frequency relationship in the normal and failing human heart in vivo. *Circulation* 2001; 104: 2318–23.

Cotton JM, Kearney MT and Shah AM. Nitric oxide and myocardial function in heart failure: friend or foe? *Heart.* 2002 December; 88(6): 564–566.

Cox J, Neuhauser N, Michalski A, Scheltema RA, Olsen JV and Mann M. Andromeda: a peptide search engine integrated into the MaxQuant environment. *J. Proteome Res.* 2011; 10: 1794–1805.

Crabtree MJ, Tatham AL, Hale AB, Alp NJ, Channon KM. Critical role for tetrahydrobiopterin recycling by dihydrofolate reductase in regulation of endothelial nitric-oxide synthase coupling: relative importance of the de novo biopterin synthesis versus salvage pathways. *J. Biol. Chem.* 2009; 284: 28128–28136.

Craig R and Beavis RC. TANDEM: matching proteins with mass spectra. *Bioinformatics.* 2004; 20: 1466-7.

Crimi E, Taccone FS, Infante T, Scolletta S, Crudele V and Napoli C. Effects of intracellular acidosis on endothelial function: an overview. *Journal of critical care.* 2012; 27 (2): 108-118.

- Crisafulli C, Galuppo M and Cuzzocrea S. Effects of genetic and pharmacological inhibition of TNF- α in the regulation of inflammation in macrophages. *Pharmacological Research*. 2009; 60 (4): 332-340.
- Crosswhite P and Sun Z. Nitric oxide, oxidative stress and inflammation in pulmonary arterial hypertension. *Journal of hypertension*. 2010; 28 (2): 201.
- Culic O, Gruwel ML, Schrader J. Energy turnover of vascular endothelial cells. *Am. J. Physiol*. 1997; 273: C205–C213.
- Culotta E and Koshland DE Jr. NO news is good news. *Science*. 1992; 258 (5090): 1862-1865.
- Daff S. NO synthase: structures and mechanisms. *Nitric Oxide*. 2010; 23 (1): 1-11.
- Dalle-Donne I, Scaloni A, Giustarini D, Cavarra E, Tell G, Lungarella G, Colombo R, Rossi R and Milzani A. Proteins as biomarkers of oxidative/nitrosative stress in diseases: the contribution of redox proteomics. *Mass spectrometry reviews*. 2005; 24 (1): 55-99.
- Dandona P, Aljada A, Chaudhuri A, Mohanty P and Garg R. Metabolic Syndrome A Comprehensive Perspective Based on Interactions Between Obesity, Diabetes, and Inflammation. *Circulation*. 2005; 111 (11): 1448-1454.
- Danilic S, Bitterman H, Rahat MA, Kinarty A, Rosenzweig D, Nitza L. Hypoxia inactivates inducible nitric oxide synthase in mouse macrophages by disrupting its interaction with α -actinin 4. *J Immunol*. 2003; 171: 3225–3232.
- Davalos A, Fernandez-Hernando C, Sowa G, Derakhshan B, Lin MI, Lee JY, Zhao H, Luo R, Colangelo C and Sessa WC. Quantitative proteomics of caveolin-1 regulated proteins: characterization of PTRF/cavin-1 in endothelial cells. *Molecular & Cellular Proteomics*. 2010.
- Davidson SM and Duchon MR. Endothelial Mitochondria. Contributing to Vascular Function and Disease. *Circulation Research*. 2007; 100: 1128-1141.
- Davignon J, Ganz P. Role of endothelial dysfunction in atherosclerosis. *Circulation*. 2004; 109: 27–32.
- Declercq W, Denecker G, Fiers W and Vandenaebroeck P. Cooperation of both TNF receptors in inducing apoptosis: involvement of the TNF receptor-associated factor binding domain of the TNF receptor 75. *J. Immunol*. 1998; 161: 390 - 399.
- Deedwania PC. Hypertension and diabetes: new therapeutic options. *Archives of Internal Medicine*. 2000; 160 (11): 1585.
- De Palma C, Meacci E, Perrotta C, Bruni P and Clementi E. Endothelial nitric oxide synthase activation by tumor necrosis factor α through neutral sphingomyelinase 2, sphingosine kinase 1, and sphingosine 1 phosphate receptors: a novel pathway relevant to the pathophysiology of endothelium. *Arterioscler. Thromb. Vasc. Biol*. 2006; 26: 99–105.
- De Vriese AS, Verbeuren TJ, Van de Voorde J, Lameire NH and Vanhoutte PM. Endothelial dysfunction in diabetes. *Br. J. Pharmacol*. 2000; 130: 963–974.

- Deanfield JE, Halcox JP, Rabelink TJ. Endothelial function and dysfunction: Testing and clinical relevance. *Circulation* 2007; 115: 1285–1295.
- Defer N, Azroyan A, Pecker F and Pavoine C. TNFR1 and TNFR2 signaling interplay in cardiac myocytes. *Journal of Biological Chemistry*. 2007; 282 (49): 35564-35573.
- Dejana E. Endothelial cell-cell junctions: happy together. *Nat Rev Mol Cell Biol*. 2004; 5: 261–270.
- Dela Paz NG, Simeonidis S, Leo C, Rose DW and Collins T. Regulation of NF- κ B-dependent gene expression by the POU domain transcription factor. *J. Biol. Chem.* 2007; 282: 8424–8434.
- Demiryurek AT, Karamsetty MR, McPhaden AR, Wadsworth RM, Kane KA and MacLean MR. Accumulation of Nitrotyrosine Correlates with Endothelial NO Synthase in Pulmonary Resistance Arteries During Chronic Hypoxia in the Rat. *Pulmonary Pharmacology & Therapeutics*. 2000; 13: 157–165.
- Denko NC. Hypoxia, HIF1 and glucose metabolism in the solid tumour. *Nat Rev Cancer*. 2008; 705–713.
- Deshpande NN, Sorescu D, Seshiah P, et al. Mechanism of hydrogen peroxide–induced cell cycle arrest in vascular smooth muscle. *Antioxid Redox Signal*. 2002; 4: 845– 854.
- Desideri G, Bravi MC, Tucci M, Croce G, Marinucci MC, Santucci A, Alesse E and Ferri C. Angiotensin II Inhibits Endothelial Cell Motility Through an AT1-Dependent Oxidant-Sensitive Decrement of Nitric Oxide Availability. *Arterioscler Thromb Vasc Biol*. 2003; 23: 1218-1223.
- Desjardins F, Delisle C and Gratton JP. Modulation of the cochaperone AHA1 regulates heat-shock protein 90 and endothelial NO synthase activation by vascular endothelial growth factor. *Arteriosclerosis, thrombosis, and vascular biology*. 2012; 32 (10): 2484-2492.
- Diaz N, Frei B, Vita JA, Keaney Jr. JF. Antioxidants and atherosclerotic heart disease. *New England Journal of Medicine*. 1997; 337: 408–416.
- Dib H, Chafey P, Clary G, Federici C, Le Gall M, Dwyer J, Gavard J *et al*. Proteomes of umbilical vein and microvascular endothelial cells reflect distinct biological properties and influence immune recognition. *Proteomics*. 2012; 12 (15-16): 2547-2555.
- Diesen DL and Kuo PC. Nitric Oxide and Redox Regulation in the Liver: Part I. General Considerations and Redox Biology in Hepatitis. Research Review. *Journal of Surgical Research*. 2010; 162 (1): 95–109.
- Dignat-George F and Boulanger CM. The many faces of endothelial microparticles. *Arteriosclerosis, thrombosis, and vascular biology*. 2011; 31 (1): 27-33.
- Dikalov SI, Dikalova AE, Bikineyeva AT, Schmidt HH, Harrison DG, Griendling KK. Distinct roles of Nox1 and Nox4 in basal and angiotensin II-stimulated superoxide and hydrogen peroxide production. *Free Radic Biol Med*. 2008; 45(9): 1340–1351.

- Ding Y, Vaziri ND, Coulson R, Kamanna VS and Roh DD. Effects of simulated hyperglycemia, insulin, and glucagon on endothelial nitric oxide synthase expression. *American Journal of Physiology-Endocrinology And Metabolism*. 2000; 279 (1): E11-E17.
- DiStasi MR and Ley K. Review. Opening the flood-gates: how neutrophil-endothelial interactions regulate permeability. *Trends in Immunology*. 2009; 30 (11): 547–556.
- Divchev D and Schieffer B. The secretory phospholipase A2 group IIA: a missing link between inflammation, activated renin-angiotensin system, and atherogenesis? *Vasc Health Risk Manag*. 2008; 4(3): 597–604.
- D'Orleans-Juste P. Enzymatic pathways involved in the generation of endothelin-11–31 from exogenous big endothelin-1 in the rabbit aorta. *Br J Pharmacol*. 2006; 148: 527–535.
- Doughan AK, Harrison DG and Dikalov SI. Molecular Mechanisms of Angiotensin II–Mediated Mitochondrial Dysfunction Linking Mitochondrial Oxidative Damage and Vascular Endothelial Dysfunction. *Circulation research*. 2008; 102 (4): 488-496.
- Douni E and Kollias G. A critical role of the p75 tumor necrosis factor receptor (p75TNF-R) in organ inflammation independent of TNF, lymphotoxin α , or the p55 TNF-R. *J. Exp. Med*. 1998; 188: 1343 - 1352.
- Downey JM, Omar B, Ooiwa H and McCord J. Superoxide dismutase therapy for myocardial ischemia. *Free Radical Res. Commun*. 1991; 12–13: 703–720.
- Du XL, Edelstein D, Dimmeler S, Ju Q, Sui C and Brownlee M. Hyperglycemia inhibits endothelial nitric oxide synthase activity by posttranslational modification at the Akt site. *J Clin Invest*. 2001; 108: 1341 –1348.
- Dudek SM and Garcia JGN. Cytoskeletal regulation of pulmonary vascular permeability. *J. Appl. Physiol*. 2001; 91: 1487-1500.
- Dumas E, Martel C, Neagoe PE, Bonnefoy A and Sirois MG. Angiopoietin-1 but not angiopoietin-2 promotes neutrophil viability: Role of interleukin-8 and platelet-activating factor. *Biochimica et Biophysica Acta (BBA) - Molecular Cell Research*. 2012; 1823 (2): 358–367.
- Dvorak AM, Kohn S, Morgan ES, Fox P, Nagy JA, Dvorak HF. The vesiculo-vacuolar organelle (VVO): a distinct endothelial cell structure that provides a transcellular pathway for macromolecular extravasation. *J Leukoc Biol*. 1996; 59: 100–115.
- Dvorak AM, Feng D. The vesiculo-vacuolar organelle (VVO). A new endothelial cell permeability organelle. *J Histochem Cytochem*. 2001; 49: 419–432.
- Dweik RA. Nitric oxide, hypoxia, and superoxide: the good, the bad, and the ugly!. *Thorax*. 2005; 60 (4): 265-267.
- Dyrlund TF, Poulsen ET, Scavenius C, Nikolajsen CL, Thogersen IB, Vorum H, Enghild JJ. Human Cornea Proteome: Identification and Quantitation of the Proteins of the Three Main Layers Including Epithelium, Stroma, and Endothelium. *J. Proteome Res*. 2012; 11: 4231-4239.

- Egert S, Kannenberg F, Somoza V, Erbersdobler HF and Wahrburg U. Dietary α -linolenic acid, EPA, and DHA have differential effects on LDL fatty acid composition but similar effects on serum lipid profiles in normolipidemic humans. *The Journal of nutrition*. 2009; 139 (5): 861-868.
- Eggermann J, Kliche S, Jarmy G, Hoffmann K, Mayr-Beyrle U, Debatin KM, Waltenberger J and Beltinger C. Endothelial progenitor cell culture and differentiation in vitro: a methodological comparison using human umbilical cord blood. *Cardiovascular research*. 2003; 58 (2): 478-486.
- Ehara S, Ueda M, Naruko T, Haze K, Itoh A, Otsuka M, et al. Elevated levels of oxidized low density lipoprotein show a positive relationship with the severity of acute coronary syndromes. *Circulation* 2001; 103: 1930– 2.
- Ehara S, Ueda M, Naruko T, Haze K, Matsuo T, Ogami M, et al. Pathophysiological role of oxidized low-density lipoprotein in plaque instability in coronary artery diseases. *J Diabetes Complications*. 2002; 16: 60 – 4.
- El-Haroun H, Clarke DL, Deacon K, Bradbury D, Clayton A, Sutcliffe A and Knox AJ. IL-1 β , BK, and TGF- β 1 attenuate PGI₂-mediated cAMP formation in human pulmonary artery smooth muscle cells by multiple mechanisms involving p38 MAP kinase and PKA. *American Journal of Physiology-Lung Cellular and Molecular Physiology*. 2008; 294 (3): L553-L562.
- Elkington PT, O’Kane CM, Friedland JS. The paradox of matrix metalloproteinases in infectious disease. *Clin. Exp. Immunol*. 2005; 142: 12-20.
- El-Remessy AB, Abou-Mohamed G, Caldwell RW and Caldwell RB. High glucose-induced tyrosine nitration in endothelial cells: role of eNOS uncoupling and aldose reductase activation. *Investigative ophthalmology & visual science*. 2003; 44 (7): 3135-3143.
- Erickson SL, Desauvage FJ, Kikly K, Carvermoore K, Pittsmeek, S, Gillet N, Sheehan KCF, Schreiber RD, Goeddel DV and Moore MW. Decreased sensitivity to tumor-necrosis-factor but normal T-cell development in TNF receptor-2-deficient mice. *Nature*. 1994; 372 : 560–563.
- Esmon CT and Esmon NL. The link between vascular features and thrombosis. *Annu Rev Physiol*. 2011; 73: 503–514.
- Esper RJ, Nordaby RA, Vilarino JO, Paragano A, Cacharon JL, Machado RA. Endothelial dysfunction: a comprehensive appraisal. *Cardiovasc Diabetol*. 2006; 5: 4.
- Estrada-Bernal A, Sanford SD, Sosa LJ, Simon GC and Hansen KC. Functional complexity of the axonal growth cone: a proteomic analysis. *PloS one*. 2012; 7 (2): e31858.
- Farooqui AA and Horrocks LA. Phospholipase A₂-Generated Lipid Mediators in the Brain: The Good, the Bad, and the Ugly. *The Neuroscientist*. 2006; 12 (3): 245-260.
- Faustman D and Davis M. TNF receptor 2 pathway: drug target for autoimmune diseases. *Nat Rev Drug Discov*. 2010; 9: 482-493.
- Feldman AM and McNamara D. Myocarditis. *N Engl J Med*. 2000; 343: 1388–1398.
- Feletou M and Vanhoutte PM. Endothelial dysfunction: a multifaceted disorder. *Am. J. Physiol.Heart Circ. Physiol*. 2006; 291: H985–H1002.

- Félétou M, Vanhoutte PM. Endothelium-dependent hyperpolarizations: past beliefs and present facts. *Ann Med.* 2007; 39: 495–516.
- Ferrara N, Gerber HP and LeCouter J. The biology of VEGF and its receptors. *Nature medicine.* 2003; 9 (6): 669-676.
- Fetalvero KM, Martin KA and Hwa J. Cardioprotective prostacyclin signaling in vascular smooth muscle. *Prostag Other Lipid Mediat.* 2007; 82: 109-118.
- Fickling SA, Leone AM, Nussey SS, Vallance P & Whitley GSJ. Synthesis of NG,NG-dimethylarginine by human endothelial cells. *Endothelium.* 1993; 1: 137-140.
- Fickling SA, Holden DP, Cartwright JE, Nussey SS, Vallance P, Whitley G. Regulation of macrophage nitric oxide synthesis by endothelial cells: a role for NG, NG dimethylarginine. *Acta Physiol Scand.* 1999; 167: 145–150.
- Fish JE, Yan MS, Matouk CC, St. Bernard R, Ho JJD, Gavryushova A, Srivastava D and Marsden PA. Hypoxic Repression of Endothelial Nitric-oxide Synthase Transcription Is Coupled with Eviction of Promoter Histones. *The Journal of Biological Chemistry.* 2010; 285 (2): 810–826.
- Fleming I, Michaelis UR, Bredenkotter D, et al. Endothelium-derived hyperpolarizing factor synthase (Cytochrome P450 2C9) is a functionally significant source of reactive oxygen species in coronary arteries. *Circ Res.* 2001; 88: 44 –51.
- Förstermann U, Munzel T. Endothelial nitric oxide synthase in vascular disease: from marvel to menace. *Circulation* 2006; 113: 1708–1714.
- Förstermann U and Sessa WC. Nitric oxide synthases: regulation and function. *European heart journal.* 2012; 33 (7): 829-837.
- Fournier NM, Lee B, Banasr M, Elsayed M and Duman RS. Vascular endothelial growth factor regulates adult hippocampal cell proliferation through MEK/ERK-and PI3K/Akt-dependent signaling. *Neuropharmacology.* 2012; 63 (4): 642-652.
- Francis SH, Busch JL, Corbin JD and Sibley D. cGMP-dependent protein kinases and cGMP phosphodiesterases in nitric oxide and cGMP action. *Pharmacol. Rev.* 2010; 62: 525–563.
- Franzén B, Duvefelt K, Jonsson C, Engelhardt B, Ottervald J, Wickman M, Yang Y, Schuppe-Koistinen I. Gene and protein expression profiling of human cerebral endothelial cells activated with tumor necrosis factor- α . *Molecular Brain Research.* 2003; 115: 130–146.
- Freed JK and Greene AS. Proteomic Analysis of Shear Stress-Mediated Protection from TNF- α in Endothelial Cells. *Microcirculation.* 2010; 17(4): 259–270.
- Frey RS, Rahman A, Kefer JC, Minshall RD, Malik AB. PKC- ζ regulates TNF- α -induced activation of NADPH oxidase in endothelial cells. *Circ Res.* 2002; 90: 1012–1019.
- Frezza C and Gottlieb E. Mitochondria in cancer: not just innocent bystanders. *Semin Cancer Biol.* 2009; 19: 4–11.

Furchgott RF, Zawadzki JV. The obligatory role of endothelial cells in the relaxation of arterial smooth muscle by acetylcholine. *Nature*.1980; 288: 373–376.

Furie B and Furie BC. Mechanisms of Thrombus Formation. *N Engl J Med*. 2008; 359: 938-949.

Furukawa S, Fujita T, Shimabukuro M, Iwaki M, Yamada Y, Nakajima Y, Nakayama O, Makishima M, Matsuda M and Shimomura I. Increased oxidative stress in obesity and its impact on metabolic syndrome. *J. Clin. Invest*. 2004; 114: 1752–1761.

Galis ZS, Muszynski M, Sukhova GK, et al. Enhanced expression of vascular matrix metalloproteinases induced in vitro by cytokines and in regions of human atherosclerotic lesions. *Ann N Y Acad Sci*. 1995; 748: 501–507.

Ganda A, Onat D, Demmer RT, Wan E, Vittorio TJ, Sabbah HN, Colombo PC. Venous Congestion and Endothelial Cell Activation in Acute Decompensated Heart Failure. *Current Heart Failure Reports*. 2010; 7 (2): 66-74.

Gao X, Belmadani , Picchi A. et al. Tumor necrosis factor- α induces endothelial dysfunction in Leprdb mice. *Circulation*. 2007; 115: 245–254.

Gardner G, Banka CL, Roberts KA, Mullick AE, Rutledge JC. Modified LDL-mediated increases in endothelial layer permeability are attenuated with 17 beta-estradiol. *Arteriosclerosis Thrombosis and Vascular Biology*. 1999; 19: 854–861.

Gath I, Gödtel-Armbrust U and Förstermann U. Expressional downregulation of neuronal-type NO synthase I in guinea pig skeletal muscle in response to bacterial lipopolysaccharide. *FEBS Lett*. 1997; 410: 319–323.

Gaur U and Aggarwal BB. Regulation of proliferation, survival and apoptosis by members of the TNF superfamily. *Biochem. Pharmacol*. 2003; 66 (8): 1403–8.

Gawaz M, Langer H and May AE. Platelets in inflammation and atherogenesis. *Journal of Clinical Investigation*. 2005; 115 (12): 3378-3384.

Geiger M, Stone A, Mason SN, Oldham KT and Guice KS. Differential nitric oxide production by microvascular and macrovascular endothelial cells. *Am J Physiol*. 1997;273 (1 Pt 1): L275-81.

Ghosh S and Hayden MS. Celebrating 25 years of NF- κ B research. *Immunological reviews*. 2012; 246 (1): 5-13.

Gielen S, Sandri M, Erbs S and Adams V. Exercise-Induced Modulation of Endothelial Nitric Oxide Production. *Current Pharmaceutical Biotechnology*. 2011; 12 (9): 1375-1384(10).

Gielis JF, Lin JY, Wingler K, Van Schil PEY, Schmidt HH and Moens AN. Pathogenetic role of eNOS uncoupling in cardiopulmonary disorders. *Free Radical Biology and Medicine*. 2011; 50 (7): 765–776.

Gillham JC, Myers JE, Baker PN and Taggart MJ. TNF- α alters nitric oxide- and endothelium-derived hyperpolarizing factor-mediated vasodilatation in human omental arteries. *Hypertens.Pregnancy*. 2008; 27: 29–38.

- Girgis RE, Li D, Zhan X, Garcia JGN, Tudor RM, Hassoun PM and Johns RA. Attenuation of chronic hypoxic pulmonary hypertension by simvastatin. *American Journal of Physiology-Heart and Circulatory Physiology*. 2003; 285: 3: H938-H945.
- Gleissner CA, von Hundelshausen P and Ley K. Brief Reviews. Platelet Chemokines in Vascular Disease. *Arteriosclerosis, Thrombosis, and Vascular Biology*. 2008; 28: 1920-1927.
- Gonenc A, Hacışevki A, Griffiths HR, Torun M, Bakkaloglu B and Simsek B. Free radical reaction products and antioxidant capacity in beating heart coronary artery surgery compared to conventional bypass. *Biochemistry (Moscow)*. 2011; 76 (6): 677-685.
- Goodwin BL, Solomonson LP and Eichler DC. Argininosuccinate synthase expression is required to maintain nitric oxide production and cell viability in aortic endothelial cells. *J. Biol. Chem.* 2004; 279: 18353–18360.
- Goodwin BL, Pendleton LC, Levy MM, Solomonson LP and Eichler DC. Tumor necrosis factor- α reduces argininosuccinate synthase expression and nitric oxide production in aortic endothelial cells. *Am. J. Physiol. Heart Circ. Physiol.* 2007; 293: H1115–H1121.
- Goracci G, Balestrieri ML and Nardicchi V. Metabolism and Functions of Platelet-Activating Factor (PAF) in the Nervous Tissue. *Handbook of Neurochemistry and Molecular Neurobiology*. 2010; 311-352 .
- Görlach A, Brandes RP, Bassus S, et al. Oxidative stress and expression of p22phox are involved in the up-regulation of tissue factor in vascular smooth muscle cells in response to activated platelets. *Faseb J.* 2000; 14: 1518–1528.
- Gourdin MJ, Bree B and De Kock M. Review. The impact of ischaemia-reperfusion on the blood vessel. *European Journal of Anaesthesiology*. 2009; 26 (7): 537-547.
- Gräfe M, Auch-Schwelk W, Hertel H, Terbeek D, Steinheider G, Loebe M and Fleck E. Human cardiac microvascular and macrovascular endothelial cells respond differently to oxidatively modified LDL. *Atherosclerosis*. 1998; 137 (1): 87-95.
- Granger D, Rodrigues SF, Yildirim A and Senchenkova EY. Microvascular responses to cardiovascular risk factors. *Microcirculation*. 2010a; 17 (3): 192-205.
- Granger DN and Senchenkova E. Chapter 7: Leukocyte–Endothelial Cell Adhesion. *Inflammation and the Microcirculation*. 2010b.
- Gratton JP, Bernatchez P and Sessa WC. Caveolae and caveolins in the cardiovascular system. *Circ. Res.* 2004; 94: 1408–1417.
- Graven KK and Farber HW. Endothelial cell hypoxic stress proteins. *J. Lab. Clin. Med.* 1998; 132 (6): 456-463.
- Graven KK, Zimmerman LH, Dickson EW, Weinhouse GL, Farber HW. Endothelial cell hypoxia associated proteins are cell and stress specific. *J. Cell. Physiol.* 1993; 157 (3): 544-54.
- Greenacre SA and Ischiropoulos H. Tyrosine nitration: localization, quantification, consequences for protein function and signal transduction. *Free Radic. Res.* 2001; 34: 541/581.

- Greenberg S, Xie J, Wang Y. et al. Tumor necrosis factor- α inhibits endothelium-dependent relaxation. *J. Appl. Physiol.* 1993; 74: 2394–2403.
- Greene AL, Rutherford MS, Regal RR, Flickinger GH, Hendrickson JA, Giulivi C, Mohrman ME, Fraser DG and Regal JF. Arginase activity differs with allergen in the effector phase of ovalbumin-versus trimellitic anhydride-induced asthma. *Toxicol. Sci.* 2005; 88: 420–433.
- Gregersen N and Bross P. Protein misfolding and cellular stress: an overview. In *Protein Misfolding and Cellular Stress in Disease and Aging*. 2010; pp. 3-23.
- Grell M, Becke FM, Wajant H, Mannel DN and Scheurich P. TNF receptor type 2 mediates thymocyte proliferation independently of TNF receptor type 1. *Eur. J. Immunol.* 1998; 28: 257 - 263.
- Griendling KK, Sorescu D, Lassègue B, Ushio-Fukai M. Modulation of Protein Kinase activity and gene expression by reactive oxygen species and their role in vascular physiology and pathophysiology. *Arterioscler Thromb Vasc Biol.* 2000a; 20: 2175–2183.
- Griendling KK, Sorescu D, Ushio-Fukai M. NAD(P)H oxidase: role in cardiovascular biology and disease. *Circ Res.* 2000b; 86: 494 –501.
- Griendling KK and FitzGerald GA. Review: Clinical Cardiology: New Frontiers. Oxidative Stress and Cardiovascular Injury. Part I: Basic Mechanisms and In Vivo Monitoring of ROS. *Circulation.* 2003; 108: 1912-1916.
- Griffith TM. Endothelium-dependent smooth muscle hyperpolarization: do gap junctions provide a unifying hypothesis? *Br J Pharmacol.* 2004; 141: 881–903.
- Grivennikov SI and Karin M. Dangerous liaisons: STAT3 and NF- κ B collaboration and crosstalk in cancer. *Cytokine & growth factor reviews.* 2010; 21 (1): 11-19.
- Grover-Páez F and Zavalza-Gómez AB. Endothelial dysfunction and cardiovascular risk factors. *Diabetes Research and Clinical Practice.* 2008; 84 (1); 1-10.
- Guicciardi ME, Bronk SF, Werneburg NW, Yin X-M, Gores GJ. Bid Is Upstream of Lysosome-Mediated Caspase 2 Activation in Tumor Necrosis Factor α -Induced Hepatocyte Apoptosis. *Gastroenterology* 2005; 129(1): 269 – 284.
- Gupta AK, Joshi MB, Philippova M, Erne P, Hasler P, Hahn S and Resink TJ. Activated endothelial cells induce neutrophil extracellular traps and are susceptible to NETosis-mediated cell death. *FEBS letters.* 2010; 584 (14): 3193-3197.
- Guzik TJ, Mussa S, Gastaldi D, et al. Mechanisms of increased vascular superoxide production in human diabetes mellitus, role of NAD(P)H oxidase and endothelial nitric oxide synthase. *Circulation* 2002; 105: 1656–1662.
- Guzy RD and Schumacker PT. Oxygen sensing by mitochondria at complexIII: the paradox of increased reactive oxygen species during hypoxia. *Exp Physiol.* 2006; 91.5: 807–819.

- Haas MJ and Mooradian AD. Regulation of high-density lipoprotein by inflammatory cytokines: establishing links between immune dysfunction and cardiovascular disease. *Diabetes/Metabolism Research and Reviews*. 2010; 26 (2): 90–99.
- Haddad JJ and Hisham LH. Cytokines and the regulation of hypoxia-inducible factor (HIF)-1 α . *International immunopharmacology*. 2005; 5 (3): 461-483.
- Hadi AR, Carr CS and Al Suwaidi J. Endothelial Dysfunction: Cardiovascular Risk Factors, Therapy, and Outcome. *Vasc Health Risk Manag*. 2005: 1(3): 183–198.
- Halcox JP, Schenke WH, Zalos G, et al. Prognostic value of coronary vascular endothelial dysfunction. *Circulation*. 2002; 106(6): 653-8.
- Hall JL, Wang X, Adamson V, Zhao Y and Gibbons GH. Overexpression of Ref-1 inhibits hypoxia and tumor necrosis factor–induced endothelial cell apoptosis through nuclear factor- κ B–independent and–dependent pathways. *Circulation research*. 2001; 88 (12): 1247-1253.
- Hall CN and Garthwaite J. What is the real physiological NO concentration in vivo? *Nitric Oxide*. 2009; 21: 92–103.
- Hamburg NM, Vita JA. Endothelial dysfunction in atherosclerosis: mechanisms of impaired nitric oxide bioactivity. In: Loscalzo J (ed). *Molecular Mechanisms of Atherosclerosis*. London: Taylor and Francis 2005: 95–110.
- Harlan JM. Endothelial activation and dysfunction in sepsis. *In Endothelial Dysfunction and Inflammation*. Springer Basel. 2010: pp. 1-13.
- Harris AL. Hypoxia—a key regulatory factor in tumour growth. *Nat Rev Cancer*. 2002; 2: 38–47.
- Harris MB, Blackstone MA, Ju H, Venema VJ and Venema RC. Heat-induced increases in endothelial NO synthase expression and activity and endothelial NO release. *Am. J. Physiol. Heart Circ. Physiol*. 2003; 285: H333–340.
- Harrison D, Griendling KK, Landmesser U, Hornig B and Drexler H. Role of oxidative stress in atherosclerosis. *Am J Cardiol*. 2003a; 91: 7A–11A.
- Harrison DG, Cai H, Landmesser U and Griendling KK. Interactions of angiotensin II with NAD (P) H oxidase, oxidant stress and cardiovascular disease. *Journal of the renin-angiotensin-aldosterone system: JRAAS*. 2003b; 4 (2): 51-61.
- Hase H, Legarda-Addison D, Seed B, Ting AT, Varughese L, Yang M. B cell maturation antigen, the receptor for a proliferation-inducing ligand and B cell-activating factor of the TNF family, induces antigen presentation in B cells. *J. Immunol*. 2005; 175: 2814-24.
- Haseloff RF, Krause E, Bigl M, Mikoteit K, Stanimirovic D, Blasig IE. Differential protein expression in brain capillary endothelial cells induced by hypoxia and posthypoxic reoxygenation. *Proteomics*. 2006; 6: 1803-1809.
- Hattori Y, Campbell EB and Gross SS. Argininosuccinate synthetase mRNA and activity are induced by immunostimulants in vascular smooth muscle. Role in the regeneration or arginine for nitric oxide synthesis. *J. Biol. Chem*. 1994; 269: 9405–9408.

- Hayashida K, Kume N, Murase T, Minami M, Nakagawa D, Inada T, et al. Serum soluble lectin-like oxidized low-density lipoprotein receptor-1 levels are elevated in acute coronary syndrome: a novel marker for early diagnosis. *Circulation*. 2005; 112: 812–8.
- Haynes WG, Strachan FE, Gray GA, Webb DJ. Forearm vasoconstriction to endothelin-1 is mediated by ETA and ETB receptors in vivo in humans. *J Cardiovasc Pharmacol*. 1995; 26 (3): S40–S43.
- Heemskerk S, Masereeuw R, Russel FGM and Pickkers P. Review. Selective iNOS inhibition for the treatment of sepsis-induced acute kidney injury. *Nature Reviews Nephrology*. 2009; 5: 629–640.
- Heiss EH, Schachner D, Werner ER and Dirsch VM. Active NF-E2-related factor (Nrf2) contributes to keep endothelial NO synthase (eNOS) in the coupled state: role of reactive oxygen species (ROS), eNOS, and heme oxygenase (HO-1) levels. *J. Biol. Chem*. 2009; 284: 31579–31586.
- Hendrickx J, Doggen K, Weinberg EO, Van Tongelen P, Franssen P and De Keulenaer GW. Molecular diversity of cardiac endothelial cells in vitro and in vivo. *Physiol. Genomics*. 2004; 19: 198–206.
- Herrera M and Garvin JL. Angiotensin II stimulates thick ascending limb NO production via AT2 receptors and Akt1-dependent nitric-oxide synthase 3 (NOS3) activation. *Journal of Biological Chemistry*. 2010a; 285 (20): 14932–14940.
- Herrera MD, Mingorance C, Rodriguez R, et al. Endothelial dysfunction and aging: an update. *Ageing Res Rev*. 2010b; 9: 142–152.
- Heusch G, Post H, Michel MC, et al. Endogenous nitric oxide and myocardial adaptation to ischemia. *Circ Res* 2000; 87: 146–52.
- Hicklin DJ and Ellis LM. Role of the vascular endothelial growth factor pathway in tumor growth and angiogenesis. *Journal of Clinical Oncology*. 2005; 23 (5): 1011–1027.
- Hidalgo M, Le Bouffant R, Bello V, Buisson N, Cormier P, Beaudry M and Darribere T. The translational repressor 4E-BP mediates hypoxia-induced defects in myotome cells. *Journal of Cell Science*. 2012; 125: 3989–4000.
- Higuchi M and Aggarwal BB. TNF induces internalization of the p60 receptor and shedding of the p80 receptor. *J. Immunol*. 1994; 152: 3550 - 3558.
- Hien TT, Oh WK, Hung NP, Oh SJ, Lee MY and Kang KW. Nectandrin B Activates eNOS Phosphorylation in Endothelial Cells: Role of the AMP-activated Protein Kinase/estrogen Receptor α /phosphatidylinositol 3-kinase/Akt Pathway. *Molecular Pharmacology*. 2011; mol.111.073502.
- Hijdra D, Vorselaars ADM, Grutters JC, Claessen AME and Rijkers GT. Differential expression of TNFR1 (CD120a) and TNFR2 (CD120b) on subpopulations of human monocytes. *Journal of Inflammation*. 2012; 9 (1): 38.

Hill BG, Dranka BP, Bailey SM, Lancaster Jr JR and Darley-Usmar VM. What Part of NO Don't You Understand? Some Answers to the Cardinal Questions in Nitric Oxide Biology. *The Journal of Biological Chemistry*. 2010; 285: 19699-19704.

Hill-Kapturczak N, Kapturczak MH, Block ER, Patel JM, Malinski T, Madsen KM, Tisher CC. Angiotensin II-stimulated nitric oxide release from porcine pulmonary endothelium is mediated by angiotensin IV. *J Am Soc Nephrol*. 1999; 10(3): 481-91.

Hiraoka E, Kawashima S, Takahashi T, Rikitake Y, Kitamura T, Ogawa W, Yokoyama M. TNF-alpha induces protein synthesis through PI3-kinase-Akt/PKB pathway in cardiac myocytes. *Am J Physiol Heart Circ Physiol*. 2001; 280(4): H1861-8.

Hirata K, Miki N, Kuroda Y, Sakoda T, Kawashima S and Yokoyama M. Low concentration of oxidized lowdensity lipoprotein and lysophosphatidylcholine up-regulate constitutive nitric oxide synthase mRNA expression in bovine aortic endothelial cells. *Circ. Res*. 1995; 6: 958-962.

Hoffmann A, Gloe T and Pohl U. Hypoxia-induced upregulation of eNOS gene expression is redox-sensitive: a comparison between hypoxia and inhibitors of cell metabolism. *J Cell Physiol*. 2001; 188(1): 33-44.

Hoffmann A, Levchenko A, Scott ML, Baltimore D. The I κ B-NF- κ B Signaling Module: Temporal Control and Selective Gene Activation. *Science*. 2002; 298 (5596): 1241-1245.

Hojlund K, Yi Z, Hwang H, Bowen B, Lefort N, Flynn CR, Langlais P, Weintraub ST and Mandarino LJ. Characterization of the Human Skeletal Muscle Proteome by One-dimensional Gel Electrophoresis and HPLC-ESI-MS/MS. *Molecular and Cellular Proteomics*. 2008; 7: 257-267.

Holland SM. Chronic granulomatous disease. *Clinical reviews in allergy & immunology*. 2010; 38 (1): 3-10.

Holvoet P, Vanhaecke J, Janssens S, Van de Werf F, Collen D. Oxidized-LDL and malondialdehyde-modified LDL in patients with acute coronary syndromes and stable coronary artery disease. *Circulation*. 1998; 98: 1487-1494.

Holvoet P, Mertens A, Verhamme P, Bogaerts K, Beyens G, Verhaeghe R, Collen D, Muls E, Vande Werf F. Circulating oxidized-LDL is a useful marker for identifying patients with coronary artery disease. *Arteriosclerosis Thrombosis and Vascular Biology*. 2001; 21: 844-848.

Holyer I. The role of platelets and their associated recruitment mechanisms, in intestinal ischaemia reperfusion injury. *PhD diss., University of Birmingham*, 2011.

Hsieh PCH, Davis ME, Lisowski LK, Lee RT. Endothelial-cardiomyocyte interactions in cardiac development and repair. *Annu Rev Physiol*. 2006; 68: 51-66.

Hsueh WA, Lyon CJ, Quinones MJ. Insulin resistance and the endothelium. *Am J Med*. 2004; 117: 109-117.

Huang PL, Huang Z, Mashimo H, Bloch KD, Moskowitz MA, Bevan JA, Fishman MC. Hypertension in mice lacking the gene for endothelial nitric oxide synthase. *Nature*. 1995; 377: 239-242.

Huang PL. Endothelial nitric oxide synthase and endothelial dysfunction. *Curr Hypertens Rep.* 2003; 5: 473–480.

Huang DW and Lempicki RA. Systematic and integrative analysis of large gene lists using DAVID bioinformatics resources. *Nature Protocols.* 2009; 4 (1): 44–57.

Huang CY, Yeh JS, Shih CM, Lin FY, Kao YT, Tsao NW, Hsiao WT, Chen JW, Chang NC and Shyu KG. The Association between Serum Asymmetric Dimethylarginine and Coronary Atherosclerotic Plaque in an Asymptomatic Population. *Immunology, Endocrine & Metabolic Agents-Medicinal Chemistry.* 2012; 12 (3): 236-243.

Hurd TR, DeGennaro M and Lehmann R. Redox regulation of cell migration and adhesion. *Trends in cell biology.* 2012; 22 (2): 107-115.

Husson A, Brasse-Lagnel C, Fairand A, Renouf S and Lavoigne A. Argininosuccinate synthetase from the urea cycle to the citrulline-NO cycle. *Eur. J. Biochem.* 2003; 270: 1887–1899.

Iaccarino G, Ciccarelli M, Sorriento D, et al. AKT participates in endothelial dysfunction in hypertension. *Circulation* 2004; 109: 2587–2593.

Ignarro LJ, Buga GM, Wood KS, Byrns RE, Chaudhuri G. Endothelium-derived relaxing factor produced and released from artery and vein is nitric oxide. *Proc Natl Acad Sci USA.* 1987; 84: 9265–9269.

Ikner A and Ashkenazi A. TWEAK induces apoptosis through a death-signaling complex comprising receptor-interacting protein 1 (RIP1), Fas-associated death domain (FADD), and caspase-8. *Journal of Biological Chemistry.* 2011; 286 (24): 21546-21554.

Ikonen E and Parton RG. Caveolins and Cellular Cholesterol Balance. *Traffic.* 2000; 1 (3): 212–217.

Imrie H, Abbas A and Kearney M. Insulin resistance, lipotoxicity and endothelial dysfunction. *Biochimica et Biophysica Acta (BBA)-Molecular and Cell Biology of Lipids.* 2010; 1801 (3): 320-326.

Inoue T, Hoshi K, Yaguchi I, Iwasaki Y, Takayanagi K and Morooka S. Serum levels of circulating adhesion molecules after coronary angioplasty. *Cardiology.* 1999; 91: 236–242.

Ioannidou S, Deinhardt K, Miotla J, Bradley J, Cheung E, Samuelsson S, Ng YS, Shima DT. An in vitro assay reveals a role for the diaphragm protein PV-1 in endothelial fenestra morphogenesis. *Proc Natl Acad Sci U S A.* 2006; 103: 16770–16775.

Irwin W, Mak S, Mann DL, Qu R, Penninger JM, Yan A, Dawood F, Wen FW, Shou Z and Liu P. Tissue expression and immunolocalization of tumor necrosis factor- α in postinfarction dysfunctional myocardium. *Circulation.* 1999; 99: 1492–1498.

Isenberg JS, Romeo MJ, Yu C, Yu CK, Nghiem K, Monsale J, Rick ME, Wink DA, Frazier WA and Roberts DB. Thrombospondin-1 stimulates platelet aggregation by blocking the antithrombotic activity of nitric oxide/cGMP signaling. *Hemostasis, Thrombosis and Vascular Biology.* 2008; 111 (2): 613-623.

Ito A, Tsao PS, Adimoolam S, Kimoto M, Ogawa T & Cooke JP. Novel mechanism for endothelial dysfunction: dysregulation of dimethylarginine dimethylaminohydrolase. *Circulation*. 1999; 99: 3092-3095.

Iwai N, Hanai K, Tooyama I, Kitamura Y and Kinoshita M. Regulation of neuronal nitric oxide synthase in rat adrenal medulla. *Hypertension*. 1995; 25: 431-436.

Iwasaki T, Hayasaki-Kajiwara Y, Shimamura T, Naya N, Nakajima M. Endothelin receptor subtype antagonist activity of S-0139 in various isolated rabbit and canine arteries. *Eur J Pharmacol*. 2000; 400: 255-262.

Jagielska J, Kapopara PR, Salguero G, Scherr M, Schütt H, Grote K, Schieffer B and Bavendiek U. Interleukin-1 Assembles a Proangiogenic Signaling Module Consisting of Caveolin-1, Tumor Necrosis Factor Receptor-Associated Factor 6, p38-Mitogen-Activated Protein Kinase (MAPK), and MAPK-Activated Protein Kinase 2 in Endothelial Cells. *Arteriosclerosis, thrombosis, and vascular biology*. 2012; 32 (5): 1280-1288.

Jang JJ, Ho HK, Kwan HH, Fajardo LF, Cooke JP. Angiogenesis is impaired by hypercholesterolaemia: role of asymmetric dimethylarginine. *Circulation*. 2000; 102: 1414-1419.

Jantzen F, Koneman S, Wolff B., et al. Isoprenoid depletion by statins antagonizes cytokine-induced down-regulation of endothelial nitric oxide expression and increases NO synthase activity in human umbilical vein endothelial cells. *J. Physiol. Pharmacol*. 2007; 58: 503-514.

Jennings LK. Mechanisms of platelet activation: need for new strategies to protect against platelet-mediated atherothrombosis. *Thromb Haemost*. 2009; 102 (2): 248-257.

Ji Y, Anderson DJ and Bennett BM. Endothelial cell apoptosis as a mechanism of endothelial dysfunction in nitrate tolerance. *cGMP*. 2003; 1: 0026.

Jiang J, Fu W, Wang X, Lin PH, Yao Q and Chen C. HIV gp120 induces endothelial dysfunction in tumour necrosis factor- α -activated porcine and human endothelial cells. *Cardiovasc Res*. 2010; 87 (2): 366-374.

Jiang X, Yang Z, Chandrakala AN, Pressley D and Parthasarathy S. Oxidized Low Density Lipoproteins-Do We Know Enough About Them? *Cardiovascular drugs and therapy*. 2011; 25 (5): 367-377.

Jin HG, Yamashita H, Nagano Y, Fukuba H, Hiji M, Ohtsuki T, Takahashi T, Kohriyama T, Kaibuchi K and Matsumoto M. Hypoxia-induced upregulation of endothelial small G protein RhoA and Rho-kinase/ROCK2 inhibits eNOS expression. *Neuroscience Letters*. 2006; 408 (1): 62-67.

Jin RC and Loscalzo J. Vascular nitric oxide: formation and function. *Journal of blood medicine*. 2010; 1: 147.

Jin CZ, Jang JH, Kim HJ, Wang Y, Hwang IC, Sadayappan S, Park BM *et al*. Myofilament Ca²⁺ Desensitization Mediates Positive Lusitropic Effect of Neuronal Nitric Oxide Synthase in Left Ventricular Myocytes from Murine Hypertensive Heart. *Journal of molecular and cellular cardiology*. 2013.

Johannes and Lamaze C. Clathrin-Dependent or Not: Is It Still the Question? *Traffic*. 2002; 3 (7): 443–451.

Juonala M, Viikari JS, Alfthan G, Marniemi J, Kahonen M, Taittonen L, Laitinen T and Raitakari OT. Brachial artery flow-mediated dilation and asymmetrical dimethylarginine in the cardiovascular risk in young Finns study. *Circulation*. 2007; 116: 1367–1373.

Justice JM, Tanner MA and Myers PR. Endothelial Cell Regulation of Nitric Oxide Production During Hypoxia in Coronary Microvessels and Epicardial Arteries. *Journal of Cellular Physiology*. 2000; 182: 359–365.

Kamijikkoku S, Murohara T, Tayama S, Matsuyama K, Honda T, Ando M and Hayasaki K. Acute myocardial infarction and increased soluble intercellular adhesion molecule-1: a marker of vascular inflammation and a risk of early restenosis? *Am Heart J*. 1998; 136: 231–236.

Kathuria H, Cao YX, Ramirez MI, Williams MC. Transcription of the caveolin-1 gene is differentially regulated in lung type I epithelial and endothelial cell lines. A role for ETS proteins in epithelial cell expression. *Biol Chem*. 2004; 279: 30028–30036.

Katusi ZS. Mechanisms of endothelial dysfunction induced by aging role of arginase I. *Circulation research*. 2007; 101 (7): 640-641.

Kavdia M and Popel AS. Contribution of nNOS- and eNOS-derived NO to microvascular smooth muscle NO exposure. *J Appl Physiol*. 2004; 97(1): 293-301.

Keaney JF Jr., Guo Y, Cunningham D, Shwaery GL and Vita JA. Vascular incorporation of alpha-tocopherol prevents endothelial dysfunction due to oxidized LDL by inhibiting protein kinase C stimulation. *J. Clin. Invest*. 1996; 98: 386–394.

Kessler P, Popp R, Busse R and Schini-Kerth VB. Proinflammatory mediators chronically downregulate the formation of the endothelium-derived hyperpolarizing factor in arteries via a nitric oxide/cyclic GMP-dependent mechanism. *Circulation*. 1999; 99: 1878–1884.

Kiechl S, Werner P, Knoflach M and Willeit J. Subclinical Atherosclerosis, Markers of Inflammation, and Oxidative Stress. *Ultrasound and Carotid Bifurcation Atherosclerosis*. 2012; 4: 487-509.

Kiefer FN, Berns H, Resink TJ and Bategay EJ. Hypoxia enhances vascular cell proliferation and angiogenesis in vitro via rapamycin (mTOR)-dependent signaling. *The FASEB Journal*. 2002; 16 (8): 771-780.

Kielstein JT, Impraim B, Simmel S, Bode-Böger SM, Tsikas D, Frölich JC, Höper MM, Haller H & Frölich JC. Cardiovascular effects of systemic nitric oxide synthase inhibition with asymmetrical dimethylarginine in humans. *Circulation*. 2004; 109: 172-177.

Kieszko R, Krawczyk P, Chocholska S, Bojarska-Junak A, Jankowska O, Król A, Roliński J, Milanowski J. Tumor necrosis factor receptors (TNFRs) on T lymphocytes and soluble TNFRs in different clinical courses of sarcoidosis. *Respir Med* 2007, 101:645-654.

Kietzmann T and Görlach A. Reactive oxygen species in the control of hypoxia-inducible factor-mediated gene expression. *In Seminars in cell & developmental biology*. 2005; 16 (4): 474-486.

- Kim F, Gallis B and Corson MA. TNF- α inhibits flow and insulin signaling leading to NO production in aortic endothelial cells. *Am J Physiol Cell Physiol*. 2001; 280: C1057–C1065.
- Kim HJ, Tsoy I, Park JM, Chung J, Shin SC and Chan KC. Anthocyanins from soybean seed coat inhibit the expression of TNF- α -induced genes associated with ischemia/reperfusion in endothelial cell by NF- κ B-dependent pathway and reduce rat myocardial damages incurred by ischemia and reperfusion in vivo. *FEBS Letters*. 2006a; 580 (5): 1391–1397.
- Kim J, Tchernyshyov I, Semenza GL and Dang CV. HIF-1-mediated expression of pyruvate dehydrogenase kinase: a metabolic switch required for cellular adaptation to hypoxia. *Cell Metab*. 2006b; 3: 177–185.
- Kimoto M, Whitley GS, Tsuji H & Ogawa T. Detection of NG,NG-dimethylarginine dimethylaminohydrolase in human tissues using a monoclonal antibody. *J. Biochem*. 1995; 117: 237-238.
- Kinlay S and Ganz P. Role of endothelial dysfunction in coronary artery disease and implications for therapy. *Am J Cardiol*. 1997; 80(9A): 11I-16I.
- Kita T, Nagano Y, Yokode M, Ishii K, Kume N, Ooshima A, *et al*. Probucol prevents the progression of atherosclerosis in Watanabe heritable hyperlipidemic rabbit, an animal model for familial hypercholesterolemia. *Proc Natl Acad Sci U S A*. 1987; 84: 5928– 31.
- Kita T. LOX-1, a Possible Clue to the Missing Link Between Hypertension and Atherogenesis. *Circ Res*. 1999; 84: 1113-1115.
- Kluge MA, Fettermann JL and Vita JA. Mitochondria and endothelial function. *Circ. Res*. 2013; 112: 1171-1188.
- Kneilling M, Mailhammer R, Hültner L, Schönberger T, Fuchs K, Schaller M, Bukala D *et al*. Direct crosstalk between mast cell–TNF and TNFR1-expressing endothelia mediates local tissue inflammation. *Blood*. 2009; 114 (8): 1696-1706.
- Koch S and Claesson-Welsh L. Signal Transduction by Vascular Endothelial Growth Factor Receptors. *Cold Spring Harb Perspect Med*. 2012;2:a006502.
- Kolář F and Ošťádal B. Molecular mechanisms of cardiac protection by adaptation to chronic hypoxia. *Physiol Res*. 2004; 53 (1): S3-S13.
- Kolluru GK, Tamilarasan KP, Rajkumar AS, Priya SG, Rajaram M, Saleem NK, Majumder S, Jaffar Ali BM, Illavazagan G and Chatterjee S. Nitric oxide/cGMP protects endothelial cells from hypoxia-mediated leakiness. *European journal of cell biology*. 2008; 87 (3): 147-161.
- Kolluru GK, Siamwala JH and Chatterjee S. Review. eNOS phosphorylation in health and disease *Biochimie*. 2010; 92 (9): 1186–1198.
- Konig P, Dedio J, Muller-Esterl W and Kummer W. Distribution of the novel eNOS-interacting protein NOSIP in the liver, pancreas, and gastrointestinal tract of the rat. *Gastroenterology*. 2002; 123: 314–324.

- König P, Dedio J, Oess S, Papadakis T, Fischer A, Müller-Esterl W and Kummer W. NOSIP and its interacting protein, eNOS, in the rat trachea and lung. *J. Histochem. Cytochem.* 2005; 53: 155–164.
- Kostourou V, Robinson SP, Cartwright JE, Whitley GS. Dimethylarginine dimethylaminohydrolase I enhances tumour growth and angiogenesis. *Br J Cancer.* 2002; 87: 673–680.
- Kostourou V, Robinson SP, Whitley GS, Griffiths JR. Effects of overexpression of dimethylarginine dimethylaminohydrolase on tumor angiogenesis assessed by susceptibility magnetic resonance imaging. *Cancer Res.* 2003; 63: 4960–4966.
- Krempf TK, Maas R, Sydow K, Meinertz T, Böger RH, Kähler J. Elevation of asymmetric dimethylarginine in patients with unstable angina and recurrent cardiovascular events. *Eur Heart J.* 2005; 26(18): 1846–1851.
- Kugiyama K, Kerns SA, Morrisett JD, Roberts R and Henry PD. Impairment of endothelium-dependent arterial relaxation by lysolecithin in modified low-density lipoproteins. *Nature.* 1990; 344: 160–162.
- Kuhr F, Lowry J, Zhang Y, Brovkovich V and Skidgel RA. Differential regulation of inducible and endothelial nitric oxide synthase by kinin B1 and B2 receptors. *Neuropeptides.* 2010; 44 (2): 145-154.
- Kumar A, Takada Y, Boriek AM and Aggarwal BB. Nuclear factor- κ B: its role in health and disease. *J. Mol. Med.* 2004; 82: 434–448.
- Kumar SD, Krishnamurthy K, Manikandan J, Pakeerappa PN and Pushparaj PN. Deciphering the key molecular and cellular events in neutrophil transmigration during acute inflammation. *Bioinformation.* 2011; 6 (3): 111.
- Kume N, Arai H, Kawai C, Kita T. Receptors for modified low-density lipoproteins on human endothelial cells: different recognition for acetylated low-density lipoprotein and oxidized low-density lipoprotein. *Biochim Biophys Acta.* 1991; 1091: 63–7.
- Kunieda T, Minamino T, Nishi J, Tateno K, Oyama T, Katsuno T, Miyauchi H *et al.* Angiotensin II induces premature senescence of vascular smooth muscle cells and accelerates the development of atherosclerosis via a p21-dependent pathway. *Circulation.* 2006; 114 (9): 953-960.
- Kunsch C, Medford RM. Oxidative stress as a regulator of gene expression in the vasculature. *Circ Res.* 1999; 85: 753–766.
- Kuster GM, Lancel S, Zhang J, Communal C, Trucillo MP, Lim CC, Pfister O *et al.* Redox-mediated reciprocal regulation of SERCA and Na⁺-2⁺ exchanger contributes to sarcoplasmic reticulum Ca²⁺ depletion in cardiac myocytes. *Free Radical Biology and Medicine.* 2010; 48 (9): 1182-1187.
- Kuzkaya N, Weissmann N, Harrison DG, *et al.* Interaction of peroxynitrite, tetrahydrobiopterin, ascorbic acid, and thiols. *J Biol Chem.* 2003; 278: 22546–22554.
- Kwaan HC, Samama MM. The significance of endothelial heterogeneity in thrombosis and hemostasis. *Semin Thromb Hemost.* 2010; 36: 286–300.

- La Sala A, Pontecorvo L, Agresta A, Rosano G and Stabile E. Regulation of collateral blood vessel development by the innate and adaptive immune system. *Trends In Molecular Medicine*. 2012; 18 (8): 494–501.
- Labrecque L, Royal I, Surprenant DS, Patterson C, Gingras D and Beliveau R. Regulation of vascular endothelial growth factor receptor-2 activity by caveolin-1 and plasma membrane cholesterol. *Mol Biol Cell*. 2003; 14: 334–347.
- Laemmli UK. Cleavage of Structural Proteins during the Assembly of the Head of Bacteriophage T4. *Nature*. 1970; 227: 680 – 685.
- Lahoz C, Mostaza JM. Atherosclerosis as a systemic disease. *Rev Esp Cardiol* 2007; 60(2): 184-95.
- Lam CF, Peterson TE, Richardson DM, Croatt AJ, d'Uscio LV, Nath KA and Katusic ZS. Increased blood flow causes coordinated upregulation of arterial eNOS and biosynthesis of tetrahydrobiopterin. *Am. J. Physiol. Heart Circ. Physiol*. 2006; 290: H786–793.
- Lamas S, ed. Nitric oxide, cell signaling, and gene expression. Vol. 19. *CRC Press*, 2010.
- Lambert IH, Pedersen SF and Poulsen KA. Activation of PLA2 isoforms by cell swelling and ischaemia/hypoxia. *Acta Physiologica*. 2006; 187 (1-2): 75-85.
- Lambeth JD. NOX enzymes and the biology of reactive oxygen. *Nat Rev Immunol*. 2004; 4: 181–189
- Landmesser U, Dikalov S, Price SR, McCann L, Fukai T, Holland SM, Mitch WE and Harrison DG. Oxidation of tetrahydrobiopterin leads to uncoupling of endothelial cell nitric oxide synthase in hypertension. *J. Clin. Invest*. 2003; 111: 1201–1209.
- Landmesser U, Harrison DG, Drexler H. Oxidant stress – a major cause of reduced endothelial nitric oxide availability in cardiovascular disease. *Eur J Clin Pharmacol*. 2006; 63: 13–19.
- Lassègue B, Sorescu D, Szöcs K, et al. Novel gp91phox homologues in vascular smooth muscle cells: nox1 mediates angiotensin II–induced superoxide formation and redox-sensitive signaling pathways. *Circ Res*. 2001; 88: 888–894.
- Lau DCW, Dhillon B, Yan H, Szmitko PE and Verma S. Adipokines: molecular links between obesity and atherosclerosis. *American Journal of Physiology-Heart and Circulatory Physiology*. 2005; 288 (5): H2031-H2041.
- Layland J, Li J-M, Shah AM. Role of cyclic GMP-dependent protein kinase in the contractile response to exogenous nitric oxide in isolated cardiac myocytes. *J Physiol* 2002; 540.2: 457–67.
- Lecour S, Suleman N, Deuchar GA, Somers S, Lacerda L, Huisamen B and Opie LH. Pharmacological Preconditioning With Tumor Necrosis Factor- α Activates Signal Transducer and Activator of Transcription-3 at Reperfusion Without Involving Classic Prosurvival Kinases (Akt and Extracellular Signal–Regulated Kinase). *Circulation*. 2005; 112: 3911-3918.
- Lee SB, Cho ES, Yang HS, Kim H and Um HD. Serum withdrawal kills U937 cells by inducing a positive mutual interaction between reactive oxygen species and phosphoinositide 3-kinase. *Cell. Signal*. 2005; 17: 197–204.

Lee HS, Lee MJ, Kim H, Choi SK, Kim JE, Moon HI, Park WH. Curcumin inhibits TNF α -induced lectin-like oxidised LDL receptor-1 (LOX-1) expression and suppresses the inflammatory response in human umbilical vein endothelial cells (HUVECs) by an antioxidant mechanism. *Journal of Enzyme Inhibition and Medicinal Chemistry*. 2010; 25 (5): 720-729.

Lee JS, Park SY, Thapa D, Kim AR, Shin HM and Kim JA. 1HMC05, Herbal Formula, Inhibits TNF- α -Induced Inflammatory Response in Human Umbilical Vein Endothelial Cells. *Evidence-Based Complementary and Alternative Medicine*. 2011; Article ID 974728, 11 pages.

Leiper JM, Santa Maria J, Chubb A, MacAllister RJ, Charles IG, Whitley GS & Vallance P. Identification of two human dimethylarginine dimethylaminohydrolases with distinct tissue distributions and homology with microbial arginine deiminases. *Biochem. J*. 1999; 343: 209-214.

Leiper J, Murray-Rust J, McDonald N & Vallance P. S-Nitrosylation of dimethylarginine dimethylaminohydrolase regulates enzyme activity: further interactions between nitric oxide synthase and dimethylarginine dimethylaminohydrolase. *Proc. Natl. Acad. Sci. U.S.A.* 2002; 99: 13527-13532.

Lekakis J, Abraham P, Balbarini A, Blann A, Boulanger CM, Cockcroft J, Cosentino F, Deanfield J, Gallino A, Ikonomidis I, Kremastinos D, Landmesser U, Protogerou A, Stefanadis C, Tousoulis D, Vassalli G, Vink H, Werner N, Wilkinson I and Vlachopoulos C. Methods for evaluating endothelial function: a position statement from the European Society of Cardiology Working Group on Peripheral Circulation. *European Journal of Cardiovascular Prevention & Rehabilitation*. 2011; 18(6): 775–789.

Lemarié CA and Schiffrin EL. The angiotensin II type 2 receptor in cardiovascular disease. *J Renin Angiotensin Aldosterone Syst*. 2010; 11(1): 19–31.

Lemoine S, Buléon C, Rouet R, Ivascau C, Babatasi G, Massetti M, Gérard JL and Hanouz JL. Bradykinin and adenosine receptors mediate desflurane induced postconditioning in human myocardium: role of reactive oxygen species. *BMC anesthesiology*. 2010; 10 (1): 12.

Lerman A and Zeiher AM. Endothelial Function. Cardiac Events. Contemporary Reviews in Cardiovascular Medicine. *Circulation*. 2005; 111: 363-368.

Levi M and van der Poll T. Inflammation and coagulation. *Critical care medicine*. 2010; 38: S26-S34.

Levitan I, Volkov S, Subbaiah PV. Oxidized-LDL: diversity, patterns of recognition, and pathophysiology. *Antioxidants and Redox Signaling*. 2010; 13: 39–75.

Ley K, Laudanna C, Cybulsky MI, Nourshargh S. Getting to the site of inflammation: the leukocyte adhesion cascade updated. *Nat Rev Immunol*. 2007; 7(9): 678–689.

Li D and Mehta JL. Antisense to endothelial ox-LDL receptor LOX-1 inhibits ox-LDL-mediated upregulation of MCP-1 expression and monocyte adhesion to human coronary artery endothelial cells. *Circulation*. 2000; 101: 2889–96.

Li C and Jackson RM. Reactive species mechanisms of cellular hypoxia-reoxygenation injury. *American Journal of Physiology-Cell Physiology*. 2002; 282 (2): C227-C241.

- Li C, Issa R, Kumar P, Hampson IN, Lopez-Novoa JM, Bernabeu C and Kumar S. CD105 prevents apoptosis in hypoxic endothelial cells. *Journal of cell science*. 2003; 116 (13): 2677-2685.
- Li D, Liu L, Chen H, Sawamura T, Mehta JL. LOX-1 mediates oxidized LDL-induced the expression and activation of matrix metalloproteinases (MMPs) in human coronary artery endothelial cells. *Circulation* 2003a; 107: 612–7.
- Li D, Liu L, Chen H, Sawamura T, Mehta JL. LOX-1, an oxidized LDL endothelial receptor, induces CD40/CD40L signaling in human coronary artery endothelial cells. *Arterioscler Thromb Vasc Biol* 2003b; 23: 816– 21.
- Li D and Mehta JL. Editorial. Oxidized LDL, a critical factor in atherogenesis. *Cardiovascular Research*. 2005; 68: 353 – 354.
- Li JM, Fan LM, Christie MR, et al. Acute tumor necrosis factor alpha signaling via NADPH oxidase in microvascular endothelial cells: role of p47phox phosphorylation and binding to TRAF4. *Mol Cell Biol*. 2005; 25:2320–2330.
- Li YSJ, Haga JH and Chien S. Review. Molecular basis of the effects of shear stress on vascular endothelial cells. *Journal of Biomechanics*. 2005; 38 (10): 1949–1971.
- Li J, Zhao X, Li X, Lerea KM and Olson SC. Angiotensin II type 2 receptor-dependent increases in nitric oxide synthase expression in the pulmonary endothelium is mediated via a Gαi3/Ras/Raf/MAPK pathway. *Am J Physiol Cell Physiol*. 2007a; 292: C2185–C2196.
- Li JM, Fan LM, George VT and Brooks G. Nox2 regulates endothelial cell cycle arrest and apoptosis via p21^{cip1} and p53. *Free Radical Biology and Medicine*. 2007b; 43 (6): 976-986.
- Li H and Lin X. Positive and negative signaling components involved in TNF-α-induced NF-KB activation. *Cytokine*. 2008; 41: 1-8.
- Li J, Zou Y, Ge J, Zhang D, Guan A, Wu J and Li L. The Effects of G-CSF on Proliferation of Mouse Myocardial Microvascular Endothelial Cells. *International journal of molecular sciences*. 2011; 12 (2): 1306-1315.
- Li H, Li J, Wang Y and Yang T. Proteomic analysis of effluents from perfused human heart for transplantation: identification of potential biomarkers for ischemic heart damage. *Proteome Science*. 2012; 10: 21.
- Liao JK, Shin WS, Lee WY and Clark SL. Oxidized low-density lipoprotein decreases the expression of endothelial nitric oxide synthase. *J. Biol. Chem*. 1995; 270: 319–324.
- Liao L and Granger DN. Modulation of oxidized low-density lipoprotein-induced microvascular dysfunction by nitric oxide. *American Journal of Physiology*. 1995; 268: H1643–H1650.
- Libby P, Ridker PM, Maseri A. Inflammation and atherosclerosis. *Circulation*. 2002; 150: 1135–1143.
- Liew FY, Pitman NI and McInnes IB. Disease-associated functions of IL-33: the new kid in the IL-1 family. *Nature Reviews Immunology*. 2010; 10 (2): 103-110.

- Limaye V and Vadas M. The vascular endothelium: structure and function. *Mechanisms of Vascular Disease. A Textbook for Vascular Surgeons*. 2007; 1: 1-14.
- Little PJ, Ivey ME and Osman N. Endothelin-1 Actions on Vascular Smooth Muscle Cell Functions As a Target for the Prevention of Atherosclerosis. *Current Vascular Pharmacology*. 2008; 6 (3): 195-203(9).
- Liu L and Simon MC. Regulation of transcription and translation by hypoxia. *Cancer Biology and Therapy*. 2004; 3 (6): 492-497.
- Liu L, Cash TP, Jones RG, Keith B, Thompson CB and Simon MC. Hypoxia induced energy stress regulates mRNA translation and cell growth. *Mol. Cell*. 2006; 21 (4): 521-531.
- Liu Y, Ma Y, Wang R, Xia C, Zhang R, Lian K, Tao L, et al. Advanced glycation end products accelerate ischemia/reperfusion injury through receptor of advanced end product/nitrative thioredoxin inactivation in cardiac microvascular endothelial cells. *Antioxidants & redox signalling*. 2011; 15(7), 1769 - 78.
- Liu G, Place AT, Chen Z, Brovkovych VM, Vogel SM, Muller WA, Skidgel RA, Malik AR and Minshall RD. ICAM-1-activated Src and eNOS signaling increase endothelial cell surface PECAM-1 adhesivity and neutrophil transmigration. *Blood*. 2012; 120 (9): 1942-1952.
- Lo LW, Cheng JJ, Chiu JJ, Wung BS, Liu YC and Wang DL. Endothelial exposure to hypoxia induces Egr-1 expression involving PKC α -mediated Ras/Raf-1/ERK1/2 pathway. *Journal of cellular physiology*. 2001; 188 (3): 304-312.
- Locksley RM, Killeen N, Lenardo MJ. The TNF and TNF receptor superfamilies: integrating mammalian biology. *Cell*. 2011; 104: 487-501.
- Lopez A, Lorente JA, Steingrub J, Bakker J, McLuckie M, Willatts S, Brockway, Anzueto A, Holzapfel L, Breen D, Silverman MS, Takala J, Donaldson J, Arneson C, Grove G, Grossman S and Grover R. Multiple-center, randomized, placebo-controlled, double-blind study of the nitric oxide synthase inhibitor 546C88: effect on survival in patients with septic shock. *Crit. Care Med*. 2004; 32: 21-30.
- López JA and Chen J. Pathophysiology of venous thrombosis. *Thromb Res*. 2009; 123 (Suppl 4): S30-4.
- Loyer X, Gomez AM, Milliez P, Fernandez-Velasco M, Vangheluwe P, Vinet L, Charue D, Vaudin E, Zhang W, Sainte-Marie Y, Robidel E, Marty I, Mayer B, Jaisser F, Mercadier JJ, Richard S, Shah AM, Benitah JP, Samuel JL, Heymes C. Cardiomyocyte overexpression of neuronal nitric oxide synthase delays transition toward heart failure in response to pressure overload by preserving calcium cycling. *Circulation* 2008; 117: 3187-3198.
- Lu D, Maulik N, Moraru II, et al. Molecular adaptation of vascular endothelial cells to oxidative stress. *Am J Physiol*. 1993; 264: C715-C722.
- Lu TM, Ding YA, Lin SJ, Lee WS, Tai HC. Plasma levels of asymmetrical dimethylarginine and adverse cardiovascular events after percutaneous coronary intervention. *Eur Heart J*. 2003; 24: 1912-1919.

- Lu L, Yang PY, Rui YCH, Kang H, Zhang J, Zhang JP and Feng WH. Comparative proteome analysis of rat brain and coronary microvascular endothelial cells. *Physiol. Res.* 2007; 56: 159-167.
- Luan ZG, Zhang H, Yang PT, Ma XC, Zhang C and Guo RX. HMGB1 activates nuclear factor- κ B signaling by RAGE and increases the production of TNF- α in human umbilical vein endothelial cells. *Immunobiology.* 2010; 215 (12): 956-962.
- Lucas R, Juillard P, Decoster E, Redard M, Burger D, Donati Y, Giroud C, Monsohinard C, Dekesel T, Buurman WA, Moore MW, Dayer JM, Fiers W, Bluethmann H and Grau GE. Crucial role of tumor necrosis factor (TNF) receptor 2 and membrane-bound TNF in experimental cerebral malaria. *Eur. J. Immunol.* 1997a; 27: 1719 - 1725.
- Lucas R, Lou JN, Juillard P, Moore M, Bluethmann H and Grau GE. Respective role of TNF receptors in the development of experimental cerebral malaria. *J. Neuroimmunol.* 1997b; 72: 143 - 148.
- Lucas R, Garcia I, Donati YRA, Hribar M, Mandriota SJ, Giroud C, Buurman WA, Fransen L, Suter PM, Nunez G, Pepper MS and Grau GE. Both TNF receptors are required for direct TNF-mediated cytotoxicity in microvascular endothelial cells. *Eur. J. Immunol.* 1998; 28: 3577 - 3586.
- Luo D, Luo Y, He Y, et al. Differential functions of tumor necrosis factor receptor 1 and 2 signaling in ischemia-mediated arteriogenesis and angiogenesis. *Am J Pathol.* 2006; 169: 1886-1898.
- Luscher TF and Vanhoutte PM. The Endothelium: Modulator of Cardiovascular Function. *Boca Raton, FL, CRC Press.* 1990.
- Ma ZC, Gao Y, Wang J, Zhang XM and Wang SQ. Proteomic analysis effects of ginsenoside Rg1 on human umbilical vein endothelial cells stimulated by tumor necrosis factor- α . *Life sciences.* 2006; 79 (2): 175-181.
- Maas R, Schulze F, Baumert J, Lowel H, Hamraz K, Schwedhelm E, Koenig W, Boger RH. Asymmetric dimethylarginine, smoking, and risk of coronary heart disease in apparently healthy men: Prospective analysis from the population-based Monitoring of Trends and Determinants in Cardiovascular Disease/Kooperative Gesundheitsforschung in der Region Augsburg study and experimental data. *Clin. Chem.* 2007; 53: 693-701.
- MacAllister R, Whitley G, Vallance P. Effects of guanidino and uremic compounds on nitric oxide pathways. *Kidney Int.* 1994; 45: 737-742.
- MacAllister RJ, Parry H, Kimoto MT, Russell RJ, Hodson H, Whitley GS & Vallance P. Regulation of nitric oxide synthesis by dimethylarginine dimethylaminohydrolase. *Br. J. Pharmacol.* 1996; 119: 1533-1540.
- MacEwan DJ. TNF ligands and receptors: a matter of life and death. *British Journal of Pharmacology.* 2002; 135: 855 - 875.
- Mackay F, Loetscher H, Stueber D, Gehr G, Lesslauer W: Tumor necrosis Factor α (TNF- α)-induced cell adhesion to human endothelial cells is under dominant control of one TNF receptor type, TNF-R55. *J Exp Med* 1993, 177:1277-1286.

- MacNaul KL and Hutchinson NI. Differential expression of iNOS and cNOS mRNA in human vascular smooth muscle cells and endothelial cells under normal and inflammatory conditions. *Biochem. Biophys. Res. Commun.* 1993; 196: 1330–1334.
- Madamanchi NR, Vendrov A, Runge MS. Oxidative stress and vascular disease. *Arterioscler Thromb Vasc Biol.* 2005; 25: 29–38.
- Madge LA, Kluger MS, Orange JS and May MJ. Lymphotoxin-alpha 1 beta 2 and LIGHT induce classical and noncanonicalNF-kappa B-dependent proinflammatory gene expression in vascular endothelial cells. *J. Immunol.* 2008; 180: 3467–3477.
- Malan D, Elischer A, Hesse M, Wickström SA, Fleischmann BK and Bloch W. Deletion of integrin linked kinase in endothelial cells results in defective RTK signaling caused by caveolin 1 mislocalization. *Development.* 2013; 140 (5): 987-995.
- Mallat Z and Tedgui A. Regulatory T cell responses: potential role in the control of atherosclerosis. *Current opinion in lipidology.* 2005; 16 (5): 518-524.
- Manalo DJ, Rowan A, Lavoie T, Natarajan L, Kelly BD, Shui QY, Garcia JGN and Semenza GL. Transcriptional regulation of vascular endothelial cell responses to hypoxia by HIF-1. *Blood.* 2005; 105 (2): 659-669.
- Mancia G, De Backer G, Dominiczak A, Cifkova R, Fagard R, Germano G, Grassi G, Heagerty AM, Kjeldsen SE, Laurent S, Narkiewicz K, Ruilope L, Rynkiewicz A, Schmieder RE, *et al.* 2007 Guidelines for the Management of Arterial Hypertension: The Task Force for the Management of Arterial Hypertension of the European Society of Hypertension (ESH) and of the European Society of Cardiology (ESC). *J Hypertens.* 2007; 25: 1105–1187.
- Manea A, Manea SA, Gafencu AV and Raicu M. Regulation of NADPH oxidase subunit p22(phox) by NF-kB in human aortic smooth muscle cells. *Arch. Physiol. Biochem.* 2007; 113: 163–172.
- Manea A, Manea SA, Gafencu AV, Raicu M and Simionescu M. AP-1-dependent transcriptional regulation of NADPH oxidase in human aortic smooth muscle cells: role of p22phox subunit. *Arterioscler. Thromb. Vasc. Biol.* 2008; 28: 878–885.
- Manes T, Zheng D, Tognin S, Woodard AS, Marchisio PC and Languino LR. vβ3 integrin expression up-regulates cdc2, which modulates cell migration. *J. Cell Biol.* 2003; 161 (4): 817-826.
- Manna SK and Aggarwal BB. Interleukin-4 downregulates both forms of tumor necrosis factor receptor and receptor-mediated apoptosis, NF-kB, AP-1, and c-Jun N-terminal kinase-comparison with interleukin-13. *J. Biol. Chem.* 1998; 273: 33333 - 33341.
- Manning BD and Cantley LC. AKT/PKB signaling: navigating downstream. *Cell.* 2007; 129 (7): 1261-1274.
- Manukhina EB, Downey HF and Mallet RT. Role of Nitric Oxide in Cardiovascular Adaptation to Intermittent Hypoxia. *Exp Biol Med (Maywood).* 2006; 231 (4): 343-365.
- Marcus NJ, Philippi NR, Bird CE, Li YL, Schultz HD and Morgan BJ. Effect of AT1 receptor blockade on intermittent hypoxia-induced endothelial dysfunction. *Respiratory Physiology & Neurobiology.* 2012; 183 (2): 67–74.

- Martínez-Ruiz A, Cadenasa S and Lamas S. Review Article. Nitric oxide signaling: Classical, less classical, and nonclassical mechanisms. *Free Radical Biology and Medicine*. 2011; 51 (1): 17–29.
- Martyn KD, Frederick LM, von Loehneysen K, Dinauer MC, Knaus UG. Functional analysis of Nox4 reveals unique characteristics compared to other NADPH oxidases. *Cell Signal*. 2006; 18(1): 69–82.
- Mas M. A Close Look at the Endothelium: Its Role in the Regulation of Vasomotor Tone. *European Urology Supplements*. 2009; 8 (2): 48–57.
- Masaki T, Kimura S, Yanagisawa M, Goto K. Molecular and cellular mechanism of endothelin regulation. Implications for vascular function. *Circulation*. 1991; 84: 1457–1468.
- Massion PB, Feron O, Dessy C and Balligand JL. Nitric oxide and cardiac function: ten years after, and continuing. *Circ Res*. 2003; 93(5): 388–398.
- Matsumoto T, Kakami M, Noguchi E, Kobayashi T and Kamata K. Imbalance between endothelium-derived relaxing and contracting factors in mesenteric arteries from aged OLETF rats, a model of type 2 diabetes. *Am J Physiol Heart Circ Physiol*. 2007; doi:10.1152/ajpheart.00229.
- Mattapally S and Banerjee SK. Nitric oxide: Redox balance, protein modification and therapeutic potential in cardiovascular system. *IIOABJ*. 2011; 2: 29-38.
- Mattson MP and Meffert MK. Roles for NF- κ B in nerve cell survival, plasticity, and disease. *Cell Death & Differentiation*. 2006; 13 (5): 852-860.
- Mayr M, Mayr U, Chung YL, Yin X, Griffiths JR and Xu Q. Vascular proteomics: linking proteomic and metabolomics changes. *Proteomics*. 2004; 4: 3751-3761.
- Mazzocchi G, Rossi GP, Malendowicz LK, Champion HC, Nussdorfer GG. Endothelin-11–31, acting as an ETA-receptor selective agonist, stimulates proliferation of cultured rat zona glomerulosa cells. *FEBS Lett*. 2000; 487: 194–198.
- McCabe TJ, Fulton D, Roman LJ, Sessa WC. Enhanced Electron Flux and Reduced Calmodulin Dissociation May Explain “Calcium-independent” eNOS Activation by Phosphorylation. *J. Biol. Chem*. 2000; 275: 6123–6128.
- McDermott JR. Studies on the catabolism of Ng-methylarginine, Ng, Ng-dimethylarginine and Ng, Ng-dimethylarginine in the rabbit. *Biochem J*. 1976; 154: 179–184.
- McMurtry MS and Michelakis ED. Coronary Heart Disease. *Endothelium Biology*. 2012: 219 – 237.
- Medvedev AE, Espevik T, Ranges G and Sundan A. Distinct roles of the two tumor necrosis factor (TNF) receptors in modulating TNF and lymphotoxin α effects. *J. Biol. Chem*. 1996; 271: 9778 - 9784.
- Mehta JL and Li DY. Inflammation in ischemic heart disease: response to tissue injury or a pathogenetic villain? *Cardiovasc Res*. 1999; 43: 291–299.

- Mehta JL, Li D, Chen H, Joseph J, Romeo F. Inhibition of LOX-1 by statins may relate to upregulation of eNOS. *Biochem Biophys Res Commun*. 2001; 289: 857–61.
- Mehta PK and Griendling KK. Angiotensin II cell signalling: physiological and pathological effects in the cardiovascular system. *Am J Physiol Cell Physiol*. 2007; 292: C82–97.
- Meldrum DR, Cleveland JC, Cain BS, Meng X and Harken AH. Increased myocardial TNF α in a crystalloid-perfused model of cardiac ischemia–reperfusion injury. *Ann Thorac Surg*. 1998a; 65: 439–443.
- Meldrum DR, Meng X, Dinarello CA, Ayala A, Cain BS, Shames BD, Ao L, Banerjee A and Harken AH. Human myocardial tissue TNF α expression following acute global ischemia in vivo. *J Mol Cell Cardiol*. 1998b; 30: 1683–1689.
- Mendis S, Puska P and Norrving B. Global Atlas on cardiovascular disease prevention and control 2011. *World Health Organization, Geneva* 2011.
- Mertens S, Noll T, Spahr R, Krutzfeldt A and Piper HM. Energetic response of coronary endothelial cells to hypoxia. *Am. J. Physiol*. 1990; 258: H689–H694.
- Meziani F, Tesse A and Andriantsitohaina R. Microparticles are vectors of paradoxical information in vascular cells including the endothelium: role in health and diseases. *Pharmacol Rep*. 2008; 60 (1): 75-84.
- Michell BJ, Chen Z, Tiganis T, Stapleton D, Katsis F, Power DA, Sim AT, Kemp BE. Coordinated Control of Endothelial Nitric-oxide Synthase Phosphorylation by Protein Kinase C and the cAMP-dependent Protein Kinase. *J. Biol. Chem*. 2001; 276: 17625–17628.
- Michiels C, Arnould T and Remacle J. Endothelial cell responses to hypoxia: initiation of a cascade of cellular interactions. Review. *Biochimica et Biophysica Acta*. 2000; 1497; 1-10.
- Millar TM, Phan V and Tibbles LA. ROS generation in endothelial hypoxia and reoxygenation stimulates MAP kinase signaling and kinase-dependent neutrophil recruitment. *Free Radical Biology and Medicine*. 2007; 42 (8): 1165–1177.
- Min J, Jin YM, Moon JS, Sung MS, Ahn S and Jo I. Through the Tax-Responsive Element in Endothelial Cells Hypoxia-Induced Endothelial NO Synthase Gene Transcriptional Activation Is Mediated. *Hypertension*. 2006; 47: 1189-1196.
- Minor RLJ, Myers PR, Guerra RJ, Bates JN and Harrison DG. Diet-induced atherosclerosis increases the release of nitrogen oxides from rabbit aorta. *J. Clin. Invest*. 1990; 86: 2109–2116.
- Miwa D, Sakaue T, Inoue H, Takemori N, Kurokawa M, Fukuda S, Omi K, Goishi K and Higashiyama S. Protein kinase D2 and heat shock protein 90 beta are required for BCL6-associated zinc finger protein mRNA stabilization induced by vascular endothelial growth factor-A. *Angiogenesis*. 2013: 1-14.
- Mizukami Y, Kohgo Y and Chung DC. Hypoxia Inducible Factor-1-independent pathways in tumor angiogenesis. *Clinical Cancer Research*. 2007; 13 (19): 5670-5674.

- Moccia F, Berra-Romani R, Tanzi F. Update on vascular endothelial Ca(2+) signalling: A tale of ion channels, pumps and transporters. *World J Biol Chem.* 2012; 26; 3(7): 127-58.
- Mochizuki M, Tsuchie Y, Yamada N, Miyake Y and Osawa T. Effect of Sesame Lignans on TNF- α -Induced Expression of Adhesion Molecules in Endothelial Cells. *Bioscience, Biotechnology, and Biochemistry.* 2010; 74 (8): 1539-1544.
- Modesti PA, Vanni S, Morabito M, Modesti A, Marchetta M, Gamberi T, Sofi F *et al.* Role of Endothelin-1 in Exposure to High Altitude Acute Mountain Sickness and Endothelin-1 (ACME-1) Study. *Circulation.* 2006; 114 (13): 1410-1416.
- Mohan S and Fung HL. Article. Mechanism of Cellular Oxidation Stress Induced by Asymmetric Dimethylarginine. *Int. J. Mol. Sci.* 2012; 13(6): 7521-7531.
- Molema G. Heterogeneity in endothelial responsiveness to cytokines, molecular causes, and pharmacological consequences. *Semin Thromb Hemost.* 2010; 36: 246–264.
- Moller DS, Lind P, Strunge B and Pedersen EB. Abnormal vasoactive hormones and 24-hour blood pressure in obstructive sleep apnea. *American Journal of Hypertension.* 2003; 16: 274–280.
- Monaghan-Benson E and Burrige K. The regulation of vascular endothelial growth factor-induced microvascular permeability requires Rac and reactive oxygen species. *Journal of Biological Chemistry.* 2009; 284 (38): 25602-25611.
- Moncada S: Nitric oxide in the vasculature: physiology and pathophysiology. *Ann N Y Acad Sci.* 1997; 811: 60–67.
- Moncada S, Higgs EA. The discovery of nitric oxide and its role in vascular biology. *Br J Pharmacol.* 2006; 147 (Suppl 1): S193– S201.
- Moore C, Tymvios C and Emerson M. Functional regulation of vascular and platelet activity during thrombosis by nitric oxide and endothelial nitric oxide synthase. *Thrombosis and Haemostasis.* 2010; 104 (2): 191-419.
- Moosmayer D, Dinkel A, Gerlach E, Hessabi B, Grell M, Pfizenmaier K and Scheurich P. Coexpression of the human TNF receptors tr60 and TR80 in insect cells-analysis of receptor complex-formation. *Lymphokine Cytokine Res.* 1994; 13: 295 - 301.
- Morgan MJ and Liu Z. Crosstalk of reactive oxygen species and NF- κ B signaling. *Cell research.* 2010; 21 (1): 103-115.
- Morrell NW, Adnot S, Archer SL, Dupuis J, Lloyd Jones P, MacLean MR, McMurtry IF *et al.* Cellular and molecular basis of pulmonary arterial hypertension. *Journal of the American College of Cardiology.* 2009; 54 (1s1): S20-S31.
- Mudau M. Endothelial dysfunction in cardiac microvascular endothelial cells: an investigation into cellular mechanisms and putative role of oleanolic acid in reversing endothelial dysfunction. *MSC thesis.* December 2010.

- Mudau M, Genis A, Lochner A, Strijdom H. Endothelial dysfunction: the early predictor of atherosclerosis. *Cardiovasc J Afr.* 2012; 23(4): 222-31.
- Muller WA. Review. Mechanisms of Transendothelial Migration of Leukocytes. *Circulation Research.* 2009; 105: 223-230.
- Murad F. Shattuck Lecture: Nitric oxide and cyclic GMP in cell signaling and drug development. *N Engl J Med.* 2006; 355:2003–2011.
- Murdoch CE, Alom-Ruiz SP, Wang M, Zhang M, Walker S, Yu B, Brewer A and Shah AM. Role of endothelial Nox2 NADPH oxidase in angiotensin II-induced hypertension and vasomotor dysfunction. *Basic Res Cardio.* 2011; 106:527–538.
- Muschel RJ, Bernhard EJ, Garza L, McKenna WG, Koch CJ. Induction of apoptosis at different oxygen tensions: evidence that oxygen radicals do not mediate apoptotic signaling. *Cancer Res.* 1995;55:995–998.
- Mustafa AK, Sikka G, Gazi SK, Steppan J, Jung SM, Bhunia AK, Barodka VM, Gazi KF, Barrow RK, Wang R, Amzel LM, Berkowitz DE and Snyder SH. Integrative Physiology. Hydrogen Sulfide as Endothelium-Derived Hyperpolarizing Factor Sulfhydrates Potassium Channels. *Circulation Research.* 2011; 109: 1259-1268.
- Muzaffar S, Shukla N, Angelini G, et al. Nitroaspirins and morpholinonydnonimine but not aspirin inhibit the formation of super-oxide and the expression of gp91phox induced by endotoxin and cytokines in pig pulmonary artery vascular smooth muscle cells and endothelial cells. *Circulation.* 2004; 110: 1140–1147.
- Nabi IR and Le PU. Caveolae/raft-dependent endocytosis. *JCB.* 2003; 161 (4): 673-677.
- Nacci C, Tarquinio M and Montagnani M. Molecular and clinical aspects of endothelial dysfunction in diabetes. *Internal and Emergency Medicine.* 2009; 4 (2): 107-116.
- Namdar M, Gebhard C, Studiger R, Shi Y, Mocharla P, Schmied C, Brugada P, Lüscher TF and Camici GG. Globotriaosylsphingosine accumulation and not alpha-galactosidase-a deficiency causes endothelial dysfunction in Fabry disease. *PLoS one.* 2012; 7 (4): e36373.
- Naruse K, Shimizu K, Muramatsu M, Toki Y, Miyazaki Y, Okumura K, Hashimoto H, Ito T. Long-term inhibition of NO synthesis promotes atherosclerosis in the hypercholesterolemic rabbit thoracic aorta. PGH2 does not contribute to impaired endothelium-dependent relaxation. *Arterioscler Thromb.* 1994; 14: 746–752.
- Nathan C. Neutrophils and immunity: challenges and opportunities. Review. *Nature Reviews Immunology.* 2006; 6: 173-182.
- Naudé PJW, den Boer JA, Luiten PGM and Eisel ULM. Tumor necrosis factor receptor cross-talk. *FEBS Journal.* 2011; 278 (6): 888-898.
- Navarro-Antolin J, Lopez-Munoz MJ, Klatt P, Soria J, Michel T, Lamas S. Formation of peroxynitrite in vascular endothelial cells exposed to cyclosporine A. *FASEB J.* 2001; 15: 1291-1293.

- Nazarewicz RR, Bikineyeva A and Dikalov SI. Rapid and Specific Measurements of Superoxide Using Fluorescence Spectroscopy. *Journal of biomolecular screening*. 2013; 18 (4): 498-503.
- Nediani C, Raimondi L, Borchi E and Cerbai E. Nitric oxide/reactive oxygen species generation and nitroso/redox imbalance in heart failure: from molecular mechanisms to therapeutic implications. *Antioxidants & redox signaling*. 2011; 14 (2): 289-331.
- Neill S, Bright J, Desikan R, Hancock J, Harrison J and Wilson I. Nitric oxide evolution and perception. *J. Exp. Bot.* 2008; 59 (1): 25-35.
- Nijs J, Meeus M, De Meirleir K. Chronic musculoskeletal pain in chronic fatigue syndrome: recent developments and therapeutic implications. *Man Ther.* 2006; 11 (3): 187-91.
- Nishida M, Carley WW, Gerritsen M, Ellingsen O, Kelly RA, Smith TW. Isolation and characterization of human and rat cardiac microvascular endothelial cells. *Am J Physiol Heart Circ Physiol*. 1993; 264: 639-652.
- Nishikimi T, Nakao K and Kangawa K. Adrenomedullin in Heart Failure: Molecular Mechanism and Therapeutic Implication. *Current Hypertension Reviews*. 2011; 7 (4): 273-283.
- Nishiyama M, Takahara Y, Masaki T, Nakajima N, Kimura S. Pharmacological heterogeneity of both endothelin ETA- and ETB-receptors in the human saphenous vein. *Jpn J Pharmacol*. 1995; 69: 391-398.
- Niwa Y, Nagata N, Oka M, Toyoshima T, Akiyoshi H, Wada T, Nakaya Y. Production of nitric oxide from endothelial cells by 31-amino-acid-length endothelin-1, a novel vasoconstrictive product by human chymase. *Life Sci*. 2000; 67: 1103-1109.
- Niwa K, Inanami O, Yamamori T, et al. Roles of protein kinases C delta in the accumulation of P53 and the induction of apoptosis in H₂O₂-treated bovine endothelial cells. *Free Radic Res*. 2002; 36: 1147-1153.
- Norberg ESO and Zhivotovsky B. Mitochondrial regulation of cell death: processing of apoptosis-inducing factor (AIF). *Biochemical and biophysical research communications*. 2010; 396 (1): 95-100.
- North AJ, Star RA, Brannon TS, Ujiie K, Wells LB, Lowenstein CJ, Snyder SH and Shaul PW. Nitric oxide synthase type I and type III gene expression are developmentally regulated in rat lung. *Am. J. Physiol*. 1994; 266: L635-L641.
- Nurden AT. Platelets, inflammation and tissue regeneration. *Thromb Haemost* 2011; 105 (Suppl 1): S13-S33.
- O'Donnell VB, Taylor KB, Parthasarathy S, et al. 15-Lipoxygenase catalytically consumes nitric oxide and impairs activation of guanylate cyclase. *J. Biol. Chem*. 1995; 274: 20083-20091.
- Obal D, Dai S, Keith FR, Dimova N, Kingery J, Zheng YT, Zweier J et al. Cardiomyocyte-restricted overexpression of extracellular superoxide dismutase increases nitric oxide bioavailability and reduces infarct size after ischemia/reperfusion. *Basic research in cardiology*. 2012; 107 (6): 1-14.

Ogawa T, Kimoto M, Watanabe H, Sasaoka K. Metabolism of NG NG-dimethylarginine and NG NG dimethylarginine in rats. *Arch Biochem Biophys.* 1987; 252: 526–537.

Ogawa T, Kimoto M and Sasaoka K. Purification and properties of a new enzyme, NG, NG-dimethylarginine dimethylaminohydrolase, from rat kidney. *J. Biol. Chem.* 1989; 264: 10205–10209.

Olechnowicz SWZ and Peet DJ. Homo sapiens endothelial PAS domain protein. *Homo.* 2010.

Olken NM and Marletta MA. NG-methyl-L-arginine functions as an alternate substrate and mechanism-based inhibitor of nitric oxide synthase. *Biochemistry.* 1993; 32: 9677–9685.

Olszewska-Pazdrak B, Hein TW, Olszewska P and Carney DH. Chronic hypoxia attenuates VEGF signaling and angiogenic responses by downregulation of KDR in human endothelial cells. *American Journal of Physiology - Cell Physiology.* 2009; 296: C1162-C1170.

Ortega AL, Mena S and Estrela JM. Oxidative and Nitrosative Stress in the Metastatic Microenvironment. *Cancers* 2010, 2(2), 274-304.

Østergaard L, Stankevicius E, Andersen MR, Eskildsen-Helmond Y, Ledet T, Mulvany MJ and Simonsen U. Diminished NO release in chronic hypoxic human endothelial cells. *American Journal of Physiology-Heart and Circulatory Physiology.* 2007; 293 (5): H2894-H2903.

Osto E, Cosentino F. The role of oxidative stress in endothelial dysfunction and vascular inflammation. In: Ignarro LJ (ed). *Nitric Oxide: Biology and Pathobiology.* 2nd edn. London: Academic Press 2010: 705–754.

Otrock, Zaher K., Jawad A. Makarem, and Ali I. Shamseddine. Vascular endothelial growth factor family of ligands and receptors: review. *Blood Cells, Molecules, and Diseases.* 2007; 38 (3): 258-268.

Oudega M. Molecular and cellular mechanisms underlying the role of blood vessels in spinal cord injury and repair. *Cell and Tissue Research.* 2012; 349 (1): 269 – 288.

Ouedraogo R, Gong Y, Berzins B, Wu X, Mahadev K, Hough K, Chan L, Goldstein BJ and Scalia R. Adiponectin deficiency increases leukocyte-endothelium interactions via upregulation of endothelial cell adhesion molecules in vivo. *Journal of Clinical Investigation.* 2007; 117 (7): 1718-1726.

Oyadomari S, Gotoh T, Aoyagi K, Araki E, Shichiri M and Mori M. Coinduction of endothelial nitric oxide synthase and arginine recycling enzymes in aorta of diabetic rats. *Nitric Oxide.* 2001; 5: 252–260.

Pablos JL, Santiago B, Tsay D, Singer MS, Palao G, Galindo M and Rosen SD. A HEV-restricted sulfotransferase is expressed in rheumatoid arthritis synovium and is induced by lymphotoxin-alpha/beta and TNF-alpha in cultured endothelial cells. *BMC Immunol.* 2005; 6: 6.

Pacher P, Beckman JS and Liaudet L. Nitric Oxide and Peroxynitrite in Health and Disease. *Physiol Rev.* 2007; 87(1): 315–424.

- Pae HO, Son Y, Kim NH, Jeong HJ, Chang KC and Chung HT. Role of heme oxygenase in preserving vascular bioactive NO. *Nitric Oxide*. 2010; 23 (4): 251-257.
- Pak O, Aldashev A, Welsh D and Peacock A. The effects of hypoxia on the cells of the pulmonary vasculature. *ERJ*. 2007; 30 (2): 364-372.
- Paleolog EM, Delasalle SA, Buurman WA and Feldmann M. Functional activities of receptors for tumor necrosis factor-alpha on human vascular endothelial cells. *Blood*. 1994; 84 (8): 2578-2590.
- Palm F, Onozato ML, Luo Z and Wilcox CS. Dimethylarginine dimethylaminohydrolase (DDAH): expression, regulation, and function in the cardiovascular and renal systems. *AJP – Heart*. 2007; 293 (6): H3227-H3245.
- Paniagua OA, Bryant MB, Panza JA. Role of endothelial nitric oxide in shear stress-induced vasodilation of human microvasculature: diminished activity in hypertensive and hypercholesterolemic patients. *Circulation*. 2001; 103: 1752–1758.
- Papandreou I, Cairns RA, Fontana L, Lim AL and Denko NC. HIF-1 mediates adaptation to hypoxia by actively downregulating mitochondrial oxygen consumption. *Cell Metab*. 2006; 3: 187–197.
- Paravicini TM and Touyz RM. Redox signaling in hypertension. *Cardiovascular Research*. 2006; 71: 247–258.
- Park Y, Capobianco S, Gao X, Falck JR, Dellsperger KC and Zhang C. Role of EDHF in Type 2 diabetes-induced endothelial dysfunction. *Am. J. Physiol. Heart Circ. Physiol*. 2008.
- Parmley LA, Elkins ND, Fini MA, Liu YE, Repine JE and Wright RM. α -4/ β -1 and α -L/ β -2 integrins mediate cytokine induced lung leukocyte-epithelial adhesion and injury. *British Journal of Pharmacology*. 2007; 152 (6): 915–929.
- Parton RG, Simons K. The multiple faces of caveolae. *Nat Rev Mol Cell Biol*. 2007; 8: 185–194.
- Parton RG and del Pozo MA. Review. Caveolae as plasma membrane sensors, protectors and organizers. *Nature Reviews Molecular Cell Biology*. 2013; 14: 98-112.
- Partridge J, Carlsen H, Enesa K, Chaudhury H, Zakkar M, Luong L, Kinderlerer A *et al*. Lamina shear stress acts as a switch to regulate divergent functions of NF- κ B in endothelial cells. *The FASEB Journal*. 2007; 21 (13): 3553-3561.
- Patel SD, Waltham M, Wadoodi A, Burnand KG and Smith A. The role of endothelial cells and their progenitors in intimal hyperplasia. *Ther Adv Cardiovasc Dis*. 2010; 4: 129.
- Pavlovic D, Hall AR, Kennington EJ, Aughton K, Boguslavskiy A, Fuller W, Despa S, Bers DM and Shattock MJ. Nitric oxide regulates cardiac intracellular Na⁺ and Ca²⁺ by modulating Na/K ATPase via PKC ϵ and phospholemman-dependent mechanism. *Journal of molecular and cellular cardiology*. 2013.
- Pearlstein DP, Ali MH, Mungai PT, Hynes KL, Gewertz BL and Schumacker PT. Role of Mitochondrial Oxidant Generation in Endothelial Cell Responses to Hypoxia. *Arteriosclerosis, Thrombosis, and Vascular Biology*. 2002; 22: 566-573.

- Pecchi E, Dallaporta M, Jean A, Thirion S and Troadec JD. Review: Prostaglandins and sickness behavior: Old story, new insights. *Physiology & Behavior*. 2009; 97: 279–292.
- Pennathur S and Heinecke JW. Oxidative stress and endothelial dysfunction in vascular disease. *Current diabetes reports*. 2007; 7 (4): 257-264.
- Pennica D, Lam VT, Mize NK, Weber RF, Lewis M, Fendly BM, Lipari mT and Goeddel DV. Biochemical-properties of the 75-kDa tumor-necrosis-factor receptor \pm characterization of ligand-binding, internalization, and receptor phosphorylation. *J. Biol. Chem*. 1992; 267: 21172 - 21178.
- Perrault R and Zahradka P. Molecular Defects in Cardiovascular Disease. *Vascular Dysfunction in Heart Disease*. 2011; Part 3, 283-303.
- Phillips SA, Olson EB, Morgan BJ and Lombard JH. Chronic intermittent hypoxia impairs endothelium-dependent dilation in rat cerebral and skeletal muscle resistance arteries. *American Journal of Physiology: Heart and Circulatory Physiology*. 2004; 286: H388–H393.
- Picchi A, Gao X, Belmadani S. et al. Tumor necrosis factor- α induces endothelial dysfunction in the prediabetic metabolic syndrome. *Circ. Res*. 2006; 99: 69–77.
- Pietrogrande MC, Marchetti N, Dondi F and Righetti PG. Spot overlapping in two-dimensional polyacrylamide gel electrophoresis separations: A statistical study of complex protein maps. *Electrophoresis*. 2002; 23 (2): 283-291.
- Pilz RB and Casteel DE. Regulation of gene expression by cyclic GMP. *Circ. Res*. 2003; 93: 1034–1046.
- Pinsky DJ, Naka Y, Liao H, Oz MZ, Wagner DD, Mayadas TN, Johnson RC *et al*. Hypoxia-induced exocytosis of endothelial cell Weibel-Palade bodies. A mechanism for rapid neutrophil recruitment after cardiac preservation. *Journal of Clinical Investigation*. 1996; 97 (2): 493.
- Piper HM, Spahr R, Mertens S, Krutzfeldt A, Watanabe H. Microvascular endothelial cells from heart. In: Piper HM (editor). Cell culture techniques in heart vessel and research. *Springer-Verlag*. 1990: 158-173.
- Ploppa A, Schmidt V, Hientz A, Reutershan J, Haeberle H and Nohé B. Mechanisms of leukocyte distribution during sepsis: an experimental study on the interdependence of cell activation, shear stress and endothelial injury. *Critical Care*. 2010; 14 (6): R201.
- Pober JS, Min W. Endothelial cell dysfunction, injury and death. *Handb Exp Pharmacol*. 2006: 135–156.
- Polotsky VY, Savransky V, Bevans-Fonti S, Reinke C, Li J, Grigoryev DN, Shimonda LA. Intermittant and sustained hypoxia induce a similar gene expression profile in human aortic endothelial cells. *Physiol. Genomics*. 2010; 41: 306-314.
- Polunovsky VA, Wendt CH, Ingbar DH, et al. Induction of endothelial cell apoptosis by TNF alpha: modulation by inhibitors of protein synthesis. *Exp Cell Res*. 1994; 214(2): 584-94.

- Porasuphatana S. Formation of the reactive iron-oxo intermediate during the biosynthesis of nitric oxide by neuronal nitric oxide synthase and its possible mechanism in the generation of secondary free radicals. 2001.
- Porteu F and Hieblot C. Tumor-necrosis-factor induces a selective shedding of its p75-receptor from human neutrophils. *J. Biol. Chem.* 1994; 269: 2834 - 2840.
- Potenza MA, Gagliardi S, Nacci C, et al. Endothelial dysfunction in diabetes: From mechanisms to therapeutic targets. *Curr Med Chem.* 2009; 16: 94–112.
- Pottiez G, Deracinois B, Duban-Deweere S, Cecchelli R, Fenart L, Karamanos Y and Flahaut C. A large-scale electrophoresis- and chromatography-based determination of gene expression profiles in bovine brain capillary endothelial cells after the re-induction of blood-brain barrier properties. *Proteome Science.* 2010; 8: 57.
- Pou S, Keaton L, Surichamorn W, Rosen GM. Mechanism of superoxide generation by neuronal nitric oxide synthase. *J Biol Chem.* 1999; 274: 9573–9580.
- Prabhakar NR and Semenza GL. Adaptive and maladaptive cardiorespiratory responses to continuous and intermittent hypoxia mediated by hypoxia-inducible factors 1 and 2. *Physiological Reviews.* 2012; 92 (3): 967-1003.
- Presley T, Vedam K, Velayutham M, Zweier JL, Ilangovan G. Activation of Hsp90-eNOS and increased NO generation attenuate respiration of hypoxia-treated endothelial cells. *Am. J. Physiol. Cell. Physiol.* 2008; 295: C1281-C1291.
- Pretorius S, Stewart S and Sliwa K. Lessons from the Heart of Soweto Study and future directions. *SAHeart.* 2011; 8:104-113.
- Prieto CP, Krause BJ, Quezada Q, Martin RS, Sobrevia L and Casanello P. Hypoxia-reduced nitric oxide synthase activity is partially explained by higher arginase-2 activity and cellular redistribution in human umbilical vein endothelium. *Placenta.* 2011; 32 (12): 932-940.
- Pritchard KA, Groszek L, Smalley DM et al. Native lowdensity lipoprotein increases endothelial cell nitric oxide synthase generation of superoxide anion. *Circ Res.* 1995; 77: 510–18.
- Puranik R, Celermajer DS. Smoking and endothelial function. *Progr Cardiovasc Dis* 2003; 45: 443–458.
- Qin H, Huang CH, Mao L, Xia HY, Kalyanaraman B, Shao J, Shan GQ and Zhu BZ. Molecular Mechanism of Metal-independent Decomposition of Lipid Hydroperoxide 13-HPODE by Halogenated Quinoid Carcinogens. *Free Radical Biology and Medicine.* 2013.
- Qingdong K and Costa M. Hypoxia-inducible factor-1 (HIF-1). *Molecular pharmacology.* 2006; 70 (5): 1469-1480.
- Quintero M, Colombo SL, Godfrey A and Moncada S. Mitochondria as signaling organelles in the vascular endothelium. *PNAS.* 2006; 103 (14): 5379-5384.
- Quyyumi AA, Dakak N, Andrews NP, et al. Contribution of nitric oxide to metabolic coronary vasodilation in the human heart. *Circulation.* 1995; 92(3): 320-6.

- Rabilloud T. Mitochondrial proteomics : analysis of a whole mitochondrial extract with two-dimensional electrophoresis. *Methods Mol Biol.* 2008; 432: 83-100.
- Radomski MW, Vallance P, Whitley G, Foxwell N and Moncada S. Platelet adhesion to human vascular endothelium is modulated by constitutive and cytokine induced nitric oxide. *Journal Cardiovasc Res.* 1993; 27(7): 1380-2.
- Rafikov R, Fonseca FV, Kumar S, Pardo D, Darragh C, Elms S, Fulton D and Black SM. eNOS activation and NO function: Structural motifs responsible for the posttranslational control of endothelial nitric oxide synthase activity. *J Endocrinol.* 2011; 210(3): 271–284.
- Rajagopalan S, Kurz S, Münzel T, et al. Angiotensin II mediated hypertension in the rat increases vascular superoxide production via membrane NADH/NADPH oxidase activation: contribution to alterations of vasomotor tone. *J Clin Invest.* 1996; 97: 1916–1923.
- Raman CS, Li H, Martasek P, Kral V, Masters BS and Poulos TL. Crystal structure of constitutive endothelial nitric oxide synthase: a paradigm for pterin function involving a novel metal center. *Cell.* 1998; 95: 939–950.
- Ramasamy S, Parthasarathy S and Harrison DG. Regulation of endothelial nitric oxide synthase gene expression by oxidized linoleic acid. *Journal of Lipid Research.* 1998; 39: 268–276.
- Raphael J, Gozal Y, Navot N and Zuo Z. Hyperglycemia inhibits anesthetic-induced postconditioning in the rabbit heart via modulation of phosphatidylinositol-3-kinase/Akt and endothelial nitric oxide synthase signaling. *Journal of cardiovascular pharmacology.* 2010; 55 (4): 348-357.
- Raspaglio G, Filippetti F, Prislei S, Penci R, De Maria I, Cicchillitti L, Mozzetti S, Scambia G, and Ferlini C. Hypoxia induces class III beta-tubulin gene expression by HIF-1alpha binding to its 3' flanking region. *Gene.* 2008; 409 (1-2): 100-108.
- Rastaldo R, Pagliaro P, Cappello S, Penna C, Mancardi D, Westerhof N and Losano G. Nitric oxide and cardiac function. *Life sciences.* 2007; 81; (10): 779-793.
- Rathore R, Zheng YM, Niu CF, Liu QH, Korde A, Ho YS and Wang YX. Hypoxia activates NADPH oxidase to increase [ROS] i and [Ca²⁺] i through mitochondrial ROS–PKCε signaling axis in pulmonary artery smooth muscle cells. *Free radical biology & medicine.* 2008; 45 (9): 1223.
- Rautureau Y and Schiffrin EI. Endothelin in hypertension: an update. *Current opinion in nephrology and hypertension.* 2012; 21 (2): 128-136.
- Ray, Julie Basu. Oxygen regulation of vascular smooth muscle cell proliferation and survival. *PhD diss., University of Toronto, 2009.*
- Rebuffat P, Malendowicz LK, Neri G, Nussdorfer GG. Endothelin-11–31 acts as a selective ETA-receptor agonist in the rat adrenal cortex. *Histol Histopathol.* 2001; 16: 535–540.
- Reed JC. Mechanisms of Apoptosis. *Am J Pathol.* 2000; 157(5): 1415–1430.
- Ren S, Shatadal S, Shen GX. Protein kinase C-beta mediates lipoprotein-induced generation of PAI-1 from vascular endothelial cells. *Am J Physiol.* 2000; 278: E656.

- Renault F, Formstecher E, Callebaut I, Junier MP, Chneiweiss H. The multifunctional protein PEA-15 is involved in the control of apoptosis and cell cycle in astrocytes. *Biochemical Pharmacology*. 2003; 66 (8): 1581–1588.
- Reuter S, Gupta SC, Chaturvedi MM and Aggarwal BB. Oxidative stress, inflammation, and cancer: How are they linked? Review Article. *Free Radical Biology and Medicine*. 2010; 49 (11): 1603–1616.
- Revil T, Pelletier J, Toutant J, Cloutier A, Chabot B. Heterogeneous Nuclear Ribonucleoprotein K Represses the Production of Pro-apoptotic Bcl-xS Splice Isoform. *J Biol Chem*. 2009; 284 (32): 21458–21467.
- Rey S and Semenza GL. Hypoxia-inducible factor-1-dependent mechanisms of vascularization and vascular remodelling. *Cardiovascular research*. 2010; 86 (2): 236-242.
- Rhee SG, Chang TS, Jeong W and Kang D. Methods for detection and measurement of hydrogen peroxide inside and outside of cells. *Molecules and cells*. 2010; 29 (6): 539-549.
- Richardson MR, Lai X, Witzmann FA and Yoder MC. Venous and arterial endothelial proteomics: mining for markers and mechanisms of endothelial diversity. *Expert Rev. Proteomics*. 2010; 7 (6): 823-831.
- Rimbach G, Valacchi G, Canali R and Virgili F. Macrophages stimulated with IFN- γ activate NF- κ B and induce MCP-1 gene expression in primary human endothelial cells. *Mol. Cell. Biol. Res. Commun*. 2000; 3: 238–242.
- Rizzo V, Morton C, DePaola N, Schnitzer JE and Davies PF. Recruitment of endothelial caveolae into mechanotransduction pathways by flow conditioning in vitro. *Am J Physiol Heart Circ Physiol*. 2003; 285: H1720–H1729.
- Robertson KE, McDonald RA, Oldroyd KG, Nicklin SA and Baker AH. Prevention of coronary in-stent restenosis and vein graft failure: Does vascular gene therapy have a role?. *Pharmacology & therapeutics*. 2012.
- Robey RB and Hay N. Is Akt the “Warburg kinase”?—Akt-energy metabolism interactions and oncogenesis. *Semin Cancer Biol*. 2009; 19: 25–31.
- Rocha VZ and Libby P. Obesity, inflammation, and atherosclerosis. *Nat. Rev. Cardiol*. 2009; 6, 399–409.
- Rodriguez JM, Glozak MA, Ma Y and Cress WD. Bok, Bcl-2-related ovarian killer, is cell cycle-regulated and sensitizes to stress-induced apoptosis. *Journal of Biological Chemistry*. 2006; 281 (32): 22729-22735.
- Rodríguez-Juárez E and Aguirre SC. Relative sensitivity of soluble guanylate cyclase and mitochondrial respiration to endogenous nitric oxide at physiological oxygen concentration. *Biochem. J*. 2007; 405: 223–231.
- Rodriguez-Rodriguez R, Stankevicius E, Herrera MD, Ostergaard L, Andersen MR, Ruiz-Gutierrez V, Simonsen U. Oleic acid induces relaxation and calcium-independent release of endothelium-derived nitric oxide. *Br J Pharmacol*. 2008; 155: 535-546.

- Roe MR and Griffin TJ. Gel-free mass spectrometry-based high throughput proteomics: Tools for studying biological response of proteins and proteomes. *Proteomics*. 2006; 6 (17): 4678-4687.
- Rossi GP, Andreis PG, Colonna S, Albertin G, Aragona F, Belloni AS and Nussdorfer GG. Endothelin-1[1–31]: A Novel Autocrine-Paracrine Regulator of Human Adrenal Cortex Secretion and Growth. *The Journal of Clinical Endocrinology & Metabolism*. 2002; 87(1): 322–328.
- Ruef J, Moser M, Kübler W and Bode C. Induction of endothelin-1 expression by oxidative stress in vascular smooth muscle cells. *Cardiovascular Pathology*. 2001; 10 (6): 311-315.
- Rus A, Peinado A, Castro L and Del Moral L. Lung eNOS and iNOS are Reoxygenation Time-Dependent Upregulated After Acute Hypoxia. *The Anatomical Record*. 2010; 293 (6): 1089–1098.
- Russwurm M and Koesling D. NO activation of guanylyl cyclase. *EMBO J*. 2004; 23: 4443–4450.
- Sack MN. Tumor necrosis factor- α in cardiovascular biology and the potential role for anti-tumor necrosis factor- α therapy in heart disease. *Pharmacology & Therapeutics*. 2002; 94 (1–2): 123–135.
- Saeed SA, Waqar MA, Waqar M, Kazmi SF, Basit A and Ahmad N. Nitric Oxide Signalling and Its Role in the Activation of Human Blood Platelets. *Chemical Society of Pakistan*. 2007; 29 (4).
- Saito S, Hirata Y, Emori Imai T Y, Marumo F. Angiotensin II activates endothelial constitutive nitric oxide synthase via AT1 receptors. *Hypertens Res*. 1999; 19: 201–206.
- Salt IP, Morrow VA, Brandie FM, Connell JMC and Petrie JR. High glucose inhibits insulin-stimulated nitric oxide production without reducing endothelial nitric-oxide synthase Ser1177 phosphorylation in human aortic endothelial cells. *Journal of Biological Chemistry*. 2003; 278 (21): 18791-18797.
- Sano M, Minamino T, Toko H, Miyauchi H, Orimo M, Qin Y, Akazawa H et al. p53-induced inhibition of Hif-1 causes cardiac dysfunction during pressure overload. *Nature*. 2007; 446 (7134): 444-448.
- Santos CXC, Anilkumar N, Zhang M, Brewer AC, Shah AM. Redox signalling in cardiac myocytes. *Free Radic. Biol. Med*. 2011; 50 (7): 777-793.
- Sasaki N, Sato T, Ohler A, O'Rourke B, Marban E. Activation of mitochondrial ATPdependent potassium channels by nitric oxide. *Circulation* 2000; 101(4): 439-45.
- Satoh M, Nakamura M, Satoh H, Saitoh H, Segawa I and Hiramori K. Expression of tumor necrosis factor-alpha-converting enzyme and tumor necrosis factor-alpha in human myocarditis. *J Am Coll Cardiol*. 2000; 36: 1288–1294.
- Saussede-Aim J and Dumontet C. Regulation of tubulin expression: Multiple overlapping mechanisms. *Int. J. Med. Med. Sci*. 2009; 1 (8): 290-296.
- Sawamura T, Kume N, Aoyama T, Moriwaki H, Hoshikawa H, Ariba Y, et al. An endothelial receptor for oxidized low-density lipoprotein. *Nature*. 1997; 886: 73–7.

- Sawamura T. LOX-1, a lectin-like oxidized LDL receptor identified from endothelial cells, in endothelial dysfunction. *Int Congr.* 2004; 1262: 531–534.
- Scalera F. Intracellular glutathione and lipid peroxide availability and the secretion of vasoactive substances by human umbilical vein endothelial cells after incubation with TNF- α . *Eur J Clin Invest.* 2003; 33: 176–182.
- Schafer A and Bauersachs J. Endothelial Dysfunction, Impaired Endogenous Platelet Inhibition and Platelet Activation in Diabetes and Atherosclerosis. *Current Vascular Pharmacology.* 2008; 6 (1): 52-60(9).
- Scheller K, Dally I, Hartmann N, Münst B, Braspenning J and Walles H. Upcyte[®] Microvascular endothelial cells repopulate decellularized scaffold. *Tissue Engineering Part C: Methods.* 2012; 19 (1): 57-67.
- Schiffrin EL. Vascular endothelin in hypertension. *Vascular Pharmacology.* 2005; 43 (1): 19–29.
- Schildknecht and Ullrich V. Review. Highlight on Peroxynitrite and Reactive Nitrogen Species. Peroxynitrite as regulator of vascular prostanoid synthesis. *Archives of Biochemistry and Biophysics.* 2009; 484 (2): 183–189.
- Schilling K, Opitz N, Wiesenthal A, Oess S, Tikkanen R, Muller-Esterl W and Icking A. Translocation of endothelial nitric-oxide synthase involves a ternary complex with caveolin-1 and NOSTRIN. *Mol. Biol. Cell.* 2006; 17: 3870–3880.
- Schmidt K, Klatt P, Graier WF, Kostner GM and Kukovetz WR. High-density lipoprotein antagonizes the inhibitory effects of oxidized low-density lipoprotein and lysolecithin on soluble guanylyl cyclase. *Biochem. Biophys. Res. Commun.* 1992; 82: 302–308.
- Schmidt TS and Alp NJ. Mechanisms for the role of tetrahydrobiopterin in endothelial function and vascular disease. *Clinical Science.* 2007. 113: p. 47-63.
- Schmitz EJ, Potteck H, Schüppel M, Manggau M, Wahyudin E and Kleuser B. Sphingosine 1-phosphate protects primary human keratinocytes from apoptosis via nitric oxide formation through the receptor subtype S1P3. *Molecular and Cellular Biochemistry.* 2012; 371 (1-2): 165-176.
- Schnabel R, Blankenberg S, Lubos E, Lackner KJ, Rupprecht HJ, Espinola-Klein C, Jachmann N, Post F, Peetz D, Bickel C, Cambien F, Tiret L, Munzel T. Asymmetric dimethylarginine and the risk of cardiovascular events and death in patients with coronary artery disease: results from the *AtheroGene Study.* *Circ Res.* 2005; 97: e53–e59.
- Schricker K, Potzl B, Hamann M and Kurtz A. Coordinate changes of renin and brain-type nitric-oxide-synthase (b-NOS) mRNA levels in rat kidneys. *Pfluegers Arch.* 1996; 432: 394–400.
- Schulz E, Schuhmacher S and Münzel T. When Metabolism Rules Perfusion. AMPK-Mediated Endothelial Nitric Oxide Synthase Activation. *Circulation Research.* 2009; 104: 422-424.
- Seidel M, Billert H and Kurpisz M. Regulation of eNOS expression in HCAEC cell line treated with opioids and proinflammatory cytokines. *Kardiol. Pol.* 2006; 64: 153–158.

Seko Y, Takahashi N, Yagita H, Okumura K and Yazaki Y. Expression of cytokine mRNAs in murine hearts with acute myocarditis caused by coxsackievirus b3. *J Pathol.* 1997; 183: 105–108.

Semenza GL, Jiang BH, Leung SW, Passantino R, Concordet JP, Maire P, Giallongo A. Hypoxia response elements in the aldolase A, enolase 1, and lactate dehydrogenase A gene promoters contain essential binding sites for hypoxia-inducible factor 1. *J. Biol. Chem.* 1996; 271 (51): 32529-32537.

Semenza GL. HIF-1: mediator of physiological and pathophysiological responses to hypoxia. *Journal of Applied Physiology.* 2000; 88 (4): 1474-1480.

Semenza GL. Hypoxia-inducible factor 1: Regulator of mitochondrial metabolism and mediator of ischemic preconditioning. *Biochim. Biophys. Acta.* 2011; 1813 (7): 1263-1268.

Serrander L, Cartier L, Bedard K, Banfi B, Lardy B, Plastre O, Sienkiewicz A, Forro L, Schlegel W, Krause KH. NOX4 activity is determined by mRNA levels and reveals a unique pattern of ROS generation. *Biochem J.* 2007; 406(1): 105–114.

Serviddio G, Romano AD, Cassano T, Bellanti F, Altomare E and Vendemiale G. Principles and therapeutic relevance for targeting mitochondria in aging and neurodegenerative diseases. *Current pharmaceutical design.* 2011; 17 (20): 2036-2055.

Shah AM, MacCarthy PA. Paracrine and autocrine effects of nitric oxide on myocardial function. *Pharmacol Ther* 2000; 86: 49–86.

Shao D, Park JES and Wort SJ. The role of endothelin-1 in the pathogenesis of pulmonary arterial hypertension. *Pharmacological Research.* 2011; 63 (6): 504-511.

Shen HM and Pervaiz S. TNF receptor superfamily-induced cell death: redox-dependent execution. *The FASEB Journal.* 2006; 20 (10): 1589-1598.

Shen Y, Guo W, Wang Z, Zhang Y, Zhong L and Zhu Y. Protective Effects of Hydrogen Sulfide in Hypoxic Human Umbilical Vein Endothelial Cells: A Possible Mitochondria-Dependent Pathway. *Int. J. Mol. Sci.* 2013; 14: 13093-13108.

Shibuya N, Mikami Y, Kimura Y, Nagahara N, Kimura H. Vascular endothelium expresses 3-mercaptopyruvate sulfurtransferase and produces hydrogen sulfide. *J Biochem.* 2009; 146: 623–626.

Shimizu Y, Sakai M, Umemura Y and Ueda H. Immunohistochemical localization of nitric oxide synthase in normal human skin: expression of endothelial-type and inducible-type nitric oxide synthase in keratinocytes. *J. Dermatol.* 1997; 24: 80–87.

Shimoda LA and Polak J. Hypoxia. 4. Hypoxia and ion channel function. *American Journal of Physiology-Cell Physiology.* 2011; 300 (5): C951-C967.

Shimokawa H and Tsutsui M. Nitric oxide synthases in the pathogenesis of cardiovascular disease. *Pflügers Archiv-European Journal of Physiology.* 2010; 459 (6): 959-967.

Shostak HDC, Lemasters JJ, Edgell CJ, Herman B. Role of ICE-like proteases in endothelial cell hypoxic and reperfusion injury. *Biochem Biophys Res Commun.* 1997; 231: 844–847.

- Siamwala JH, Majumder S, Tamilarasan KP, Muley A, Reddy SH, Kolluru GK, Sinha S and Chatterjee S. Simulated microgravity promotes nitric oxide-supported angiogenesis via the iNOS–cGMP–PKG pathway in macrovascular endothelial cells. *FEBS letters*. 2010; 584 (15): 3415-3423.
- Silvagno F, Xia H and Bredt DS. Neuronal nitric oxide synthase-m, an alternatively spliced isoform expressed in differentiated skeletal muscle. *J. Biol. Chem.* 1996; 271: 11204–11208.
- Simionescu M, Simionescu N, Palade GE. Morphometric data on the endothelium of blood capillaries. *J Cell Biol.* 1974; 60: 128–152.
- Simionescu M. Implications of Early Structural-Functional Changes in the Endothelium for Vascular Disease. *Arteriosclerosis, Thrombosis, and Vascular Biology*. 2007; 27: 266-274.
- Simon A, Plies L, Habermeier A, Martine U, Reining M and Closs EI. Role of neutral amino acid transport and protein breakdown for substrate supply of nitric oxide synthase in human endothelial cells. *Circ. Res.* 2003; 93: 813–820.
- Sirker A, Zhang M and Shah AM. NADPH oxidases in cardiovascular disease: insights from in vivo models and clinical studies. *Basic Res Cardiol.* 2011; 106: 735–747.
- Sitia S, Tomasoni L, Atzeni F, Ambrosio G, Cordiano C, Catapano A, Tramontana S, Perticone SF, Naccarato P, Camici P, Picano E, Cortigiani L, Bevilacqua M, Milazzo L, Cusi D, Barlassina C, Sarzi-Puttini C and Turiel M. Review. From endothelial dysfunction to atherosclerosis. *Autoimmunity Reviews*. 2010; 9 (12): 830–834.
- Sliwa K, *et al.* Spectrum of heart disease and risk factors in a black urban population in South Africa (the Heart of Soweto Study): a cohort study. *Lancet* 2008;371:915-22.
- Slowik MR, De Luca LG, Fiers W and Pober JS. Tumor necrosis factor activates human endothelial cells through the p55 tumor necrosis factor receptor but the p75 receptor contributes to activation at low tumor necrosis factor concentration. *The American journal of pathology*. 1993; 143 (6): 1724.
- Smith CI, Birdsey GM, Anthony S, Arrigoni FI, Leiper JM, Vallance P. Dimethylarginine dimethylaminohydrolase activity modulates ADMA levels, VEGF expression, and cell phenotype. *Biochem Biophys Res Commun*. 2003; 308: 984–989.
- Smith DD, Tan X, Tawfik O, Milne G, Stechschulte DJ and Dileepan KN. Increased aortic atherosclerotic plaque development in female apolipoprotein E-null mice is associated with elevated thromboxane A₂ and increased prostacyclin production. *J Physiol and Pharmacol*. 2010; 61 (3): 309-316.
- Smolka M, Zhou H and Aebersold R. Quantitative protein profiling using two-dimensional gel electrophoresis, isotope-coded affinity tag labeling, and mass spectrometry. *Molecular & Cellular Proteomics*. 2002; 1 (1): 19-29.
- So T, Soroosh P, Eun SY, Altman A and Croft M. Antigen-independent signalosome of CARMA1, PKC θ , and TNF receptor-associated factor 2 (TRAF2) determines NF- κ B signaling in T cells. *Proceedings of the National Academy of Sciences*. 2011; 108, (7): 2903-2908.

- Sobrevia L A, Nadal D, Yudilevich L and Mann GE. Activation of L-arginine transport (system y+) and nitric oxide synthase by elevated glucose and insulin in human endothelial cells. *The Journal of physiology*. 1996; 490 (3): 775-781.
- Södergren A, Karp K, Boman K, Eriksson C, Lundström E, Smedby T, Söderlund L, Rantapää-Dahlqvist S, Wällberg-Jonsson S. Atherosclerosis in early rheumatoid arthritis: very early endothelial activation and rapid progression of intima media thickness. *Arthritis Research & Therapy*. 2010, 12:R158.
- Solaini G, Baracca A, Lenaz G and Sgarbi G. Hypoxia and mitochondrial metabolism. *Biochim. Biophys. Acta*. 2010; 1797: 1171-1177.
- Soldatos G, Cooper ME, Jandeleit-Dahm KAM. Advanced-glycation end products in insulin-resistant states. *Curr Hypertens Rep*. 2005; 7: 96–102.
- Son D, Kojima I, Inagi R, Matsumoto M, Fujita T, Nangaku, M. Chronic hypoxia aggravates renal injury via suppression of Cu/Zn-SOD: A proteomic analysis. *Am. J. Renal Physiol*. 2008; 294: F62-F72.
- Song W, Lu X, eng Q. Tumor necrosis factor- α induces apoptosis via inducible nitric oxide synthase in neonatal mouse cardiomyocytes. *Cardiovasc Res* 2000; 45: 595 – 602.
- Sorescu D and Griendling KK. Reactive oxygen species, mitochondria, and NAD(P)H oxidases in the development and progression of heart failure. *Congest. Heart Failure*. 2002; 8: 132–140.
- Sotgia F, Martinez-Outschoorn UE, Howell A, Pestell RG, Pavlides S and Lisanti MP. Caveolin-1 and cancer metabolism in the tumor microenvironment: markers, models, and mechanisms. *Annual Review of Pathology: Mechanisms of Disease*. 2012; 7: 423-467.
- Sowa G. Caveolae, Caveolins, Cavins, and Endothelial Cell Function: New Insights. *Front Physiol*. 2011; 2: 120.
- Spahr R, Krutzfeldt A, Mertens S, Siegmund B and Piper HM. Fatty acids are not an important fuel for coronary microvascular endothelial cells. *Mol. Cell. Biochem*. 1989; 88: 59–64.
- Spiecker M, Darius H, Kaboth K, et al. Differential regulation of endothelial cell adhesion molecule expression by nitric oxide donors and antioxidants. *J Leuko Biol*. 1998; 63: 732–739.
- Spindler V, Schlegel N, Waschke J. Role of GTPases in control of microvascular permeability. *Cardiovascular Research*. 2010; 87: 243-253.
- Sprague AH and Khalil RA. Inflammatory Cytokines in Vascular Dysfunction and Vascular Disease. *Biochem Pharmacol*. 2009; 15; 78(6): 539–552.
- Sprong H, van der Sluijs P and van Meer G. How proteins move lipids and lipids move proteins. *Nature Reviews. Molecular Cell Biology*. 2001; 2 (7): 504-513.
- Stan RV, Kubitzka M, Palade GE. PV-1 is a component of the fenestral and stomatal diaphragms in fenestrated endothelia. *Proc Natl Acad Sci USA*. 1999; 96: 13203–13207.

- Stan RV, Tkachenko E, Niesman IR. PV1 is a key structural component for the formation of the stomatal and fenestral diaphragms. *Mol Biol Cell*. 2004; 15: 3615–3630.
- Stan RV. Structure of caveolae. *Biochim Biophys Acta*. 2005; 1746: 334–348.
- Stan RV. Endothelial stomatal and fenestral diaphragms in normal vessels and angiogenesis. *J Cell Mol Med*. 2007; 11: 621–643.
- Stanton RC. Glucose-6-phosphate dehydrogenase, NADPH, and cell survival. *IUBMB Life* 2012; 64 (5): 362-369.
- Stefanec T. Endothelial Apoptosis: Could It Have a Role in the Pathogenesis and Treatment of Disease? *Chest* 2000; 117: 841-854.
- Stempien-Otero A, Karsan A, Cornejo CJ, Xiang H, Eunson T, Morrison RS, Kay M, Winn R, Harlan, J. Mechanisms of hypoxia-induced endothelial cell death. Role of p53 in apoptosis. *J. Biol. Chem*. 1999; 274 (12): 8039-45.
- Stenmark, Kurt R., et al. Hypoxia, leukocytes, and the pulmonary circulation. *Journal of Applied Physiology*. 2005; 98.2: 715-721.
- Stenmark KR, Fagan KA and Frid MG. Reviews. Hypoxia-Induced Pulmonary Vascular Remodeling Cellular and Molecular Mechanisms. *Circulation Research*. 2006; 99: 675-691.
- Stenvinkel P. Endothelial dysfunction and inflammation – is there a link? *Nephrol Dial Transplant*. 2001; 16: 1968–1971.
- Stephen SL, Freestone K, Dunn S, Twigg MW, Homer-Vanniasinkam S, Walker JH, Wheatcroft SB and Ponnambalam S. Review Article. Scavenger Receptors and Their Potential as Therapeutic Targets in the Treatment of Cardiovascular Disease. *International Journal of Hypertension*. 2010. 21 pages.
- Strijdom, H., Muller, C., and Lochner, A., Direct intracellular nitric oxide detection in isolated adult cardiomyocytes: flow cytometric analysis using the fluorescent probe, diaminofluorescein. *J. Mol. Cell Cardiol*. 2004; 37 (4): 897–902.
- Strijdom H, Jacobs S, Suzel H, Page C, Lochner A. Nitric oxide production is higher in rat cardiac microvessel endothelial cells than ventricular cardiomyocytes in baseline and hypoxic conditions: a comparative study. *FASEB J* 2006;20:14-316.
- Strijdom H, Chamane N, Lochner A. Nitric oxide in the cardiovascular system: a simple molecule with complex actions. *Cardiovasc J Afr*. 2009a; 20: 303-310.
- Strijdom H, Friedrich SO, Hattingh S, Chamane N and Lochner A. Hypoxia-induced regulation of nitric oxide synthase in cardiac endothelial cells and myocytes and the role of the PI3-K/PKB pathway. *Molecular and Cellular Biochemistry*. 2009b; 321 (1-2): 23–35.
- Strijdom H, Lochner A. Cardiac endothelium: More than just a barrier! *SA Heart* 2009c; 6(3):174-185.

- Stroka KM, Levitan I and Aranda-Espinoza H. Ox-LDL and substrate stiffness promote neutrophil transmigration by enhanced endothelial cell contractility and ICAM-1. *Journal of Biomechanics*. 2012; 45: 1828–1834.
- Stumpe T, Decking UK, Schrader J. Nitric oxide reduces energy supply by direct action on the respiratory chain in isolated cardiomyocytes. *Am J Physiol Heart Circ Physiol* 2001; 280(5): H2350-6.
- Sudjarwo SA, Hori M, Tanaka T, Matsuda Y, Okada T, Karaki H. Subtypes of endothelin ETA and ETB receptors mediating venous smooth muscle contraction. *Biochem Biophys Res Commun*. 1994; 200: 627–633.
- Suh Y, Arnold RS, Lassègue B, et al. Cell transformation by the superoxide-generating oxidase mox1. *Nature*. 1999; 401: 79–82.
- Sumpio BE, Riley JT and Dardik A. Cells in focus: endothelial cell. *The International Journal of Biochemistry & Cell Biology*. 2002; 34 (12): 1508–1512.
- Sydow K and Munzel T. ADMA and oxidative stress. *Atheroscler. Suppl*. 2003; 4: 41–51.
- Szabo C. Multiple pathways of peroxynitrite cytotoxicity. *Toxicol. Lett*. 2003; 140–141: 105–112.
- Szmitko PE, Wang C-H, Weisel RD, et al. New markers of inflammation and endothelial cell activation, part 1. *Circulation* 2003; 108: 1917–1923.
- Szotowska B, Antoniak S, Goldin-Lang P, Tran QV, Pels K, Rosenthal P, Bogdanov VY, Borchert HH, Schultheiss HP and Rauch. Antioxidative treatment inhibits the release of thrombogenic tissue factor from irradiation- and cytokine-induced endothelial cells. *Cardiovasc Res*. 2007; 73 (4): 806-812.
- Tabata T, Mine S, Kawahara C, Okada Y and Tanaka Y. Monocyte chemoattractant protein-1 induced scavenger receptor expression and monocyte differentiation into foam cell. *Biochem Biophys Res Commun*. 2003; 305: 380–385.
- Tada H, Thompson CI, Recchia FA, Loke KE, Ochoa M, Smith CJ, Shesely EG, Kaley G, Hintze TH. Myocardial glucose uptake is regulated by nitric oxide via endothelial nitric oxide synthase in Langendorff mouse heart. *Circ Res* 2000; 86(3): 270-4.
- Taddei S, Ghiadoni L, Virdis A, Versari D, Salvetti A. Mechanisms of endothelial dysfunction: clinical significance and preventive non-pharmacological therapeutic strategies. *Curr Pharm Des* 2003; 9: 2385–2402.
- Taguchi S, Oimuma T and Yamada T. A comparative study of cultured smooth muscle cell proliferation and injury, utilizing glycated low density lipoproteins with slight oxidation, antu-oxidation, or extensive oxidation. *Atheroscler Thromb*. 2000; 7: 132–137.
- Tahawi Z, Orolinova N, Joshua IG, Bader M and Fletcher EC. Altered vascular reactivity in arterioles of chronic intermittent hypoxic rats. *Journal of Applied Physiology*. 2001; 90: 2007–2013.

- Taipale M, Jarosz DF and Lindquist S. Review. HSP90 at the hub of protein homeostasis: emerging mechanistic insights. *Nature Reviews Molecular Cell Biology*. 2010; 11: 515–528.
- Tajsic T and Morrell NW. Cellular and Molecular Mechanisms of Pulmonary Vascular Smooth Muscle Cell Proliferation. *Textbook of Pulmonary Vascular Disease*. 2011, Part 1, 323-334.
- Takac I, Schroder K, Zhang L, Lardy B, Anilkumar N, Lambeth JD, Shah AM, Morel F, Brandes RP. The E-loop Is Involved in Hydrogen Peroxide Formation by the NADPH Oxidase Nox4. *J Biol Chem*. 2011; 286(15): 13304–13313.
- Tamargo J, Caballero R, Gómez R and Delpón E. Cardiac electrophysiological effects of nitric oxide. *Cardiovascular research*. 2010; 87 (4): 593-600.
- Tang N, Wang L, Esko J, Giordano FJ, Huang Y, Gerber HP, Ferrara N and Johnson RS. Loss of HIF-1 α in endothelial cells disrupts a hypoxia-driven VEGF autocrine loop necessary for tumorigenesis. *Cancer cell*. 2004; 6 (5): 485-495.
- Tang EH, Vanhoutte PM. Endothelial dysfunction: a strategic target in the treatment of hypertension? *Pflugers Arch*. 2010; 459(6): 995–1004.
- Tanner FC, Noll G, Boulanger CM and Luscher TF. Oxidized low-density lipoproteins inhibits relaxation of porcine coronary arteries: Role of scavenger receptor and endothelium-derived nitric oxide. *Circulation*. 1991; 83: 2012–2020.
- Tey BT, Yap KC, Yamaji H, Ali AM and Tan WS. Supplementation of Phosphatidylcholine Protects the Hybridoma Cells from Apoptosis Induced by Serum Withdrawal. *In Animal Cell Technology: Basic & Applied Aspects*. 2010; 73-76.
- Thorburn A. Review article. Death receptor-induced cell killing. *Cellular Signalling*. 2004; 16: 139–144.
- Thorin E and Webb DJ. Endothelium-derived endothelin-1. *Pflügers Archiv-European Journal of Physiology*. 2010; 459 (6): 951-958.
- Tiede LM, Cook EA, Morse B and Fox HS. Oxygen matters: tissue culture oxygen levels affect mitochondrial function and structure as well as responses to HIV viroproteins. *Cell Death and Disease*. 2011; 2: e246.
- Tomasian D, Keaney JF, Vita JA. Antioxidants and the bioactivity of endothelium-derived nitric oxide. *Cardiovasc Res*. 2000; 47(3); 426-35.
- Torre-Amione G, Kapadia S, Lee J, Durand JB, Bies RD, Young JB and Mann DL. Tumor necrosis factor- α and tumor necrosis factor receptors in the failing human heart. *Circulation*. 1996; 93 (4): 704-711.
- Toshima S, Hasegawa A, Kurabayashi M, Itabe H, Takano T, Sugano J, Shimamura K, Kimura J, Michishita I, Suzuki T, Nagai R. Circulating oxidized low density lipoprotein levels. A biochemical risk marker for coronary heart disease. *Arteriosclerosis Thrombosis and Vascular Biology*. 2000; 20: 2243–2247.

- Tousoulis D, Kampoli AM, Papageorgiou CNT and Stefanadis C. The role of nitric oxide on endothelial function. *Current vascular pharmacology*. 2012; 10 (1): 4-18.
- Touyz RM and Schiffrin EL. Signal transduction mechanisms mediating the physiological and pathophysiological actions of angiotensin II in vascular smooth muscle cells. *Pharmacol Rev*. 2000; 52: 639–72.
- Trimarchi H. The endothelium and hemodialysis. *Special Problems in hemodialysis patients. Riejska: InTech*. 2011; 167-192.
- Trochu JN, Bouhour JB, Kaley G, Hintze TH. Role of endothelium-derived nitric oxide in the regulation of cardiac oxygen metabolism: implications in health and disease. *Circ Res* 2000; 87(12): 1108-17.
- Troncoso Brindeiro CM, da Silva AQ, Allahdadi KJ, Youngblood V and Kanagy NL. Reactive oxygen species contribute to sleep apnea-induced hypertension in rats. *American Journal of Physiology: Heart and Circulatory Physiology*. 2007; 293: H2971–H2976.
- Tsai AL, Berka V, Martin F, Ma X, van den Akker F, Fabian M and Olson JS. Is Nostoc H-NOX a NO sensor or redox switch?. *Biochemistry*. 2010; 49 (31): 6587-6599.
- Tsihlis ND, Oustwani CS, Vavra AK, Jiang Q, Keefer LK and Kibbe MR. Nitric Oxide Inhibits Vascular Smooth Muscle Cell Proliferation and Neointimal Hyperplasia by Increasing the Ubiquitination and Degradation of UbcH10 Cell. *Biochemistry and Biophysics*. 2011; 60 (1-2): 89-97.
- Tsou HK, Su CM, Chen HT, Hsieh MH, Lin CJ, Lu DY, Tang CH and Chen YH. Integrin-Linked Kinase Is Involved in TNF- α -Induced Inducible Nitric-Oxide Synthase Expression in Myoblasts. *Journal of Cellular Biochemistry*. 2010; 109: 1244–1253.
- Tsutsui M, Shimokawa H, Morishita T, Nakashima Y and Yanagihara N. Development of genetically engineered mice lacking all three nitric oxide synthases. *J. Pharmacol. Sci.* 2006; 102: 147–154.
- Tsutsui M, Shimokawa H, Otsuji Y, Ueta Y, Sasaguri Y and Yanagihara N. Nitric oxide synthases and cardiovascular diseases insights from genetically modified mice. *Circ. J.* 2009; 73: 986–993.
- Ueda S, Kato S, Matsuoka H, Kimoto M, Okuda S, Morimatsu M, Imaizumi T. Regulation of cytokine-induced nitric oxide synthesis by asymmetric dimethylarginine: role of dimethylarginine dimethylaminohydrolase. *Circ Res*. 2003; 92: 226–233.
- Ueno S, Sano A, Kotani K, Kondoh K, Kakimoto Y. Distribution of free methylarginines in rat tissues and in the bovine brain. *J Neurochem*. 1992; 59: 2012–2016.
- Umbrello M, Dyson A, Feelisch M and Singer M. The key role of nitric oxide in hypoxia: hypoxic vasodilation and energy supply-demand matching. *Antioxidants & redox signaling*. 2013.
- Ungvari Z, Labinskyy N, Gupte S, Chander PN, Edwards JG and Csiszar A. Dysregulation of mitochondrial biogenesis in vascular endothelial and smooth muscle cells of aged rats. *Am. J. Physiol. Heart Circ. Physiol.* 2008; 294: H2121-H2128.

Ushio-Fukai M, Zafari AM, Fukui T, et al. p22phox is a critical component of the superoxide-generating NADH/NADPH oxidase system and regulates angiotensin II-induced hypertrophy in vascular smooth muscle cells. *J Biol Chem.* 1996; 271: 23317–23321.

Uzel G and Holland SM. Phagocyte deficiencies. *Clinical immunology principles and practice.* 2012; 1: 37-1.

Valavanidis A, Vlachogianni T and Fiotakis K. Tobacco Smoke: Involvement of Reactive Oxygen Species and Stable Free Radicals in Mechanisms of Oxidative Damage, Carcinogenesis and Synergistic Effects with Other Respirable Particles. *Int. J. Environ. Res. Public Health* 2009, 6(2), 445-462.

Valez V, Cassina A, Batinic-Haberle I, Kalyanaraman B, Ferrer-Sueta G and Radi R. Peroxynitrite formation in nitric oxide-exposed submitochondrial particles: detection, oxidative damage and catalytic removal by Mn-porphyrins. *Archives of biochemistry and biophysics.* 2012.

Vallance P, Leone A, Calver A, Collier J & Moncada S. Endogenous dimethylarginine as an inhibitor of nitric oxide synthesis. *J. Cardiovasc. Pharmacol.* 1992a; 20(suppl. 12): S60-S62.

Vallance P, Leone A, Calver A, Collier J and Moncada S. Accumulation of an endogenous inhibitor of NO synthesis in chronic renal failure. *Lancet.* 1992b; 339: 572-575.

Vallance P and Leiper J. Dimethylaminohydrolase Pathway Cardiovascular Biology of the Asymmetric Dimethylarginine:Dimethylarginine. *Arterioscler Thromb Vasc Biol.* 2004; 24: 1023-1030.

Van den Beucken T, Koritzinsky M and Wouters BG. Translational control of gene expression during hypoxia. *Cancer Biology and Therapy.* 2006; 5 (7): 749-755.

Van den Oever IAM, Raterman HG, Nurmohamed MT and Simsek S. Endothelial Dysfunction, Inflammation, and Apoptosis in Diabetes Mellitus. *Mediators of Inflammation.* 2010; Volume 2010, Article ID 792393, 15 pages.

Van den Tweel ERW, Nijboer C, Kavelaars A, Heijnen CJ, Groenendaal F and van Bela F. Expression of nitric oxide synthase isoforms and nitrotyrosine formation after hypoxia-ischemia in the neonatal rat brain. *Journal of Neuroimmunology.* 2005; 167 (1–2): 64–71.

Van der Laan PA, Reardon CA and Getz GS. Site Specificity of Atherosclerosis. Site-Selective Responses to Atherosclerotic Modulators. *Arteriosclerosis, Thrombosis, and Vascular Biology.* 2004; 24: 12-22.

Van Nieuw Amerongen GP, Minshall RD and Malik AB. Caveolae and Signaling in Pulmonary Vascular Endothelial and Smooth Muscle Cells. *In Textbook of Pulmonary Vascular Disease.* 2011; 273-285.

Vandenabeele P, Declercq W, Beyaert R, Fiers W. Two tumour necrosis factor receptors: structure and function. *Trends Cell Biol.* 1995; 5: 392-9.

Vanhoutte PM. Ageing and endothelial dysfunction. *Eur Heart J Suppl* 2002; 4: A8–A17.

- Vanhoutte PM. Endothelial Dysfunction The First Step Toward Coronary Arteriosclerosis. *Circ J.* 2009; 73: 595 – 601.
- Vasquez-Vivar J, Kalyanaraman B, Martasek P et al. Superoxide generation by endothelial nitric oxide synthase: the influence of cofactors. *Proc. Natl. Acad. Sci. U.S.A.* 1998; 95: 9220–9225.
- Vasquez-Vivar J, Martasek P, Whitsett J, Joseph J and Kalyanaraman B. The ratio between tetrahydrobiopterin and oxidized tetrahydrobiopterin analogues controls superoxide release from endothelial nitric oxide synthase: an EPR spin trapping study. *Biochem. J.* 2002; 362: 733–739.
- Veal EA, Day AM and Morgan BA. Hydrogen peroxide sensing and signaling. *Molecular cell.* 2007; 26 (1): 1-14.
- Veal E and Day A. Hydrogen peroxide as a signaling molecule. *Antioxidants & redox signalling.* 2011; 15 (1): 147-151.
- Verma S and TJ Anderson. Clinician Update. Fundamentals of Endothelial Function for the Clinical Cardiologist. *Circulation.* 2002; 105: 546-549.
- Versari D, Daghini E, Viridis A, et al. Endothelium-dependent contractions and endothelial dysfunction in human hypertension. *Br J Pharmacol* 2009a; 157: 527–536.
- Versari D, Daghini E, Viridis A, Ghiadoni L and Taddei S. Endothelial Dysfunction as a Target for Prevention of Cardiovascular Disease. *Diabetes Care.* 2009b; 32 (2): S314-321.
- Victor VM, Rocha M, Esplugues JV and Fuente MDI. Role of Free Radicals in Sepsis: Antioxidant Therapy. *Current Pharmaceutical Design.* 2005; 11 (24): 3141-3158(18).
- Vidal F, Colomé C, Martínez-González J and Badimon L. Atherogenic concentrations of native low-density lipoproteins down-regulate nitric-oxide-synthase mRNA and protein levels in endothelial cells. *European journal of biochemistry.* 1998; 252 (3): 378-384.
- Vila-Petrof MG, Kim SH, Pepe S, et al. Endogenous nitric oxide mechanisms mediate the stretch dependence of Ca²⁺ release in cardiomyocytes. *Nat Cell Biol* 2001; 3: 867–73.
- Villanueva C and Giulivi C. Subcellular and cellular locations of nitric oxide synthase isoforms as determinants of health and disease. *Free Radical Biology and Medicine.* 2010; 49 (3): 307–316.
- Viñals F and Pouysségur J. Confluence of Vascular Endothelial Cells Induces Cell Cycle Exit by Inhibiting p42/p44 Mitogen-Activated Protein Kinase Activity. *Mol. Cell. Biol.* 1999; 19 (4): 2763-2772.
- Viridis A, Duranti E and Taddei S. Oxidative stress and vascular damage in hypertension: role of angiotensin II. *International journal of hypertension.* 2011.
- Vizzard MA, Erdman SL, Förstermann U and de Groat WC. Ontogeny of nitric oxide synthase in the lumbosacral spinal cord of the neonatal rat. *Dev. Brain Res.* 1994; 81: 201–217.
- Vogel RA, Corretti MC. Estrogens, progestins and heart disease: can endothelial function divine the benefit? *Circulation.* 1998; 97(13): 1223-6.

- Volonte D, Galbiati F, Pestell RG and Lisanti MP. Cellular stress induces the tyrosine phosphorylation of caveolin-1 (Tyr(14)) via activation of p38 mitogen-activated protein kinase and c-Src kinase. Evidence for caveolae, the actin cytoskeleton, and focal adhesions as mechanical sensors of osmotic stress. *J Biol Chem.* 2001; 276: 8094–8103.
- Von Ballmoos MW, Yang Z, Völzmann J, Baumgartner I, Kalka C and Di Santo S. Endothelial progenitor cells induce a phenotype shift in differentiated endothelial cells towards PDGF/PDGFR β axis-mediated angiogenesis. *PLoS one.* 2010; 5 (11): e14107.
- Von Haehling S, Bode-Böger SM, Martens-Lobenhoffer J, Rauchhaus M, Schefold JC, Genth-Zotz S, Karhausen T, Ciccoira M, Anker SD and Doehner W. Elevated Levels of Asymmetric Dimethylarginine in Chronic Heart Failure: A Pathophysiologic Link Between Oxygen Radical Load and Impaired Vasodilator Capacity and the Therapeutic Effect of Allopurinol. *Clinical Pharmacology & Therapeutics.* 2010; 88: 506-512.
- Von Löhneysen K, Noack D, Wood MR, Friedman JS and Knaus UG. Structural insights into Nox4 and Nox2: motifs involved in function and cellular localization. *Molecular and cellular biology.* 2010; 30 (4): 961-975.
- Voyta JC, Via DP, Butterfield CE and Zetter BR. Identification and isolation of endothelial cells based on their increased uptake of acetylated-low density lipoprotein. *The Journal of cell biology.* 1984; 99 (6): 2034-2040.
- Wagner S, Rokita AG, Anderson ME and Maier LS. Redox regulation of sodium and calcium handling. *Antioxidants & Redox Signaling.* 2013; 18 (9): 1063-1077.
- Wajant H, Pfizenmaier K, Scheurich P. Tumor necrosis factor signaling. *Cell Death Differ.* 2003; 10 (1): 45–65.
- Walczak H. TNF and ubiquitin at the crossroads of gene activation, cell death, inflammation, and cancer. *Immunological reviews.* 2011; 244, (1): 9-28.
- Walczynski J, Lyons S, Jones N and Breitwieser W. Sensitisation of c-MYC-induced B-lymphoma cells to apoptosis by ATF2. *Oncogene.* 2013.
- Walford GA, Moussignac RL, Scribner AW, Loscalzo J and Leopold JA. Hypoxia Potentiates Nitric Oxide-mediated Apoptosis in Endothelial Cells via Peroxynitrite-induced Activation of Mitochondria-dependent and -independent Pathways. *Journal of Biological Chemistry.* 2004; 279: 4425-4432.
- Wallerath T, Gath I, Aulitzky WE, Pollock JS, Kleinert H and Förstermann U. Identification of the NO synthase isoforms expressed in human neutrophil granulocytes, megakaryocytes and platelets. *Thromb. Haemost.* 1997; 77: 163–167.
- Walmsley SR, Print C, Farahi N, Peyssonnaud C, Johnson RS, Cramer T, Sobolewski A, Condliffe AM, Cowburn AS, Johnson N and Chilvers ER. Hypoxia-induced neutrophil survival is mediated by HIF-1 α -dependent NF- κ B activity. *JEM.* 2005; 201 (1): 105-115.
- Wang P, Ba ZF, Chaudry IH. Administration of tumor necrosis factor-alpha in vivo depresses endothelium-dependent relaxation. *Am J Physiol.* 1994; 266: H2535–H2541.

- Wang B, Kondo S, Shivji GM, Fujisawa H, Mak TW and Sauder DN. Tumour necrosis factor receptor II (p75) signalling is required for the migration of Langerhans' cells. *Immunology*. 1996; 88: 284 - 288.
- Wang Y, Goligorsky MS, Lin M, Wilcox JN and Marsden PA. A novel, testis-specific mRNA transcript encoding an NH₂-terminal truncated nitric-oxide synthase. *J. Biol. Chem.* 1997; 272: 11392–11401.
- Wang Y, Wu TR, Cai S, Welte T and Chin YE. Stat1 as a Component of Tumor Necrosis Factor Alpha Receptor 1-TRADD Signaling Complex To Inhibit NF- κ B Activation. *Mol. Cell. Biol.* 2000; 20 (13): 4505-4512.
- Wang L, Lim EJ, Toborek M and Hennig B. The role of fatty acids and caveolin-1 in tumor necrosis factor α -induced endothelial cell activation. *Metabolism*. 2008; 57 (10): 1328–1339.
- Wang CY, Monzingo AF, Hu S, Schaller TH, Robertus JD and Fast W. Developing Dual and Specific Inhibitors of Dimethylarginine Dimethylaminohydrolase-1 and Nitric Oxide Synthase: Toward a Targeted Polypharmacology To Control Nitric Oxide. *Biochemistry*, 2009, 48 (36), pp 8624–8635.
- Wang Y. Vascular biology of the placenta. *In Colloquium Series on Integrated Systems Physiology: from Molecule to Function*. 2010; 2 (1): 1-98.
- Wang L, Chen Q, Li G and Ke D. Ghrelin stimulates angiogenesis via GHSR1a-dependent MEK/ERK and PI3K/Akt signal pathways in rat cardiac microvascular endothelial cells. *Peptides*. 2012; 33 (1): 92-100.
- Warnholtz A, Nickenig G, Schulz E *et al.* Increased NADH-oxidase-mediated superoxide production in the early stages of atherosclerosis: evidence for involvement of the renin-angiotensin system. *Circulation*. 1999; 99: 2027–2033.
- Warnholtz A, Mollnau H, Oelze M, *et al.* Antioxidants and endothelial dysfunction in hyperlipidemia. *Curr Hypertens Rep*. 2001; 3: 53–60.
- Watson SP. Platelet activation by extracellular matrix proteins in haemostasis and thrombosis. *Curr Pharm Des*. 2009; 15(12): 1358–1372.
- Watt AP, Schock BC and Ennis M. Neutrophils and Eosinophils: Clinical Implications of their Appearance, Presence and Disappearance in Asthma and COPD. *Current Drug Targets - Inflammation & Allergy*. 2005; 4 (4): 415-423(9).
- Weakley SM, Jiang J, Kougiias P, Lin PH, Yao Q, Brunicardi FC, Gibbs RA and Chen C. Role of Somatic Mutations in Vascular Disease Formation. *Expert Rev Mol Diagn*. 2010; 10(2): 173–185.
- Weibel ER and Palade GE. New cytoplasmic components in arterial endothelia. *JCB*. 1964; 23 (1): 101 – 112.
- Weigand L, Sylvester JT and Shimoda LA. Mechanisms of endothelin-1-induced contraction in pulmonary arteries from chronically hypoxic rats. *American Journal of Physiology-Lung Cellular and Molecular Physiology*. 2006; 290 (2): L284-L290.

- Weigand L, Shimoda LA and Sylvester JT. Enhancement of myofilament calcium sensitivity by acute hypoxia in rat distal pulmonary arteries. *American Journal of Physiology-Lung Cellular and Molecular Physiology*. 2011; 301 (3): L380-L387.
- Weljie AM and Jirik FR. Hypoxia-induced metabolic shifts in cancer cells: moving beyond the Warburg effect. *The international journal of biochemistry & cell biology*. 2011; 43 (7): 981-989.
- Wenger RH. Cellular adaptation to hypoxia: O₂-sensing protein hydroxylases, hypoxia-inducible transcription factors, and O₂-regulated gene expression. *The FASEB journal*. 2002; 16 (10): 1151-1162.
- Wennerberg K, Rossman KL, Der CJ. The Ras superfamily at a glance. *Journal of Cell Science*. 2005; 118: 843-846.
- Whitman EM, Pisarcik S, Luke T, Fallon M, Wang J, Sylvester JT, Semenza GL and Shimoda LA. Endothelin-1 mediates hypoxia-induced inhibition of voltage-gated K⁺ channel expression in pulmonary arterial myocytes. *American Journal of Physiology-Lung Cellular and Molecular Physiology*. 2008; 294 (2): L309-L318.
- Wilkins RC, Kutzner BC, Truong M, Sanchez-Dardon J, McLean JRN. Analysis of radiation induced apoptosis in human lymphocytes: Flow cytometry using annexin V and propidium iodide versus neutral comet assay. *Cytometry*. 2002; 48: 14-19.
- Williams MR, Azcutia V, Newton G, Alcaide P, Luscinskas FW. Emerging mechanisms of neutrophil recruitment across the endothelium. *Trends Immunol*. 2011; 32(10): 461-469.
- Wimalasundera R, Fexby S, Regan L, Thom SA and Hughes AD. Effect of tumour necrosis factor- α and interleukin 1 β on endothelium-dependent relaxation in rat mesenteric resistance arteries in vitro. *Br. J. Pharmacol*. 2003; 138: 1285-1294.
- Wink DA, Hines HB, Cheng RYS, Switzer CH, Flores-Santana W, Vitek MP, Ridnour LA and Colton CA. Nitric oxide and redox mechanisms in the immune response. *Journal of leukocyte biology*. 2011; 89 (6): 873-891.
- Wolle J, Ferguson E, Keshava C, Devall LJ, Boschelli DH, Newton RS, Saxena U. Inhibition of tumor necrosis factor induced human aortic endothelial cell adhesion molecule gene expression by an alkoxybenzo[b]thiophene-2-carboxamide. *Biochem Biophys Res Commun*. 1995;214:6-10.
- Wong ML, Whelan F, Deloukas P, Whittaker P, Delgado M, Cantor RM, McCann SM and Licinio J. Phosphodiesterase genes are associated with susceptibility to major depression and antidepressant treatment response. *Proc. Natl Acad. Sci. USA*. 2006; 103: 15124-15129.
- Wong WT, Ng CH, Tsang SY, Huang Y and Chen ZY. Relative contribution of individual oxidized components in ox-LDL to inhibition on endothelium-dependent relaxation in rat aorta. *Nutrition, Metabolism and Cardiovascular Diseases*. 2011; 21 (3): 157-164.
- World Health Organisation (WHO). Global health risks: Mortality and burden of disease attributable to selected major risks. *WHO 2009*.

- Wouters BG, van den Beucken T, Magagnin MG, Koritzinsky M, Fels D and Koumenis C. Control of the hypoxic response through regulation of mRNA translation. *Semin. Cell Dev. Biol.* 2005; 16: 487-501.
- Wu Y and Zhou BP. TNF- α /NF- κ B/Snail pathway in cancer cell migration and invasion. *British journal of cancer.* 2010; 102 (4): 639-644.
- Xia Z, Liu M, Wu Y, et al. N-acetylcysteine attenuates TNF-alpha-induced human vascular endothelial cell apoptosis and restores eNOS expression. *Eur J Pharmacol.* 2006; 550: 134-142.
- Xie L, Hattori Y, Tume N and Gross SS. The preferred source of arginine for high-output nitric oxide synthesis in blood vessels. *Semin. Perinatol.* 2000; 24: 42-45.
- Xu J, He L, Ahmed SH, Chen SW, Goldberg MP, Beckman JS and Hsu CY. Oxygen-Glucose Deprivation Induces Inducible Nitric Oxide Synthase and Nitrotyrosine Expression in Cerebral Endothelial Cells. *Stroke.* 2000; 31: 1744-1751.
- Xu W, Kaneko FT, Zheng S, Comhair SA, Janocha AJ, Goggans T, Thunnissen FB, Farver C, Hazen SL, Jennings C, Dweik RA, Arroliga AC and Erzurum SC. Increased arginase II and decreased NO synthesis in endothelial cells of patients with pulmonary arterial hypertension. *FASEB J.* 2004; 18: 1746-1748.
- Xu Y, Buikema H, van Gilst WH and Henning RH. Caveolae and endothelial dysfunction: Filling the caves in cardiovascular disease. *European Journal of Pharmacology.* 2008; 585 (2-3): 256-260.
- Xu Q, Metzler B, Jahangiri M and Mandal K. Molecular chaperones and heat shock proteins in atherosclerosis. *American Journal of Physiology-Heart and Circulatory Physiology.* 2012; 302 (3): H506-H514.
- Yamada E. The fine structure of the gall bladder epithelium of the mouse. *J. Biophys. Biochem. Cytol.* 1955; 1: 445-457.
- Yan G, You B, Chen SP, Liao JK, Sun J. Tumor necrosis factor-alpha downregulates endothelial nitric oxide synthase mRNA stability via translation elongation factor 1-alpha 1. *Circ Res.* 2008; 103: 591-597.
- Yang CM, Chien CS, Hsiao LD, Pan SL, Wang CC, Chiu CT, et al. Mitogenic effect of oxidized low-density lipoprotein on vascular smooth muscle cells mediated by activation of Ras/Raf/MEK/MAPK pathway. *Br J Pharmacol.* 2001; 132: 1531-41.
- Yang Z, Ming X-Z. Recent advances in understanding endothelial dysfunction in atherosclerosis. *Clin Med Res.* 2006; 4: 53-65.
- Yang G, Wu L, Jiang B, Yang W, Qi J, Cao K, Meng Q, Mustafa AK, Mu W, Zhang S, Snyder SH, Wang R. H₂S as a physiologic vasorelaxant: hypertension in mice with deletion of cystathionine gamma-lyase. *Science.* 2008; 322: 587-590.
- Yang G, Lucas R, Caldwell R, Yao L, Romero MJ, Caldwell RW. Novel mechanisms of endothelial dysfunction in diabetes. *J Cardiovasc Dis Res.* 2010; 1(2): 59-63.

- Yang Y, Tang LQ and Wei W. Prostanoids receptors signaling in different diseases/cancers progression. *Journal of Receptors and Signal Transduction*. 2013: 1-14.
- Ye Q, Dai H, Sarria R, Guzman J, Costabel U. Increased expression of tumor necrosis factor receptors in cryptogenic organizing pneumonia. *Respir Med*. 2010; 105: 292-297.
- Yokoyama T, Vaca L, Rossen RD, Durante W, Hazarika P and Mann DL. Cellular basis for the negative inotropic effects of tumor necrosis factor- α in the adult mammalian heart. *J Clin Invest*. 1993; 92: 2303–2312.
- Yokoyama T, Nakano M, Bednarczyk JL, McIntyre BW, Entman M, Mann DL. Tumor necrosis factor- α provokes a hypertrophic growth response in adult cardiac myocytes. *Circulation*. 1997; 95: 1247–1252.
- Yokoyama M. Oxidant stress and atherosclerosis. *Curr Opin Pharmacol*. 2004; 4: 110–115.
- Yoshizumi M, Perrella MA, Burnett Jr JC and Lee ME. Tumor necrosis factor downregulates an endothelial nitric oxide synthase mRNA by shortening its half-life. *Circ Res*. 1993; 73: 205–209.
- Yu M, Chen DM, Hu G and Wang H. Proteomic response analysis of endothelial cells of human coronary artery to stimulation with carbachol. *Acta Pharmacol. Sin*. 2004; 25 (9): 1124-30.
- Yuan ZM, Chen BY, Wang PX, Li SY, Chen YL and Dong LX. Changes of angiotensin II and its receptor during the development of chronic intermittent hypoxia-induced hypertension in rats. *Zhonghua Jie He He Hu Xi Za Zhi*. 2004; 27: 577–580.
- Zafari AM, Ushio-Fukai M, Minieri CA, et al. Arachidonic acid metabolites mediate angiotensin II-induced NADH/NADPH oxidase activity and hypertrophy in vascular smooth muscle cells. *Antioxid Redox Signal*. 1999; 1: 167–179.
- Zeibig S, Li Z, Wagner S, et al. Effect of the ox-LDL binding protein Fc-CD68 on plaque extension and vulnerability in atherosclerosis. *Circ Res*. 2011; 108(6): 695–703.
- Zembowicz A, Tang J and Wu KK. Transcriptional induction of endothelial nitric oxide synthase type III by lysophosphatidylcholine. *J Biol Chem*. 1995; 270: 17006–17010.
- Zhang J, Patel JM, Li YD and Block ER. Proinflammatory cytokines downregulate gene expression and activity of constitutive nitric oxide synthase in porcine pulmonary artery endothelial cells. *Res Commun Mol Pathol Pharmacol*. 1997; 96: 71–87.
- Zhang C, Hein TW, Wang W et al. Activation of JNK and xanthine oxidase by TNF- α impairs nitric oxide-mediated dilatation of coronary arteries. *J Mol Cell Cardiol* 2006a; 40: 247-257.
- Zhang C, Xu X, Potter B J. et al. TNF- α contributes to endothelial dysfunction in ischemia/reperfusion injury. *Arterioscler. Thromb. Vasc. Biol*. 2006b; 26: 475–480.
- Zhang M, Kho AL, Anilkumar N, Chibber R, Pagano PJ, Shah AM and Cave AC. Glycated Proteins Stimulate Reactive Oxygen Species Production in Cardiac Myocytes Involvement of Nox2 (gp91phox)-Containing NADPH Oxidase. *Circulation*. 2006; 113 (9): 1235-1243.

- Zhang DX and Gutterman DD. Mitochondrial reactive oxygen species-mediated signaling in endothelial cells. *Am J Physiol Heart Circ Physiol*. 2007; 292: H2023-H2031.
- Zhang C. The role of inflammatory cytokines in endothelial dysfunction. *Basic research in cardiology*. 2008; 103 (5): 398-406.
- Zhang H, Park Y, Wu J, Chen XP, Lee S, Yang S, Dellsperger KC and Zhang C. Role of TNF- α in vascular dysfunction. *Clinical Science*. 2009; 116: 219–230.
- Zhang W, Rojas M, Lilly B, Tsai NT, Lemtalsi T, Liou GI, Caldwell RW and Caldwell RB. NAD(P)H Oxidase-Dependent Regulation of CCL2 Production during Retinal Inflammation. *IOVS*. 2009 50 (6): 30333 -3040.
- Zhang P, Hu X, Xu X, Chen Y and Bache RJ. Cell Biology/Signaling. Dimethylarginine Dimethylaminohydrolase 1 Modulates Endothelial Cell Growth Through Nitric Oxide and Akt. *Arteriosclerosis, Thrombosis, and Vascular Biology*. 2011; 31: 890-897.
- Zhang Z, Li W, Sun D, Zhao L, Zhang R, Wang Y, Zhou X, Wang H and Cao F. Toll-like receptor 4 signaling in dysfunction of cardiac microvascular endothelial cells under hypoxia/reoxygenation. *Inflammation Research*. 2011; 60 (1): 37-45.
- Zhang GL, Dai DZ, Zhang C and Dai Y. Apocynin and raisanberine alleviate intermittent hypoxia induced abnormal StAR and 3 β -HSD and low testosterone by suppressing endoplasmic reticulum stress and activated p66Shc in rat testes. *Reproductive Toxicology*. 2013; 36: 60–70.
- Zhao W, Zhang J, Lu Y, Wang R. The vasorelaxant effect of H(2)S as a novel endogenous gaseous K(ATP) channel opener. *EMBO J*. 2001; 20: 6008–6016.
- Zhong H, De Marzo AM, Laughner E, Lim M, Hilton DA, Zagzag D, Buechler P, Isaacs WB, Semenza GL, Simons JW. Overexpression of hypoxia-inducible factor 1 α in common human cancers and their metastases. *Cancer Res*. 1999; 59: 5830–5835.
- Zhong L, You J and Sun Q. The role of NF- κ B in the TNF- α -induced endothelial cell apoptosis. *Zhonghua Yixue Zazhi*. 1999; 79: 863–866.
- Zhou J, Schmid T, Schnitzer S and Brüne B. Tumour hypoxia and cancer progression. *Cancer Lett*. 2006; 237: 10–21.
- Zhou W, Li S, Wan N, Zhang Z, Guo R, Chen B. Effects of various degrees of oxidative stress induced by intermittent hypoxia in rat myocardial tissues. *Respirology*. 2012; 17: 821-829.
- Zimmermann K, Opitz N, Dedio J, Renne C, Muller-Esterl W and Oess S. NOSTRIN: a protein modulating nitric oxide release and subcellular distribution of endothelial nitric oxide synthase. *Proc. Natl. Acad. Sci*. 2002; 99: 17167–17172.
- Ziolo MT, Kohr MJ and Wang H. Nitric oxide signaling and the regulation of myocardial function. *Journal of molecular and cellular cardiology*. 2008; 45 (5): 625.
- Zoccali C, Bode-Böger SM, Mallamaci F, Benedetto FA, Tripepi G, Malatino L, Cataliotti A, Bellanuova I, Fermo I, Frölich JC & Böger RH. Asymmetric dimethylarginine (ADMA): an

endogenous inhibitor of nitric oxide synthase predicts mortality in end-stage renal disease (ESRD). *Lancet*. 2001; 358: 2113-2117.

Zou MH, Cohen RA and Ullrich V. Peroxynitrite and vascular endothelial dysfunction in diabetes mellitus. *Endothelium*. 2004; 11 (2): 89-97.